Studies in Mechanobiology,
Tissue Engineering and Biomaterials 8

Meital Zilberman *Editor*

Active Implants and Scaffolds for Tissue Regeneration

Springer

Studies in Mechanobiology, Tissue Engineering and Biomaterials

Volume 8

Series Editor
Dr. Amit Gefen
Department of Biomedical Engineering,
The Iby and Aladar Fleischman Faculty of Engineering
Tel Aviv University
69978 Ramat Aviv
Israel
e-mail: gefen@eng.tau.ac.il

Further volumes of this series can be found on our homepage:
http://www.springer.com/series/8415

Meital Zilberman
Editor

Active Implants and Scaffolds for Tissue Regeneration

Springer

Editor
Prof. Dr. Meital Zilberman
Faculty Engineering
Department of Biomedical Engineering
Tel Aviv University
Tel Aviv
Israel
e-mail: meitalz@eng.tau.ac.il

ISSN 1868-2006 e-ISSN 1868-2014

ISBN 978-3-642-18064-4 e-ISBN 978-3-642-18065-1

DOI 10.1007/978-3-642-18065-1

Springer Heidelberg Dordrecht London New York

Cover design: WMXDesign GmbH, Heidelberg

Printed on acid-free paper

Springer is part of Springer Science+Business Media (www.springer.com)

I would like to dedicate this book to those who have always stood by my side with love, patience and understanding.
My parents, who provided the opportunities.
My husband Noam and our children Gil and Ron, the lights of my life.

Preface

Biomaterials science is the study of the application of materials to problems in biology and medicine. It is a field characterized by medical needs, basic research, and advanced technological developments. Tissue engineering is a relatively new field which began as a sub-field of biomaterials, and is described as an interdisciplinary field that applies the principles of engineering and life sciences to the development of biological materials that restore, maintain, or improve tissue function or a whole organ. Drug delivery is the method or process of administering a pharmaceutical compound to achieve a therapeutic effect in humans or animals. Controlled release systems, such as microspheres, have been developed and studied in order to enable release of bioactive agents in a controlled desired manner for periods of time which range from several days to several years. These systems serve for various biomedical applications, such as treatment of cancer, treatment of infections, enhancing tissue growth, etc.

When the three above-mentioned fields, i.e. biomaterials, tissue engineering and drug delivery are combined, a new approach in the field of implants and scaffolds for tissue regeneration is achieved. In this regard, biomedical implants with improved clinical performance have recently been developed and studied. The current book focuses on such new emerging novel implants, termed active implants, which are actually drug or protein-eluting implants that induce healing effects, in addition to their regular function. It is the first book to describe a broad range of active implants in terms of matrix formats, incorporated drugs and their release profiles from the implants, as well as cell-implant interactions and functions.

This book contains 18 chapters which are divided into four sections. The first section focuses on drug-eluting implants, namely stents, wound dressings, bioadhesives and RNA interference enhanced implants, which release hydrophilic or hydrophobic active agents to the surrounding tissue. The second section is dedicated to scaffolds for bone regeneration. A broad range of polymeric structures, composites and nanostructured scaffolds are described. The third section focuses on scaffolds based on natural polymers, such as alginate, hyaluronic acid and chitosan derivatives and fucoidan, for soft tissue regeneration. The last part

describes unique synthetic polymeric systems that can be beneficial for active implants. These include new polylactones, thermosensitive polymers, mucoadhesives and intrinsically conducting polymers. The 18 chapters in this book were written by well-known experts in the field of biomaterials, tissue engineering and drug delivery, who conduct their work in 10 different countries. They present the frontier of knowledge in active implants and scaffolds for tissue regeneration.

Prof. Dr. Meital Zilberman

Contents

Part I
Drug-Eluting Implants

Novel Composite Antibiotic-Eluting Structures for Wound Healing Applications

Jonathan J. Elsner, Israela Berdicevsky, Adaya Shefy-Peleg and Meital Zilberman

Abstract There are various wounds with tissue loss. These include burn wounds, wounds caused as a result of trauma, diabetic ulcers and pressure sores. Every year in the United States more than 1.25 million people experience burns and 6.5 million experience various chronic skin ulcers. In burns, infection is the major complication after the initial period of shock and it is estimated that about 75% of the mortality following burn injuries is related to infections. Wound dressings aim to restore the milieu required for skin regeneration by protecting the wound from environmental threats, including penetration of bacteria, and by maintaining a moist healing environment. A wide variety of wound dressing products targeting various types of wounds and different aspects of the wound healing process are currently available on the market. Ideally, a dressing should be easy to apply and remove, and its design should meet both physical and mechanical requirements; namely water absorbance and transmission rate, handleability and strength. Although silver-eluting wound dressings are available for addressing the problem of infection, there is growing evidence of the deleterious effects of such dressings in delaying the healing process due to cellular toxicity. In this chapter wound dressings with controlled release of bioactive agents are discussed. Our novel biodegradable antibiotic-eluting wound dressings are described in details and the engineering aspects in the design are emphasized. The composite material which is based on a biodegradable fibrous polyglyconate mesh bonded with a porous Poly-(DL-lactic-co-glycolic acid) matrix, is designed to protect the wound until it is no longer needed, after which it dissolves away by chemical degradation into

J. J. Elsner · A. Shefy-Peleg · M. Zilberman (✉)
Department of Biomedical Engineering, Tel-Aviv University, 69978 Tel-Aviv, Israel
e-mail: meitalz@eng.tau.ac.il

I. Berdicevsky
Department of Microbiology, Technion – Israel Institute of Technology, 32000 Haifa, Israel

Stud Mechanobiol Tissue Eng Biomater (2011) 8: 3–37
DOI: 10.1007/8415_2011_66

Published Online: 16 February 2011

non-toxic products. These new composite wound dressings are advantageous in that they provide better protection against infection, enable faster wound healing and reduce the need for frequent dressing changing.

1 Introduction

The skin is regarded as the largest organ of the body and has many different functions. Wounds with tissue loss include burn wounds, wounds caused as a result of trauma, diabetic ulcers and pressure sores. The regeneration of damaged skin includes complex tissue interactions between cells, extracellular matrix (ECM) molecules and soluble mediators in a manner that results in skin reconstruction. The moist, warm, and nutritious environment provided by wounds, together with diminished immune functioning secondary to inadequate wound perfusion, may allow build-up of physical factors such as devitalized, ischemic, hypoxic, or necrotic tissue and foreign material, all of which provide an ideal environment for bacterial growth [34].

Infection is defined as a homeostatic imbalance between the host tissue and the presence of microorganisms at concentrations that exceeds 10^5 organisms per gram of tissue or the presence of beta-hemolytic streptococci [74, 82]. The main goal of treating the various types of wound infections should be to reduce the bacterial load in the wound to a level at which wound healing processes can take place. Otherwise, the formation of an infection can seriously limit the wound healing process, can interfere with wound closure and may even lead to bacteremia, sepsis and multi-system failure. Evidence of bacterial resistance is on the rise, and complications associated with infections are therefore expected to increase in the general population.

Various wound dressings aim to restore the milieu required for skin regeneration and to protect the wound from environmental threats and penetration of bacteria. Although traditional gauze dressings offer some protection against bacteria, this protection is lost when the outer surface of the dressing becomes moistened by wound exudates or external fluids. Furthermore, traditional gauze dressings exhibit low restriction of moisture evaporation which may lead to dehydration of the wound bed. This may lead to adherence of the dressing, particularly as wound fluid production diminishes, causing pain and discomfort to the patient during removal. Most modern dressings are designed according to the well-accepted bilayer structural concept: an upper dense ‘skin’ layer to prevent bacterial penetration and a lower spongy layer designed to adsorb wound exudates and accommodate newly formed tissue. Unfortunately, dressing material adsorbed with wound discharges provides conditions that are also favorable for bacterial growth. This has given rise to a new generation of wound dressings with improved curative properties that provide a local antimicrobial effect by eluting various germicidal compounds.

Local delivery of antibiotics and disinfectants addresses the major disadvantages of the systemic approach, namely poor penetration into ischemic and

necrotic tissue typical of post-traumatic and postoperative tissue, renal and liver complications, and need for hospitalized monitoring [59, 65] by maintaining a high local antibiotic concentration for an extended duration of release without causing systemic toxicity [26, 70, 84]. The effectiveness of such devices is strongly dependent on the rate and manner in which the drug is released [81]. These are determined by the host matrix into which the antibiotic is loaded, the type of drug/disinfectant and its clearance rate. If the agent is released quickly, the entire drug could be released before the infection is arrested. If release is delayed, infection may set in further, thus making it difficult to manage the wound. The release of antibiotics at levels below the minimum inhibitory concentration (MIC) may lead to bacterial resistance at the release site and intensify infectious complications [24, 25]. A local antibiotic release profile should therefore generally exhibit a considerable initial release rate in order to respond to the elevated risk of infection from bacteria introduced during the initial shock, followed by a sustained release of antibiotics at an effective level, long enough to inhibit latent infection [65]. This chapter introduces types of cutaneous wounds and then describes the main features of wound dressings based on both synthetic and natural polymers. Part of it then focuses on our new concept of antibiotic-eluting composite structures for wound healing applications.

2 Cutaneous Wounds

The primary function of the skin is to serve as a protective barrier against the environment. The skin has two anatomic layers, each with a separate function. The superficial, epidermal layer is a barrier to bacteria and vapor (moisture loss). The dermal layer deep to the epidermis provides protection from mechanical trauma and the elasticity and mechanical integrity of the skin. Blood vessels providing nutrition to the epidermal layer run within the dermis. After skin loss, epidermal cells regenerate from deep within dermal appendages, such as hair follicles and sweat glands. The skin's function as a barrier to infection and fluid loss is lost with injury. Loss of the integrity of large portions of the skin as a result of injury or illness may lead to major disability or even death. Every year in the United States more than 1.25 million people experience burns and 6.5 million experience chronic skin ulcers caused by pressure, venous stasis, or diabetes mellitus [69]. The treating physician must compensate with appropriate fluid management and local wound care.

2.1 Burns

It is estimated that 1.25 million burn injuries occur every year in the US. Approximately 450,000 of these cases visit hospital emergency departments and

4,500 die annually of thermal related injuries (American Burn Association). Burn injuries are among the most complex and harmful physical injuries to evaluate and manage. The multiple treatment algorithms for burn wounds and resuscitation require quantification of the extent of the burn. Although many new modalities are becoming available to assess burn depth, such as laser Doppler and dielectric measurements, assessment by an experienced practitioner is currently the most reliable judge of burn depth. A simplistic description of burn type and depth is presented in Table 1.

The two most important problems encountered clinically with burn victims are dehydration and infection. Despite considerable advancements in burn wound care and infection control practices, infection remains the leading cause of death in this group of patients an it is estimated that about 75% of the mortality following burn injuries is related to infections rather than to osmotic shock and hypovolemia [38, 61].

Clearly the best coverage for wounds requiring serious reconstruction is natural skin taken from the individual himself (an autograft). However, in clinical practice this is not always possible, particularly in large total body surface area burns, as there is often an insufficient amount of skin for autografting available at the time of burn excision, or the physiological condition of the patient precludes the harvesting of skin. Allografts and xenografts can be used to provide temporary wound coverage, but there are issues with graft rejection, availability, and the possibility of disease transfer.

Although burn wound surfaces are sterile immediately following thermal injury, colonization with autogenous microorganisms (originating from the skin, gastrointestinal and respiratory flora) or through contact with the contaminated environment (water, air, and healthcare workers) generally occurs within 48 h [1, 20]. The typical burn wound is initially colonized predominantly with Gram-positive organisms, which are replaced by antibiotic-susceptible Gram-negative organisms within approximately 1 week after the burn injury. If wound closure is delayed and the patient becomes infected, thus requiring treatment with broad-spectrum antibiotics, these floras may be replaced by yeasts, fungi, and antibiotic-resistant bacteria [68]. *Staphylococcus aureus* (*S. aureus*) *and Pseudomonas aeruginosa* (*P. aeruginosa*) are the most frequently isolated organisms in most burn units [68]. Systemic treatment against infection is limited by inadequate wound perfusion which restricts migration of host immune cells and the delivery of antimicrobial agents to the wound. In this case the local concentration of the antibiotics may be insufficient and may lead to bacterial resistance. The widespread application of a topical antimicrobial agent on the open burn wound surface can substantially reduce the microbial load and risk of infection [50]. However, it requires frequent changes of the dressing material which causes inconvenience to the patient and comprises a financial burden to the healthcare system.

Table 1 Classification of burns based on depth characteristics [27, 77]

Burn severity	Cause/appearance	Treatment	Healing time
First degree	Caused by flame flash or ultraviolet exposure. Red, swollen, and painful. The burned area whitens (blanches) when lightly touched but does not develop blisters Epithelium is intact	Require no specific care	Necrotic epidermis will generally slough within 1 or 2 days, revealing intact epidermis
Second degree	Caused by scald (spill), flame, oil, grease. Pink or red, swollen, and painful, blisters that may ooze a clear fluid. The burned area may blanch when touched. Loss of the epidermis and a portion of the dermis.	Superficial burns generally heal spontaneously with local wound care. Deep burns should be treated like 3rd degree burns	Superficial burns heal within 10–14 days. Deep dermal burns usually take more than 3 weeks to heal.
Third degree	Scald (immersion), flame, steam, oil, grease, chemical, high-voltage electricity Usually not painful. skin may be red, white, waxy or charred black Loss of the tissue through the dermis including the hair follicles and sweat glands and extending into the hypodermis Notable absence of tissue edema compared with surrounding second-degree burned area	Surgical debridement (removal of dead skin). Treatment with skin graft or other skin replacement.	Small third-degree wounds (those of <2 cm) may heal spontaneously by ingrowth from the wound edges, requiring 6 weeks, and the wound may never heal completely and always result in a generous scar. Larger wounds will not heal without surgery
Fourth degree	Direct exposure of skin to open flame. Electrical, electrical shock	Full thickness wound extending through the subcutaneous soft tissue to tendon, muscle or bone	Associated with limb loss or the need for complex reconstruction

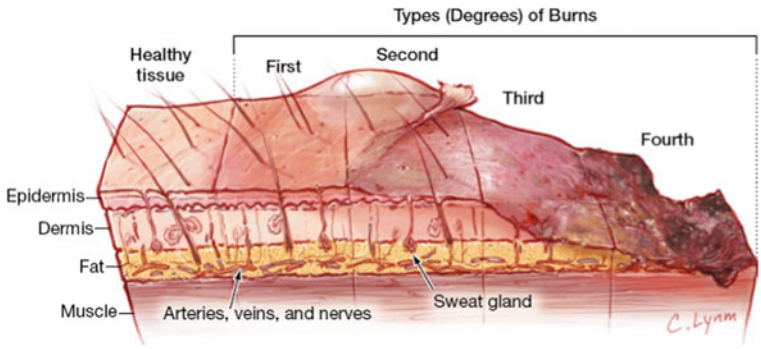

2.2 Ulcers Associated with Pressure and Arterial and Venous Diseases

An ulcer is an area of loss of the epithelium, with acute or chronic inflammation in the underlying connective tissue. In an acute ulcer, the epithelium is lost and there is edema, congestion, and polymorphonuclear leukocyte infiltration in the underlying tissue. In a chronic ulcer, there may be exuberant proliferation of young capillaries with plump fibroblasts and chronic inflammatory cells including lymphocytes and macrophages (granulation tissue).

Ulceration of the lower limb affects 1% of the adult population and 3.6% of people older than 65 years [46]. Venous disease, arterial disease, and neuropathy cause over 90% of lower limb ulcers. Venous ulcers most commonly occur above the medial or lateral malleoli. Arterial ulcers often affect the toes or shin or occur over pressure points. Neuropathic ulcers tend to occur on the sole of the foot or over pressure points. Apart from necrobiosis lipoidica, diabetes is not a primary cause of ulceration but often leads to ulceration through neuropathy or ischaemia, or both. Ulcers are usually treated with elastic compression bandaging with a simple non-adherent dressing underneath. The bandages should be changed once or twice a week, and the healing rate depends on the initial size of the ulcer, but 65–70% of ulcers heal within 6 month [46].

2.3 The Biology of Wound Healing

Wound healing is a dynamic, interactive process involving soluble mediators, blood cells, ECM, and parenchymal cells. Wound healing has three phases: inflammation, tissue formation, and tissue remodeling—that overlap in time [4, 28]:

(i) Inflammation

The first stage of wound repair occurs immediately after tissue damage, and components of the coagulation cascade, inflammatory pathways and immune system are needed to prevent ongoing blood and fluid losses, to remove dead and devitalized (dying) tissues and to prevent infection. Haemostasis is achieved initially by the formation of a platelet plug, followed by a fibrin matrix, which becomes the scaffold for infiltrating cells as demonstrated in Fig. 1a. Neutrophils are then recruited to the wound in response to the activation of complement, the degranulation of platelets and the products of bacterial degradation.

(ii) New tissue formation

The second stage of wound repair occurs 2–10 days after injury and is characterized by cellular proliferation and migration of different cell types. The first event is the migration of epithelial cells and fibroblasts to the injured area to replace damaged and lost tissue. These cells regenerate from the margins, rapidly growing over the wound under the dried scab (clot) (Fig. 1b).

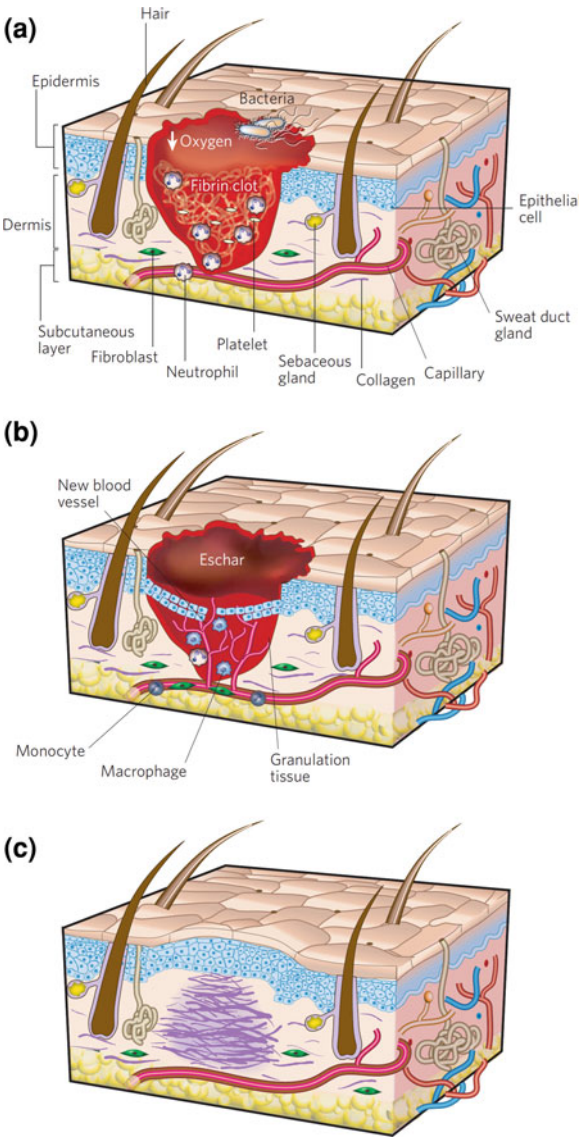

Fig. 1 Schematic representation of the phases of wound healing: **a** infiltration of neutrophils into the wound area, **b** invasion of wound area by epithelial cells, **c** epithelium completely covers the wound, and many of the capillaries and fibroblasts, formed at early stages have all disappeared [28]

The proliferative phase occurs almost simultaneously or just after the migration phase (Day 3 onwards) and basal cell proliferation, which lasts for between 2 and 3 days. Granulation tissue is formed by the in-growth of capillaries and lymphatic vessels into the wound and collagen is synthesized by fibroblasts giving the skin strength and form. By the fifth day, maximum formation of blood vessels and granulation tissue has occurred. Further epithelial thickening takes place until collagen bridges the wound. The fibroblast proliferation and collagen synthesis

continues for up to 2 weeks by which time blood vessels decrease and oedema recedes. In the later part of this stage, some of the fibroblasts are stimulated by macrophages differentiate into myofibroblasts. Myofibroblasts are contractile cells that, over time, bring the edges of a wound together. Fibroblasts and myofibroblasts interact and produce ECM, mainly in the form of collagen, which ultimately forms the bulk of the mature scar.

(iii) Remodeling

Remodeling begins 2–3 weeks after injury and lasts for a year or more. During this stage, all of the processes activated after injury wind down and cease. Most of the endothelial cells, macrophages and myofibroblasts undergo apoptosis or exit from the wound, leaving a mass that contains few cells and consists mostly of collagen and other extracellular-matrix proteins (Fig. 1c). In addition, over 6–12 months, the acellular matrix is actively remodeled from a mainly type III collagen backbone to one predominantly composed of type I collagen. This process is carried out by matrix metalloproteinases that are secreted by fibroblasts, macrophages and endothelial cells, and it strengthens the repaired tissue. However, the tissue never regains the properties of uninjured skin.

3 Wound Dressings with Controlled Release of Antibacterial Agents

A range of dressing formats based on films, hydrophilic gels and foams are available or have been investigated [86, 88]. Films and gels have a limited absorbance capacity and are recommended for light to moderately exudating wounds, whereas foams are highly absorbent and have a high water vapor transmission rate and are therefore considered more suitable for wounds with moderate to heavy exudation [4]. The characteristics of the latter are controlled by the foam texture, pore size, and dressing thickness.

3.1 Wound Dressings Based on Synthetic Polymers

Wound dressings that provide an inherent antimicrobial effect by eluting germicidal compounds have been developed to respond to the aforementioned problems associated with conventional topical treatments with ointments and creams. Wound dressings that incorporate iodine (Iodosorb® by Smith & Nephew), chlorohexidime (Biopatch® by Johnson & Johnson) or most frequently silver ions (e.g., Acticoat® by Smith & Nephew, Actisorb® by Johnson & Johnson and Aquacel® by ConvaTec) as active agents are available on the market. Such dressings are designed to provide controlled release of the active agent through a slow but sustained release mechanism which helps avoid toxicity yet ensures delivery of a therapeutic dose to the wound. Acticoat® (Smith and Nephew), for instance, is a

3-ply gauze dressing made of an absorbent rayon polyester core, with upper and lower layers of a nano-crystalline silver-coated high density polyethylene mesh. It is applied wet and is then moistened with water several times daily to allow the release of the silver ions so as to provide an antimicrobial effect for 3 days [21].

Despite frequent usage, there is growing evidence that silver is highly toxic to keratinocytes and fibroblasts and may delay burn wound healing if applied indiscriminately to healing tissue areas [7, 13, 57]. In order to address this issue, the silver in Actisorb® (Johnson & Johnson) is impregnated into an activated charcoal cloth, after which it is encased in a nylon sleeve which does not enable the silver in the product to be freely released at the wound surface but nevertheless eradicates bacteria that adsorb onto the activated charcoal component.

Another substantial disadvantage of the majority of the available synthetic wound dressings is the fact that similarly to textile wound dressings, the necessary change of dressings may be painful and increases the risk of secondary contamination. Bioresorbable dressings may successfully address this shortcoming, since they do not need to be removed from the wound surface once they have fulfilled their role. Biodegradable film dressings made of synthetic lactide-ε-caprolactone copolymers [35] are available for clinical use under the brand names of Topkin® (Biomet, Europe) and Oprafol® (Lohmann & Rauscher, Germany). During the hydrolytic degradation process the pH shifts towards the acidic range, with pH values as low as 3.6 measured in vitro [35]. Although these two dressings do not contain antibiotic agents, it is claimed that the low pH values induced by the polymer's degradation help reduce bacterial growth [78] and also promote epithelialization [14]. Furthermore, local lactate concentrations may stimulate local collagen synthesis [32]. Film dressings are better suited for small wounds, since they lack an absorbing capacity and are impermeable to water vapors and gases, which may cause accumulation of wound fluids on larger wound surfaces.

3.2 Wound Dressings Based on Natural Polymers

Only a handful of natural materials: collagen [66], chitosan/chitin [48] and alginate [75] are already available on the market as either main or additional components to the dressing structure which are able to impact the local wound environment beyond moisture management and to elicit a cellular response. Collagen is the main structural protein of the ECM, and was one of the first natural materials to be utilized for skin reconstruction and dressing applications. Collagen-based products have been available commercially for over a decade. They come in a variety of set-ups ranging from gels, pastes and powders to more elaborate sheets, sponges, and composite structures [66]. Biological materials such as collagen and chitosan have been reported to perform better than conventional and synthetic dressings in accelerating granulation tissue formation and epithelialization [8, 64, 71]. Chitosan has also been documented as displaying considerable intrinsic antibacterial activity against a broad spectrum of bacteria [51].

Gentamicin-eluting collagen sponges have been found useful in both partial-thickness and full-thickness burn wounds. Collatamp® (Innocoll GmbH, Germany), Sulmycin®-Implant (Schering-Plough, USA) and Septocoll® (Biomet Merck, Germany) are examples of such products which have been found to accelerate both granulation tissue formation and epithelialization. Because these products elute gentamicin, they also protect the recovering tissue from potential infection or re-infection [64, 65]. A comprehensive clinical study of gentamicin-collagen sponges demonstrated their ability to induce high local concentrations of gentamicin (up to 9,000 μg/mL) at the wound site for at least 72 h while serum levels remained well below the established toxicity threshold of 10–12 μg/mL [65]. However, the release of antibiotics directly from natural polymers suffers from several disadvantages. First, most natural polymers are hydrophilic and cannot counteract rapid release of the small antibiotic molecules upon water uptake, unless they are highly cross-linked. Second, natural polymers undergo in vivo degradation by proteases. The incorporated drug is thus released by a combination of diffusion and natural enzymatic breakdown of the protein, and is dependent on the biochemical wound setting. Consequently, the active agent is rapidly released from these materials [39, 71].

Simple collagen sponge entrapment systems are characterized by high drug release upon the wetting of the sponge, typically within 1–2 h of application. Sripriya et al. [71] have suggested improving the release profile of such systems by using succinylated collagen which can create ionic bonds with the cationic antibiotic ciprofloxacin so as to restrain its diffusion. It is claimed that in this way ciprofloxacin release corresponds to the nature of the wound in line with the amount of wound exudates absorbed in the sponge. Effective in vitro release from their system was found to last 5 days, and was proven successful in controlling infection in rats. Other studies have aimed to better control drug release or improve wound healing properties by combining collagen with other synthetic or natural biodegradable elements. Prabu et al. [58] focused on achieving a more sustained release of the antimicrobial agent and described a dressing made from a mixture of collagen and PCL loaded with gentamicin and amikacin, whereas Shanmugasundaram et al. [67] chose to impregnate collagen with alginate microspheres loaded with the antibacterial agent silver sulfadiazine (AgSD).

Other studies which focused on improving wound healing capabilities tried to incorporate tobramycin, ciprofloxacin [56] and AgSD [44] into collagen–hyaluronan based dressings. The two latter studies did not show conclusive evidence of improved healing properties compared to their control. However, hyaluronan, a structure-stabilizing component of the ECM, is thought to play a role in several aspects of the healing process with hyaluronan-based dressings, and exhibited promising results in the management of chronic wounds such as venous leg ulcers [11, 76].

A wide range of studies describe the employment of the polysaccharide chitosan and its partially deacetylated derivative chitin as structural materials analogous to collagen for wound dressings. Both materials offer good wound protection and have also been found to promote wound healing without excessive

granulation tissue and scar formation [10]. Chitosan has also been documented as displaying considerable intrinsic antibacterial activity against a broad spectrum of bacteria [51]. Ignatova et al. [33] reported the electrospinning of chitosan with PVA into non-woven nano-fiber mats with good in vitro bactericidal activity against *S. aureus* and *Escherichia coli* (*E. coli*). Another interesting fibrous form which combines the polysaccharides chitosan and alginate was reported by Knill et al. [41], who developed a composite structure of calcium alginate filaments coated with chitosan, utilizing the cationic interaction of chitosan with the anionic nature of alginate to bond the two together. It has been suggested that the core alginate fiber may manage excess exudates whereas chitosan would provide antibacterial, haemostatic and wound healing properties. In this case too, antibacterial testing of the fibers demonstrated an antibacterial effect. Several attempts to improve the chitosan dressing's antibacterial capabilities by incorporating various agents such as AgSD [48], chlorhexidine diacetate [63] and minocycline hydrochloride [2] have been reported.

3.3 The Relevant Antibacterial Agents

Silver ions, which are the most commonly used topical antimicrobial agent in burn wound care products, do not discriminate between cells involved in the healing process and pathogenic bacteria. Several recent tissue culture studies have shown that silver ions can cause lethal damage to both keratinocytes and fibroblasts [7, 53, 55, 57]. Such tests are probably a severe estimate, since rapid inactivation by chloride and protein occur in the wound, in the clinical environment [57]. However, the inactivation of silver ions concomitantly reduces their antibacterial potency. Since the bacterial and cellular toxic silver dose is within a similar range (7–55 mg/mL) [57], it has been suggested that silver-based products should be used with caution in situations where rapidly proliferating cells may be harmed, such as in superficial burns and the application of cultured cells [55, 57].

Despite growing evidence of bacterial resistance, antibiotics still represent an effective and selective treatment option against bacterial infections. The incorporation of broad-spectrum antibiotics such as gentamicin, ceftazidime or mafenide acetate in wound dressings can help reduce the bio-burden in the wound bed and thus prevent infection and accelerate wound healing. Aminoglycosides such as gentamicin are often used as prophylaxis when skin excisions and transplantation are undertaken. However, aminoglycosides have a narrow therapeutic index and are known for their potential nephro- and ototoxicity when used systemically, such that frequent drug and renal function monitoring are mandatory [79]. Ceftazidime is a third generation cephalosporin antibiotic that is very active against Gram-negative bacteria, including *P. aeruginosa*, and is a suitable antibiotic for the prophylaxis and therapy of bacterial infections in patients with severe burns [73, 79]. Mafenide is particularly appropriate in cases of burn wounds, since it

Table 2 Physicochemical properties of the antibiotics used in the study [6]

Antibiotic agent	Molecular weight (g/mol)	Water solubility (mg/mL)	Antibacterial spectrum
Gentamicin sulphate	477.6	100	Effective against a broad spectrum of Gram-positive and Gram-negative bacteria
Ceftazidime pentahydrate	546.6	5	A third-generation cephalosporin which displays a broad spectrum activity against Gram-positive and Gram-negative bacteria. Unlike most third-generation agents, it is active against *Pseudomonas aeruginosa*
Mafenide acetate	246.3	250	Bacteriostatic for many Gram-negative and Gram-positive organisms, including *Pseudomonas aeruginosa* and certain strains of anaerobes. Mafenide is highly soluble and diffuses into and through eschar producing a marked reduction in the number of bacteria present, even in avascular tissue of second- and third-degree burns

exhibits excellent antimicrobial activity and the best eschar penetration of any antibacterial agent [72]. However, mafenide causes severe side effects, especially when applied to large areas [52]. The controlled release of this antibiotic, alone or in combination with the other antibiotics reported in this study, may help prevent the occurrence of complications associated with conventional topical antibiotic treatment. The physicochemical properties of three these water soluble antibiotics are brought in Table 2. Their release directly to the wound, and in a controlled manner, should enable reaching a high local concentration while avoiding systemic toxicity, and therefore we chose to use them in our study which is presented in the following sub-chapter.

4 Novel Composite Antibiotic-Eluting Wound Dressings

The previous section shows that there is currently no available synthetic dressing that combines the advantages of occlusive dressings with biodegradability and intrinsic topical antibiotic treatment. In order to obtain this combination of properties we have recently developed and studied a composite wound dressing based on the concept of core/shell (matrix) composite structures. Its characteristics are described here.

Composites are made up of individual materials, matrix and reinforcement. The matrix component supports the reinforcement material by maintaining its relative positions and the reinforcement material imparts its special mechanical properties to enhance the matrix properties. Taken together, both materials synergistically produce properties unavailable in the individual constituent materials, allowing the designer to choose an optimum combination. In our application, a reinforcing

polyglyconate mesh affords the necessary mechanical strength to the dressing, while the porous Poly (DL-lactic-co-glycolic acid) (PDLGA) binding matrix is aimed to provide adequate moisture control and release of antibiotics in order to protect the wound bed from infection and promote healing. Both structural constituents are biodegradable, thus enabling easy removal of the wound dressing from the wound surface once it has fulfilled its role. This new structural concept in the field of wound healing is presented in Fig. 2.

The freeze-drying of inverted emulsions technique which was used to create the porous binding matrix is unique in its ability to preserve the liquid structure in the solid state [85]. The viscous emulsion, consisting of a continuous PDLGA/chloroform solution phase and a dispersed aqueous drug solution, formed good contact with the mesh during the dip-coating process. Consequently, an unbroken solid porous matrix was deposited by the emulsion following freeze-drying (Fig. 2b). The freeze-drying of inverted emulsions technique has several advantages. First, it enables attaining a thin uninterrupted barrier, which unlike mesh or gauze alone can better protect the wound bed against environmental threats and dehydration. Second, it entails very mild processing conditions which enable the incorporation of sensitive bioactive agents such as antibiotics [15, 87] and even growth factors [85] to help reduce the bio-burden in the wound bed and accelerate wound healing.

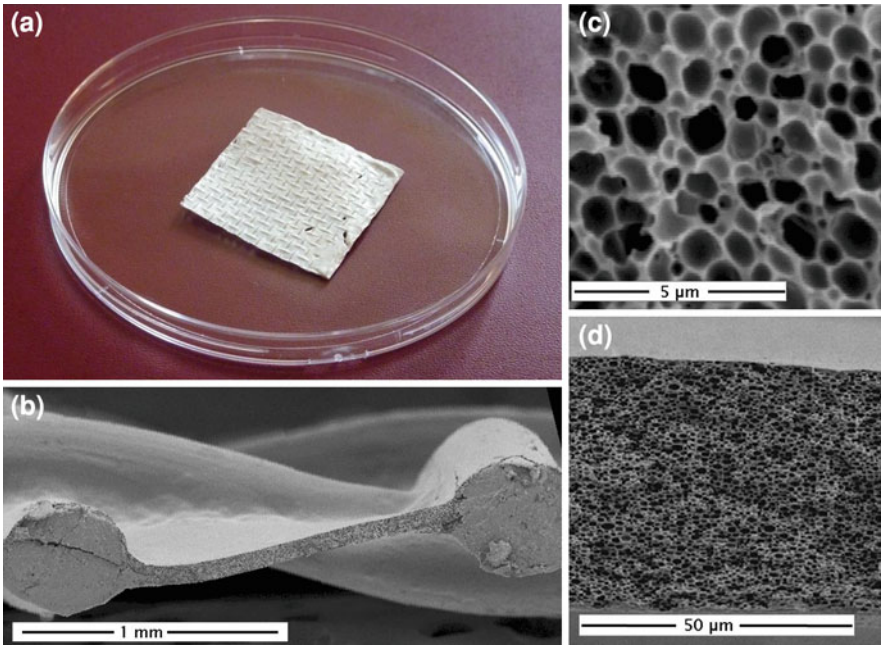

Fig. 2 The structure of the biodegradable composite wound dressing composed of polyglyconate fibers surrounded by a continuous PDLGA porous matrix: **a** Photograph of the wound dressing, **b** cross-sectional cryo-fractured SEM image showing two fibers and the binding matrix between them, **c**, **d** the microstructure of the porous matrix [18]

Third, the microstructure of the freeze-dried matrix can be customized through modifications of the emulsion's formulation to exhibit different attributes, namely different porosities or drug release profiles. Such structuring effects are described in this chapter. The mechanical and physical properties of these new wound dressings and their biological performance are also presented. Finally, a guinea pig model was used to evaluate the effectiveness of these antibiotic-eluting dressings and the main conclusions are brought here.

4.1 Structure-Controlled Release Effects

The controlled release of antibiotics from wound dressings is challenging, since various related design considerations need to be addressed. Specifically, porosity which is desired to provide adequate gaseous exchange and absorption of wound exudates [48] may act as a two-edged sword; allowing rapid water penetration which typically leads to a rapid release of the water soluble active agent within several hours to several days [40, 71]. Structural effects on the controlled release of gentamicin and ceftazidime from our composite structures were extensively studied [15, 17] and the most important results are presented here.

The emulsion's formulation parameters which determine the porous matrix structure and also the resulting properties are the organic:aqueous (O:A) phase ratio, the drug content in the aqueous phase, the polymer content in the organic phase, the polymer's initial molecular weight (MW) and also surfactants incorporated in the emulsion so as to increase its stability. The characteristic features of our studied samples are presented in Table 3. The basic formulations were used for the microstructure-release profile study. A highly interconnected porous structure poses almost no restriction to outward drug diffusion once water penetrates the matrix, and drug release in this case is most probably governed by the rate of water penetration into the matrix. Hence, the antibiotic release from our reference formulation (formulation 1, Fig. 3a, open circle) clearly demonstrates the prominent effect of pore connectivity on the burst release of the antibiotics, i.e. release of drug within the first 6 h. Samples with relatively low emulsion's O:A phase ratio (up to 8:1) typically demonstrate much pore connectivity (Fig. 3b) and their in vitro release patterns display a burst release of approximately 95% (Fig. 3a, open circle). In contradistinction, porous shell structures derived from higher O:A phase ratios (for example 12:1), display reduced pore connectivity and a lower pore fraction (Fig. 3c and Table 3), resulting in a significant half-fold decrease in the burst release of antibiotics to approximately 45% (Fig. 3a, open triangle).

An increase in the polymer's MW from 100 to 240 kDa resulted in a tremendous effect on the shell microstructure. The porosity of the shell in this case was reduced to only 16% (Fig. 3d and Table 3). Since high viscosity increases the shear forces during the process of emulsification and also reduces the tendency of droplets to move, it is expressed in a significantly smaller pores and relatively thick polymeric domain between them. These changes in microstructure reduced

Table 3 Structural characteristics of the ceftazidime-loaded porous matrix [16]

	Formulation	O:A	Drug loading* (w/w) (%)	Polymer content in the organic phase**(w/v) (%)	Polymer MW (kDa)	Surfactant**	Freeze-dried emulsion	
							Porosity (%)	Pore diameter (μm)
Basic formulations	1. Reference	6:1		15	100	None	68	1.5 ± 0.6
	2. High O:A	12:1	5	15	100	None	45	1.6 ± 0.4
	3. High Polymer Content	6:1	5	20	100	None	22	1.2 ± 0.9
	4. High Polymer MW	6:1	5	15	240	None	16	0.5 ± 0.4
Formulations with surfactants	5. BSA1: Ref, stabilized with BSA	6:1	5	15	83	BSA (1% w/v in the aqueous phase)	63	1.4 ± 0.3
	6. BSA2: High O:A, stabilized with BSA	12:1	5	15	83	BSA (1% w/v in the aqueous phase)	35	1.4 ± 0.3
	7. SPAN: High O:A, stabilized with Span	12:1	5	15	83	Span80 (1% w/v in the organic phase)	45	1.1 ± 0.3

* Relative to the polymer weight

** Relative to the liquid phase volume (organic or aqueous)

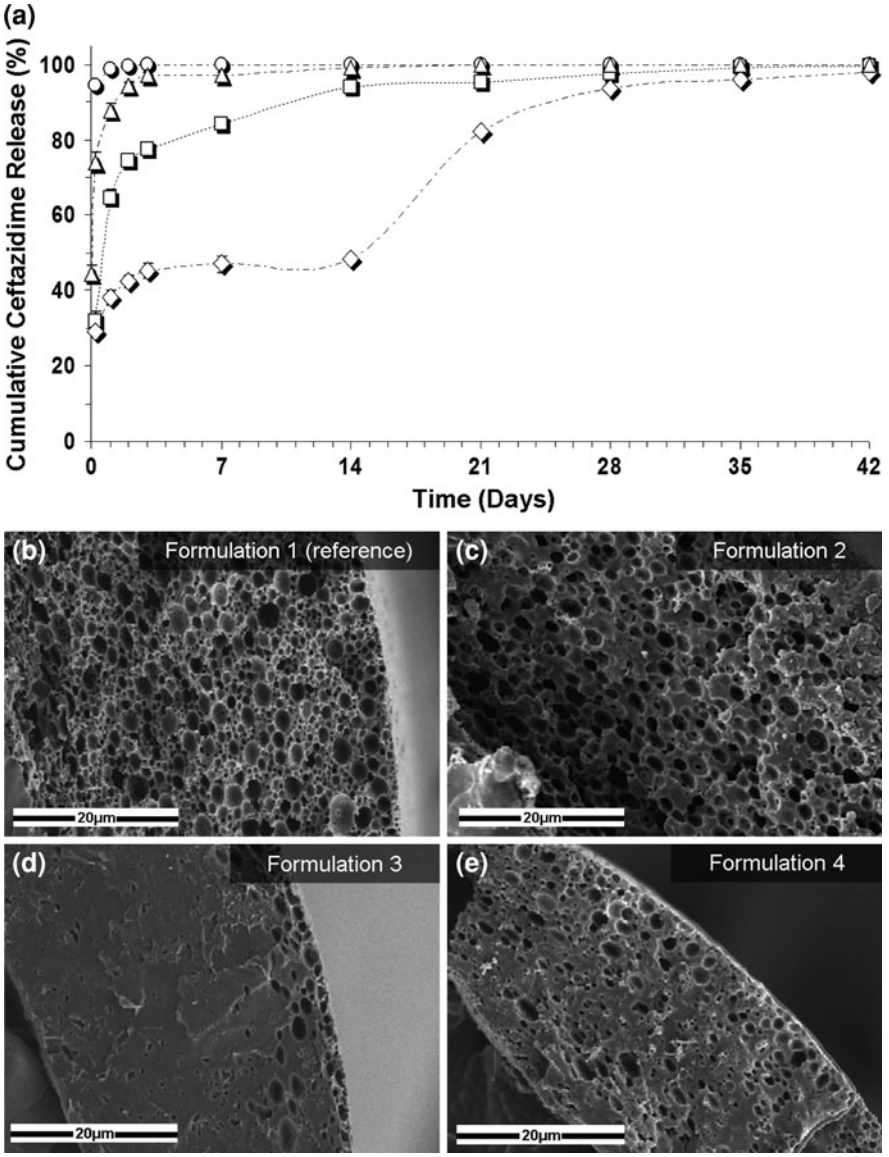

Fig. 3 **a** Controlled release of the antibiotic drug ceftazidime from composite structures based on various formulations. *open circle*—the reference formulation (formulation 1): 5% w/w ceftazidime and 15% w/v polymer (75/25 PDLGA, MW = 100 kDa), O:A = 6:1, *open triangle*—formulation 2: increased O:A phase ratio (12:1), *open square*—formulation 3: increased polymer MW (240 kDa), and *open diamond*—formulation 4: increased polymer content in the organic phase (20%). **b–e** SEM fractographs showing the effect of a change in the emulsion's formulation parameters on the microstructure of the binding matrix for formulations 1–4, respectively [16]

the burst release of the encapsulated antibiotics to approximately 30% and enabled a continuous moderate release over a period of 1 month (Fig. 3a, open square).

Finally, an increase in the emulsion's polymer content to 20% w/v also resulted in a dramatic decrease in the burst release (Fig. 3a, open diamond). A higher polymer content in the organic phase results in denser polymer walls between pores after freeze-drying (Fig. 3e) and therefore poses better constraint on the release of drugs out of pores. Interestingly, samples containing a 20% polymer content exhibited a three-phase release pattern: an initial burst release, a continuous release at a declining rate during the first 2 weeks until release of 50% of the encapsulated drug, followed by a third phase of release of a similar nature reaching 99% release after 42 days. The second phase of release is governed by diffusion, whereas the third phase is probably governed by degradation of the host polymer which enables trapped drug molecules to diffuse out through newly formed elution paths. In other cases described thus far, drug release was governed primarily by diffusion, since almost the entire amount of drug was released before polymer degradation would in fact be able to affect the release profile. Thus, when drug diffusion out of the shell is restricted as in the case of high polymer content, and a considerable amount of drug still remains within the porous matrix, polymer degradation will contribute to further release the antibiotics, which leads to an additional release phase.

Other modifications to the emulsion formulation included the addition of surfactants. Surfactants promote stabilization of the emulsion by reduction of interfacial tension between the organic and aqueous phases, resulting in refinement of the microstructure. We examined three matrix formulations loaded with surfactants (listed in Table 3), which display distinctly different micro-structural features (Fig. 4a–c and Table 3). The effect of the O:A phase ratio was examined on formulations containing bovine serum albumin (BSA) as surfactant. As expected, a higher O:A phase ratio, i.e., lower aqueous phase quantity, resulted in a smaller porosity of the solid structure. However, both microstructures were homogenous and characterized by a similar average pore size. The stabilization effect of Span 80 was even higher than that obtained using BSA, and therefore resulted in a smaller pore size (Table 3). The release profile of antibiotics from wound dressings varied considerably with the changes in formulation (Fig. 4d). Ceftazidime release from the dressings based on the BSA1 formulation was relatively short, reaching almost complete release of the encapsulated drug within 24 h. An increase in the emulsion's O:A phase ratio from 6:1 to 12:1 reduced the burst release. Specifically, burst release values of 97 and 57% were recorded after 6 h for formulations BSA1 and BSA2, respectively, after which the release of the antibiotics from BSA2 dressings continued for 5 days at a decreasing rate. The ceftazidime release profile from the SPAN formulation was totally different. It exhibited a low burst release of 6% during the first 6 h of incubation and then a release pattern of a nearly constant rate for 10 days. Surfactant incorporation can contribute to the achievement of more than merely a stabilizing effect, by binding to antibiotics and thus counteracting drug depletion. We have found, for instance, that dressings containing mafenide in combination with albumin as surfactant display a lower burst release and a moderate release rate [15].

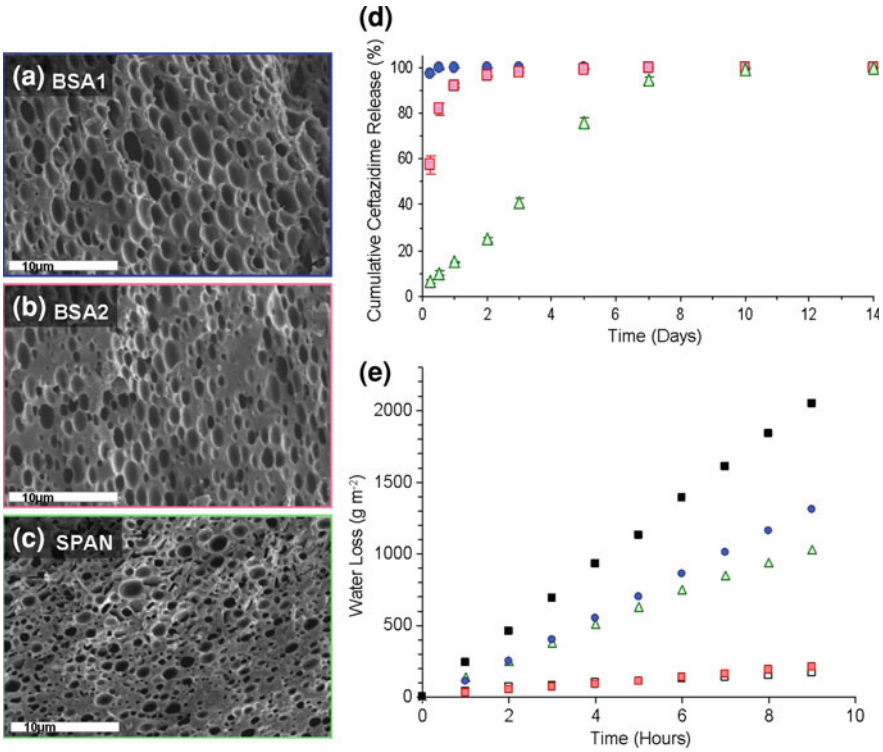

Fig. 4 **a**–**c** SEM fractographs demonstrating the microstructure of wound dressings based on formulations BSA1 (*filled circle*), BSA2 (*light shaded filled square*) and SPAN (*filled triangle*), respectively. **d** The controlled release of the antibiotic drug ceftazidime and **e** water loss, corresponding to each sample, together with water loss from a dense (non-porous) PDLGA (50/50, MW 100 kDa) film (*dark shaded filled square*) and from an uncovered surface (*open square*) [16]

In summary, we demonstrated the release of antibiotic contents at high (>90%), intermediate (40–60%) and low (∼5%) burst release rates and release spans ranging from several days to three weeks. The versatility of the drug release profiles was obtained through the effects of the inverted emulsion's formulation parameters on the porous structure. In particular, lower burst release rates and longer elution durations can be achieved through structuring towards a reduced pore size, pore connectivity and total porosity.

4.2 Physical and Mechanical Properties

4.2.1 Moisture Management

Successful wound healing requires a moist environment. Two parameters must therefore be determined: the water uptake ability of the dressing and the water

vapor transmission rate (WVTR) through the dressing. An excessive WVTR may lead to wound dehydration and adherence of the dressing to the wound bed, whereas a low WVTR might lead to maceration of healthy surrounding tissue and buildup of a back pressure and pain to the patient. A low WVTR may also lead to leakage from the edges of the dressing which may result in dehydration and bacterial penetration [4, 60]. It has been claimed that a wound dressing should ideally possess a WVTR in the range of 2,000–2,500 g/m^2/day, half of that of a granulating wound [60]. In practice; however, commercial dressings do not necessarily conform to this range, and have been shown to cover a larger spectrum of WVTR, ranging from 90 (Dermiflex®, J&J [80] to 3,350 g/m^2/day (Beschitin®, Unitika [48]). Clearly, the WVTR is related to the structural properties (thickness, porosity) of the dressing as well as to the chemical properties of the material from which it is made.

In this part of the study, we examined the specific emulsion formulations that included surfactants (BSA1, BSA2, SPAN, see Table 3). These were chosen based on emulsion stability and resultant microstructure (Fig. 4a–c), and also on drug release profiles (Fig. 4d). Evaporative water loss through the various dressings (Fig. 4e) was linearly dependant on time ($R^2 > 0.99$ in all cases), resulting in a constant WVTR, between 480–3,452 g/m^2/day, depending on the formulation (Table 4). These results demonstrate how the WVTR can be customized based on modifications of the porous matrix's microstructure. The lowest value is similar to that reported for film type dressings (e.g. Tegaderm, 491 ± 44 g/m^2/day) [42], while the highest value is similar to that of foam type dressings (e.g. Lyofoam, 3,052 ± 684 g/m^2/day) [42]. Further investigation of O:A phase ratios between 6:1 and 12:1 with albumin may generate a WVTR specifically in the 2,000–2,500 g/m^2/day range. A WVTR of 2,641 ± 42 g/m^2/day which was achieved for 12:1 O:A with the surfactant Span 80 (formulation 7) is close to this range and seems the most appropriate.

Water uptake by the wound dressing may occur either as the result of water entry into accessible voids in the porous matrix structure (hydration effect), or as the polymer matrix material gradually uptakes water and swells (swelling effect). Our water uptake patterns for wound dressings based on formulations (5) and (6) demonstrated both these effects (Fig. 5). Both types of wound dressing demonstrated a 3-stage water uptake pattern. Examination of the water uptake process through temporal micro-structural changes in the polymeric matrix sheds light on these stages, as follows:

Table 4 Water vapor transmission rates, calculated for various wound dressings [16]

Dressing type	WVTR (g/m^2/day)
Dense (nonporous) film	356 ± 106
BSA1	3,452 ± 116
BSA2	480 ± 69
SPAN	2,641 ± 42
Open surface	6,329 ± 765

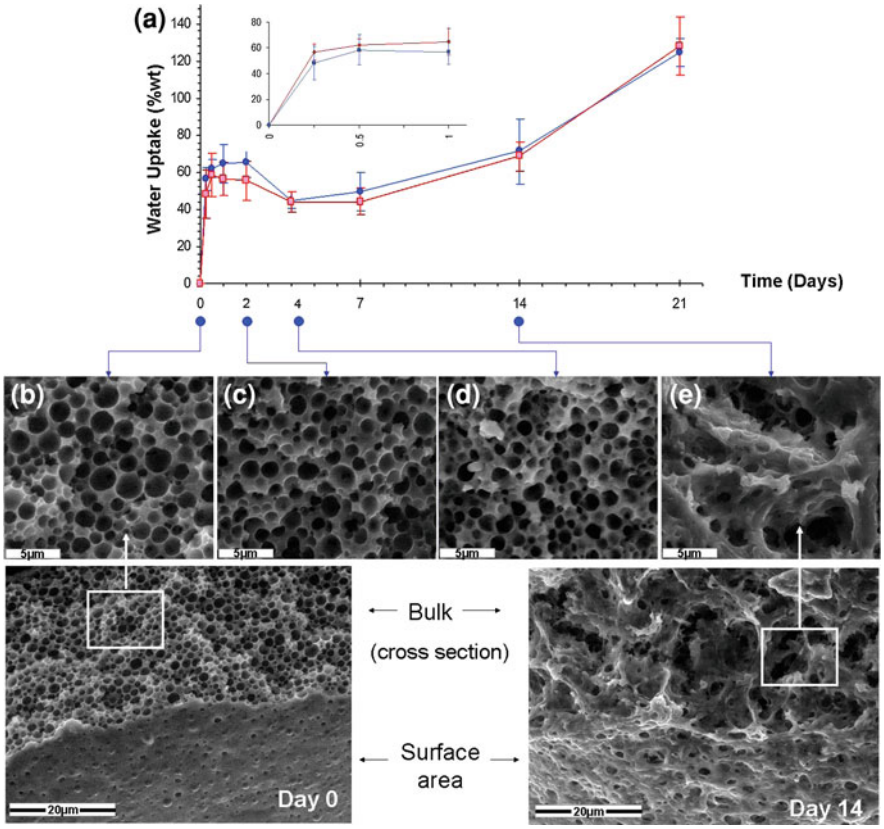

Fig. 5 **a** Water uptake by two dressing formulations containing: 5% w/w ceftazidime, 15% w/v polymer (50/50 PDLGA, MW 100 kDa), stabilized with 1% w/v BSA: (*filled circle*) BSA1 (O:A = 6:1) and (*filled square*) BSA2 (O:A = 12:1), **b–e** E-SEM fractographs of BSA1, recorded during the water uptake experiment at 0 (**b**), 2 (**c**), 4 (**d**) and 14 days (**e**). In addition, larger domains of (**b**) and (**e**) are presented [17]

Stage 1. (governed by hydration): during this stage of water uptake a quick flux of water associated with hydration of the porous structures was measured within 6 h after immersion in PBS for both types of dressings, as demonstrated in Fig. 5a. Water content then plateaued at values of 65% for the BSA1 formulation with the higher porosity (63%) and 55% for the BSA2 formulation with the smaller porosity (35%).

Stage 2. A small decrease in water content during days 2–4, probably due to gradual shrinkage of pore walls and reorganization of the porous matrix (Fig. 5b–d). Such changes could be provoked by a combined effect of the polymer's glass transition temperature which is very close to the incubation temperature (37°C) in combination with a softening effect of water on the polymer. It has been shown, for instance, that amorphous electrospun PDLGA fibrous mats undergo drastic

shrinkage after 1 day of in vitro incubation due to the relaxation of extended amorphous chains [89]. A 26% decrease in the void fraction of the polymer matrix (Fig. 5e) evidently caused a reduction in the water volume contained within the matrix ($\sim$20%) during this phase.

Stage 3. (governed by swelling): After the fourth day of immersion in the aqueous medium, water uptake increased gradually and similarly for both types of dressing over the duration of 3 weeks, ultimately reaching a two-fold increase. The process of swelling is dependent on the polymer's water affinity. Since PDLGA is not as hydrophilic as hydrogels or natural polymers used in this application, swelling occurred slowly. It is believed that the swelling effect was enhanced over time as hydrophilic end groups became more abundant due to polymer degradation by hydrolysis. This stage is also characterized by gradual thickening of the polymer walls due to the increased water uptake and creation of larger voids in the matrix due to polymer degradation (Fig. 5e). The combination of these two changes, which occurred in parallel, resulted is a coarser microstructure.

4.2.2 Mechanical Properties

The mechanical properties of a wound dressing are an important factor in its performance, whether it is to be used topically to protect cutaneous wounds or as an internal wound support, e.g. for surgical tissue defects or hernia repair. Furthermore, in the clinical setting, appropriate mechanical properties of dressing materials are needed to ensure that the dressing will not be damaged by handling. Porous structures typically possess inferior mechanical properties compared to dense structures, yet in wound healing applications porosity is an essential requirement for diffusion of gasses, nutrients, cell migration and tissue growth. Most wound dressings are therefore designed according to the bi-layer composite structure concept and consist of an upper dense "skin" layer to protect the wound mechanically and prevent bacterial penetration and a lower spongy layer designed to adsorb wound exudates and accommodate newly formed tissue. Our new dressing design integrates both structural/mechanical and functional components (e.g., drug release and moisture management) in a single composite layer [17]. It combines relatively high tensile strength and modulus together with good flexibility (elongation at break). It actually demonstrated better mechanical properties than most other dressings currently used or studied, as demonstrated in Table 5.

The initial mechanical properties of natural polymers such as collagen or gelatin can be satisfactory. However, considerable degradation of these properties is expected to occur rapidly due to hydration [62] and enzymatic activity [43]. The results of the 3 weeks degradation study of our wound dressings show a significant decrease only in Young's modulus (Fig. 6). The maximal stress and strain of our composite wound dressing (24 MPa and 55%, respectively) are dictated mainly by the mechanical properties of the reinforcing fibers which fail first during breakage. At these time periods they are not subjected to considerable degradation, which

Table 5 Mechanical properties of various wound dressings [17]

Material/format	Elastic modulus (MPa)	Tensile strength (MPa)	Elongation at break (%)
BSA1 (composite polyglyconate mesh, coated with PDLGA porous matrix)	126 ± 27	24.2 ± 4.5	55 ± 5
Electrospun poly-(L-lactide-*co*-ε-caprolactone) (50:50) mat [45]	8.4 ± 0.9	4.7 ± 2.1	960 ± 220
Electrospun gelatin mat [45]	490 ± 52	1.6 ± 0.6	17.0 ± 4.4
Electrospun collagen mat [62]		11.4 ± 1.2	
Resolut® LT regenerative membrane (Gore). Glycolide fiber mesh coated with an occlusive PDLGA membrane [49]		11.7	20
Kaltostat® (ConvaTec) Calcium/sodium alginate fleece [9]	1.3 ± 0.2	0.9 ± 0.1	10.8 ± 0.4

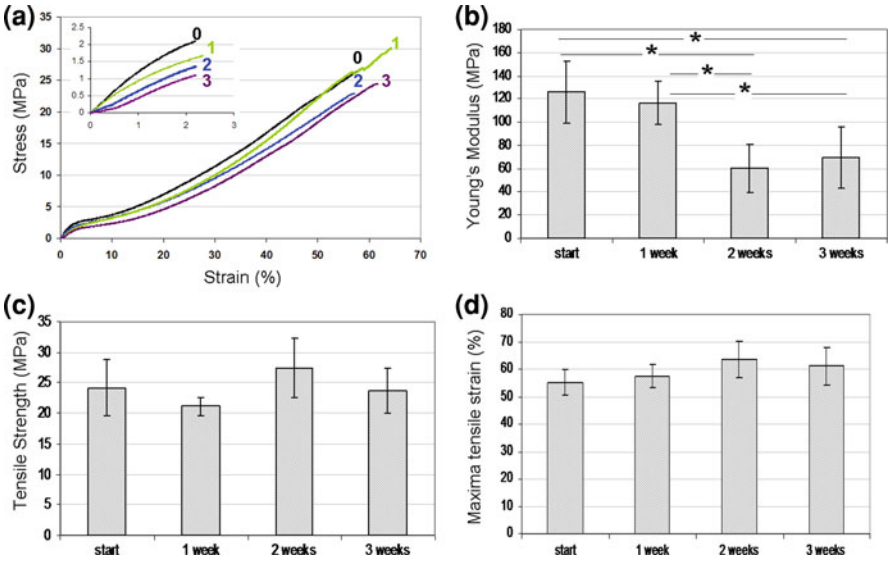

Fig. 6 **a** Tensile stress–strain curves for wound dressings immersed in water for 0 (–0–), 1 (–1–) 2 (–2–), and 3 (–3–), weeks, **b** Young's modulus, **c** tensile strength and **d** maximal tensile strain as a function of immersion time. Comparison was made using ANOVA and significant differences are indicated (*asterisk*) [17]

explains the constancy in these properties. In contradistinction, the Young's modulus of the dressings is considerably affected by the properties of the binding matrix that makes up the largest part of the cross-sectional area. The degradation of the matrix material which is clearly in progress after 2 weeks of exposure to PBS (Fig. 5e) thus leads to a decrease in Young's modulus. The mechanical properties of our wound dressings are superior to those reported before, and remain

good even after 3 weeks of degradation (Young's modulus of 69 MPa, maximal stress 24 MPa and maximal strain 61%), as demonstrated in Fig. 6.

It should also be mentioned that delamination of the fiber-matrix interface may affect the integrity of the wound dressing as well as barrier properties. We have therefore examined the effect of degradation on the interface and found that the dressing material maintained its integrity for the duration of at least 2 weeks exposure to aqueous medium, despite a gradual ongoing process of degradation of the matrix component. SEM observations (Fig. 7) showed high quality fiber-matrix interface, i.e. contact between the two components still exists as degradation proceeds [17].

In summary, the mechanical properties of our wound-dressing structures were found to be superior, combining relatively high tensile strength and ductility, which changed only slightly during 3 weeks of incubation in an aqueous medium. The parameters of the inverted emulsion as well as the type of surfactant used for stabilizing the emulsion were found to affect the microstructure of the binding matrix and the resulting physical properties, i.e., water absorbance and water vapor transmission rate.

4.3 Biological Performance

4.3.1 Bacterial Inhibition

The strategy of drug release to a wound depends on the condition of the wound. After the onset of an infection, it is crucial to immediately respond to the presence of large numbers of bacteria ($>10^5$ CFU/mL) which may already be present in the biofilm [30], and which may require antibiotic doses of up to 1,000 times those needed in suspension [12, 23]. Following the initial release, sustained release at an effective level over a period of time can prevent the occurrence of latent infection. We have shown that the proposed system can comply with these requirements (sect. 4.1).

The time-dependent antimicrobial efficacy of these antibiotic-eluting wound dressing formulations was tested in vitro by the following two complementary methods:

1. The corrected zone of inhibition test (CZOI) [18], which is also termed the disc diffusion test. According to this method presence of bacterial inhibition in an area that exceeds the dressing material (CZOI >0) can be considered beneficial. This method gives a good representation of the clinical situation, where the dressing material is applied to the wound surface, allowing the drug to diffuse to the wound bed. The results from this method are dependent on the rate of diffusion of the active agent from the dressing, set against the growth rate of the bacterial species growing on the lawn, and are highly dependent on the physicochemical environment.

2. A release study from selected wound dressings in the presence of bacteria was also performed, in order to study the effect of drug release on the kinetics of

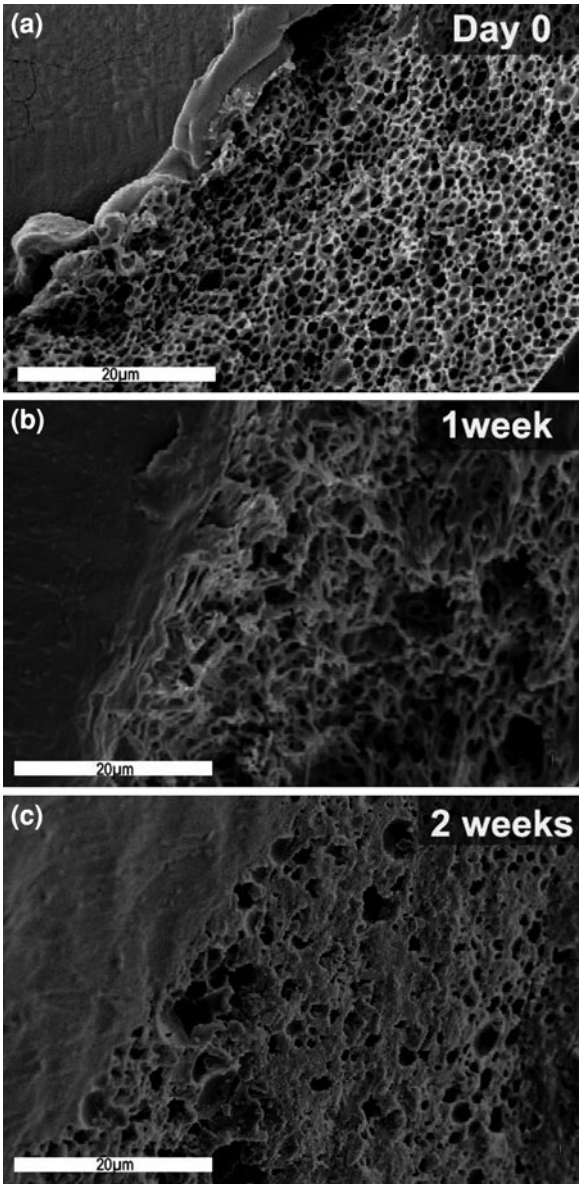

Fig. 7 SEM fractographs demonstrating the interface between the reinforcing fiber and porous matrix for specimens based on formulation BSA1, immersed in aqueous medium for: **a** start point, **b** 1 week, and **c** 2 weeks [17]

residual bacteria [18]. This method, which is termed viable counts, provide valuable information on the kill rate, which is a key comparator for different formulations and physicochemical conditions.

The bacterial strains *S. aureus*, *Staphylococcus albus (S. albus)* and *P. aeruginosa* were used in this study. The results for wound dressings stabilized with BSA are presented in Figs. 8, 9 and 10. Wound dressings containing gentamicin demonstrated excellent antimicrobial properties over 2 weeks, with

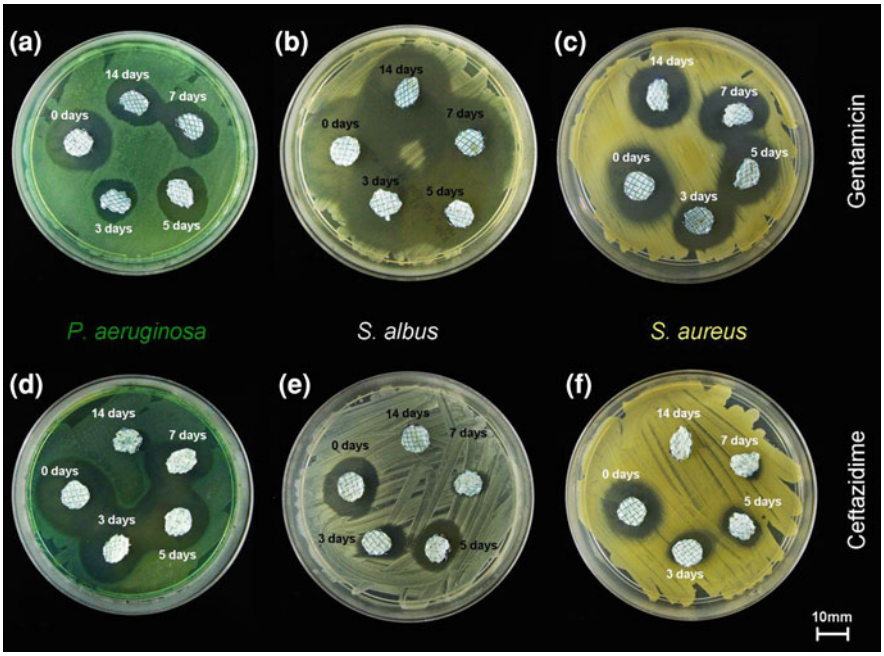

Fig. 8 The inhibition of *P. aeruginosa*, *S. albus* and *S. aureus* growth around wound dressings based on the emulsion formulations containing 10% gentamicin or 10% ceftazidime and stabilized with 1% BSA, PBS incubation times prior to the test are indicated next to each sample [18]

bacterial inhibition zones extending well beyond the dressing margin at most times (Figs. 8 and 9). Interestingly, inhibition zones around dressing materials containing gentamicin remained close to constant over time and for the different drug loads. The largest CZOI were measured for the Gram-positive bacteria (*S. aureus*. and *S. albus*) and especially for *S.albus*. Despite having the lowest minimal inhibitory concentration (MIC) (Table 6), The Gram-negative *P. aeruginosa* was least inhibited, and exhibited the smallest CZOI (Figs. 8 and 9). This was not the case for ceftazidime-loaded materials, for which CZOI were found to decrease over time, and with lower drug loads. In contradistinction to gentamicin-loaded materials, ceftazidime was found to be most effective against *P. aeruginosa* and less effective against *S. albus* and *S. aureus*, and in good correlation with their MIC's (Table 6).

The CZOI was also evaluated for dressing materials with a reduced burst release, stabilized by Span, focusing on the mid-range 10% antibiotic loading ratio. Samples containing gentamicin exhibited similar inhibition zones to those shown when BSA was used as surfactant. In contradistinction, both the magnitude and the duration of the inhibition effect of ceftazidime-loaded materials were reduced [18].

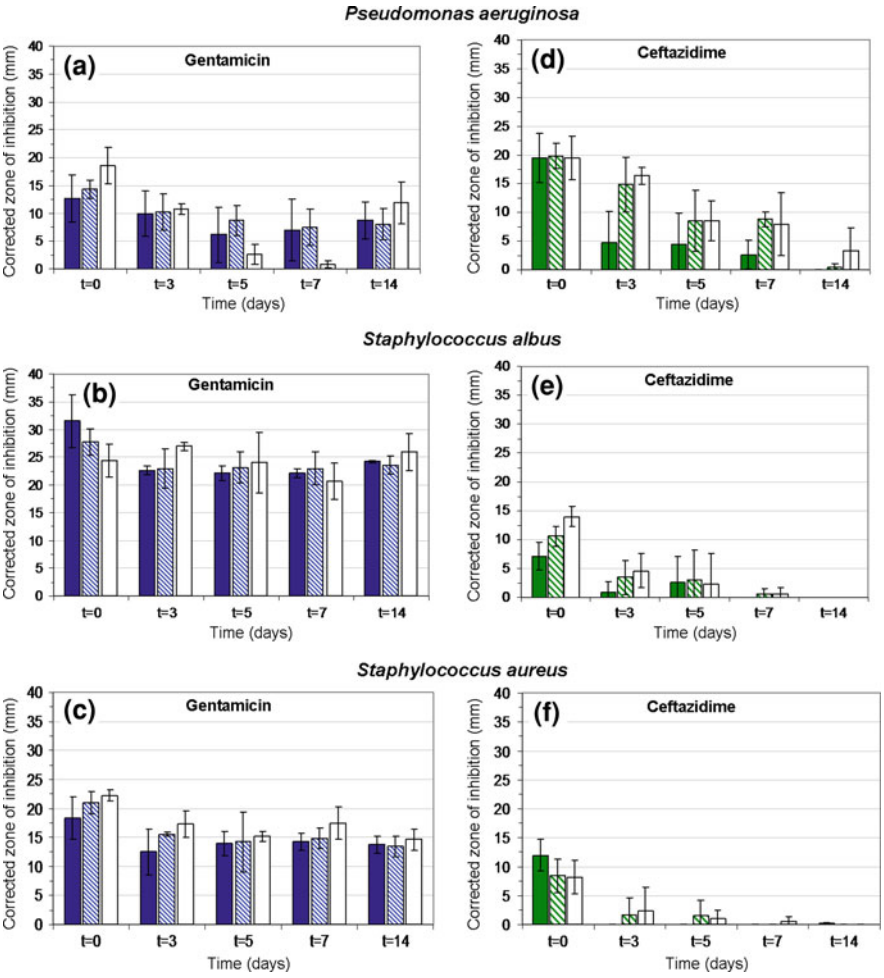

Fig. 9 Histograms showing the effect of drug release on corrected zone of inhibition (CZOI) around (1% w/v) BSA loaded wound dressings ($n = 3$) containing 5% (w/w) (*filled square*), 10% (w/w) (▨) and 15% (w/w) (*open square*) drug, as a function of pre-incubation time in PBS: **a–c**—gentamicin-loaded wound dressings, **d–f**—ceftazidime-loaded dressings. The bacterial strain (*P. aeruginosa*, *S. albus* and *S. aureus*) is indicated [18]

Table 6 Minimum inhibitory concentrations of antibiotics [18]

Microorganism	MIC (μg/mL)	
	Gentamicin	Ceftazidime
Pseudomonas aeruginosa	2.5	6.3
Staphylococcus albus	3	12.5
Staphylococcus aureus	6.3	12.5

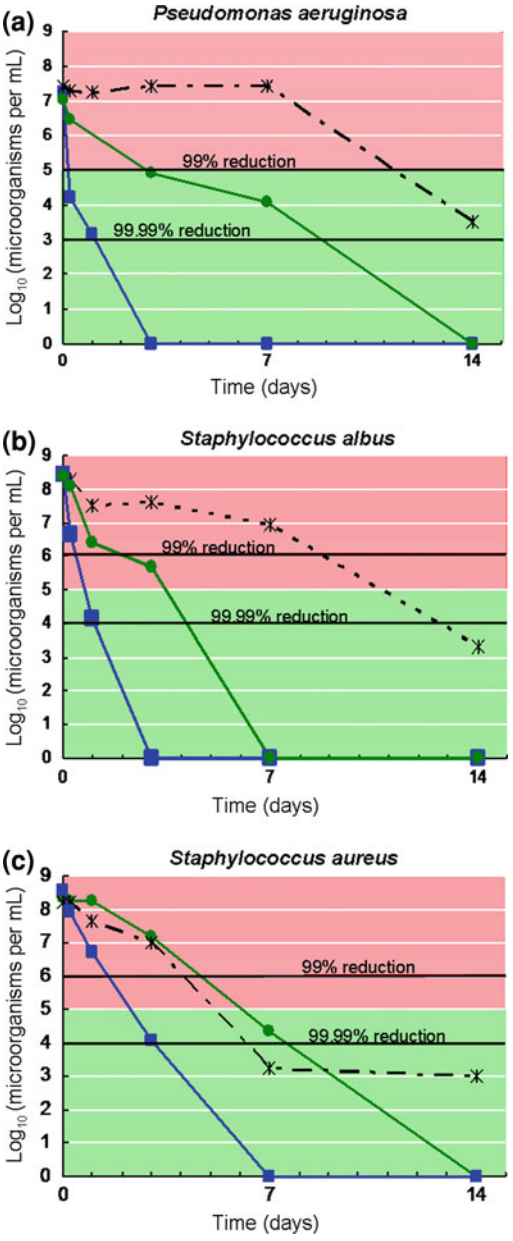

Fig. 10 Number of colony forming units (CFU) versus time, when initial concentrations of 10^7–10^8 CFU/mL were used: **a** *P. aeruginosa*, **b** *S. albus* and **c** *S. aureus*. The releasing wound dressing discs ($D = 10$ mm) were derived from 1% (w/v) BSA-stabilized emulsions containing 10% (w/w) gentamicin (*filled square*) or 10% (w/w) ceftazidime (*filled circle*). Bacteria in the presence of PBS only served as control (*asterisk*) [18]

The purpose of the viable counts experiments was to monitor the effectiveness of cumulative antibiotic release from the wound dressings in terms of the residual bacteria compared to initial bacterial inoculations of 10^7–10^8 CFU/mL which correspond to severe infection. This investigation focused on samples based on

BSA-stabilized emulsions containing 10% antibiotics. Bacteria present in PBS only served as the control. Curves describing the decrease in the number of bacteria due to antibiotic release also demonstrate the superiority of gentamicin-loaded dressing materials over ceftazidime (Fig. 10). High bacterial inoculations of 10^7–10^8 CFU/mL were decreased by 99.99% after 1 (*P. aeruginosa* and *S. albus*) to 3 days (*S. aureus*) in the presence of the gentamicin-loaded wound dressing material. Under similar conditions, the ceftazidime-loaded dressing material demonstrated a 99% decrease in *P. aeruginosa* and *S. albus* only after 3 days, and its effect on *S. aureus* was even lower.

4.3.2 Cell Cytotoxicity

In order to complete the results of bacterial inhibition, it is also necessary to ensure that the dressing material we developed is not toxic to the cells that participate in the healing process. Previous studies have shown that dressing materials may impose a toxic effect on cells, caused by the dressing material itself, its processing, or due to the incorporation of antimicrobials [13, 55]. We assessed cell viability by observations of cell morphology, and by use of the Alamar-Blue assay, which is comparable to the MTT assay in measuring changes in cellular metabolic activity [29]. This method involves the addition of a non-toxic fluorogenic redox indicator to the culture medium. The oxidized form of AB has a dark blue colour and little intrinsic fluorescence. When taken up by cells, the dye becomes reduced and turns red. This reduced form of AB is highly fluorescent. The extent of the AB conversion, which is a reflection of cell viability, can be quantified spectrophotometrically at wavelengths of 570 and 600 nm. The AB assay is advantageous in that it does not necessitate killing the cells (as in the MTT assay), thus enabling day by day monitoring of the cell cultures. The AB assay was performed on human fibriblast cell cultures before introducing the dressing materials and then every 24 h for 3 days.

We saw no difference in the appearance of the cell cultures over the 3 days during which they were exposed to the dressing material devoid of antibiotics. The AB assay also shows a stable preservation of cellular viability. Thus, we are assured that the dressing material itself and its processing by freeze-drying of inverted emulsions do not inflict a toxic effect. Similar results were obtained for all the dressing materials containing antibiotics. No more than a 10% reduction in the metabolic activity of cell cultures was measured and in most cases metabolic activity even increased as the cells became more confluent (Fig. 11). These results are promising, when compared to studies reporting the similar testing of commonly used silver-based dressing materials. Burd et al. [7] and Paddle-Leinek et al. [55] have reported that such dressings induce a mild to severe cytotoxic effect on keratinicytes and fibroblasts grown in culture, which correlated with the silver released to the culture medium. Specifically, it was shown that commercial dressings such as Acticoat™, Aquacel® Ag and Contreet® Ag reduce fibroblast viability in culture by 70% or more [55]. All silver dressings were shown to delay

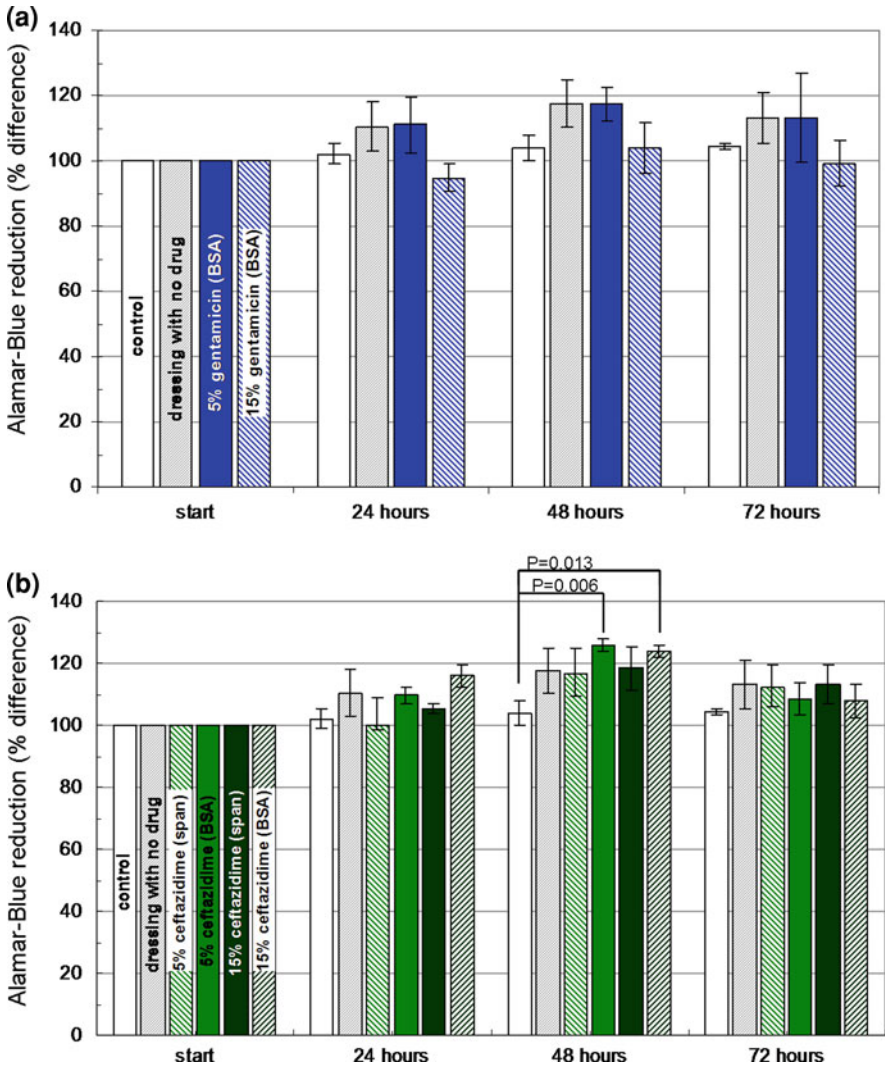

Fig. 11 Histograms demonstrating changes in the viability of dermal fibroblast cultures (Alamar Blue assay) in the presence of wound dressing discs ($D = 10$ mm): **a** BSA-stabilized wound dressings ($n = 3$) containing 5 or 15% (w/w) gentamicin, **b** BSA and Span stabilized wound dressings containing 5 or 15% ceftazidime. Dressing materials devoid of antibiotics and pristine cell cultures served as control [18]

wound reepithelialization in an explant culture model, and Aquacel® Ag and Contreet® Ag were found to significantly delay reepithelialization in a mouse excisional wound model [7]. These findings emphasize the superiority of the proposed new antibiotic-eluting wound dressings over dressings loaded with silver ions.

In summary, both types of microbiological studies showed that the investigated antibiotic-eluting wound dressings are highly effective against the three relevant bacterial strains. Despite severe toxicity to bacteria, the dressing material was not found to have a toxic effect on cultured fibroblasts, indicating that the new antibiotic-eluting wound dressings represent an effective and selective treatment option against bacterial infection.

4.4 In vivo Study

The guinea pig is often used as a dermatological and infection model [3, 36, 54, 83]. Research on guinea pigs has included topical antibiotic treatment [5], delivery of delayed-release antibiotics [22], and investigation of wound dressing materials [37, 47]. A deep partial skin thickness burn is an excellent wound model for the evaluation of wound healing, not only for contraction and epithelialization of the peripheral area such as in third degree burns, but also for evaluation of the recovery of skin appendages, to serve as the main source for the re-epithelization, which completes the healing process. The metabolic response to severe burn injury in guinea pigs is very similar to that of the human post-burn metabolic response [31]. Furthermore, bacterial colonization and changes within the complement component of the immune system in human burn victims is analogous to guinea pigs affected by severe burns [3]. Such a model was therefore used in the current study to evaluate the effectiveness of our novel composite antibiotic-eluting wound dressing.

Our in vivo evaluation of the antibiotic-eluting wound dressings in a contaminated wound demonstrated its ability to accelerate wound healing compared to an unloaded format of the wound dressing and a non-adherent dressing material (Melolin®). Faster epithelialization of the wound was measured in both release strategies, fast antibiotic release (such as in Fig. 4d, filled square) and slow antibiotic release (such as in Fig. 4d, filled triangle), but was significantly better for animals treated with the slow release rate. The results are described in detail elsewhere [19 (submitted)]. From a practical aspect, faster epithelialization leads to less pain to the patient, shorter hospitalization, a better healing quality. The new current dressing material shows promising results. It does not require bandage changes and offers a potentially valuable and economic approach for treating the life-threatening complication of burn-related infections.

5 Conclusion

This chapter presents an overview of wound dressings with controlled release of antibacterial agents. These include wound dressings based on both types of polymers, synthetic and natural. A special part of this chapter focused on our novel biodegradable occlusive wound dressings, based on a polyglyconate mesh and a

porous PDLGA binding matrix. These composite dressings were prepared by dip-coating woven meshes in inverted emulsions, followed by their freeze-drying. Their in vitro investigation focused on the microstructure, mechanical and physical properties and the release profiles of the antibiotic drugs and their effects on bacterial inhibition. The main results were brought here, with emphasis on engineering aspects related to wound dressings. Our new composite structures demonstrated combination of good mechanical properties with desired physical properties and adjustable controlled release of the antibiotic drugs from the binding matrix, which resulted in impressive bacterial inhibition effect and biocompatibility. Hence, these new wound dressings are potentially very useful as burn and ulcer dressings with enhanced protection against infection and reduce the need for frequent dressing changing. Furthermore, we have shown that modifications in the emulsion formulation enables adapting the desired properties to the wound characteristics, and may thus enhance wound healing. New designs based on structured wound dressings may thus advance the therapeutic field of wound healing.

Acknowledgments The authors are grateful to the Israel Science Foundation (ISF, grant no. 1312/07) and to the Israel Ministry of Health (grant no. 3-3943) for supporting this research.

References

1. Altoparlak, U., Erol, S., Akcay, M.N., Celebi, F., Kadanali, A.: The time-related changes of antimicrobial resistance patterns and predominant bacterial profiles of burn wounds and body flora of burned patients. Burns **30**(7), 660–664 (2004)
2. Aoyagi, S., Onishi, H., Machida, Y.: Novel chitosan wound dressing loaded with minocycline for the treatment of severe burn wounds. Int. J. Pharm. **330**, 138–145 (2007)
3. Bjornson, A.B., Bjornson, H.S., Lincoln, N.A., Altemeier, W.A.: Relative roles of burn injury, wound colonization, and wound infection in induction of alterations of complement function in a guinea pig model of burn injury. J. Trauma **24**, 106–115 (1984)
4. Boateng, J.S., Matthews, K.H., Stevens, H.N., Eccleston, G.M.: Wound healing dressings and drug delivery systems: a review. J. Pharm. Sci. **97**(8), 2892–2923 (2008)
5. Boon, R.J., Beale, A.S., Sutherland, R.: Efficacy of topical mupirocin against an experimental Staphylococcus aureus surgical wound infection. J. Antimicrob. Chemother. **16**, 519–526 (1985)
6. Budavari, S.: The Merck index: an encyclopedia of chemicals, drugs, and biologicals. Rahway, N.J.: Merck & Co. 1 (various pagings) (1989)
7. Burd, A., Kwok, C.H., Hung, S.C., Chan, H.S., Gu, H., Lam, W.K., Huang, L.: A comparative study of the cytotoxicity of silver-based dressings in monolayer cell, tissue explant, and animal models. Wound Repair Regen. **15**(1), 94–104 (2007)
8. Campos, M.G., Rawls, H.R., Innocentini-Mei, L.H., Satsangi, N.: In vitro gentamicin sustained and controlled release from chitosan cross-linked films. J. Mater. Sci. **20**(2), 537–542 (2009)
9. Chiu, C.T., Lee, J.S., Chu, C.S., Chang, Y.P., Wang, Y.J.: Development of two alginate-based wound dressings. J. Mater. Sci. Mater. Med. **19**(6), 2503–2513 (2008)
10. Chung, L.Y., Schmidt, R.J., Hamlyn, P.F., Sagar, B.F., Andrews, A.M., Turner, T.D.: Biocompatibility of potential wound management products: fungal mycelia as a source of chitin/chitosan and their effect on the proliferation of human F1000 fibroblasts in culture. J. Biomed. Mater. Res. **28**, 463–469 (1994)

11. Colletta, V., Dioguardi, D., Di Lonardo, A., Maggio, G., Torasso, F.: A trial to assess the efficacy and tolerability of Hyalofill-F in non-healing venous leg ulcers. J. Wound Care **12**, 357–360 (2003)
12. Costerton, J.W., Stewart, P.S., Greenberg, E.P.: Bacterial biofilms: a common cause of persistent infections. Science **284**(5418), 1318–1322 (1999)
13. Dover, R., Otto, W.R., Nanchahal, J., Riches, D.J.: Toxicity testing of wound dressing materials in vitro. Br. J. Plast. Surg. **48**(4), 230–235 (1995)
14. Eisinger, M., Lee, J.S., Hefton, J.M., Darzynkiewicz, Z., Chiao, J.W., de Harven, E.: Human epidermal cell cultures: growth and differentiation in the absence of differentiation in the absence of dermal components or medium supplements. Proc. Natl. Acad. Sci. USA **76**, 5340–5344 (1979)
15. Elsner, J.J., Zilberman, M.: Antibiotic eluting bioresorbable composite fibers for wound healing applications: microstructure, drug delivery and mechanical properties. Acta Biomater. **5**(8), 2872–2883 (2009)
16. Elsner, J.J., Zilberman, M.: Novel antibiotic-eluting wound dressings: an in vitro study and engineering aspects in the dressing's design. J. Tissue Viability **19**(2), 54–66 (2010)
17. Elsner, J.J., Shefy-Peleg, A., Zilberman, M.: Novel biodegradable composite wound dressings with controlled release of antibiotics: microstructure, mechanical and physical properties. J. Biomed. Mater. Res. Part B, Appl. Biomater. **93**(2), 425–435 (2010)
18. Elsner, J.J., Berdicevsky, I., Zilberman, M.: In vitro microbial inhibition and cellular response to novel biodegradable composite wound dressings with controlled release of antibiotics. Acta Biomater. **7**(1), 325–336 (2011)
19. Elsner, J.J., Ullmann, Y., Egozi, D., Berdicevsk, I., Shefy-Peleg, A., Zilberman, M.: Novel biodegradable composite wound dressings with controlled release of antibiotics: results in a guinea pig burn model. (submitted)
20. Erol, S., Altoparlak, U., Akcay, M.N., Celebi, F., Parlak, M.: Changes of microbial flora and wound colonization in burned patients. Burns **30**(4), 357–361 (2004)
21. Fraser, J.F., Bodman, J., Sturgess, R., Faoagali, J., Kimble, R.M.: An in vitro study of the anti-microbial efficacy of 1% silver sulphadiazine and 0.2% chlorhexidine digluconate cream, 1% silver sulphadiazine cream and a silver coated dressing. Burns **30**, 35–41 (2004)
22. Galandiuk, S., Wrightson, W.R., Young, S., Myers, S., Polk Jr., H.C.: Absorbable, delayed release antibiotic beads reduce surgical wound infection. Am. Surg. **63**, 831–835 (1997)
23. Gilbert, P., Collier, P.J., Brown, M.R.: Influence of growth rate on susceptibility to antimicrobial agents: biofilms, cell cycle, dormancy, and stringent response. Antimicrob. Agents Chemother. **34**(10), 1865–1868 (1990)
24. Gold, H.S., Moellering Jr., R.C.: Antimicrobial-drug resistance. N. Engl. J. Med. **335**, 1445–1453 (1996)
25. Gransden, W.R.: Antibiotic resistance. Nosocomial gram-negative infection. J. Med. Microbiol. **46**, 436–439 (1997)
26. Gristina, A.G.: Biomaterial-centered infection: microbial adhesion versus tissue integration. Science **237**, 1588–1595 (1987)
27. Grunwald, T.B., Garner, W.L.: Acute burns. Plast. Reconstr. Surg. **121**(5), 311–319 (2008)
28. Gurtner, G.C., Werner, S., Barrandon, Y., Longaker, M.T.: Wound repair and regeneration. Nature **453**(7193), 314–321 (2008)
29. Hamid, R., Rotshteyn, Y., Rabadi, L., Parikh, R., Bullock, P.: Comparison of alamar blue and MTT assays for high through-put screening. Toxicol. In vitro **18**(5), 703–710 (2004)
30. Harrison-Balestra, C., Cazzaniga, A.L., Davis, S.C., Mertz, P.M.: A wound-isolated Pseudomonas aeruginosa grows a biofilm in vitro within 10 hours and is visualized by light microscopy. Dermatol. Surg. **29**(6), 631–635 (2003)
31. Herndon, D.N., Wilmore, D.W., Mason, A.D.: Development and analysis of a small animal model simulating the human postburn hypermetabolic response. J. Surg. Res. **25**, 394–403 (1978)
32. Hutchinson, F.G., Furr, B.J.: Biodegradable polymers for the sustained release of peptides. Biochem. Soc. Trans. **13**, 520–523 (1985)

33. Ignatova, M., Starbova, K., Markova, N., Manolova, N., Rashkov, I.: Electrospun nano-fibre mats with antibacterial properties from quaternised chitosan and poly(vinyl alcohol). Carbohydr. Res. **341**, 2098–2107 (2006)
34. Jones, S.A., Bowler, P.G., Walker, M., Parsons, D.: Controlling wound bioburden with a novel silver-containing Hydrofiber dressing. Wound Repair Regen. **12**, 288–294 (2004)
35. Jürgens, C., Schulz, A.P., Porté, T., Faschingbauer, M., Seide, K.: Biodegradable films in trauma and orthopedic surgery. Eur. J. Trauma **2**, 160–171 (2006)
36. Kaufman, T., Lusthaus, S.N., Sagher, U., Wexler, M.R.: Deep partial thickness burns: a reproducible animal model to study burn wound healing. Burns **16**, 13–16 (1990)
37. Kawai, K., Suzuki, S., Tabata, Y., Taira, T., Ikada, Y., Nishimura, Y.: Development of an artificial dermis preparation capable of silver sulfadiazine release. J. Biomed. Mater. Res. **57**, 346–356 (2001)
38. Keen III, E.F., Robinson, B.J., Hospenthal, D.R., Aldous, W.K., Wolf, S.E., Chung, K.K., Murray, C.K.: Incidence and bacteriology of burn infections at a military burn center. Burns **36**(4), 461–468 (2010)
39. Kilian, O., Hossain, H., Flesch, I., Sommer, U., Nolting, H., Chakraborty, T., Schnettler, R.: Elution kinetics, antimicrobial efficacy, and degradation and microvasculature of a new gentamicin-loaded collagen fleece. J. Biomed. Mater. Res. **90**(1), 210–222 (2009)
40. Kim, H.W., Knowles, J.C., Kim, H.E.: Porous scaffolds of gelatin-hydroxyapatite nanocomposites obtained by biomimetic approach: characterization and antibiotic drug release. J. Biomed. Mater. Res. B Appl. Biomater. **74**(2), 686–698 (2005)
41. Knill, C.J., Kennedy, J.F., Mistry, J., Miraftab, M., Smart, G., Groocock, M.R., Williams, H.J.: Alginate fibres modified with unhydrolysed and hydrolysed chitosans for wound dressings. Carbohydr. Polym. **55**, 65–76 (2004)
42. Lamke, L.O.: The influence of different "skin grafts" on the evaporative water loss from burns. Scand. J. Plast. Reconstr. Surg. **5**(2), 82–86 (1971)
43. Lee, S.B., Kim, Y.H., Chong, M.S., Hong, S.H., Lee, Y.M.: Study of gelatin-containing artificial skin V: fabrication of gelatin scaffolds using a salt-leaching method. Biomaterials **26**(14), 1961–1968 (2005)
44. Lee, S.H., Szinai, I., Carpenter, K., Katsarava, R., Jokhadze, G., Chu, C.C., Huang, Y., Verbeken, E., Bramwell, O., De Scheerder, I., Hong, M.K.: In vivo biocompatibility evaluation of stents coated with a new biodegradable elastomeric and functional polymer. Coron. Artery Dis. **13**, 237–241 (2002)
45. Lee, J., Tae, G., Kim, Y.H., Park, I.S., Kim, S.H., Kim, S.H.: The effect of gelatin incorporation into electrospun poly(L-lactide-co-epsilon-caprolactone) fibers on mechanical properties and cytocompatibility. Biomaterials **29**(12), 1872–1879 (2008)
46. London, N.J., Donnelly, R.: ABC of arterial and venous disease. Ulcerated lower limb. BMJ, **10**:320(7249), 1589–1591 (2000)
47. Mazurak, V.C., Burrell, R.E., Tredget, E.E., Clandinin, M.T., Field, C.J.: The effect of treating infected skin grafts with Acticoat on immune cells. Burns **33**, 52–58 (2007)
48. Mi, F.L., Wu, Y.B., Shyu, S.S., Schoung, J.Y., Huang, Y.B., Tsai, Y.H., Hao, J.Y.: Control of wound infections using a bilayer chitosan wound dressing with sustainable antibiotic delivery. J. Biomed. Mater. Res. **59**, 438–449 (2002)
49. Milella, E., Ramires, P.A., Brescia, E., La Sala, G., Di Paola, L., Bruno, V.: Physicochemical, mechanical, and biological properties of commercial membranes for GTR. J. Biomed. Mater. Res. **58**(4), 427–435 (2001)
50. Murphy, K.D., Lee, J.O., Herndon, D.N.: Current pharmacotherapy for the treatment of severe burns. Exp. Opin. Pharmacoth. **4**(3), 369–384 (2003)
51. Muzzarelli, R., Tarsi, R., Filippini, O., Giovanetti, E., Biagini, G., Varaldo, P.E.: Antimicrobial properties of N-carboxybutyl chitosan. Antimicrob. Agents Chemother. **34**, 2019–2023 (1990)
52. Noronha, C., Almeida, A.: Local burn treatment—topical antimicrobial agents. Annals of Burns and Fire Disasters; XIII (4): (2000)

53. Ong, S.Y., Wu, J., Moochhala, S.M., Tan, M.H., Lu, J.: Development of a chitosan-based wound dressing with improved hemostatic and antimicrobial properties. Biomaterials **29**(32), 4323–4332 (2008)
54. Orenstein, A., Klein, D., Kopolovic, J., Winkler, E., Malik, Z., Keller, N., Nitzan, Y.: The use of porphyrins for eradication of Staphylococcus aureus in burn wound infections. FEMS Immunol. Med. Microbiol. **19**, 307–314 (1997)
55. Paddle-Ledinek, J.E., Nasa, Z., Cleland, H.J.: Effect of different wound dressings on cell viability and proliferation. Plast. Reconstr. Surg. **117**(7 Suppl), 110S–120S (2006)
56. Park, S.N., Kim, J.K., Suh, H.: Evaluation of antibiotic-loaded collagen-hyaluronic acid matrix as a skin substitute. Biomaterials **25**, 3689–3698 (2004)
57. Poon, V.K.M., Burd, A.: In vitro cytotoxity of silver: implication for clinical wound care. Burns **30**(2), 140–147 (2004)
58. Prabu, P., Dharmaraj, N., Aryal, S., Lee, B.M., Ramesh, V., Kim, H.Y.: Preparation and drug release activity of scaffolds containing collagen and poly(caprolactone). J. Biomed. Mater. Res. A **79**, 153–158 (2006)
59. Price, J.S., Tencer, A.F., Arm, D.M., Bohach, G.A.: Controlled release of antibiotics from coated orthopedic implants. J. Biomed. Mater. Res. **30**, 281–286 (1996)
60. Queen, D., Gaylor, J.D., Evans, J.H., Courtney, J.M., Reid, W.H.: The preclinical evaluation of the water vapour transmission rate through burn wound dressings. Biomaterials **8**(5), 367–371 (1987)
61. Revathi, G., Puri, J., Jain, B.K.: Bacteriology of burns. Burns **24**(4), 347–349 (1998)
62. Rho, K.S., Jeong, L., Lee, G., Seo, B.M., Park, Y.J., Hong, S.D., Roh, S., Cho, J.J., Park, W.H., Min, B.M.: Electrospinning of collagen nanofibers: effects on the behavior of normal human keratinocytes and early-stage wound healing. Biomaterials **27**(8), 1452–1461 (2006)
63. Rossi, S., Marciello, M., Sandri, G., Ferrari, F., Bonferoni, M.C., Papetti, A., Caramella, C., Dacarro, C., Grisoli, P.: Wound dressings based on chitosans and hyaluronic acid for the release of chlorhexidine diacetate in skin ulcer therapy. Pharm. Dev. Technol. **12**, 415–422 (2007)
64. Ruszczak, Z.: Effect of collagen matrices on dermal wound healing. Adv. Drug Del. Rev. **55**(12), 1595–1611 (2003)
65. Ruszczak, Z., Friess, W.: Collagen as a carrier for on-site delivery of antibacterial drugs. Adv. Drug Deliv. Rev. **55**, 1679–1698 (2003)
66. Ruszczak, Z., Schwartz, R.A.: Collagen uses in dermatology—an update. Dermatology **199**(4), 285–289 (1999)
67. Shanmugasundaram, N., Sundaraseelan, J., Uma, S., Selvaraj, D., Babu, M.: Design and delivery of silver sulfadiazine from alginate microspheres-impregnated collagen scaffold. J. Biomed. Mater. Res. B Appl. Biomater **77**, 378–388 (2006)
68. Sharma, B.R.: Infection in patients with severe burns: causes and prevention thereof. Infect. Dis. Clin. North Am. **21**(3), 745–759 (2007)
69. Singer, A.J., Clark, R.A.: Cutaneous wound healing. N. Engl. J. Med. **341**(10), 738–746 (1999)
70. Springer, B.D., Lee, G.C., Osmon, D., Haidukewych, G.J., Hanssen, A.D., Jacofsky, D.J.: Systemic safety of high-dose antibiotic-loaded cement spacers after resection of an infected total knee arthroplasty. Clin. Orthop. Relat. Res. **427**, 47–51 (2004)
71. Sripriya, R., Kumar, M.S., Sehgal, P.K.: Improved collagen bilayer dressing for the controlled release of drugs. J. Biomed. Mater. Res. B Appl. Biomater. **70**, 389–396 (2004)
72. Stefanides Sr., M.M., Copeland, C.E., Kominos, S.D., Yee, R.B.: In vitro penetration of topical antiseptics through eschar of burn patients. Ann. Surg. **183**(4), 358–364 (1976)
73. Stiver, H.G., Goldring, A.M., Snelling, C.F., Ronald, A.R., Robertson, G.A., Goldsand, G., Dawson, L.: Ceftazidime therapy versus aminoglycoside therapy in patients with gram-negative burn wound infections. J. Burn Care Rehabil. **8**(1), 19–22 (1987)
74. Sussman, C., Bates-Jensen, B.M.: Wound care: a collaborative practice manual for physical therapists and nurses, 2nd edn. Aspen Publishers, Gaithersburg (2001)

75. Suzuki, Y., Tanihara, M., Nishimura, Y., Suzuki, K., Yamawaki, Y., Kudo, H., Kakimaru, Y., Shimizu, Y.: In vivo evaluation of a novel alginate dressing. J. Biomed. Mater. Res. **48**(4), 522–527 (1999)
76. Taddeucci, P., Pianigiani, E., Colletta, V., Torasso, F., Andreassi, L., Andreassi, A.: An evaluation of Hyalofill-F plus compression bandaging in the treatment of chronic venous ulcers. J. Wound Care **13**, 202–204 (2004)
77. USA Burn Support Organization Burn Association website: http://www.usburn.org/Pages/Treatment.htm
78. Varghese, M.C., Balin, A.K., Carter, D.M., Caldwell, D.: Local environment of chronic wounds under synthetic dressings. Arch. Dermatol. **122**, 52–57 (1986)
79. Walstad, R.A., Aanderud, L., Thurmann-Nielsen, E.: Pharmacokinetics and tissue concentrations of ceftazidime in burn patients. Eur. J. Clin. Pharmacol. **35**(5), 543–549 (1988)
80. Wu, P., Fisher, A.C., Foo, P.P., Queen, D., Gaylor, J.D.: In vitro assessment of water vapour transmission of synthetic wound dressings. Biomaterials **116**(3), 171–175 (1995)
81. Wu, P., Grainger, D.W.: Drug/device combinations for local drug therapies and infection prophylaxis. Biomaterials **27**, 2450–2467 (2006)
82. Xu, R.X., Sun, X., Weeks, B.S.: Burns Regenerative Medicine and Therapy. Karger, Basel, New York (2004)
83. Yannas, I.V., Burke, J.F., Orgill, D.P., Skrabut, E.M.: Wound tissue can utilize a polymeric template to synthesize a functional extension of skin. Science **215**, 174–176 (1982)
84. Zalavras, C.G., Patzakis, M.J., Holtom, P.: Local antibiotic therapy in the treatment of open fractures and osteomyelitis. Clin. Orthop. Relat. Res. **427**, 86–93 (2004)
85. Zilberman, M.: Novel composite fiber structures to provide drug/protein delivery for medical implants and tissue regeneration. Acta Biomater. **3**(1), 51–57 (2007)
86. Zilberman, M., Elsner, J.J.: Antibiotic-eluting medical devices for various applications—a review. J. Controlled Release **130**, 202–215 (2008)
87. Zilberman, M., Golerkansky, E., Elsner, J.J., Berdicevsky, I.: Gentamicin-eluting bioresorbable composite fibers for wound healing applications. J. Biomed. Mater. Res.—part A **89**(3), 654–666 (2009)
88. Zilberman, M., Kraitzer, A., Grinberg, O., Elsner, J.J.: Drug-eluting medical implants, Part III Chap. 11. In: Schafer-Korting, M. (ed.) Handbook of Experimental Pharmacology, vol. 197, pp. 299–341. Drug Delivery, Springer, (2010)
89. Zong, X., Ran, S., Kim, K.S., Fang, D., Hsiao, B.S., Chu, B.: Structure and morphology changes during in vitro degradation of electrospun poly(glycolide-co-lactide) nanofiber membrane. Biomacromolecules **4**(2), 416–423 (2003)

Tissue Adhesives as Active Implants

Boaz Mizrahi, Christopher Weldon and Daniel S. Kohane

Abstract Tissue adhesives are substances that hold tissues together, and could be broadly applicable in medicine and surgery. In appropriate circumstances, such materials could be attractive alternatives to sutures and staples since they can be applied more quickly, causes less pain and may require less equipment. In addition, there is no risk to the practitioner from sharp instruments (Singer et al., Acad. Emerg. Med. 5(2):94, 1998), and they may obviate the need for suture removal (Coulthard et al., Cochrane Database Syst. Rev. 5:CD004287, 2010). An ideal surgical tissue adhesive should allow rapid adhesion and maintain strong and close apposition of wound edges for an amount of time sufficient to allow wound healing. It should not interfere with body's natural healing mechanisms and should degrade without producing an excessive localized or generalized inflammatory response (Mobley et al., Facial Plast. Surg. Clin. North Am. 10(2):147, 2002). The clinical and scientific potential of adhesives can be enhanced by a variety of functionalities that may not be directly related to their function as glues or sealants. Here we will review adhesives in general, with an emphasis on enhancements

B. Mizrahi, C. Weldon and D. S. Kohane (✉)
Department of Anesthesia and Perioperative Medicine, Division of Critical Care, Children's Hospital Boston, 300 Longwood Avenue, Bader 6, Boston, MA 02115, USA
e-mail: Daniel.Kohane@childrens.harvard.edu

B. Mizrahi
Department of Chemical Engineering, Massachusetts Institute of Technology, Cambridge, MA 02139, USA

B. Mizrahi
Operations Research Center, Massachusetts Institute of Technology, Cambridge, MA 02139, USA

C. Weldon
Department of Surgery, Children's Hospital Boston, 300 Longwood Avenue, Fegan 3, Boston, MA 02115, USA

Stud Mechanobiol Tissue Eng Biomater (2011) 8: 39–56
DOI: 10.1007/8415_2010_48

Published Online: 11 January 2011

that render those otherwise passive materials "active". We note that some glues also have intrinsic secondary functionalities that can be direct or indirect consequences of their primary function, but that is not the focus of this chapter. (For example, they may augment local hemostasis directly, or by improving tissue apposition, without affecting clotting mechanisms (Reece et al., Am. J. Surg. 182(2 Suppl):40S, 2001)).

1 Categories of Adhesives

Tissue adhesives hold tissues together (and therefore are glues) but also can serve as barriers to leakage (and therefore can be sealants) when used for wound closure [74]. Achieving a strong bond (Fig. 1) is dependent upon obtaining close contact between the tissue(s) to be bonded and the glue (adhesive strength), and on the integrity of the glue (cohesive strength of the material) [47]. Consequently the causes of glue failure [67] can include: (1) adhesive failure—where the material detaches from the tissue and (2) cohesive failure—where the adhesive fails within itself. Even if the glue functions well, the tissue itself may tear; this may occur when both adhesive and cohesive forces are too strong.

Tissue adhesives can be divided into three main chemical categories: cyanoacrylates, fibrin sealant, and other cross-linkable polymers. They can be administered for a variety of clinical indications including wound closure [26], fistula repair, including in the bowel, blood vessels and bronchi [70], retinal fixation [30] and others. Cyanoacrylates are the strongest ($\sim$68 kPa**,** [2]) and are widely used for wound closure. Fibrin based materials, being weaker ($\sim$13 kPa, [2]) are applied as a sealant in many surgical procedures in conjunction with suturing. Hydrogels, collagen compounds, peptides and polyethylene glycol (PEGs)-based materials are also considered weak (4–17 kPa, [2]) and are therefore used as topical wound dressings or as sealants where mechanical properties are of less concern than with internal injuries (where wound dehiscence could be disastrous).

Below we detail a number of compounds used as glues. The list is not intended to be exhaustive but to provide a framework for the subsequent discussion of active glues.

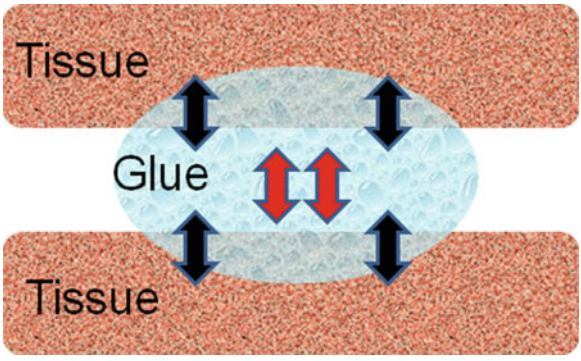

Fig. 1 Types of glue strength: adhesive strength between the glue and the tissue (*black arrow*), and cohesive strength within the glue (*red arrow*)

1.1 Cyanoacrylates

Cyanoacrylates were first synthesized in 1949 [3] and were first reported as tissue adhesives ten years later [18]. They are produced synthetically by condensation between cyanoacetic acid and a suitable alcohol followed by the Knoevenagel reaction [68]. The alcohol group will determine the nature of the final monomer by controlling the length of the side chain (e.g. by using methanol or octanol, 2-methyl cyanoacrylate or 2-octyl cyanoacrylate will be formed, respectively). The cyanoacetate oil formed is reacted with paraformaldehyde to form cyanoacrylate oligomers. High vacuum ($\sim$0.7 mm Hg) and heat (150–180°C) are applied and depolymerization is carried out to produce clear and colorless liquids monomers. Usually, further purification by repeated vacuum distillations is utilized to get a medical grade material [33]. Since these monomers are highly reactive, polymerization inhibitors are added at this stage to prevent the monomers from hardening (polymerize) while being stored. Although polymerization may occur by one of three mechanisms—anionic (Fig. 2), zwitterionic or free radical—the first two mechanisms mentioned are strongly favored in vivo [86] by hydroxide or amine groups presented in the body, ultimately resulting in strong chains holding the two tissues' surfaces together.

Although cyanoacrylates are considered very strong and effective, their use—particularly within tissues—is limited by tissue toxicity, including necrosis, which occurs in the immediate vicinity of the cyanoacrylates. The toxicity of cyanoacrylate glues has been attributed to several factors including:

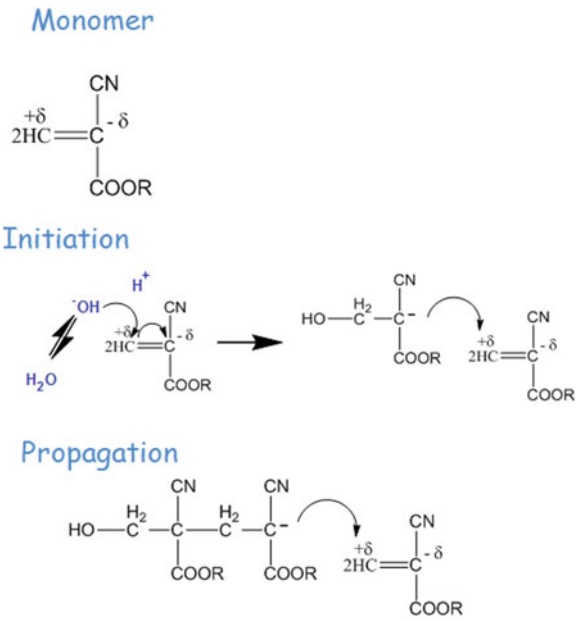

Fig. 2 The polymerization of cyanoacrylate tissue glue

direct toxicity of monomers such as methyl-2-cyanoacrylate [39] or of byproducts such as cyanoacetate and formaldehyde [87], insufficient tissue vascularization [2], and the heat from the exothermic nature of the reaction [21]. In addition, it has been postulated that the polymerization of the monomers may be initiated by the -NH_2 groups of glycosides or amino acids present on cell surfaces [42] thus damaging membrane lipids [84]. A second concern limiting the use of cyanoacrylates in tissues stems from the fact that they are hard and brittle, hence they may have insufficient flexibility for the dynamic nature of in vivo conditions [40]. As a result, cyanoacrylates are currently limited to external or temporary applications.

In general, the smaller the molecular weight of the side group, the quicker the rate of degradation. Accordingly, it has been shown that monomers with higher molecular weights may result in slower production of byproducts with resultant decreased inflammatory response [38]. This difference may be reflected in the fact that n-2-butyl cyanoacrylate (Histoacryl®), a monomer with a four carbon alkyl side chain, was not approved for the US market, while 2-octyl cyanoacrylate (Dermabond®), a monomer with an eight carbon alkyl side chain, was approved for use in the United States after it proved to be less toxic than cyanoacrylates with shorter side chains [79].

Cyanoacrylate tissue glues have found multiple uses. They have been used in the management of corneal perforations, corneal melts and wound leaks [2]. The cornea glue may also improve visual outcomes by obviating the need for sutures, which are associated with inducing astigmatism. In addition, they may create a more watertight seal, decreasing the risk of infection, thus reducing the chance of devastating intraocular infections such as endophthalmitis [5]. In dermatology, cyanoacrylate glues provide a flexible water-resistant coating with improved cosmetic outcomes. It was also found that patients, in particular children, prefer the concept of being "glued" over sutures and clips [9]. Recently, Dermabond was found to be superior for skin closure after repairing congenital cleft lip with or without associated palate defects [17]. In mammoplasties, Dermabond® was effective, safe, and had better cosmetic results than sutures [77]. Operative times and costs were also decreased, while patient satisfaction increased compared to traditional techniques.

1.2 In Situ Cross-linking Polymers

1.2.1 Fibrin Glue/Sealant

Fibrin tissue glue was first introduced in 1909 as an hemostatic agent, and was first used as an adhesive material in 1940 [78]. Fibrin based tissue adhesives are composed of purified fibrinogen and thrombin, and form a bond via the physiological cascade of coagulation (Fig. 3). Some additives such as Factor XIII, fibronectin,

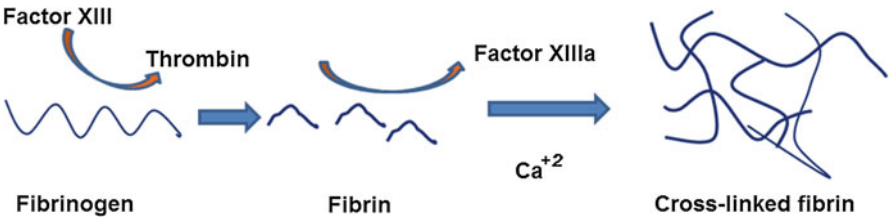

Fig. 3 Formation of cross-linked fibrin from fibrinogen

calcium chloride and the anti-fibrinolytic aprotinin may also be added to inhibit tissue fibrinolysis, and to control gelling time [4, 11, 89].

Since fibrin tissue adhesives are prepared from pooled human blood, there has been concern for potential viral transmission, in particular of hepatitis and human immunodeficiency virus (HIV) [24]. However, parvovirus (B19) has been the only documented virus transmitted from fibrin sealants to date [36]. Nowadays, these products are carefully screened so that the risk of viral transmission is considered minuscule compared to the risk with other biomaterials taken from donors [70].

Although fibrin glues are considered less toxic than cyanoacrylates their low adhesive strength limits their use in many surgical procedures [2]**.** For example, the strength of cystotomy closure with fibrin glue and 2-octyl cyanoacrylate were compared in a porcine model [50]. At 4 weeks postoperatively, the bladders were filled with saline to 200 mm Hg pressure and the cystotomy scars inspected for evidence of leakage. Four of six of the pigs treated with fibrin glue leaked, while none in the cyanoacrylate group had evidence of wound compromise. Ultimately, three pigs treated with fibrin glue died from urine leakage.

As a sealant, however, fibrin glue is very successful, especially in conjunction with sutures or clips. It has been used clinically in many settings including: anal fistulae closure to preserve sphincter function [94], prevention of esophageal leakage and stricture after esophageal reconstruction from caustic injury [75], prevention of cerebral spinal fluid leakage after durotomy during lumbar spinal surgery [35], hernia repairs [62], posterolateral spinal fusions [96], nerve anastomoses [90] and in cardiovascular surgeries [6].

1.2.2 Other In Situ Cross-linking Polymers

Water soluble polymers forming a three dimensional (3D) network at the site of injection have been used as tissue adhesives due to their safety, mechanical properties and ease of application. Cross-linking prevents early dissolution of the material in the body, and maintains cohesive integrity. Since it may be desirable that tissue adhesives degrade after healing has occurred, these compounds will frequently contain labile bonds in their backbone or in the cross-linking domains [28].

Several polymers, synthetic and natural, have been proposed for tissue adhesion, including poly(ethylene glycol) (PEG) [19], chitosan [43], laser- and

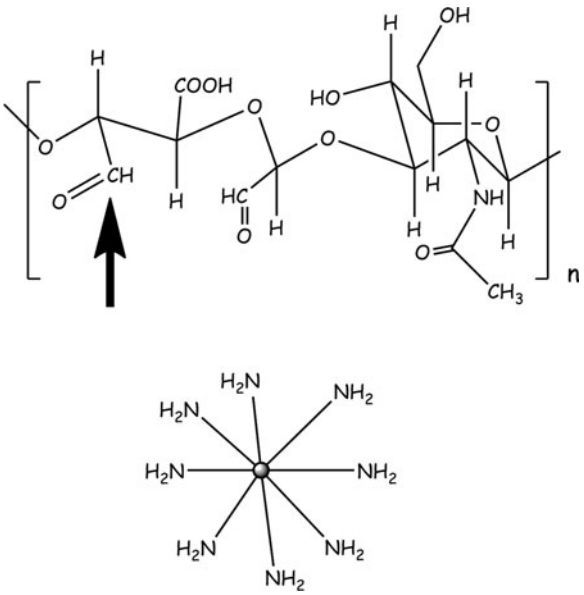

Fig. 4 Oxidized dextran (aldehyde is indicated by an *arrow*) and aminated star-shaped polyethylene glycol

non-laser-activated protein solders [1], porcine gelatin, glutaraldehyde mixed with collagen [49, 53] to name but a few examples. In situ cross-linking polymer systems can form non-self assembling systems (e.g. UV-light/irradiation) or can form spontaneously without the need of external triggers [85]. The bond formed between the two polymeric chains (cross-linking) can be covalent or can depend on weaker bonds, such as hydrogen bonds, van der Waals forces, ionic interactions or a molecule's side chain interactions [71]. Similarly, adhesive forces between the gel and the tissue can be due to covalent bonds formed between functional groups on one of the polymers (e.g. aldehyde) or by weak van der Waals or hydrogen bonds interactions (e.g. PEG compounds).

BioGlue® (Cryolife, Kennesaw, GA) is a surgical adhesive used in cardiovascular surgery, approved by the FDA and the EU as an adjunct in human vascular and pulmonary repair surgery [29]. It is composed of purified bovine serum albumin (BSA) and glutaraldehyde. The two components are dispensed by a delivery system comprised of a double-chambered syringe and an applicator apparatus. Once dispensed, the components are mixed within the applicator tip (a mixer) where the cross-linking begins. The glutaraldehyde molecules bond with the BSA molecules and, upon application to the tissue create an elastic seal independent of the body's clotting mechanism [48]. A pilot study [31] aimed to determine the feasibility of using BioGlue® to achieve hemostasis and to prevent urine leakage suggested that this glue provides adequate hemostasis during renal surgery, and decreased blood loss, transfusion rates and operative times.

Another two-component system [59] is made of aminated star-PEG (a star-shaped poly[ethylene glycol]) and high-molecular-weight dextran-aldehyde (Fig. 4). The two polymers are administered as viscous aqueous solutions that are

delivered through a dual-chambered syringe connected to a single injection needle, thus separating the compounds until the time of administration. Upon mixing, imide bonds are spontaneously formed through a Schiff-base reaction between the amine groups in the PEG molecule and the aldehyde groups of the dextran moieties. As a result, a network is formed in seconds. Cohesion strength is created by cross-linking between polymer chains, while adhesion forces are created by the reaction between the aldehyde and the amine groups in tissue. The aldehydes of the dextran are in excess of the amine groups in the star-PEG since they are responsible for both cohesion and adhesion. The adhesive mechanics of this glue varied with aldehyde content and with tissue type. For example: increasing aldehyde content from 8.8 to 14 and 20% resulted in moduli of 100, 500 and 744 kPa, respectively. Likewise, when moduli were measured for different tissues using a dextran with 20% aldehyde content, the highest modulus was measured in the duodenum, followed by the liver, heart and lung (724 ± 86 kPa, 431 ± 15, 296 ± 60 and 72 ± 7 kPa, respectively). Thus, it was concluded that different tissues may require specific surgical sealants when applied.

PEG-based sealants have gained interest in recent years because they are considered safe, easy to apply, and very effective in sealing suture lines when cross-linked [19]. In order to provide a tight seal, PEGs can be cross-linked by chemical agents or by visible light. An example is the commercial product FocalSeal® (FocalSeal, Focal, Inc., Lexington, MA) which is composer of an eosin primer and an aqueous polymeric solution [69]. The primer is applied first, is absorbed by the tissue, and auto-cross-links. A polymeric solution composed of PEG is applied and cured by visible light (450–550 nm) [2]. FocalSeal®was effective in minimally invasive cardiac surgery, where limited exposure and tight quarters make accurate suturing difficult. This product was also found to be effective for sealing bronchial and parenchymal air leaks [37] and preventing leakage from the cut pancreas (the pancreatic stump) [83].

The preceding systems formed glues spontaneously upon application or mixing. Some, such as chitosan containing azide groups and lactose moieties [63] employ a triggering agent. After ultraviolet light (UV) irradiation, an aqueous solution of this material was used to glue two pieces of sliced ham to each other [65]. The binding strength of the chitosan hydrogel prepared from 30 to 50 mg/mL solutions was similar to that of fibrin glue. However, it was more effectively in sealing air leakage from pinholes on isolated small intestine, aorta, and from incisions on the isolated trachea. Neither the tested gel nor its pre-crosslinked solution showed any cytotoxicity in cell culture of human skin fibroblasts, coronary endothelial cells, and smooth muscle cells. In vivo, all mice survived for at least 1 month after implantation of 200 μL of photocrosslinked chitosan gel or intraperitoneal administration of the pre-crosslinked solution.

The catechol functionality of L-3,4-dihydroxyphenylalanine (DOPA) is thought to be responsible for the ability of marine mussels to form strong bonds with a range of substrates, a property shared by DOPA-coated surfaces [44]. DOPA moieties have been conjugated to polymers and peptides in efforts to develop tissue adhesives [81, 88]. However, the adhesive strength of these biomaterials

have not shown higher adhesive strength than that of fibrin sealant This is believed to be the result of two major factors: (1) low adhesion forces due to intra- and/or intermolecular cross-linking reactions rather than with the surrounding tissue [45], and (2) the soft, flexible nature of hydrogel networks [66] that limits the cohesion forces within the material.

2 Active Tissue Glues

2.1 Tissue Adhesives Releasing Drugs

Tissue adhesives, in addition to being utilized as glues or sealants, can be used as drug delivery systems. The architecture of the material can be engineered to release its contents in the desired pattern directly to the target site. Local release by the glue enables the administration of controlled dosages, reducing the risk of adverse drug effects. Moreover, patient compliance with these drugs is assured as the agents are delivered at the time of the procedure and then released without the need for active participation on the patient's part. The release and the clinical benefits of several drug classes have been investigated utilizing this model, including antibiotics, chemotherapy, analgesics, growth factors, and gene vectors to name but a few. In some of these applications the adhesives are not used as glues or sealants, but simply as drug delivery (depot) systems.

2.1.1 Antibiotic Impregnated Glues

High local antibiotic concentrations at a wound site could prevent local infections (e.g. of surgical wounds) by providing local drug concentrations far in excess of what could be achieved by conventional dosing methods. A variety of formulations have been developed to achieve that goal. For example, vancomycin, teicoplanin, cephalothin and gentamicin added to the thrombin component of a fibrin glue [51] were released from that matrix for over 96 h in vitro, and exhibited antibacterial activity against clinical isolates of *S. epidermidis*. Similarly, amikacin released from a fibrin sealant/polyurethane mixture implanted subcutaneously in the anterior abdominal region of rats [60] was detectable in blood for 24 h, while the same dose given intravenously cleared after only 4 h. Moreover, peak local concentrations of amikacin in tissue near the glues were 210 times higher than when the drug was given systemically. A glue composed of aldehyde-modified dextran and poly (L-lysine) was able to reduce bacterial counts in adjacent subcutaneously implanted Dacron grafts inoculated with methicillin-resistant *S. aureus* [16, 56]. About 95% of the total antibiotic was released over 72 h (Fig. 5), and the local tissue concentration of vancomycin remained above the minimum inhibitory concentration throughout this period.

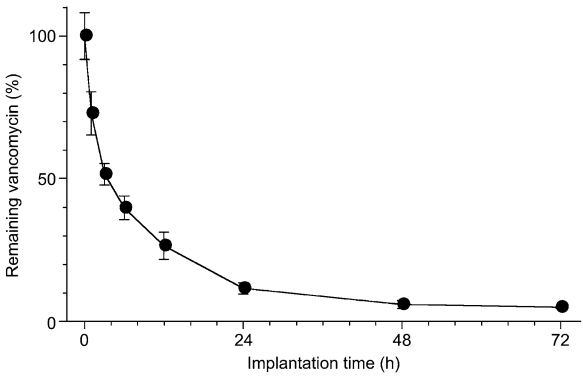

Fig. 5 Percentage of vancomycin remaining in aldehyde-modified dextran and poly (L-lysine) disks at time points after subcutaneously implantation. Reproduced with permission from Elsevier [56]

2.1.2 Release of Local Anesthetics from Fibrin Glue

A combination of fibrin glue and the local anesthetic lidocaine was developed to treat postoperative breast pain after subpectoral breast augmentation [97]. Although breast pain was observed for 1 week postoperatively for all groups, pain reported by patients in the group treated with the combination was significantly lower than that reported by patients who received lidocaine or fibrin glue alone. No complications were observed in any of the patients who participated in this study. Similarly, a fibrin glue containing lidocaine was used to relieve pain after tonsillectomy [41]. Tonsillar fossae were covered with fibrin glue containing lidocaine (dissolved in the thrombin solution) immediately after tonsillectomy. Patients began to eat normally after 3.78 days in the group administered with regular fibrin sealant compared to 2.83 days when the fibrin with lidocaine was used. In addition, the mean postoperative period for which analgesic administration was necessary decreased from 4.91 to 2.88 days when lidocaine was incorporated in the glue.

2.1.3 Release of Chemotherapy from Photocrosslinkable Chitosan Tissue Adhesives

In the management of cancer patients, local delivery may provide a high local concentration of anti-tumor drugs with decreased incidence of the side effects observed with systemic therapy [23]. A photocrosslinkable chitosan tissue adhesive (see Sect. 1.2.2 of this chapter) has been developed to deliver the antineoplastic drug paclitaxel [27, 63]. About 40% of the paclitaxel was released from the hydrogel into media (phosphate buffered saline) within 1 day in vitro, after which gradual release occurred for 3 days. The paclitaxel-containing hydrogel inhibited the growth of subcutaneous tumors induced with Lewis lung cancer (3LL) cells more effectively than those treated with plain chitosan gel or free paclitaxel injected subcutaneously at the tumor, for at least 11 days. Furthermore,

the paclitaxel-containing chitosan hydrogel markedly reduced the number of CD34-positive vessels in subcutaneous 3LL tumors, indicating a strong inhibition of angiogenesis.

2.1.4 Delivery of Growth Factors and Genetic Material from Tissue Adhesives

Although producing a system that releases biomacromolecules from a tissue adhesive can seem relatively simple (e.g. mixing one in the other), the macromolecules may have complex interactions with the surrounding matrix [80]. For example [13], when transforming growth factor beta-1 (TGF-β1) was added to fibrin sealant, release was much slower when fibrinogen concentrations were increased, suggesting a binding affinity of TGF-β1 with the fibrinogen. Varying the thrombin concentration though, had a lesser effect.

A matrix to promote wound healing has been developed by incorporating recombinant human epidermal growth factor (rhEGF) into a photocross-linkable mixture of glycidyl methacrylated chitooligosaccharide and di-acrylated Pluronic F127 [15]. When this hydrogel was administered to dorsal burn wounds in the rat, epidermal differentiation was significantly enhanced compared to plain hydrogel. The in vitro release profiles of rhEGF were dependent on the degradation rates of the hydrogels (Fig. 6).

Fibrin sealant has also been used to release nerve growth factor (NGF) into the site of end-to-end sutured peripheral nerve. Stained sections revealed significantly increased regenerated nerve fibers distal to the anastomosis compared to groups that received NGF or fibrin sealant alone. Similarly, fibrin sealant containing glia-derived neutropic factor (GDNF) had a greater in vivo effect on neuron growth than did the free factor or the sealant alone [14, 91].

Fibrin sealant has been used to release adenoviral vectors encoding ß-galactosidase [7]. Vectors released from fibrin resulted in higher numbers of rabbit cartilage cells expressing ß-galactosidase in vivo than with vector alone.

2.2 Intrinsic Activities of Glues

2.2.1 The Anti-bacterial Properties of Cyanoacrylates

The antimicrobial properties of cyanoacrylate tissue adhesives were first reported in 1983 [25]. A link has been established between the polymerization process and the antimicrobial properties, in particular against Gram-positive microorganisms [72], perhaps by action against the bacterial cell wall [22, 76]. Similarly, 2-ethyl cyanoacrylate monomers applied onto the surface of bacteria cultures [73] inhibit the growth of *S. aureus* and *S. pneumoniae* (both Gram positive). A possible explanation to the higher sensitivity of the Gram-positive bacteria might be the

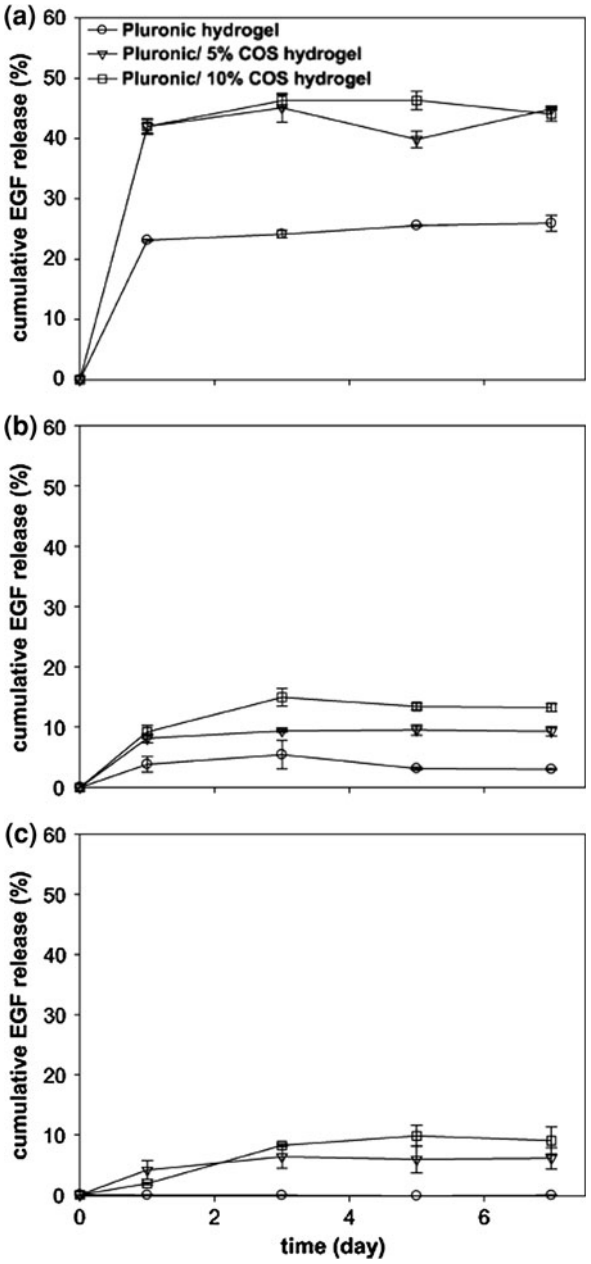

Fig. 6 Release profiles of rhEGF from a mixture of glycidyl methacrylated chitooligosaccharide and di-acrylated Pluronic F127 with photo-irradiation times of 2 min (**a**), 5 min (**b**), and 10 min (**c**). The polymeric concentration of all hydrogels was 20% (w/w). Reproduced with permission from John Wiley and Sons [15]

strong electronegative charge on the cyanoacrylate monomer that reacts with the positively charged carbohydrate capsule of Gram-positive organisms [34]. While cyanoacrylates have less effect on Gram negatives, 2-ethyl cyanoacrylate monomers did kill Escherichia coli [73].

2.2.2 Anti-bacterial Barriers

2-octyl cyanoacrylate films have been shown to be effective barriers to bacteria, fungi, and yeast in vitro [58]. The barrier property of cyanoacrylate bandage was also seen in a wound model in swine [52]. *S. aureus* or Pseudomonas aeruginosa were inoculated on one side of a test bandage placed over a wound. Significantly lower numbers of inoculated bacteria were found among the cyanoacrylate bandage group compared with other groups treated with standard or hydrocolloid bandages.

2.2.3 Glues with Wound-Healing and Other Tissue-Active Properties

Photocrosslinkable chitosan is strong, elastic and is considered more effective in sealing air leakages than fibrin glue [64]. It can stop bleeding within 30 s of UV-irradiation and firmly adhere the cut edges of two pieces of skin [32]. It can also induce wound contraction and accelerate wound closure and healing [10]. Histological findings suggest that chitin and chitosan stimulate the migration of mononuclear and polymorphonuclear cells and accelerate angiogenesis and the formation of connective tissue [55]. Other studies [46, 61] suggest that chitosans posses antibacterial properties, owing to the cationic amines interacting with negatively charged residues on the bacterial cell surface [95].

Experiments performed in our lab [92] suggest that some caution may be advisable in using chitosan and UV-cross-linkable chitosan in some contexts. Although in vitro experiments showed neither attractive interactions between the gels and the cells nor a proliferative or marked toxic effect, the same material applied in the peritoneal cavity of rabbits caused a granulomatous reaction in all animals, with resultant adhesion formation ("adhesion" in this context meaning an undesirable sticking together of tissues). Although chitosan's adhesive and other proinflammatory properties may be beneficial in some biomedical applications, this may not be true in all contexts.

Chitin and chitosan gels have inhibitory effects on tumor angiogenesis and metastasis [12, 57], and can inhibit tumor cell proliferation by inducing apoptosis [57].

2.2.4 Glues for Islet Cell Immobilization

There is a great need for medical adhesives that effectively function on wet tissue surfaces with minimal tissue and cell response. A star shape PEG core with DOPA endgroups was suggested as a system for cell immobilization [8]. When aqueous solutions of this polymer were oxidized with $NaIO_4$, each DOPA endgroup covalently attached to a neighboring DOPA, forming a 3D hydrogel structure. Donor islet cells were placed into the PEG-DOPA aqueous solution which was then oxidized. The encapsulated cells were then implanted in type 1 diabetic mice

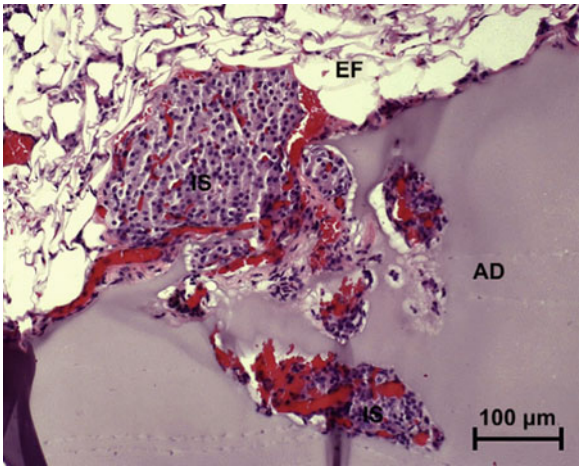

Fig. 7 Photomicrograph of hematoxylin and eosin (H&E)-stained tissue explants demonstrating star-PEG-DOPA adhesive-mediated islet cell attachment to the epididymal fat pad surface. *AD*. adhesive, *IS* islet, *EF* epididymal fat tissue. Reproduced with permission from Elsevier [8]

(Fig. 7). This adhesive material maintained an intact interface with the supporting tissue for up to 1 year. The cells encapsulated within were able to maintain normoglycemia for over 100 days.

3 Conclusions and Future Directions

Surgical adhesives are attractive alternatives to sutures and staples [20]. They allow rapid adhesion and maintain strong and close apposition of wound edges [54]. In some cases, the tissue glues themselves contribute directly to the process of wound healing. A major potential advantage of tissue glues is their ability to release drugs directly to the wound. In this chapter, we presented the release of several drugs from various classes of tissue adhesives, with emphasis on the chemical and the physical properties of each system.

There is a great variety of adhesives, to which a range of active properties can be imparted. Further studies will be required to determine whether these new materials will translate into the clinical arena. The potential to modify these materials has barely been tapped. For example, the incorporation of nanomaterials [93] and/or of components that would allow triggered release of compounds [82] could further enhance their properties.

References

1. Al-qahtani, J.M., McLean, I.W., et al.: Preliminary in vitro study of the histological effects of low fluence 193-nm excimer laser irradiation of corneal tissue. J. Refract. Surg. **17**(2), 105–109 (2001)

2. Lauto, A., Mawad, D., et al.: Adhesive biomaterials for tissue reconstruction. J. Chem. Technol. Biotechnol. **83**, 464–472 (2008)
3. Ardis, A.: Preparation of monomeric alkyl a-cyanoacrylates. US Patent 2,467,926 (1949)
4. Atrah, H.I.: Fibrin glue. BMJ **308**(6934), 933–934 (1994)
5. Bernard, L., Doyle, J., et al.: A prospective comparison of octyl cyanoacrylate tissue adhesive (dermabond) and suture for the closure of excisional wounds in children and adolescents. Arch. Dermatol. **137**(9), 1177–1180 (2001)
6. Borst, H.G., Haverich, A., et al.: Fibrin adhesive: an important hemostatic adjunct in cardiovascular operations. J. Thorac. Cardiovasc. Surg. **84**(4), 548–553 (1982)
7. Breen, A., Dockery, P., et al.: Fibrin scaffold promotes adenoviral gene transfer and controlled vector delivery. J. Biomed. Mater. Res. A **89**(4), 876–884 (2009)
8. Brubaker, C.E., Kissler, H., et al.: Biological performance of mussel-inspired adhesive in extrahepatic islet transplantation. Biomaterials **31**(3), 420–427 (2010)
9. Bruns, T.B., Worthington, J.M.: Using tissue adhesive for wound repair: a practical guide to dermabond. Am. Fam. Physician **61**(5), 1383–1388 (2000)
10. Burkatovskaya, M., Castano, A.P., et al.: Effect of chitosan acetate bandage on wound healing in infected and noninfected wounds in mice. Wound Repair Regen. **16**(3), 425–431 (2008)
11. Canonico, S.: The use of human fibrin glue in the surgical operations. Acta. Biomed. **74**(Suppl 2), 21–25 (2003)
12. Carreno-Gomez, B., Duncan, R.: Evaluation of the biological properties of soluble chitosan and chitosan microspheres. Int. J. Pharm. **48**(2), 231–240 (1997)
13. Catelas, I., Dwyer, J.F., et al.: Controlled release of bioactive transforming growth factor beta-1 from fibrin gels in vitro. Tissue Eng. Part C Methods. **14**(2), 119–128 (2008)
14. Cheng, H., Hoffer, B., et al.: The effect of glial cell line-derived neurotrophic factor in fibrin glue on developing dopamine neurons. Exp. Brain Res. **104**(2), 199–206 (1995)
15. Choi, J.S., Yoo, H.S.: Pluronic/chitosan hydrogels containing epidermal growth factor with wound-adhesive and photo-crosslinkable properties. J. Biomed. Mater. Res. A **95A**(2), 564–573 (2010)
16. Cirioni, O., Giacometti, A., et al.: Prophylactic efficacy of topical temporin A and RNAIII-inhibiting peptide in a subcutaneous rat pouch model of graft infection attributable to staphylococci with intermediate resistance to glycopeptides. Circulation **108**(6), 767–771 (2003)
17. Collin, T.W., Blyth, K., et al.: Cleft lip repair without suture removal. J. Plast. Reconstr. Aesthet. Surg. **62**(9), 1161–1165 (2009)
18. Coover, H.W., Joyner, F.B., et al.: Chemistry and performance of cyanoacrylate adhesives. J. Soc. Plast. Eng. **15**, 413–417 (1959)
19. Cosgrove, G.R., Delashaw, J.B., et al.: Safety and efficacy of a novel polyethylene glycol hydrogel sealant for watertight dural repair. J. Neurosurg. **106**(1), 52–58 (2007)
20. Coulthard, P., Esposito, M., et al.: Tissue adhesives for closure of surgical incisions. Cochrane Database Syst. Rev. **5**, CD004287 (2010)
21. DaCruz, D.: Full-thickness skin necrosis of the fingertip after application of superglue. J. Hand Surg. Am. **29**(1), 159 (2004). Author reply 159
22. de Almeida Manzano, R.P., Naufal, S.C., et al.: Antibacterial analysis in vitro of ethyl-cyanoacrylate against ocular pathogens. Cornea **25**(3), 350–351 (2006)
23. Dhanikula, A.B., Panchagnula, R.: Localized paclitaxel delivery. Int. J. Pharm. **183**(2), 85–100 (1999)
24. Durham, L.H., Willatt, D.J., et al.: A method for preparation of fibrin glue. J. Laryngol. Otol. **101**(11), 1182–1186 (1987)
25. Eiferman, R., Snyder, J.: Antibacterial effect of cyanoacrylate glue. Arch. Ophthalmol. **101**(6), 958–960 (1983)
26. Ghoreishian, M., Gheisari, R., et al.: Tissue adhesive and suturing for closure of the surgical wound after removal of impacted mandibular third molars: a comparative study. Oral Surg. Oral Med. Oral Pathol. Oral Radiol. Endod. **108**(1), e14–e16 (2009)

27. Guo, K., Chu, C.C.: Controlled release of paclitaxel from biodegradable unsaturated poly(ester amide)s/poly(ethylene glycol) diacrylate hydrogels. J. Biomater. Sci. Polym. Ed. **18**(5), 489–504 (2007)
28. Hennink, W.E., van Nostrum, C.F.: Novel crosslinking methods to design hydrogels. Adv. Drug Deliv. Rev. **54**(1), 13–36 (2002)
29. Herget, G.W., Kassa, M., et al.: Experimental use of an albumin-glutaraldehyde tissue adhesive for sealing pulmonary parenchyma and bronchial anastomoses. Eur. J. Cardiothorac. Surg. **19**(1), 4–9 (2001)
30. Hesse, L., Schanze, T., et al.: Implantation of retina stimulation electrodes and recording of electrical stimulation responses in the visual cortex of the cat. Graefes Arch. Clin. Exp. Ophthalmol. **238**(10), 840–845 (2000)
31. Hidas, G., Kastin, A., et al.: Sutureless nephron-sparing surgery: use of albumin glutaraldehyde tissue adhesive (BioGlue). Urology **67**(4), 697–700 (2006). Discussion 700
32. Ishihara, M., Nakanishi, K., et al.: Photocrosslinkable chitosan as a dressing for wound occlusion and accelerator in healing process. Biomaterials **23**(3), 833–840 (2002)
33. Jaffe, H., Wade, C.W., et al.: Synthesis and bioevaluation of alkyl 2-cyanoacryloyl glycolates as potential soft tissue adhesives. J. Biomed. Mater. Res. **20**(2), 205–212 (1986)
34. Jang, C.H., Park, H., et al.: Antibacterial effect of octylcyanoacrylate against methicillin-resistant *Staphylococcus aureus* isolates from patients with chronic suppurative otitis media. In Vivo **22**(6), 763–765 (2008)
35. Jankowitz, B.T., Atteberry, D.S., et al.: Effect of fibrin glue on the prevention of persistent cerebral spinal fluid leakage after incidental durotomy during lumbar spinal surgery. Eur. Spine J. **18**(8), 1169–1174 (2009)
36. Joch, C., Witzke, G., Groner, A., et al.: Clinical safety of fibrin sealants. Presented at the IXth World Conference of Cardio-Thoracic Surgeons, Lisbon, Portugal (1999)
37. Jones, D.R., Stiles, B.M., et al.: Pulmonary segmentectomy: results and complications. Ann. Thorac. Surg. **76**(2), 343–348 (2003). Discussion 348–349
38. Kaplan, M., Baysal, K.: In vitro toxicity test of ethyl 2-cyanoacrylate, a tissue adhesive used in cardiovascular surgery, by fibroblast cell culture method. Heart Surg. Forum **8**(3), E169–E172 (2005)
39. Kawamura, S., Hadeishi, H., et al.: Arterial occlusive lesions following wrapping and coating of unruptured aneurysms. Neurol. Med. Chir. (Tokyo) **38**(1), 12–18 (1998). Discussion 18–19
40. Kimura, K.N., Sugiura, K.N.: Adhesive composition. US patent 4321180, Application no. 06/209253, 23 March 1982
41. Kitajiri, S., Tabuchi, K., et al.: Relief of post-tonsillectomy pain by release of lidocaine from fibrin glue. Laryngoscope **111**(4 Pt 1), 642–644 (2001)
42. Kulkarni, R.K., Bartak, D.E., et al.: Initiation of polymerization of alkyl 2-cyanoacrylates in aqueous solutions of glycine and its derivatives. J. Polym. Sci. A1 **9**(10), 2977–2981 (1971)
43. Lauto, A., Hook, J., et al.: Chitosan adhesive for laser tissue repair: in vitro characterization. Lasers Surg. Med. **36**(3), 193–201 (2005)
44. Lee, B.P., Dalsin, J.L., et al.: Synthesis and gelation of DOPA-modified poly(ethylene glycol) hydrogels. Biomacromolecules **3**(5), 1038–1047 (2002)
45. Lee, B.P., Huang, K., et al.: Synthesis of 3, 4-dihydroxyphenylalanine (DOPA) containing monomers and their co-polymerization with PEG-diacrylate to form hydrogels. J. Biomater. Sci. Polym. Ed. **15**(4), 449–464 (2004)
46. Lee, D.S., Jeong, S.Y., et al.: Antibacterial activity of aminoderivatized chitosans against methicillin-resistant *Staphylococcus aureus* (MRSA). Bioorg. Med. Chem. **17**(20), 7108–7112 (2009)
47. Dean, M.J.: Treatise on Adhesion and Adhesives, vol. 7. Marcel Dekker Inc., New York (1991)
48. Manabe, T., Okino, H., et al.: In situ-formed, tissue-adhesive co-gel composed of styrenated gelatin and styrenated antibody: potential use for local anti-cytokine antibody therapy on surgically resected tissues. Biomaterials **25**(27), 5867–5873 (2004)

49. Marchini, M., Ortolani, F., et al.: Collagen-glutaraldehyde interaction as revealed by the D-banding of negatively stained fibrils and computer-drawn band patterns. Eur. J. Histochem. **37**(4), 363–373 (1993)
50. Marcovich, R., Williams, A.L., et al.: Comparison of 2-octyl cyanoacrylate adhesive, fibrin glue, and suturing for wound closure in the porcine urinary tract. Urology **57**(4), 806–810 (2001)
51. Marone, P., Monzillo, V., et al.: Antibiotic-impregnated fibrin glue in ocular surgery: in vitro antibacterial activity. Ophthalmologica **213**(1), 12–15 (1999)
52. Mertz, P.M., Davis, S.C., et al.: Barrier and antibacterial properties of 2-octyl cyanoacrylate-derived wound treatment films. J. Cutan. Med. Surg. **7**(1), 1–6 (2003)
53. Milkes, D.E., Friedland, S., et al.: A novel method to control severe upper GI bleeding from metastatic cancer with a hemostatic sealant: the CoStasis surgical hemostat. Gastrointest. Endosc. **55**(6), 735–740 (2002)
54. Mobley, S.R., Hilinski, J., et al.: Surgical tissue adhesives. Facial Plast. Surg. Clin. North Am. **10**(2), 147–154 (2002)
55. Mori, T., Okumura, M., et al.: Effects of chitin and its derivatives on the proliferation and cytokine production of fibroblasts in vitro. Biomaterials **18**(13), 947–951 (1997)
56. Morishima, M., Marui, A., et al.: Sustained release of vancomycin from a new biodegradable glue to prevent methicillin-resistant *Staphylococcus aureus* graft infection. Interact Cardiovasc. Thorac. Surg. **11**(1), 52–55 (2010)
57. Murata, J., Saiki, I., et al.: Inhibitory effect of chitin heparinoids on the lung metastasis of B16-BL6 melanoma. Jpn. J. Cancer Res. **80**(9), 866–872 (1989)
58. Narang, U., Mainwaring, L., et al.: In vitro analysis for microbial barrier properties of 2-octyl cyanoacrylate-derived wound treatment films. J. Cutan. Med. Surg. **7**(1), 13–19 (2003)
59. Artzi, N., Baker, A.B., Shazly, T., et al.: Aldehyde-amine chemistry enables modulated biosealants with tissue-specific adhesion. Adv. Mater. **21**, 3399–3403 (2009)
60. Nishimoto, K., Yamamura, K., et al.: Subcutaneous tissue release of amikacin from a fibrin glue/polyurethane graft. J. Infect. Chemother. **10**(2), 101–104 (2004)
61. No, H.K., Park, N.Y., et al.: Antibacterial activity of chitosans and chitosan oligomers with different molecular weights. Int. J. Food Microbiol. **74**(1–2), 65–72 (2002)
62. Novik, B., Hagedorn, S., et al.: Fibrin glue for securing the mesh in laparoscopic totally extraperitoneal inguinal hernia repair: a study with a 40-month prospective follow-up period. Surg. Endosc. **20**(3), 462–467 (2006)
63. Obara, K., Ishihara, M., et al.: Controlled release of paclitaxel from photocrosslinked chitosan hydrogels and its subsequent effect on subcutaneous tumor growth in mice. J. Control Release **110**(1), 79–89 (2005)
64. Ono, K., Ishihara, M., et al.: Experimental evaluation of photocrosslinkable chitosan as a biologic adhesive with surgical applications. Surgery **130**(5), 844–850 (2001)
65. Ono, K., Saito, Y., et al.: Photocrosslinkable chitosan as a biological adhesive. J. Biomed. Mater. Res. **49**(2), 289–295 (2000)
66. Park, K., Shalaby, W., et al.: Biodegradable hydrogels for drug delivery. Technomic Publishing Co., Inc., Lancaster (1993)
67. Quinn, J.V.: Tissue Adhesive in Clinical Medicine, BC Decker Inc., Hamilton (2005), p. 2.
68. Ramachary, D.B., Anebouselvy, K., et al.: Direct organocatalytic asymmetric heterodomino reactions: the Knoevenagel/Diels-Alder/epimerization sequence for the highly diastereoselective synthesis of symmetrical and nonsymmetrical synthons of benzoannelated centropolyquinanes. J. Org. Chem. **69**(18), 5838–5849 (2004)
69. Ranger, W.R., Halpin, D., et al.: Pneumostasis of experimental air leaks with a new photopolymerized synthetic tissue sealant. Am. Surg. **63**(9), 788–795 (1997)
70. Reece, T.B., Maxey, T.S., et al.: A prospectus on tissue adhesives. Am. J. Surg. **182**(2 Suppl), 40S–44S (2001)
71. Roldo, M., Hornof, M., et al.: Mucoadhesive thiolated chitosans as platforms for oral controlled drug delivery: synthesis and in vitro evaluation. Eur. J. Pharm. Biopharm. **57**(1), 115–121 (2004)

72. Romero, I.L., Malta, J.B., et al.: Antibacterial properties of cyanoacrylate tissue adhesive: Does the polymerization reaction play a role? Indian J. Ophthalmol. **57**(5), 341–344 (2009)
73. Romero, I.L., Paiato, T.P., et al.: Different application volumes of ethyl-cyanoacrylate tissue adhesive can change its antibacterial effects against ocular pathogens in vitro. Curr. Eye Res. **33**(10), 813–818 (2008)
74. Ryou, M., Thompson, C.C.: Tissue adhesives: a review. Tech. Gastrointest. Endosc. **8**(1), 33–37 (2006)
75. Saldana-Cortes, J.A., Larios-Arceo, F., et al.: Role of fibrin glue in the prevention of cervical leakage and strictures after esophageal reconstruction of caustic injury. World J. Surg. **33**(5), 986–993 (2009)
76. Schembri, M.A., Dalsgaard, D., et al.: Capsule shields the function of short bacterial adhesins. J. Bacteriol. **186**(5), 1249–1257 (2004)
77. Scott, G.R., Carson, C.L., et al.: Dermabond skin closures for bilateral reduction mammaplasties: a review of 255 consecutive cases. Plast. Reconstr. Surg. **120**(6), 1460–1465 (2007)
78. Sierra, D.H., Saltz, R.: Surgical Adhesives and Sealants. Technomic Publishing Company, Inc., Lancaster (1996)
79. Singer, A.J., Hollander, J.E., et al.: Prospective, randomized, controlled trial of tissue adhesive (2-octylcyanoacrylate) vs standard wound closure techniques for laceration repair. Stony Brook Octylcyanoacrylate Study Group. Acad. Emerg. Med. **5**(2), 94–99 (1998)
80. Spicer, P.P., Mikos, A.G.: "Fibrin glue as a drug delivery system." J. Control. Release (2010)
81. Sun, C.J., Srivastava, A., et al.: Halogenated DOPA in a marine adhesive protein. J. Adhes. **85**(2–3), 126–138 (2009)
82. Timko, B.P., Dvir, T., et al.: Remotely triggerable drug delivery systems. Adv. Mater. 22(44), 4925–4943 (2010)
83. Torchiana, D.F.: Polyethylene glycol based synthetic sealants: potential uses in cardiac surgery. J. Card. Surg. **18**(6), 504–506 (2003)
84. Tseng, Y.C., Tabata, Y., et al.: In vitro toxicity test of 2-cyanoacrylate polymers by cell culture method. J. Biomed. Mater. Res. **24**(10), 1355–1367 (1990)
85. Van Tomme, S.R., Storm, G., et al.: In situ gelling hydrogels for pharmaceutical and biomedical applications. Int. J. Pharm. **355**(1–2), 1–18 (2008)
86. Vauthier, C., Dubernet, C., et al.: Poly(alkylcyanoacrylates) as biodegradable materials for biomedical applications. Adv. Drug Deliv. Rev. **55**(4), 519–548 (2003)
87. Vote, B.J., Elder, M.J.: Cyanoacrylate glue for corneal perforations: a description of a surgical technique and a review of the literature. Clin. Experiment Ophthalmol. **28**(6), 437–442 (2000)
88. Wang, J., Liu, C., et al.: Co-polypeptides of 3, 4-dihydroxyphenylalanine and L-lysine to mimic marine adhesive protein. Biomaterials **28**(23), 3456–3468 (2007)
89. Wang, M.-C., Pins, G.D., et al.: Preparation of fibrin glue: the effects of calcium chloride and sodium chloride. Mater. Sci. Eng. C **3**(2), 131–135 (1995)
90. Wieken, K., Angioi-Duprez, K., et al.: Nerve anastomosis with glue: comparative histologic study of fibrin and cyanoacrylate glue. J. Reconstr. Microsurg. **19**(1), 17–20 (2003)
91. Wood, M.D., Borschel, G.H., et al.: Controlled release of glial-derived neurotrophic factor from fibrin matrices containing an affinity-based delivery system. J. Biomed. Mater. Res. A **89**(4), 909–918 (2009)
92. Yeo, Y., Burdick, J.A., et al.: Peritoneal application of chitosan and UV-cross-linkable chitosan. J. Biomed. Mater. Res. A **78**(4), 668–675 (2006)
93. Yeo, Y., Ito, T., et al.: In situ cross-linkable hyaluronan hydrogels containing polymeric nanoparticles for preventing postsurgical adhesions. Ann. Surg. **245**(5), 819–824 (2007)
94. Yeung, J.M., Simpson, J.A., et al.: Fibrin glue for the treatment of fistulae in ano—a method worth sticking to? Colorectal Dis. **12**(4), 363–366 (2010)
95. Young, D.H., Kauss, H.: Release of calcium from suspension-cultured glycine max cells by chitosan, other polycations, and polyamines in relation to effects on membrane permeability. Plant Physiol. **73**(3), 698–702 (1983)

96. Zarate-Kalfopulos, B., Estrada-Villasenor, E., et al.: Use of fibrin glue in combination with autologous bone graft as bone enhancer in posterolateral spinal fusion. An experimental study in New Zealand rabbits. Cir. Cir. **75**(3), 201–205 (2007)
97. Zhibo, X., Miaobo, Z.: Effect of sustained-release lidocaine on reduction of pain after subpectoral breast augmentation. Aesthet. Surg. J. **29**(1), 32–34 (2009)

Electrospun Drug-Eluting Fibers for Biomedical Applications

Mădălina V. Natu, Hermínio C. de Sousa and Maria H. Gil

Abstract Electrospinning is a simple and versatile method to produce fibers using charged polymer solutions. As drug delivery systems, electrospun fibers are an excellent choice because of easy drug entrapment, high surface area, morphology control and biomimetic characteristics. Various drugs and biomolecules can be easily encapsulated inside or on fiber surface either during electrospinning or through post-processing of the fibers. Multicomponent fibers have attracted special attention because new properties and morphologies can be easily obtained through the combination of different polymers. The factors that affect the drug release such as construct geometry and thickness, diameter and porosity, composition, crystallinity, swelling capacity, drug loading, drug state, drug molecular weight, drug solubility in the release medium, drug–polymer–electrospinning solvent interactions are discussed. Mathematical models of drug release from electrospun fibers are reviewed and strategies to attain zero-order release and control of burst stage are considered. Finally, some results concerning release control in bicomponent fibers composed of poly(ε-caprolactone) and Lutrol F127 (poly(oxyethylene-b-oxypropylene-b-oxyethylene) are presented. The properties of the bicomponent fibers were studied in order to determine the effect of electrospinning processing on crystallinity, hydrophilicity and degradation. Acetazolamide and timolol maleate were loaded in the fibers in different concentrations in order to determine the effect of drug solubility in polymer, drug state, drug loading and fiber

M. V. Natu (✉) · H. C. de Sousa · M. H. Gil
Department of Chemical Engineering, University of Coimbra,
Pólo II, Pinhal de Marrocos, 3030-290 Coimbra, Portugal
e-mail: mada@eq.uc.pt

H. C. de Sousa
e-mail: hsousa@eq.uc.pt

M. H. Gil
e-mail: hgil@eq.uc.pt

Stud Mechanobiol Tissue Eng Biomater (2011) 8: 57–85
DOI: 10.1007/8415_2010_56

Published Online: 10 February 2011

composition on morphology, drug distribution and release kinetics. Such electrospun drug eluting fibers can be used as basic elements of various implants and scaffolds for tissue regeneration.

1 What is Electrospinning?

Electrospinning is a method of producing fibers with diameters ranging from micrometer to nanometer scale by accelerating a jet of charged polymer solution/melt in an electric field. Recently, this technology has been expanding due to the simplicity of the process and the various materials that can be used. Fibers can be produced from either natural or synthetic polymers. Such fibers have diverse applications including filtration, catalysis, textiles, composite materials, biomedicine (wound dressings, drug delivery, tissue engineering, cosmetics), sensors, electronic devices, liquid crystals, photovoltaic cells and much more [1, 2].

Usually, the experimental set-up consists of a high voltage power supply connecting an electrode with needle-like geometry (through which the polymer solution is ejected) to the collector electrode. The polymer solution is pumped at the desired flow rate using a syringe pump. A diagram presenting the most common electrospinning set-up is shown in Fig. 1.

Recent works suggest that the most important mechanism of electrospinning is a rapidly whipping/bending fluid jet [3]. The jet instability is produced by the competition between surface tension and charge repulsion, in which the destabilizing effect of charge repulsion is responsible for the stretching of the fluid jet and simultaneous decrease in the jet diameter. Surface tension has a stabilizing effect leading to the cessation of stretching and attaining a limiting terminal jet diameter. The process can be decomposed into five components: fluid charging, formation of the cone-jet, thinning of the steady jet, onset and growth of jet instabilities and fiber

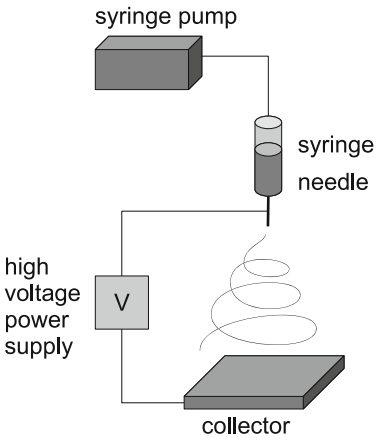

Fig. 1 Basic electrospining set-up

collection [4]. Several process parameters (voltage, nozzle to collector distance, polymer flow rate, spinning environment) and solution parameters (concentration–viscosity, conductivity, surface tension, solvent volatility) can be manipulated in order to obtain the desired properties of the fibers such as fiber diameter and morphology. Moreover, the fibers can be collected with a multitude of collectors producing fiber mats that contain either aligned or unoriented fibers [5].

2 Electrospun Fibers as Drug Delivery Systems

Electrospun fibers have been shown to function as drug delivery systems because of high surface area (which enhances mass transfer), similar topography and porosity to the extracellular matrix making them ideal candidates as active implants/scaffolds. The easy control of the macrostructure (oriented or arranged randomly, fiber mat porosity) and the microstructure (individual fiber porosity) will determine both the bulk physico-chemical properties and the biological response to the implant/scaffold. Variuos drugs ranging from low molecular agents to proteins and even cells [6] can be easily encapsulated inside or on the surface of the fibers depending on the application. Some disadvantages include drug loading that is limited by the drug solubility in the electrospining solution or burst effect due to surface deposited drug.

Drug delivery systems can be classified according to different criteria [7, 8]. The most common one is to classify with respect to the rate control mechanism. These classifications may also be applied to drug-containing polymeric fibers:

- Drug diffusion controlled systems: diffusion can take place either through the bulk polymer as in bicomponent mixed fibers or through a barrier as in core–shell fibers
- Solvent diffusion controlled systems: drug release is determined by the rate of polymer swelling
- Chemically controlled systems: either polymer erosion or enzymatic/hydrolytic polymer degradation control the drug release rate
- Regulated systems: the application of a magnetic field or another external stimulus can trigger the release (as in composite fibers containing magnetic particles)

The active ingredient can be loaded either during electrospinning or during post-processing of the electrospun fibers. In the former case, the drug is either co-dissolved with the polymers in the electrospinning solution or the drug is loaded in particles that will be co-electrospun with the polymers [9–11]. The later case includes various modalities of drug loading: fiber soaking in the drug solution, drug impregnation using supercritical fluids technology [12], loading in previously molecular imprinted fibers [13, 14], functionalization of the fiber surface through grafting copolymerization [15] and subsequent drug/protein binding [16, 17].

By electrospinning, the drug is usually entrapped as solid particles inside or on the surface of the fibers. According to the type of solid–solid or polymer–drug mixture, the drug loaded fibers can be classified as:

- Solid solutions: the drug is dissolved at molecular level in the polymer
- Solid dispersions: the drug is distributed in the polymer as either crystalline or amorphous aggregates
- Phase-separated systems or reservoir systems: the drug is contained inside the core of the fiber or encapsulated in particles, that are surrounded by a polymer shell (as in core–shell constructs or composite fibers, see Sect. 2.1)

2.1 Multicomponent Fibers

Multicomponent fibers have attracted special attention because new properties can be obtained through the combination of different materials. Synthetic polymers with good processability and good mechanical properties can be mixed with natural hydrophilic polymers producing an increase in cellular attachment and biocompatibility [5]. Unfortunately, sometimes the solvent that is used to dissolve both polymers can damage the structure of the natural polymer or phase separation can worsen the mechanical properties. One possible solution is to incorporate function-regulating biomolecules (DNA, growth factors) in synthetic polymers to increase bioactivity [17] or to modify the structure of the polymer before electrospinning [18].

Multicomponent fibers can be obtained mainly by two techniques [19, 20] as shown in Fig. 2: electrospinning of polymers solution in a single-needle configuration (if a mixture of polymers is co-dissolved in the electrospinning solution) or a multi-needle configuration (in which the polymer solutions are separated in parallel or concentric syringes) and post-treatment of the electrospun fibers (which can include either coating with other inorganic/polymer layers [16, 21], grafting [15], crosslinking [22], chemical vapour deposition [23] or functionalization with other (bio)polymers [17]).

In addition to the combination of physico-chemical properties that arise from using various components, there can be obtained a variety of fiber morphologies as presented in Fig. 3 such as core–shell fibers, micro/nanotubes, interpenetrating phase morphologies (matrix dispersed or co-continuous fibers) [24, 25], nanoscale morphologies (spheres, rods, micelles, lamellae, vesicle tubules, and cylinders) obtained by self-assembly of block copolymers [26], multilayers (either with different composition or different fiber diameter) [27, 28]. Moreover, the fiber morphology can be further controlled after electrospinning by selective removal of one component using thermal treatment [29] or dissolution [30].

Many of the fiber constructs are supposed to work as implants/tissue scaffolds besides functioning as drug delivery devices. Good mechanical properties are required in order to preserve the structural integrity of the implant. Crosslinking

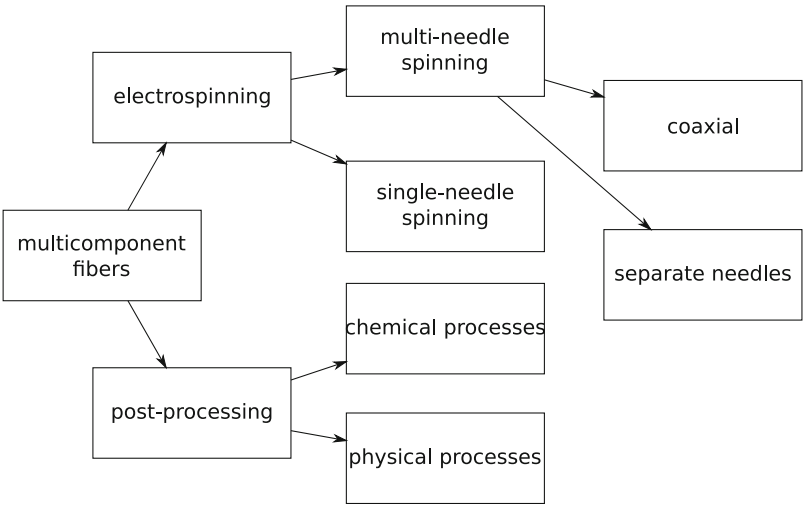

Fig. 2 Preparation methods for multicomponent fibers

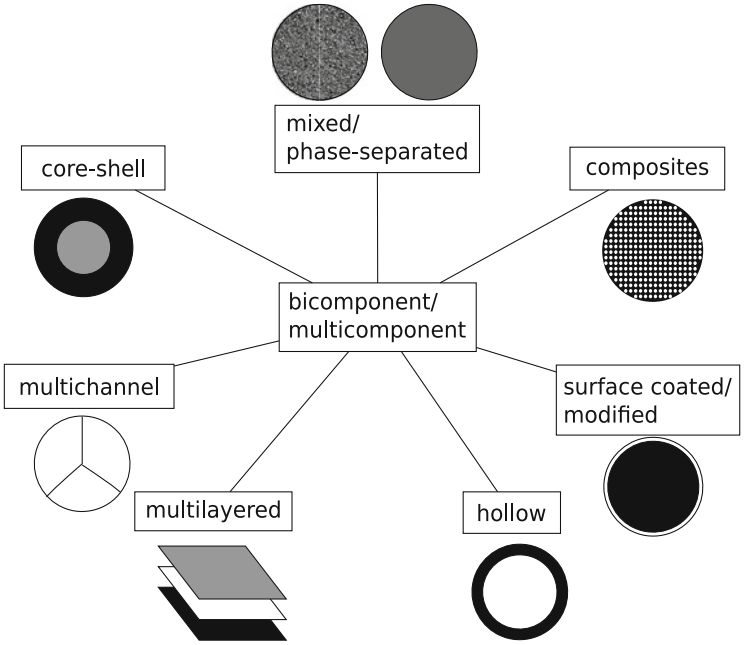

Fig. 3 Various fiber constructs types

[31], thermal interfiber bonding (accomplished near the melting temperature of the electrospun polymer and impregnated with a hydrogel that maintains the structure of the scaffold against shrinkage) in order to improve biomechanical properties

[32] or continuous alignment of electrospun fiber yarn obtained by self-bundling electrospinning and further treated by drawing and annealing to improve tensile strength [33] are just some of the available post-processing techniques.

2.2 Release Control of Drug Loaded Fibers

Fibers can be easily loaded with drug in a similar fashion as multicomponent fibers (Sect. 2.1), the drug being an extra component. By blend electrospinnning, the drug or drug vehicle (such as microspheres [9], nanoparticles [10, 11]) is mixed or phase-separated with the polymer phase and by coaxial electrospinnning, the drug is contained either in the core or in the shell. The advantage of encapsulating the drug in the core or in a vehicle is that usually burst release is minimized/avoided since the drug has longer diffusional paths [11] and the protection of active agents (such as proteins) that are sensitive to organic solvents can be achieved. Moreover, it does not require good interaction between the polymer and drug, but it must show sufficient interfacial compatibility in order to prevent delamination [34]. In contrast, for the cases of drugs loaded by blend electrospinning, poor interaction between the drug and polymer affects the drug distribution in the polymer matrix and consequently the release behavior [35, 36]. Incorporation of bioactive agents that are usually water soluble and can not be dissolved in the same solvent as the polymer (usually organic solvents) can be performed by emulsion electrospining [35, 37].

Various post-treatment modalities exist in order to further control the fiber drug release. These can be grouped in two main categories: physical and chemical. The first category includes functionalization of electrospun fibers with biomolecules using coating [16], subcritical carbon dioxide impregnation of electrospun fibers with which it is possible to load drugs and obtain more sustained release profiles in comparison to loading through soaking in drug solution [12]. The second category consists of coating electrospun fiber by chemical vapour deposition in order to prolong the release and avoid burst effect [23], molecular imprinting of fibers (either by loading the template molecule [13] or by loading molecularly imprinted particles [14] inside the fibers during electrospinning) that can selectively rebind the target molecule (biological receptor molecule) and produce targeted drug delivery.

Drug delivery systems are intended to deliver well controlled amounts of drug between the minimum effective level and the toxic level during a predetermined time interval [7]. Control of burst effect is essential either to avoid toxicity or to ensure immediate action at the targeted location (as in the case of antibiotics [38]). These are the reasons why the factors that affect the release rate should be considered when designing a new fiber drug delivery system:

- Fiber construct geometry (fiber mats or multilayers) and thickness: the drug deposited in single layers is released faster than from multilayers either because

the drug layers are intercalated with non-drug layers that function as barrier to drug release [39] or because the inner layers are not equally exposed to the release medium [40]

- Fiber diameter and porosity: a thinner or more porous fiber implies a bigger surface and consequently accelerates the release [41]. However, thicker, but more porous fibers release drug faster than thinner, less porous fibers [42]
- Fiber composition: the choice of a degradable polymer will allow release control through a hydrolytic [40] or enzymatic mechanism [36]. Besides, blending various components leads to modulating release capacity [42] either by improving fiber wetting properties (using hydrophilic polymers [43, 44]) or aiding incorporation of drug. In this case, it is possible to avoid burst effect by blending polymers with amphiphilic copolymers which can be compatible with both the drug and the initial incompatible polymer [38]
- Fiber crystallinity: initial polymer crystallinity influences the drug release (it blocks the release of the drug from the crystalline domains due to limited water uptake). When the release of drug from the amorphous domains or from the fiber surface is finished, no more drug is released [45]. Moreover, there is an increase in crystallinity during drug release (the drug works as a plasticizer, the polymer chains gain more mobilility and as it is leached out, they crystallize), which decreases the release of residual drug [46]
- Fiber mat swelling: water uptake by fibers or by the (macro)pores created between fibers will speed up drug release [47] as the dissolution of drug molecules is the initial step in the release process [48]
- Drug loading: higher loadings will produce faster release ([41, 46, 47, 49, 50]); on one hand, at high loadings, there is more surface segregated drug that dissolves fast and on the other hand, there is an increase in porosity during drug elution proportional to the initial amount of drug [46, 41]
- Drug state: in general, drug release was shown to be more sustained, when drug is incorporated in amorphous state [50, 51], than when drug is loaded in crystalline state [52]. Moreover, it was shown that, even when the drug is in amorphous state, the drug release was faster from the solid solution than from the amorphous dispersion [53]
- Drug molecular weight: drugs with smaller volumes will be released faster since they diffuse faster through the aqueous pores created by the water uptake in the fiber [42, 54]
- Drug solubility in the release medium: usually, the higher drug solubility, the faster the release [42]
- Drug–polymer–solvent interaction: solubility and compatibility of drugs with the polymer and/or the electrospinning solvent is essential since it ensures proper drug incorporation inside the fibers and not on the fiber surface [35, 47, 36]. Phase separation between the drug and polymer will produce amorphous or crystalline drug at the fiber surface leading to faster release [55]. Moreover, the interaction between drug and the polymer can block the crystallization of the drug in the fibers, if so desired [53] and can even determine sustained release of

drugs that are present in crystalline state because of hydrogen bonding to the polymer [54]

However, in order to predict the outcome of drug release from fibers, it is important to consider the interaction among the various factors in such a complex system. We have already discussed how the drug state controls drug release. However, sometimes high drug loadings are needed for long term applications. Usually, at high loads, the drug will crystallize and/or phase-separate from the polymer and form conglomerates that will produce a heterogeneous distribution of the drug inside the fibers [35, 56] or deposition on the fiber surface [55]. Thus, in long term release applications where high amounts of loaded drug are required, a compromise must be found between loading and release rate that change in contrary directions [57]. Careful consideration should also be paid when selecting best pair of polymer and drug, although some applications require material properties that may not match in terms of compatibility the drugs used in the treatment of the targeted diseases.

2.3 Release Modeling

As summarized in Table 1, a multitude of drug/biomolecules loaded fibers have already been produced. They have been produced either from polymers (synthetic and natural) or inorganic compounds. Most of the release mechanisms were attributed to drug diffusion (as it is the case for most non-biodegradable, non-erodible polymers), solvent diffusion (as in the case of natural polymers that are usually hydrophilic [58]), polymer erosion (as in the case of erodible (bio)polymers [53, 54]), polymer degradation (as for hydrolytic or enzymatic degradable polymers) or external triggers (like a magnetic field). In the release system governed by drug diffusion, one has to consider two cases, one in which the diffusion takes place through the bulk of polymer (bulk diffusion) or through a membrane/layer (barrier diffusion, similar to the reservoir devices as in the case of core–shell fibers, composite fibers or multilayered constructs). There are cases in which several mass transport mechanisms superpose. However, in most cases, there is only one that is the "rate-limiting" step. For example, in the case in which diffusion is coupled with chemical reaction (in most cases, hydrolysis), if diffusion is faster than the chemical reaction, then mass transfer is controlled by the polymer degradation [59] and when diffusion is not much faster than reaction, then diffusion and degradation superpose [40]. In some systems, the release process is composed of sequential stages, with each stage being controlled by a different phenomenon. For example, in the first stage you can have the drug release controlled by the polymer erosion and subsequent diffusion, followed by polymer degradation control stage [60].

Related to core–shell fibers, we can consider two controlling phenomena: diffusion through the polymer shell (barrier diffusion) or partition of the drug from

Table 1 Literature examples

Polymer	Drug [loading (%, by weight)]	Construct	Rel. mechanism	Rel. kinetics	Studied rel. time	Refs.
PCL	Heparin (0.05, 0.5)	Unicomponent	Bulk diffusion	$t^{0.5}$	14 days	[49]
PCL	Metronidazole benzoate (5, 10, 15)	Unicomponent	Bulk diffusion	$\sim t^{0.5}$	20 days	[50]
PCL, PLA	Tetracycline (2), chlorotetracycline hydrochloride (2), amphotericin B (1)	Unicomponent, bicomponent	Bulk diffusion	na	1.5 h	[42]
PCL-co-EEP	NGF (0.0123), FITC-BSA (4.08)	Unicomponent	Bulk diffusion	$\sim t^{0.5}$	90 days	[35]
PEG-b-PLLA	BCNU (5, 10, 20)	Unicomponent	Bulk diffusion	$t^{0}.5$	70 h	[46]
PLGA	Paclitaxel (9.1)	Unicomponent	Bulk diffusion, hydrolytic degradation	t^{0}	80 days	[40]
PDLLA	Tetracycline (2), chlorotetracycline (2)	Unicomponent	Bulk diffusion, polymer swelling	$\sim t^{0.5}$	50 h	[47]
PDLLA	Paracetanol (2, 5, 8)	Unicomponent	Bulk diffusion, hydrolytic degradation	na	350 h	[41]
PLLA	Paclitaxel (15), doxorubicin hydrochloride (1.6), doxorubicin base (1.6)	Unicomponent	Bulk diffusion, enzymatic degradation	t^{0}	4 h	[36]
PLLA	Lidocaine hydrochloride (40, 80), mupirocin (3.75, 7.5)	Unicomponent	Bulk diffusion	na	72 h	[52]
PLLA	Rifampin (15, 25, 50), paclitaxel (na), doxorubicin hydrochloride (na)	Unicomponent, bicomponent	Enzymatic degradation	t^{0}	7 h	[64]
PLA-POE-PLA	Paracetamol (2)	Unicomponent	Bulk diffusion, pH responsive degradation	na	144 h	[65]
PLGA	Paclitaxel (9.2, 9.9)	Unicomponent	Bulk diffusion, hydrolytic degradation	$t^{0.5}$	60 days	[51]

(continued)

Table 1 (continued)

Polymer	Drug [loading (%, by weight)]	Construct	Rel. mechanism	Rel. kinetics	Studied rel. time	Refs.
PLGA, PEG-b-PLA	Cefoxitin sodium (1, 5)	Unicomponent	Bulk diffusion	na	150 h	[38]
PU	Itraconazole (10, 40), ketanserin (10)	Unicomponent	Biphasic diffusion	$t^{0.5}$	20 h	[55]
PVA	Sodium salicylate (10, 20), diclofenac sodium (10, 20), naproxen (10, 20), indomethacin (10, 20)	Unicomponent	Bulk diffusion, polymer erosion		24 h	[54]
PVP	Ibuprofen (20, 33.3)	Unicomponent	Polymer erosion	na	180 s	[53]
CA	Vitamin A (0.5), vitamin E (5)	Unicomponent	Bulk diffusion	$t^{0.5}$	24 h	[54]
CA	Curcumin (5, 10, 15, 20)	Unicomponent	Bulk diffusion	$t^{0.5}$	50 h	[67]
HPMC	Itraconazole (20, 40)	Unicomponent	Bulk diffusion	na	3.4 h	[68]
gelatin	*Centella asiatica* extract (5, 10, 20, 30)	Unicomponent	Bulk diffusion, polymer erosion	na	7 days	[58]
PDLLA/HA	RhBMP-2 (0.00015-0.00016)	Bicomponent	Bulk diffusion, hydrolytic degradation	na	60 days	[43]
PCL, Res	Ketoprofen ($\sim$5)	Bicomponent	Bulk diffusion	na	360 h	[69]
PLLA/PEI, PLLA/PLL	Cytochrome C (na)	Bicomponent	Diffusion	na	29 days	[44]
PLA, PEVA	Tetracycline hydrochloride (5, 25)	Bicomponent	Bulk diffusion	na	120 h	[45]
PCL, PEO, PLLA, PLGA	Lysozyme (na)	Bicomponent	Bulk diffusion, polymer erosion	na	300 h	[60]
PCL, PEG	BSA (1.96, 3.12, 5.56), lysozyme (na)	Core–shell	Barrier diffusion	na	27 days	[70]
PCL	Resveratrol (4, 6, 8, 10), gentamycin sulfate (10, 20, 30, 40)	Core–shell	Enzymatic degradation	$\sim t^0$	180 h	[56]

(continued)

Table 1 (continued)

Polymer	Drug [loading (%, by weight)]	Construct	Rel. mechanism	Rel. kinetics	Studied rel. time	Refs.
PLA-co-CL	TPPS (1), ChroB (1)	Multilayers	Bulk diffusion, barrier diffusion	sigmoidal	7 h	[39]
PCL, LDH	Diclofenac sodium (0.49, 1.47, 2.45, 4.9)	Composite	Ionic exchange	$t^{0.5}$	250 days	[71]
PLLA, Ca-alginate	BSA microsphere (na)	Composite	Barrier diffusion	na	120 h	[9]
PLGA, PLA-PEG-PLA	DNA nanoparticle (na)	Composite	Hydrolytic degradation, solvent diffusion	na	7 days	[10]
PLGA/PEDOT	Dexamethasone (na)	Hollow fibers	External trigger	pulsed	1,300 h	[72]

PDLLA poly(D,L-lactide), *PEG* poly(ethylene glycol), *PLLA* poly(L-lactic acid), *PDLLA-co-GA* poly-(D,L-lactide-co-glycolide), *PLA-POE-PLA* poly(D,L-lactic acid) poly(orthoester) triblock copolymer, *PLA-PEG-PLA* poly(lactic acid) poly(ethylene glycol) triblock copolymer, *PEG-b-PLLA* pol(etylene glycol) poly(L-lactic acid) diblock copolymer, *HPMC* hydroxypropylmethylcellulose, *PVP* poly(vinylpyrrolidone), *PCL* poly(ε-caprolactone), *Res* Tecophilic Resin HP-60D-60, *PEI* Poly(ethylene imine), *PLL* Poly(L-lysin), *PEVA* poly(ethylene-co-vinyl acetate), *PLA-co-CL* poly(L-lactide-co-ε-caprolactone), *PEO* poly(ethylene oxide), *PEDOT* poly(3,4-ethylenedioxythiophene), *PU* polyurethane, *HA* hydroxylapatite, *LDH* Mg–Al hydrotalcite clay, *SPI* soy protein isolate, *CA* cellulose acetate, *BSA* bovine serum albumin, *FITC-BSA* fluorescein isothiocyanate conjugate bovine, *NGF* recombinant human β-nerve growth factor, *BCNU* 1,3-bis(2-chloroethyl)-1-nitrosourea, *RhBMP-2* recombinant human bone morphogenetic protein-2, *TPPS* 5,10,15,20-tetraphenyl-21H,23H-porphinetetrasulfonic acid disulfuric acid, *ChroB* 2,6-dichloro-4-hydroxy-3,3-dimethylfuchsone-5,5-dicarboxylic acid disodium salt), *AITC* allyl isothiocyanate

the core to the shell. The diffusion through the shell polymer should not be too slow, otherwise this diffusion will be rate-limiting step. In this instance, the system behaves as monolith fibers and not core–shell fibers (reservoir system). Shell porosity must also be carefully controlled since the drug from the core will be released through water-filled channels rather than through the barrier/shell polymer [34]. Composite fibers that contain drug vehicles such as microspheres and nanoparticles (see Sect. 2.2) are also a type of reservoir system (double barrier system) in which the drug molecules have to diffuse through longer pathways: the polymer comprising the vehicle and the "shell" polymer [11].

Drug diffusion (more precisely solid state diffusion) was mentioned earlier as one of the most common mechanisms of drug release. There are models that consider diffusion of solutes in polymers insignificant in comparison with diffusion in water-filled spaces in between polymer chains, so they assume that water uptake and subsequent solubilization of the drug is an important step in the release process and it is the solvated molecule that is actually diffusing [61]. This is the assumption behind biphasic diffusion that includes an initial diffusion phase through the polymer (either amorphous or semi-crystalline) and a second diffusion phase through water-filled pores formed in the fiber due to polymer swelling/chain rearrangement or polymer recrystallization [55, 62].

The power law equation, which was developed considering that the main mechanism for drug release is drug diffusion through the polymer or solvent diffusion inside the polymer that produces polymer relaxation/chain rearrangement (Eq. 1) is the most widely used equation in works concerning drug release:

$$\frac{m_t}{m_{\text{tot}}} = a_0 + kt^n \tag{1}$$

where m_t/m_{tot} is the fractional release of the drug at time t,a_0 is a constant, representing the percentage of burst release, k is the kinetic constant and n is the release exponent, indicating the mechanism of drug release (which can either be Fickian drug diffusion or polymer relaxation or an intermediate case combining the two [63]).

Other models consider different phenomena that control the release such as desorption due to the fact that under the assumption of diffusion control, 100% release of the drug is expected, but this was not verified experimentally. In the desorption model, the release is not controlled by diffusion, but by the desorption of the drug from fiber pores or from the fiber surface. Thus, only the drug on the fiber and pore surfaces can be released, whereas the drug from the bulk can only be released when the polymer starts to degrade. These assumptions are similar to the theory of mobile agent, that can be released by diffusion and the immobilized agent, that can be released through degradation [59].

The Eq. 2 is based on a pore model, in which the effective drug diffusion coefficient, D_{eff} is considered and not the actual diffusion coefficient in water, D (with $D_{\text{eff}}/D \ll 1$) because desorption from the pore is the rate limiting step and not drug diffusion in water, which is relatively fast.

$$\frac{m_t}{m_{tot}} = \alpha\left[1 - \exp\left(-\frac{\pi^2}{8}\frac{t}{\tau_r}\right)\right] \quad (2)$$

where the porosity factor $\alpha = m_{s0}/(m_{s0} + m_{b0}) < 1$, with m_{s0} and m_{b0} being the initial amount of drug at the fiber surface and the initial amount of drug in the fiber bulk, respectively; m_t is the drug amount released at time t, while the total initial amount of drug in the fiber is $m_{tot} = m_{s0} + m_{b0}$ and τ_r is the characteristic time of the release process [73].

Various release kinetics exist and the most desirable one is the zero-order kinetics in which the drug is released at constant rate, independent of concentration gradient (see Fig. 4). Usually, zero-order kinetics is achieved for reservoir systems such as core–shell fibers or composite fibers (see Table 1) in which the drug is properly encapsulated in the core of the fiber or in other vehicles (micro/nanoparticles). Burst stage in this kind of system is diminished (or non-existent) because there is no drug deposited on the surface of the fibers. As the controlling release phenomena is drug partition from one phase to another and not diffusion, there is no decrease in release rate over time as expected in a diffusion-controlled system (the release rate depends on the concentration gradient and on the length of diffusion path; as release proceeds, the concentration gradient decreases and the diffusion length increases and both contribute to slowing down the release rate).

Other strategies to attain zero-order release include polymer degradation controlled release (either accompanied by erosion or not) because then drug is released due to polymer chain cleavage [36, 40]. The drug is released either because the diffusion paths are shortened as degradation takes place (surface degradation) or because porosity is increased due to the leaching of degradation products (bulk degradation) [7]. Another strategy to obtain constant release rate is the use of multilayered constructs [39], in which sequential electrospinning is used to obtain drug loaded layers surrounded by barrier layers.

Burst effect can be determined by fiber porosity [34], poor drug solublity in electrospinning solvent [47], poor drug solubility in polymer [36], high drug solubility in release medium [42], heterogeneous drug distribution [35] or surface segregated drug [45]. Most of the times, the selection of the polymer and of the drug depends on the properties of the fiber mat and the targeted disease. Thus, the burst

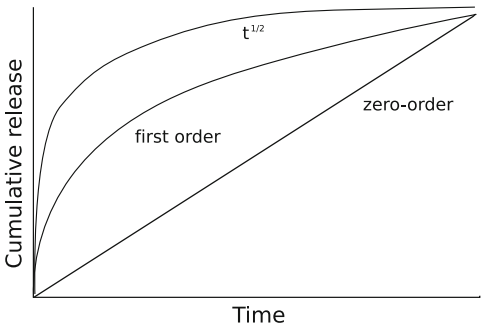

Fig. 4 Types of release kinetics

stage can only be controlled in unicomponent/monolith fibers by manipulating the process parameters and not by the material choice. Ensuring a homogeneous drug distribution [49] (usually by encapsulating drug in amorphous state [50, 46]), low drug loadings [50], or coating the drug loaded fibers [16] are some simple techniques to diminish burst if so desired.

3 Results

In this chapter we are presenting some results concerning release control in bicomponent fibers composed of poly(ε-caprolactone), PCL and Lutrol F127 (Lu, poly(oxyethylene-b-oxypropylene-b-oxyethylene)), both semi-crystalline (co)polymers. The properties of the bicomponent fibers were studied in order to determine the effect of electrospinning processing on crystallinity, hydrophilicity and degradation. As both polymers are semi-crystalline, we could test the effect of such organization on the loading and release of drugs. Acetazolamide and timolol maleate were loaded in the fibers in different concentrations (below and above the drug solubility limit in polymers) in order to determine the effect of drug solubility in polymer, drug state, drug loading and fiber composition on fiber morphology, drug distribution and release kinetics. A diffusion model and a desorption model (see Sect. 2.3) were fit to the release data in order to determine the release mechanism.

3.1 Fiber Mat Degree of Crystallinity, Drug Solubilitity in Polymer and Drug State

Solid-state drug polymer solubility and miscibility were shown to influence the drug encapsulation and correlate to drug release [74]. Timolol maleate (experimental water solubility =2.74 mg/ml [75]) and acetazolamide (experimental water solubility =0.98 mg/ml [76]) were chosen because of different hydrophilic/hydrophobic character that would allow us to understand how the interactions between the drug and polymers contribute to drug release. The drug solubility is expected to influence the loading and the state of the drug in the fibers as a higher solubility ensures higher loading of drugs in amorphous state. Thus, fibers with low and high drug loadings were prepared corresponding to drug percentages below and above the drug solubility limit, respectively. As a measure of drug–polymer interaction [77], the drug solubility in polymers was determined by differential scanning calorimetry (DSC) method and the obtained results are presented in Table 2. Acetazolamide had higher solubility than timolol maleate in all fiber compositions probably because of enhanced interaction with the hydroxyl/carboxyl groups of the polymers. Furthermore, a tendency of increase in solubility

Table 2 Degree of crystallinity and drug solubility in polymer(*, no processing)

Sample	Loading (%, w/w)	$T_m(^\circ C)$	Rel. degree of crystallinity (%)	Drug solubility (%)
Acetazolamide	–	271.14		–
Timolol maleate	–	205.60		–
PCL	0	60.06 (0.29)	51.37 (0.84)	–
25/75 Lu/PCL	0	51.65 (1.37), 59.38 (0.20)	50.97 (2.03)	–
50/50 Lu/PCL	0	52.36 (0.67), 59.50 (0.17)	54.83 (1.90)	–
Lu*	0	55.57 (0.64)	68.51 (2.12)	–
PCL, timolol	0.88 (0.01)	60.28	48.22 (0.86)	4.48 (1.11)
25/75 Lu/PCL, timolol	0.86 (0.02)	56.22	54.71	5.14 (0.94)
50/50 Lu/PCL, timolol	0.88 (0.04)	55.48 (0.21), 61.28 (0.26)	59.89 (0.24)	6.97 (1.86)
PCL, acetazolamide	1.24 (0.28)	59.99 (0.15)	49.76 (2.87)	16.53 (2.1)
25/75 Lu/PCL, acetazolamide	1.55 (0.60)	57.64 (2.98), 58.15 (2.93)	55.04 (0.29)	15.94 (4.81)
50/50 Lu/PCL, acetazolamide	1.16 (0.20)	54.19 (0.08), 60.20 (0.00)	58.94 (0.06)	14.81 (0.8)
PCL, timolol	7.60 (0.32)	60.52	45.96	–
25/75 Lu/PCL, timolol	6.99 (0.19)	54.36 (0.61), 60.94 (0.21)	52.82 (4.27)	–
25/75 Lu/PCL, acetazolamide	12.67 (0.35)	53.69 (0.87), 60.93 (0.22)	48.15 (4.03)	–

was noticed when PCL ratio was increased. An opposite trend was observed for timolol maleate when an increase in solubility was obtained with decrease in PCL content. We will discuss in Sect. 3.4 how the solubility affects the drug release.

The polymer degree of crystallinity is known to play an important role in determining water uptake and drug release. Drug release is faster from amorphous than from crystalline regions for semi-crystalline polymers because the lamellae behave as barriers to the diffusion of water and drug [45, 79]. In the case of amorphous polymers, the drug can act as a plasticizer and as it is leached out, the mobile polymer chains rearrange themselves and crystallize [46]. The crystallized matrix becomes microporous [78] and the subsequent drug diffusion takes place through water-filled pores. The polymers used in this work are semi-crystalline and the obtained fibers are expected to be semi-crystalline too. DSC analysis confirmed this hypothesis showing a single or two melting peaks corresponding to the melting of either PCL or Lu. The relative degree of crystallinity of drug loaded fibers is presented in Table 2, where it can be seen that the fibers showed similar degrees of crystallinity regardless the type of loaded drug. The drug appeared to be in amorphous state in fibers with low drug loadings as proven by the absence of drug melting peak (images not shown). In fibers with high loadings, part of the drug was in crystalline form as confirmed by morphological analysis (Sect. 3.2), while the DSC scans of these sample were not conclusive because the peak

corresponding to drug melting was masked by fiber degradation process (that starts at around 250°C).

3.2 Morphological Analysis and Drug Mapping

Morphological differences between samples loaded with the two drugs above or below the solubility limit were assessed by scanning electron microscopy (Fig. 5). In Fig. 5a and b surface images of fibers that contain acetazolamide above solubility limit are shown. As the loaded mass of drug was above the solubility limit in the polymer, the drug was expected to be in crystalline form as confirmed by the images where drug crystals were visible outside or inside the fibers. On the other hand, no crystals were observed in the fibers that contain drug in low loadings (Fig. 5c) suggesting that the drug was in amorphous state in the fibers in agreement with DSC analysis results (Sect. 3.1).

Electron probe microanalysis was performed in order to assess the drug distribution inside the fiber mats. The surface mapping of timolol loaded fibers (Fig. 6b, c) showed relatively homogeneous drug distribution regardless of composition, while the surface mapping of acetazolamide fibers (Fig. 6a) indicate the presence of drug conglomerates probably due to higher loading. When the drug is above the solubility limit, it will phase-separate and crystallize [56, 35].

3.3 Water Contact Angle, Swelling Capacity and Mass Loss

Water contact angle is determined by both chemical composition and surface morphology [80]. The surface roughness of the fibrous mat results in air entrapment between fibers, and as such the fiber mats usually present higher contact angle than films with the same composition [81]. Swelling takes place in two different regions of porosity (Fig. 7): water diffuses first in the pores between fibers and later in the fibers themselves.

In a fiber mat there are regions in between the fibers that can be occupied by water molecules, while in films or compacts these regions have significantly smaller surface. PCL fibers were highly hydrophobic (a water contact angle of 123.18 (0.98)), while the bicomponent fibers were highly hydrophilic (25/75 Lu/PCL had a water contact angle of 18.28 (4.07), while 50/50 Lu/PCL had one of 16.25 (2.16)). These results were surprising since in a previous work films with the same compositions presented contact angles in the range 50 to 62° [82]. In bicomponent fibers, the trapped air between the fibers and pores at the fiber surface is easily removed by the incoming water molecules because the water soluble component (Lu) is leaching out. In PCL fibers that showed an increase in water contact angle from 62 (for films) to 123, probably the hydrophobic nature of surface chemical groups (PDLLA was shown to enrich its fiber surface with

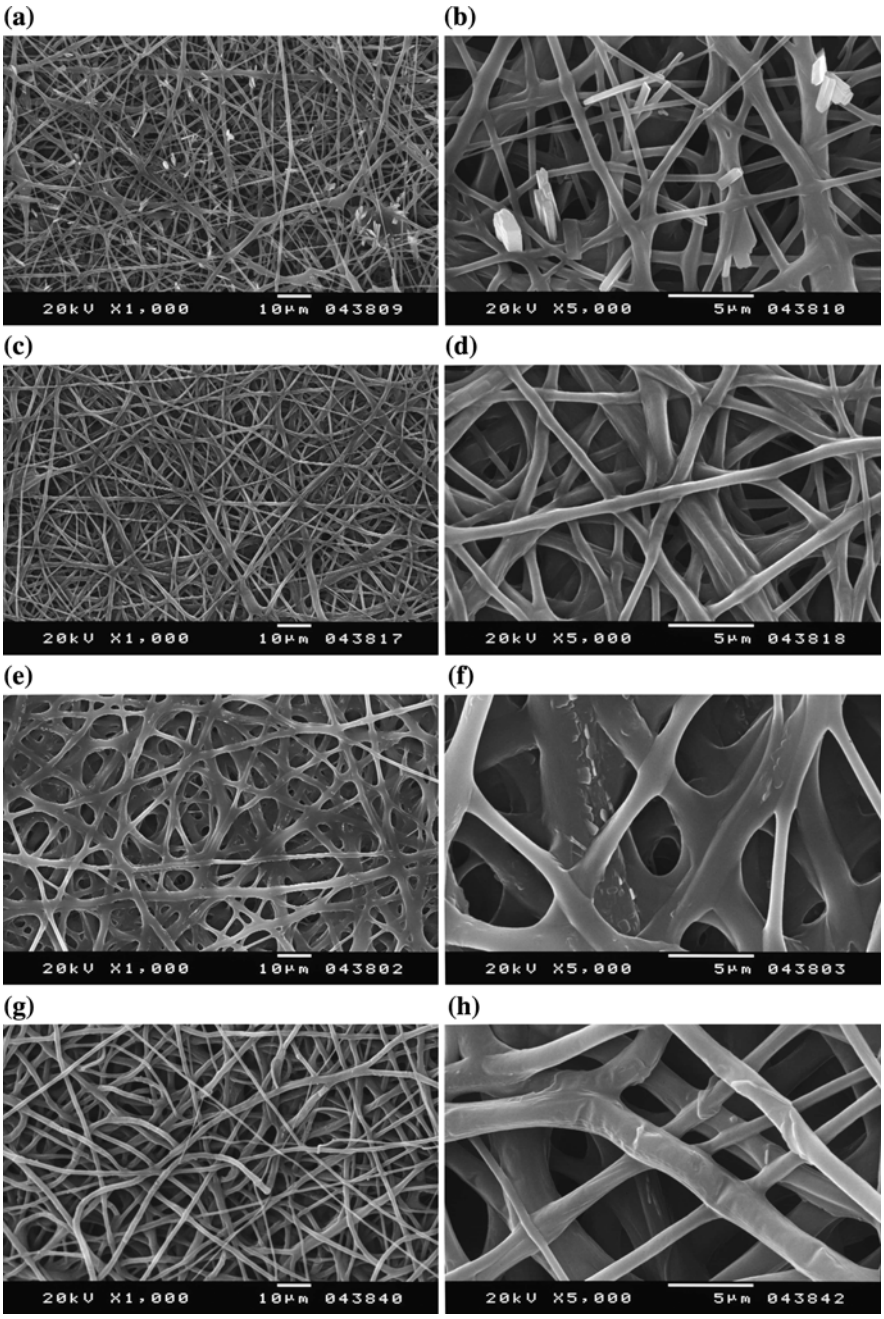

Fig. 5 SEM micrographs of various drug load fibers. **a**, **b** 25/75 Lu/PCL, acetazolamide, high load; **c**, **d** 25/75 Lu/PCL, acetazolamide, low load; **e**, **f** PCL, timolol, high load; **g**, **h** PCL, timolol, low load

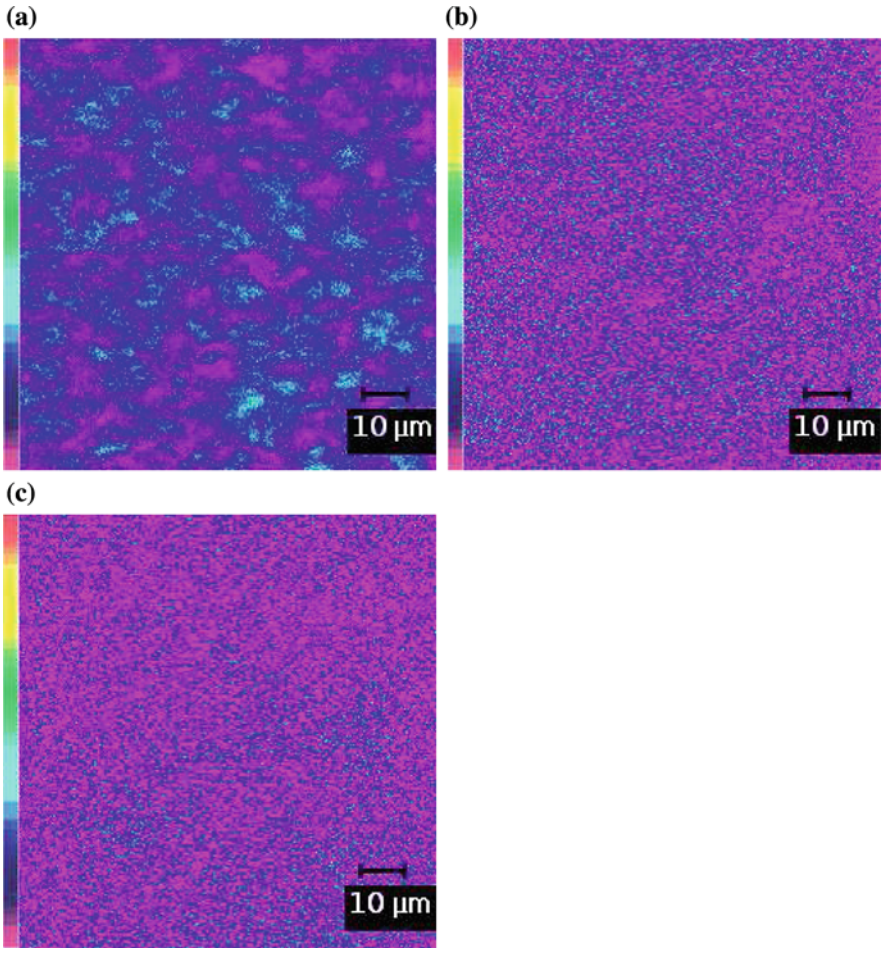

Fig. 6 Sulphur mapping of high loading fibers. **a** 25/75 Lu/PCL, acetazolamide; **b** PCL, timolol (reprinted from [57]); **c** 25/75 Lu/PCL, acetazolamide (reprinted from [57]), (the *scale bar* represents a gradient from 0% (*pink*) to 100% (*red*) sulphur content

hydrophobic groups [80]) and the trapped air create a barrier to water penetration. Consequently, PCL fibers absorbed water gradually (see Fig. 8a, while the bicomponent fibers presented a sudden increase in water content during the first day (79.0% for 50/50 Lu/PCL and 68.5% for 25/75 Lu/PCL), followed by a constant value thereafter as Lu content in the fiber was diminished due to dissolution.

The mass loss plot (Fig. 8b) showed an initial increase in mass loss for bicomponent fibers (42.5% for 50/50 Lu/PCL and 16.6% for 25/75 Lu/PCL), while PCL fibers presented insignificant mass loss (0.45%). Mass loss of PCL is detectable only after the molecular weight reaches a value of 10,000 g/mol [83]

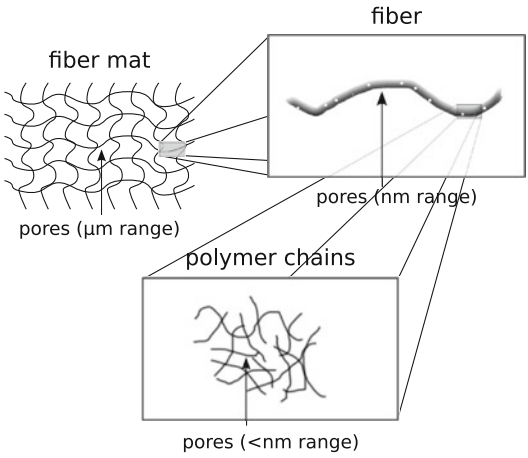

Fig. 7 Regions of porosity in a fiber mat

and thus the initial high mass loss of the bicomponent fibers can only be attributed to the dissolution of Lu as the sample with higher Lu content had the highest mass loss.

The morphology of aged fibers (immersed in PBS during 3 days) was also investigated in order to determine the change in fiber structure. In Fig. 9a, it can be noticed the smooth surface of the fibers, while in Fig. 9e pores were observed that were formed due to the dissolution and leaching of Lu. A different appearance was shown by 25/75 Lu/PCL fiber mat (Fig. 9f), where the fibers appeared more wrinkled in comparison with the initial ones and no pores were visible, probably because of lower Lu content.

3.4 Drug Release

We previously showed how the fiber morphology and drug deposition were affected by the drug state in the fibers: when drug was in amorphous state, it was incorporated inside the fibers, while the drug present in amounts above the solubility limit crystallized inside and on the fiber surface (as shown in Fig. 5b). In Fig. 10a and b, the cumulative percentage of released acetazolamide and timolol maleate from fibers with low drug content is presented, while in Fig. 11a, the released drug for fibers with high loadings is shown. It was noticed that fibers with high drug loading presented burst release in contrast with low drug content fibers that showed a more sustained release. The former contained drug crystals at the fiber surface or inside the fibers that were not totally encapsulated and were instantaneously "released", suggesting that the predominant mechanism of release was drug dissolution. On the other hand, in the low loadings fibers, the drug was amorphous and dissolved in the fiber, and as such the release was governed by diffusion.

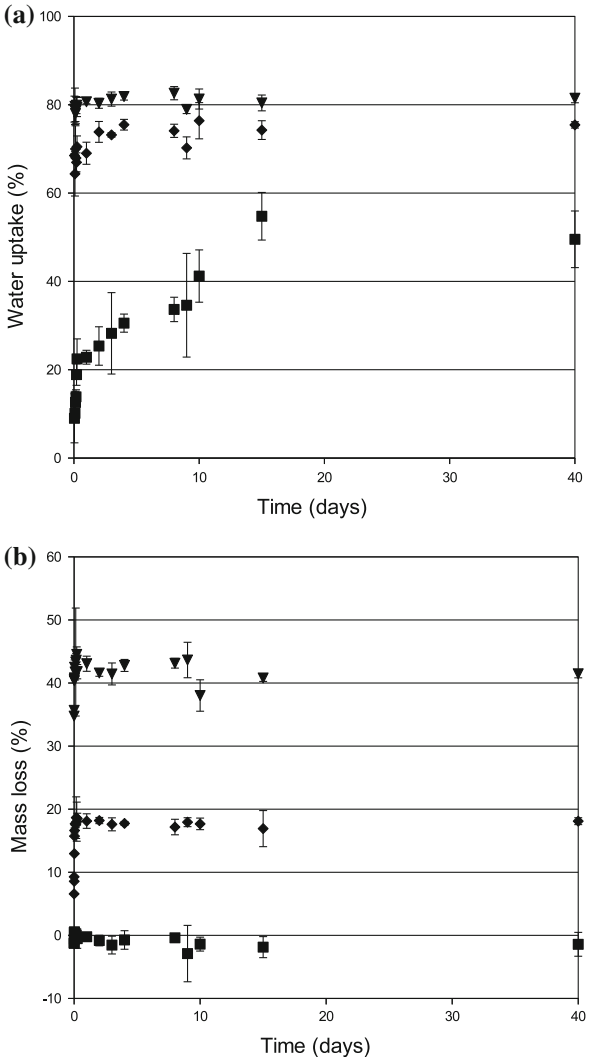

Fig. 8 Water uptake **a** and mass loss **b** of *black square* PCL, *black lozenge* 25/75 Lu/PCL, *black triangle down* 50/50 Lu/PCL

Drug solubility in polymer as well as drug solubility in solution are important as they control the partitioning of the drug from the polymer toward the elution medium [48]. For the same type of fibers, higher percentages of timolol maleate were released in comparison with acetazolamide (for example, in the case of PCL fibers, $\alpha = 45.96$ (2.92) for timolol and $\alpha = 35.14$ (1.43) for acetazolamide). This can be explained by the combined effect of lower polymer solubility and higher water solubility of timolol maleate in contrast with acetazolamide that has higher polymer solubility and lower water solubility. High drug loading and sustained release were observed for formulations using drugs with higher solubility in the

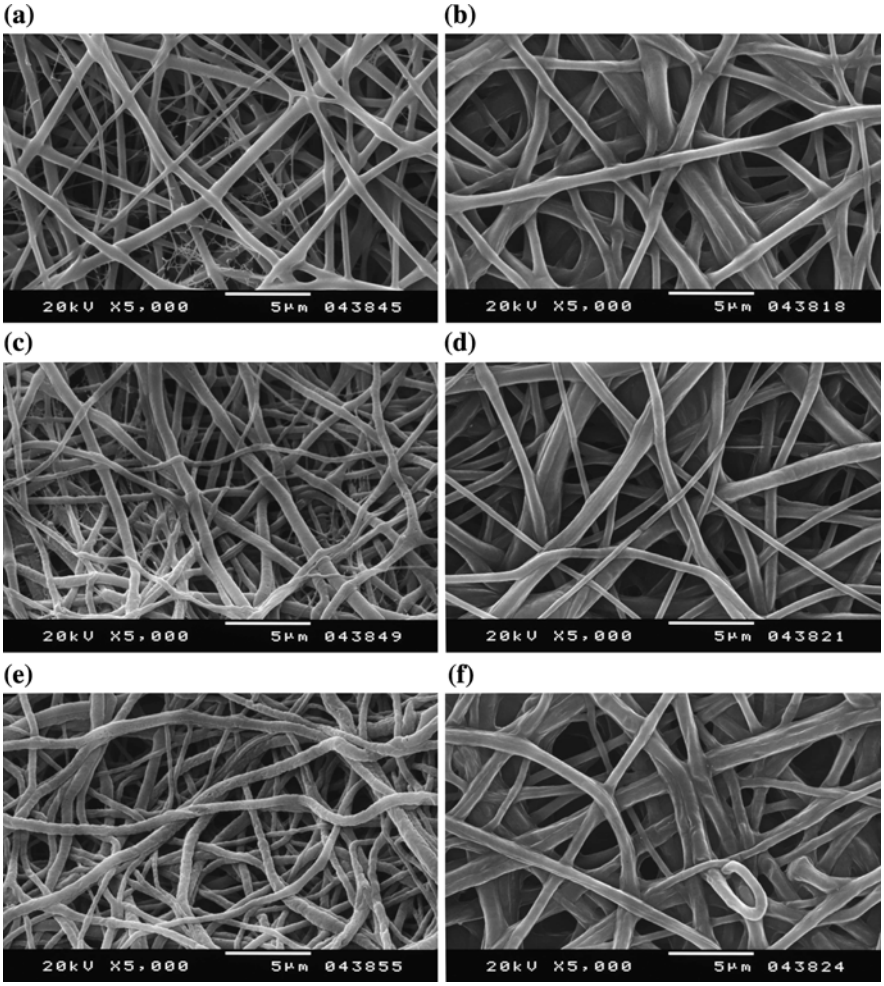

Fig. 9 SEM micrographs of **a** initial 50/50 Lu/PCL (reprinted from [57]), **b** initial 25/75 Lu/PCL (reprinted from [57]), **c** 50/50 Lu/PCL after 2 days, **d** 25/75 Lu/PCL after 2 days, **e** 50/50 Lu/PCL after 3 days (reprinted from [57]), **f** 25/75 Lu/PCL after 3 days (reprinted from [57])

polymer [74]. The compatibility between drug and polymer is indeed important as it ensures sustained release when the drug is completely encapsulated and dissolved in the fiber [45].

Fiber composition influenced the release kinetics as drug was slowly released from PCL fibers when compared to bicomponent fibers regardless of the drug type (lower α and k for PCL fiber with timolol than for 25/75 Lu/PCL and 50/70 Lu/PCL fibers with timolol, see Table 3). Certainly, as erosion was very fast (see Sect. 3.3), various pores were created and the drug was released through

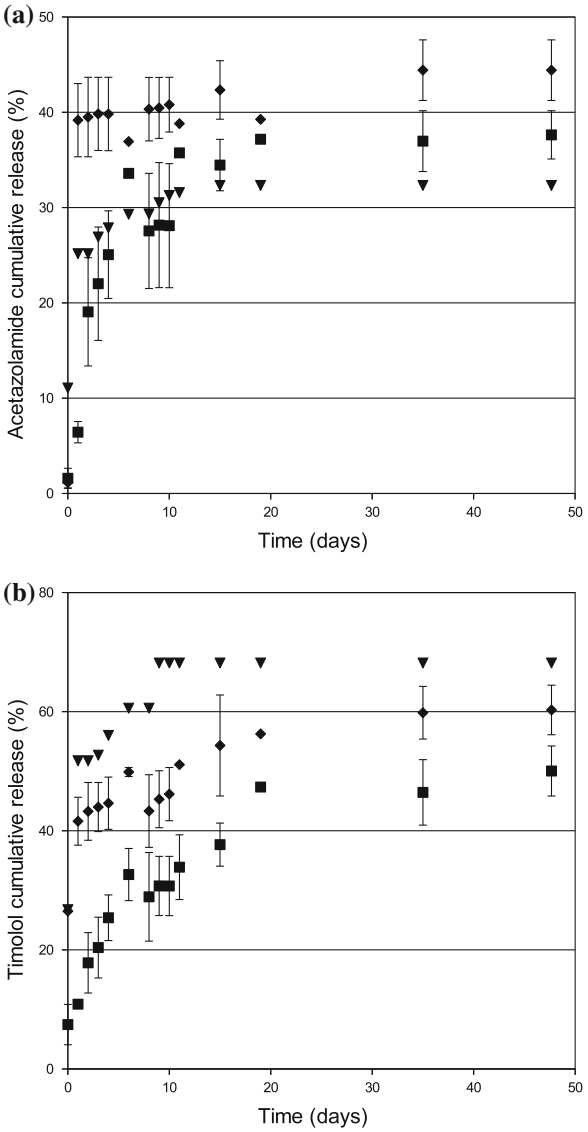

Fig. 10 Cumulative release of acetazolamide **a** and timolol maleate **b** from *filled square* PCL, *blacklozenge* 25/75 Lu/PCL, *blacktriangledown* 50/50 Lu/PCL

water-filled pores much faster than from amorphous and crystalline regions of PCL fibers that presented lower porosity [34, 55, 62].

A steady state was attained (after approximately 10 days for bicomponent fibers and after 20 days for PCL fibers) without total release of loaded drug (cumulative release percentages smaller than 100%). A fraction of the drug was desorbed from the pores surface and then it diffused through water filled pores, while another portion of the drug was trapped between crystalline areas [49, 50] (and

Table 3 Drug loading and model parameters determined by non-linear regression (*, high drug loading samples)

Sample	Desorption model			Power law			
	α	τ (days)	Adj R^2	a_0	k(day^{-n})	n	Adj R^2
PCL, timolol	45.96 (2.92)	7.94 (0.03)	0.86	5.08 (3.63)	11.51 (3.23)	0.37 (0.06)	0.92
25/75 Lu/PCL, timolol	50.41 (2.95)	0.87 (0.76)	0.00	26.93 (2.71)	12.58 (2.72)	0.26 (0.05)	0.90
50/50 Lu/PCL, timolol	64.60 (2.99)	1.10 (0.40)	0.33	26.34 (3.74)	25.97 (4.09)	0.15 (0.03)	0.90
PCL, timolol*	87.29 (0.46)	0.02 (6.51)	0.55				
25/75 Lu/PCL, timolol*	98.55 (0.27)	0.01 (8.66)	0.40				
PCL, acetazolamide	35.14 (1.43)	4.11 (0.05)	0.92	0.00 (4.76)	17.09 (4.88)	0.24 (0.06)	0.82
25/75 Lu/PCL, acetazolamide	40.59 (0.62)	0.37 (1.48)	0.96	1.16 (1.66)	36.60 (1.92)	0.03 (0.01)	0.98
50/50 Lu/PCL, acetazolamide	30.50 (1.16)	0.91 (0.46)	0.54	10.99 (1.06)	14.49 (1.18)	0.12 (0.02)	0.96
25/75 Lu/PCL, acetazolamide*	98.08 (0.24)	0.05 (0.59)	0.99				

inaccessible to water) and can only be released by polymer degradation (which is insignificant during the time scale of release experiment) [73, 59]. This was not the case for the high drug loading fibers where release was almost complete in the time frame of the experiment. At high loadings, only a small portion of drug was trapped (approximately 10% in the case of PCL, see Fig. 11a). As drug was in higher amount, additional regions of porosity were created after drug dissolution and diffusion besides those created by water uptake and polymer erosion, increasing surface area and enhancing drug release [46, 41].

The release kinetics and regression analysis results suggested a three stage release mechanism, with different steps depending on fiber composition. Dissolution of the surface deposited drug (this stage triggered burst release) was followed by drug desorption and subsequent diffusion through water-filled pores (created either due to Lu leaching or polymer recrystallization [78]), while the last stage was controlled by polymer degradation. In bicomponent fibers, the polymer erosion stage was dominant during the initial part of the drug release and it was replaced by the above-mentioned three stage mechanism as soon as Lu was leached out from the fibers.

4 Summary and Conclusion

Electrospinning is a method of obtaining fibers by stretching a polymer droplet using an electrical field. This technology has being expanding due to its simplicity and versatility. In the field of drug delivery, electrospun fibers are an excellent choice because of easy drug entrapment, high surface area, morphology control

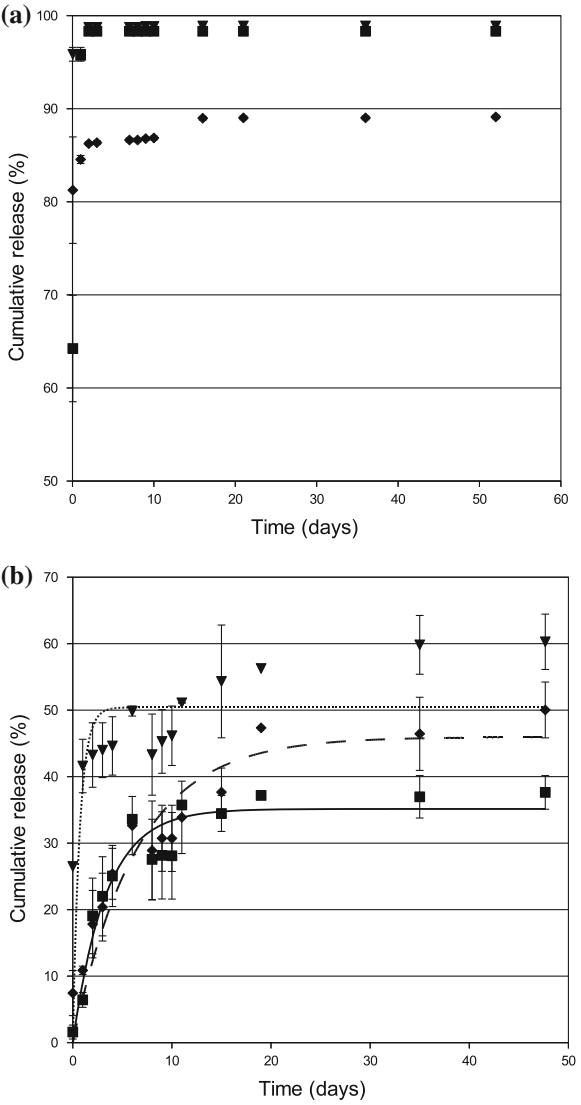

Fig. 11 Cumulative release of high loadings fibers **a** from *black square* 25/75 Lu/PCL with acetazolamide, *blacklozenge* PCL with timolol, *blacktriangledown* 25/75 Lu/PCL with timolol and cumulative release of low loadings fibers and curves corresponding to non-linear fit of Eq. 2) **b** from *blacksquare* PCL with acetazolamide, *blacklozenge* PCL with timolol, *blacktriangledown* 25/75 Lu/PCL with timolol

and biomimetic characteristics. Multicomponent fibers have attracted special attention because new properties can be obtained through the combination of different materials. There are several factors that can be manipulated in order to control the drug release from electrospun fibers. Fiber construct geometry and thickness, fiber diameter and porosity, fiber composition, fiber crystallinity, fiber swelling capacity, drug loading, drug state, drug molecular weight, drug solubility in the release medium, drug–polymer–electrospinning solvent compatibility are some of the process variables that can be optimised during method development.

We presented in this chapter how drug release control can be achieved in bicomponent fibers through the manipulation of drug solubility in polymer, drug state and loading. The restraint of burst stage is essential in order to avoid toxicity at the implantation site and to ensure long-term delivery. Fibers were obtained by electrospinning of two semi-crystalline (co)polymers, PCL and Lu, and were loaded with two drugs, acetazolamide and timolol maleate, in concentrations below and above the drug solubility limit in polymer. Morphological analysis showed that fibers with high drug loadings (above solubility limit) had drug crystals inside and outside the fibers, while fibers with low drug content (below solubility limit) had drug encapsulated in amorphous form.

The high loadings fibers showed higher extent of burst and shorter periods of release than low drug content fibers, suggesting that loading and drug encapsulation in either crystalline or amorphous form are interrelated and control the release rate, especially in the burst stage. Thus, in long term release applications where high amounts of loaded drug are desirable, a compromise must be found in order to balance the loading and release rate that seem to vary in opposite directions according to the present study. Timolol maleate was released faster than acetazolamide in the same type of fibers and at similar loadings, indicating that drug solubility in polymer influenced the partition of drug between polymer and elution medium. The fiber composition also controlled drug release, since release was slower from PCL fibers than from bicomponent fibers regardless of the drug type. By choosing the polymers making up the bicomponent fibers and their ratio, the magnitude of the various release stages can be controlled, attaining the desired release kinetics.

Acknowledgments FCT (Fundação para a Ciência e a Tecnologia) financial support is acknowledged by Mădălina V. Natu (SFRH/BD/30198/2006).

References

1. Fridrikh, S.V., Yu, J.H., Brenner, M.P., Rutledge, G.C.: Controlling the fiber diameter during electrospinning. Phys. Rev. Lett. doi:10.1103/PhysRevLett.90.144502 (2003)
2. Huang, Z.-M., Zhang, Y.-Z., Kotaki, M., Ramakrishna, S.: A review on polymer nanofibers by electrospinning and their applications in nanocomposites. Comp. Sci. Tech. (2003). doi:10.1016/S0266-3538(03)00178-7
3. Hohman, M.M., Shin, M., Rutledge, G., Brenner, M.P.: Electrospinning and electrically forced jets. I. Stability theory. Phys. Fluids. (2001). doi:10.1063/1.1383791
4. Rutledge, G.C., Fridrikh, S.V.: Formation of fibers by electrospinning. Adv. Drug Deliv. Rev. (2007). doi:10.1016/j.addr.2007.04.020
5. McClure, M.J., Sell, S.A., Ayres, C.E., Simpson, D.G., Bowlin, G.L.: Electrospinning-aligned and random polydioxanone-polycaprolactone-silk fibroin-blended scaffolds: geometry for a vascular matrix. Biomed. Mater. (2009). doi:10.1088/1748-6041/4/5/055010
6. Lopez-Rubio, A., Sanchez, E., Sanz, Y., Lagaron, J.M.: Encapsulation of living bifidobacteria in ultrathin PVOH electrospun fibers. Biomacromolecules (2009). doi:10.1021/bm900660b
7. Heller, J.: Drug delivery systems. In: Ratner, B.D., Hoffman, A.S., Schoen, F.J., Lemons, J.E. (eds.) Biomaterials Science: An Introduction to Materials in Medicine, 1st edn. Academic Press, London (1996)

8. Cussler, E.L.: Diffusion Mass Transfer in Fluid Systems. Cambridge University Press, New York (1997)
9. Qi, H., Hu, P., Xu, J., Wang, A.: Encapsulation of drug reservoirs in fibers by emulsion electrospinning: morphology characterization and preliminary release assessment. Biomacromolecules (2006). doi:10.1021/bm060264z
10. Liang, D., Luu, Y.K., Kim, K., Hsiao, B.S., Hadjiargyrou, M., Chu B.: In vitro non-viral gene delivery with nanofibrous scaffolds. Nucl Acids Res. (2005). doi:10.1093/nar/gni171
11. Wang, Y., Wang, B., Qiao, W., Yin T.: A novel controlled release drug delivery system for multiple drugs based on electrospun nanofibers containing nanoparticles. J. Pharm. Sci. (2010). doi:10.1002/jps.22189
12. Ayodeji, O., Graham, E., Kniss, D., Lannutti, J., Tomasko, D.: Carbon dioxide impregnation of electrospun polycaprolactone fibers. J Sup Fluids. (2007). doi:10.1016/j.supu.2006.09.011
13. Chronakis, I.S., Milosevic, B., Frenot, A., Ye, L.: Generation of molecular recognition sites in electrospun polymer nanofibers via molecular imprinting. Macromolecules (2006). doi: 10.1021/ma052091w
14. Chronakis, I.S., Jakob, A., Hagstrom, B., Ye, L: Encapsulation and selective recognition of molecularly imprinted theophylline and 17β-estradiol nanoparticles within electrospun polymer nanofibers. Langmuir (2006). doi:10.1021/la0613880
15. Ma, Z., Kotaki, M., Ramakrishna, S.: Surface modified nonwoven polysulphone (PSU) fiber mesh by electrospinning: a novel affinity membrane. J. Membr. Sci. (2006). doi: 10.1016/j.memsci.2005.07.038
16. Casper, C.L., Yang, W., Farach-Carson, M.C., Rabolt, J.F.: Coating electrospun collagen and gelatin fibers with Perlecan domain I for increased growth factor binding. Biomacromolecules (2007). doi:10.1021/bm061003s
17. Casper, C.L., Yamaguchi, N., Kiick, K.L., Rabolt, J.F.: Functionalizing electrospun fibers with biologically relevant macromolecules. Biomacromolecules (2005). doi: 10.1021/bm050007e
18. Skotak, M., Leonov, A.P., Larsen, G., Noriega, S., Subramanian, A.: Biocompatible and biodegradable ultrafine fibrillar scaffold materials for tissue engineering by facile grafting of L-lactide onto chitosan. Biomacromolecules (2008). doi:10.1021/bm800158c
19. Sawicka, K.M., Gouma, P.: Electrospun composite nanofibers for functional applications. J. Nanopart. Res. (2006). doi:10.1007/s11051-005-9026-9
20. Liang, D., Hsiao, B.S., Chu, B.: Functional electrospun nanofibrous scaffolds for biomedical applications. Adv. Drug Deliv .Rev. (2007). doi:10.1016/j.addr.2007.04.021
21. Lee, J.A., Krogman, K.C., Ma, M., Hill, R.M., Hammond, P.T., Rutledge, G.C.: Highly reactive multilayer-assembled TiO_2 coating on electrospun polymer nanofibers. Adv. Mater. (2009). doi:10.1002/adma.200802458
22. Lee, S.J., Yoo, J.J., Lim, G.J., Atala, A., Stitzel, J.: In vitro evaluation of electrospun nanofiber scaffolds for vascular graft application. J. Biomed. Mater. Res A. (2007). doi: 10.1002/jbm.a.31287
23. Zeng, J., Aigner, A., Czubayko, F., Kissel, T., Wendorff, J.H., Greiner, A: Poly(vinyl alcohol) nanofibers by electrospinning as a protein delivery system and the retardation of enzyme release by additional polymer coatings. Biomacromolecules (2005). doi:10.1021/bm0492576
24. Bogntizki, M., Frese, T., Steinhart, M., Greiner, A., Wendorff, J.H.: Preparation of fibers With nanoscaled morphologies: electrospinning of polymer blends. Polym. Eng. Sci. (2001). doi:10.1002/pen.10799
25. Wei, M., Kang, B., Sung, C., Mead, J.: Core–sheath structure in electrospun nanofibers from polymer blends. Macromol. Mater. Eng. (2006). doi:10.1002/mame.200600284
26. Kalra, V., Kakad, P.A., Mendez, S., Ivannikov, T., Kamperman, M., Joo, Y.L.: Self-assembled structures in electrospun poly(styrene-block-isoprene) fibers. Macromolecules (2006). doi:10.1021/ma052643a
27. Vaz, C.M., van Tuijl, S., Bouten, C.V.C., Baaijens, F.P.T.: Design of scaffolds for blood vessel tissue engineering using a multi-layering electrospinning technique. Acta Biomater. (2005). doi:10.1016/j.actbio.2005.06.006

28. Pham, Q.P., Sharma, U., Mikos, A.G.: Electrospun poly(E-caprolactone) microfiber and multilayer nanofiber/microfiber scaffolds: characterization of scaffolds and measurement of cellular infiltration. Biomacromolecules (2006). doi:10.1021/bm060680j
29. Hong, C.K., Yang, K.S., Oh, S.H., Ahn, J.-H., Cho, B.-H., Nah, C.: Effect of blend composition on the morphology development of electrospun fibres based on PAN/PMMA blends. Polym. Int. (2008). doi:10.1002/pi.2481
30. You, Y., Youk, J.H., Lee, S.W., Min, B.-M., Lee, S.J., Park, W.H.: Preparation of porous ultrafine PGA fibers via selective dissolution of electrospun PGA/PLA blend fibers. Mater. Lett. (2006). doi:10.1016/j.matlet.2005.10.007
31. Sisson, K., Zhang, C., Farach-Carson, M.C., Chase, D.B., Rabolt, J.F.: Evaluation of cross-linking methods for electrospun gelatin on cell growth and viability. Biomacromolecules (2009). doi:10.1021/bm900036s
32. Lee, S.J., Oh, S.H., Liu, J., Soker, S., Atala, A., Yoo, J.J.: The use of thermal treatments to enhance the mechanical properties of electrospun poly(ε-caprolactone) scaffolds. Biomaterials (2008). doi:10.1016/j.biomaterials.2007.11.024
33. Wang, X., Zhang, K., Zhu, M., Hsiao, B.S.., Chu, B.: Enhanced mechanical performance of self-bundled electrospun fiber yarns via post-treatments. Macromol. Rapid Commun. (2008). doi:10.1002/marc.200700873
34. Tiwari, S.K., Tzezana, R., Zussman, E., Venkatraman, S.S.: Optimizing partition-controlled drug release from electrospun core–shell bers. Int. J. Pharm. (2010). doi:10.1016/j.ijpharm.2010.03.021
35. Chew, S.Y., Wen, J., Yim, E.K.F., Leong, K.W.: Sustained release of proteins from electrospun biodegradable fibers. Biomacromolecules (2005). doi: 10.1021/bm0501149
36. Zeng, J., Yang, L., Liang, Q., Zhang, X., Guan, H., Xu, X., Chen, X., Jin, X.: Influence of the drug compatibility with polymer solution on the release kinetics of electrospun fiber formulation. J. Con. Rel. (2005). doi:10.1016/j.jconrel.2005.02.024
37. Xu, X., Yang, L., Xu, X., Wang, X., Chen, X., Liang, Q., Zeng, J., Jing, X.: Ultrafine medicated fibers electrospun from W/O emulsions. J. Con. Rel. (2005). doi:10.1016/j.jconrel.2005.07.021
38. Kim, K., Luu, Y.K., Chang, C., Fang, D., Hsiao, B.S., Chu, B., Hadjiargyro, M.: Incorporation and controlled release of a hydrophilic antibiotic using poly(lactide-co-glycolide)-based electrospun nanofibrous scaffolds. J. Con. Rel. (2004). doi:10.1016/j.jconrel.2004.04.009
39. Okuda, T., Tominaga, K., Kidoaki, S.: Time-programmed dual release formulation by multilayered drug-loaded nanober meshes. J. Con. Rel. (2009). doi:10.1016/j.jconrel.2009.12.029
40. Ranganath, S.H., Wang, C.-H.: Biodegradable microfiber implants delivering paclitaxel for post-surgical chemotherapy against malignant glioma. Biomaterials (2008). doi:10.1016/j.biomaterials.2008.04.002
41. Cui, W., Li, X., Zhu, X., Yu, G., Zhou, S., Weng, J.: Investigation of drug release and matrix degradation of electrospun poly($_{D,L}$-lactide) fibers with paracetanol inoculation. Biomacromolecules (2006). doi:10.1021/bm060057z
42. Buschle-Diller, G., Cooper, J., Xie, Z., Wu, Y., Waldrup, J., Ren, X.: Release of antibiotics from electrospun bicomponent fibers. Cellulose (2007). doi:10.1007/s10570-007-9183-3
43. Nie, H., Soh, B.W., Fu, Y.-.C, Wang, C.-H.: Three-dimensional fibrous PLGA/HAp composite scaffold for BMP-2 Delivery. Biotech. Bioeng. (2007). doi:10.1002/bit.21517
44. Maretschek, S., Greiner, A., Kissel, T.: Electrospun biodegradable nanofiber nonwovens for controlled release of proteins. J. Con. Rel. (2008). doi:10.1016/j.jconrel.2008.01.011
45. Kenawy, E.-R., Bowlin, G.L., Manseld, K., Layman, J., Simpson, D.G., Sanders, E.H., Wnek, G.E.: Release of tetracycline hydrochloride from electrospun poly(ethylene-co-vinylacetate), poly(lactic acid), and a blend. J. Con. Rel. (2002). doi:10.1016/S0168-3659(02)00041-X
46. Xu, X., Chen, X., Xu, X., Lu, T., Wang, X., Yang, L., Jing, X.: BCNU-loaded PEG-PLLA ultrafine fibers and their in vitro antitumor activity against glioma C6 cells. J. Con. Rel. (2006). doi:10.1016/j.jconrel.2006.05.031

47. Xie, Z., Buschle-Diller, G.: Electrospun Poly(D,L-lactide) fibers for drug delivery: the influence of cosolvent and the mechanism of drug release. J. Appl. Polym. Sci. (2009). doi: 10.1002/app.31026
48. Chien Y.W. (1992) Novel Drug Delivery Systems. Marcel Dekker, New York
49. Luong-Van, E., Grndahl, L., Chua, K.N., Leong, K.W., Nurcombe, V., Cool, S.M.: Controlled release of heparin from poly(ε-caprolactone) electrospun fibers. Biomaterials (2006). doi:10.1016/j.biomaterials.2005.10.028
50. Zamani, M., Morshed, M., Varshosaz, J., Jannesari, M.: Controlled release of metronidazole benzoate from poly(ε-caprolactone) electrospun nanobers for periodontal diseases. Eur. J. Pharm. Biopharm. (2010). doi:10.1016/j.ejpb.2010.02.002
51. Xie, J., Wang, C.-H.: Electrospun micro- and nanofibers for sustained delivery of paclitaxel to treat C6 glioma in vitro. Pharm. Res. (2006). doi:10.1007/s11095-006-9036-z
52. Thakur, R.A., Florek, C.A., Kohn, J., Michniak, B.B.: Electrospun nanobrous polymeric scaffold with targeted drug release proles for potential application as wound dressing. Int. J. Pharm. (2008). doi:10.1016/j.ijpharm.2008.07.033
53. Yu, D.-G., Shen, X.-X., Branford-White, C., White, K., Zhu, L.-M., Annie Blig S.W.: Oral fast-dissolving drug delivery membranes prepared from electrospun polyvinylpyrrolidone ultrafine fibers. Nanotechnology, (2009). doi:10.1088/0957-4484/20/5/055104
54. Taepaiboon, P., Rungsardthong, U., Supaphol, P.: Drug-loaded electrospun mats of poly(vinyl alcohol) fibres and their release characteristics of four model drugs. Nanotechnology (2006). doi:10.1088/0957-4484/17/9/041
55. Verreck, G., Chun, I., Rosenblatt, J., Peeters, J., Van Dijck, A., Mensch, J., Noppe, M., Brewste, M.E.: Incorporation of drugs in an amorphous state into electrospun nanofibers composed of a water-insoluble, nonbiodegradable polymer. J. Con. Rel. (2003). doi:10.1016/S0168-3659(03)00342-0
56. Huang, Z.-M., He, C.-L., Yang, A., Zhang, Y., Han, X.-J., Yin, J., Q.W Encapsulating drugs in biodegradable ultrafine fibers through co-axial electrospinning. J. Biomed. Mater. Res. (2005). A. doi:10.1002/jbm.a.30564
57. Natu, M.V., de Sousa, H.C., Gil, M.H.: Effects of drug solubility, state and loading on controlled release in bicomponent electrospun fibers. Int. J. Pharm. (2010). doi:10.1016/j.ijpharm.2010.06.045
58. Sikareepaisan, P., Suksamrarn, A., Supaphol, P.: Electrospun gelatin fiber mats containing a herbal—*Centella asiatica*—extract and release characteristic of asiaticoside. Nanotechnology, (2008). doi:10.1088/0957-4484/19/01/015102
59. Tzafriri, A.R.: Mathematical modeling of diffusion-mediated release from bulk degrading matrices. J. Con. Rel. (2000). doi:10.1016/S0168-3659(99)00174-1
60. Kim, T.G., Lee, D.S., Park, T.G.: Controlled protein release from electrospun biodegradable fiber mesh composed of poly(ε-caprolactone) and poly(ethylene oxide). Int. J. Pharm. (2007). doi:10.1016/j.ijpharm.2007.01.040
61. Perale, G., Arosio, P., Moscatelli, D., Barri, V., Mller, M., Maccagnan, S., Masi, M.: A new model of resorbable device degradation and drug release: transient 1-dimension diffusional model. J. Con. Rel. (2009). doi:10.1016/j.jconrel.2009.02.014
62. Zong, X., Ran, Sh., Kim, K.-S., Fang, D., Hsiao, B.S., Chu B.: Structure and morphology changes during in vitro degradation of electrospun poly(glycolide-co-lactide) nanofiber membrane. Biomacromolecules (2003). doi:10.1021/bm025717o
63. Peppas, N.A., Brannon-Peppas, L.: Water diffusion and sorption in amorphous macromolecular systems and foods. J. Food Eng. (1994). doi:10.1016/0260-8774(94)90030-2
64. Zeng, J., Xu, X., Chen, X., Liang, Q., Bian, X., Yang, L., Jin, X.: Biodegradable electrospun fibers for drug delivery. J. Con. Rel. (2003). doi:10.1016/S0168-3659(03)00372-9
65. Qi, M., Li, X., Yang, Y., Zhou, S.: Electrospun fibers of acid-labile biodegradable polymers containing ortho ester groups for controlled release of paracetamol. Eur. J. Pharm. Biopharm. (2008). doi:10.1016/j.ejpb.2008.05.003

66. Taepaiboon, P., Rungsardthong, U., Supaphol, P.: Vitamin-loaded electrospun cellulose acetate nanober mats as transdermal and dermal therapeutic agents of vitamin A acid and vitamin E. Eur. J. Pharm. Biopharm. (2007). doi:10.1016/j.ejpb.2007.03.018
67. Suwantong, O., Opanasopit, P., Ruktanonchai, U., Supaphol, P.: Electrospun cellulose acetate ber mats containing curcumin and release characteristic of the herbal substance. Polymer (2007). doi:10.1016/j.polymer.2007.11.019
68. Verreck, G., Chun, I., Peeters, J., Rosenblatt, J., Brewste, M.E.: Preparation and characterization of nanofibers containing amorphous drug dispersions generated by electrostatic spinning. Pharm. Res. (2003) doi:10.1023/A:1023450006281
69. Kenawy, E.-R., Abdel-Hay, F.I., El-Newehy, M.H., Wnek, G.E.: Processing of polymer nanobers through electrospinning as drug delivery systems. Mater. Chem. Phys. (2009). doi: 10.1016/j.matchemphys.2008.07.081
70. Jiang, H., Hu, Y., Li, Y., Zhao, P., Zhu, K., Che, W.: A facile technique to prepare biodegradable coaxial electrospun nanofibers for controlled release of bioactive agents. J. Con. Rel. (2005). doi:10.1016/j.jconrel.2005.08.006
71. Tammaro, L., Russo, G., Vittoria, V.: Encapsulation of diclofenac molecules into Poly(ε-caprolactone) electrospun fibers for delivery protection. J. Nanomater. (2009). doi: 10.1155/2009/238206
72. Abidian, M.R., Kim, D.-H., Martin, D.C.: Conducting-polymer nanotubes for controlled drug release. Adv. Mater. (2006). doi:10.1002/adma.200501726
73. Srikar, R., Yarin, A.L., Megaridis, C.M., Bazilevsky, A.V., Kelley, E.: Desorption-limited mechanism of release from polymer nanofibers. Langmuir. (2008). doi:10.1021/la702449k
74. Panyam, J., Williams, D., Dash, A., Leslie-Pelecky, D., Labhasetwar, V.: Solid-state solubility influences encapsulation and release of hydrophobic drugs from PLGA/PLA nanoparticles. J. Pharm. Sci. (2004). doi:10.1002/jps.20094
75. Drug card for timolol (DB00373), DrugBank database. http://www.drugbank.ca/drugs/DB00373. Cited 27 May 2010
76. Drug card for acetazolamide (DB00819), DrugBank database. http://www.drugbank.ca/drugs/DB00819. Cited 27 May 2010.
77. Marsac, P.J., Li, T., Taylor L.S.: Estimation of drug–polymer miscibility and solubility in amorphous solid dispersions using experimentally determined interaction parameters. Pharm. Res. (2009). doi:10.1007/s11095-008-9721-1
78. Miyajima, M., Koshika, A., Okada, J., Ikeda, M., Nishimura, K.: Effect of polymer crystallinity on papaverine release from poly(L-lactic acid) matrix. J. Con. Rel. (1997). doi: 10.1016/S0168-3659(97)00081-3
79. Jeong, J.-C., Lee, J., Cho, K.: Effects of crystalline microstructure on drug release behavior of poly(ε-caprolactone) microspheres. J. Con. Rel. (2003). doi:10.1016/S0168-3659(03)00367-5
80. Cui, W., Li, X., Zhou, S., Weng, J.: Degradation patterns and surface wettability of electrospun brous mats. Polym. Degrad. Stab. (2008). doi:10.1016/j.polymdegradstab.2007.12.002
81. Kang, M., Jung, R., Kim, H.-S., Jin, H.-J.: Preparation of superhydrophobic polystyrene membranes by electrospinning. Colloids Surf. A Physicochem. Eng. Asp. (2008). doi: 10.1016/j.colsurfa.2007.04.122
82. Natu, M.V., Gil, M.H., de Sousa, H.C.: Supercritical solvent impregnation of poly(ε-caprolactone)/poly(oxyethylene-b-oxypropylene-b-oxyethylene) and poly(ε-caprolactone)/poly(ethylene-vinyl acetate) blends for controlled release applications. J. Sup. Fluids (2008). doi:10.1016/j.supflu.2008.05.006
83. Hglund, A., Hakkarainen, M., Albertsson, A.-C.: Degradation profile of poly(ε-caprolactone)-the influence of macroscopic and macromolecular biomaterial Design. J. Macromol. Sci. A. doi:10.1080/10601320701424487 (2007)

Novel Coating Technologies of Drug Eluting Stents

Dennis Douroumis and Ichioma Onyesom

Abstract In the last decade, drug eluting (DES) stent have been introduced as a useful tool in modern interventional cardiology. A wide variety of stent platforms are already in the market or under development undergoing clinical evaluation. The stent characteristics including stent design, coating strategies and pharmacological agents are related to different rates of restenosis. In this chapter we emphasise the current coating technologies employed for drug and delivery-vehicle material deposition onto the stent surface. A discussion about the existing platforms, recent developments and clinical outcomes is also included.

1 Introduction

Drug eluting stents (DES) have played a key role in interventional cardiology for the treatment of vascular diseases in the last 20 years. One of the most common vascular diseases is atherosclerosis which is a leading cause of death in the western world. Atherosclerosis is characterized by narrowing and/or occlusion of the arteries that supply blood to tissues of the heart [26, 80, 90] where a necrotic core of foam cells, dead cells and fat is formed, surrounded by a fibrotic cap of smooth muscle cells, proteoglycans, collagen, and calcium in the intima of large and medium size arteries. The development of these lesions will finally lead to artery narrowing and consequently in reduction of oxygen and blood to the heart causing patient inschemia and angina pectoris (chest discomfort, pain, tightness or

D. Douroumis (✉) · I. Onyesom
University of Greenwich, School of Science, Medway Campus,
Chatham Maritime, Kent, ME4 4TB, UK
e-mail: d.douroumis@gre.ac.uk

Stud Mechanobiol Tissue Eng Biomater (2011) 8: 87–125
DOI: 10.1007/8415_2010_54

Published Online: 5 February 2011

pressure) and further may result to heart attack, stroke or kidney failure [53]. When this blockage occurs in the coronary artery it can lead to myocardial infraction and death.

One of the main treatments to cure atherosclerosis is the implementation of a procedure called percutaneous transluminal coronary angioplasty (PCTA) that can restore the obstruction or the narrowing of a blood vessel. In this procedure the stent which is mounted in a balloon catheter is inserted into the artery placed at the site of the initial blockage. Balloon angioplasty was introduced in 1979 when Andreas Gruentzig [36, 45] successfully achieved the first PCTA using a balloon catheter. However, PCTA can cause injury to the blood vessels termed restenosis and particularly in-stent resteonosis [59, 62] as occasionally some patients develop a re-narrowing after coronary stenting. Restenosis is developed by the implantation of the stent and it is mainly characterized by neoitimal proliferation where proliferating cells grow inmost to the vessel and elastic recoil of the vascular wall [18, 55].

Several studies have demonstrated the efficiency of DES to reduce vessel blockage due to restenosis by delivering therapeutic agents [74, 111, 112]. The DES can provide localized drug delivery and ensure the delivery of the effective dosage on the target site due to the direct contact with the vessel walls. The Cypher® stent developed by Cordis was the first DES that reached the market [105, 127] and it was approved in 2003 by the Food and Drug Administration (FDA). Its breakthrough technology was proved advantageous compared to the bare metal stents (BMS) that caused thrombogenic effects and high mortality to patients receiving BMS. Indeed the RAVEL trial (randomized study with the sirolimus-eluting Velocity balloon-expandable stent in the treatment of patients with de novo native coronary artery lesions) performed on 238 patients and SIRIUS (a multicenter, randomized, double-blind study of the sirolimus-eluting balloon expandable stent in the treatment of patients with de novo native coronary artery lesions) ($n = 1{,}100$) trials showed significant reduction of neointimal growth [75, 99]. These large scale randomized trials confirmed the antirestenotic effect of DES.

The successful development of DES requires the involvement of a multidisciplinary group of scientists and can be simplified in three basic components: stent design, coating strategies and pharmacological agent [107]. The stent coating is an important factor for stent design affecting both angiographic and clinical data [48]. The existence of a coating substrate on the strut surface influences thrombogenicity as a result of delayed healing and hypersensitivity reactions [76, 124]. Thus the stent surface has a major impact on vascular responses such as platelet and leukocyte deposition at stent sites, smooth muscle cell migration, proliferation, production of cellular matrix and at the end of neointimal hyperplasia formation [40]

Research efforts are now directed at coating strategies for prevention of restenosis and coating strategies for improving biocompatibility [1]. The first direction is related to the applied coating techniques since several approaches have been used to coat the drug on the stent surface and control the release kinetics. In order to develop effective DES, it is important to precisely control the drug release kinetics to avoid bulk release and the drug must be in an effective dosage form at the target site. It is now evident that antirestenotic drugs need to be delivered in 3 weeks to

prevent smooth muscle cell migration and proliferation [3, 118] since the initiation of both processes takes place a day after balloon angioplasty for at least 2 weeks [115]. Therefore, a drug carrier, usually a polymer, has to be blended and coated on the stent strut to deliver the active substance directly to the endothelial walls approximately for 3 weeks [46, 52]. This chapter will discuss the features and applications of various stent coating methods including novel approaches that have been employed from industry and researchers to improve the quality of DES. We will also focus on the novel coating materials (e.g. polymers, inorganic materials) with anti-inflammatory, anti-thrombogenic activity and improved biocompatibility.

2 Drug Eluting Stents

2.1 What is Drug Eluting Stent?—Stent Structure

A DES can be defined as a localized small expandable, slotted metal tube (Fig. 1) inserted into a vessel coated with pharmacological agent that is used to provide structural support for a vessel after the intervention and to allow slow release of that particular drug at the stent implantation site [25]. The rationale behind the development of DES is: (a) to control and reduce smooth muscle cell growth and migration and (b) to prevent inflammatory response which is the cause of in-stent restenosis and neointimal proliferation [1, 61]. The advantages offered by DES include clinical benefits such as avoiding excessive exposure of drugs with systemic toxicity by providing effective drug concentrations in the surrounding tissues [61,

Fig. 1 The cobalt chromium NEMO^{TM} reservoir stent

65]. Additionally, DES bypass first pass metabolism facilitating administration of higher concentration of drug with no significant side effect (Intravascular stent).

The physical structure of the stent can have an impact on DES performance. Three primary performance factors [13, 65, 89, 107] drive stent design: radial strength to minimize vessel recoil, flexibility to facilitate stent delivery and conformability to improve vessel wall opposition. The last factor has become particularly important as it plays a significant role on uniform delivery of antirestenotic drugs to the diseased vessel segment.

The radial strength is important since displaying or compressing plague with only a balloon may leave the artery susceptible to vessel recoil or acute closure. A stent provides scaffolding to prevent vessel's recoil and helps maintain luminal diameter and one of the key attributes to determining stent ability to resist vessel's recoil is its metal composition. Currently available stents use a composition of metal alloys which include stainless steel (liberte stent), cobalt chromium (CoCr) (vision stent) and cobalt nickel (driver stent). The selection of specific metal composition often involves a performance standard. For example, stainless steel maybe selected for improved biocompatibility, strength and durability but may not have the same radiopacity of other alloys. Specific benefits from one alloy to another are not quite clear at the moment although they might impart benefits. The radial strength and vessel recoil resistance are also a function of stent geometry and strut thickness [12, 82]. Over the last decade the stent strut thickness has been decreased by 40% and many DES now feature struts less than 0.0038–0.0032″.

Another benefit of the evolution of stent design is the improvement of stent flexibility [67, 107]. Over time, stents have been moved from highly connected closed patterns to more open structures with fewer strut connections. The initial closed designs were extremely strong but stent were difficult to deliver. To improve stent flexibility and deliverability the shape and the connections of the stent strut became the focus. The gradual decrease of the stent struts and their connections resulted improved flexibility. A new innovative hybrid design featuring unique geometric shapes was introduced to further minimize vessel recoil. These hybrid designs use thinner struts to uniformly distribute compressive forces and reduce vessel recoil. In essence these hybrid designs helped to deliver a combination of radial strength, low stent profile and excellent flexibility. Another important property was the more uniform vessel coverage, an important factor in DES design. Many of the open cell designs present large areas between struts which may improve flexibility over closed cell designs but may also lead to gaps or areas of inconsistent vessel coverage. Stents with small cell areas may help to improve vessel coverage and promote uniform drug distribution.

2.2 Importance of DES Coating

There is an enormous number of coating technologies applied on the surface of DES, some of them already used for commercial products and others under

development. DES are usually coated by polymers [1] incorporating a pharmacological agent to reduce adverse effects mentioned previously.

The implemented coating technology should provide a safe, uniform, reproducible, accurate and cost effective coating on the stent surface for a wide range of carriers and active agents. Incomplete coating on the strut surface results in roughening of stent surface, increase strut thickness and lack of uniformity that consequently can lead to increased risk of restenosis as it was observed in gold coating [51, 103]. Another concern is the bridging which is the forming of a film across the open space (slots) between structural members of the device and occurs when coating stents with less open construction. The bridging is undesirable because it can interfere with the mechanical performance of the stent such as expansion during deployment in a vessel lumen. The created brides may rapture upon expansion and provide sites that activate platelet adhesion by creating flow disturbances in the adjacent heamodynamic environment or pieces of the film may break off and cause further complications. Bridging of the open slots may also prevent cell migration thus complicating the endothelial cell encapsulation of the stent.

In some cases the coating technologies could be problematic in that there is a significant amount of material lost during the process when most of the incorporated active agents are quite costly. Similarly the same technologies can limit the coating level failing to achieve high drug loading. The coating method can itself exclude a class of pharmaceutical agents due to the operational principles. For example, many coating devices operate by using organic solvents to dissolve the polymers and water insoluble active agents. Hence, it is impossible that can be used for loading of water soluble drugs. The coating technology should be suitable to control accurately the coating thickness, along to the longitudinal axes of the tubular wall, to optimize the release of the active substance. There are quite a few occasions where the amount of the active substance has to be increased in the end sections of the stent surface as compared to the middle part to reduce the risk of restenosis. The coating of both the abluminal and luminal or only the abluminal surface of the stent body requires the employment of the appropriate technique. As we will discuss later reservoir systems are designed to deliver more than one drugs in a controllable manner in different time intervals.

In a study reported by Virmani et al. and Hwang et al. [47, 128] a case of late-stage thrombosis of a patient who had two overlapping Cypher^{TM} stents was described. The analysis showed thrombus at the entrance of the distal stent with evidence of inflammatory cells in the subluminal tissue. Interestingly, in the proximal stent, a few small polymer pieces were found separated from the stent surrounded by giant cell. It was not unclear whether this was due to the preparation procedure the authors concluded that localized hypersensitivity to the polymer was responsible for the occlusion. However, the existence of separated polymers on the stent surface is a strong indication of incomplete coating.

2.3 Polymer and Drug Aspects

In addition to stent design, the polymer technology is proven to be a key aspect on DES performance. Originally polymers have not been used as a necessary component of DES. In the first DES generation only anti-restenotic active substances were coated directly on the stent surface [47, 99]. The lack of a protecting polymer layer caused the drug layer to crack and delaminated from the stent with significant impact on the quality and consistency of the clinical results. The polymer coatings were added to DES to protect the drug during the manufacturing, delivering to the lesion and expansion [47]. For instance, some drugs may degrade or lose their activity when exposed to the blood flow for a period of time. Another reason was to allow consistent drug dose to be applied to the entire stent and control the drug amount/time that is released from the stent.

Although polymers are an essential component of DES they vary in their mechanical characteristics. The ideal coatings for DES require mechanical integrity in a smooth uniform fashion and vascular compatibility to avoid additional inflammatory response or vessel injury. The polymer should also be designed and manufactured to deliver the drug loading in a controlled, consistent manner. Briefly, two different approaches, for storing and releasing anti-restenotic drugs have been explored: reservoir [22, 56, 107] and matrix systems. In the reservoir systems the drug is loaded in voids and the polymers may be mixed with the drug or used to coat the drug by tailoring the drug release from the stent. Alternatively, matrix systems incorporate the drug into the polymer during the polymer process distributing the drug through the entire thickness of final polymer coating.

The clinical efficacy of DES has been evaluated in relation to the polymer properties. In a study, five degradable and three non-degradable polymers were dip coated to study the inflammatory responses [124]. The study revealed that poly (ortho ester), poly (caprolactone), poly (hydroxy butyrate valerate), as well as the non-degradable poly (urethane) and poly (dimethyl siloxane) caused severe inflammatory reactions. Only in the case of the biodegradable PLGA, a copolymer of poly (ethylene oxide) and poly (butylenes terephthalate) less severe responses were observed. A number of polymers used in DES showed extensive inflammatory responses after implantation in coronary arteries and only high molecular weight, slow degradable polymer such as poly-l lactic acid showed acceptable heamocompatibility and histocompatibility in porcine and human coronary arteries [64, 96].

A variety of drugs used in DES includes immune-suppressive agents (sirolimus, tacrolimus, biolimus B9, everolimus and zotarolimus), cellular proliferation agents (paclitaxel, actinonycin D), anti-inflammatory agents (dexamethasone), antibodies and prohealing agents. For most of the active agents the mechanism of action has been studied and it is well know. Rapamycin (sirolimus) is a macrocyclic lactone with immune-suppressive properties and it is known to inhibit proliferation and migration of smooth muscle cells. On a subcellular level rapamycin inhibits the

mammalian target of rapamycin by binding to the FK-binding protein 12. As a result rapamycin increases thrombin and tumor necrosis factor-a [109, 110]. For these reasons rapamycin has been incorporated in the commercial Cypher stent (Cordis, Warren, New Jersey) with clinical studies showing almost complete abolition of neointimal growth [105]. The profound effect on restenosis and revascularization in several clinical trials (RAVEL, SIRIUS, E-SIRIUS, and C-SIRIUS) has confirmed the efficacy of Rapamycin in DES.

Paclitaxel is a lipophilic diterpenoid that acts as an immune-suppressive and anti-proliferative agent and it also a well know in cancer treatment. It is a potent anti-microtubule agent that binds to the β-subunit of the tubulin heterodimer, promoting tubulin polymerization, cell cycle arrest, and ultimately, inhibition of vascular smooth muscle cell migration and proliferation [20, 104]. The latter takes place by blocking cell proliferation in the G1- or M-phase of the cell cycle. Furthermore, paclitaxel activates the c-JunNH2-terminal kinase [108, 132] an important mediator of endothelial and monocytic tissue factor induction. Therefore, paclitaxel enhances tissue factor expression and activity in endothelial when introduced in DES [28]. Paclitaxel has been incorporated as the active component in several available commercial stents such as TAXUS^{TM} (Boston Scientific, Natick, Massachusetts).

Similarly, Everolimus and Zotarolimus which are Rapamycin synthetic analogues with similar activity have been successfully used as antirestenotic agents in DES [50, 69, 95]. Both substances bind to cytosolic FK-506 binding protein-12 and inhibit the proliferation of smooth muscle cells and T-cells. The Xience V (Abbott Vascular, Santa Clara, California) everolimus-eluting stent (EES) and the Endeavor (Medtronic Vascular, Santa Rosa, California) zotarolimus-eluting stent (ZES) both consist of a CoCr platform loaded with a non-erodible polymer and with a permanent polymer (phosphorylcholine) respectively, are two examples of commercial DES with proved clinical efficacy. A wide variety of DES are already in clinical use or under investigation while research is focused in the development of the stent platform, the pharmacological agent, the drug carrier vehicle and the coating technology.

3 Coating Technologies of DES

3.1 Dip Coating

Stents are typically coated by simple dip coating of the stent in a single drug/polymer(s) solution [138]. In a simplistic approach a drug solution is prepared in an organic solvent miscible with the polymer carrier solution at a concentration range. The polymers can both be biodegradable or non-biodegradable with the appropriate adhesion on the metal surface and rate controlling properties. Alternatively, the stent is modified to contain micropores or channels [137] and is dipped into the drug solution of a volatile organic solvent (acetone, methylene chloride) for sufficient time to allow solution to permeate into the pores. The

dipping solution can be further concentrated to improve the loading efficiency. After solvent has been allowed to evaporate the drug coated stent is dipped for a short time. In the final step a polymer solution is applied to the stent be repeating the dipping process. This outer layer of polymer acts as diffusion controller for the drug release.

However, the above dipping methods were accepted for early stent designs that were of opened construction fabricated from wires [135] or ribbons. The reason was that these approaches could provide relatively low coating weights (about 4% polymer) without bridging the open space between structural parts of the stent. In addition, the application of multiple dip coats from low concentration solutions often has the effect of reaching a limiting loading level as equilibrium is reached between the solution concentration and the amount of coating, with or without pharmaceutical agent, deposited on the stent. There also cases where the stent coating requires high concentration coatings (about 15%) or multiple polymer layers. Thus, the dip-coating method was developed to allow coating thickness of 10–15 μm by Ethicon Inc. (New Jersey, US).

The stent is positioned on an undersized mandrel after been cleaned by sonication in an organic solvent. A small amount of the drug/polymer solution is dropped on the stent surface to coat thoroughly the stent. Once the mandrel motor turns on, the mandrel rotates at high speed for a few seconds to through off any excess solution from the stent and to provide the proper distribution of the coating solution on the stent surface. The stent is then moved into a new, clean position on the mandrel to remove the surplus solution from the inner stent walls. The process is repeated a few times, after which time the conformal coating is already dry and non-sticky. In terms of the process, important polymer solution parameters include viscosity, solvent evaporation rate and several others. Finally, a coating cure step takes place within 24 h and the stent is placed in a saturated water atmosphere under vacuum at ambient temperature.

This approach [135] has been employed to coat the Cypher™ stent developed by Cordis Corporation (Miami US). It was the first drug-eluting stent that obtained commercial approval by the US FDA granted in April 2003 aiming to improve coronary luminal diameter in patients with symptomatic ischemic disease due to discrete de novo lesions of length $\leq$30 mm in native coronary arteries with a vessel diameter of $\geq$2.5 to $\leq$3.5 mm. The device components consists of the BX VELOCITY balloon expandable coronary stent premounted on a delivery system the RAPTOR over the wire or the RAPTORRAIL rapid exchange. The approved drug eluting stent contains a nominal sirolimus content of 70–314 μg while the inactive ingredients contain a subcoat of parylene C and a basecoat of two non-erodible polymers polyethylene-co-vinyl acetate (PEVA) and poly n-butyl methacrylate (PBMA). The hydrophobic parylene C subcoat is applied on the stent surface by chemical vapour deposition method that requires high temperature and low pressure conditions. The rationale of this primer coating is to develop stent elasticity and long lasting adherence. The FDA has already approved Parylene C (Class VI polymer) for medical implants [39] due to its excellent biostability and biocompatibility [32, 92]. The PEVA and PBMA polymers are mixed with

sirolimus at a ratio of 67 and 33%, respectively, and this subcoat is applied to the parylene treated stent. A drug free topcoat solution of PBMA polymer is applied onto the drug reservoir layer to provide a slow-release formulation. The presence of the topcoat renders the Cypher stent a diffusion controlled device.

Dip coating has been used to apply the phosphorylcholine polymer drug carrier on the BiodivYsio™ (Biocompatibles Ltd. UK), ZoMaxx (Abbott Vascular, US) and Endeavor™ (Medtronic Inc. US). The phosphorylcholine polymer drug carrier [16], known simply as PC-1036 or PC, is neutral, zwitterionic, naturally occurring phospholipid polymer, composed of the polymers 2-methacryloyloxyethyl phosphorylcholine (MPC), lauryl methacrylate (LMA), hydroxypropyl methacrylate (HPMA), and trimethoxysilylpropyl methacrylate (TSMA) in the molar ratios of MPC (23%), LMA(47%), HPMA(25%), and TSMA(5%). It not a biodegradable polymer but it is biostatic and biocompatible [134], being a natural component of the cell membrane. PC-polymers are typically applied to a medical device through a simple dip or spray coating process using organic or aqueous solvent systems. This allows for application of a suitably soluble active by either applying a mixture of the active with the coating, or, because the polymers are hydrogels, simply swelling the coating in a solution of the drug after application. As the polymers may be cross-linked through a curing process, post coating, it is possible to incorporate materials of widely different solubility properties into the coating and to control the elution of the active. The ZoMaxx stent uses the Tri-Maxx stainless steel–tantalum stent platform to deliver zotarolimus 10 μg/mm via the PC technology. After 9 months, the ZoMaxx stent clinical studies showed high rate implantation success (99%), low rates of subacute (0.5%) and late (0%) stent thrombosis. It also showed less neointimal inhibition than the Taxus stent, as demonstrated by higher in-stent late loss and restenosis by QCA and neointimal volume obstruction by intravascular ultrasound. The second-generation Endeavor ZES uses the CoCr Driver stent platform loaded with PC polymer which releases 95% of zotarolimus, within 14 days. The superiority of ZES [29] compared with BMS was demonstrated in the, randomized ENDEAVOR II Study (n = 1,197), which reported significantly lower in-stent late loss and angiographic binary restenosis at 9 month follow-up with ZES and significantly lower target lesion revascularization (TLR) out to 5 years of follow-up. Rates of death, myocardial infraction, and stent thrombosis remained comparable between both stents throughout follow-up. In the comparison with other DES, data have indicated a relatively poorer performance of ZES compared with paclitaxel (PES) and sirolimus (SES) eluting stent at short-term follow-up, as indicated by significantly higher late loss and numerically greater TLR. Further follow-up outcomes have been more supportive after the observed reductions in the absolute difference in TLR between ZES and SES/PES. For instance, in the ENDEAVOR III study, the 2.8% absolute difference in TLR between ZES and SES at 1 year was reduced to 1.6% at 5 years, whereas in the ENDEAVOR IV study, the absolute difference in TLR between ZES and PES was 1.3 and 0.5% at 1 and 3 years, respectively. Although at only medium term follow-up, these results suggest the absence of the "late-catch" phenomenon with ZES.

An alternative dipping process [83] is the preparation of an aqueous polymeric emulsion where the stent is dipped and then is removed to evaporate water until a uniform coating is formed. The emulsion is mainly produced by emulsion polymerization process at 75–100°C by combining polymer monomers, initiators and surfactants. The active substance is usually dissolved in the emulsion or it is dispersed if it is not water soluble. The dipping process is repeated several times to adjust the desired coating thickness while the aqueous phase of the emulsion does not dissolve the coating layers upon successive dipping. Although dip coating has been used extensively it can be problematic as polymeric coatings are applied from solutions of one or more polymers in one or more organic solvents in order to control the release of the active agent. These solvents prevent repeated dipping to build up the desired amount of coating as the solvent will re-dissolved the coating applied during the previous dipping.

3.1.1 Polymer Free Dip Coating

A polymer free drug eluting stent [44], Debiostent®, developed by Debiotech to overcome polymer coated associated pitfalls. The coating consists of biocompatible nano-structured ceramic material such as TiO_2, Al_2O_3 or IrO_2 combining different types of porosities disposed in a fully controllable mode at the stent surface. Because of the highly porous coating, a high drug loading efficiency is achieved with full controllable drug elution kinetics or even selective drug loading options. The coating layer acts as drug reservoir representing up to 30% of the total coating volume and drug loading can reach up to 10 mg/mm^2. By adjusting the layer thickness, pore size and turtuosity then elution times can be then controlled to provide the desired patterns. The stent coating is conducted using Debiotech's proprietary technology for example by depositing a pre-coating a soft hydrophilic layer followed by deposition of the temporary particles. The deposition process for the final coating depends on the coating precursors and also the desired coating properties. In all case the coating is deposited in several sub-layers and the coating precursors (e.g. water) are removed with thermal treatment. This approach allows formation of thicker and crack-free coatings. It is preferable to use nano-powders or sol–gel approaches because they reduce the application of high temperatures for obtaining crystalline coatings. As a result metal stents do not undergo phase transitions that could have an effect on the mechanical or shape memory properties.

The obtained inorganic coatings are built upon a network of cavities with sizes varying from nanometer to micrometer scales. The particles are linked together by multiple channels of particles with highly accurate particle size. The drug loading is conducted by dip coating of the stent in the appropriate solution. Because of the controllable pore size different actives can be loaded depending on their molecular size. For example layers with different porosities can be coated that will allow selective drug adsorption. The developed porous Debiostent® stent is expected to

offer a new DES platform with desirable drug elution properties and favorable clinical outcomes. At the moment is has not been under clinical evaluation.

3.2 Spray Coating

Spray coating of DES is among the most common approaches to apply a drug/polymer matrix on the strut surface [1]. A typical spray coating system includes a spray nozzle and a pump that supplies the coating material from the reservoir to the nozzle. The drug/polymer or polymer solution is ejected from the nozzle in the form of microdroplets applied to the surface of the stent. For example, a block copolymer and the drug can be dissolved in a mixture of organic solvents (e.g. toluene, tetrahydrofuran) to a final concentration of 1%. The solution is placed in a syringe pump and fed to a spray nozzle while the stent device is mounted on a rotated mandrel. To ensure a uniform coating the nozzle moves along the stent surface while spraying for one or more passages until the desired coat thickness is achieved. The coated stent is then cured in a preheated oven for 3 h at 65–70°C.

Such a spray coating device [87] was employed to coat the commercial TAXUS™ EXPRESS^{2}™ paclitaxel (PTx) eluting stent (Boston Scientific, Natick, Massachusetts). The TAXUS technology consists of discrete PTx nanoparticles (1 mcg/mm^2) embedded in a thermoplastic elastomer poly(styrene-b-isobutyl-b-styrene) (SIBS) called Translute™ [88]. This stent also incorporates a stainless steel platform where PTx is released from the Translute polymer matrix directly into arterial walls without going through the rate-controlling membrane, providing a diffusion controlled matrix system. The in vitro release studies demonstrated various release patterns depending on the PTx loading amounts (Fig. 2). The Taxus™ family of stents were the second DES platform approved by the FDA in March 2004 in the US [127] and the drug contents of the stents were approximately 50–200 μg. The clinical performance of the TAXUS™ stent system has been widely studied [17, 35, 111, 112] and it was found to have a profound effect on reducing restenosis rates compared to BMS models. The TAXUS IV trials presented a dramatic reduction in restenosis rates when compared to BMS after 9 months, 7.9 versus 26.6%, respectively [127].

The aforementioned coating methods in some cases have been proved inefficient and unreliable as they produce defective coatings with a damaged or waving or uneven strut layers. In addition, a significant coating amount is lost during the spray process. Therefore, more sophisticated spray coating devices have been employed for stent coating such the one described below from Abbott Cardiovascular Systems (Santa Clara, CA) [125]. Initially, the uncoated stent is weighted through an automated system on a microbalance and then it is placed for aligning on a conical shape support. By using a digital image recorder the stent is aligned at the appropriate position. The reason is that while the coating substance is ejected by the spray nozzle it is not uniformly distributed in the cloud of the spray nozzle. The concentration of the coating substance is higher in the area along or near the

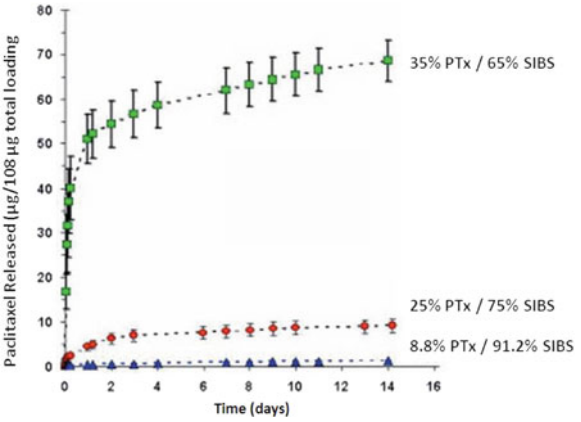

Fig. 2 *In vitro* kinetic drug-release profiles of PTx from SIBS polymer stent coatings containing 8.8, 25, and 35% PTx (w/w) over 14 days in PBS–Tween20 at 37°C. Data are an average from three stents at each time point (with permission from Ranade et.al 2004)

longitudinal axis of the nozzle. As the distance from the axis of the nozzle increases, the concentration of the coating substance decreases. Thus it is desirable to place the stent in a cloud area that has the highest concentration in order to increase the coating efficiency. The stent alignment will facilitate coating efficiency and prevent inconsistent or uneven patterns on the stent surface. The coating is applied be feeding a gas and a liquid through a nozzle that consists of a gas-assisted mixing atomizer. The nozzle deposits the coating materials onto the stent in the form of fine droplets. Process parameters that affect droplet size include the viscosity of the solution, surface tension of the solvent, solution feed rate and atomization pressure. During the coating operation the stent rotates about its central longitudinal axis and can also translate axially or linearly though the spraying cloud. After a selected number of passes through the spraying cloud the deposited coating substance is aloud to dry or subjected to further spraying. The spraying and drying steps can be repeated until a desired amount (or thickness) of coating materials is deposited on the stent. This helps to avoid excessive applications of coating material and create a plurality of coating layers. The drying process depends on the solvent nature and various energy sources such as conventional or infrared or UV ovens are used to remove residual solvents.

This spray coating process has been used to coat the XIENCE V® everolimus-eluting coronary stent system (Abbott Vascular, Santa Clara, CA, USA). The XIENCE V® is consists of either the MULTI-LINK VISION® or the MULTI-LINK MINI VISION® coronary stent system coated with a formulation containing everolimus, the active ingredient, embedded in a non-erodible polymer mixture. This mixture consists of PBMA, a polymer that adheres to the CoCr stent and drug coating, and PVDF-HFP, which is comprised of vinylidene fluoride and hexafluoropropylene monomers as the drug matrix layer containing everolimus. PBMA is a homopolymer with a molecular weight (Mw) of 264–376 kDa and PVDF-HFP is a non-erodible semi-crystalline random copolymer with a molecular weight (Mw) of 254–293 kDa. The drug matrix copolymer is mixed with everolimus (83%/17% w/w polymer/everolimus ratio) and applied to the entire PBMA

coated stent surface. The drug load is 100 μg/cm^2 without the presence of a layer. In 2008 a pivotal clinical trial SPIRIT II was designed to compare the XIENCE V and TAXUS EXPRESS2 in US and Japan. The results demonstrated that angiographic in-segment late loss was considerably less for the Xience V stent compared to the Taxus stent. In addition a significant reduction in major adverse cardiac events for the Xience V than for the Taxus stent with 43.2 and 41.7% after 9 and 12 months, respectively [113].

An advanced spray coating technology [126] has been developed by Biosensors International Ltd. to produce accurate and precise coatings to avoid imperfections such as excessive coating, creation of meniscus or bridging on the stent surface. Similarly to the previous device the stent is placed on a support element while a dispensing head (nozzle) moves along the axis of the rotating stent applying the coating material. Prior stent coating the stent is placed on a mandrel and then positioned in focus under an imaging system. A line camera is used to produce a two-dimensional image that will be further processed. The imaging system is connected to a control unit which operates by using a series of algorithms. For this purpose a step sequence is introduce to apply (i) a segmentation algorithm to determine the area occupied by the stent elements, (ii) a skeletonization algorithm to determine the points of intersections of the stent skeletal elements, (iii) a path-traversal algorithm to determine the paths along the skeletal elements and (iv) a speed and position algorithm to determine the relative speeds and positions of the dispenser head as it travels along the stent.

In essence, the main functions of the operating system is to determine the traversal paths by which the dispenser head is moved over the stent elements and also to determine the speed and position variations in order to optimize the deposited coating. The imaging system supplies a signal information in the form of light transmition followed by a segmentation process (histogram based pixel classification) to produce a grayscale image. This image is used for the sceletonization process to reflect the stent structure and then the skeleton image is translated into an in-memory sequence of points to define the traversal path. The speed and position algorithms play also a major role in the coating process as they control a number of key functions. For example, they control the coating parameters such as motion speed, dispensing flow rate and number of passes. They also used to adjust the coating thickness between links and bands by controlling the number of layers. An important function of these algorithms is the variation of the coating trajectories over wider struts. When the strut becomes wider the algorithms enable multiple passes by deviating the trajectory of the dispensing head from the centre of the strut and shifting it closer to either edge of the strut. Another feature of the operating system is the ability to control the distance between the tip (typically 20–60 μm) of the dispensing nozzle and the stent in order to affect the coating deposition. When there is a requirement for less coating on specific strut areas e.g. thinner parts, sharp turn or stent crowns, the operating system is programmed to increase the motion speed without altering the flow rate.

This unique precision automated coating approach was implemented to coat Biomatrix Flex^{TM} a new generation (Grube et al. 2006) DES developed by

Biosensors International. An improved mechanical stainless steel platform was coated with an abluminal biodegradable polylactic acid (PLA) polymer and Biolimus A9^{TM} (Fig. 3). The improved flexibility, trackability (ability of the stent plus delivery system to navigate through the vessel to reach the lesion) and larger initial cell opening (i.e. the area between the struts when fully extended) due to the employment of curved connectors achieves reduced turbulence and arterial wall injury. The active agent Biolimus is a highly lipophilic, semi-synthetic sirolimus analogue with an alkoxy-alkyl group replacing hydrogen at position 42-O [33]. At a cellular level, biolimus presents similar pharmacological effects to sirolimus where it forms a complex with intracellular FKBP-12, which binds to the mammalian target of rapamycin and reversibly inhibits cell-cycle transition of proliferating smooth muscle cells. The abluminal coating of PLA is absorbed with 6–9 months (Fig. 4) as polymer degrades over time [19, 34] to lactic acid. Biolimus is more lipophilic than sirolimus presenting faster cellular uptake with excellent immunosuppressant and anti-inflammatory properties. The 1 and 3 years randomised clinical trials LEADERS [97, 136] suggested that the Biomatrix Flex^{TM} showed improved safety and efficacy compared to Cypher Select^{TM} (J&J). When compared to both 1 and 3 years results there was a diverging trend towards a

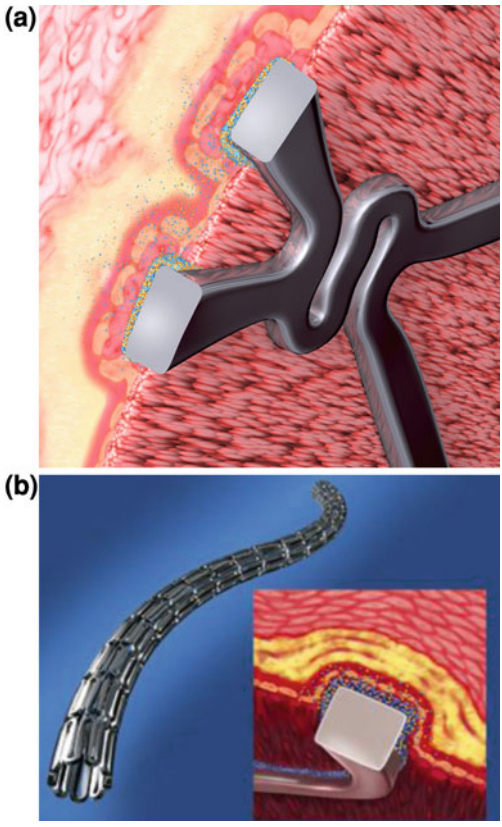

Fig. 3 Abluminal coating of Biomatrix Flex^{TM} **a** coated with biodegradable PLA and Biolimus BA9, **b** Juno stent platform (courtesy of by Biosensors Int.)

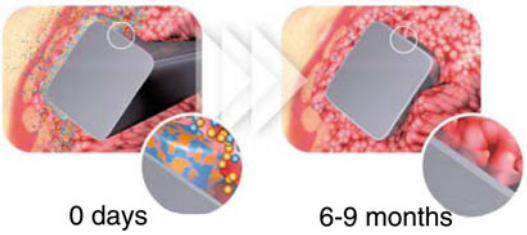

Fig. 4 Abluminal coating of Biomatrix Flex™ absorbed after 6–9 months (courtesy of by Biosensors Int.)

lower rate of MACE (15.7 vs. 19.0%; *P* value for superiority = 0.09) in patients treated with BioMatrix Flex versus those treated with Cypher Select. In addition, the very late thrombosis (VLST) was reduced to 0.2% for BioMatrix Flex out to 3 years, compared with 0.9% for Cypher Select observed within the same period.

3.2.1 Polymer Free Coatings

An innovative coating system called Transluminal Stent Coating Machine (SCM), [8] has been developed by Transluminal GmbH (Germany) for polymer free coating DES. Interestingly, this is the only technology reported up to date that can be used for individual stent coating a few moments prior to stent implantation and for immediate use. An important advantage is that the device allows physicians to decide as to which active substances and which dose are to be applied to coat the stent depending on the patient's particular situation. The SCM device consists (Fig. 5a, b) of a reusable base station, an exchangeable cartridge mounted in a drive unit within the station, a holder and a spray nozzle. The whole process takes place within the cartridge which is placed in the station. A catheter with a stent at the front end is fitted into the cartridge. The cartridge can be sealed in a sterile manner during the stent coating to prevent contamination. A transport carriage is connected with the spray nozzle and moves on the longitudinal axis to spray the inserted stent. Furthermore, the selected active agent is filled in a syringe which can travel simultaneously with the spray nozzle pressed by a piston. The coating process is initialized by the advancement of the drug into a mobile, positionable ring containing three jet units, which allow for uniform delivery of the drug onto the stent surface. At the end of the coating process the stent is dried by applying compressed air. The stents are usually coated with 0.5, 1.0 and 2.0% rapamycin solutions. An additional advantage of the technology is that the syringe can be replaced by a new one which contains a different pharmacological agent. Moreover, SMC provides short coating times with freshly coated stents without the need for long term storage.

The SCM was employed to coat the Yukon Choice^{DES+} stainless steel (316 LVM) stent with sirolimus in the absence of polymer. In the Yukon platform the stent surface contains micro-pores to enable adsorption of various active substances. The coating solution fills the pores by creating a uniform layer after evaporation of the solvent. Clinical studies carried out to evaluate the safety and efficiency of these polymer free stents compared to BMS [43, 133] of polymer

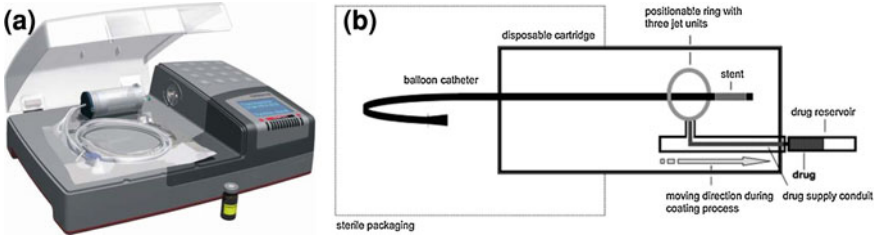

Fig. 5 **a** The Yukon Stent Coating Machine (courtesy of Transluminal GmbH), **b** Schematic overview of the Yukon disposable stent cartridge holding a premounted microporous stent (with permission from [133]

coated stents (Byme et al. 2009; [72]. Patients were treated with commercially available permanent-polymer (Cypher and Taxus stent) and polymer-free (Translumina). The results showed an ongoing late luminal loss (LLL) beyond 6–8 months after the index procedure was observed following DES implantation with 0.12 ± 0.49, 0.17 ± 0.50, 0.01 ± 0.42, and 0.13 ± 0.50 mm in permanent-polymer RES, polymer-free RES, and permanent-polymer PES groups, respectively. The absence of permanent polymer from the DES platform appeared to militate against this late reduction in antirestenotic efficacy [14].

In another randomized clinical trial [72] patients received polymer-coated rapamycin-eluting stents (Cypher, Cordis) and nonpolymer rapamycin-eluting stents (Yukon, Translumina) to examine neointimal thickness, stent strut coverage, and protrusion at 90 days. The mean neointimal thickness for the polymer-coated rapamycin-eluting stent was significantly less than the nonpolymer rapamycin-eluting stent but as a result coverage was not homogenous, with >10% of struts being uncovered. High-resolution imaging allowed development of the concept of the protrusion index, and >25% of struts protruded into the vessel lumen with the polymer coated rapamycin-eluting stent compared with <5% with the non polymer rapamycin-eluting. Nevertheless, the placement of polymer-free stents coated on-site with rapamycin was proved feasible and safe with a dose-dependent efficacy in restenosis prevention.

3.2.2 Ultrasonic Atomizing Spray Coating

The usage of ultrasonic atomizing spray nozzles is an innovative approach to deliver continuous and uniform stent coatings (Fig. 6). This is a technology developed by Sono-Tek Corp. (New York, US). There are two principal ultrasonic nozzle designs [9, 58] that can be used for stent coating (Fig. 7a–d). Both designs rely on the use of a high frequency ultrasonic atomizing nozzle combined with a low-pressure gas stream to shape the low velocity drops into a narrow, soft spray beam. The operating frequency of both designs is approximately 120 kHz. In the first design (nozzle A—AccuMist Stent) compressed gas, typically at 1 psi, is introduced into the diffusion chamber of the gas shroud, which produces a

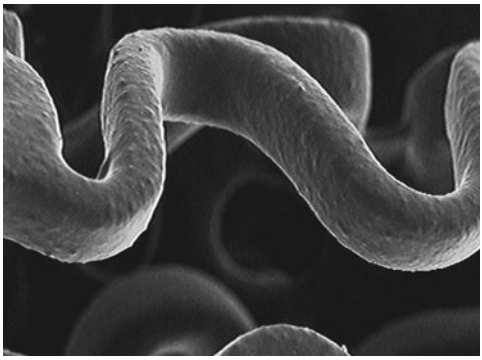

Fig. 6 Drug loaded coated stent by ultrasonic atomization spray (courtesy of Sono-Tek Corp)

uniformly distributed flow of air around the nozzle stem**.** The ultrasonically produced spray at the tip of the stem is immediately entrained in the gas stream. An adjustable focusing mechanism on the gas shroud allows complete control of spray width. The spray envelope is conical with a slight bow or hourglass shape and by moving the focus-adjust mechanism the width of the bow can be manipulated to optimize the spray pattern. The distance between nozzle and substrate varies from a few millimetres to approximately a few centimetres. The narrowest beam diameter achievable at the focal plane is approximately 1.75 mm and the median diameter from 13–70 μm.

The second design (nozzle B—MicroMist Nozzle) delivers feeding liquid to the atomizing surface through an externally mounted isolated hypotube. The gas is fed through the nozzle orifice and the gas stream creates a very narrow spray beam of about 0.5 mm. An important feature of this nozzle design is that the liquid feed is external and completely isolated from the nozzle vibrations up to the time that atomization occurs. As a result, high degree of spray stability and a greater degree of reproducibility from one spray cycle to the next is achieved. The size of the produced microdroplets depends on the operating frequency, varying from 13–38 μm. The droplets achieved with ultrasonic spray have a very tight drop distribution size, allowing better penetration of complex stent geometries and therefore more uniform coverage of all strut surfaces.

Unlike pressure nozzles, ultrasonic nozzles allow for independent control of flow rate, spray velocity and drop size. Very low flow rates can be achieved while maintaining a high degree of repeatability and without compromising spray performance. These tighter process controls maximize the effectiveness and quality of production volume stent coating processes.

Ultrasonic atomization can take place when a liquid film is placed on a smooth surface that is set into vibrating motion perpendicular to the surface. The liquid *d* absorbs some of the vibrational energy, which is transformed into capillary waves. The ampltitude of the vibrations is increased until acritical amplitude is eventually reached. At this point the capillary waves collapse and liquid droplets are ejected from the nozzles of the degenerating waves normal to the atomizing

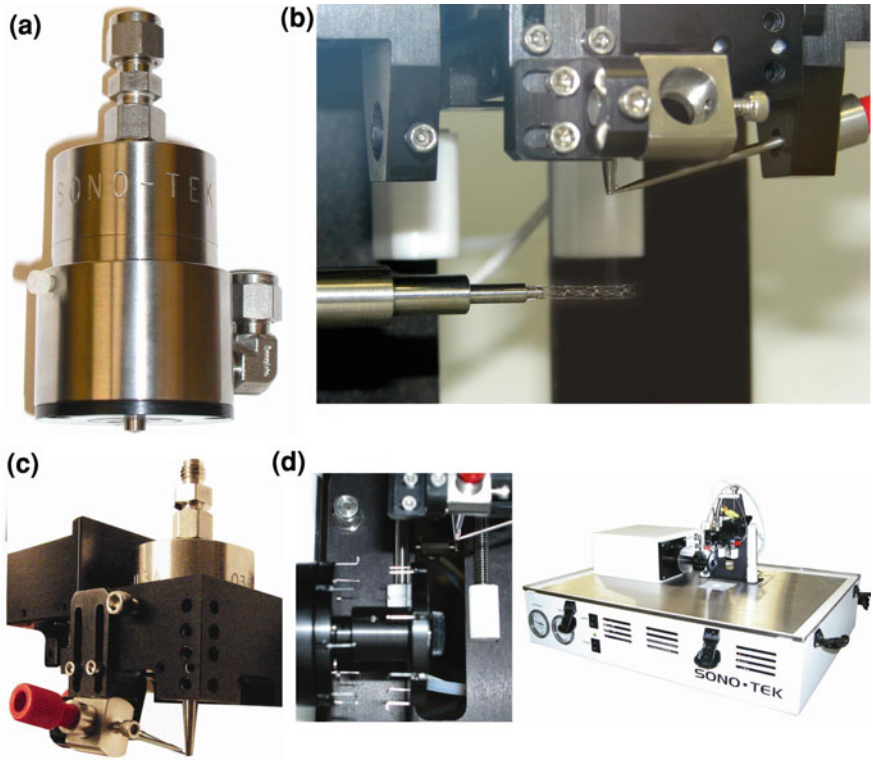

Fig. 7 **a** Accoumist nozzle configuration, **b** micromist nozzle configuration, **c** micromist stent coating process, **d** medicoat sinus coating device used for stent coating (courtesy of Sono-Tek Corp)

surface. The number median drop diameter ($D_{N,0.5}$) is inversely proportional to the vibration frequency (f) to the two-thirds power according to Eq. (1):

$$D_{0.5} = 0.34\left(\frac{8\pi\sigma}{\rho f^2}\right)^{1/3} \tag{1}$$

where σ is surface tension of the liquid, and ρ is its density. As a result, the droplets formed in this atomization process exhibit a mathematically defined size that is based on the kHz of a given nozzle. The vibrational energy of the nozzle provides inherent non-clogging benefits as agglomerated particles are broken up during the atomization process and solutions are kept homogenously mixed during the coating process, further improving uniformity and functionality of coatings on small surfaces.

In a typical experimental setup the sprayed liquid consists of the polymer/drug system dissolved in a suitable organic solvent (e.g. THF, acetone, DMAC, toluene, chloroform) and diluted to approximately 0.5–2% by weight. Preferably, high

vapour pressure solvents are used to facilitate the drying process. By varying rotational speed, distance of the spray from the stent, and number of traverses (and therefore flow rate), a process can be optimized to produce the best coatings and maximum material transfer efficiency. In some instances stent coating is conducted in a nitrogen environment due to the better liquid flow characteristics such as lower surface tension of the liquid as it contacts the stent surface.

Ultrasonic spray coating has been reported in several studies of coated stents. A parylene C-primed Driver stent (Medtronic Inc., US) was coated using ultrasonic spraying [120] with a blend of newly synthesized polymers (n-butyl methacrylate, N-vinyl pyrrolidinone and n-hexyl methacrylate and zotarolimus (65/35 w/w). The cytotoxicity and porcine coronary artery model studies conducted by Udipi et al. showed robust coating and flexibility along with excellent zotarolimus deliverability. Studies of cumulative elution over a 28-day period have shown that an initial burst of drug is released from the drug–polymer complex over the first 48 h which slows asymptotically to a sustained release rate over subsequent weeks (Fig. 8). The results were also confirmed by-*vivo* studies.

In another study 316L stainless steel stents were coated with curcumin and PLGA at three different doses by ultrasonic spray [84]. Surface morphology studies showed that the coating was very smooth and uniform without cracks or webbings between struts but also had the ability to withstand the compressive and tensile strains (absence of delamination or destruction) imparted without cracking from the stent during the expansion process. After loading curcumin in the PLGA coating, the roughness of the stent was greater than for the PLGA-only-coated stent, with an average roughness of curcumin-eluting stent about 0.55 nm. However, no drug particles can be seen on the stent surfaces from the SEM and AFM images indicating that curcumin can be mixed with PLGA at the molecular level using an ultrasonic atomization spray method. The same researchers (Pan et al.) developed rapamycin/curcumin-loaded PLGA (poly(d,l-lactic acid-co-glycolic acid)) stents by using again ultrasonic atomization in another study [85] to obtain again fine coatings without any webbings and "bridges" between struts. Recently, [86] developed an emodin/PLGA eluting stent by using ultrasonic atomization

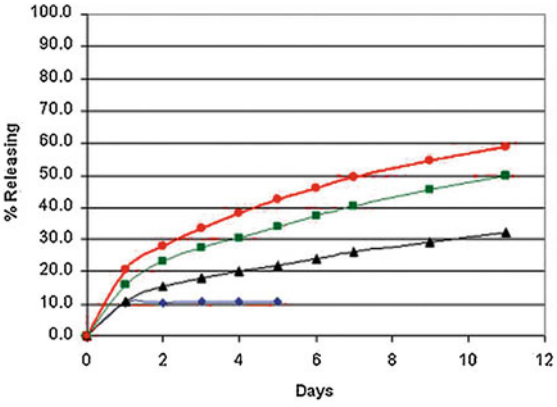

Fig. 8 Elution profiles of zotarolimus drug from coatings based on C10 (◆) and C19 (■) polymers and C10:C19 (30:70) (▲) and C10:C19:PVP (27:63:10) (●) polymer blends (with permission from Udipi et al. 2007)

similar to the MediCoat^{TM}PSI. Although the surface analysis of the emodin coated stents showed rough surface due to drug polymer incompatibility, the coatings retained their physical integrity after balloon expansion tests.

3.2.3 ElectroNanospray

ElectroNanospray^{TM} (ENS) is a proprietary Nanocopoeia's Inc. Technology that produces precise, ultra-pure nanoparticles varying from 2–200 nm. This technology [24] allows coating of polymer and pharmacological agents on the surface of stents. ElectroNanospray^{TM} technology operates in a 'cone jet' mode and produces airborne nanoparticles from a solution or colloidal suspension of drug loaded nanoparticles to target and coat stent struts. A device comprises of a syringe pump is used to feed the solution in microcapillary tubes exposed to high electric field. The field is established between the tip of the capillary, and the stent that is grounded or oppositely charged. The applied voltage creates non-uniform electric field causes the liquid meniscus to form a conical shape created by the balance between the surface tension force and the electrical force on the cone. The sprayed particles are fragmented due to the instability of the liquid jet and form positively charged nanoparticles that repulse each other in the gas phase facilitating solidification as discrete nanometer-sized objects. The produced particles are highly uniform and the spraying device can process a broad range of chemical and biological agents irrespectively of the solvent phase. Preliminary coating studies carried out with polyisobutylenepolystyrene (*arb*IBS) block copolymer and sirolimus sprayed on a stainless steel stent surface by ENS. Real-time imaging analysis showed that the smooth film has a highly mobile drug phase consistent with nano-sized particles. It was also observed that nanoparticles from domains with higher drug concentrations contribute to the initial burst release.

3.3 Plasma Coatings

Chemical vapour deposition (CVD) is a state of the art chemical process used to produce high purity and performance solid materials. The CVD process is often used for the fabrication of thin films of integrated circuits in the semiconductor industry. When the process involves thin film deposition from a gas state to a solid state on a substrate is called plasma-enhanced chemical vapour deposition (PECVD). The aim of the process is to use gaseous agents of the deposited elements through the creation of a plasma (ionized gas) that promotes chemical reactions on the substrate surface. Typically, PECVD of inorganic materials requires high temperatures and/or high powers to generate the appropriate electric field. However, polymer CVD approaches have also been reported to modify surfaces with thin coating of insoluble polymers such as methacrylate polymers [15] or other electrically conductive polymers [6]. Plasma coatings have been

employed as an alternative coating technology for DES either with inorganic materials or organic polymers especially in case where solutions cannot be used. It is out of the scope of this chapter to emphasize the PECVD process and the technology as it can be found elsewhere [10, 11]. However, a few details of the processing will be described in the various approaches below.

3.3.1 Silicon Carbide Coatings

Silicon carbide SiC is an amorphous n-doped hydrogenated semiconductor and it appears to be a promising material to improve the biocompatibility of metal stents [1, 121]. It is well know for the antithrombogenic properties including reduced platelet deposition, leukocytes and monocytes after stent coating [71, 94]. It is known that blood proteins adsorb at the surface of BMS to induce thrombosis due to degradation. One of the main reaction mechanisms is the interaction of fibrinogen which decomposes into fibrin monomers on the metal surface. As a result an electron transfer process from fibrinogen to the stent surface induces the release of fibrinpeptides and thrombus formation.

A method called PROBIO® coating, developed by Biotronik (Germany), utilises the PECVD technique [41] to deposit a thin film ($\sim$80 nm) to coat a variety of metal stents such as stainless steel, nitinol (Astron®) and super alloy cobalt chromium (L-605, PRO-kinetic). In the case of silicon carbide the cracking components, consisting of silane (SiH_4), methane (CH_4) and phosphine (PH_3), are chemically activated and bound to the surface. The activated molecules react at the stent's surface to form a-SiC:H film which covers completely the struts and hides the underlying stent surface. The application of the silicon carbide coating prevents the diffusion of nickel (90% compared to uncoated stents) and other substances into the blood and surrounding tissue [93]. In addition SiC coatings improve hemocompatibility and endothelialisation. The SiC stents developed by Biotronik are not DES and clinical trials showed mixed results. In a 6-month clinical follow up the SiC stents showed the presence of endothelialisation [49] while in a latter study a greater neointimal hyperplasia was observed [114]. Further to this, a comparison between SiC stents with 316L NIR stents (Boston Scientific, US) concluded low rate of major adverse coronary events with no explicit superiority [1, 122]. Thus, the development of DES with inorganic coating is a prerequisite for superior clinical outcomes as described next.

3.3.2 Diamond-like Carbon

Diamond-like carbon (DLC) is another promising coating that has attract attention as candidate for thromboresistant coating on metal stents due to its high hardness, low frictional coefficient chemical inertness, high electrical resistivity, excellent smoothness and especially for the tissue biocompatibility [91].

A uniform coating of the inner and outer stainless steel surface with DLC by a specially developed plasma-induced cold deposition technique (PICDT) was

introduced from PlasmaChem GmbH (Germany) to develop a DLC stent called BioDiamond® DLC. This approach provides high quality ultra-thin (50–150 nm), uniform coating which is extremely sturdy, smooth and flexible. By overcoming the Faraday cage effect the PICDT technology allows the generation of diamond-like surfaces (Fig. 9) in the inner lumen of the stent compared to other sputtering/plasma approaches. As a result the diamond-like coated surface of the BioDiamond stent builds up a barrier against the heavy metal ions diffusion of nickel and chromium ions into the surrounding tissue and the blood stream. In addition the stent is constructed for high flexibility and low recoil due to the "Flexible" and "Dense" segments (F- and D-segments) were F-segments are responsible for stent's flexibility and D-segments for high stability after expansion. The BioDiamond®. DLC stent presents another two unique features. It is made from non-annealed steel which is mechanically much stronger than any annealed one which allows using very thin walls (30–50 μm instead of standard 100 μm). The stent is "asymmetrically" polished thus it is much thinner in the middle as at both ends thus it begins to open from the middle not from the ends as any other stent and provide no "thorn trauma" by end-pins. The next generation of BioDiamond® family stent is the DES BioDiamond®-TRIO where drug layers, separated by ultra-thin biodegradable membranes, are assembled onto DLC platform. Such approach allows the "programmed" sequential release of different drugs.

A Biodiamond stent includes four coating layers consisting of a first adhesive layer that binds on the stent, a second semi elastic layer that absorbs any mechanical or thermal expansion stress, a third DLC layer and finally a biocompatible anti-thrombogenic heparin-like, top-layer, which comes in direct contact to the blood/tissue. In vitro studies demonstrated that there is a remarkable reduction of thrombogenic potential and increase of the time until stent occlusion (TSO) by the addition of the heparin coating. The top-layer is also loaded with a water soluble antibiotic that is delivered within a few hours in the artery walls. The rationale behind this approach is to take an advantage of the deep cracks formed in the vessel walls during the stent implantation. These cracks are consider as "transporting channels" to deliver the water soluble drug deep into the vessel wall (Adventium) which is responsible for restenosis but which is normally is not approachable for eluted drug. After few hours these channels are healed and

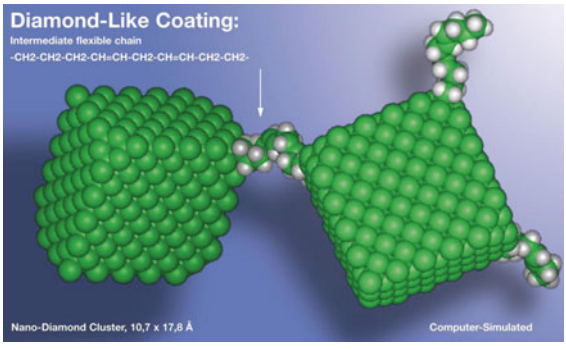

Fig. 9 Three dimensional structure of Diamond Like Carbon (courtesy of PlasmaChem GmbH)

closed. After relatively rapid release of the top-layer, the under-layer which is loaded with a lipophilic drug is activated to initiate slowly release of the second drug. In a model study on mini-pigs with over-stretched vessels it was shown that the application of a second layer is approximately 30–40% more effective compared to a single layer of a lipophilic drug (PlasmaChem unpublished data).

5The presence of the DLC layer inhibits the release of cytotoxic and allergenic heavy metal ions from metal surface resulting reduced thrombogenicity [37] and enhanced biocompatibility [117]. The clinical trial results indicated that major adverse cardiac events (MACE) were significantly reduced with DLC stents in 6 months follow-up and no acute thrombosis or restenosis could be observed [5].

The Janus tacrolimus-eluting Carbostent™ system (Sorin Biomedica, Italy) is a unique DES coated with a Carbofilm™ coating that imparts excellent biocompatibility and thromboresistance [4]. The metal stent has multiple reservoir grooves or sculptures on the external surface loaded with tacrolimus. A thin carbon film is applied by triode sputtering vacuum deposition at relatively low temperature [123]. In the triode sputtering device, an ionization chamber generates a plasma beam of an inert gas containing positively charged ions of high energy. The carbon atoms sputtered from the pyrolitic turbostatic carbon source by the bombarding ions of the plasma beam are deposited on the stent surface. To avoid exposure to high temperatures generated from the plasma, the stent is insulated from the ionization chamber. Tacrolimus is loaded into the reservoirs by a melting process without the need for a polymeric coating [119]. The drug is protected under the sculptured stent design and variable dose distribution is achieved by filling the sculptures with different amount of drug(s). Animal studies showed 50% release of tacrolimus in a month and maximum artery concentration in the first few days. In Jupiter I clinical trials the Janus Carbostent™ demonstrated reduced neointinal proliferation and inflammation [4, 73].

3.3.3 Plasma Polymerized Polymer Coatings

Recent developments of plasma enhanced chemical vapor deposition (PECVD) revealed the applicability of the technology on stent coating. This method has been reported for parylene and its derivatives know as poly(para-xylylene) [31]. Parylene has found several applications as conformal insulator and especially as a sub-coating on Cypher® stent. This is Class IV polymer with excellent biocompatibility and negligible toxicity. The advantages of PECVD technology include the formation of substrate independent, dry and smooth thin organic layers on the stent surface. Early plasma polymerization studies of 2-chloroparacyclophan showed a decrease of platelet adhesion at 20% compared to 85% of the BMS [57]. The ultra thin polymeric coating was further treated with sulfur dioxide plasma to obtain a more hydrophilic surface and new functional groups. In a latter study, a radio-frequency plasma polymerization process, with oxygen as the carrier gas to deposit poly-butyl methacrylate (PPBMA) on a 316L stainless steel stent surface [140]. The coated stents showed improved blood compatibility with reduced

platelet adhesion. The PPBMA coating was found intact and strong enough to withstand external forces after stent expansion.

A smart approach of PECVD coating involves protein immobilization or other biomolecules by covalent attachment onto the stent polymer coated surface. In a recent study tropoelastin was immobilized on a stainless steel surface [139]. Tropoelastin is an extracellular matrix protein and a precursor of elastin that mediates endothelial cell growth and regulates smooth cell infiltration. A thin acetylene film was plasma polymerized on stainless steel surfaces and a horseradish peroxidase was used as a probe to covalently attach tropoelastin. The results showed improved biocompatibility by promoting endothelial cell attachment and proliferation relative to uncoated stainless steel and polymerized controls. The experimental findings of this study clearly indicate that immobilization of biomolecules on stent surfaces is feasibly.

In a latest study, pulsed plasma polymerization of polymeric allylamine (P-PPAm) was employed to coat stainless steel stents and prepare heparin immobilized strut surfaces [7]. Polymeric P-PPAm possesses high density of primary amine groups which can facilitate covalent immobilization with biomolecules. On the other hand, heparin is a strong anticoagulant and antithrombotic molecule that can successfully improve stent hemocompatibility [129]. The plasma polymerization process was further developed though a negative bias voltage to improve the cross linking degree. In addition, NH_3 was mixed with allylamine vapour as a precursor gas to compensate the decrease of amine groups caused by the vacuum thermal treatment. Coated allylamine films showed high density of amine groups, resistance in hydrolysis and resistance on stent expansion. The films were sufficiently flexible and no cracking or peeling was observed. The in vitro hemocompatibility was assessed by estimating the hemolysis ratio (<1%) and platelet adhesion which was remarkably reduced. Further evaluation was followed by implanting bare 316L SS disks and Hep–Th–P-PPAm coated disks in dog for 30 and 90 days. The results indicated that the heparin-immobilized P-PPAm surface successfully inhibits thrombus formation by growing a homogeneous and intact shuttle-like endothelium on its surface.

3.4 Electrostatic Stent Coatings

3.4.1 Electrostatic Dry Powder Deposition

The electrostatic application of powder material is already know. Methods have been developed in the fields of electrophotography, electrography, paintings and plastics. This approach has been applied to coat DES by depositing a dry polymeric layer on the stent surface followed by fusion to produce a uniform and smooth layer. Some of the advantages of the electrostatic application are the ability to coat both the luminal and abluminal surfaces, accurate and reproducible deposited amounts or multiple coating layers to create a specific release profile.

The active substances ca n be applied in a separate layer or with the polymeric material as a blend or encapsulated microparticles. However, the technology is limited by the heat resistance of the active substance especially when elevated polymer fusion temperatures are required.

A novel electrostatic dry powder deposition technology (EDPDT) has been developed by Phoqus Pharmaceuticals Ltd. (UK) [38]. The technology can be used for any stent type as metal substrates present high conductivity. The powder material is electrostatically charged while an electric field of the same potential is present in the region between the stent and the coating device. According to this platform the powder particle size should be in the range of 10–20 μm. Usually the electrostatic charge is applied by triboelectric charging or corona charging and the electric field is provided by a bias steady DC voltage. Further development of the electric field is achieved by superimposing of an alternative voltage. The stent is placed in a distance of 0.5–5 mm from the charged powder. Once the stent is placed at a fixed position at earth potential the bias voltage (1–2 kV) generates an electric field between the stent and the dry powder. The powder is then driven onto the stent surface by the interaction of the electric field and builds up an electric charge by reducing the field. The coating process continues until the electric field is so small that the driving of the powder on the stent surface is substantially terminated. At the end of the coating process the dry powder is converted into a coherent film by heating using infrared radiation or convection heating.

Recently, the EDPDT was introduce to coat bare metal Cypher® stents with sirolimus encapsulated polymeric microspheres [77]. The aim of this study was to compare the EDPDT coated stent with the commercial Cypher® in terms of dissolution patterns and hemocompatibility. In contrast to Phoqus coating methodology, a spray gun (Sure Coat®, Nordson Ltd. UK) is used for the coating studies. By regulating operating parameters such as voltage, atomizing air flow rate, and coating times the rapamycin polymeric microparticles are coated on the stent surface. The applied voltage generates a high-strength electrostatic field between the electrode in the nozzle and the grounded stent. An electrically charged cloud is then created by spraying the microparticles. A continuous and uniform layer is formed by applying infrared radiation at 80–100°C.

Microparticles were prepared by a supercritical aerosol solvent extraction system (ASES) using a combination of supercritical N_2 and CO_2 fluids. Optimization of the ASES process produced particles with 2.5–3.5 μm and high sirolimus drug loading (DL) of 28–30%. ASES provided microparticles free of emulsifiers and negligible residual solvents. By applying the appropriate coating, the authors were able to present coatings with thickness of 6.2 μm interestingly, the fusion temperatures did not have an effect on sirolimus structure and no isomeric transformation was observed after ^{1}H NMR studies. The EDPDT approach gave similar release patterns to Cypher® stent even in the absence of a topcoat (Fig. 10). However, the most important finding of this study was the reduced platelet adhesion of the EDPDT coated stents similar to the commercial product. These results suggesting that EDPDT could efficiently used for the development of DES.

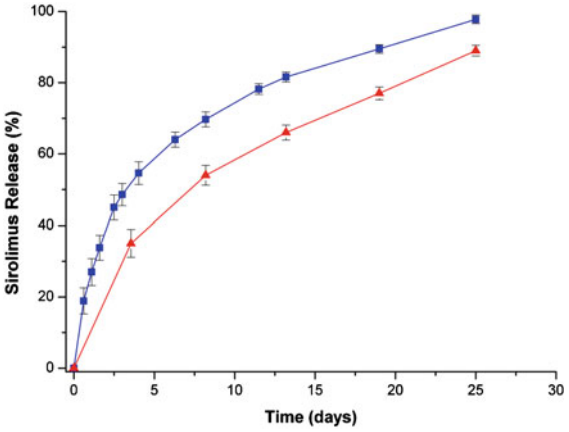

Fig. 10 Release profiles of EDPDT-coated (■) and Cypher® stents (▲), respectively, n = 3 (with permission from Nukala et. al 2009)

3.5 Ink-jet Coating

In the last decade, ink-jet printing technology has being used in a wide range of manufacturing applications such as electrical,optical, sensors, medical diagnostics, drug delivery and packaging [130]. Although ink-jet technology is know for the use in office printers, the controllable microdespensing of fluids renders it attractive for coating applications on medical devices. The main feature of the technology is the production of controllable and reproducible droplets in a jet stream that can be directed to exact locations on the stent surface. Thus, it can be advantageous especially for DES where the active substances are very expensive and the wastage should be negligible. Ink jet technology produces very complex coatings that could be multilayer, with different drug and polymer solutions in each layer. The layer thickness can be varied to produce different release kinetics at different locations along the stent. Ink jetting can tightly control and maintain dug concentration on the luminal surfaces crating a fine layer without webbings or bridges.

The ink jet technologies fall in two main categories called continuous mode and demand mode. In the continues mode, the pressurized fluid is forced through an orifice (50–80 μm diameter) to create a liquid jet that breaks up in small droplets due to surface tension (Rayleigh instability). The application of a single frequency disturbance to the jet, at the correct frequency, generates droplets of reproducible size and velocity. The disturbance is amplified by a piezoelectric dispenser that creates pressure oscillations in the fluid. To control the droplet uniformity and size an electrostatic field is created through a chargeable electrode. The electrode is located near the orifice and induces a charge on the produced droplet by applying a high voltage. This type of ink-jet printing is called “continuous” because the droplets are continuously produced with various trajectories depending on the applied charge. The droplets are formed in 80–100 kHz with a particle size from 20 to 150 μm.

In the drop-on-demand ink jetting the fluid is maintained at ambient pressure and the piezoelectric transducer produces a drop only when needed. The

transducer creates pressure waves through volumetric changes in the coating fluid. The pressure waves travel to the orifice and then are converted to fluid velocity that creates an ejected droplet from the orifice [2, 23]. In this mode the formed droplets have a particle size diameter similar to the orifice that varies from 20 to 120 μm while the operational frequency is in the 4–12 kHz range.

A continuous mode ink jetting was applied to coat zotarolimus (ABT-578) and phosphorylcholine-linked methacrylate tetracopolymer (PC polymer) on a stainless steel stent [116]. The stent was placed on a rotatable mandrel and the jet stream was positioned to be tangent to the cylindrical surface that passes through the centre of the strut thickness. The authors used an "off-axis" and "on-axis" coating technique to avoid tight dimensional tolerances and part to part exactness in positional accuracy. The jetting nozzle produced droplets of 60–70 μm when isobutanol was used as solvent and 50 μm for ethanol. The stent rotated around its longitudinal axis and translated along its length to create helical patterns. By using ink jet coating an accurate amount of 100 μg ABT-578 (± 0.6 μg) was loaded on the stent surface with a yield efficiency of 91% (± 2%). To demonstrate the capability of the ink-jet technology, a stent was totally coated by the same group with paclitaxel-PC solution containing coumarin. The same stent was coated only on the struts wrapping towards the right using a solution containing rhodamine red. In this way individual drops were dispensed at the desired locations and the stent was coated with different drug amounts per unit area (for details see, http://www.microfab.com/techtexolowanology/biomedical/Stents.html).

The ink jet coating technology was applied to coat the Medstent™, paclitaxel DES made by Conor Medsystems (Palo Alto, US) [27]. A polymer/drug solution consisted of polylactide co-glycolide (PLGA) and palcitaxel was shot through a piezoelectric microdispenser with a 40 μm orifice on a special designed stainless steel stent. Two biodegradable PLGA grades with lactic acid to glycolic acid ratios of 50:50 and 85:15 were dissolved at 5% for PLGA 85:15 and 10% for PLGA 50:50, while paclitaxel concentrations varied from 1–3%. This unique stent design (Fig. 11) presents ductile hinges that connect the stent struts to sinusoidal "bridges". The ductile hinges carry the stent deformation during the balloon expansion and the struts do not deform. The struts act as passive elements and hence can be cored with holes or cavities for drug delivery without affecting the strut strength. The passive struts can be filled with drug containing polymers in various configurations to control the release kinetics. For example, different lactic acid/glycolic acid ratios, polymer top coats, number of layers layer thickness or even solvent were found to influence kinetics. Paclitaxel kinetics were chosen to simulate first and zero order release kinetics where 60% (95 μg total) of the drug was release in 24 h and the rest by 15–20 days.

Clinical studies were undertaken to evaluate CoStar in humans using six different formulations. In the PISCES (paclitaxel in-stent controlled elution study) [100] clinical study patients ($n = 244$) with de novo lesions received BMS or one of the six formulations. The formulation varied on paclitaxel dose, duration of elution ad directionality (bidirectional or monodirectional abluminal). In the 6 months follow-up, no improvement was observed for a period of 10 days over BMSs. The

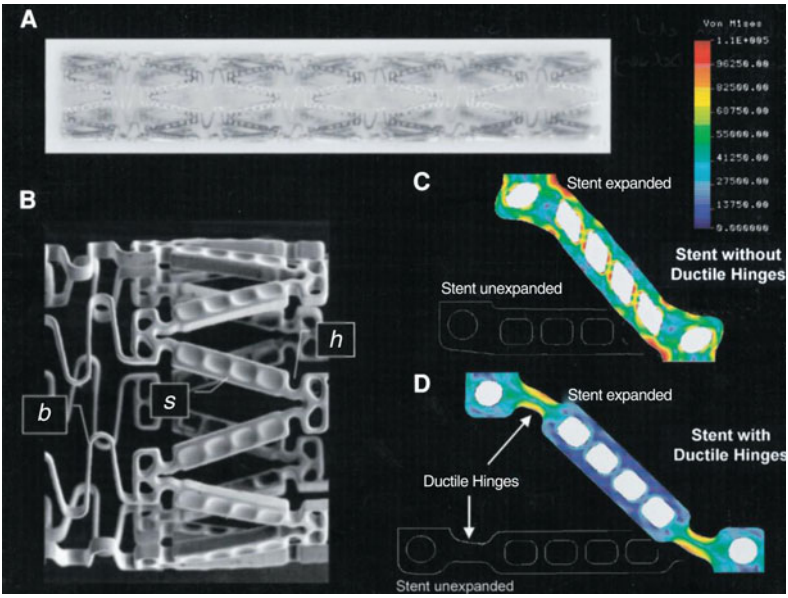

Fig. 11 **A**, 3/15 mm Conor stent metallic backbone. **B**, SEM of section of stent. *s* indicates struts with laser-cut holes, two thirds of which are filled PLGA polymer inlays; *h*, ductile hinges, and *b*, sinusoidal bridges. **C** and **D**, Finite element analysis of diameter expansion of stents with honeycombed struts without (**C**) and with (**D**) ductile hinges. Stent unexpanded (black and white) and stent expanded (color). Color-coded units are Von Mises shear stress (with permission from [27]

directionality of paclitaxel release did not show any significant effect and the superior inhibition of neointimal hyperplasia was attributed to the longer release duration.

The ink jet coating technology was applied to Conor/CoStar® stent (Cobalt chromium) a later version of the Medstent™ platform. Clinical studies on the Costar stent named EuroSTAR (European Cobalt Chromium Stent with Antiproliferative for Restenosis Trial), concluded equivalent results to the current DES [98]. The Conor reservoir platform was acquired by Cordis in 2007 to develop the NEVO™ drug eluting stent. NEVO™ contains sirolimus as the pharmacological agent that can be released in various patterns (multiple bi-directional and multiple or single luminal). This reservoir design (Fig. 12) allows drug delivery from a stent with a surface that is 75% bare metal upon insertion and which becomes purely bare metal following drug delivery and polymer bioresorption in approximately 3 months.

In a recent 6 months randomized clinical trial [81], the NEVO sirolimus-eluting coronary stent had significantly lower in-stent late lumen loss compared to Taxus Liberte®. Specifically, late lumen loss was reduced by 64% in the NEVO arm as compared to the Taxus Liberte® arm (0.13 mm compared to 0.36 mm, $p < 0.001$). In-stent late lumen loss, which is tissue growth within a stent, reduces the diameter

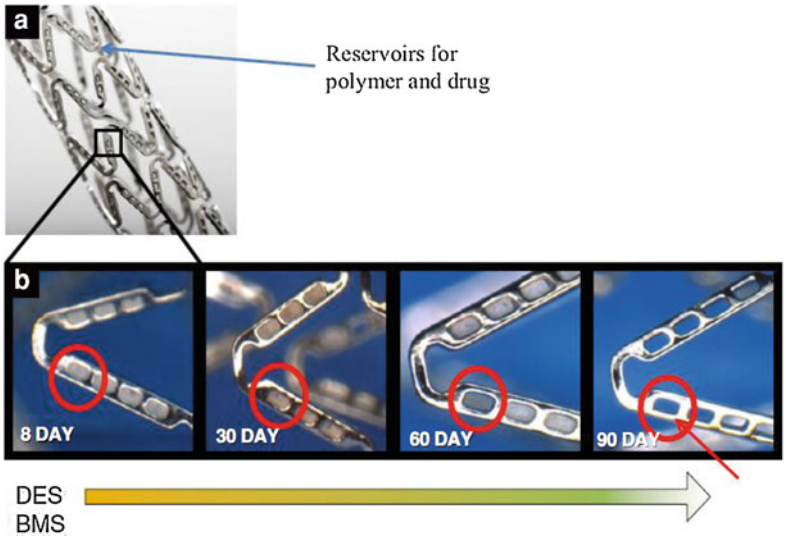

Fig. 12 **a** The NEVO cobalt chromium stent, which has an open-cell design and unique reservoirs that contain a biodegradable polymer and sirolimus mix that **b** completely biodegrades within 90 days (with permission from Garg and [97]

of the lumen thus restricting blood flow through the stent and can potentially lead to major adverse coronary events, also known as MACE. In addition, NEVO also showed superior angiographic results to the Taxus Liberte® Stent in reducing restenosis at 6 months. Angiographic restenosis was reduced 86% (1.1% in the NEVO arm compared to 8.0% in the Taxus Liberte arm, $p < 0.002$). NEVO also reduced the incidence of MACE (major adverse coronary events) by more than 40% compared to the Taxus Liberte stent (4.1 vs. 7.0%, respectively; $p = 0.226$) and presented lower rates of events with respect to target lesion revascularization (1.6% for NEVO vs. 3.2% for the Taxus Liberte stent; $p = 0.33$)

3.6 Electrochemical Deposition (Electrocoating)

Electrocoating is another process that has been reported for stent coating. This electrochemical process requires a conduction surface such as stent for deposition of the desired material. More specifically, stent coating can be achieved by electropolymerization which engages the electrochemical oxidation of a monomer, such as pyrrole or phenol, resulting the deposition of an organic polymer coating on the metal surface. This coat can be conducting or insulating depending on the polymer that is formed. This is a relatively new approach for stent coating and there a few studies reported up to date.

Recently Shaulov et al. [102] reported an electrochemical reduction of 4-(2-bromoethyl) benzenediazonium tetrafluoroborate (BrD) on a SS stent and the

formation of a carbon–metal covalent bond. The reduction produces parasubstituted phenyl radicals that are highly reactive species and tend to bind to a wide range of metals and carbonaceous materials. In a second step, methyl methacrylate was polymerized onto the grafted surface by atom-transfer radical to form poly(methyl methacrylate) (PMMA) brushes. A drug-in-polymer matrix [poly(*n*-butylmethacrylate) (PBMA)/poly(ethylene-*co*-vinyl acetate) (PEVA)/paclitaxel] was spray coated on the polymerized layer. This covalently attached layer was found to improved significantly the drug-in-polymer matrix adhesion to the SS stent backbone providing a durable and stable DES.

In another study [60] by the same group diazonium salt 4-(1-dodecyloxy)-phenyldiazonium tetrafluoroborate (C12-phenyldiazonium) was electrocoated on stainless steel and CoCr stents. This material was applied as basecoat and found to be a superior adhesive promoter for polymeric coatings applied onto metallic stents. The electrocoated metallic stents were spray-coated with a second polymeric film of single-layer coating SIBS/paclitaxel matrix, or double-layer coating PBMA/PEVA/paclitaxel matrix. C12-phenyldiazonium was synthesized and electrocoated on metallic stents and plates to produce an insulating layer. The electrodiposition takes place through an irreversible reaction forming a covalently attached ultra thin layer ranging from 5–10 nm. In vivo and in vitro evaluation showed very good biocompatibility and absence of substantial adverse effects.

Similar electrocoating studies conducted by the same group to deposit non-biodegradable polymer coating based on N-(2-carboxyethyl)pyrrole (PPA) and butyl ester of PPA (BuOPy) [78] and blend of three different pyrrole derivatives *N*-methylpyrrole (*N*-me), *N*-(2-carboxyethyl)pyrrole (PPA), and the butyl ester of *N*-(2-carboxyethyl)pyrrole (BuOPy) [79]. These studies demonstrated that electropolymerization can be used to apply adhesive basecoats to develop durable DES but further evaluation is required to prove the clinical safety of electrodiposition.

3.7 Layer-by Layer Stent Coatings

New developments in nanotechnology have found ground for applications on coating and drug delivery of DES. In this instance thin polymeric coatings in the nanometer scale can be applied on the stent surfaces through a layer-by-layer assembly (LBL) technology. LBL technology has been used to immobilize macromolecules on stents by absorption of oppositely charged polymers and drugs [21]. Some of the advantages of LBL assemblies include easy preparation, adhesion on strut surfaces, adaptable shapes and sizes but most importantly improved biocompatibility.

An excellent example of LBL assembly is the Carmeda® Bioactive Surface (CBAS®, Carmeda AB, Sweden) heparin based surface-modification technology with clinically proved non-thrombogenicity, hemocompatibility and long term stability. In this water based process a layer by layer base matrix of a cationic amino polymer (polyethyleneimine) is absorbed to the metal surface followed by a an

anionic polymer (dextran sulfate) and another polyethyleneimine layer. Potentially, further layers are applied to optimize functional characteristics and surface coverage of the stent struts. A reactive aldehyde group of partially degraded heparin is covalently attached to the functional amino groups of the third layer. Heparin is attached by a single bond at one terminus (end point) and thus the immobilized molecules that extend from the surface into the liquid phase interact with blood components. The heparin activity of the coated stent is measured according to its ability to bind antithrombin III with high affinity and were approximately 15% of the end point-attached heparin molecules will carry the high affinity antithrombin III-binding site [42]. CBAS technology has already found application in two commercial Cordis Corp. products, the PALMAZ-SCHATZ™ Balloon-Expandable Stent and the BX Velocity® stent with Hepacoat. The BElgian NEtherlands STENT (BENESTENT) Study [101] clinical trial analyzed the outcome of elective stent implantation compared to balloon angioplasty in both large and small vessels. Despite the highly successful outcome with aggressive angioplasty and bailout stenting in this study, the relative risks of angiographic restenosis (0.54%), major cardiac events at 6 months (0.66%), and target-lesion revascularisation (0.60%) in the patients assigned clinical but not angiographic follow-up confirm the substantial superiority of stenting to angioplasty in this population. In the HOPE clinical trial [66] (HEPACOAT coating) the primary end point of stent thrombosis at 30 days occurred in 2 of 200 patients (1%): in one after blunt chest trauma and in the other in the setting of essential thrombocytosis. Major adverse cardiac events (death, myocardial infarction, target lesion revascularization, and coronary artery bypass grafting) were observed at 30 days in 5 of 200 (2.5%) patients. These clinical outcomes confirmed that heparin provides additional protection against stent thrombosis.

The LBL assemblies have been investigated by various research groups to enable naked plasmid DNA coating on heparin layers [131], immobilization of chitosan/heparin layers [68], anti-CD34 antibody functionalized multilayer of haparin/collagen [54] and plasmid pDNA coating on derivitized hyluronic acid [63].Further in vivo evaluation proved that LBL assemblies could significantly promote re-endothelialization demonstrate, inhibited neointimal hyperplasia and improved anticoagulation properties. Thus, LBL coating can be used as a robust and viable coating approach for the development of DES.

4 Conclusion and Future Aspect

Although DES have been proved beneficial in modern interventional cardiology concerns have been raised regarding their long–term safety [30]. In this chapter we describe several stent platforms including DES with biodegradable polymers, DES with non-erodible polymers, DES with inorganic coatings and DES with novel coatings. Recent trends also suggest the development of fully biodegradable polymeric or metallic stents with early promising results. Nevertheless, the science behind these new technologies should be developed and further clinical evaluation

is required. An abundance of clinical data evidently indicates the superiority of DES to bare-metal stents in reducing the rate of restenosis without increased risk for stent thrombosis. However, the polymers on the stent struts are believed to cause late-stent thrombosis, since stent struts or drug(s) alone are not likely to cause this late phenomenon. The reason is that stent struts of current DESs are usually made from the same materials used for BMSs, and the amount of the pharmacological agent(s) on the struts is generally negligible after 1 year after stenting. Hence, future developments of DES could include new bioresorbable and biocompatible polymers that can deliver new active substances or combinations of those. Reservoir DES seems to be a promising DES due to the ability to deliver multiple drugs in a specified sequence, and the ability to program the timing and spatial distribution patterns of drug release. Furthermore, DES with inorganic coatings or porous surfaces are likely to promote enhanced endothelialisation. These DES platforms could possibly address the phenomenon of late thrombosis and deliver superior clinical outcomes. Finally, the application of the previously described novel coating technologies has a noticeable effect on the coating quality and release mechanism. Coating uniformity, smoothness and thickness are fully controlled by the aforementioned technologies. Most importantly, the freedom to choose a combination of pharmacological agents at the desired dosage depending on the patient characteristics is an attractive feature for interventional cardiologists.

References

1. Acharya, G., Park, K.: Mechanisms of controlled drug release from drug-eluting stents. Adv Drug Deliv Rev. **58**, 387–401 (2006)
2. Adams, R.L., Roy, J.: A one dimensional numerical model of a drop-on-demand ink jet. J. Appl. Mech. **53**, 193–197 (1986)
3. Babapulle, M.N., Eisenberg, M.J.: Coated stents for the prevention of restenosis: Part II. Circulation **106**, 2859–2866 (2002)
4. Bartorelli, A.L., Trabattoni, D., Fabbiocchi, F., Montorsi, P., de Martini, S., Calligaris, G., Teruzzi, G., Galli, S., Ravagnani, P.: Synergy of passive coating and targeted drug delivery: the tacrolimus-eluting Janus CarboStent. Interv. Cardiol. **16**, 499–505 (2003)
5. Batyraliev, T.A., Samko, A.N., Pershukov, I.V., Niazova-Karben, Z.A., Levitskiĭ, I.V., Ozgul, S., Serchelik, A., Pia, Iu, Besnili, F., Dinler, G., Aialp, M.R.: Immediate and long-term results of implantation of the coronary stent "BioDiamond". Ter. Arkh. **74**, 57–60 (2002)
6. Baxamusa, S.H., Im, S.G., Gleason, K.K.: Initiated and oxidative chemical vapor deposition: a scalable method for conformal and functional polymer films on real substrates. Phys. Chem. Chem. Phys. **14**, 5227–5240 (2009)
7. Bayram, C., Mizrak, A.K., Aktürk, S., Kurşaklioğlu, H., Iyisoy, A., Ifran, A., Denkbaş, E.B.: In vitro biocompatibility of plasma-aided surface-modified 316L stainless steel for intracoronary stents. Biomed. Mater. **5**(5), 055007 (2010)
8. Behnisch, B., Epple, K., Einhellig, S.: Device for applying substances onto medical implants in particular stents. Patent WO2004091684
9. Berger, H.L., Mowbray, D.F., Copeman, R.A., Rusell, R.J.: Ultrasonic atomizing nozzle and method. Patent US 2007/0176017 (A1) (2007)

10. Bolz, A.: Applications of thin-film technology in biomedical engineering. In: Wise, D.L., Trantolo, D.J., et al. (eds.) Encyclopedic Handbook of Biomaterials and Bioengineering: Materials and Applications. Marcel Dekker, New York (1995)
11. Bolz, A., Schaldach, M.: Artificial heart valves: improved blood compatibility by PECVD a-SiC:H coating. Artif. Organs **14**(4), 260–269 (1990)
12. Briguori, C., Sarais, C., Pagnotta, P., Liistro, F., Montorfano, M., Chieffo, A., Sgura, F., Corvaja, N., Di Mario, C., Colombo, A.: In-stent restenosis in small coronary arteries: impact of strut thickness. J. Am. Coll. Cardiol. **40**, 403–409 (2002)
13. Burke, S.E., Kuntz, R.E., Schwartz, L.B.: Zotarolimus (ABT-578) eluting stents. Adv. Drug Deliv. Rev. **58**(3), 437–446 (2006)
14. Byrne, R.A., Iijima, R., Mehilli, J., Pinieck, S., Bruskina, O., Schömig, A., Kastrati, A.: Durability of antirestenotic efficacy in drug-eluting stents with and without permanent polymer. JACC Cardiovasc. Interv. **2**(4), 291–299 (2009)
15. Chen, G., Gupta, M., Chan, K., Gleason, K.K.: Initiated chemical vapor deposition of poly(furfuryl methacrylate). Macromol. Rapid Commun. **28**, 2205–2209 (2007)
16. Chevalier, B., Di Mario, C., Neumann, F.J., Ribichini, F., Urban, P., Popma, J.J., Fitzgerald, P.J., Cutlip, D.E., Williams, D.O., Ormiston, J., Grube, E., Whitbourn, R., Schwartz, L.B., Investigators, ZoMaxx I.: A randomized, controlled, multicenter trial to evaluate the safety and efficacy of zotarolimus-versus paclitaxel-eluting stents in de novo occlusive lesions in coronary arteries The ZoMaxx I trial. JACC Cardiovasc. Interv. **1**, 524–532 (2008)
17. Chieffo, A., Colombo, A.: Polymer-based paclitaxel-eluting coronary stents clinical results in de novo lesions. Herz **29**(2), 147–151 (2004)
18. Costa, M.A., Simon, D.I.: Molecular basis of restenosis and drug-eluting stents. Circulation **111**, 2257–2273 (2005)
19. Costa, R.A., Lansky, A.J., Abizaid, A., Mueller, R., Tsuchiya, Y., Mori, K., et al.: Angiographic results of the first human experience with the biolimus A9 drug-eluting stent for de novo coronary lesions. Am. J. Cardiol. **98**, 443–446 (2006)
20. Crown, J., O'Leary, M.: The taxanes: an update. Lancet **355**, 1176–1178 (2000)
21. Decher, G.F.: nanoassemblies: toward layered polymeric multicomposites. Science **277**, 1232–1237 (1997)
22. Deconinck, E., Sohier, J., De Scheerder, I., Van den Mooter, G.: Pharmaceutical aspects of drug eluting stents. J. Pharm. Sci. **97**(12), 5047–5060 (2008)
23. Dijksman, J.F.: Hydrodynamics of small tubular pumps. J. F luid Mech. **139**, 173–191 (1984)
24. Dong, J., Frethem, C., Haugstad, G., Hoerr, R.A., Foley, J.D., Matuszewski, M.J., Puskas, J.E.: Effect of the Coating morphology on the drug release from engineered drug-polymer nanocomposites. 31st Annual International Conference of the IEEE EMBS Minneapolis, Minnesota, USA, September 2–6 (2009)
25. Fattoria, F., Piva, T.: Drug-eluting stents in vascular intervention. Lancet **361**(9353), 247–249 (2003)
26. Faxon, D., Fuster, V.: Atherosclerotic vascular disease conference: writing group III: Pathophysiology. Circulation **109**, 2617–2625 (2004)
27. Finkelstein, A., McLEan, D., Kar, S., et al.: Local drug delivery via a coronary stent with programmable release kinetics. Circulation **107**, 777–784 (2003)
28. Finn, A.V., Kolodgie, F.D., Harnek, J., Guerrero, L.J., Acampado, E., Tefera, K., Skorija, K., Weber, D.K., Gold, H.K., Virmani, R.: Differential response of delayed healing and persistent inflammation at sites of overlapping sirolimus- or paclitaxel-eluting stents. Circulation **112**, 270–278 (2005)
29. Garg, S., Serruys, P.W.: Coronary stents: looking forward. J. Am. Coll. Cardiol. **56**(10 Suppl), S43–S78 (2010)
30. Garg, S., Serruys, P.W.: Coronary stents: current status. J. Am. Coll. Cardiol. **56**, S1–S42 (2010)
31. Gorham, W.F.: A new, general synthetic method for the preparation of linear poly-p-xylelenes. J. Polym. Sci. Part A1 **4**(12), 3027–3347 (1966)

32. Greiner, A.: Poly(p-xylylene)s (Structure, Properties, and Applications), The Polymeric Materials Encyclopedia. CRC Press, Bocca Raton (1996)
33. Grube, E., Buellesfeld, L.: BioMatrix Biolimus A9-eluting coronary stent: a next-generation drugeluting stent for coronary artery disease. Expert Rev. Med. Devices **3**, 731–741 (2006)
34. Grube, E., Hauptmann, K.E., Buellesfeld, L., Lim, V., Abizaid, A.: Six-month results of a randomized study to evaluate safety and efficacy of a biolimus A9 eluting stent with a biodegradable polymer coating. EuroIntervention **1**, 53–57 (2005)
35. Grube, E., Silber, S., Hauptmann, K.E., Mueller, R., Buellesfeld, L., Gerckens, U., Russell, M.E.: TAXUS I: Six- and twelve-month results from a randomized, double-blind trial on a slow-release paclitaxel-eluting stent for de novo coronary lesions. Circulation **107**(1), 38–42 (2003)
36. Gruentzig, A.: Transluminal dilation of coronary artery stenosis. Lancet **1**, 263 (1978)
37. Gutensohn, K., Beythien, C., Bau, J., Fenner, T., Grewe, P., Koester, R., Padmanaban, K., Kuehnl, P.: In vitro analyses of diamond-like carbon coated stents. Reduction of metal ion release, platelet activation, and thrombogenicity. Thromb. Res. **15**, 577–585 (2000)
38. Hallett, M.D., Whiteman, M., Stringer, I.J., Green, L.: Coating of surgical devices. Patent WO/2005/014069. (2005)
39. Hanefeld, P., Westedt, U., Wombacher, R., Kissel, T., Schaper, A., Wendorff, J.H., Greiner, A.: Coating of poly(p-xylylene) by PLA-PEO-PLA triblock copolymers with excellent polymer-polymer adhesion for stent applications. Biomacromolecules **7**(7), 2086–2090 (2006)
40. Hara, H., Nakamura, M., Palmaz, J.C., Schwartz, R.S.: Role of stent design and coatings on restenosis and thrombosis. Adv. Drug Deliv. Rev. **58**(3), 377–386 (2006)
41. Harder, C., Rzany, A., Schaldach, M.: Coating of vascular stents with antithrombogenic amorphous silicon carbide. Prog. Biomed. Res. **4**, 71–77 (1999)
42. Hardhammar, P.A., Beusekom, H.M.M.V., Emanuelsson, H.U., Hofma, S.H., Albertsson, P.A., Verdouw, P., Boersma, E., Serruys, P.W.: Reduction in thrombotic events with heparin-coated Palmaz–Schatz stents in normal porcine coronary arteries. Circulation **90**, 423–430 (1996)
43. Hausleiter, J., Kastrati, A., Wessely, R., et al.: Prevention of restenosis by a novel drug-eluting stent system with a dose-adjustable, polymer-free, on-site stent coating. Eur. Heart J. **26**, 1475–1481 (2005)
44. Hofmann, H., Neftel, F., Piveteau, L.D.: Reinforced porous coating. Patent WO2007/0311972 (A1) (2007)
45. Hurst, J.W.: The first coronary angioplasty as described by Andreas Gruentzig. Am. J. Cardiol. **57**, 185–186 (1986)
46. Hwang Chao-Wei, A.B., Wu, D., Edelman, E.R.: Impact of transport and drug properties on the local pharmacology of drug eluting stents. Int. J. Cardiovasc. Interv. **5**, 7–12 (2003)
47. Hwang, C.W., Wu, D., Edelman, E.R.: Physiological transport forces govern drug distribution for stent-based delivery. Circulation **104**, 600–605 (2001)
48. Joner, M., Finn, A.V., Farb, A., Mont, E.K., Kolodgie, F.D., Ladich, E., et al.: Pathology of drug-eluting stents in humans: delayed healing and late thrombotic risk. J. Am. Coll. Cardiol. **48**, 193–202 (2006)
49. Kalnins, U., Erglis, A., Dinne, I., Kumsars, I., Jegere, S.: Clinical outcomes of silicon carbide coated stents in patients with coronary artery disease. Med. Sci. Monit. **8**, 116–120 (2002)
50. Kandzari, D.E., Leon, M.B., Popma, J.J., Fitzgerald, P.J., O'Shaughnessy, C., Ball, M.W., et al.: Comparison of zotarolimus-eluting and sirolimus-eluting stents in patients with native coronary artery disease: a randomized controlled trial. J. Am. Coll. Cardiol. **48**, 2440–2447 (2006)
51. Kastrati, A., Schomig, A., Dirschinger, J., et al.: Increased risk of restenosis after placement of gold-coated stents. Results of a randomized trial comparing gold-coated with uncoated steel stents in patients with coronary artery disease. Circulation **101**, 2478–2483 (2000)

52. Keuhler, M., Braun Melsungen, B.: Chapter 15: Overview of drug delivery coatings. In: Camenzind, E., De Scheerder, I.K. (eds.) Local Drug Delivery for Coronary Artery Disease, Established and Emerging Application, pp. 127–137. Taylor and Francis, New York (2005)
53. Khan, I.A., Patravale, V.B.: The intra-vascular stent as a site-specific local drug deliver system. Drug Develop Ind. pharm. **32**, 52–78 (2005)
54. Kim, T.G., Lee, Y., Park, T.G.: Controlled gene-eluting metal stent fabricated by bio-inspired surface modification with hyaluronic acid and deposition of DNA/PEI polyplexes. Int. J. Pharm. **384**, 181–188 (2010)
55. King, S., Meier, B.: Interventional treatment of coronary heart disease and peripheral vascular disease. Circulation **102**, IV81–IV86 (2000)
56. Kukreja, N., Onuma, Y., Daemen, J., Serruys, P.W.: The future of drug-eluting stents. Pharmacol. Res. **57**(3), 171–180 (2008)
57. Lahann, J., Klee, D., Thelen, H., Bienert, H., Vorwerk, D., Höcker, H.: Improvement of haemocompatibility of metallic stents by polymer coating. J. Mater. Sci. Mater. Med. **10**(7), 443–448 (1999)
58. Leiby, M.W., Cerul, J.J., Berger, H.L.: Process for coating three-dimensional substrates with thin organic films and products. Patent WO03072269(A1) (2003)
59. Lemos, P.A., Saia, F., Ligthart, J.M., Arampatzis, C.A., Sianos, G., Tanabe, K., et al.: Coronary restenosis after sirolimus-eluting stent implantation: morphological description and mechanistic analysis from a consecutive series of cases. Circulation **108**, 257–260 (2003)
60. Levy, Y., Tal, N., Tzemach, G., Weinberger, J., Domb, A.J., Mandler, D.: Drug-eluting stent with improved durability and controllability properties, obtained via electrocoated adhesive promotion layer. J. Biomed. Mater. Res. B Appl. Biomater. 91:819–823 (2009)
61. Liistro, F., Bolognes, L.: Drug-eluting stents. Heart Drug **3**(1), 203–213 (2003)
62. Liistro, F., Stankovic, G., Mario, C.D., Takagi, T., Chieffo, A., Moshiriet, S., et al.: First clinical experience with a paclitaxel derivate-eluting polymer stent system implantation for in-stent restenosis: immediate and long-term clinical and angiographic outcome. Circulation **105**, 1883–1886 (2002)
63. Lin, Q., Ding, X., Qiu, F., Song, X., Fu, G., Ji, J.: In situ endothelialization of intravascular stents coated with an anti-CD34 antibody functionalized heparin-collagen multilayer. Biomaterials **31**, 4017–4025 (2010)
64. Lincoff, A.M., Furst, J.G., Ellis, S.G., et al.: Sustained local delivery of dexamethasone by a novel intravascular eluting stent to prevent restenosis in the porcine coronary injury model. J. Am. Coll. Cardiol. **29**, 808–816 (1997)
65. McLean, D.R., Eiger, N.L.: Stent design: implications for restenosis. Rev. Cardiovasc. Med. **3**(Suppl 5), S16–S22 (2002)
66. Mehran, R., Aymong, E.D., Ashby, D.T., et al.: Safety of an aspirin-alone regimen after intracoronary stenting with a heparin-coated stent: final results of the HOPE (HEPACOAT and an antithrombotic regimen of aspirin alone) study. Circulation **108**, 1078–1083 (2003)
67. Meireles, G., Lemos, P.A., Ambrose, J.A., Ribeiro, E., Horta, P., Perin, M., Ramires, J., Martinez, E.: Luminal recovery from six to twelve months after implantation of "thicker strut" coronary stents. Am. J. Cardiol. **93**, 210–213 (2004)
68. Meng, S., Liu, Z., Shen, L., Guo, Z., Chou, L.L., Zhong, W., Du, Q., Ge, J.: The effect of a layer-by-layer chitosan-heparin coating on the endothelialization and coagulation properties of a coronary stent system. Biomaterials **30**, 2276–2283 (2009)
69. Meredith, I.T., Ormiston, J.A., Whitbourn, R., Kay, P., Muller, D., Bonan, R., et al.: First-in-human study of the Endeavor ABT-578-eluting phosphorylcholine-encapsulated stent system in de novo native coronary artery lesions: endeavor I trial. EuroIntervention **1**, 157–164 (2005)
70. Microfab technology, biomedical applications: stents, http://www.microfab.com/techtexolowanology/biomedical/Stents.html.

71. Monnink, S.H., van Boven, A.J., Peels, H.O., et al.: Siliconcarbide coated coronary stents have low platelet and leukocyte adhesion during platelet activation. J. Investig. Med. **47**, 304–310 (1999)
72. Moore, P., Barlis, P., Spiro, J., Ghimire, G., Roughton, M., Di Mario, C., Wallis, W., Ilsley, C., Mitchell, A., Mason, M., Kharbanda, R., Vincent, P., Sherwin, S., Dalby, M.: A randomized optical coherence tomography study of coronary stent strut coverage and luminal protrusion with rapamycin-eluting stents. JACC Cardiovasc. Interv. **2**(5), 437–444 (2009)
73. Morice, M.C., Bestehorn, H.P., Carrie, D., Macaya, C., Aengevaeren, W., Wijns, W., et al.: Direct stenting of de novo coronary stenoses with tacrolimuseluting versus carbon coated carbostents. The randomized JUPITER II trial. EuroIntervention **2**, 45–52 (2006)
74. Morice, M.C., Serruys, P.W., Sousa, J.E., et al.: A randomized comparison of a sirolimus-eluting stent with a standard stent for coronary revascularization. N. Engl. J. Med. **346**(23), 1773–1780 (2002)
75. Moses, J.W., Leon, M.B., Popma, J.J., et al.: Sirolimus-eluting stents versus standard stents in patients with stenosis in a native coronary artery. N. Engl. J. Med. **349**, 1315–1323 (2003)
76. Nebeker, J.R., Virmani, R., Bennett, C.L., Hoffman, J.M., Samore, M.H., Alvarez, J., et al.: Hypersensitivity cases associated with drug-eluting coronary stents: a review of available cases from the Research on Adverse Drug Events and Reports (RADAR) project. J. Am. Coll. Cardiol. **47**, 175–181 (2006)
77. Nukala, R.K., Boyapally, H., Slipper, I.J., Menhdam, A., Douroumis, D.: Application of electrostatic dry powder deposition technology for coating of drug eluting stents. Pharm. Res. **27**, 72–81 (2010)
78. Okner, R., Oron, M., Tal, N., Nyska, A., Kumar, N., Mandler, D., Domb, A.J.: Electrocoating of stainless steel coronary stents for extended release of paclitaxel. J. Biomed. Mater. Res. A **88**, 427–436 (2009)
79. Okner, R., Shaulov, Y., Tal, N., Favaro, G., Domb, A.J., Mandler, D.: Electropolymerized tricopolymer based on N-pyrrole derivatives as a primer coating for improving the performance of a drug-eluting stent. ACS Appl. Mater. Interfaces **1**(4), 758–767 (2009)
80. Orford, J., Selwyn, A.: The comparative pathobiology of atherosclerosis and restenosis. Am. J. Cardiol. **86**, 6H–11H (2000)
81. Ormiston, J.A, Abizaid, A., Spertus, J., Fajadet, J., Mauri, L., Schofer, J., Verheye, S., Dens, J., Thuesen, L., Dubois, C., Hoffmann, R., Wijns, W., Fitzgerald, P.J., Popma, J.J., Macours, N., Cebrian, A., Stoll, H.P., Rogers, C., Spaulding, C.: NEVO ResElution-I Investigators. Six-month results of the NEVO Res-Elution I (NEVO RES-I) trial: a randomized, multicenter comparison of the NEVO sirolimus-eluting coronary stent with the TAXUS Liberté paclitaxel-eluting stent in de novo native coronary artery lesions. Circ. Cardiovasc. Interv. **3**, 556–564 (2010)
82. Pache, J., Kastrati, A., Mehilli, J., Schuhlen, H., Dotzer, F., Hausleiter, J., Fleckenstein, M., Neumann, F.J., Sattelberger, U., Schmitt, C., Muller, M., Dirschinger, J., Schomig, A.: Intracoronary stenting and angiographic results: strut thickness effect on restenosis outcome (ISAR-STEREO-2) trial. J. Am. Coll. Cardiol. **41**, 1283–1288 (2003)
83. Pallasana, N.V., Mead, B.: Method of coating medical devices. Patent EP 1440701(A1) (2004)
84. ChJ, Pan, Tang, J.J., Weng, Y.J., Wang, J., Huang, N.: Preparation, characterization and anticoagulation of curcumin-eluting controlled biodegradable coating stents. J. Control Release **116**, 42–49 (2006)
85. Pan, C.J., Tang, J.J., Shao, Z.Y., Wang, J., Huang, N.: Improved blood compatibility of rapamycin-eluting stent by incorporating curcumin. Colloids Surf. B Biointerfaces **59**(1), 105–111 (2007)
86. Pan, C.J., Wang, J., Huang, N.: Preparation, characterization and in vitro anticoagulation of emodin-eluting controlled biodegradable stent coatings. Colloids Surf. B Biointerfaces **77**, 155–160 (2010)
87. Pinchuk, L., Nott, S., Schwarz, M., Kamath, K.: Drug delivery compositions and medical devices containing block copolymer. Patent US2002107330 (A1) (2005)

88. Ranade, S.V., Miller, K.M., Richard, R.E., Chan, A.K., Allen, M.J., Helmus, M.N.: Physical characterization of controlled release of paclitaxel from the TAXUS Express2 drug-eluting stent. J. Biomed. Mater. Res. A **71**(4), 625–634 (2004)
89. Rodgers, C.D.: Drug-eluting stents: role of stent design, delivery vehicle, and drug selection. Rev. Cardiovasc. Med. **5**, S10–S15 (2002)
90. Ross, R.: Atherosclerosis-an inflammatory disease. N. Engl. J. Med. **340**, 115–126 (1999)
91. Roy, R.K., Lee, K.R.: Biomedical applications of diamond-like carbon coatings: a review. J. Biomed. Mater. Res. B Appl. Biomater. **83**, 72–84 (2007)
92. Schäfer, O., Brink-Spalink, F., Schmidt, C., Wendorff, J.H., Witt, C., Kissel, T., Greiner, A.: Synthesis and properties of-phenylalkyl-substituted poly(p-xylylene)s prepared by base-induced 1, 6-dehydrohalogenation. Macromol. Chem. Phys. **200**(8), 1942–1949 (1999)
93. Schmehl, J.M., Harder, C., Wendel, H.P., Claussen, C.D., Tepe, G.: Silicon carbide coating of nitinol stents to increase antithrombogenic properties and reduce nickel release. Cardiovasc. Revasc. Med. **9**(4), 255–262 (2008)
94. Schuler, P., Assefa, D., Ylanne, J., Basler, N., Olschewski, M., Ahrens, I., et al.: Adhesion of monocytes to medical steel as used for vascular stents is mediated by the integrin receptor Mac-1 (CD11b/CD18; alphaM beta2) and can be inhibited by semiconductor coating. Cell. Commun. Adhes. **10**(1), 17–26 (2003)
95. Schuler, W., Sedrani, R., Cottens, S., Haberlin, B., Schulz, M., Schuurman, H.J., et al.: SDZ RAD, a new rapamycin derivative: pharmacological properties in vitro and in vivo. Transplantation **64**, 36–42 (1997)
96. Schwartz, R.S., Huber, K.C., Murphy, J.G., et al.: Restenosis and the proportional neointimal response to coronary artery injury: results in a porcine model. J. Am. Coll. Cardiol. **19**, 267–274 (1992)
97. Serruys, P.: BIOMATRIX: First report from the three–year LEADERS trial. In: Transcatheter Cardiovascular Therapeutics 22nd Annual Scientific Symposium. Washington DC, USA (2010)
98. Serruys, P.W.: The new CoStar ^{TM} stent: 12 month results with the new DES technology. European Paris Course on Revascularization, Paris (2005)
99. Serruys, P.W., Degertekin, M., Tanabe, K., Abizaid, A., Sousa, J.E., Colombo, A., Guagliumi, G., Wijns, W., Lindeboom, W.K., Ligthart, J., Feyter, P.J., Morice, M.C.: Intravascular ultrasound findings in the multicenter, randomized, double-blind RAVEL: RAndomized study with the sirolimus-eluting VElocity balloon-expandable stent in the treatment of patients with de novo native coronary artery Lesions trial. Circulation **106**(7), 798–803 (2002)
100. Serruys, P.W., Sianos, G., Abizaid, A., et al.: The effect of variable dose and release kinetics on neointimal hyperplasia using a novel paclitaxel-eluting stent platform: the paclitaxel in-stent controlled elution study (PISCES). J. Am. Coll. Cardiol. **46**(2), 253–260 (2005)
101. Serruys, P.W., Van Hout, B., Bonnier, H., et al.: Randomised comparison of implantation of heparin-coated stents with balloon angioplasty in selected patients with coronary artery disease (Benestent II). Lancet **352**, 673–681 (1998)
102. Shaulov, Y., Okner, R., Levi, Y., Tal, N., Gutkin, V., Mandler, D., Domb, A.J.: Poly(methyl methacrylate) grafting onto stainless steel surfaces: application to drug-eluting stents. ACS Appl. Mater. Interfaces **1**(11), 2519–2528 (2009)
103. Reifart, N., Morice, M.C., Silber, S., Benit, E., Hauptmann, K.E., de Sousa, E., Webb, J., Kaul, U., Chan, C., Thuesen, L., Guagliumi, G., Cobaugh, M., Dawkins, K.: The NUGGET study: NIR ultra gold-gilded equivalency trial. Catheter Cardiovasc Interv. 62, 18–25 (2004)
104. Sollott, S.J., Cheng, L., Pauly, R.R., Jenkins, G.M., Monticone, R.E., Kuzuya, M., Froehlich, J.P., Crow, M.T., Lakatta, E.G., Rowinsky, E.K., Kinsella, J.L.: Taxol inhibits neointimal smooth muscle cell accumulation after angioplasty in the rat. J. Clin. Invest. **95**, 1869–1876 (1995)
105. Sousa, J.E., Costa, M.A., Abizaid, A., Abizaid, A.S., Feres, F., Pinto, I.M.F., et al.: Lack of neointimal proliferation after implantation of sirolimus-coated stents in human coronary

arteries: a quantitative coronary angiography and three-dimensional intravascular ultrasound study. Circulation **103**, 192–195 (2001)
106. Sousa, J.E., Costa, M.A., Abizaid, A.C., Rensing, B.J., Abizaid, A.S., Tanajura, L.F., Kozuma, K., Van Langenhove, G., Sousa, A.G.M.R., Falotico, R., Jaeger, J., Popma, J.J., Serruys, P.W.: Sustained suppression of neointimal proliferation by sirolimus-eluting stents. Circulation **104**, 2007–2011 (2001)
107. Sousa, J.E., Serruys, P.W., Costa, M.A.: New frontiers in cardiology: drug-eluting stents: Part I. Circulation **107**(17), 2274–2279 (2003)
108. Stahli, B.E., Camici, G.G., Steffel, J., Akhmedov, A., Shojaati, K., Graber, M., Luscher, T.F., Tanner, F.C.: Paclitaxel enhances thrombin-induced endothelial tissue factor expression via c-Jun terminal NH_2 kinase activation. Circ. Res. **99**, 149–155 (2006)
109. Steffel, J., Latini, R.A., Akhmedov, A., Zimmermann, D., Zimmerling, P., Luscher, T.F., Tanner, F.C.: Rapamycin, but not FK-506, increases endothelial tissue factor expression: implications for drug-eluting stent design. Circulation **112**, 2002–2011 (2005)
110. Steffel, J., Luscher, T.F., Tanner, P.C.: Tissue factor in cardiovascular diseases: molecular mechanisms and clinical implications. Circulation **112**, 2002–2011 (2006)
111. Stone, G.W., Ellis, S.G., Cox, D.A., et al.: A polymer-based, paclitaxel-eluting stent in patients with coronary artery disease. N. Engl. J. Med. **350**(3), 221–231 (2004)
112. Stone, G.W., Ellis, S.G., Cox, D.A., et al.: One-year clinical results with the slow-release, polymer-based, paclitaxel-eluting TAXUS stent: the TAXUS-IV trial. Circulation **109**(16), 1942–1947 (2004)
113. Stone, G.W., Midei, M., Newman, W., Sanz, M., Hermiller, J.B., Williams, J., Farhat, N., Mahaffey, K.W., Cutlip, D.E., Fitzgerald, P.J., Sood, P., Su, X., Lansky, A.J.: Comparison of an everolimus-eluting stent and a paclitaxel-eluting stent in patients with coronary artery disease: a randomized trial. JAMA **299**, 1903–1913 (2008)
114. Tanajura, L.F., Abizaid, A.A., Feres, F., Pinto, I., Mattos, L., Staico, R., et al.: Randomized intravascular ultrasound comparison between patients that underwent amorphous hydrogenated silicon-carbide coated stent deployment versus uncoated stent. JACC **41**(6), 58 (2003)
115. Tanner, F.C., Yang, Z.Y., Duckers, E., Gordon, D., Nabel, G.J., Nabel, E.G.: Expression of cyclin-dependent kinase inhibitors in vascular disease. Circ. Res. **82**, 396–403 (1998)
116. Tarcha, P., Verlee, D., Hui, H., Setesak, J., Antohe, B., Radulescu, D., Wallace, D.: The application of ink-jet technology for the coating and loading of drug-eluting stents. Ann. Biomed. Eng. **35**, 1791–1799 (2007)
117. Thomson, L.A., Law, F.C., Rushton, N.: Biocompatibility of diamond-like carbon coating. Biomaterials **12**, 37–40 (1991)
118. Topol, E.J., Serruys, P.W.: Frontiers in interventional cardiology. Circulation **98**, 1802–1820 (1998)
119. Tsujino, I., Ako, J., Honda, Y., Fitzgerald, P.J.: Drug delivery via nano-, micro and macroporous coronary stent surfaces. Expert Opin. Drug Deliv. **4**, 287–295 (2007)
120. Udipi, K., Chen, M., Cheng, P., Jiang, K., Judd, D., Caceres, A., Melder, R.J., Wilcox, J.N.: Development of a novel biocompatible polymer system for extended drug release in a next-generation drug-eluting stent. J. Biomed. Mater. Res. A **85**(4), 1064–1071 (2008)
121. Unverdorben, M., Sattler, K., Degenhardt, R., Fries, R., Abt, B., Wagner, E., et al.: Comparison of silicon carbide coated stent versus a noncoated stent in humans: the Tenax-versus Nir-stent Study. J. Interv. Cardiol. **16**(4), 325–333 (2003)
122. Unverdorben, M., Sippel, B., Degenhardt, R., Sattler, K., Fries, R., Abt, B., et al.: Comparison of a silicon carbide-coated stent versus a noncoated stent in human beings: the Tenax versus Nir stent study's long-term outcome. Am. Heart J. **145**(4), E17 (2003)
123. Vallana, F., Arru, P.: Method and apparatus for forming prosthetic device having a biocompatible carbon film thereon. US patent 5,084,151 (1992)
124. Van der Giessen, W.J., Lincoff, A.M., Schwartz, R.S., Van Beusekom, H.M., Serruys, P.W., Holmes Jr, D.R., et al.: Marked inflammatory sequelae to implantation of biodegradable and nonbiodegradable polymers in porcine coronary arteries. Circulation **94**, 1690–1697 (1996)

125. VanSciver, J., Cheng, Y., Glenn, B.D. et al.: System and method for coating a stent. Patent WO2008156920 (2008)
126. Vecerina, I., Pham, V.: Automated coating apparatus and method. Patent WO2009065087 (2009)
127. Venkatraman, S., Boey, F.: Release profiles in drug eluting stents: issues and uncertainties. J. Control Release **120**, 149–160 (2007)
128. Virmani, R., Guagliumi, G., Farb, A., Musumeci, G., Grieco, N., Motta, T., et al.: Localized hypersensitivity and late coronary thrombosis secondary to a sirolimus-eluting stent: should we be cautious? Circulation **109**, 701–705 (2004)
129. Vrolix, M.C.M., Legrand, V.M., Reiber, J.H.C., Grollier, G., Schalij, M.J., Brunel, P., et al.: Heparin-coated Wiktor stents in human coronary arteries (MENTOR trial). Am. J. Cardiol. **86**, 385–389 (2000)
130. Wallace, D., Cooley, P., Antohe, B., Hayes, D., Chen, T.: Ink jet technology for manufacturing and instrument applications. Proceedings, 20th workshop on micromachining, micromechanics and microsystems, Toulouse, France (2009)
131. Walter, D.H., Cejna, M., Diaz-Sandoval, L., Willis, S., Kirkwood, L., Stratford, P.W., Tietz, A.B., Kirchmair, R., Silver, M., Curry, C., Wecker, A., Yoon, Y.S., Heidenreich, R., Hanley, A., Kearney, M., Tio, F.O., Kuenzler, P., Isner, J.M., Losordo, D.W.: Local gene transfer of phVEGF-2 plasmid by gene-eluting stents. Circulation **110**, 36–45 (2004)
132. Wang, T.H., Wang, H.S., Ichijo, H., Giannakakou, P., Foster, J.S., Fojo, T., Wimalasena, J.: Microtubule-interfering agents activate c-Jun N-terminal kinase/stress-activated protein kinase through both Ras and apoptosis signal-regulating kinase pathways. J. Biol. Chem. **273**, 4928–4936 (1998)
133. Wessely, R., Hausleiter, J., Michaelis, C., Jaschke, B., Vogeser, M., Milz, S., Behnisch, B., Schratzenstaller, T., Renke-Gluszko, M., Stöver, M., Wintermantel, E., Kastrati, A., Schömig, A.: Inhibition of neointima formation by a novel drug-eluting stent system that allows for dose-adjustable, multiple, and on-site stent coating. Arterioscler. Thromb. Vasc. Biol. **25**, 1–6 (2005)
134. Whelan, D.M., van der Giessen, W.J., Krabbendam, S.C., van Vliet, E.A., Verdouw, P.D., Serruys, P.W., van Beusekom, H.M.: Biocompatibility of phosphorylcholine coated stents in normal porcine coronary arteries. Heart **83**, 338–345 (2000)
135. Wiktor, D.M.: Intravascular radially expandable stent and method of implant. US patent 4,886,062 (1989)
136. Windecker, S., Serruys, P.W., Wandel, S., Buszman, P., Trznadel, S., Linke, A., Lenk, K., Ischinger, T., Klauss, V., Eberli, F., Corti, R., Wijns, W., Morice, M.C., di Mario, C., Davies, S., van Geuns, R.J., Eerdmans, P., van Es, G.A., Meier, B., Jüni, P.: Biolimus-eluting stent with biodegradable polymer versus sirolimus-eluting stent with durable polymer for coronary revascularisation (LEADERS): a randomised non-inferiority trial. Lancet **372**(9644), 1163–1173 (2008)
137. Wright, C., Llanos, G.H., Rakos, R., King, K.: Stent with local rapamycin delivery. Patent EP095038 (A2) (1999)
138. Wright, C., Llanos, G.H., Rakos, R., King, K.: Modified stent useful for delivery of drugs along stent strut. US Patent 6,273,913 (2001)
139. Yin, Y., Wise, S.G., Nosworthy, N.J., Waterhouse, A., Bax, D.V., Youssef, H., Byrom, M.J., Bilek, M.M., McKenzie, D.R., Weiss, A.S., Ng, M.K.: Covalent immobilisation of tropoelastin on a plasma deposited interface for enhancement of endothelialisation on metal surfaces. Biomaterials **30**, 1675–1681 (2009)
140. Yuan, Y., Liu, C., Yin, M.: Plasma polymerized n-butyl methacrylate coating with potential for re-endothelialization of intravascular stent devices. J. Mater. Sci. Mater. Med. **19**, 2187–2196 (2008)

Polyesteramide Coatings for Drug Eluting Stents: Controlling Drug Release by Polymer Engineering

Mikael Trollsas, Bozena Maslanka, Nam Pham, Qing Lin, Syed Hossainy, Shaw Ling Hsu and Michael Huy Ngo

Abstract Bioresorbable vascular scaffolds may revolutionize the field of interventional cardiology and to optimize the clinical outcome it is critical to select coating materials that can control the drug release, maintain coating integrity, and have long term biocompatibility. Polyesteramides have great coating properties, have shown promise in biomedical applications, and their thermo-mechanical properties are easily modified by changing the molecular structure. In this paper a series of polyester amides with various chemical structures, specifically synthesized to optimize the everolimus release rate and the mechanical integrity of drug eluting stent coatings are reported. The obtained data shows that the drug release rate of a lipohilic drug is highly dependent on the molecular structure and more specifically to the polarity, water uptake, and the molecular mobility of the polymer used. The effect on drug release of both the molecular weight and the dry and wet glass transition temperatures of the polymer was demonstrated. In addition, it was demonstrated that minimal changes in a polymers molecular structure showed significant impact on the drug release rate.

M. Trollsas (✉) · B. Maslanka · N. Pham · Q. Lin · S. Hossainy · M. H. Ngo
Abbott Vascular, Abbott Laboratories, 3200 Lakeside Drive,
Santa Clara, CA 95054, USA
e-mail: mikael.trollsas@av.abbott.com

S. L. Hsu
Department of Polymer Science and Engineering, Room A125,
Conte Research Center, University of Massachusetts at Amherst,
120 Governors Drive, Amherst, MA 01003, USA

Stud Mechanobiol Tissue Eng Biomater (2011) 8: 127–143
DOI: 10.1007/8415_2010_57

Published Online: 5 February 2011

1 Introduction

The successful formulation of drug eluting stents has so far mainly been combinations of anti-proliferative drugs, such as paclitaxcel or rapamycin derivatives, with a polymeric drug eluting reservoir in the form of a coating [1]. The formulation of a drug eluting stent may at first, seems as a relatively simple task, but in fact considerable development and innovation has been required to find polymer coatings with the desired combination of biological, chemical, physical and mechanical properties [1–5].

Bioabsorbable polymers are commonly used in controlled drug delivery applications in the form of particles, gels, coatings, etc. [6, 7] and have recently received a lot of attention in the field of drug eluting bioresorbable vascular scaffolds (BVS). The family of lactic acid, glycolic acid, and caprolactone homo- and co-polymers (PLA, PLGA, PCL) are commonly used in medical products and are the preferred materials in many of these applications because of their proven biocompatibility, tunable degradation, and the possibility to control their synthesis [7–12]. Numerous synthetic methods have been developed to control the preparation of advanced polymer architectures using these monomers [11–18]. However, tuning release of highly lipophilic drugs and peptides from α-hydroxy acid polyesters such as PLA and PLGA is difficult due to the chemical nature and low water uptake of these polymers [1–4, 6–10, 19, 20].

Polyester amides (PEA) form an alternative class of bioabsorbable polymers, in which the molecular structure readily is altered, Scheme 1 [21–34]. Katsarava has outlined how various electrophilic diacid monomers can be combined with nucleophilic amino acid monomers to form PEA with various glass transition temperatures [21, 22] and also shown that the incorporation of L-phenyalanine [23, 24] or dianhydrohexitoles [25] are potential ways of altering the degradation rate of this class of polymers. Work with unsaturated polyesteramides [26, 27], and more recently hyperbranched polyesteramides [28, 29] synthesized from commercially available dicarboxylic acids and multi-hydroxyl primary amines have been reported as novel biodegradable materials. The use of PEA in medical applications such as polymer coated stent has been evaluated [30], and recently microencapsulation [31] as well as model drug-release studies from non-covalent nano-adducts of PEA in combination with poly(ethylene glycol) were reported [32]. Numerous studies have also been focused on combining PEA polymers with various aliphatic polyesters [33, 34].

In this manuscript we present the development of PEA with high glass transition temperatures (>45°C) specifically designed to be used in drug eluting stent coatings. The possibility to easily alter the chemical structure of PEA allows simultaneous optimization of coating integrity post sterilization and drug release properties. Ideally, these coatings should be thin to reduce both degradation time and build up of degradation products in the arteries. In addition, we will discuss the intrinsic properties required to control drug release from a polymer material. The influence of polymer polarity, water uptake, drug/polymer miscibility,

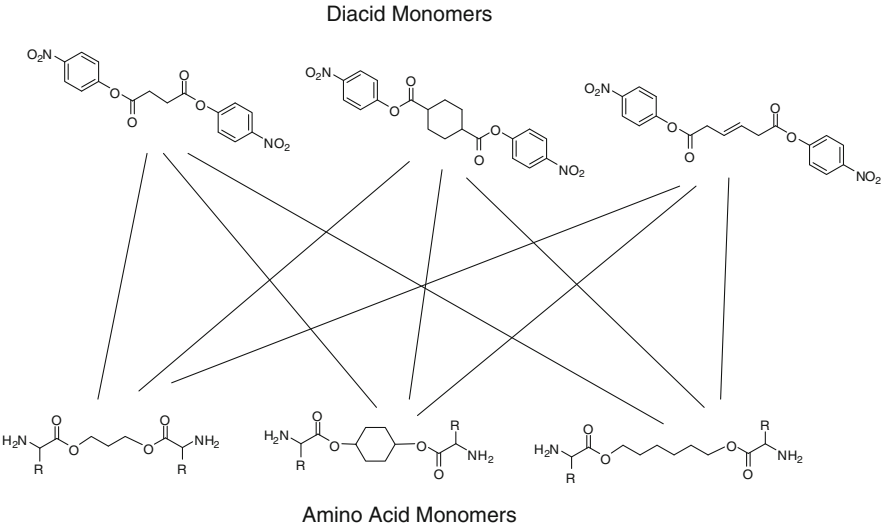

Scheme 1 Schematic over view of the polyesteramide polymerization method using di-pnitrophenyl esters of dicarboxylic acids (Diacid Monomers) and di-p-toluene sulfonic acid salts of bis (a-amino acid) alkylene diesters (Amino Acid Monomers)

and polymer rigidity on controlling drug release will be discussed. The polymer polarity as well as the polymer rigidty, are both controlled by the size of side groups and the connector chain lengths. The polymer rigidity can also be modified by altering the ratio of linear and cyclic units in the main chain without affecting the polymer polarity, which will shine more light on the mechanism of hydrophobic drug release from a thin polymer coating.

2 Experimental Methods

2.1 Materials

Everolimus (40-*O*-(2-hydroxy)ethyl-rapamycin) was delivered from Novartis. Bare metal stents (3.0 mm × 12 mm) were supplied internally at Abbott Vascular. PEA polymers were synthesized in house according to previously published methods using di-*p*-nitrophenyl esters of dicarboxylic acids and di-*p*-toluene sulfonic acid salts of bis (a-amino acid) alkylene diesters, Scheme 1 [22, 23]. The monomers were carefully purified by repeated re-crystalizations from ethanol or methanol and carefully dried for 48 h under vacuum. The purified monomers were mixed in perfect stochiometric amounts, to generate high molecular weight polymers, with a minimal amount of DMF as the solvent, and a small excess of triethylamine, which was used as the base during the room temperature polymerization. All raw materials were purchased from Sigma–Aldrich.

2.2 Methods

Drug and polymer were dissolved in ethanol and spray-coated in multiple passes to achieve the specific drug dose and coating thickness (D:P 1:5, drug dose 56 μg, coating thickness 5 μm). PEA structures were confirmed by the analysis of ^{1}H NMR. Molecular weight (Mw) data was acquired by GPC method using polystyrene standard. Glass transition (Tg) was measured by differential scanning calorimetry (DSC). Scanning electron microscopy (SEM) was used to evaluate the coating integrity, and drug release rates were measured by HPLC utilizing a United States Pharmacopeia Type VII apparatus in porcine serum media using sink conditions. The release rate results are the average result of three samples, each sample was measured in duplicates. Swelling measurements were made by recording the weight increase of drug- and polymer-coated stents after they were immersed in saline at 37°C. The wet Tg measurements were performed after exposing polymer coated substrates for various humidity conditions for 24 h at 37°C.

3 Results and Discussion

3.1 Leucine Based PEA

Scheme 2 outlines the structures of four new PEA polymers with various glass transition temperatures (Tg). Common building blocks for all polymers are leucine and adipate (four methylene units), although **PEA-II** is made from sebacinate (eight methylene units) and **PEA-III** is based on phenylalanine. Three different diols, propanediol, hexanediol, and cyclohexanediol were used. As observed in Table 1 all these polymers have a similar molecular weight and the only polymer with a Tg outside the range of 42–49°C is **PEA-III**, which is made from 100% cyclic diols. All other changes of molecular structure has little influence on the glass transition temperature and this correlates well with results reported by Katsarava for PEA structures with only linear segment in the main chain [21].

Interestingly, although the structures of the four polymers are fairly similar, the amount everolimus released after 24 h in porcine serum from the various polymers vary dramatically, from 0.8% (**PEA-III**) to 99.5% (**PEA-I**), Table 1.

The very rapid burst release observed in **PEA-I** likely indicate that the drug and the polymer are not ideally mixed. This could be due to poor miscibility of the two, or be related to their relative solubility in ethanol, which was used as the spray coating solvent. However, from the results observed for the other polymers, it is clear that increasing hydrophobicity of the polymer helps to control drug diffusion and achieve a more sustained drug release. Alternatively, drug diffusion can be controlled by reducing polymer chain mobility or more simply explained by increasing the glass transition temperatures. **PEA-III** has a significantly higher Tg

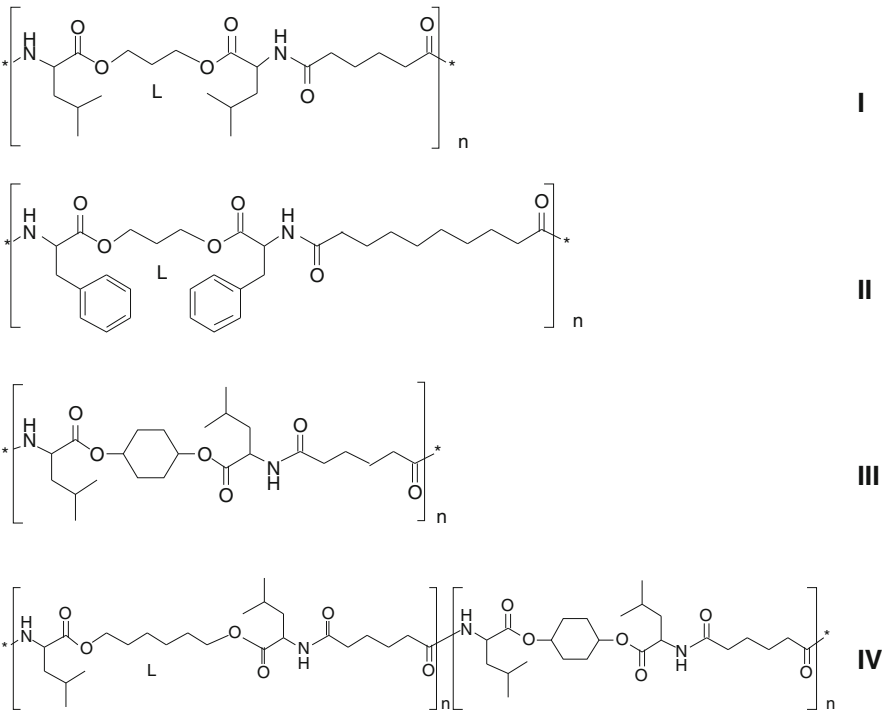

Scheme 2 The chemical structures of **PEA-I**, **PEA-II**, **PEA-III**, and **PEA-IV**

Table 1 Molecular weight (kD), Tg (°C), and everolimus release rates (%) after 1- and 3-days from four different PEA polymers

Polymers	Mw (kD)	Tg (°C)	1-Day RR (%)	3-Day RR (%)
PEA-I	48.0	48.5	95.5	99.7
PEA-II	52.7	42.5	44.3	64.6
PEA-III	43.1	82.0	0.8	7.2
PEA-IV	61.0	45.5	41.8	70.9

due to the higher percentage of cyclic structures in the polymer main chain and as a result drug release is slowed down. The short linkages in the main chain gives **PEA-III** a high glass transition temperature (82°C) and as result it becomes more brittle and less suitable as a stent coating, Fig. 1.

An ideal polymer from a release rate perspectives is therefore likely more similar to **PEA-II** or **PEA-IV**. **PEA-IV** synthesized from a mixture of cyclohexanediol and hexanediol, has worse coating integrity then **PEA-II** but provides an opportunity to tune release by combining cyclics with a hydrophobic structure. The drug release from **PEA-IV** is too fast for an ideal DES coating [1–5], where the target release after 3 days is in the range of 20–40% to allow for an elution of approximately 80% after 4 weeks when a limus drug is used. The structure of

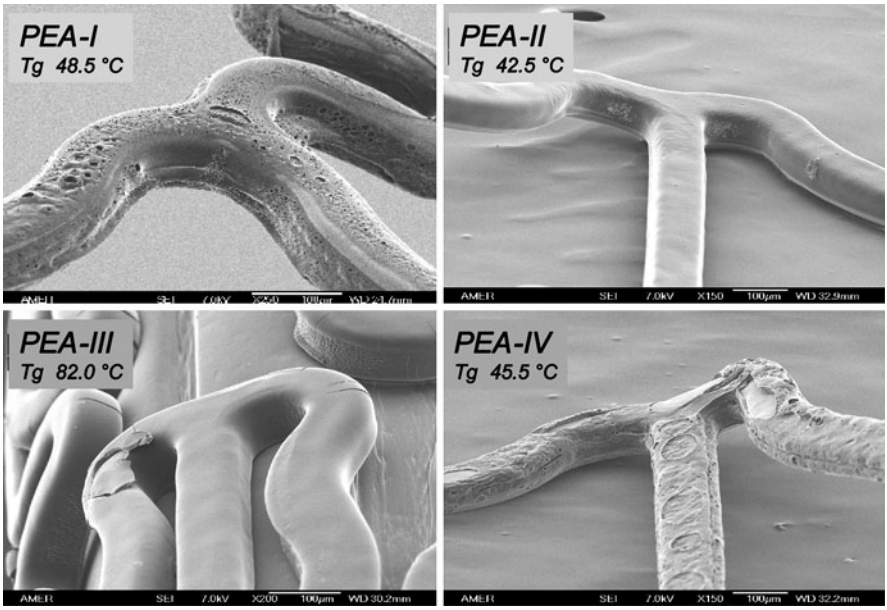

Fig. 1 Coating integrity and glass transition temperatures, Tg (°C), of **PEA-III** after crimping, and of **PEA-I**, **PEA-II**, and **PEA-IV** after crimping, sterilization, passing through a tortuous path, expansion, and simulated use for an hour at 37°C in physiologic buffer solution (PBS)

PEA-IV was therefore changed by altering the ratio of the flexible units (hexane diol) and the more rigid cyclic units (cyclohexane diol), as well as by using a more hydrophobic linker, sebacinate instead of adipate.

The new polymers (**PEA-V**, **PEA-VI**, **PEA-VII**, **PEA-VIII**), were synthesized using different ratios of cyclohexanediol and hexanediol (m/n), Table 2, and as the data in Table 3 show, the ratio of cyclic to linear units has a significant impact on the glass transition temperature and also on the drug release rate once the dry glass transition temperature starts to approach physiologic temperature.

The glass transition temperatures reported in Table 3 are for the dry polymers and does thus not take into account any plasticization caused by swelling in the drug release media. Although the PEA polymers have an in general hydrophobic nature the water uptake is significant as observed by swelling measurements. The swelling for **PEA-VI** and **PEA-VIII** when applied as drug coatings on a stent was measured over time and found to be 6 and 3%, respectively after 24 h and 15 and 6%, respectively after 7 days, Fig. 2. These measurements do not exclude any loss of drug in these coatings, which means that the true swelling of the polymers in reality should be slightly higher. As expected this type of water uptake plasticizes the polymer and as a result reduces the glass transition temperature of the polymer and the coating. The reduction of the Tg was measured at various humidity levels for **PEA-V**, **PEA-VI**, and **PEA-VIII** and for the latter two the Tg were in

Table 2 Hexanediol and cycylohexanediol ratios for **PEA-V**, **PEA-VI**, **PEA-VII**, and **PEA-VIII**

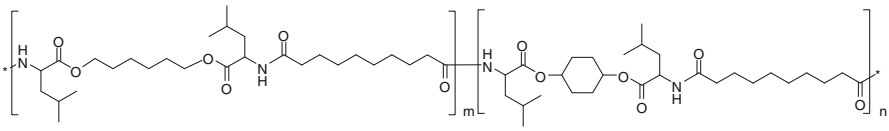

Polymer	Hexane diol—*n* (%)	Cyclohexane diol—*m* (%)
PEA-V	75	25
PEA-VI	50	50
PEA-VII	25	75
PEA-VIII	0	100

Table 3 Molecular weight (kD), Tg (°C), and everolimus release rates (%) after 1- and 3-days for **PEA-V**, **PEA-VI**, **PEA-VII**, and **PEA-VIII**

Polymer	Hexane/cyclohexane (%)	Mw (kD)	Tg (°C)	1-Day RR (%)	3-Day RR (%)
PEA-V	**75/25**	83.8	31	n/a	n/a
PEA-VI	**50/50**	50.0	55	12.5	24.2
PEA-VII	**25/75**	68.7	72	4.7	7.1
PEA-VIII	**0/100**	52.3	83	4.6	7.2

The bold values are part of the name/structures of the polymers and not measured values

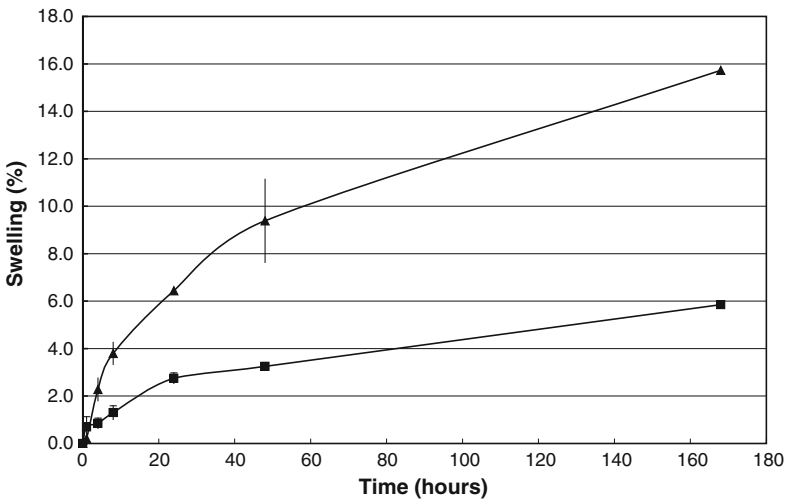

Fig. 2 Swelling of **PEA-VI** (*black triangle*) and **PEA-VIII** (*black square*) DES coatings in PBS over time

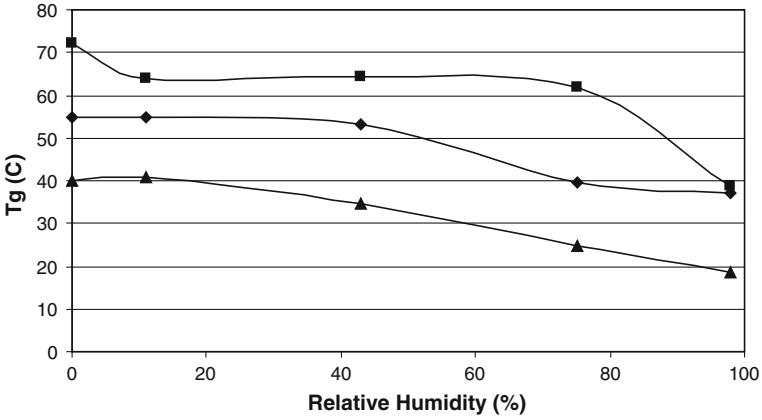

Fig. 3 Change in glass transition temperatures, Tg (°C), for **PEA-V** (*black triangle*), **PEA-VI** (*black diamond*), and **PEA-VIII** (*black square*) coatings after being exposed to various relative humidity levels (%) for 24 h

the range of physiological temperature at 100% humidity while the wet Tg for the more flexible **PEA-V** was found to be slightly below 20°C, Fig. 3.

As this data suggest the molecular mobility, observed as a change in glass transition temperature for the dry polymers, seems to have a significant impact on the drug release rate. This can be concluded as all the polymers in Table 2 have a very similar macroscopic polarity. They all have basically the same type and concentration of functional groups and a very similar ratio of atoms in the main chain. They also have a very similar molecular weight and the only real difference between the three polymers is the molecular mobility around the main chain provided by altering the ratio of hexane diol and cyclohexane diol building blocks. This change in molecular mobility is observed and confirmed by the variation in glass transition temperature, Table 2.

The coating integrity for this group of polymer after simulated use can be observed in Fig. 4, which shows that both **PEA-VI** and **PEA-VII** have outstanding mechanical properties and are ideal from that perspective to be used as drug eluting stent coatings. **PEA-VIII** on the other hand is too brittle with its high concentration of cyclics for this application, as coating defects are potential risk for thromboembolic events. The reduction of Tg observed for **PEA-VIII** in contact with blood or water is kinetically too slow for having a useful effect prior to the deployment of the stent in the vasculature.

3.2 Alanine Based PEA

The molecular mobility around a polymers main chain can alternatively be modified by altering the size of the pendant groups. Leucine, which provides

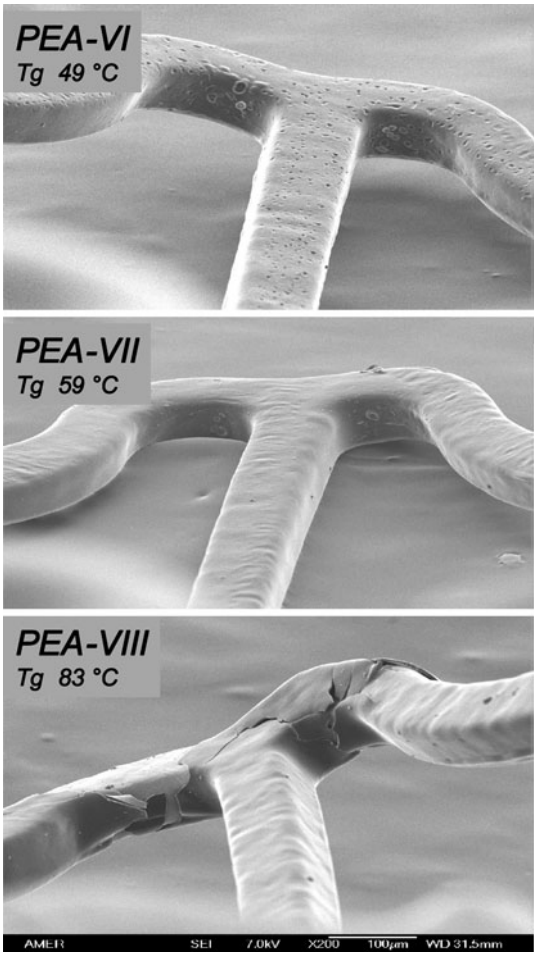

Fig. 4 Coating integrity and glass transition temperatures, Tg (°C), of **PEA-VI**, **PEA-VII**, and **PEA-VIII** after crimping, sterilization, passing through a tortuous path, expansion, and simulated use for an hour at 37°C in physiologic buffer solution (PBS)

the PEA polymers with pendant iso-butyl groups was therefore replaced in **PEA-VI** (**PEA-Leucine**) by alanine, which provides the PEA with pendant methyl groups. Two new polymers were synthesized, one which had 100% alanine (**PEA-Alanine**) and one which had 50% alanine and 50% leucine (**PEA-50:50 Alanine-Leucine**), Scheme 3. In the **PEA-50:50 Alanine-Leucine** all leucine monomers also contained hexanediol, while all alanine monomers were made from cyclohexanediol.

To understand the influence of this side group modification the two new polymers were compared to **PEA-VI**, Table 4. Also, the molecular weight of the polymer were targeted to be in the same range (100–140 kD) and in addition similar glass transition temperatures ranging from 45 to 55°C were observed, which indicate that the molecular mobility should not have been significantly changed. Figure 5 shows that the small change in polymer structure had minor

PEA – Alanine

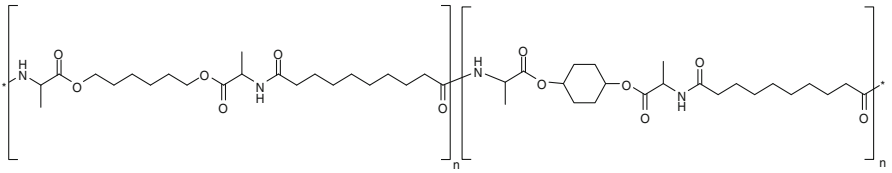

PEA- 50:50 Alanine: Leucine

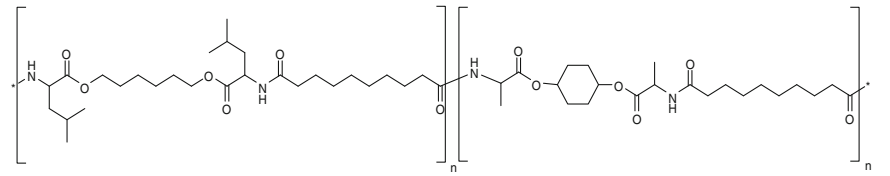

Scheme 3 The chemical structures of **PEA-Alanine** and **PEA-50:50 Alanine:Leucine**

Table 4 Methyl/iso-butyl ratio, molecular weight (kD), Tg (°C), and everolimus release rate (%) after 1-day for **PEA-Leucine** (**PEA-VI**), **PEA 50:50 Alanine-Leucine**, and **PEA-Alanine**

Polymer	Methyl/iso-butyl ratio	Mw (kD)	Tg (°C)	1-Day RR (%)
PEA-Leucine (PEA-VI)	**0/100**	135.0	55	5
PEA 50:50 Alanine-Leucine	**50/50**	145.3	51	39
PEA-Alanine	**100/0**	104	55	99

The bold values are part of the name/structures of the polymers and not measured values

effect on the DES coating integrity, although the **PEA-Alanines** seems to swell somewhat more, which is confirmed by the data in Table 5.

However, most interestingly this small change in molecular structure, which had little impact on the mechanical properties of the coating, had a very dramatic impact on the everolimus release rate. The drug release rate observed for the pure alanine polymer was significantly faster than for the corresponding leucine polymer (**PEA-VI**), while the polymer with a 50:50 ratio of alanine and leucine had a drug release rate right in between the two other polymers, Fig. 6. The more lipophilic **PEA-VI** with pendant iso-butyl groups releases only 5% of the drug after 24 h, while the less lipophilic **PEA Alanine** with pendant methyl group released more than 90% of the drug during the same time frame using the same drug dose and drug:polymer ratio. Table 5 suggest that this rapid release of the drug for the Alanine PEA is driven by a high degree of water uptake, which is 45% after 24 h at 98% relative humidity of 37°C, while for PEA-Leucine the same uptake is approximately 14%. These water uptakes result in wet Tg's of 0 and 37°C for PEA-Alanine and PEA-Leucine, respectively.

The variation of the polymer architecture possible by altering the concentration of alanine and leucine monomers, allows the molecular mobility to stay relatively

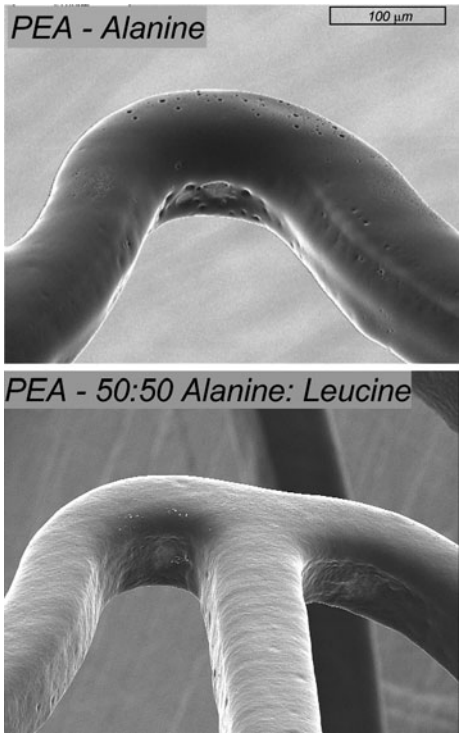

Fig. 5 Coating integrity of **PEA-Alanine**, and **PEA-50:50 Alanine-Leucine** after crimping, sterilization, passing through a tortuous path, expansion, and simulated use for an hour at 37°C in physiologic buffer solution (PBS)

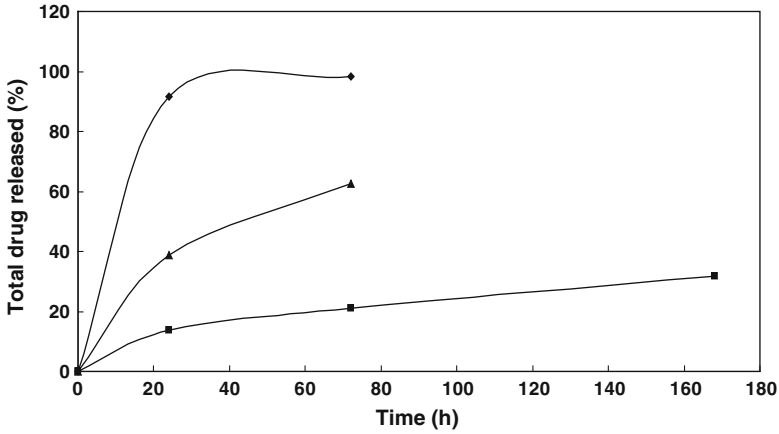

Fig. 6 Everolimus release profile in porcine serum from DES coatings based on **PEA-Leucine** (**PEA-VI**) (*black square*), **PEA 50:50 Alanine-Leucine** (*black triangle*), and **PEA-Alanine** (*black diamond*), formulated with a drug/polymer ratio of 1:5 and a total dose of 100 μg/cm^2

Table 5 Water uptake after 24 h exposure to various relative humidity levels at 37°C for **PEA-Leucine** (**PEA-VI**), **PEA 50:50 Alanine-Leucine**, and **PEA-Alanine**

Relative humidity (%)	Water uptake (%)		
	PEA-Leucine (PEA-VI)	**PEA 50:50 Alanine-Leucine**	**PEA-Alanine**
11	0	3	1
43	1	4	10
75	12	16	17
98	14	22	45

constant as observed by the dry Tg, while changing the polymer polarity indicates that water uptake and drug polymer miscibility is an extremely critical parameter for controlling drug release. These three polymers provide a useful tool to separate the effect of molecular polarity from the effect of molecular mobility with respect to drug delivery.

3.3 Adipate Based PEA

The impact of polymer drug miscibility was also partly the rationale to why the sebacinate linker was selected over the shorter and less lipophilic adipate linker to be used in the polymers for DES coating applications. Figure 7 shows the everolimus release rates for a family of PEA polymers synthesized in our laboratory. All polymers in Fig. 7 had very different molecular structures but were except for

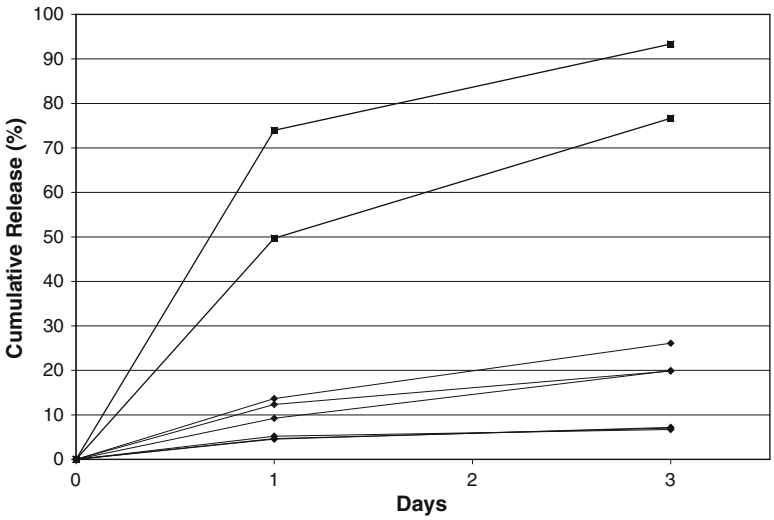

Fig. 7 Everolimus release profile in porcine serum from DES coatings based on various **PEA-adipate** (*black square*), and **PEA-sebacinate** (*black diamond*). All coatings were formulated with a drug/polymer ratio of 1:5 and a total dose of 100 μg/cm^2

Table 6 Adipate/sebacinate ratio, molecular weight (kD), Tg (°C), and everolimus release rate (%) after 1-day for **PEA-VI**, **PEA-IX**, and **PEA-X**

Polymer	Adipate/sebacinate ratio	Mw (kD)	Tg (°C)	1-Day RR (%)
PEA-VI	**0/100**	135.0	55	5
PEA-IX	**50/50**	153	60	10
PEA-X	**100/0**	100	68	50

The bold values are part of the name/structures of the polymers and not measured values

two all made using sebacinate. The other two polymers had adipate linkers and the impact of this difference was very clear with respect to the drug release rate as can be observed in Fig. 7.

To understand the impact of using adipate versus sebacinate in more detail two new polymers were synthesized, **PEA-IX** and **PEA-X**. In **PEA-X** all the sebacinate used in **PEA-VI** were replaced with adipate, and in **PEA-IX** 50% of the sebacinate in **PEA-VI** were replaced by adipate. To make the comparison possible the molecular weight was kept in the same range, 100–150 kD. Different from the alanine modification the adipate/sebacinate change increased the Tg a few degrees when the shorter adipate linkers were used, Table 6. Comparing the drug release rate for these three polymers confirmed the observation that the more lipophilic structure is preferred to control the drug release rate of lipophilic drugs such as everolimus.

The change to adipate increases the release rate dramatically even though the molecular mobility is actually reduced as observed with the higher Tg. The lower molecular mobility is likely responsible for the initially slower water uptake observed for **PEA-X** (adipate) relative to **PEA-VI** (sebacinate), Fig. 8. However, the less hydrophobic nature of the adipate polymer results in a higher water uptake 32 versus 14% for the sebacinate polymer after 24 h at 98% humidity at 37°C, Table 7. The higher water uptakes makes drug release less controllable from

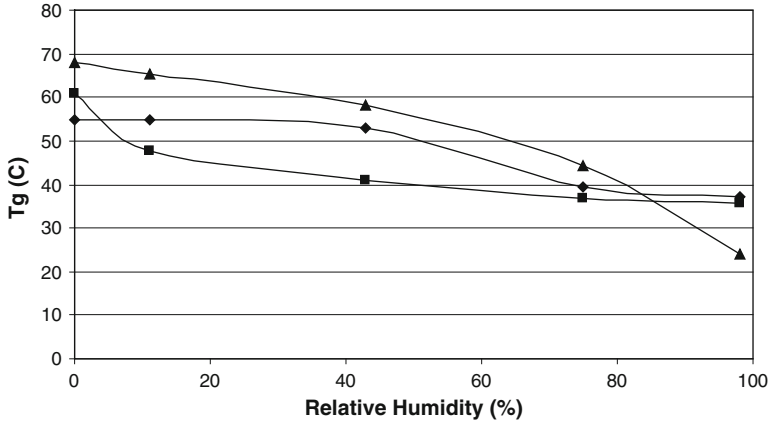

Fig. 8 Change in glass transition temperatures, Tg (°C), for **PEA-VI** (*black diamond*), **PEA-IX** (*black square*), and **PEA-X** (*black triangle*), coatings after being exposed to various relative humidity levels (%) for 24 h

Table 7 Water uptake after 24 h exposure to various relative humidity levels at 37°C for **PEA-VI**, **PEA-IX**, and **PEA-X**

Relative humidity (%)	Water uptake (%)		
	PEA-VI	**PEA-IX**	**PEA-X**
11	0	10	2
43	1	15	6
75	12	18	16
98	14	19	32

adiapte polymers and as pointed out above the adipate polymers are also less flexible than the sebacinate polymers, which makes them less suitable for DES applications with respect to coating integrity as well.

3.4 Molecular Weight of PEA

The data in Table 2 also indicate that the molecular weight may have an impact on the drug release rate. This was further demonstrated by synthesizing **PEA-V** with the 50/50 ratio of cyclohexanediol/hexanediol with various molecular weights. As can be observed in Table 8, although the molecular weight of **PEA-V** varied from 50 to 146.8 kD no significant change in glass transition was observed. However, although the glass transition temperature was held constant, a significant impact on the drug release was observed as a function of the molecular weight and in particular as the release started to be more restricted at higher molecular weights. This observation correlates well with the result above (Table 2) and confirms the hypothesis that molecular mobility of the polymer chains or the polymers free volume has a significant impact on the drug release rate. A higher molecular weight is less mobile than a lower molecular weight and provides a method to control the drug release for system where the drug and the polymer have good miscibility.

Since molecular weight in addition provides an impact on both the mechanical integrity and the resorption rate of a bioabsorbable material, it is necessary to carefully optimize this attribute to generate an ideal bioresorbable DES coating. Table 9 confirms that the molecular weight was stable throughout these studies for PEA-VI and that hydrolysis of the polymer backbone should not have had an impact on any of these experiments.

Table 8 Molecular weight (kD), Tg (°C), and everolimus release rates (%) after 1- and 3-days of **PEA-VI** polymers with different molecular weights

PEA-VI			
Mw (kD)	Tg (°C)	1-Day RR (%)	3-Day RR (%)
50.0	55	12.5	24.2
73.4	49	9.2	19.9
100.8	55	13.8	21.1
146.8	55	5.4	12

Table 9 Molecular weight (Daltons) and Mass Loss (%) for a **PEA-VI** DES coating with everolimus after being immersed in PBS at 37°C for 0, 2, 4, and 8 weeks

PEA-VI		
Time (weeks)	Mw (Daltons)	Mass loss (%)
0	49,500	0
2	48,400	0.8
4	44,300	1
8	44,000	5

4 Conclusion

It was demonstrated that PEA can be designed to have outstanding coating and controlled release properties that can potentially be used for complex medical application such as a drug eluting stent coatings. By modifying the molecular structure of PEA it was shown that they provide an excellent ability to tune water uptake and to control the release of small lipophilic drugs. In addition, the influence of polymer polarity and polymer rigidity on controlling drug release was demonstrated. By altering the molecular structure of PEA it provides a unique toolbox to understand the intrinsic mechanism of what controls hydrophobic drug release from thin polymer coatings, small polymer particles, and likely polymer gels.

Acknowledgments Gina Zhang is acknowledged for her help with drug release characterization.

References

1. Venkatraman, S., Boey, F.: Release profiles in drug-eluting stents: Issues and uncertainties. J. Control. Release **120**, 149–160 (2007)
2. Acharya, G., Park, K.: Mechanisms of controlled drug release from drug-eluting stent. Adv. Drug Deliv. Rev. **58**, 387–401 (2006)
3. Burt, H.M., Hunter, W.L.: Drug-eluting stents: A multidisciplinary success story. Adv. Drug Deliv. Rev. **58**, 350–357 (2006)
4. Commendeur, S., Van Beusekom, H.M.M., Van der Giessen, W.J.: Polymers, drug release, and drug-eluting stents. J. Interven. Cardiol. **19**, 500–506 (2006)
5. Ellis, J.T., Kilpatrick, D.L., Consigny, P., Prabhu, S., Hossainy, S.F.A.: Therapy considerations in drug eluting stents. Crit. Rev. Ther. Drug Carr. Syst. **22**, 1–25 (2004)
6. Lewis, A.L., Vick, T.A., Collias, A.C.M., Hughes, L.G., Palmer, R.R., Leppard, S.W., Furze, J.D., Taylor, A.S., Stratford, P.W.: Stratford "Phosphorylcholine-based polymer coatings for stent drug delivery. J. Mater. Sci.: Mater. Med. **12**, 865–870 (2001)
7. Langer, R.: New methods of drug delivery. Science **249**, 1527–1533 (1990)
8. Das, G.S., Rao, G.H.R., Wilson, R.F., Chandy, T.: Colchicine encapsulation within poly(ethyleneglycol)-coated poly(lactic acid)/poly(-caprolactone) microspheres-controlled release studies. Drug Deliv. **7**, 129–138 (2000)
9. Pitt, C.G.: Poly (ε-caprolactone) and its copolymers" in Biodegradable Polymers as Drug Delivery Systems. In: Langer, R., Chasin, M. (eds.) Biodegradable Polymers as Drug Delivery Systems, pp. 71–120. Marcel Dekker, New York, NY (1990)

10. Gref, R., Minamitae, Y., Peracchia, M.T., Trubetskoy, V., Torchillin, V., Langer, R.: Biodegradable long-circulating polymeric nanospheres. Science **263**, 1600–1603 (1994)
11. Albertsson, A.C., Varma, I.K.: Recent developments in ring opening polymerization of lactones for biomedical applications. Biomacromolecules **4**, 1466–1486 (2003)
12. Dechy-Cabaret, O., Martin-Vaca, B., Bourissou, D.: Controlled ring-opening polymerization of lactide and glycolide. Chem. Rev. **104**, 6147–6176 (2004)
13. Mecerreyes, D., Moineau, G., Dubois, P., Jerome, R., Hedrick, J.L., Hawker, C.J., Malmström, E.E., Trollsås, M.: Simultaneous dual living polymerizations: a novel approach to block and graft copolymers. Angew. Chem. **37**, 1274 (1998)
14. Hawker, C.J., Hedrick, J.L., Malmström, E.E., Trollsås, M., Mecerreyes, D., Moineau, G., Dubois, P., Jerome, R.: Dual living polymerizations from a double headed initiator. Macromolecules **31**, 213 (1998)
15. Trollsås, M., Hedrick, J.L., Mecerreyes, D., Dubois, P., Jerome, R., Ihre, H., Hult, A.: Versatile and controlled synthesis of star and branched macromolecules by dendritic initiation. Macromolecules **30**, 8508 (1997)
16. Trollsås, M., Hedrick, J.L.: Dendrimer-like star polymers. J. Am. Chem. Soc. **120**, 4644 (1998)
17. Hedrick, J., Trollsas, M., Hawker, C., Atthoff, B., Claesson, H., Heise, A., Miller, R., Mecerreyes, D., Jerome, R., Dubois, P.: Dendrimer-like star and block amphiphilic copolymers by combination of ring-opening and atom transfer radical polymerization. Macromolecules **31**, 8691 (1998)
18. Trollsås, M., Atthoff, B., Claesson, H., Hedrick, J.L.: Layered dendritic block copolymers. Angew. Chem. Int. Ed. Engl. **37**, 3132 (1998)
19. Bates, F.S.: Polymer-polymer phase-behavior. Science **251**, 898–905 (1991)
20. Fredrickson, G.H., Bates, F.S.: Block copolymers-Designer soft materials. Phys. Today **52**, 32–38 (1999)
21. Katsarava, R., Beridze, V., Arabuli, N., Kharadze, D.: Amino acid-based bioanalogous polymers. Synthesis and study of regular poly(ester amide)s based on bis(α-amino acid), α-ω-alkylene diesters, and aliphatic dicarboxylic acids. J. Polym. Sci. A: Polym. Chem. **37**, 391–407 (1999)
22. Kharadze, D., Kirmelashvili, L., Medzmariashvili, N., Beridze, V., Tsitlanadze, G., Tugushi, D., Chu, C.C., Katsarava, R.: Synthesis and α-chymotrypsinolysis of regular poly(ester amides) based on phenylalanine, diols, and terephthalic acid. Polym. Sci. A **41**, 883–890 (1999)
23. Arabuli, N., Tsitlanadze, G., Edilashvili, L., Kharadze, D., Goguadze, T., Beridze, V., Gomurashvili, Z., Katsarava, R.: Heterochain polymers based on natural amino-acids - synthesis and enzymatichydrolysis of regular poly(ester-amide)s based on bis(L-phenylalanine) a,w-alkylene diesters and adipic acid. Macromol. Chem. Phys. **195**, 2279–2289 (1994)
24. Tsitlanadze, G., Kviria, T., Katsarava, R., Chu, C.C.: Biodegradation of amino acid based poly(ester amide)s: in vitro study using potentiometric titration. J. Mater. Sci.: Mater. Med. **15**, 185–190 (2004)
25. Gomurashvili, Z., Kricheldorf, H.R., Katsarava, R.: Amino acid based bioanalogous polymers. synthesis and study of new poly(ester amide)s composed of hydrophobic a-amino acids and dianhydrohexitoles. J. Macromol. Sci. Pure Appl. Chem. **A37**, 215–227 (2000)
26. Guo, K., Chu, C.C., Chkhaidze, E., Katsarava, R.: Synthesis and characterization of novel biodegradable unsaturated poly(ester-amide)s. Polym. Sci. A **43**, 1463–1477 (2005)
27. Perez-Rodriguez, A., Alla, A., Fernandez-Santin, J.M., Munoz-Guerra, S.: Poly(ester amide)s derived from tartaric and succinic acids: changes in structure and properties upon hydrolytic degradation. J. Appl. Polym. Sci. **78**, 486–494 (2000)
28. Li, X., Lu, X., Lin, Y., Zhan, J., Li, Y., Liu, Z., Chen, X., Liu, S.: Synthesis and characterization of hyperbranched poly(ester-amide)s from commercially available

dicarboxylic acids and multihydroxyl primary amines. Macromolecules **39**, 7889–7899 (2006)
29. Li, X., Su, Y., Chen, Q., Lin, Y., Tong, Y., Li, Y.: Synthesis and Characterization of Biodegradable Hyperbranched Poly(ester-amide)s Based on Natural Material. Biomacromolecules **6**, 3181–3188 (2005)
30. Katsarava, R.: Active polycondensation–from peptide chemistry to amino acid based biodegradable polymers. Macromol. Symp. **199**, 419–429 (2003)
31. Vera, M., Puiggal, A., Coudane, J.: Microspheres from new biodegradable poly(ester amide)s with different ratios of L- and D-alanine for controlled drug delivery. J. Microencap. **23**(6), 686–697 (2006)
32. Legashvili, I., Nepharidze, N., Katsarava, R., Sannigrahi, B., Khan, I.: Non-covalent nano-adducts of co-poly(ester amide) and poly(ethylene glycol): preparation, characterization and model drugrelease studies. J. Biomater. Sci. Polym. Ed. **18**, 673–685 (2007)
33. Lin, Y., Zhang, K.Y., Dong, Z.-M., Dong, L.S., Li, Y.: Study of hydrogen-bonded blend of polylactide with biodegradable hyperbranched poly(ester amide). Macromolecules **40**, 6257–6267 (2007)
34. Lin, Y., Liu, X., Dong, Z., Li, B., Chen, X., Li, Y.: Amphiphilic Core-Shell Nanocarriers Based On Hyperbranched Poly(ester amide)-star-PCL : Synthesis, Characterization, and Potential as Efficient Phase Transfer Agent. Biomacromolecules **9**, 2629–2636 (2008)

RNA Interference Enhanced Implants

Morten Østergaard Andersen and Jørgen Kjems

Abstract RNA interference (RNAi) has in the last decade seen ever increasing use in cell biology as both a tool with which most cell functions can be modulated and as a natural mechanism through which cells regulate their gene expression. As RNAi can be used to direct stem cell differentiation, enhance tissue development, modulate inflammation and control other cellular phenomenon relevant to implant medicine the potential for using RNAi to enhance regenerative medicine is huge. Unfortunately, there are a number of obstacles and special concerns that need to be addressed before the use of RNAs on scaffolds and implants can go into clinical use. A number of studies have recently started to address these problems and demonstrate both the current limitations and the great promise of the technique. In this chapter we will discuss the basic principles of RNAi, it's applications in regenerative medicine and approaches to functionalize implants. We will describe various delivery methods for the inducer of RNAi, small interfering RNAs, in conjunction with scaffolds and how the application determines the delivery strategy. Finally, we describe how natural RNAi, mediated by microRNAs, can be manipulated by similar delivery techniques.

1 Introduction

Regenerative medicine is widely expected to be a corner stone of future medicine. The most common definition was coined in 1993 by Langer [57]: "Tissue engineering is an interdisciplinary field that applies the principles of engineering and

M. Ø. Andersen (✉) · J. Kjems
Department of Molecular Biology and Interdisciplinary Nanoscience Center, Aarhus University, C.F. Møllers Allé 3 (Building 1130), 8000 Aarhus, Denmark
e-mail: jk@mb.au.dk

Stud Mechanobiol Tissue Eng Biomater (2011) 8: 145–165
DOI: 10.1007/8415_2011_68

Published Online: 22 March 2011

the life sciences toward the development of biological substitutes that restore, maintain, or improve tissue function" and does so by bringing together "Isolated cells, cell supporting matrices and tissue inducing substances such as growth factors and their delivery vehicles" which still accurately describes the aim and ingredients of the field. Regenerative medicine could potentially alleviate many of the problems associated with current tissue and organ transplantation therapy, including risk of rejection and disease transmission, insufficient supply and lifelong immunosuppressant therapy with associated problems of infections and cancer. Furthermore, living tissue engineered organs could potentially replace mechanical implants when they can be created in sufficient numbers and quality. The obvious goal of tissue engineering is to grow personalized tissues and organs using cells derived from the patient (which are, therefore, immunocompatible). This is typically accomplished [97] (Fig. 1) by extracting, purifying and expanding cells from a patient. These are then seeded into a three dimensional support (commonly a solid scaffold or a gel) which works as a temporary artificial extracellular matrix. The cells are induced to produce the correct extracellular matrix, and, if stem cells are involved, to differentiate into the correct cell type(s) either before or after they are implanted back into the patient. Variations on the theme exist. Sometimes the cells are implanted without a support and migrate to and lodge at their site of action

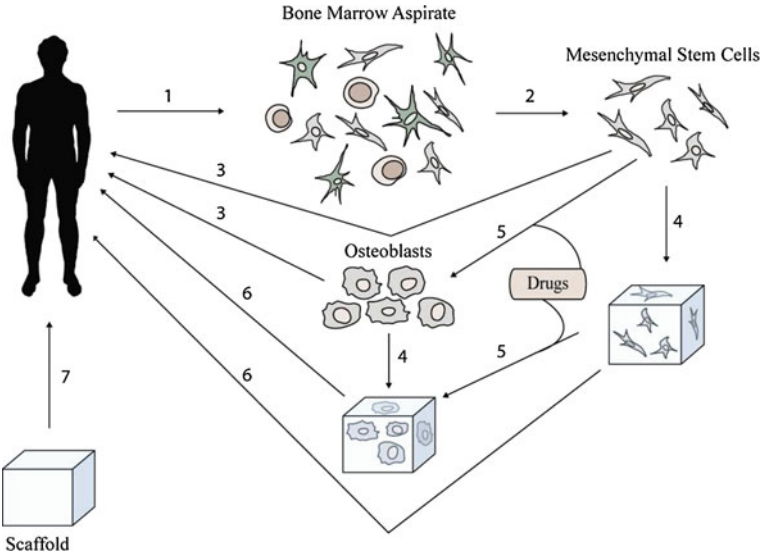

Fig. 1 Approaches to Tissue Engineering. In tissue engineering, cells are commonly extracted from the patient (1) where after the cells of interest are purified, expanded (2), and re-implanted into the patient undifferentiated (3) or after ex vivo differentiation (5). These approaches are known as cell therapy. Alternatively, the cells can be seeded in a supportive structure (4) which can be implanted without further manipulation (6). However, the cellularized scaffolds are commonly differentiated (5) before implantation (6). Finally scaffolds without cells (7) can be implanted after which the scaffold is colonized by migrating host cells

which usually is referred to as cell therapy [86]. Another approach is to simply inject progenitor cells on a matrix, but without cues, and let them differentiate according to cues provided by the in vivo environment [53]. Finally, implants can be implanted without cells and get colonized by migrating host cells [33].

Several types of organs and tissues have been grown using tissue engineering techniques. Notable examples that have been tested with success in patients include bladders [5] and airways [64]. However, the tissues and organs previously engineered successfully were all relatively simple, and included only one or two cell types. The regenerated airway consisted of a decellularized matrix cylinder seeded with chondrocytes on the outside and epithelial cells on the inside while the bladder consisted of a decellularized matrix or collagen/poly-glycolide sphere seeded with urothelial cells on the inside and smooth muscle cells on the outside. In both examples two cell types could be applied, since they were separated physically by a wall. In most tissues such as liver, skin, kidney, pancreas, and the central nervous system many cell types are in contact with each other but still separated in distinct structures. Although previous attempts have been made to create skin tissue by seeding different cells in layers it was found that the cells migrated and mixed [76]. Therefore, in order to create such tissues, other approaches are needed. One reported strategy utilizes "printing" different cell types in spatially different locations using a bioplotter [31, 59]. An obvious advantage of this approach over traditional loading of cells onto a structure is that high throughput as well as complex geometries can be achieved. Several problems, however, are connected with this approach [67] such as the adverse effects the printing process may have on the cells [93]. Furthermore, by seeding pre-differentiated cells on a scaffold one can miss the important functions that some stem cells perform while differentiating, such as depositing extracellular matrix, an ability cells sometimes loose when fully differentiated [6]. There is, therefore, a need for active implants that can influence the differentiation of cells spatially in a scaffold.

Other major obstacles affecting the success rate of implants is acquiring enough cells in the implant, to ensure their survival and to prevent the immune response mounted by the patient against an implant (known as the foreign body response). Few strategies address the multitude of challenges a cellularized implant is met with. One extremely versatile technique that enables control over differentiation and other cellular processes, is the potential for over expressing genes from exogenously added plasmids or silencing specific gene expression by RNAi. This chapter will focus on the latter possibility; however, many of the delivery methods are applicable to plasmids as well.

2 RNA Interference

RNAi was first discovered in plants [9] and lower animals [32] and has since been identified in higher animals including humans [29] (Fig. 2). It has subsequently become a primary tool to dissect gene function in vitro and in vivo and is being

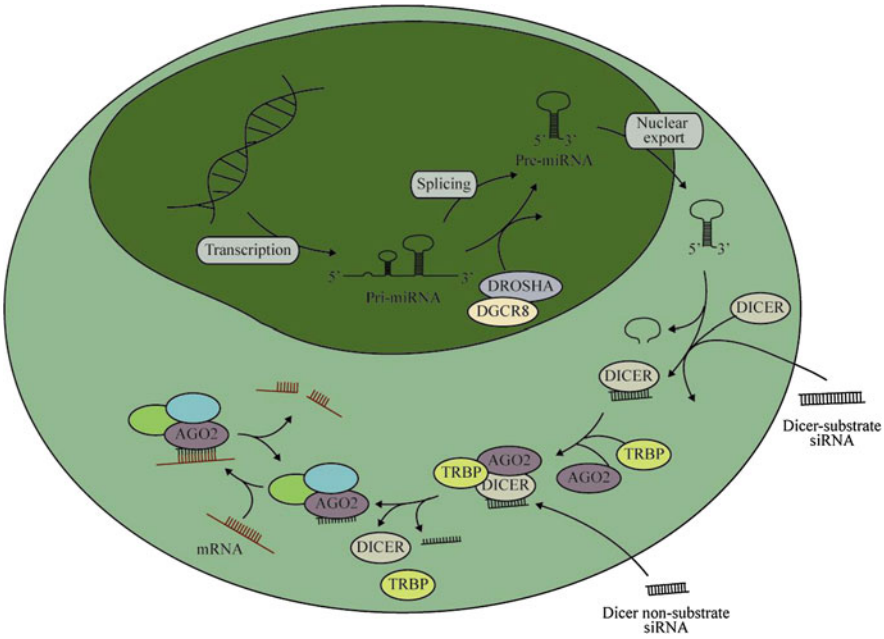

Fig. 2 RNA Interference. Pri-miRNA is transcribed in the nucleus and processed to pre-miRNA by DROSHA and DGCR8. The pre-miRNA is exported to the cytoplasm where it (or a DICER Substrate siRNA) is processed by DICER into a siRNA which can also be introduced externally as non-DICER Substrate siRNA. The DICER/siRNA complex forms the RISC loading complex together with AGO2 and TRBP. This complex transfers one of the siRNA strands to AGO2 forming the RISC complex. The loaded strand can subsequently guide RISC to mRNAs with a complementary sequence. These mRNAs are translationally inhibited, destabilized or cut (if completely complementary). The RISC complex can be reused. For a detailed review see [20]

investigated as a therapeutic strategy for many diseases [21]. While RNAi is found in all higher eukaryotes there is considerable difference in the exact mechanisms in different species. This chapter will consider the application of RNAi to mammalian cells.

The mediators of RNAi are largely based on two types of molecules; microRNA (miRNA) and small interfering RNA (siRNA), although, it is becoming difficult to distinguish between the two categories [20]. Originally it was thought the siRNAs acted through cleavage of the target mRNA while miRNAs acted through inhibition of translation and destabilization of the target mRNA. However, exogenously introduced siRNAs with incomplete complementarity to an mRNA are able to repress through the latter mechanisms of translational inhibition and mRNA destabilization while endogenously expressed miRNAs with complete complementarity to an mRNA can repress it through the former mechanism of strand cleavage [102].

The active component of RNAi is small interfering RNAs (siRNAs) that, upon transfection into the cytoplasm will cause specific degradation of complementary mRNAs. A problem plaguing all siRNA based knockdown strategies is

the off target effect which is thought to occur when the siRNA is partially complementary to untargeted mRNAs and thus inhibits these through inhibition of translation and destabilization [77]. One strategy to avoid off target effects is to avoid high siRNA concentration and by chemically modifying the RNA strands at strategic positions [16].

MicroRNAs are used extensively by eukaryotes to control mRNA activity. It is estimated that 30% of the genes in humans are under miRNA control [60] and nearly 1,000 miRNA have been characterized in humans. microRNAs are normally expressed as longer primary transcripts by Pol II and then subsequently processed in two steps into mature miRNA. Most miRNAs in mammals are not completely complementary to their mRNA targets, and therefore, repress them through translational inhibition and mRNA destabilization [66].

3 Applications to Tissue Engineering

Tight control of gene expression involved in proliferation, differentiation and the immune response are key parameters for tissue engineering. The high level of specificity provided by the RNAi technology and the potential of constraining siRNA particles to predetermined position in a scaffold make them an excellent tool for manipulating these events [22, 100].

3.1 Proliferation and Apoptosis

Controlling cell proliferation and apoptosis is particular important in the initial phase of regeneration where the cell concentration is low. However, it is important that these processes are temporary, since escape from the cell cycle and apoptosis are important processes in the later stages of tissue development [17]. Non-viral RNAi induced knockdown is usually temporary, and therefore, provides an ideal method for increasing cell numbers and survival short term. For example, silencing of the cell cycle regulator p21 has been shown to increase cellular proliferation in monolayer and scaffold culture of mesenchymal stem cells while not adversely affecting their differentiation capability [75]. In another study Bax-2 silencing in allografted neuronal precursor cells was shown to reduce apoptosis during the critical first 24 h after transplantation which led to an increase in cell numbers and transplant size [104].

3.2 Differentiation

Differentiation occurs when a stem cell specializes into a more mature cell type. It typically takes place in steps and is driven by several sequential transcription

factors. Usually a master transcription factor acts as a switch and, when expressed, drives the differentiation alone. Examples of such switches are PPARγ2 in adipogenic differentiation [89] and RUNX2 in osteogenic differentiation [54]. In line with this it has been demonstrated that osteogenic differentiation and adipogenic differentiation can be repressed by silencing the main transcription factor responsible for those pathways, RUNX2 [62] and PPARγ2 [96], respectively. Enhancement of differentiation is a more complicated matter but can be accomplished by silencing a repressor of a differentiation pathway. Although a large set of such genes have been characterized (Table 1), caution should be taken when using RNA interference to control differentiation as siRNAs may induce adipogenic differentiation non-specifically [95].

Silencing a single gene is usually not sufficient to induce full differentiation, necessitating supporting differentiation media. BCL2L2 knockdown, for example, was found to induce osteogenic gene expression but not mineralization [103]. The latter was enhanced when the BCL2L2 knockdown was combined with osteogenic media containing ascorbic acid, dexamethasone and beta-glycerol-phosphate. It appears, however, that certain siRNAs can replace specific factors in the chemical induction cocktails and still drive full differentiation. The adipogenic media components dexamethasone and IBMX can, for example, be replaced by silencing TRIB2 and Krox24, respectively [15, 70]. This indicates that a cocktail of siRNAs, at least in some instances, may be found to replace all the chemical inducers of differentiation and thus drive differentiation alone. In addition, studies that investigate the effect of combining knockdown of several inhibitors of a pathway find that much greater stimulation of differentiation can be achieved this way. For example, combining SLC12a2 and KCNT1 knockdown was found to enhance osteogenic differentiation more efficiently than if the genes were silenced individually [103].

3.3 Multi-Lineage Differentiation

Most tissues in the body are composed of different cell types arranged in highly organized geometries [72]. Constructing implants with multiple cell types is thus of great interest in tissue engineering [40]. The traditional approach to accomplish this is to seed different pre-differentiated cell types in separated regions of an implant. A different strategy is to seed one stem cell population and let the implant exert different differentiation stimuli in spatially distinct regions.

The latter concept has recently been explored using different strategies. One method is to deposit a gradient of nucleic acid over a scaffold before cell seeding. When stem cells are seeded a gradient of differentiated and undifferentiated cells develop [73]. A second method is to print nucleic acids and stem cells to different areas of a scaffold although this has so far not been tried with multiple drugs at the same time [24, 94]. We have recently developed a third method [2] (Fig. 3) where separate parts of an implant are loaded with siRNAs against either BCL2L2 or

Table 1 RNA interference targets for enhancement of differentiation

Target	Differentiation	Organism	Molecule	Vector	Ref.
GSα	Osteogenic	H. Sapiens	DNA antisense	Etoxylated PEI	[61]
WISP1 WISP2	Hepatogenic	H. Sapiens	siRNA	RNAiFect	[82]
NRSF	Neurogenic	H. Sapiens	shRNA	Lentiviral Vector	[98]
GAS6	Chondrogenic	M. Musculus	siRNA	Lipofectamine 2000	[69]
SOX9	Adipogenic Osteogenic	H. Sapiens	siRNA	"Transfection Reagent"	[91]
TRIB2	Adipogenic	M. Musculus	shRNA	Retroviral Vector	[70]
TRIB3	Adipogenic	M. Musculus	shRNA	Lentiviral Vector	[88]
KROX24	Adipogenic	M. Musculus	shRNA	Retroviral Vector	[15]
NOTCH1	Neurogenic	M. Musculus	shRNA	siPORT Lipid	[99]
TWIST1	Osteogenic	M. Musculus	siRNA	Lipofectamine 2000	[38]
HDAC7	Osteogenic	M. Musculus	shRNA	Retroviral Vector	[52]
HDAC1	Osteogenic	R. Norvegicus	shRNA	Retroviral Vector	[58]
MENIN	Myogenic	M. Musculus	shRNA	pSilencer	[7]
BCL2L2	Osteogenic	H. Sapiens	siRNA	Extreme siRNA Transfection Reagent	[103]
BCL2	Osteogenic	H. Sapiens	siRNA	Extreme siRNA Transfection Reagent	[103]
P2RY11	Osteogenic	H. Sapiens	siRNA	Extreme siRNA Transfection Reagent	[103]
ADK	Osteogenic	H. Sapiens	siRNA	Extreme siRNA Transfection Reagent	[103]
ADCY8	Osteogenic	H. Sapiens	siRNA	Extreme siRNA Transfection Reagent	[103]
GDBR1	Osteogenic	H. Sapiens	siRNA	Extreme siRNA Transfection Reagent	[103]
SLC12a2	Osteogenic	H. Sapiens	siRNA	Extreme siRNA Transfection Reagent	[103]
KCNT1	Osteogenic	H. Sapiens	siRNA	Extreme siRNA Transfection Reagent	[103]
DUSP6	Osteogenic	H. Sapiens	siRNA	Extreme siRNA Transfection Reagent	[103]
BIRC4	Osteogenic	H. Sapiens	siRNA	Extreme siRNA Transfection Reagent	[103]
GNAS	Osteogenic/ Adipogenic	H. Sapiens	siRNA	Extreme siRNA Transfection Reagent	[103]

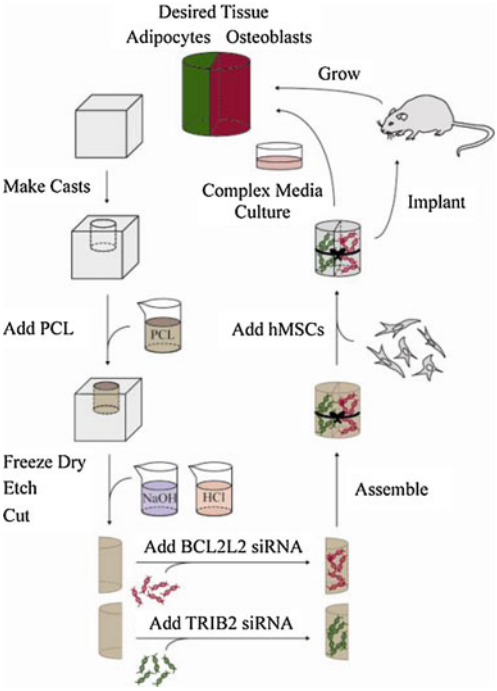

Fig. 3 Multilineage differentiation. The figure demonstrates the approach to multilineage differentiation developed in our group [2]. First casts are made wherein PCL solution is cast, frozen and lyophilized to produce scaffolds which are then surface modified and cut into smaller building blocks. These are then loaded with nanoparticles containing siRNAs against either BCL2L2 or TRIB2. The scaffolds parts are then assembled into the desired structure which is subsequently loaded with stem cells. A tissue containing adipocyte- and osteoblast-like cells in separate parts can then be grown in vitro or in vivo directed by the included siRNAs

TRIB2 promoting osteogenesis or adipogenesis, respectively. The scaffold is then seeded with stem cells and placed into complex differentiation media containing factors that support the differentiation pathways dictated by the siRNAs. Alternatively, the scaffold could be implanted after cellularization in which case differentiation happened in vivo.

3.4 Host Response

Implant induced inflammation is a major concern in tissue engineering [4]. The acute inflammation phase is triggered by the adsorption of blood proteins onto the surface of the material where they establish a provisional blood derived matrix. These proteins can function as anchors and bind immune cell surface receptors. Neutrophils and mast cells are the first immune cells to infiltrate the biomaterial structure and their excretion of chemoattractants such as the monocyte chemoattractant protein 1 (MCP-1) trigger subsequent infiltration by macrophages and other immune cells [25]. If not treated the situation usually inters a chronic inflammation phase characterized by the presence of degradative monocytes and macrophages. This phase may be followed by the formation of granulation tissue composed of fibroblast and macrophages surrounding the biomaterials. The granulation tissue then becomes a fibrous capsule effectively isolating the

biomaterial. Collectively these processes are known as the foreign body response. Decellularized extracellular matrix is particularly vulnerable to inflammation [8] as antibodies may be raised against foreign proteins or carbohydrates remaining in the product. Xenogenic matrix is especially susceptible because it contains the x-gal-epitope which is a carbohydrate present on glycoproteins and glycolipids. Humans do not have this carbohydrate and around 1% of the circulating human IgG is directed against the epitope severely limiting the potential of xenogenic scaffolds. Together these problems restrict the clinical use of decellularized tissue engineered products [84].

As mentioned, macrophages are major players in the foreign body response [3]. They secrete chemoattractants sustaining the cellular response and pro-inflammatory cytokines such as interleukin 1 and tumor necrosis factor alpha (TNFα). Furthermore, macrophages are responsible for the degradation of the biomaterial. They accomplish this by releasing degradative enzymes, acid and reactive oxygen species as well as by phagocytising material. Cytokines such as TNFα can act detrimental to the implant in several ways. They can act as chemoattractants further increasing immune cell infiltration [35], as stimulators of phagocytosis, oxygen radical production and degranulation, which degrade the implant [12], or they can interfere with stem cell differentiation [42, 56]. As macrophages are stimulated to express cytokines when they come in contact with biomaterials [27] they present very attractive targets for therapies that seek to reduce inflammation and prevent degradation of tissue engineered structures. However, one must apply such strategies carefully as immune cells, and other cells derived from haematopoietic precursors such as osteoclasts, play a major role in removing tissue damaged during implantation [37] and in remodelling the implant to achieve the correct tissue structure and composition [28]. While RNAi provides an effective means to control the production of cytokines such as TNFα in macrophages after injection in vivo [46] or if grown on substrates pre-coated with anti-TNFα siRNA particles [1] it remains to be established whether siRNA delivery from scaffolds or other implants can control the foreign body response in vivo. An alternative method for preventing implant encapsulation and failure could be to silence mTOR in fibroblasts [87]; however, such a method would require preferential delivery of siRNAs to fibroblasts instead of invading immune cells which may prove difficult. Based on these findings we suspect that RNAi will play a major role in controlling the foreign body response to implants in the future.

3.5 Other Applications

Since siRNAs can be used to target virtually any pathway there are numerous other ways in which siRNA coating could be used to enhance the function of the cells seeded on an implant. In neural injury, for example, a major problem is axonal degeneration due to factors secreted by the damaged tissue, these factors act through the neuronal gene RhoA that, therefore, represents an attractive siRNA

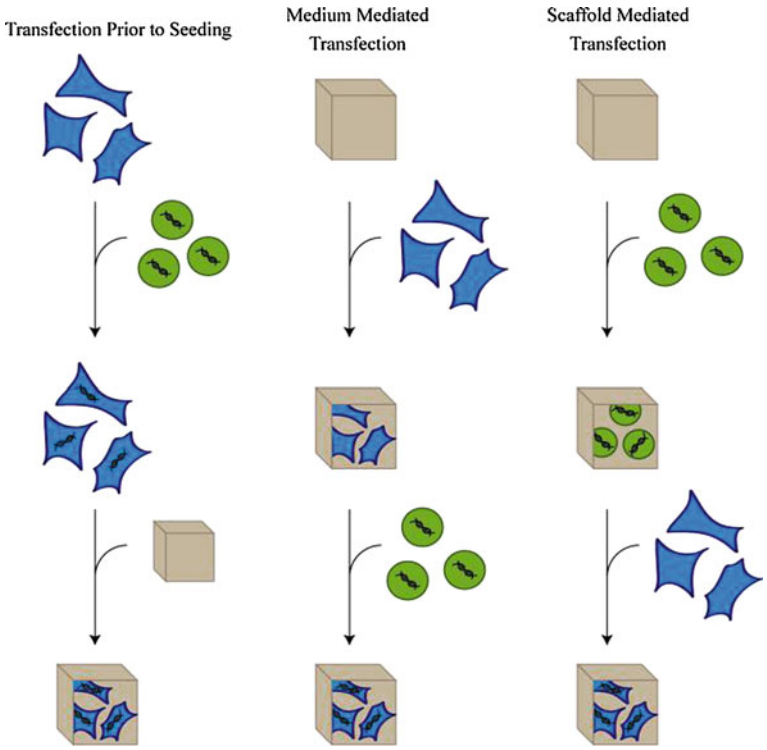

Fig. 4 Delivery strategies. RNAi can be applied to cells that are destined for implantation on a tissue engineering scaffolds in three ways. The cells can be transfected before being seeded onto a scaffold (*left*). Alternatively, the cells can be seeded onto the scaffold and the scaffold can then be placed in medium containing the RNA (*center*). Finally, the nucleic acids can be applied to a scaffold before cell seeding; the cells then take up the RNA when they are seeded onto the scaffold (*right*)

target for enhancing neurite outgrowth. Indeed, polymeric implants coated with chitosan/siRNA nanoparticles targeted to RhoA have been shown to reduce RhoA expression in seeded PC12 neural cells and the particles were able to enhance neurite outgrowth in the presence of myelin [68]. Hence, siRNA coated scaffolds may prove valuable as guides for joining damaged neuronal axons in the future.

4 Combining RNA Delivery and Implants

There are three strategies to combine cells, siRNA/plasmid and scaffolds (Fig. 4). Cells may be transfected with nucleic acids prior to seeding them into the scaffold or cells can be seeded first and then transfected via the scaffold or culture medium. All three strategies present certain advantages and disadvantages

Transfecting cells prior to scaffold seeding [22] is the easiest approach as it involves a standard transfection procedure and requires little formulated siRNA or plasmid, however, concern has been raised that transfection could leave the cells too fragile to survive the process of scaffold seeding [19]. This could especially be a problem if a seeding method that induces additional strain, such as cell printing, is used.

Alternatively, cells may be seeded first in the scaffold and subsequently transfected by adding siRNA/plasmid formulations to the culture medium [19]. This approach is essentially a standard transfection procedure and it is, therefore, relatively straight forward, however, it might result in uneven transfection efficiency with cells on the surface of the scaffold being more efficiently transfected than those in the centre of the scaffold. The severity of this problem depends on the diffusion rate within the scaffold and on how quickly the transfection reagent binds to the cells. The diffusion rate of medium within scaffolds can be increased using dynamic culturing methods such as spinner flasks or flow cells [23], however, these methods require large volumes of medium which would make the use of this strategy prohibitively expensive for siRNA delivery. Alternatively, a slowly acting transfection reagent could be employed giving it time to reach the centre of the scaffold before it interacts with cells. Unfortunately, most commercially available transfection reagents are designed to bind to cells as quickly as possible, and therefore, new delivery systems may have to be developed in order to utilize such a strategy. One could, for example, imagine a delivery system that has been partly coated with polyethylenglycol (PEG) which is known to reduce particle–cell interaction [92].

Finally, cells within the implant can be transfected by releasing the siRNA or plasmids from the matrix itself (Fig. 4). In this case the nucleic acids can either be coated onto the surface of the polymer structure were it is readily available to the cells [2] or be encapsulated within the implant during preparation [55] and be released over prolonged periods. This strategy limits the amount of drug that has to be used compared to options mentioned above. Furthermore, the cells can attach and proliferate prior to transfection which may reduce adverse effects from transfection reagent. However, delivering siRNA or DNA from a scaffold requires the interfacing of the delivery system with the structure and this usually represents another challenge that we will address below.

4.1 Delivery Methods for Scaffolds

From a pharmaceutical stand point siRNA delivery pose a number of obstacles [45]. For example, RNA is susceptible to degradation by serum nucleases and hydrolytic cleavage and siRNAs are large anionic molecules incompatible with crossing cell membranes. These problems are typically overcome by using carriers (vectors) to protect and deliver nucleotide based drugs to the cellular interior. In the case of nucleotide delivery from scaffolds, the scaffold material itself may

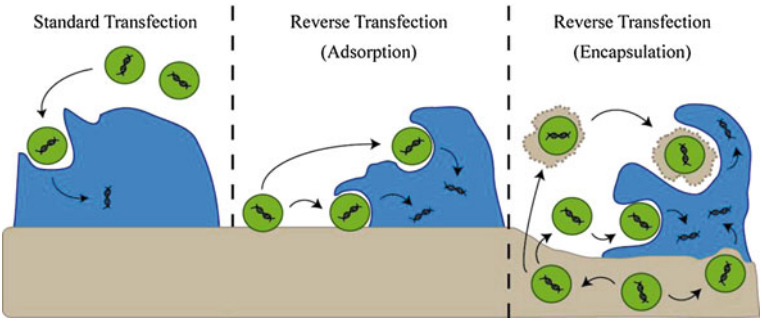

Fig. 5 Delivery methods. Nucleic acid carrying particles can be delivered to cells sitting on implants through three different routes. If a standard transfection is carried out, through the medium surrounding the scaffold, the particles will diffuse through the structure until they adsorb onto and are internalized by the cells they encounter (*left*). Alternatively, the carriers can be adsorbed onto the structure before cell seeding (*center*). In this case the cells can internalize the particles directly from the wall where they attach (known as reverse transfection). Depending on the strength of the interaction between the scaffold and the particles, the carriers may alternatively resuspend and transfect the cells from the medium (as in the *left panel*). Finally, the nucleic acids may be encapsulated within the scaffold polymer (*right*). In this case they are released continually as the matrix breaks down, the scaffold polymer may play a part in the uptake of the nucleic acids or it may be purely driven by the carrier in which case it works like reverse transfection

carry out functions ordinarily performed by the vectors. Figure 5 illustrates some of the delivery routes that can be used in tissue engineering.

In general carriers are divided into viral vectors and non-viral vectors. Viral carriers typically used together with scaffolds are based on retroviruses [26], adenoviruses [79] and adeno-associated viruses [10]. While viral vectors are generally considered more efficient than non-viral vectors they are also more cumbersome to produce and have safety issues. Retroviruses can causes insertional mutagenesis and cancer [11] while adenoviruses can cause severe immune reactions [65]. Non-viral carriers exist in a multitude of variants but vectors used for scaffold delivery are typically based upon lipids [18] or polymers [47]. Lipid carriers are primarily in the form of nucleic acid entrapping liposomes or electrostatic complexes between cationic lipids and nucleic acids (lipoplexes). Polymer based delivery is based on either dynamic polyelectrolyte complexes, known as polyplexes, formed through electrostatic interaction between a polycation and a nucleotide or on solid particles composed of a polymer matrix which can encapsulate or adsorb the nucleic acid [44]. Electrostatic complexes made with mixtures of lipids, polymers and siRNA are also used (lipopolyplexes) [78]. Lipid and polymer based vectors are also associated with various problems such as toxicity but these issues can to a certain extent be ameliorated by adjusting the chemical structure of the carrier [63].

It is important to bear in mind that most carrier systems are designed to deliver nucleotides to cells grown in monolayer culture. Interfacing such systems with implants may radically alter their properties such as transfection efficiency [39], onset of silencing [90] and duration [43]. Such behaviour is likely to depend on the

carrier and scaffold properties and the method of incorporation. Limited work has been done with siRNA delivery from implants but important lessons can be learnt from the research on scaffolds loaded with DNA. However, one most bear in mind that siRNA primarily function in the cytoplasm, whereas, plasmids need to translocate to the nucleus to be expressed.

4.2 Lessons from DNA Delivery

DNA has been delivered from scaffolds successfully into cells as part of viral vectors [83], polyplexes [39] and as a naked plasmid [50]. Interestingly adsorbing [14, 30], and encapsulating [51, 81]; naked plasmid into scaffolds appears to have an effect in several studies, despite the fact that delivery of naked plasmid is usually considered highly inefficient unless it is performed under increased hydrodynamic pressure or with electroporation [41]. Conceivably the plasmids could be carried on eroding fragments of the scaffold polymer that can then facilitate cellular binding, uptake and endosomal escape. In this case one would expect the delivery efficiency to be highly dependant on the scaffold material.

To improve delivery, polymeric DNA nanoparticles have been used extensively on scaffolds and shown great promise. Studies have shown that absorbed plasmid can be released over time [49] and greatly reduces the amount of nucleic acids needed to achieve transfection compared to delivery through the surrounding medium. The dissociation rate appears to be dependant on the polymer to plasmid ratio of the complex probably due to increased ionic interactions between the carrier and scaffold at higher carrier to DNA ratios. Furthermore, transfection efficiency was found to increase while cell proliferation decreased with higher polymer to DNA ratios.

A study [71], comparing scaffolds coated with naked plasmids with scaffolds coated with or encapsulating chitosan/plasmid nanoparticles showed that naked plasmid is released fastest and encapsulated nanoparticles slowest. The study further showed that adsorbed carriers induced a slightly higher toxicity compared to encapsulated material and that the formulation of plasmid DNA with chitosan increased expression. Therefore, for most purposes encapsulation may seem like the most attractive strategy to interface plasmid and scaffold Fig. 6.

Partly because DNA transfection has to bypass an additional barrier (the nuclear membrane) compared to siRNA transfection the percentage of transfected cells is typically lower when using DNA delivery systems [105]. This is especially true for non-dividing cells where the nuclear membrane remains intact. It would, therefore, generally be insufficient to use plasmids affecting only the transfected cells to control the development of tissue on an implant. This is especially true in applications where undifferentiated stem cells might pose a risk of oncogenicity [13]. However, when using a gene encoding payload, transfecting a small fraction of the cells may cause a major effect if the vector encodes secreted growth factors which affects the neighbouring non-transfected cells. While this strategy is useful for generating single cell

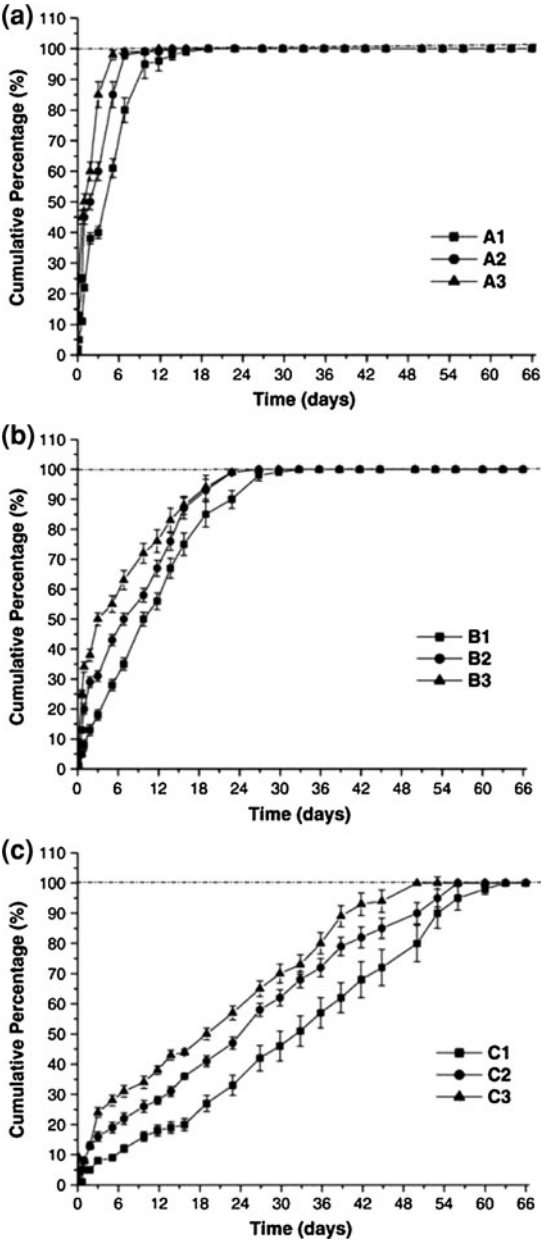

Fig. 6 Controlled release from scaffolds. The release of nucleic acids from a scaffold depends on the method of incorporation [71]. This figure shows the cumulative release of plasmid DNA that had been incorporated in three different ways into scaffolds made from poly(lactic-glycolic)acid and three different amounts of hydroxyapatite (1–3). Unprotected anionic nucleic acids adsorbed onto the anionic scaffolds are released fastest as they are most likely repelled from the surface [*top* (A1–A3)]. Cationic chitosan/nucleic acid complexes adsorbed onto the anionic scaffolds are released slower probably due to electrostatic interactions between the complexes and the scaffold [*center* (B1–B3)]. Finally, chitosan/nucleic acid complexes that were encapsulated into the scaffold are released slowest, presumably because the scaffold has to breakdown before the complexes are released [*bottom* (C1–C3)]

type tissues it is not ideal for multi-lineage differentiation applications as the forced over expression and secretion of growth factors inducing a certain type of differentiation could diffuse into a section of an implant where a different type of differentiation is desired. Delivery of siRNA only affects the transfected cells and as it is

more efficient than DNA delivery, approaching 100% [2], therefore it presents an ideal method for controlling multi-lineage differentiation.

4.3 Temporally and Spatially Controlled RNA Delivery

While one of the advantages of the siRNA is that the effect is temporary, and therefore, more easily controlled there are also drawbacks. Results indicate that temporary silencing of a differentiation repressor gene is enough to greatly enhance differentiation [2]; however, extended silencing would be necessary in certain cases. Furthermore, a delayed knockdown of a late repressor could probably be beneficial under many circumstances. In such a case one could, for example, silence first BCL2L2 to induce osteogenic differentiation and then HTRA1 to enhance mineralization in the resulting osteoblasts [36]. To achieve these effects a two phasic release system is necessary. While such a system still is to be developed for siRNA delivery there are results performed with proteins that can be used as inspiration. For example, it has been shown that two different proteins can be released sequentially from a multi-polymer composite scaffold if they are incorporated into polymers with dissimilar degradation rates [34, 101]. We believe a similar mechanism could be used with siRNA, however, one must take care that the RNA is sufficiently chemically protected to survive the duration until release.

Multilineage differentiation is possible when different siRNAs are delivered from spatially distinct regions of an implant. Achieving this effect depends on the retention of the nucleic acid carriers until they are delivered to the seeded cells. This requires an interaction between the vectors and the scaffolding material. Materials can be bound onto implants in various ways such as by covalent linkage [74], by electrostatic or hydrophobic interactions [2] or by embedding the drug into the scaffold polymer [71]. We believe any of these methods could be used together with siRNA. A conceivable alternative to using temporally delayed release in a multi-lineage differentiated implant would be to use a targeted delivery system to deliver the RNA cargo to a specific cell type at a later stage. For example, one could use the siRNAs loaded on a scaffold initially to start differentiation of seeded stem cells such as MSCs into tissue precursor cells such as pre-osteoblasts and pre-adipocytes. If, at this stage, a different RNA is needed to, for example, drive terminal differentiation of one of these cell types it could be delivered using a delivery system targeted to a receptor expressed solely on one of the precursor cell types.

5 MicroRNA Enhanced Scaffolds

The number of characterized miRNAs that appear to have a role in phenomenons important to implant function such as stem cell differentiation [48] and inflammation [85] is steadily increasing. Just like siRNAs, miRNAs are capable of

repressing or enhancing differentiation pathways, for example, miR27a and miR489 downregulates osteogenic differentiation of mesenchymal stem cells while miR148b upregulates it [80]. They can be, therefore, be used to direct cell specialization in a similar way as the siRNAs described in this chapter. Furthermore, the similar structure of miRNA precursors and a siRNA duplex mean that they can be delivered using the same delivery systems. miRNAs may in fact turn out to be superior to siRNAs for controlling cell functions as miRNAs are naturally playing an important role in these processes. The development of efficient miRNA inhibitors (anti-miRs), which are chemically modified oligonucleotides complementary to specific miRNAs, also opens up for the possibility of inhibiting miRNA function in differentiation processes. Therefore, we expect that miRNA/antimiR delivery from scaffolds will be used in the future for growing tissues.

6 Conclusion and Future Perspectives

RNAi presents an extremely attractive solution to the obstacles facing implant medicine in general and tissue engineering in particular. The delivery of siRNAs and miRNAs from scaffolds provides a versatile method for controlling stem cell differentiation, tissue functions and inflammation. Furthermore, the technique is well suited to generate complex tissues composed of multiple cell types. There are many different strategies and methods for using RNAi together with implants, a specific application may benefit from a simple transfection with one RNA but, if needed, complex delivery modes of multiple nucleic acids have been demonstrated. The number of characterised RNAs that regulate various cell functions is continually increasing, underlining the need for improved RNA delivery methods from scaffolds. In conclusion, we predict that RNAi will become as powerful a tool in implant medicine and tissue engineering as it has been for manipulating monolayer cell culture.

References

1. Andersen, M.Ø., Howard, K.A., Paludan, S.R., Besenbacher, F., Kjems, J.: Delivery of siRNA from lyophilized polymeric surfaces. Biomaterials **29**(4), 506–512 (2008)
2. Andersen, M.Ø., Nygaard, J.V., Burns, J.S., Raarup, M.K., Nyengaard, J.R., Bünger, C., Besenbacher, F., Howard, K.A., Kassem, M., Kjems, J.: siRNA nanoparticle functionalization of nanostructured scaffolds enables controlled multilineage differentiation of stem cells. Mol. Ther. **18**(11), 2018–2027 (2010)
3. Anderson, J.M., Miller, K.M.: Biomaterial biocompatibility and the macrophage. Biomaterials **5**, 5–10 (1984)
4. Anderson, J.M., Rodriguez, A., Chang, D.T.: Foreign body reaction to biomaterials. Semin. Immunol. **20**(2), 86–100 (2008)
5. Atala, A., Bauer, S.B., Soker, S., Yoo, J.J., Retik, A.B.: Tissue-engineered autologous bladders for patients needing cystoplasty. Lancet **367**(9518), 1241–1246 (2006)

6. Aubin, J.E., Liu, F., Malaval, L., Gupta, A.K.: Osteoblast and chondroblast differentiation. Bone **17**, S77–S83 (1995)
7. Aziz, A., Miyake, T., Engleka, K.A., Epstein, J.A., McDermott, J.C.: Menin expression modulates mesenchymal cell commitment to the myogenic and osteogenic lineages. Dev. Biol. **332**(1), 116–130 (2009)
8. Badylak, S.F., Gilbert, T.W.: Immune response to biologic scaffold materials. Semin. Immunol. **20**(2), 109–116 (2008)
9. Baulcombe, D.C.: RNA as a target and an initiator of post-transcriptional gene silencing in transgenic plants. Plant. Mol. Biol. **32**(1–2), 79–88 (1996)
10. Basile, P., Dadali, T., Jacobson, J., Hasslund, S., Ulrich-Vinther, M., Søballe, K., Nishio, Y., Drissi, M.H., Langstein, H.N., Mitten, D.J., O'Keefe, R.J., Schwarz, E.M., Awad, H.A.: Freeze-dried tendon allografts as tissue-engineering scaffolds for Gdf5 gene delivery. Mol. Ther. **16**(3), 466–473 (2008)
11. Baum, C., Kustikova, O., Modlich, U., Li, X., Fehse, B.: Mutagenesis and oncogenesis by chromosomal insertion of gene transfer vectors. Hum. Gene. Ther. **17**, 253–263 (2006)
12. Berkow, R.L., Wang, D., Larrick, J.W., Dodson, R.W., Howard, T.H.: Enhancement of neutrophil superoxide production by preincubation with recombinant human tumor necrosis factor. J. Immunol. **139**(11), 3783–3791 (1987)
13. Blum, B., Benvenisty, N.: The tumorigenicity of human embryonic stem cells. Adv. Cancer. Res. **100**, 133–158 (2008)
14. Bonadio, J., Smiley, E., Patil, P., Goldstein, S.: Localized, direct plasmid gene delivery in vivo: prolonged therapy results in reproducible tissue regeneration. Nat. Med. **5**(7), 753–759 (1999)
15. Boyle, K.B., Hadaschik, D., Virtue, S., Cawthorn, W.P., Ridley, S.H., O'Rahilly, S., Siddle, K.: The transcription factors Egr1 and Egr2 have opposing influences on adipocyte differentiation. Cell. Death. Differ. **16**(5), 782–789 (2009)
16. Bramsen, J.B., Pakula, M.M., Hansen, T.B., Bus, C., Langkjær, N., Odadzic, D., Smicius, R., Wengel, S.L., Chattopadhyaya, J., Engels, J.W., Herdewijn, P., Wengel, J., Kjems, J.: A screen of chemical modifications identifies position-specific modification by UNA to most potently reduce siRNA off-target effects. Nucleic Acids Res. **38**(17), 5761–5773 (2010)
17. Bran, G.M., Stern-Straeter, J., Hörmann, K., Riedel, F., Goessler, U.R.: Apoptosis in bone for tissue engineering. Arch. Med. Res. **39**(5), 467–482 (2008)
18. Capito, R.M., Spector, M.: Collagen scaffolds for nonviral IGF-1 gene delivery in articular cartilage tissue engineering. Gene. Ther. **14**(9), 721–732 (2007)
19. Carlson, M.A., Prall, A.K., Gums, J.J.: RNA interference in human foreskin fibroblasts within the three-dimensional collagen matrix. Mol. Cell. Biochem. **306**(1–2), 123–132 (2007)
20. Carthew, R.W., Sontheimer, E.J.: Origins and mechanisms of miRNAs and siRNAs. Cell **136**(4), 642–655 (2009)
21. Castanotto, D., Rossi, J.J.: The promises and pitfalls of RNA-interference-based therapeutics. Nature **457**(7228), 426–433 (2009)
22. Cheema, S.K., Chen, E., Shea, L.D., Mathur, A.B.: Regulation and guidance of cell behavior for tissue regeneration via the siRNA mechanism. Wound Repair Regen. **15**(3), 286–295 (2007)
23. Concaro, S., Gustavson, F., Gatenholm, P.: Bioreactors for tissue engineering of cartilage. Adv. Biochem. Eng. Biotechnol. **112**, 125–143 (2009)
24. Cui, X., Dean, D., Ruggeri, Z.M., Boland, T.: Cell damage evaluation of thermal inkjet printed Chinese hamster ovary cells. Biotechnol. Bioeng. **106**, 963–969 (2010)
25. Deshmane, S.L., Kremlev, S., Amini, S., Sawaya, B.E.: Monocyte chemoattractant protein-1 (MCP-1): an overview. J. Interferon Cytokine Res. **29**(6), 313–326 (2009)
26. Devroe, E., Silver, P.A.: Retrovirus-delivered siRNA. BMC Biotechnol. **28**:15 (2002)
27. Ding, T., Sun, J., Zhang, P.: Immune evaluation of biomaterials in TNF-alpha and IL-1beta at mRNA level. J. Mater. Sci. Mater. Med. **18**(11), 2233–2236 (2007)

28. Domaschke, H., Gelinsky, M., Burmeister, B., Fleig, R., Hanke, T., Reinstorf, A., Pompe, W., Rösen-Wolff, A.: In vitro ossification and remodeling of mineralized collagen I scaffolds. Tissue Eng. **12**(4), 949–958 (2006)
29. Elbashir, S.M., Harborth, J., Lendeckel, W., Yalcin, A., Weber, K., Tuschl, T.: Duplexes of 21-nucleotide RNAs mediate RNA interference in cultured mammalian cells. Nature **411**(6836), 494–498 (2001)
30. Fang, J., Zhu, Y.Y., Smiley, E., Bonadio, J., Rouleau, J.P., Goldstein, S.A., McCauley, L.K., Davidson, B.L., Roessler, B.J.: Stimulation of new bone formation by direct transfer of osteogenic plasmid genes. Proc. Natl. Acad. Sci. USA **93**(12), 5753–5758 (1996)
31. Fedorovich, N., Dewijn, J., Verbout, A., Alblas, J., Dhert, W.J.A.: Three-dimensional fiber deposition of cell-laden, viable, patterned constructs for bone tissue printing. Tissue Eng. A. **14**, 127–133 (2008)
32. Fire, A., Xu, S., Montgomery, M.K., Kostas, S.A., Driver, S.E., Mello, C.C.: Potent and specific genetic interference by double-stranded RNA in *Caenorhabditis elegans*. Nature **391**, 806–811 (1998)
33. Gamba, P.G., Conconi, M.T., Lo Piccolo, R., Zara, G., Spinazzi, R., Parnigotto, P.P.: Experimental abdominal wall defect repaired with acellular matrix. Pediatr. Sur. Int. **18**(5–6), 327–331 (2002)
34. Ginty, P.J., Barry, J.J., White, L.J., Howdle, S.M., Shakesheff, K.M.: Controlling protein release from scaffolds using polymer blends and composites. Eur. J. Pharm. Biopharm. **68**(1), 82–89 (2008)
35. Graves, D.T., Jiang, Y.: Chemokines, a family of chemotactic cytokines. Crit. Rev. Oral. Biol. Med. **6**(2), 109–118 (1995)
36. Hadfield, K.D., Rock, C.F., Inkson, C.A., Dallas, S.L., Sudre, L., Wallis, G.A., Boot-Handford, R.P., Canfield, A.E.: HtrA1 inhibits mineral deposition by osteoblasts: requirement for the protease and PDZ domains. J. Biol. Chem. **283**(9), 5928–5938 (2008)
37. Haga, M., Fujii, N., Nozawa-Inoue, K., Nomura, S., Oda, K., Uoshima, K., Maeda, T.: Detailed process of bone remodeling after achievement of osseointegration in a rat implantation model. Anat. Rec. (Hoboken) **292**(1), 38–47 (2009)
38. Hayashi, M., Nimura, K., Kashiwagi, K., Harada, T., Takaoka, K., Kato, H., Tamai, K., Kaneda, Y.: Comparative roles of Twist-1 and Id1 in transcriptional regulation by BMP signaling. J. Cell Sci. **120**(8), 1350–1357 (2007)
39. He, C.X., Tabata, Y., Gao, J.Q.: Non-viral gene delivery carrier and its three-dimensional transfection system. Int. J. Pharm. **386**(1–2), 232–242 (2010)
40. Hendriks, J., Riesle, J., van Blitterswijk, C.A.: Co-culture in cartilage tissue engineering. J. Tissue Eng. Regen. Med. **1**(3), 170–178 (2007)
41. Herweijer, H., Wolff, J.A.: Progress and prospects: naked DNA gene transfer and therapy. Gene. Ther. **10**(6), 453–458 (2003)
42. Hess, K., Ushmorov, A., Fiedler, J., Brenner, R.E., Wirth, T.: TNFalpha promotes osteogenic differentiation of human mesenchymal stem cells by triggering the NF-kappaB signaling pathway. Bone **45**(2), 367–376 (2009)
43. Holladay, C., Keeney, M., Greiser, U., Murphy, M., O'Brien, T., Pandit, A.: A matrix reservoir for improved control of non-viral gene delivery. J. Control Release **136**(3), 220–225 (2009)
44. Howard, K.A.: Delivery of RNA interference therapeutics using polycation-based nanoparticles. Adv. Drug Deliv. Rev. **61**(9), 710–720 (2009)
45. Howard, K.A., Kjems, J.: Polycation-based nanoparticle delivery for improved RNA interference therapeutics. Expert. Opin. Biol. Ther. **7**(12), 1811–1822 (2007)
46. Howard, K.A., Paludan, S.R., Behlke, M.A., Besenbacher, F., Deleuran, B., Kjems, J.: Chitosan/siRNA nanoparticle-mediated TNF-alpha knockdown in peritoneal macrophages for anti-inflammatory treatment in a murine arthritis model. Mol. Ther. **17**(1), 162–168 (2009)
47. Huang, Y.C., Simmons, C., Kaigler, D., Rice, K.G., Mooney, D.J.: Bone regeneration in a rat cranial defect with delivery of PEI-condensed plasmid DNA encoding for bone morphogenetic protein-4 (BMP-4). Gene. Ther. **12**(5), 418–426 (2005)

48. Ivey, K.N., Srivastava, D.: MicroRNAs as regulators of differentiation and cell fate decisions. Cell Stem Cell **7**(1), 36–41 (2010)
49. Jang, J.H., Bengali, Z., Houchin, T.L., Shea, L.D.: Surface adsorption of DNA to tissue engineering scaffolds for efficient gene delivery. J. Biomed. Mater. Res. A **77**(1), 50–58 (2006)
50. Jang, J.H., Rives, C.B., Shea, L.D.: Plasmid delivery in vivo from porous tissue-engineering scaffolds: transgene expression and cellular transfection. Mol. Ther. **12**(3), 475–483 (2005)
51. Jang, J.H., Shea, L.D.: Controllable delivery of non-viral DNA from porous scaffolds. J. Control Release **86**(1), 157–168 (2003)
52. Jensen, E.D., Schroeder, T.M., Bailey, J., Gopalakrishnan, R., Westendorf, J.J.: Histone deacetylase 7 associates with Runx2 and represses its activity during osteoblast maturation in a deacetylation-independent manner. J. Bone Miner. Res. **23**(3), 361–372 (2008)
53. Kim, S.S., Sun Park, M., Jeon, O., Yong Choi, C., Kim, B.S.: Poly(lactide-co-glycolide)/hydroxyapatite composite scaffolds for bone tissue engineering. Biomaterials **27**(8), 1399–1409 (2006)
54. Komori, T.: Runx2, a multifunctional transcription factor in skeletal development. J. Cell Biochem. **87**(1), 1–8 (2002)
55. Krebs, M.D., Jeon, O., Alsberg, E.: Localized and sustained delivery of silencing RNA from macroscopic biopolymer hydrogels. J. Am. Chem. Soc. **131**(26), 9204–9206 (2009)
56. Lacey, D.C., Simmons, P.J., Graves, S.E., Hamilton, J.A.: Proinflammatory cytokines inhibit osteogenic differentiation from stem cells: implications for bone repair during inflammation. osteoarthr. cartil. **17**(6), 735–742 (2009)
57. Langer, R., Vacanti, J.P.: Tissue engineering. Science **260**(5110), 920–926 (1993)
58. Lee, H.W., Suh, J.H., Kim, A.Y., Lee, Y.S., Park, S.Y., Kim, J.B.: Histone deacetylase 1-mediated histone modification regulates osteoblast differentiation. Mol. Endocrinol. **20**(10), 2432–2443 (2006)
59. Lee, W., Debasitis, J.C., Lee, V.K., Lee, J.-H., Fischer, K., Edminster, K., Park, J.-K., Yoo, S.-S.: Multi-layered culture of human skin fibroblasts and keratinocytes through three-dimensional freeform fabrication. Biomaterials **30**(8), 1587–1595 (2009)
60. Lewis, B.P., Burge, C.B., Bartel, D.P.: Conserved seed pairing, often flanked by adenosines, indicates that thousands of human genes are MicroRNA targets. Cell **120**(1), 15–20 (2005)
61. Lietman, S.A., Ding, C., Cooke, D.W., Levine, M.A.: Reduction in Gsalpha induces osteogenic differentiation in human mesenchymal stem cells. Clin. Orthop. Relat. Res. **434**, 231–238 (2005)
62. Lin, L., Chen, L., Wang, H., Wei, X., Fu, X., Zhang, J., Ma, K., Zhou, C., Yu, C.: Adenovirus-mediated transfer of siRNA against Runx2/Cbfa1 inhibits the formation of heterotopic ossification in animal model. Biochem. Biophys. Res. Commun. **349**(2), 564–572 (2006)
63. Lv, H., Zhang, S., Wang, B., Cui, S., Yan, J.: Toxicity of cationic lipids and cationic polymers in gene delivery. J. Control Release **114**(1), 100–109 (2006)
64. Macchiarini, P., Jungebluth, P., Go, T., Asnaghi, M.A., Rees, L.E., Cogan, T.A., Dodson, A., Martorell, J., Bellini, S., Parnigotto, P.P., Dickinson, S.C., Hollander, A.P., Mantero, S., Conconi, M.T., Birchall, M.A.: Clinical transplantation of a tissue-engineered airway. Lancet **372**(9655), 2023–1030 (2008)
65. Marshal, E.: Gene therapy death prompts review of adenovirus vector. Science **286**(5448), 2244–2245 (1999)
66. Mendes, N.D., Freitas, A.T., Sagot, M.F.: Current tools for the identification of miRNA genes and their targets. Nucleic Acids Res. **37**(8), 2419–2433 (2009)
67. Mironov, V., Kasyanov, V., Drake, C., Markwald, R.R.: Organ printing: promises and challenges. Reg. Med. **3**, 93–103 (2008)
68. Mittnacht, U., Hartmann, H., Hein, S., Oliveira, H., Dong, M., Pêgo, P.A., Kjems, J., Howard, K.A., Schlosshauer, B.: Chitosan/siRNA nanoparticles biofunctionalize nerve implants and enable neurite outgrowth. Nano. Lett. **10**(10), 3933–3939 (2010)

69. Motomura, H., Niimi, H., Sugimori, K., Ohtsuka, T., Kimura, T., Kitajima, I.: Gas6, a new regulator of chondrogenic differentiation from mesenchymal cells. Biochem. Biophys. Res. Commun. **357**(4), 997–1003 (2007)
70. Naiki, T., Saijou, E., Miyaoka, Y., Sekine, K., Miyajima, A.: TRB2, a mouse Tribbles ortholog, suppresses adipocyte differentiation by inhibiting AKT and C/EBPbeta. J. Biol. Chem. **282**(33), 24075–24082 (2007)
71. Nie, H., Wang, C.H.: Fabrication and characterization of PLGA/HAp composite scaffolds for delivery of BMP-2 plasmid DNA. J. Control Release **120**(1–2), 111–121 (2007)
72. Nishimura, I., Garrell, R.L., Heddrick, M., Iida, K., Osher, S., Wu, B.: Precursor tissue analogs as a tissue-engineering strategy. Tissue Eng. **9**(S1), S77–S89 (2003)
73. Phillips, J.E., Burns, K.L., Le Doux, J.M., Guldberg, R.E., García, A.J.: Engineering graded tissue interfaces. Proc. Natl. Acad. Sci. USA **105**(34), 12170–12175 (2008)
74. Pieper, J.S., Hafmans, T., Veerkamp, J.H., van Kuppevelt, T.H.: Development of tailor-made collagen-glycosaminoglycan matrices: EDC/NHS crosslinking, and ultrastructural aspects. Biomaterials **21**(6), 581–593 (2000)
75. Plasilova, M., Schonmeyr, B., Fernandez, J., Clavin, N., Soares, M., Mehrara, B.J.: Accelerating stem cell proliferation by down-regulation of cell cycle regulator p21. Plast. Reconstr. Surg. **123**(S2), 149S–157S (2009)
76. Reed, C.R., Han, L., Andrady, A., Caballero, M., Jack, M.C., Collins, J.B., Saba, S.C., Loboa, E.G., Cairns, B.A., van Aalst, J.A.: Composite tissue engineering on polycaprolactone nanofiber scaffolds. Ann. Plast. Sur. **62**(5), 505–512 (2009)
77. Scacheri, P.C., Rozenblatt-Rosen, O., Caplen, N.J., Wolfsberg, T.G., Umayam, L., Lee, J.C., Hughes, C.M., Shanmugam, K.S., Bhattacharjee, A., Meyerson, M., Collins, F.S.: Short interfering RNAs can induce unexpected and divergent changes in the levels of untargeted proteins in mammalian cells. Proc. Natl. Acad. Sci. USA **101**(7), 1892–1897 (2004)
78. Schäfer, J., Höbel, S., Bakowsky, U., Aigner, A.: Liposome-polyethylenimine complexes for enhanced DNA and siRNA delivery. Biomaterials **31**(26), 6892–6900 (2010)
79. Schek, R.M., Wilke, E.N., Hollister, S.J., Krebsbach, P.H.: Combined use of designed scaffolds and adenoviral gene therapy for skeletal tissue engineering. Biomaterials **27**(7), 1160–1166 (2006)
80. Schoolmeesters, A., Eklund, T., Leake, D., Vermeulen, A., Smith, Q., Force Aldred, S., Fedorov, Y.: Functional profiling reveals critical role for miRNA in differentiation of human mesenchymal stem cells. PLoS One **4**(5), e5605 (2009)
81. Shea, L.D., Smiley, E., Bonadio, J., Mooney, D.J.: DNA delivery from polymer matrices. Nat. Biotech. **17**, 551–554 (1999)
82. Shimomura, T., Yoshida, Y., Sakabe, T., Ishii, K., Gonda, K., Murai, R., Takubo, K., Tsuchiya, H., Hoshikawa, Y., Kurimasa, A., Hisatome, I., Uyama, T., Umezawa, A., Shiota, G.: Hepatic differentiation of human bone marrow-derived UE7T–13 cells: effects of cytokines and CCN family gene expression. Hepatol. Res. **37**(12), 1068–1079 (2007)
83. Shin, S., Salvay, D.M., Shea, L.D.: Lentivirus delivery by adsorption to tissue engineering scaffolds. Lentivirus delivery by adsorption to tissue engineering scaffolds. J. Biomed. Mater. Res. A **93**(4), 1252–1259 (2010)
84. Simon, P., Kasimir, M.T., Seebacher, G., Weigel, G., Ullrich, R., Salzer-Muhar, U., Rieder, E., Wolner, E.: Early failure of the tissue engineered porcine heart valve SYNERGRAFT in pediatric patients. Eur. J. Cardiothorac. Surg. **23**(6), 1002–1006 (2003)
85. Sonkoly, E., Pivarcsi, A.: microRNAs in inflammation. Int. Rev. Immunol. **28**(6), 535–561 (2009)
86. Strauer, B.E., Kornowski, R.: Stem cell therapy in perspective. Circulation **107**, 929–934 (2003)
87. Takahashi, H., Wang, Y., Grainger, D.W.: Device-based local delivery of siRNA against mammalian target of rapamycin (mTOR) in a murine subcutaneous implant model to inhibit fibrous encapsulation. J. Control Release **147**(3), 400–407 (2010)

88. Takahashi, Y., Ohoka, N., Hayashi, H., Sato, R.: TRB3 suppresses adipocyte differentiation by negatively regulating PPARγ transcriptional activity. J. Lipid Res. **49**, 880–892 (2008)
89. Tontonoz, P., Hu, E., Spiegelman, B.M.: Stimulation of adipogenesis in fibroblasts by PPARγ2, a lipid-activated transcription factor. Cell **79**(7), 1147–1156 (1994)
90. Viñas-Castells, R., Holladay, C., di Luca, A., Díaz, V.M., Pandit, A.: Snail1 down-regulation using small interfering RNA complexes delivered through collagen scaffolds. Bioconjug. Chem. **20**(12), 2262–2269 (2009)
91. Wang, Y., Sul, H.S.: Pref-1 regulates mesenchymal cell commitment and differentiation through Sox9. Cell. Metab. **9**(3), 287–302 (2009)
92. Wattendorf, U., Merkle, H.P.: PEGylation as a tool for the biomedical engineering of surface modified microparticles. J. Pharm. Sci. **97**(11), 4655–4669 (2008)
93. Xu, T., Jin, J., Gregory, C., Hickman, J.J., Boland, T.: Inkjet printing of viable mammalian cells. Biomaterials **23**(1), 93–99 (2005)
94. Xu, T., Rohozinski, J., Zhao, W., Moorefield, E.C., Atala, A., Yoo, J.J.: Inkjet-mediated gene transfection into living cells combined with targeted delivery. Tissue Eng. Part A **15**(1), 95–101 (2009)
95. Xu, Y., Mirmalek-Sani, S.H., Lin, F., Zhang, J., Oreffo, R.O.: Adipocyte differentiation induced using nonspecific siRNA controls in cultured human mesenchymal stem cells. RNA **13**(8), 1179–1183 (2007)
96. Xu, Y., Mirmalek-Sani, S.H., Yang, X., Zhang, J., Oreffo, R.O.: The use of small interfering RNAs to inhibit adipocyte differentiation in human preadipocytes and fetal-femur-derived mesenchymal cells. Exp. Cell. Res. **312**(10), 1856–1864 (2006)
97. Yamanouchi, K., Satomura, K., Gotoh, Y., Kitaoka, E., Tobiume, S., Kume, K., Nagayama, M.: Bone formation by transplanted human osteoblasts cultured within collagen sponge with dexamethasone in vitro. J. Bone Miner. Res. **16**(5), 857–867 (2001)
98. Yang, Y., Li, Y., Lv, Y., Zhang, S., Chen, L., Bai, C., Nan, X., Yue, W., Pei, X.: NRSF silencing induces neuronal differentiation of human mesenchymal stem cells. Exp. Cell. Res. **314**(11–12), 2257–2265 (2008)
99. Yanjie, J., Jiping, S., Yan, Z., Xiaofeng, Z., Boai, Z., Yajun, L.: Effects of Notch-1 signalling pathway on differentiation of marrow mesenchymal stem cells into neurons in vitro. Neuroreport **18**(14), 1443–1447 (2007)
100. Yao, Y., Wang, C., Varshney, R.R., Wang, D.A.: Antisense makes sense in engineered regenerative medicine. Pharm. Res. **26**(2), 263–275 (2009)
101. Yilgor, P., Tuzlakoglu, K., Reis, R.L., Hasirci, N., Hasirci, V.: Incorporation of a sequential BMP-2/BMP-7 delivery system into chitosan based scaffolds for bone tissue engineering. Biomaterials **30**(21), 3551–3559 (2009)
102. Zeng, Y., Yi, R., Cullen, B.R.: MicroRNAs and small interfering RNAs can inhibit mRNA expression by similar mechanisms. Proc. Natl. Acad. Sci. USA **100**(17), 9779–9784 (2003)
103. Zhao, Y., Ding, S.: A high-throughput siRNA library screen identifies osteogenic suppressors in human mesenchymal stem cells. Proc. Natl. Acad. Sci. USA **104**(23), 9673–9678 (2007)
104. Zhokhov, S.S., Desfeux, A., Aubert, N., Falluel-Morel, A., Fournier, A., Laudenbach, V., Vaudry, H., Gonzalez, B.J.: Bax siRNA promotes survival of cultured and allografted granule cell precursors through blockade of caspase-3 cleavage. Cell. Death Differ. **15**(6), 1042–1053 (2008)
105. Zou, S., Scarfo, K., Nantz, M.H., Hecker, J.G.: Lipid-mediated delivery of RNA is more efficient than delivery of DNA in non-dividing cells. Int. J. Pharm. **389**(1–2), 232–243 (2010)

Part II
Scaffolds for Bone Regeneration

Nanostructured Scaffolds for Bone Tissue Engineering

John Igwe, Ami Amini, Paiyz Mikael, Cato Laurencin and Syam Nukavarapu

Abstract The field of tissue engineering is an emerging discipline that applies basic principles of life sciences and engineering for the repair and restoration of human tissues and organs. Among many tissue types, bone has attracted much attention since it is the second most transplanted tissue in clinics. Bone is a complex tissue where organic and inorganic components interact to maintain an appropriate physio-chemical balance to allow for its cellular and structural functions. Treating bone loss via tissue engineering approach requires the design, fabrication and characterization of biodegradable scaffolds that display similar characteristics as the bone. Scaffolds for bone tissue engineering should have nano/micro structural features similar to the bone extracellular matrix to mimic the bone environment and support the bone cell adhesion, proliferation and differentiation. This chapter mainly focuses on the 3D nanostructured scaffold fabrication techniques and the scaffold characterization for in vitro and in vivo bone tissue engineering. Further, the chapter highlights the various effects of nanofeatures on bone forming cell performance, as well the signaling cascades induced by nanotopography.

J. Igwe · A. Amini · C. Laurencin (✉) · S. Nukavarapu (✉)
Orthopaedic Surgery, University of Connecticut, Farmington, CT, USA
e-mail: laurencin@uchc.edu

S. Nukavarapu
e-mail: syam@uchc.edu

P. Mikael · C. Laurencin · S. Nukavarapu
Chemical, Materials and Biomolecular Engineering, University of Connecticut, Storrs, CT, USA

Stud Mechanobiol Tissue Eng Biomater (2011) 8: 169–192
DOI: 10.1007/8415_2010_60

Published Online: 8 February 2011

1 Introduction

In the past three decades, tissue engineering has become one of the leading areas in the academic and industrial world, with over 33 thousand articles published on a broad range of advances and challenges in the field. The field of tissue engineering arose from the need of many clinicians and healthcare specialists to address a long standing challenge in medicine. Tissue engineering has been defined as "the application of biological, chemical, and engineering principals toward the repair, restoration, or regeneration of living tissue by using biomaterials, cells, and factors alone or in combination" [31]. Three main strategies are commonly used in tissue engineering namely, infusion of isolated cells, treatment with tissue-inducing growth factors, and implantation of scaffolds with or without the tissue-specific cells and growth factors [30, 41]. Based on the tissue type, one of the above listed strategies is preferred over other. For example, cell therapy has become a popular method to regenerate cartilage tissue. As far as bone regeneration is concerned, there is a strong need to have a three-dimensional and porous architecture, referred to a scaffold, which not only supports bone-forming cell proliferation, migration and mineralization, but also mechanically supports the bone tissue regeneration process. In addition, scaffolds are also designed to have interconnected porosity that allow for cellular ingrowth, tissue infiltration and eventually, new bone tissue formation [32].

Bone is a complex tissue that varies in arrangement and structure that work in concert and accommodates for all of its mechanical, biological and chemical functions. The unique combination of materials and structure, as well as the ability to continually regenerate, makes bone a *smart* material. However, when bone is fractured beyond the critical range, it fails to regenerate and repair itself. Therefore, the need to find a compatible treatment has been the focus and driving force for the researchers in the field of tissue engineering. Recent advances in materials technology have led to the fabrication of many biodegradable (natural and synthetic), three-dimensional porous scaffolds that are capable of adapting to the biological and mechanical needs of the repairing bone tissue. Scaffolds require several features in order to closely mimic the native bone environment. One of the important features is the scaffold topography, which is required to duplicate the ECM environment. It is becoming increasingly clear that cells on scaffolds look for topographical cues that they normally receive from the surrounding ECM and basement membranes [44, 46]. Therefore, the creation and utilization of nanostructured scaffolds is vital for the success of bone tissue engineering. In this chapter, we present an overview of currently available methods to fabricate nanostructured scaffolds and the scaffold performance evaluation using bone forming cells in vitro and pre-clinical studies will be presented.

2 Overview of Bone Morphology

2.1 Bone Tissue

Bone is a dynamic and highly vascularized tissue with a rich hierarchy. It consists of mineralized matrix and bone-forming cells. The mineralized matrix is composed of bone mineral (i.e., hydroxyapatite) and extracellular matrix (ECM). Overall, bones provide many functions including mineral homeostasis, support for the softer tissues, provide points of attachment for skeletal muscles, and locomotion. Bones also play a major role in hematopoiesis (i.e., blood cells production). Hematopoietic stem cells (HSC) reside in the medulla of the bone and give rise to different types of mature blood cells when necessary. In addition, its unique ability to regenerate and remodel throughout developmental stages makes bone the ultimate smart material [5].

To fulfill all of its various functions, bone has evolved into a highly specialized composite of natural materials that has an anisotropic characteristic and exhibits a rich hierarchical cellular structure consisting of up to seven levels of organization. The different hierarchical levels of bone include macrostructure, microstructure, sub-microstructure, and the ultrastructural level [49]. The basic bone hierarchical level (as shown in Fig. 1) is at the whole bone and in most parts of the body it

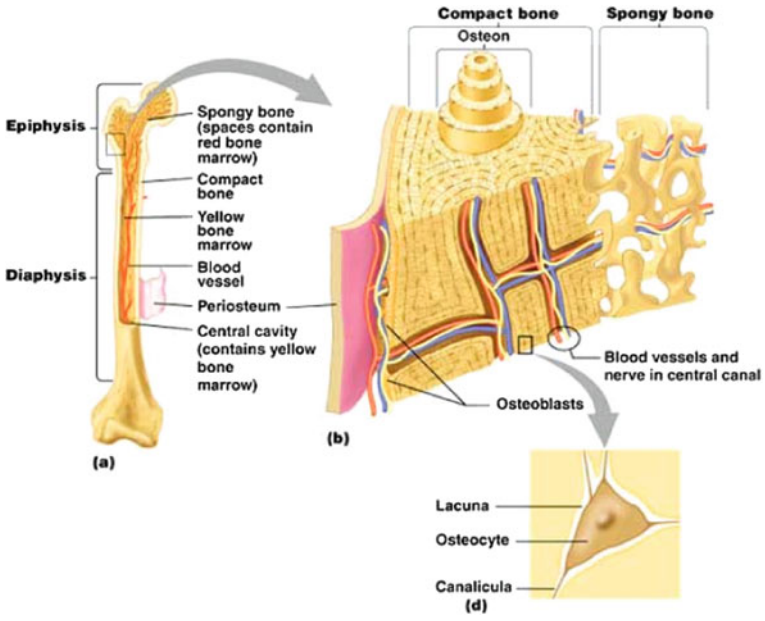

Fig. 1 Illustration of the two basic hierarchical structures of bone. A cross-sectional image showing compact and trabecular regions of the bone tissue. http://www.personal.psu.edu/staff/m/b/mbt102/bisci4online/bone/bone4.htm

consists of an external compact cortical region, which makes up 80% of total skeleton and an internal spongy trabecular region, which makes up 20% of total skeleton [29].

The cortical bone primarily consists of the Haversian system, which in turn is comprised of concentric lamella of bone matrix, osteons and a central Haversian canal, where blood vessels and nerves pass. The Haversian canals are interconnected by Volkmann canals. Within the bone matrix exists structures called lacunae, each of which contains an osteocyte (Fig. 1). Canaliculi are fine tunnels in between the lacunae, and allow for osteocytes communication.

2.2 Extracellular Matrix

Although bone is made up of different cell types, such as osteoblasts, osteocytes and osteoclasts, the majority, more than ninety percent, of cortical and trabecular bone is composed of a matrix. This matrix is best explained at the microstructure level, where mineralized collagen fibrils are arranged in planar sheet or lamellae, each approximately 3–7 μm wide. Trabecular bone is composed of irregular, sinuous, convolutions of lamellae, whereas the cortical bone is composed of regular, cylindrical shaped lamellae, 3–8 sheets, called the osteons [6, 7, 14, 27]. The osteons are about 200–250 μm diameter and can be arranged parallel or perpendicular to the long axis of bone or in a less well-organized fashion with no distinguished pattern as in woven bone. These arrangements play a major role in the unique properties of bone.

The final level of bone hierarchy is the nanostructure (as shown in Fig. 2), where the collagen fibers are surrounded and infiltrated with mineral. The primary mineral in bone is hydroxyapatite, which grows within discrete areas on the

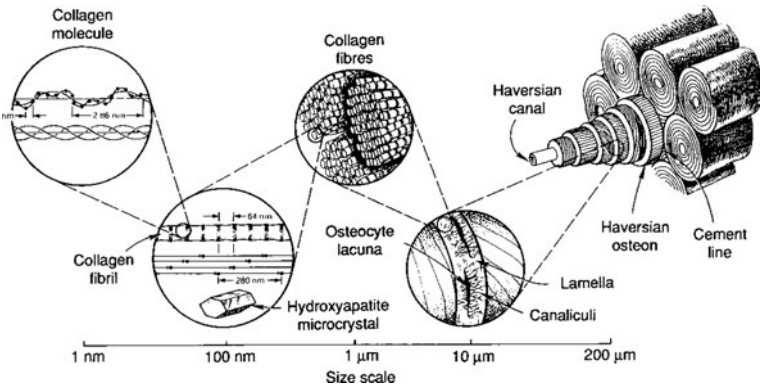

Fig. 2 Hierarchical structure of compact bone. Fibrous, laminar, particulate and porous structure is present at different size scales. Adapted from Lakes et al. [22]

collagen fibers in plate-like crystals. The apatite crystals are about 2–3 nm and mainly composed of calcium and phosphate, which contribute to its molecular formula, $Ca_5(PO_4)_3(OH)$.

As previously mentioned, ECM occupies the majority of the osseous tissue, and therefore, is considered a major element that influences bone cell behavior and development. It is well established that cells receive topographical cues from the surrounding ECM [54]. Such cell–ECM interactions spread and reach out to include neighboring cells providing a neat systematic network. The systematic network is enhanced by the diversity of molecules and receptors that constitutes the ECM such as, transmembrane glycoproteins, proteoglycans, and glycolipids.

3 Biodegradable Scaffolds

3.1 Scaffolds for Bone Tissue Engineering

As described in pervious sections, the ECM is a complex material that has a rich hierarchy of arranged collagen and laminin fibrils at the micrometer scale, and glycoproteins, proteoglycans and glycolipids at the nanometer scale. One of the strategies for bone regeneration utilizes biodegradable scaffolds, which can serve as a temporary matrix for tissue in growth. A scaffold is nothing but a three-dimensional and porous structure that supports tissue regeneration with degradation rate matching the defect healing rate. This way, the scaffold will disappear by the time the defect is completely healed. With the scaffold-based bone regeneration, the extent of tissue regeneration depends on how well the tissue forming cells adhere and grow on a biodegradable scaffold. The cell compatibility of a scaffold can be very well achieved by just duplicating the native tissue ECM structure. Therefore, it is important to design scaffolds with ECM-like features. In addition, scaffolds for bone regeneration should also satisfy the general scaffold properties such as tissue compatibility and tissue matching mechanical properties.

Many synthetic polymers, such as poly lactic acid (PLA), poly glycolic acid (PGA), poly(lactide-*co*-glycolide) (PLGA), polyphosphazenes and polyanhydrides and natural polymers, such as chitosan, hylouroic acid, and alginate have been extensively studied as biodegradable materials. These materials are fabricated into 3D scaffolds through many different techniques, which include freeze drying, solid free-form fabrication, solvent casting, particulate leaching, gas foaming and microsphere sintering [38]. Although all these techniques produce three-dimensional and porous scaffolds adequate to support cellular adhesion and proliferation, they still lack the topographical features that simulate the native tissue ECM matrix. In the next section, a brief description of few methods used to fabricate 3D, nano-featured scaffolds that closely mimic the natural environment of the bone tissue will be discussed.

3.2 Methods to Fabricate Nano-Structured Scaffolds

A variety of fabrication techniques have been developed to achieve nano-featured scaffolds for bone tissue engineering applications. These techniques can be primarily classified into two different approaches (Table 1). The first approach involves scaffolding methods that are capable of producing three-dimensional and porous matrices with nano-features throughout the structure. Electrospinning, phase separation and self-assembly are some of the techniques often utilized. In particular, electrospinning technique has attracted wide attention due to its applicability for a variety of synthetic and natural polymers. In the latter approach, nano-features can be introduced onto any pre-fabricated scaffold via physical or chemical methods. Although, this is relatively an easy approach, the introduced nano-features are only limited to scaffold surface. The following is a brief description of some of the important nano-featured scaffold fabrication methods.

3.2.1 Electrospinning

Electrospinning is a spinning method to generate submicron to nanometer scale fibers from polymer melts or solutions. It is a physical process to obtain fibers from a bulk polymer of interest under the applied electric field. The spinning setup consists of a syringe pump, high-voltage power supply and collector. During electrospinning the applied electric potential (order of kilovolts), between the syringe pump and collector, induces charge separation in the polymer drop that is sitting at the tip of the syringe pump. When the charge separation and the associated electrostatic force overcome the polymer's surface tension, the polymer droplet will be drawn into micro- and nano-size fibers towards the collector. During this process the solvent used to dissolve the polymer of interest will evaporate and ultimately the polymer fibers are deposited onto collector. These

Table 1 Approaches and specific methods to create nano-featured scaffolds for bone tissue engineering

Approaches	Specific methods	Advantages/disadvantages
Scaffolding methods	Electrospinning	Nano-fibrous Ability to make bone like composition
	Thermally induced phase separation	Bulk approach
	Self assembly	Mechanically not compatible to bone
Pre-fabricated scaffold modification methods	Physical Printing Lithography	Can address the mechanical compatibility by choosing a weight-bearing scaffold
	Chemical Selective etching Chemical patterning	Limited to surface

fine fibers are collected and shaped according to the desired geometry. In this process, the fiber size is controlled by changing spinning parameters, such as polymer concentration, solvent selection, applied voltage and distance between the syringe pump and collector. While generating nanostructured scaffolds, the electrospinning technique has also been utilized to encapsulate bone specific growth factors (BMP-2, BMP-7, VEGF) and antibacterial agents (tetracycline, gentamycin sulphate) [45]. Although electrospinning seems like an ideal fabrication technique to create nano-structured scaffolds, the technique has limitations in terms of the scaffold size and shape required for clinical applications [47].

3.2.2 Phase Separation

Another method that is used to fabricate nano-featured 3D porous scaffolds is phase separation, specifically, thermally induced phase separation (TIPS). TIPS method is briefly described as dissolving the polymer of interest in a solvent at high temperature. Then, the phase separation into two phases is induced by lowering the temperature of solution, where one has a high polymer concentration and the other has a low polymer concentration. To make a porous scaffold, the low polymer concentration phase is removed by exchange, evaporation, or sublimation of solvent, leaving behind the high polymer concentration phase as a 3D construct. Therefore, as one can predict, porosity and fiber size can be controlled by varying the amount of solvent, temperature, and/or polymer concentration. However, this technique is limited to only highly crystalline polymers, such as PLLA [36].

3.2.3 Molecular Self Assembly

Self assembly is the spontaneous building of biologically friendly molecules into a structurally stable and well-organized motif/construct. The molecules interact with each other through hydrogen bonding, ionic bonding, hydrophilic interactions, or van der Waals interactions. Some commonly used molecules include peptides, proteins, and lipids. Although molecular self-assembly method is useful to produce biocompatible, nano-fibrous scaffolds with nano-topography that mimics to a certain degree to the natural ECM in its size and functionality, the design of self-assembling peptide fragments require complex combinatorial chemistry approaches [67].

The above described scaffolding methods have been successfully utilized to create nano-featured scaffolds. These scaffolds have clearly supported osteoblast growth and in vitro bone formation significantly higher than the control scaffolds with no nano-features. However, majority of the nano-fibrous scaffolds lack the mechanical strength required to physically support the bone regeneration. On the other hand, a set of physical and chemical methods have been proposed to introduce nano-features onto a variety of biomaterial surfaces. Furthermore, some of the methods used in creating nanofeatures on 3D scaffolds are also useful for

delivering bioactive molecules. For instance, Wei et al. showed that recombinant BMP-7 can be encapsulated into poly (lactide-co-glycolide) (PLGA) nanospheres with an average diameter of 300 nm. This nanosphere containing growth factor was then immobilized on poly (L-lactic acid) (PLLA) 3D scaffolds with interconnecting pores using a combination of sugar sphere template leaching and phase separation techniques. The modified biomaterial surfaces have been employed to understand and establish feature size and feature density effects on osteoblast cell behavior [44, 63]. As a separate strategy, patterning or printing techniques are currently proposed to apply on to pre-fabricated and mechanically bone compatible scaffolds for effective bone tissue engineering.

4 Cell Interactions with Nanotopography

4.1 Cells that Participate in Bone Formation

4.1.1 Osteoblast Lineage Cells

Osteoblasts are the main bone-forming cells, and have been the focus of bone tissue engineering research aimed for studying bone cell interactions with biomaterials and scaffolds. The ability of many biomaterials to support osteoblast growth and differentiation is currently used as yardstick for measuring osteocompatibility of many engineered scaffolds for bone repair/regeneration.

The osteoblast lineage cells originate from the mesenchymal stem cells [2, 3, 39]. Under stimuli from growth factors, such as members of the TGF-β family and bone morphogenetic proteins (BMPs), the mesenchymal cells begin to differentiate toward the osteoblast lineage [4], starting with osteoprogenitors, osteoblasts, and finally to the osteocytes. During osteoprogenitor stage, the expression of alkaline phosphatase, bone sailoprotein and collagen type I begin to increase. In addition, core binding factor a1 (cbfa1), also known as RunX-2, are also up-regulated during osteoblast differentiation [11, 12, 24].

Mature osteoblasts express high levels of osteocalcin, alkaline phosphatase, collagen type I, osteopontin and bone sialoprotein (BSP). At this stage, they start to assume a cubodial shape, and can be seen forming a continuous layer of cells on the surface of bone tissue. The primary role of the osteoblast is to form bone, and this occurs slowly, but continuously in all living bones. It is believed that more than half of the osteoblasts that started the process of bone formation are lost due to apoptosis [18]. As the bone matrix is being mineralized, some osteoblasts are trapped within the matrix; these cells are termed as osteocytes and gradually lose most of osteoblast specific functions, including the ability to divide and secrete bone matrix [13]. Osteocytes are characterized by long fine meshwork processes that serve as a network of communication between osteocytes, and other cells within the bone tissue. In addition to the primary osteoblast cells, various

immortalized cell lines, such as MC3T3, MG-63, SaOS-2, have similar gene and protein expression profiles to osteoblasts, and are commonly used to study in vitro bone formation [25].

4.1.2 Osteoclasts

Osteoclasts are another important bone cells and are of the monocyte/macrophage linage [23, 51]. Mature osteoclasts are multinucleated giant cells, responsible for the bone resorption process [68]. They can vary from 20 to over 100 μm in size and can contain 2–50 nuclei [48, 51]. Osteoclasts are characterized by podozomes or filamentous processes, and proteases which are essential for bone resorption [52]. To resorb bone, osteoclasts attach to the surface of the bone via the formation of a specialized structure called the sealing zone. This sealing zone is rich with acidic elements that help to acidify the bone mineral component. The organic components are then removed by secretion of lysozomal enzymes [21]. Osteoclasts are activated by a combination of factors including growth factors, hormones and cytokines.

It has been reported that receptor activator of NF-κB ligand (RANKL) and macrophages colony stimulating factor (M-CSF), which are secreted by osteoblasts, are essential for osteoclasts activation. The binding of RANKL to its receptor, RANK, on the cell surface of osteoclasts is critical for signal transduction leading to osteoclasts function [26, 61]. Osteoclasts are characteristically positive for tartrate acid phosphatease staining (TRAP). The traditional role of osteoclast is in bone remodeling during bone turnover or healing of a micro-fracture. However, for critical sized bone defects, it is not yet clear if and how osteoclast participates in the healing process.

4.2 Bone Cell Interactions with Nanotopography

The goal of tissue engineering is to create structures that can support cell growth and regeneration of damaged tissues or organ. In the case of bone tissue, the fabricated scaffold needs to mimic the in vivo bone environment closely. As mentioned previously, the natural bone tissue contains both macro- and nano-scale structures that influence the function of bone cells. So far the scaffold fabrication techniques mostly focused on creating three-dimensional -porous structures that support bone tissue growth. With the emergence of nanotechnology and better scaffolding methods, scientists are now able to design and fabricate three-dimensional and porous biodegradable scaffolds with nano-scale features.

Earlier studies on nano-features were carried out on two-dimensional surfaces basically to understand the effect of nanotopography on bone forming cell adhesion and performance. Zinger et al. made a significant attempt by demonstrating

that an osteoblast derived cell line MG-63 can adhere and extend their filapods on electrochemically micro-structured surfaces with hemispherical cavities of 30 or 100 μm in diameter arranged in a hexagonal pattern [69]. In addition, Roehlecke et al. demonstrated that type I collagen-coated titanium alloy exhibits favorable effects on the initial adhesion and growth activities of osteoblasts, and resulted in a more rapid formation of focal adhesions and their associated stress fibers [50]. The results from two-dimensional studies indicate that nano-features can modulate ostesoblast function. Such studies have led researchers in tissue engineering to create and characterize three-dimensional structures wearing nano-features for bone tissue engineering applications.

4.2.1 Cell Interactions with Nano-Featured 3D Fibrous Scaffolds

Fibrous scaffolds are made to mimic the extracellular matrix component of the bone; these biodegradable materials have diverse properties differing in their surface physical, chemical and topographical parameters. As described in Sect. 1, electrospining is one of the best techniques to create nano-fibrous scaffolds. Nano-fibrous scaffolds have good potential for tissue engineering because of their ability to support adhesion, growth and differentiation of bone cells. Osteoblast cells are known to attach to surfaces through protein adsorption on the surfaces. Nano-fibrous scaffolds can provide topographical architecture necessary for protein adsorption as demonstrated by Kyung Mi Woo et al., who found that scaffolds with nano-fibrous pore walls adsorbed four times more serum proteins than scaffolds with solid pore walls [64]. It was further observed that unlike solid-walled three-dimensional scaffolds, nano-fibrous scaffolds selectively enhanced adsorption of fibronectin and vitronectin, and allowed >1.7 times of osteoblastic cell attachment than scaffolds with solid pore walls. Furthermore, $\alpha 2$ and $\beta 1$ integrins, as well as αv and $\beta 3$ integrins, were highly expressed on the surface of cells seeded on nano-fibrous scaffolds, which resulted in higher levels of phospho-Paxillin and phospho-FAK in cell lysates. In contrast, cells seeded on solid-walled scaffolds expressed significantly lower levels of these integrins, phospho-Paxillin, and phospho-FAK [65].

Osteoblast attachment is crucial for their function, thus, it is not unexpected that osteoblasts cultured on nano-fibrous scaffolds exhibit higher alkaline phosphatase activity and enhanced expression of osteoblast differentiation markers RunX2 and bone sialoprotein [65]. In addition, human amniotic fluid-derived stem cells (hAFSCs) cultured on the nanofibrous scaffolds show significantly enhanced alkaline phosphatase (ALP) activity, calcium content, and higher expression of osteogenic genes than cultures from the scaffolds bearing no nanostructures [60]. A similar trend was also demonstrated by Smith et al., who established that nano-featured poly(L-lactic acid) (PLLA) 3D scaffolds improved the osteogenic differentiation of human embryonic stem cells (hESC) with significant expression of osteocalcin mRNA after 6 weeks of 3-D culture as shown in Fig. 3, hESC-derived osteogenic progenitor cells cultured on the nano-fibrous matrix expressed higher

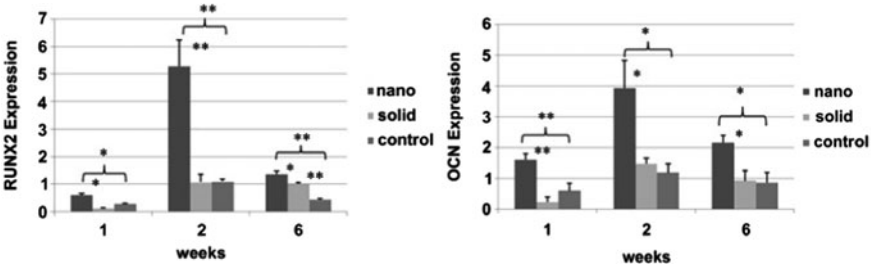

Fig. 3 Osteogenic differentiation of hESC-derived osteoprogenitors on nano-fibrous matrices (nano), flat films (solid) and 0.1% gelatin-coated tissue culture plastic (control) using quantitative PCR for Runx2 and osteocalcin, (OCN) expression. * denotes p-value < 0.05. ** denotes p-value < 0.01. Adapted from Smith et al. [59]

levels of osteogenic markers (i.e., Runx2 and osteocalcin) compared to solid walled and controls [59]. Increased osteoblastic performance was also observed with other nano-fibrous scaffolds incorporated with bioactive molecules. Studies from Wei et al. showed that BMP-7 encapsulated in PLGA nanospheres that were immobilized on interconnected macroporous scaffolds actively induced new bone formation throughout the scaffold due to the effect of nanotopography complemented with prolonged delivery of BMP-7. From these studies, it is evident that, biochemical and topographical cues presented by 3D scaffolds can enhance the bone formation of seeded stem cells, osteoprogenitor cells or osteoblasts.

4.3 Cell Signaling Cascades Induced by Nanotopography

4.3.1 Focal Adhesion Molecules

Osteoprogenitors adhere to sites of skeletal repair through the interaction of adhesion molecules present on their cell surfaces and the ECM. Several adhesion molecules have been reported for their role in cell adhesion. Research in recent years has focused on integrins, because of their presence on osteoblast surfaces, [10, 15, 16] and their importance in establishing focal adhesion. Integrins are composed of the beta and the alpha subunits, which can form several heterodimer complexes. Integrins can interact with the ECM molecules, such as the RGD tripetide motif found in fibronectin, lamininin, and vitronectin. Binding of ligands to integrins induces comformational changes that triggers intracellular signaling cascade leading to actin polymerization and subsequently cell attachment [10, 15, 16].

Cell migration is an important mechanism responsible for guiding bone cells to specific sites of bone repair or to adhere on three-dimensional scaffolds. Smith et al. demonstrated that after 2 weeks of osteogenic culture, $\alpha 2$ integrin was differently expressed (Fig. 4a), and when cells were exposed to $\alpha 2$ integrin antibodies, decreased expression of Runx2 and osteocalcin was observed on both NF matrix

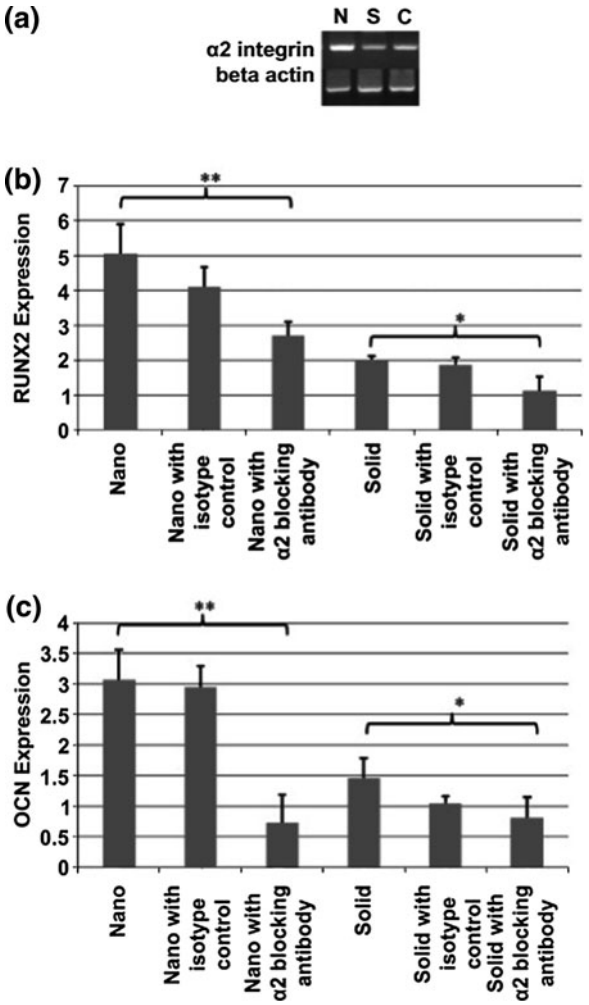

Fig. 4 Shows that α2 integrin mRNA expression was increased in cells cultured on nano-fibrous matrix **a**. Increased α2 integrin expression was correlated to increased expression of Runx2 mRNA in nano-fibrous matrix cultures **b**. * denotes p-value < 0.05. ** denotes p-value < 0.01. **c** This resulted in increased expression of osteocalcin on nano-fibrous matrix * denotes p-value < 0.05. ** denotes p-value < 0.01. Adapted from Smith et al. [59]

and flat (solid) films (Fig. 4b and c). This further indicates the positive effect of nanotopography on α2 integrin expression and consequently, improved osteogenic differentiation of these cells when cultured on nano-featured scaffolds [59].

4.3.2 Formation of Focal Adhesion Contact

Osteoblasts are anchorage-dependent cells and require attachment to a surface as a prerequisite for subsequent cellular response. To proliferate or differentiate on a biomaterial or scaffold, osteoblasts must first establish focal contacts using their microfilaments. As shown in Fig. 5, nano-topography modulates the attachment of cells to surfaces by altering their ability to form focal adhesion. Yim et al.

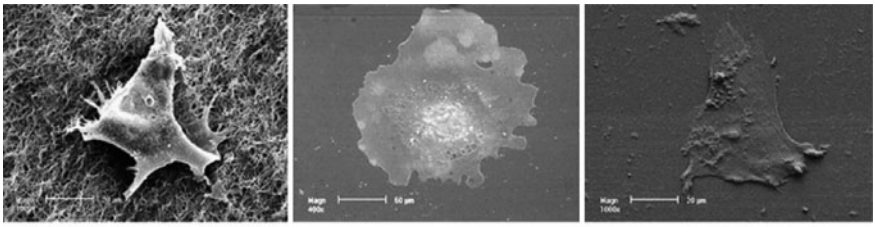

Fig. 5 SEM micrographs of osteo progenitor cells derived from hESC cultured on nano-fibrous thin matrix (nano), flat films (solid), gelatin-coated tissue culture plastic (control). Cell processes on nanostructured scaffold surface appeared more robust than the solid walled or control cultures, an indication of the positive effect of nanotopography on these cells. Scale bar = 20 μm (nano & control), 50 μm (solid). Adapted from Smith et al. [59]

demonstrated that human mesenchymal stem cells (hMSCs) cultured on 350 nm gratings of tissue-culture polystyrene (TCPS) and polydimethylsiloxane (PDMS) displayed decreased expression of integrin subunits alpha2, alpha, alpha V, beta2, beta3 and beta4 compared to the unpatterned controls [66]. In addition, they showed that the expression of cytoskeleton and FA components was also altered by the nano-topography as reflected in the mechanical properties measured by atomic force microscopy (AFM) indentation.

4.3.3 Signaling Pathways Activated by Nanotopography

Integrin activation and the formation of focal adhesion are crucial events leading to the attachment of bone cells to substrates. Before the formation of focal adhesion, some molecular interactions, such as the activation of focal adhesion kinase (FAK), a cytosolic non-receptor tyrosine kinase, occur. FAK activation is triggered by integrin signaling that results in the association of FAK with cytosolic signaling portion of integrin and subsequent phosphorylation of FAK. Once phosphorylated, FAK induces the activation of several other kinases, such as MAP kinase and PI3 kinase [53]. The role of topography has been documented; Hamilton et al. demonstrated that micro-fabricated topographies stimulated altered focal adhesion (FA) arrangements, which correlated with regions of increased tyrosine phosphorylation. It was also shown that inhibition of JAK-1 using piceatannol attenuated the phosphorylation of FAK and ERK1/2 on 30 μm deep grooves, and inhibited proliferation on all surfaces tested [17]. Furthermore, Kim et al. showed that osteoblast cells from FAK mutant mice can differentiate and are able to migrate to sites of skeletal injury [28]. However, the attachment of osteoclasts to the bone matrix was disrupted in vivo, further demonstrating the importance of FAK in osteoblast attachment.

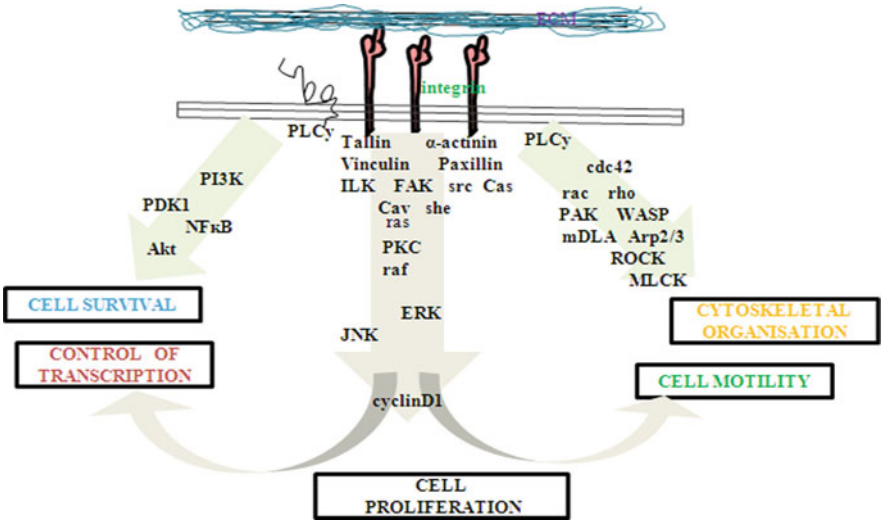

Fig. 6 The importance of integrin signaling in cell proliferation through activation of several signaling cascades linked to cell survival and migration. Modified from Siebers et al. [57]

Thus, scaffold nanotopography can influence the attachment and function of bone cells by modulating key signaling effects essential for their survival at least in vitro. Although there has been some progress in this area, the effect of the nano-feature density, size and feature type (i.e., grooves, islands, pits, etc.), on osteoblast performance is not well understood. This requires scaffold fabrication with precise control over the nano-features and, such scaffold characterization with osteoblasts and bone forming cells for establishing nano-featured scaffold applicability for bone tissue engineering applications. Furthermore, the role of osteoclast in bone tissue engineering is only beginning to be appreciated [42]. However, the effect of nanotopography on osteoclast cells and its implication for bone tissue engineering will become clearer when more results are made available in the literature (Fig. 6).

5 Nano-Structured Implants: In Vivo Studies

Current implants utilized in orthopaedic and oral maxillofacial surgeries pose various clinical problematic issues. Drawbacks include the implant loosening, wear and limited compatibility with bone in permanent metal implants. Patients experience increased costs and recovery time as a result of revision surgeries required by failed implants [58]. Additionally, the aging of the baby-boomer population and increase in life expectancy have escalated the need to search for more suitable grafts to improve the short lifetimes of the current implants, thus, decreasing the burden on patients and health care.

Ideally, in bone tissue engineering, optimal bone regeneration occurs when the implanted scaffolds mimic the native bone ECM as closely as possible. The structure of the scaffold should serve as a synthetic replica, and act as a temporary ECM in order to support cell attachment and guide three-dimensional bone tissue formation [37]. Since the two main components of bone ECM are Type I collagen fibrils and hydroxyapatite (HA) crystals, each of which are less than 50 nm in diameter, nanostructures in tissue engineering are becoming of increasing importance. Nanostructures, which include scaffolds, and controlled modifications of surface topography and composition, may help resolve existing limitations of conventional bone tissue engineering approaches and improve healing response.

While nano-featured scaffolds are in the forefront and have gained much popularity in bone tissue engineering, significant advancements are still necessary to realize their full potential in clinical use. Many in vitro studies have demonstrated nano-featured scaffolds to lead to increased osteoblast activity and bone formation, however, there have been significantly less in vivo studies reported on this topic thus far.

The following is a review of the in vivo studies conducted on nano-featured implants for bone tissue engineering. Firstly, studies on the effects of biodegradable, non-permanent nano-featured implants will be discussed. Then, the more commonly used metal implants with nano-feature modifications used in the fields of orthopaedic and oral maxillofacial surgery will be reviewed.

5.1 Nano-Featured Biodegradable Implants

As previously mentioned, the growth of replacement bone tissue using tissue engineering and regenerative medicine is an ideal and effective method for circumventing the complications of current treatments. Due to the plethora of data gained from in vitro studies, nano-featured scaffolds that more closely mimic the ECM of native bone are believed to fulfill the needs of bone tissue engineering.

This concept of textured implant surfaces enhancing the proliferation of osteoblasts and promoting bone regeneration is demonstrated by a study conducted by Harvey et al. Although not on the nano-scale, allografts with a rough surface texture elicit an increased osseous healing response (Fig. 1). By 6 weeks post-implantation, the textured allograph shows 450% new bone formation compared with non-textured allograft. Thus, grafts that display surfaces with similar roughness to that of a fracture surface have been demonstrated to be more effective in promoting new bone growth than grafts with smooth surfaces.

Moreover, on the nano-scale note, Appleford et al. investigated the differences in bone formation and angio-conductive potential of scaffolds coated with either micro-size HA (M-HA) or nano-size HA (N-HA). Histomorphometric comparisons were made between naturally forming trabecular bone, which served as their control, and defects implanted with scaffolds fabricated with M-HA and N-HA

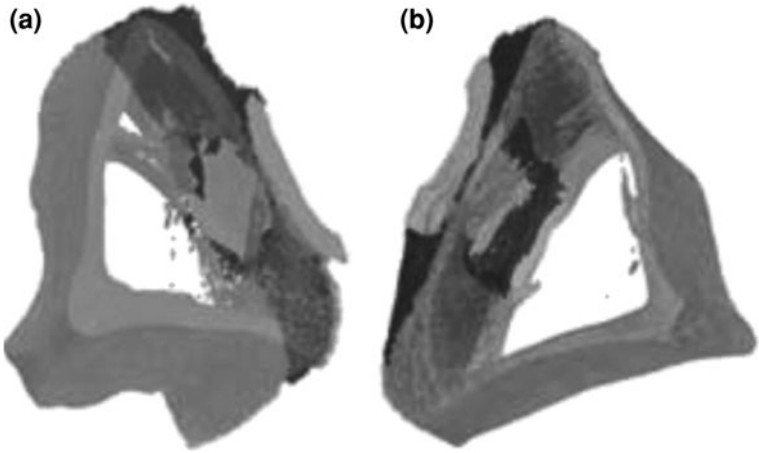

Fig. 7 Microcomputed tomographic (MicroCT) reconstruction of bilateral tibial **a** smooth surface, and **b** textured surface allograft placement of 6 weeks after initial surgery. Adapted from Harvey et al. [19]

ceramic surfaces in a canine segmental defect [1]. Although no significant differences were identified between the two HA scaffolds (Fig. 7), there was significant bone in-growth observed compared to the control. At 12 weeks, approximately 44 and 50% of the cross-sectional area was filled with mineralized bone in M-HA and N-HA scaffolds, respectively. As seen in Fig. 8, the ECM of the bone in M-HA and N-HA scaffolds was partially organized, and lamellar collagen fibrils were observed at both 3 and 12 weeks post-implantation. Substantial blood vessel infiltration, with similar distribution and diameter to that in the surrounding cortical bone, was identified in the scaffolds. Though this study did not compare the effects of M-HA and N-HA textured surfaces with a smooth surface implant, it did demonstrate the potential of textured surface HA scaffolds for regenerative bone treatments.

In addition to nano-texture modified scaffolds, nanofibrous scaffolds have also gained much attention as Type I collagen is the most abundant extracellular protein of bone and is composed of a nano-scale fibrillar structure in vivo [37]. Nano-fibrous scaffolds are highly porous, have a variable pore-size distribution, and high surface-to-volume ratio [37]. Also, nanofibers have an ultra-fine, continuous structure and have been shown to aid in cell attachment, proliferation, and differentiation.

Many biodegradable materials, such as poly (lactic acid) (PLA), poly(glycolic acid) (PGA) and poly(ε-caprolactone) (PCL), have been extensively studied as nanofiber systems for bone regeneration. Shin et al. demonstrated that PCL nanofibrous scaffolds seeded with rat bone marrow stromal cells (rBMSCs) to give rise to a bone-like appearance with sufficient cell/ECM formation on the surface of

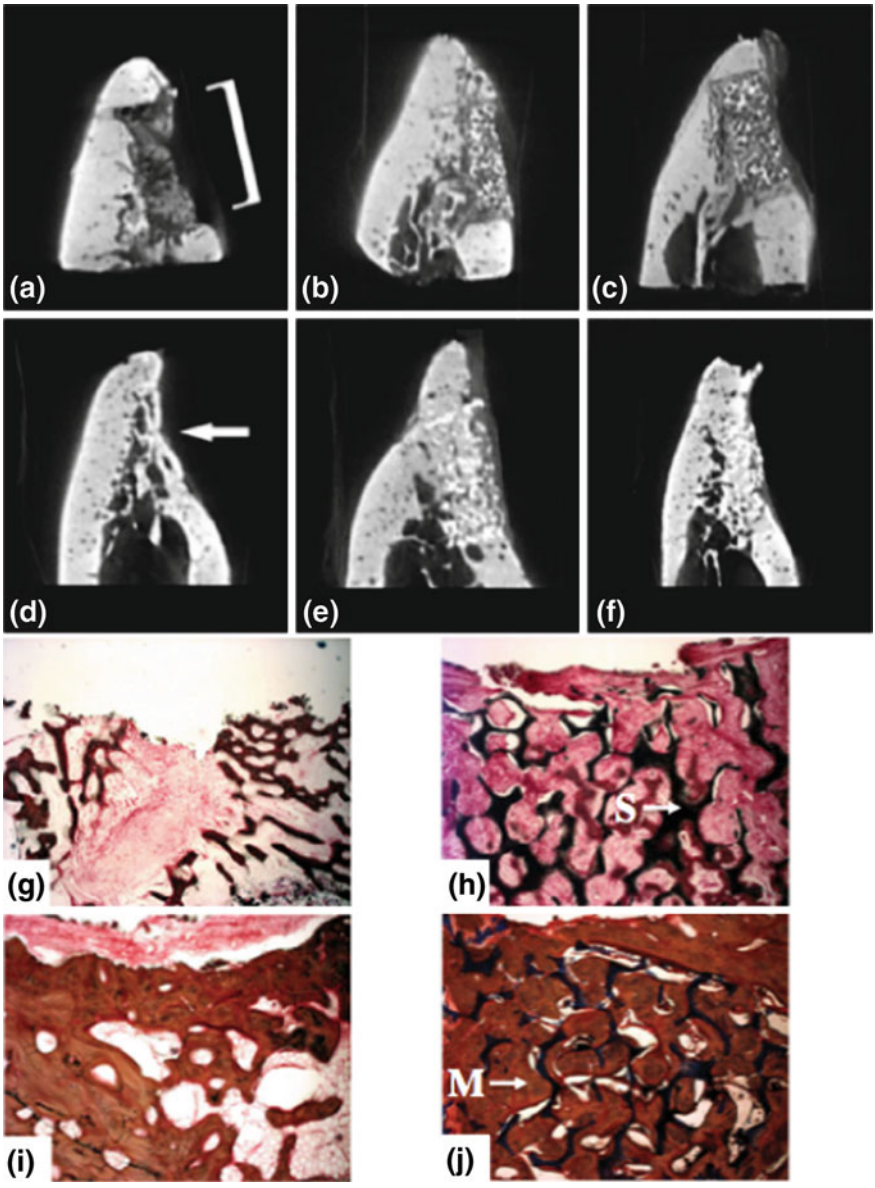

Fig. 8 MicroCT images of control defect (**a**, **d**), implanted M-HA (**b**, **e**), and N-HA (**c**, **f**) scaffolds after 3 and 12 weeks post surgery in the canine madible. Radial defect was created from the lateral surface. Control defect displayed early signs of bridging (*arrow*), whereas scaffold groups show early union and bridging with dense cortical tissue. Bone tissue cross section of control defect stained with Paragon for connective tissue (*violet*) and Alizarin Red for mineralized bone tissue (*red*) after **g** 3 and **i** 12 weeks post surgery and N-HA scaffold shown after **h** 3 and **j** 12 weeks with scaffold in *black*, 380 original magnification; (*S*, scaffold; *M*, mineralized bone). Adapted from Appleford et al. [1]

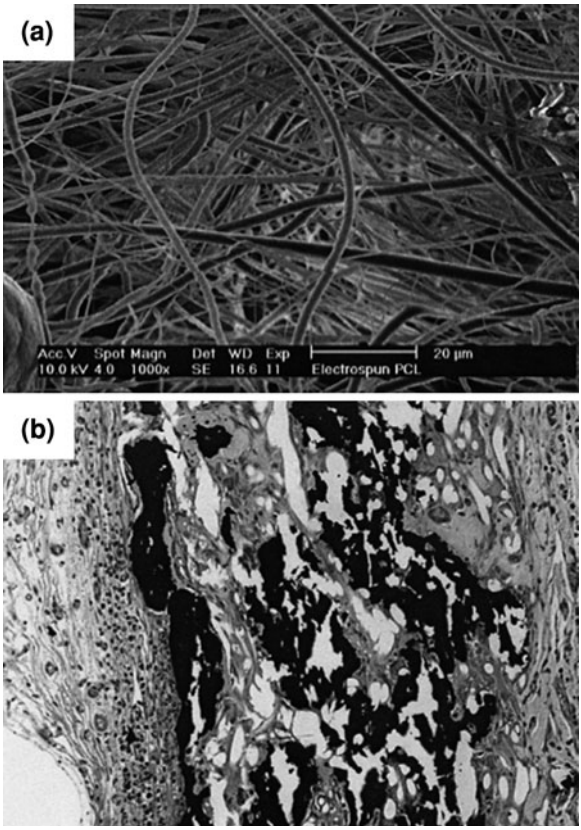

Fig. 9 **a** SEM of PCL electrospun nanofibers. The nonwoven fabric was spun from a 10 wt% PCL solution in chloroform with an applied voltage of 13 kV and a flow rate of 0.1 mL/min. The overall topography of the electrospun fibers resembles that of an extracellular matrix. **b**, **c** Histology cross-section of the explanted specimens after 4 weeks of in vitro culture and 4 weeks of implantation in the omentum of rat. **b** Osteocyte-like cells embedded in bone matrix are present (H&E; original magnification, ×3,100). **c** Mineralization has occurred throughout the specimen (von Kossa; original magnification, ×3,100). Adapted from Shin et al. [55]

the scaffold construct, mineralization, and type I collagen expression in vivo (Fig. 9) [55].

In addition, nanofibrous scaffolds composed of chitosan, a biodegradable and non-toxic natural polymer, has also been demonstrated to enhance bone regeneration. In a later study, Shin et al. studied chitosan nanofibrous scaffolds and their potential in regenerating bone in a rabbit calvarial defect model. Upon 4 weeks post-implantation within a critical-sized defect of a rabbit calvarium, the chitosan nanofibrous scaffold demonstrated almost full coverage of the defect and bone formation (Fig. 10) [56]. A significantly greater amount of bone was regenerated in the chitosan membrane group than in the control group, as seen upon histomorphometric evaluation. This study demonstrated nanofibrous membranes, specifically chitosan, to be another good candidate for a biodegradable scaffold for bone regeneration, as well as a barrier membrane that can selectively guide hard tissue growth within areas, such as the periodontal pocket.

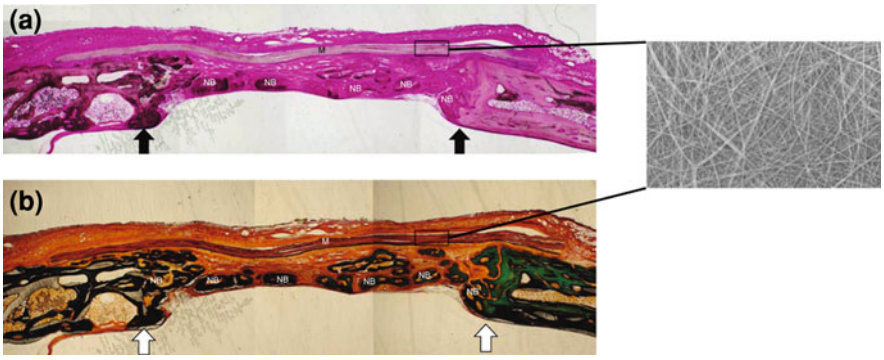

Fig. 10 Histologic view of rabbit calvarial defect covered by chitosan nanofiber membrane after 4 weeks. **a** Multiple staining (original magnification ×20). **b** Masson-Trichrome-Goldner staining (original magnification ×20). *Insert*: SEM image of a chitosan nanofiber membrane surface. *M*: chitosan nanofiber membrane; *arrows*: defect margin; *NB*: new bone. Adapted from Shin et al. [56]

5.2 Nano-Featured Permanent Implants

Titanium implants serve as a well-established, permanent treatment option, which includes orthopedic implants and endosseous dental implants used to anchor dental prostheses. Efforts to modify the surface of permanent implants, such as roughening and coating of surfaces with nano-sized particles, have significantly improved the results of clinical operations. Mechanisms responsible for the enhancement of nano-featured surfaces involves significantly improving the adsorption of proteins, adhesion of osteoblastic cells and thus, the rate of osteo-integration and healing time [33, 34, 35].

When comparing micro-rough implant surfaces to smooth implant surfaces, in vivo studies have demonstrated titanium implants with a micro-rough surfaces to exhibit a wide range of advantages. For instance, micro-rough surfaced implants achieve faster bone integration, a higher percentage of bone-implant contact, and a higher resistance to shear than titanium implants with a smooth surface [43]. The clinical advantages of implants with rough surface were observed in recently conducted clinical trials, as a significantly shorter healing time was observed for micro-rough implants.

In addition, HA coatings on orthopedic and dental implants have gained wide acceptance. It has been repeatedly demonstrated in clinic that HA coatings have osteoconductive properties, and that the fixation of HA-coated implants is better than non-coated implants following optimal surgical conditions. Significant studies also support the conclusion that the early bone growth and apposition are accelerated by implants coated with HA.

Combining the positive properties of HA and nano-featured surfaces developed for enhancing bone growth, Meirelles et al. were the first to evaluate in vivo

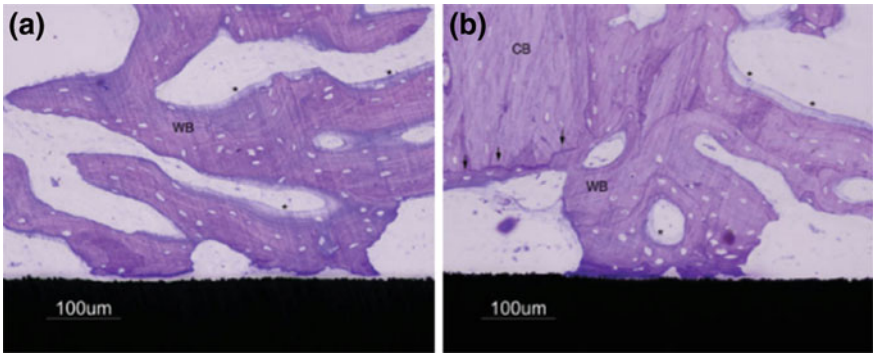

Fig. 11 Ground section of the implants (20×). **a** Uncoated implant demonstrates less bone contact than **b** nano-HA coated implant. Edges of cortical bone (CB) display signs of resorption and new bone formation (*arrows*). Osteoblasts activity (*) is strongly observed around the woven bone (WB). Adapted from Meirelles et al. [40]

bone response to nano-HA featured implants [40]. The effect of nanotopography on bone formation was examined by comparing the control electropolished (i.e. un-coated) titanium implants to implants modified with nano-HA particles. Histomorphometric evaluations showed significantly higher bone contact for the nano-HA coated implants compared to the unmodified implants after 4 weeks of healing (Fig. 11). The mean percentage calculated was 9.0% ± 6.1% for the nano-HA coated implants compared to 3.2% ± 3.6% for the uncoated implants. In a similar note, Christenson et al. examined the effects of nano-HA coated implants, specifically porous tantalum, and compared them to porous tantalum scaffolds coated with conventional grain size HA in vivo [8, 9]. Substantial osteointegration resulted after 6 weeks of implantation of scaffolds coated with nano-HA into rat calvaria, in comparison to the scaffolds coated with conventional grain size HA.

Wang et al. examined the in vivo effects of HA-coated implant surfaces created by two different techniques, plasma-spraying (PSHA) and electrochemical deposition of nano-HA (EDHA) [62]. The titanium implants, either PSHA-coated or EDHA-coated, were implanted into canine trabecular bone for up to two weeks, in order to examine the initial bone formation resulting after implantation. Both, PSHA-coated and EDHA-coated implants were found to accelerate early stage mineralization of bone tissue formation compared to un-coated implants, but PSHA-coated were more efficacious and at a much higher rate. By two weeks, the mineralized tissue apposition ratio and microstructure induced by the PSHA-coated and EDHA-coated implants were similar in vivo, but a higher surface area of EDHA-coating implants were observed, and appear to have resulted in better mechanical integration of the implant and mineralized tissue. These finding concur with a study conducted by He et al., which evaluated the effects of a EDHA-coated

titanium implants on the bone bonding. Removal torque was examined as it correlates to interfacial strength of the implants. The mean removal torque values of the EDHA-coated implants were a significant 87% higher than those of control implants after 2 weeks of healing [20]. Thus, the EDHA-coating had a beneficial effect on interfacial shear strength during the early stages of bone healing.

6 Summary and Conclusion

Advances in scaffold fabrication have led to the creation of biodegradeable scaffolds with required size of topographical features. Among them, scaffolds with nano-sized features have recently attracted much attention because they closely mimic the bone ECM structure and present native environment for the cells that participate in the tissue regeneration/repair process. Clearly, the application of nanotechnology to the scaffold-based bone repair is a new frontier in the bone tissue engineering research. The preliminary in vivo investigations indicate the strategy has great potential to improve current orthopedic biomaterials and in the development of new tissue engineering scaffolds. However, significant advancements in fabricating scaffolds with the precise nano-features and their further in vitro and in vivo characterization are necessary to realize the full potential of nano-featured scaffolds for bone tissue engineering applications.

References

1. Appleford, M.R., Oh, S., Oh, N., Ong, J.L.: In vivo study on hydroxyapatite scaffolds with trabecular architecture for bone repair. J. Biomed. Mater. Res. A **89**(4), 1019–1027 (2009)
2. Aubin, J.E.: Advances in the osteoblast lineage. Biochem. Cell Biol. **76**(6), 899–910 (1998)
3. Aubin, J.E.: Bone stem cells. J. Cell Biochem. Suppl. **30–31**, 73–82 (1998)
4. Aubin, J.E.: Regulation of osteoblast formation and function. Rev. Endocr. Metab. Disord. **2**(1), 81–94 (2001)
5. Bilezikian, J.P., Lawrence, G.R., Gideon, A.R.: Ralph Erskine Conrad Memorial Fund. Principles of Bone Biology, 2nd ed. Academic Press, New York (2002)
6. Carter, D.R.: Mechanical loading histories and cortical bone remodeling. Calcified Tissue Int. **36**, 19–24 (1984)
7. Carter, D.R., Hayes, W.C.: The compressive behavior of bone as a two-phase porous structure. J. Bone Jt. Surg. **59**(7), 954 (1977)
8. Christenson, E.M., Anseth, K.S., van den Beucken, J.J., Chan, C.K., Ercan, B., Jansen, J.A., Laurencin, C.T., Li, W.J., Murugan, R., Nair, L.S., Ramakrishna, S., Tuan, R.S., Webster, T.J., Mikos, A.G.: Nanobiomaterial applications in orthopedics. J. Orthop. Res. **25**(1), 11–22 (2007)
9. Christenson, E.M., Soofi, W., Holm, J.L., Cameron, N.R., Mikos, A.G.: Biodegradable fumarate-based polyhipes as tissue engineering scaffolds. Biomacromolecules **8**(12), 3806–3814 (2007)
10. Clover, J., Dodds, R.A., Gowen, M.: Integrin subunit expression by human osteoblasts and osteoclasts in situ and in culture. J. Cell Sci. **103**(Pt 1), 267–271 (1992)
11. Ducy, P.: Cbfa1: a molecular switch in osteoblast biology. Dev. Dyn. **219**(4), 461–471 (2000)

12. Ducy, P., Starbuck, M., Priemel, M., Shen, J., Pinero, G., Geoffroy, V., Amling, M., Karsenty, G.: A Cbfa1-dependent genetic pathway controls bone formation beyond embryonic development. Genes Dev. **13**(8), 1025–1036 (1999)
13. Franz-Odendaal, T.A., Hall, B.K., Witten, P.E.: Buried alive: how osteoblasts become osteocytes. Dev. Dyn. **235**(1), 176–190 (2006)
14. Gibson, L.J.: The mechanical behaviour of cancellous bone. J. Biomech. **18**(5), 317–328 (1985)
15. Gronthos, S., Simmons, P.J., Graves, S.E., Robey, P.G.: Integrin-mediated interactions between human bone marrow stromal precursor cells and the extracellular matrix. Bone **28**(2), 174–181 (2001)
16. Gronthos, S., Stewart, K., Graves, S.E., Hay, S., Simmons, P.J.: Integrin expression and function on human osteoblast-like cells. J. Bone Miner. Res. **12**(8), 1189–1197 (1997)
17. Hamilton, D.W., Brunette, D.M.: The effect of substratum topography on osteoblast adhesion mediated signal transduction and phosphorylation. Biomaterials **28**(10), 1806–1819 (2007)
18. Harada, S., Rodan, G.A.: Control of osteoblast function and regulation of bone mass. Nature **423**(6937), 349–355 (2003)
19. Harvey, E.J., Henderson, J.E., Vengallatore, S.T.: Nanotechnology and bone healing. J. Orthop. Trauma **24**(Suppl 1), S25–S30 (2010)
20. He, F.M., Yang, G.L., YN, Li., Wang, X.X., Zhao, S.F.: Early bone response to sandblasted, dual acid-etched and H_2O_2/HCL treated titanium implants: an experimental study in the rabbit. Int. J. Oral Maxillofac. Surg. **38**(6), 677–681 (2009)
21. Hilliard, T.J., Meadows, G., Kahn, A.J.: Lysozyme synthesis in osteoclasts. J. Bone Miner. Res. **5**(12), 1217–1222 (1990)
22. Lakes, R.S.: Materials with structural hierarchy. Nature **361**, 511–515 (1993)
23. Ibbotson, K.J., Roodman, G.D., McManus, L.M., Mundy, G.R.: Identification and characterization of osteoclast-like cells and their progenitors in cultures of feline marrow mononuclear cells. J. Cell Biol. **99**(2), 471–480 (1984)
24. Karsenty, G., Ducy, P., Starbuck, M., Priemel, M., Shen, J., Geoffroy, V., Amling, M.: Cbfa1 as a regulator of osteoblast differentiation and function. Bone **25**(1), 107–108 (1999)
25. Kartsogiannis, V., Ng, K.W.: Cell lines and primary cell cultures in the study of bone cell biology. Mol. Cell. Endocrinol. **228**(1–2), 79–102 (2004)
26. Katagiri, T., Takahashi, N.: Regulatory mechanisms of osteoblast and osteoclast differentiation. Oral Dis. **8**(3), 147–159 (2002)
27. Keller, T.S., Mao, Z., Spengler, D.M.: Young's modulus, bending strength and tissue physical properties of human compact bone. J. Orthopaedic Res. **8**(4), 592–603 (2005)
28. Kim, J.B., Leucht, P., Luppen, C.A., Park, Y.J., Beggs, H.E., Damsky, C.H., Helms, J.A.: Reconciling the roles of FAK in osteoblast differentiation, osteoclast remodeling, and bone regeneration. Bone **41**(1), 39–51 (2007)
29. Kofron, M.D.: Bone tissue engineering using an ex vivo gene therapy approach. Ph.D. Thesis, University of Virginia (2007)
30. Langer, R., Vacanti, J.P.: Tissue engineering. Science **260**(5110), 920–926 (1993)
31. Laurencin, C.T., Ambrosio, A.M., Borden, M.D., Cooper Jr., J.A.: Tissue engineering: orthopedic applications. Annu. Rev. Biomed. Eng. **1**, 19–46 (1999)
32. Laurencin, C.T., Kumbar, S.G., Nukavarapu, S.P.: Nanotechnology and orthopedics: a personal perspective. Wiley Interdiscip. Rev. Nanomed. Nanobiotechnol. **1**(1), 6–10 (2009)
33. Le Guehennec, L., Goyenvalle, E., Lopez-Heredia, M.A., Weiss, P., Amouriq, Y., Layrolle, P.: Histomorphometric analysis of the osseointegration of four different implant surfaces in the femoral epiphyses of rabbits. Clin. Oral Implants Res. **19**(11), 1103–1110 (2008)
34. Le Guehennec, L., Martin, F., Lopez-Heredia, M.A., Louarn, G., Amouriq, Y., Cousty, J., Layrolle, P.: Osteoblastic cell behavior on nanostructured metal implants. Nanomedicine (Lond) **3**(1), 61–71 (2008)
35. Le Guéhennec, L., Soueidan, A., Layrolle, P., Amouriq, Y.: Surface treatments of titanium dental implants for rapid osseointegration. Dent. Mater. **23**(7), 844–854 (2007)

36. Liu, X., Ma, P.X.: Polymeric scaffolds for bone tissue engineering. Ann. Biomed. Eng. **32**(3), 477–486 (2004)
37. Liu, X., Smith, L.A., Hu, J., Ma, P.X.: Biomimetic nanofibrous gelatin/apatite composite scaffolds for bone tissue engineering. Biomaterials **30**(12), 2252–2258 (2009)
38. Ma, P.X., Elisseeff, J.H.: Scaffolding in Tissue Engineering. Taylor & Francis/CRC Press, London/Boca Raton (2006)
39. Malaval, L., Liu, F., Roche, P., Aubin, J.E.: Kinetics of osteoprogenitor proliferation and osteoblast differentiation in vitro. J. Cell. Biochem. **74**(4), 616–627 (1999)
40. Meirelles, L., Arvidsson, A., Andersson, M., Kjellin, P., Albrektsson, T., Wennerberg, A.: Nano hydroxyapatite structures influence early bone formation. J. Biomed. Mater. Res. A **87**(2), 299–307 (2008)
41. Mooney, D.J., Mazzoni, C.L., Breuer, C., McNamara, K., Hern, D., Vacanti, J.P., Langer, R.: Stabilized polyglycolic acid fibre-based tubes for tissue engineering. Biomaterials **17**(2), 115–124 (1996)
42. Nakagawa, K., Abukawa, H., Shin, M.Y., Terai, H., Troulis, M.J., Vacanti, J.P.: Osteoclastogenesis on tissue-engineered bone. Tissue Eng. **10**(1–2), 93–100 (2004)
43. Nasatzky, E., Gultchin, J., Schwartz, Z., The role of surface roughness in promoting osteointegration. Refuat Hapeh Vehashinayim **20**(3), 8–19, 98 (2003)
44. Nukavarapu, S.P., Kumbar, S.G., Brown, J.L., Krogman, N.R., Weikel, A.L., Hindenlang, M.D., Nair, L.S., Allcock, H.R., Laurencin, C.T.: Polyphosphazene/nano-hydroxyapatite composite microsphere scaffolds for bone tissue engineering. Biomacromolecules **9**(7), 1818–1825 (2008)
45. Nukavarapu, S.P., Kumbar, S.G., Merrell, J.G., Laurencin, C.T.: Electrospun polymeric nanofiber scaffolds for tissue regeneration. Nanotechnology and Tissue Engineering: The Scaffold. Taylor & Francis, London (2008)
46. Nukavarapu, S.P., Kumbar, S.G., Nair, L.S., Laurencin, C.T.: Nanostructures for tissue engineering/regenerative medicine. Biomedical Nanostructures. Wiley, New York (2007)
47. Ramakrishna, S.: An Introduction to Electrospinning and Nanofibers. World Scientific, Singapore (2005)
48. Reddy, S.V., Roodman, G.D.: Control of osteoclast differentiation. Crit. Rev. Eukaryot. Gene Expr. **8**(1), 1–17 (1998)
49. Rho, J.Y., Kuhn-Spearing, L., Zioupos, P.: Mechanical properties and the hierarchical structure of bone. Med. Eng. Phys. **20**(2), 92–102 (1998)
50. Roehlecke, C., Witt, M., Kasper, M., Schulze, E., Wolf, C., Hofer, A., Funk, R.W.: Synergistic effect of titanium alloy and collagen type I on cell adhesion, proliferation and differentiation of osteoblast-like cells. Cells Tissues Organs **168**(3), 178–187 (2001)
51. Roodman, G.D.: Cell biology of the osteoclast. Exp. Hematol. **27**(8), 1229–1241 (1999)
52. Roodman, G.D.: Regulation of osteoclast differentiation. Ann. NY Acad. Sci. **1068**, 100–109 (2006)
53. Schlaepfer, D.D., Hanks, S.K., Hunter, T., van der Geer, P.: Integrin-mediated signal transduction linked to Ras pathway by GRB2 binding to focal adhesion kinase. Nature **372**(6508), 786–791 (1994)
54. Shekaran, A., García, A.J.: Extracellular matrix-mimetic adhesive biomaterials for bone repair. J. Biomed. Mater. Res. A **96**(1), 261–272 (2011)
55. Shin, M., Yoshimoto, H., Vacanti, J.P.: In vivo bone tissue engineering using mesenchymal stem cells on a novel electrospun nanofibrous scaffold. Tissue Eng. **10**(1–2), 33–41 (2004)
56. Shin, S.Y., Park, H.N., Kim, K.H., Lee, M.H., Choi, Y.S., Park, Y.J., Lee, Y.M., Ku, Y., Rhyu, I.C., Han, S.B., Lee, S.J., Chung, C.P.: Biological evaluation of chitosan nanofiber membrane for guided bone regeneration. J. Periodontol. **76**(10), 1778–1784 (2005)
57. Siebers, M.C., ter Brugge, P.J., Walboomers, X.F., Jansen, J.A.: Integrins as linker proteins between osteoblasts and bone replacing materials. A critical review. Biomaterials **26**(2), 137–146 (2005)

58. Smith, I.O., Liu, X.H., Smith, L.A., Ma, P.X.: Nanostructured polymer scaffolds for tissue engineering and regenerative medicine. Wiley Interdiscip. Rev. Nanomed. Nanobiotechnol. **1**(2), 226–236 (2009)
59. Smith, L.A., Liu, X., Hu, J., Ma, P.X.: The enhancement of human embryonic stem cell osteogenic differentiation with nano-fibrous scaffolding. Biomaterials **31**(21), 5526–5535 (2010)
60. Sun, H., Feng, K., Hu, J., Soker, S., Atala, A., Ma, P.X.: Osteogenic differentiation of human amniotic fluid-derived stem cells induced by bone morphogenetic protein-7 and enhanced by nanofibrous scaffolds. Biomaterials **31**(6), 1133–1139 (2010)
61. Udagawa, N., Takahash, N.: Possible role of receptor activator of Nf-kappa B ligand(RANKL) in osteoclast differentiation and function. Nippon Rinsho **60**(Suppl 3), 672–678 (2002)
62. Wang, H., Eliaz, N., Xiang, Z., Hsu, H.P., Spector, M., Hobbs, L.W.: Early bone apposition in vivo on plasma-sprayed and electrochemically deposited hydroxyapatite coatings on titanium alloy. Biomaterials **27**(23), 4192–4203 (2006)
63. Wei, G., Jin, Q., Giannobile, W.V., Ma, P.X.: The enhancement of osteogenesis by nano-fibrous scaffolds incorporating Rhbmp-7 nanospheres. Biomaterials **28**(12), 2087–2096 (2007)
64. Woo, K.M., Chen, V.J., Ma, P.X.: Nano-fibrous scaffolding architecture selectively enhances protein adsorption contributing to cell attachment. J. Biomed. Mater. Res. A **67**(2), 531–537 (2003)
65. Woo, K.M., Jun, J.H., Chen, V.J., Seo, J., Baek, J.H., Ryoo, H.M., Kim, G.S., Somerman, M.J., Ma, P.X.: Nano-fibrous scaffolding promotes osteoblast differentiation and biomineralization. Biomaterials **28**(2), 335–343 (2007)
66. Yim, E.K., Darling, E.M., Kulangara, K., Guilak, F., Leong, K.W.: Nanotopography-induced changes in focal adhesions, cytoskeletal organization, and mechanical properties of human mesenchymal stem cells. Biomaterials **31**(6), 1299–1306 (2010)
67. Yokoi, H., Kinoshita, T., Zhang, S.: Dynamic reassembly of peptide Rada16 nanofiber scaffold. Proc. Natl. Acad. Sci. USA **102**(24), 8414–8419 (2005)
68. Zaidi, M., Troen, B., Moonga, B.S., Abe, E., Cathepsin, K.: Osteoclastic resorption, and osteoporosis therapy. J. Bone Miner. Res. **16**(10), 1747–1749 (2001)
69. Zinger, O., Anselme, K., Denzer, A., Habersetzer, P., Wieland, M., Jeanfils, J., Hardouin, P., Landolt, D.: Time-dependent morphology and adhesion of osteoblastic cells on titanium model surfaces featuring scale-resolved topography. Biomaterials **25**(14), 2695–2711 (2004)

Bioactive Agent Delivery in Bone Tissue Regeneration

Aysen Tezcaner and Dilek Keskin

Abstract Bone tissue, unlike most tissues, has the ability of complete regeneration if provided with precise materials and bioactive agents. Regeneration course, however, is a highly complex process engrossing significant problems when failed. Bone grafts are indispensable in orthopedic, craniofacial and periodontal surgeries to fill the dead space, to provide support for the newly forming tissues, and to augment regeneration/treatment via its bioactive components. These multifunctional scaffolds can be categorized according to the bioactive agent they supply or by their carrier material composition. As one group of bioactive agents, growth factors, cytokines, chemokines, statins, etc. are mainly considered for regeneration of large bone defects as well as for defects in hosts with impaired regeneration capacity. The second bioactive group, antibiotics, is mostly used in clinic for infectious bone disease treatment throughout the regeneration period. They are, however, still being studied for development of more efficient forms. This chapter summarizes the most recent studies and trends in scaffolds for bone regeneration with controlled release of bioactive agents.

A. Tezcaner and D. Keskin (✉)
Department of Engineering Sciences, Middle East Technical University, Ankara, Turkey
e-mail: dkeskin@metu.edu.tr

A. Tezcaner and D. Keskin
Graduate Department of Biomedical Engineering, Middle East Technical University, Ankara, Turkey

Stud Mechanobiol Tissue Eng Biomater (2011) 8: 193–223
DOI: 10.1007/8415_2010_50

Published Online: 2 March 2011

1 State of Art in Bone Regeneration Strategies

The repair of large segmental bone defects due to trauma, osteoporosis, inflammation or tumor still remains a major challenge in orthopaedics. Clinically accepted therapies for restoring such defects involve grafting procedures and implanting biomaterials [1, 2]. Although autologous bone is a gold standard material for reconstruction of skeletal defects, allografts are also commonly used as graft materials for bone defects and nonunions. Both auto- and allo-grafts provide host osteogenic cells with osteoinductive factors, and an osteoconductive matrix essential for bone formation. However, there are critical limitations associated with the graft harvest, such as donor site morbidity, prolonged surgery time, risk of immune rejection, limited supply and late graft fracture [3].

Tissue engineering approach is becoming a promising alternative for grafting in which a biodegradable scaffold with or without bioactive molecules (i.e. growth factors, cytokines, antibiotics, etc.) is used alone or in combination with cells to regenerate a functional bone tissue (Fig. 1) [1, 4, 5]. The main purpose behind tissue engineering is to mimic natural wound healing cascade by providing suitable biochemical and mechanical cellular microenvironment which augments the proliferation and differentiation of recruited host cells or implanted cells at the defect site. Requirements for an ideal scaffold for bone tissue engineering are

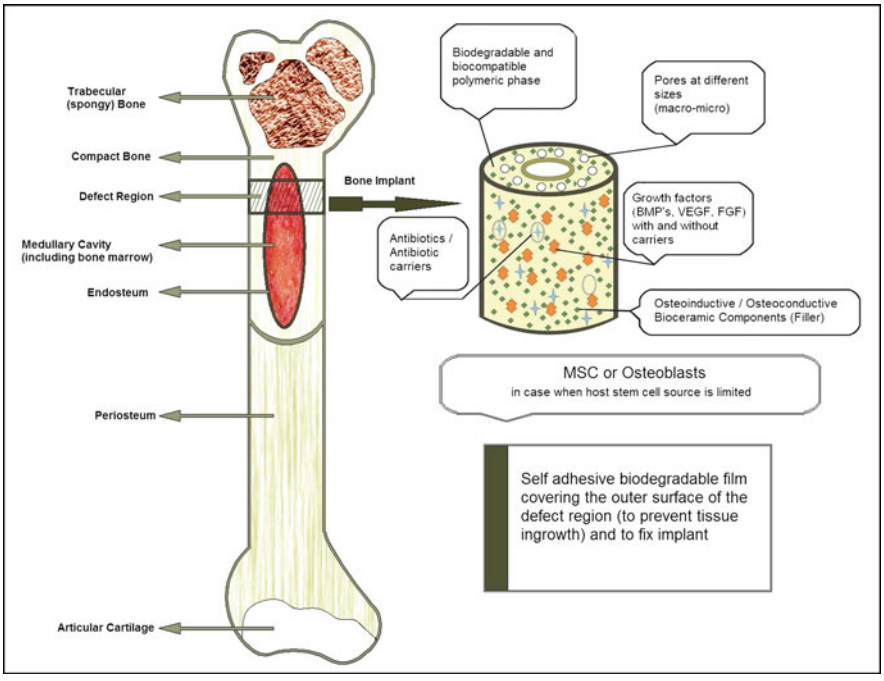

Fig. 1 Schematic representation of an ideal bioactive agent delivering bone scaffold

summarized in Table 1. Clinically available synthetic substitutes have adequate osteoconductive properties but have little or no osteoinductivity. Osteoinduction is a biological process in which the host stem cells migrate towards the carrier and differentiate into osteogenic lineage for bone formation under the control of various molecules like growth factors, cytokines, etc. The growth factors have very short half-lives owing to their susceptibility to biodegradation and easy elimination from the circulation if not protected. In clinical applications, bolus injections of bone morphogenetic protein-2 (BMP-2) by single or repeated doses resulted with loss of the growth factor through leakage and loss of its bioactivity. Additionally, need of high dose use raises the question of potential toxicity [6]. Controlled bioactive agent delivery systems can circumvent these problems. These systems can act as depots and protective environment for growth factors as well as sustaining their delivery after implantation. Besides these, in cases when defect region is contaminated by an already occuring infectious agent, delivery of antimicrobial agents is an initial must to achieve tissue regeneration. Even in the absence of a previous microbial disease, delivery of antibiotics for possible implant related infections would be a favourable approach to increase implant success.

2 Controlled Release of Bioactive Agents from Scaffolds for Bone Regeneration

Bone regeneration is a coordinated cascade of events regulated by various bioactive molecules namely cytokines, chemokines, and growth factors whose concentrations, temporal gradients, spatial gradients, sequence of their release are

Table 1 Scaffold requirements for bone regeneration

Structural requirements
Scaffold should be designable to have desired micro–macro structure considering the variety in defect sizes and shapes. The components in the scaffold should be applicable to processing methods like moulding, prototyping [103] or microrobotic deposition [20] for proper design
Scaffold should match the mechanical strength of the surrounding bone tissue at the defect site [104, 105]
Scaffold should provide multiscale homogeneous, interconnected porosity for proper osteointegration, vascularization and nutrient supply [20, 106]
Scaffold should be biodegradable, thereby eliminating the need of second surgery. Meanwhile, its degradation rate should also match with the new bone tissue formation rate [84, 90]
Biological requirements
Scaffold should be biocompatible over all its in vivo lifetime with all its initial and final forms/products [84, 86]
Scaffold should be suitable to serve as a carrier and controlled delivery system for required bioactive agents (growth factors, antibiotics, cytokines, etc.) without losing their biological activities during the desired period [30, 96]
Scaffold should provide osteoprogenitor cells or stem cells when the regeneration capacity is impaired like in the case of long term chemotherapies [19, 37]

precisely controlled [7]. Therefore, multifunctional scaffolds with sophisticated delivery strategies are needed to induce and complete bone regeneration in bone defects. These scaffolds serve the dual purposes of both cell support and delivery of bioactive agents. Such carriers are designed to provide maturation of host or transplanted cells with the delivery of single or multiple factors at the right time, dose and sequence [8–10]. The delivery of these factors in a sustained way also ensures the bioavability of bioactive agents by protecting them from degradation in the biological environment [10].

2.1 Growth Factors

Growth factors are powerful therapeutic agents. They have multimodal action (i.e., chemotactic, mitogenic, morphogenic, metabolic, apoptotic effects and their combination) depending on the concentration, exposure time and target cells [11, 12]. Many growth factors such as BMP-2, BMP-7, TGFβ-1, PDGF and FGF are known for their important role in bone formation process. However, it is reported that long term supply of these agents in the local environment is needed to achieve effective bone healing [13, 14]. High or repeated dose injections of these agents make these therapies expensive and complicated. Besides this, high doses of these agents were reported to have unwanted side effects like tissue toxicity and cancerogenicity [15]. Delivery systems, therefore, have attracted the attention of researchers to overcome these problems. Growth factors can be incorporated into the biomaterials either during or after fabrication process. Their delivery to the target tissue can be accomplished in the form of microparticles, nanoparticles [16–18] or these particles/growth factors incorporated into scaffolds [10, 19, 20]. The main concerns in these systems are the loss of their bioactivity, burst release and difficulty in sustaining their release from the carriers. Hence, various controlled delivery systems have been developed to modify the bioactive agent release properties. Some of the basic approaches are examplified in Table 2.

2.1.1 Bone Morphogenetic Proteins

Bone morphogenetic proteins (BMPs) are an important class of growth factors which can induce differentiation of mesenchymal stem cells into chondrogenic and osteogenic lineages [21, 22]. BMPs have high osteoinductive activity and they even can induce bone formation in ectopic locations [10, 14, 23]. Currently, only BMP-2 and BMP-7 are being used in clinical applications [24, 25]. As all growth factors, BMP-2 has a very short half-life and rapid in vivo clearance, therefore necessitating high dose administration. However, as noted above single or multiple injections at high doses injections result with significant loss of BMP from the site and/or its bioactivity [6]. Incorporation of BMP-2 into natural and synthetic biomaterials (collagen, gelatin, demineralized bone matrix (DBM),

Table 2 Approaches used to modify the release kinetic/profile of bioactive agents from bone scaffolds

Strategy	Release outcome	Example	Main drawback	Reference
Use of polymers as hydrophobic components in composite scaffold	Sustain the drug release from the system	PLA, PCL, PLGA/ceramic composites	Usually require organic solvents which decreases the bioactivity of proteins	Sawyer et al. and Miyai et al. [36, 88]
Use of hydrophillic components	Enhance the drug release from the system	Addition sugar molecules (mannose, lactose)	Might decrease stability and force degradation of the system	Frutos et al. [107]
Embedding the controlled release system into scaffold	Sustain the release and burst (initial fast) release	Microsphere loaded scaffolds	Use of organic solvent	De la Riva et al. and Wang et al. [19, 47]
Compaction of the system (with or without heat)	Sustain the drug release from the system	Compaction of ceramic or ceramic/polymer composites	Might decrease porosity of the sytems	Petrone et al. [108]
Coating of the delivery sytem	Sustain the drug release from the system	PLA coating of scaffolds	May delay cellular infiltration and growth	Kim et al. and Kempen et al. [10, 109]
Conjugation/immobilization	Sustain the drug release from the system	BMP or other growth factor conjugation-immobilization by chemical treatments	Might not be applicable to some bioactive agents	Benoit et al. and Zhao et al. [14, 83]
Modifying the porosity or size distribution of scaffolds	Sustain or enhance the drug release from the system	Addition of porogens like salt, sugar moieties or carboxymethyl cellulose	May weaken the mechanical properties	Xu et al. and Shi et al. [110, 111]
Increasing the initial amount of bioactive agent loading	Sustain the drug release from the system	Adding more bioactive agents to the carrier	Might increase the safe local amounts owing to burst release at early times	Patel et al. [42]
Increasing the polymer molecular weight or copolymer ratio	Sustain or enhance the drug release from the system	Using high molecular weight polymer	Prolong the in vivo degradation period of the scaffold	Mauduit and Schmidt [112, 113]
Post-loading of the bioactive agent	Fast drug release	Embedding scaffold with bioactive agent solution	Less interaction between scaffold and bioactive agent	Patel et al. [42]

Poly(lactide-co-glycolide) (PLGA), polyurethane, calcium phosphates, etc.) in different forms (foams, injectable formulations, particulates, particulates incorporated in scaffolds) have been widely studied and showed promising results [14, 26–30]. It should be noted that due to their unstable chemistry, difficulties are faced for incorporating these factors into proper carriers. BMPs are expensive molecules, therefore loading efficiency of the scaffolds is important. Apart from loading dose, obtaining sustained release pattern and retention of their bioactivity during processing and upon implantation are among the goals seeked by the researchers.

Collagen is considered as the gold standard as a delivery system for BMPs. It can be applied as gels, films and sponges. It has high binding affinity for BMPs and its osteoconductive properties also make it ideal for treating bone defects. Main concerns related with collagen are the risk of immunogenicity and transmission of prion or other disease causing agents. Clinical uses of recombinant human BMP-2 (rhBMP-2) on collagen sponges have been approved in USA with strict regulations for spinal fusion procedures in mature patients with degenerative disks and in treatment of acute, open fractures and tibial shaft. Similarly, rhBMP-7 with bovine collagen has obtained Humanitarian Device Exemption FDA approval for applications in: (1) recalcitrant long bone unions where autograft cannot be used and alternative treatments have failed, and (2) compromised patients requiring revisional posterolateral lumbar spinal fusion whose bone marrow can not be harvested or successful fusion is not expected [1].

Demineralized bone matrix (DBM) is suitable for bone regeneration due to its similarity to human bone matrix as well as for its osteoinductive and osteoconductive properties. DBM has been widely used for healing of large bone defects and for filling cranial defects [31–33]. Chen et al. [27] engineered rhBMP-2 by adding a collagen-binding peptide domain (CPD) to N-terminal of the protein and imprengated into DBM carrier for minimizing the potential adverse effects of high dose. The retained percentage of rhBMP-2 with CPD was found higher than that of rhBMP-2 in DBM carrier in accordance with the loading dose. The in vitro functional assay was in correlation with these results in which the biological activity of engineered rhBMP-2 was higher than original rhBMP-2. The group reported that better bone formation took place in comparison to control groups (DBM, rhBMP-2) both ectopically (subcutaneous implantation in rats) and orthopically (in critical size defects of rabbit mandibles). In another study of the group, they used specific binding between anti-polyhistidine antibody covalently linked to DBM and engineered rhBMP-2 with six histidine tags (hisBMP-2) to enhance loading capacity and design a controlled delivery system for the growth factor [14]. The noncovalent binding between antibody and its ligand achieved a sustained in vitro release of rhBMP-2. Functional in vitro assays proved the osteogenic differentiation capacity of the his-BMP-2 immobilized in DBM scaffolds. Accordingly, in vivo studies showed that the designed system induced more ectopic bone formation than the control group (hisBMP/DBM scaffold).

BMP-7 with its known osteogenic potential is in clinical use. In the work of Burastero et al. [9] the bone regeneration potential of in vitro expanded human

bone marrow derived mesenchymal stem cells (BMMSc) and human recombinant BMP-7 (hrBMP-7) mixed with Orthoss® was investigated in a critical size segmental bone defect created in hind limbs of athymic rats. They also investigated whether pretreatment of BMMSc with different doses of cyclic ADP ribose (cADPR), an intracellular calcium mobilizer (2 or 10 μM) or BMP-7 (0.2 or 1 μg/ml) affected the differentiation and proliferation of these cells. They found that rhBMP-7 slightly reduced cell number at two doses whereas cADPR increased proliferation of these cells in a concentration-dependent manner. An interesting finding of the study is that the combination of CADPR and hrBMP-7 induced expression of osteogenic markers (i.e. ALP, osteopontin, Runt-related transcriptional factor-2) in the absence of differentiation factors. The group conducted two separate sets of in vivo experiments to decide radiographically the minimal BMMSc cell number (2×10^6/graft) and minimum hrBMP-7 dose (80 μg/graft) for bone formation. With this cell number and rhBMP-7 dose they investigated the bone regeneration potential of cells and rBMP-7 alone and together. 16 weeks after transplanation they observed that combining BMMSc with BMP-7 in Orthoss® improved bone regeneration in defects.

Apart from collagen, synthetic polymers, calcium phosphates, hyaluronic acid, etc. based carrier systems are often used for in vitro and in vivo studies, but none has been approved for clinical applications as growth factor carrier yet. The synthetic polymers can be tailor made according to the need by changing molecular weights, configuration and conformation of polymer chains, degradation rates, and delivery forms. However, inefficient binding of growth factors to synthetic polymers, possible inflammatory reactions at the implantation site due to degradation products, unpredicted in vivo release pattern of growth factors hamper the clinical use of synthetic polymers as carriers for growth factors. Either composites of different polymers and/or ceramics are used to combine the positive effects of each to solve the problems associated with polymeric scaffolds [34–36]. Alternatively, polymeric scaffolds can be modified using different chemical, physical techniques for stable attachment of the growth factors [37, 38]. Kempen et al. [10] used three polymers (gelatin, PLGA and poly(propylene fumarate)-PPF) in the design of the carrier to achieve sustained rhBMP-2 delivery for bone regeneration. rhBMP-2 was incorporated into gelatin hydrogels, PLGA microspheres, PLGA microspheres embedded in PPF scaffolds and microspheres embedded in PPF scaffolds surrounded by a gelatin hydrogel. PPF, a crosslinkable linear polyester with suitable mechanical properties was used to prepare a three-dimensional carrier to control over the rhBMP-2 release from PLGA microspheres. Among all experimental groups, two composite groups with microspheres showed significantly more bone formation in a rat subcutaneous implantation model over 12 weeks. This finding was also in correlation with in vitro cell culture studies conducted with preosteoblast W20-17 cells. In vitro release and bioactivity tests (alkaline phosphatase activity of cells) showed that prolonged bioactive rhBMP-2 release was observed only from the two composite groups. Embedding rhBMP-2 loaded microspheres in a three-dimensional scaffold with or without a gelatin

coating enhanced the retention of in vitro and in vivo bioactivity of BMP as well as ensuring its controlled release.

In another recent study, surface plasma treatment was used to achieve good binding of rhBMP-2 onto the biomaterial without losing its biological activity at the same time. Among different plasma treatments, oxygen plasma treatment of PLGA films for 10 min gave the highest rhBMP binding. It was also reported that this immobilized rhBMP-2 retained its biological activity in vitro [38].

Calcium phosphate ceramics are also among the promising bone substitute materials with their osteoconductive property. However, their use is mostly limited to the nonload bearing bone defect reconstructions [39] due to their low mechanical strength. Besides that long bioresorption rate raised the questions over using these materials alone. On the other hand, they have high bonding affinity for growth factors [40] which makes them suitable for use in controlled delivery systems. Thus, mean retention time (MRT) of these labile factors increases after incorporation in this biomaterial. The release of growth factors from these systems depends on the resorption rate of calcium phosphates which in turn depends on both implant-related factors (composition such as HA/TCP ratio) and host related factors (species-specific, implantation site, dimension, etc.) [40]. Therefore, there is still need of further investigation on calcium phosphate delivery systems for the large scale clinical applications to be realized.

The action of growth factors are time- and concentration-dependent. The growth factor gradients created also provide spatial and directional cues in the extracellular matrix for the cells. Focus in the recent studies with scaffolds and particulate delivery systems has been put on the control of the loading dose, spatial distribution and sequential delivery of the growth factors to both understand natural tissue growth process and to mimick the natural microenvironment for achieving regeneration [17, 19]. Wang et al. used a gradient making system to produce single concentration gradients for rhBMP-2 and rhIGF-I or to create reverse gradients of rhBMP-2/rhIGF-I within alginate gels and porous silk scaffolds using growth factor loaded PLGA or silk microspheres. They have also encapsulated hMSCs homogeneously while developing the gradient distribution of microspheres within these scaffolds. hMSCs carrying scaffolds were incubated in a medium containing both osteogenic and chondrogenic components and were shown to exhibit osteogenic and chondrogenic differentiation along the concentration gradients of rhBMP-2 and reverse gradients of rhBMP-2/rhIGF-I. The group reported that silk microspheres were more efficient as delivery system for rhBMP-2 and rhIGF-I to induce hMSC osteogenesis whereas rhBMP-2 and rhIGF-I singly or dual loaded PLGA microsphere systems were found efficient for chondrogenic differentiation of hMSCs along their concentration gradients. It was concluded that alginate gel system did not exhibit an efficient carrier system property for osteochondrogenesis as porous silk scaffolds did.

For achieving local gradients of growth factors Ionescu et al. [41] recently developed an approach for the creation of multi-factor delivering anisotropic nanofibrous PCL scaffolds. The group incorporated PLGA microspheres loaded with BSA and chondroitin sulfate separately or together into nanofibrous scaffold

by entrapping them between fibers not within them. This processing technique involved delivering microspheres in sacrificial PEO fibers after which the fibers were removed form the scaffold by washing with 50% ethanol. It was shown that mechanical properties of these scaffolds did not change significantly with the incorporated microsphere amount and multi-factor release profiles from these scaffolds were indifferent than those from free microspheres.

Recent developments in the delivery systems involve preparation of carrier systems which deliver several bioactive agents. One of the earliest example for dual delivery system was the work of Simmons et al. [37] in which rhBMP-2 and transforming growth factor-β3 (TGFβ3) were incorporated either individually or in combination into alginate gels. These alginate carriers were covalently modified with RGD-containing peptides to control cell behavior. The group also used gamma irradiation to change degradation of the alginate carrier. They transplanted MSC seeded alginate gel implants subcutaneously that were either gamma irradiated or non-irradiated. It was reported that individual delivery of rhBMP-2 or TGFβ3 resulted in negligible bone tissue while growth factors delivered together at low protein concentrations induced significant bone formation.

In the recent years, to maintain a sustained delivery of the bioactive agents from the scaffold these agents are encapsulated into particles which then are incorporated into three-dimensional carrier systems. Patel et al. [42] reported that dual delivery of vascular endothelial growth factor (VEGF) and BMP-2 from gelatin microparticles embedded in porous scaffolds had a positive effect on repair of a rat cranial defect. This work is discussed in detail under Sect. 2.1.2. Considering the mechanism and timing of actions of BMP-2 and BMP-7 in bone healing, Hasirci's group designed combined sequential delivery systems for these two growth factors. They aimed early BMP-2 release followed by release of BMP-7 [16, 43]. In the work of Basmanav et al. [44] these growth factors were encapsulated in microspheres of polyelectrolyte complexes of alginic acid and poly(4-vinyl pyridine) that were crosslinked with different degrees by changing the crosslinking temperature. These microspheres were then embedded in porous PLGA scaffolds. They showed the positive effect of co-administration and sequential delivery of these factors on differentiation of bone marrow mesenchymal stem cells (in terms of increase in ALP activity with time) in vitro. In their recent work, the group embedded BMP-2 loaded PLGA and BMP-7 loaded poly(3-hydroxy-co-3-hydroxyvalerate) (PHBV) nanospheres into and onto the fibers of wet spun chitosan and chitosan-poly(ethylene oxide) (PEO) scaffolds. The group reported that chitosan-based scaffolds with nanospheres made up of two types of polymers with different protein release profiles ensures the early BMP-2 release and longer term BMP-7 release. For in vitro cell culture studies, the group encapsulated both BMP-2 and BMP-7 into PLGA nanospheres and embedded them in alginate-based scaffolds. They observed that release of BMPs led to the highest ALP level in MSC but supressed their proliferation.

Choi et al. [30] used a coaxial electro-dropping method by which core–shell structured microcapsules were prepared using two immiscible polymers, alginate and PLGA. They included dexamethasone and BMP-2 alternatively either to core

or shell domain of microcapsules to obtain different release profiles for the two osteogenic factors (burst release of biomolecule loaded in PLGA core being suppressed). In vitro studies showed that the gene expression levels of osteogenic markers of MSC were significantly upregulated when the cells were cultured with these constructs. It can be seen that dual delivery systems preferably those with a control on the release rate and pattern of several factors hold promise for bone tissue engineering.

There is a consensus among researchers that scaffold architecture must have interconnected macroporosity on the order of at least 100 μm for cellular infiltration and nutrient/waste transport in tissue engineering applications. On the contrary, Lan Levengood et al. [20] recently reported that cells can populate and form bone in pores significantly smaller than what has been reported in the literature. The focus of their work was to investigate the effect of rhBMP-2 and multiscale porosity (macro- and microscales) together on osteointegration. In the study, rhBMP-2 loaded gelatin microparticles were used for incorporating the growth factor into biphasic calcium phosphate (BCP) scaffolds having multiscale porosity. The group implanted rhBMP-2 free and loaded BCP scaffolds to noncritical size defects created in porcine mandibulars. They observed that rhBMP-2 improved osteointegration on the microscale but not at the macroscale. Both cells and bone formation were observed in the micropores. The group further concluded that rhBMP-2 was not required for cell migration and bone formation in the micropores. They proposed that acquired osteoinductivity in the micropores of BCP scaffolds could be due to biological apatite formation along with coprecipitation of endogenous growth factors during the process thus stimulating osteoprogenitor cell chemotaxis and differentiation. It can be noted that multiscale porosity has a potential for improving osteointegration of the implants which still needs further investigation.

Lastly, it should be noted that although BMP-2 has been approved by FDA, its use in treatments for long term involves high expenses. Therefore, researchers focus on other agents that induce BMP-2 production by the host cells. For example, alendronate, one of the most common osteoporosis drug was found to stimulate the BMP-2 gene activation of adipose derived stem cells seeded onto PLGA scaffolds to which alendronate was injected for a period [2]. This property of alendronate has been shown previously on osteoblasts and MSCs. This approach can lower both the overall treatment budget and minimize unwanted side effects of the use of growth factors at high doses. Yet, there is no local controlled delivery system for this drug.

2.1.2 VEGF

Bone is a highly vascularized tissue. Insufficient bone vascularity leads to decreased bone formation and mass in disease/trauma conditions [44]. Therefore, angiogenic growth factors such as vascular endothelial growth factor (VEGF) have gained increasing attention due to its critical role in angiogenesis [45, 46]. VEGF

is a potent angiogenic growth factor and causes proliferation and migration of endothelial cells. In vivo half-life of VEGF is given as 50 min [47].

It was shown that apart from physiological angiogenesis, VEGF also plays a significant role in bone regeneration. VEGF indirectly induces proliferation and differentiation of osteoblasts by stimulating endothelial cells to produce osteoanabolic growth factors such as insulin-like growth factor I (IGF-1) and endothelin-1 (ET-1) [48] which causes chemotaxis [49] and differentiation of osteoblasts [46].

Vascularization is essential for nourishing the biomaterial implantation site with oxygen, nutrients, soluble factors, and osteoprogenitor cells and to ensure the removal of metabolites. Especially in large defects, the diffusion process of nutrients is limited by an effective distance of 150–200 μm from blood vessels [50]. Hence, bone regeneration strategies involving biomaterials should consider the issue of angiogenesis.

VEGF was shown to promote vascularization of polymer and calcium phosphate based bone substitute materials [51, 52]. The study of Kaigler et al. [52] reported that VEGF scaffolds had the ability to enhance neovascularization and bone regeneration in irradiated osseous defects using a mouse critical-sized segmental femur defect model. They demonstrated that combination therapy of human bone marrow stromal cells (hBMSC) and VEGF in porous poly(DL-lactic acid) (PLA) scaffolds resulted with significant bone regeneration in contrast to the PLA and PLA + hBMSC groups in a mouse critical-sized segmental femur defect model. The results suggest that this combination therapy can be considered for treatment of lost and damaged bone tissue of cancer patients after radiation treatment and resective surgery. Another group coated PLGA and alginate porous VEGF releasing scaffolds with Bioglass 45S (BG) (both osteoconductive and osteoinductive) to enhance bone regeneration and integration with the host tissue [34]. BG-coated scaffolds released roughly over 60% of their VEGF contents during 1st day and the rest over 2 weeks. BG at low concentrations in the coating showed angiogenic capacity alone both in vitro and in vivo by a proliferative effect on endothelial cells. However, it did not result any positive effect on the differentiation of human mesenchymal stem cells in vitro. It was observed that bone mineral density increased in BG-coated VEGF releasing scaffolds in comparison to BG-coated scaffolds in vivo with improved blood vessel density. In vivo results pointed the potentially additive effect of bioactive glass coating of a VEGF releasing system on angiogenesis and bone regeneration.

The burst release of high amounts of VEGF is not desired after biomaterial implantation since it increases vascular permeability, causes vessel leakage and induces the formation of non-functional blood vessels [53]. A recent study by Wernike et al. [54] showed that both mode and dose of local VEGF delivery are critical parameters controlling the efficacy of VEGF loaded implants in terms of proper vascularization and osteointegration. The group used biphasic calcium phosphate (BCP) ceramics to study the effect of dose and release kinetics of VEGF for bone regeneration in a critical size cranial defect. They coated BCP discs with VEGF (1 and 5 μg/ml) either by superficial adsorption or coprecipitation methods. With coprecipitation, a sustained delivery of VEGF with a minimized burst was

observed for both doses in comparison to superficial adsorption. In vivo investigations revealed that sustained release of VEGF mediated by osteoclast through their action on the scaffolds promoted a dose dependent biomaterial vascularization, osseointegration, and bone formation. On the other hand, short-term VEGF release following superficial adsorption resulted in a temporally restricted angiogenesis and did not enhance bone formation irrespective of the dose used.

Apart from use of angiogenic factors [51] or endothelial cells [5] incorporated in the scaffolds, prevascularization of the tissue engineered construct inside muscle tissue of the host is another alternative way of solving the problem of in vivo vascularization of implants [55, 56]. Tissue enginered bone flaps (TEBFs) prevascularized in muscle tissue are mostly used in mandibular reconstructions. Zhou et al. [56] incorporated rhBMP-2 in situ into both demineralized freeze-dried bone allograft (DFDBA) and coralline hydroxyapatite (CHA) carriers prior to implantation into ambilateral latissimus dorsi muscles of Rhesus monkeys inside titanium meshes. After the validation of ossification and vascularization of the implants by radiography, angiography and histology, the tissue engineered bone flaps were removed and reimplanted into segmental mandibular defects within the titanium meshes. It was shown that apart from successful ossification of the implant, the prevascularized bone flaps were connected to the host artery and had blood supply for cells populating the construct. For in vivo applications, the group observed mandibular reconstruction with bone regeneration in both prefabricated bone flaps and in situ rhBMP-2 incorporated CHA implants, but not in rhBMP-2 incorportated or free DFDBA implants. Although the procedure for prefabricated TEBFs is time-consuming and there is a need for two operations, promising results make it worthwhile for considering this procedure in cases where bone regeneration is limited (i.e. treating patients after radiotherapy and/or chemotherapy).

Polymeric multi-growth factor release scaffolds tailored to promote angiogenesis and osteogenesis are under evaluation for development to actively stimulate bone regeneration. Patel et al. [42] recently investigated the effects of combined delivery of VEGF and BMP-2 locally from biodegradable scaffolds on bone regeneration in a critical size cranial defect. The experimental group for in vivo applications consisted of both VEGF and BMP-2 loaded gelatin microparticles entrapped in porous poly(propylene fumarate) scaffolds. Single factor delivery and unloaded composite scaffolds were used as controls in this study. Highest amount of blood vessel formation was observed for VEGF releasing scaffold. However, there was no significant difference in the vascularization among all groups. The authors suggested that VEGF dose used could be not enough for proper vascularization. Highest bone formation was found for dual delivery system at week 4 and for both BMP-2 and dual delivery systems at week 12. Additionally, complete union of the defect was observed at five out of eight rats for the dual delivery group while BMP-2 showed this result in only three out of eight rats. All of these results point that there is a synergistic effect of the dual delivery of VEGF and BMP-2 for early bone formation. It can be concluded that for the doses used in this study, VEGF does not affect the bone formation by BMP-2 directly and dual delivery of these two growth factors enhances bone bridging and defect union.

During normal bone healing, it has been shown that VEGF expression to peak in the early days while BMP expression was observed in the later following days [57–59]. Local delivery systems which provide the sequential release of these growth factors in the order of VEGF followed by BMP-2 would enhance BMP-2 induced bone regeneration. For this purpose, Kempen et al. (2009) prepared a composite delivery system consisting of BMP-2 loaded PLGA microspheres embedded in a poly(propylene) scaffold surrounded by a gelatin hydogel loaded with VEGF. This delivery system provided the initial release of VEGF followed by BMP-2. The group investigated the in vitro and in vivo release profiles single and dual composite delivery systems of VEGF and BMP2 and their effects on ectopic and orthotopic bone formation and angiogenesis in Sprague–Dawley rats. As expected, the scaffolds exhibited a large initial burst release of VEGF from the hydrogel compartment within the first 3 days and a sustained release of BMP-2 over 56-day post-implantation period. It was shown that VEGF in combination with BMP-2 enhanced ectopic bone formation compared to its single use or BMP-2's single use. Analysis of orthotropic bone formations revealed that most of VEGF/BMP-2 composite scaffolds showed circumferential cortical regeneration (Fig. 2a) with no significant quantitative differences between these groups (Fig. 2b). As seen in the figure no unions were observed for control groups (unfilled defect and empty scaffold) and VEGF loaded scaffolds. This work demonstrates that a sequential angiogenic and osteogenic growth release preferably with a more prolonged VEGF delivery from a multifunctional composite scaffold has potential in the enhancement of bone regeneration.

2.1.3 FGF

Basic fibroblast growth factor (bFGF) is one of the important growth factors for tissue regeneration and has various clinical and pharmaceutical applications owing to its pleiotrophic potential in various tissues/organs [60]. This growth factor has been shown to have important roles in osteoblast development, bone formation and vascularization. It is noted as the product of an early induced gene following mechanical stress for inducing osteogenesis and proliferation of osteogenic cells [61]. Furthermore, it has been found that this factor is highly expressed by osteoblast and mesenchymal cells for callus formation during distraction phase which was attenuated after maturation of newly formed bone [62]. Marie [63] has presented that FGF-2 has taken significant role in gene expression related with bone formation starting from MSC replication and differentiation into osteoprogenitor cells, followed by formation of mature osteoblasts and their bone matrix production and ended up in apoptosis of the osteoblasts. Marie has also concluded that the effect of FGF-2 on apoptosis is related with the differentiation stage. While it may cause reduction of apoptosis in immature osteblasts (favouring proliferation), continous signalling may promote apoptosis in more mature osteoblasts in the same population. This opposite effect depending on the maturation state of cells suggests that it should not be aimed to deliver FGF-2 from bone scaffolds for

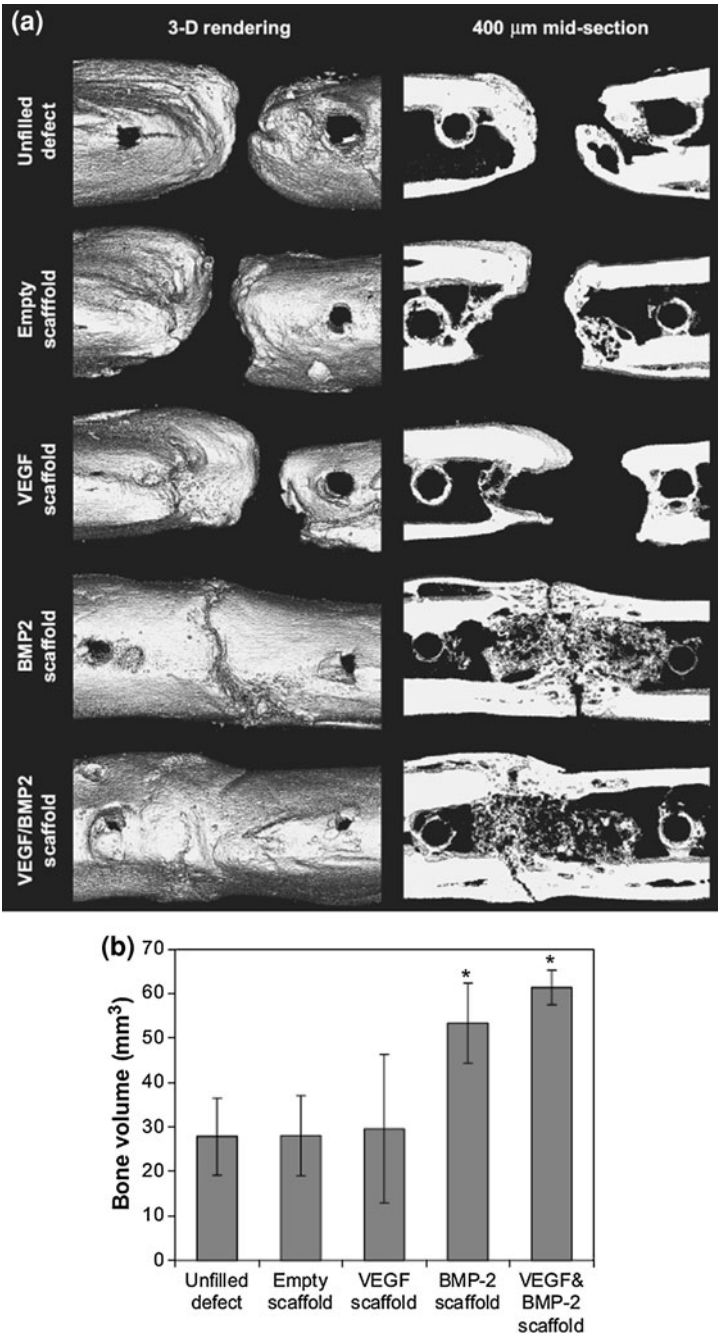

Fig. 2 Analysis of bone formation in the 5 mm critical size femoral defect model. **a** Three-dimensional μCT and 400 μm central slices of the composites in the bone defect. **b** Quantification of the bone volume in the 6 mm section between the two middle K-wires (*denotes significant difference from non-BMP-2-loaded implants at $p < 0.001$) [114] (with the permission from Elsevier)

long periods, but should be delivered in the acute phase of regeneration. Furthermore, Nakamura et al. [64] showed that FGF-2 (at low doses; 1 or 10 ng) increased ectopic bone formation induced by BMP-2 carrying collagen sponges, but had opposite effect (inhibitory effect) at high doses (100 ng or greater). Similarly, Tsurushima et al. [65] have studied HA ceramics coated with low or high doses of FGF-2. Different proliferation trend was observed with high and low doses of FGF2 in the two cell lines used in their study. While proliferation of fibroblastic cells increased with increasing dose, the proliferation of osteoblast cells decreased. Thus, it was suggested that the FGF-2 concentration must be within a certain range to stimulate osteoblast cells. Considering the importance of control over the dose of FGF-2, transfection of bone marrow mesenchymal stem cells (BMMSCs) with bFGF gene has been applied for distraction osteogenesis (endogeneous bone tissue engineering) to provide growth factors at adequate amounts to required by the target cells. The cells were suggested as a local delivery system for promoting bone regeneration after distraction. In vivo results demonstrated more effective enhancement of bone regeneration with these cells compared to untransfected BMMSCs [66].

Recently, polyphosphates (polyP, linear polymers of orthophosphate residues) have been suggested to enhance the effects of bFGF on osteogenic cells. In accordance with other studies, bFGF at low dose (1 ng/ml) together with polyP caused higher induction of cell proliferation and ALP activity compared with their single uses and controls. The effect of only FGF on cell proliferation was also in accordance with the expectations but for ALP activity, results were confusing where bFGF alone inhibited ALP activity during the entire observation period. The Poly-P and bFGF modified porous HA complexes were also evaluated in vivo. The combination group again had significantly higher bone formation compared to other groups. Single use of bFGF in vivo was again not very different from control and PolyP treated group for new bone formation. The authors suggested that these results were related with short in vivo half life of FGF, which might be extended by PolyP [67].

It has been shown that one of the most important parameters that should be taken into account is the release kinetic of FGF-2 from the carrier. A carrier that degrades slowly is expected to sustain the relase f the agents, thus extending the effective period of the growth factors. FGF-2 release from poly(2-hydroxyethyl methacrylate)-N-vinyl,2-pyrrolidone copolymer, p(HEMA-co-VP) showed the anabolic effect of FGF-2 release on bone mass following 2 months postimplantation to the rabbit femoral condyle defects. However, at 3-month period no difference from the control was observed. This result was corrrelated with release kinetic from the hydrogel providing the growth factor for about 2 months post surgery. They have also presented that the FGF-2 local delivery facilitated the bone regeneration at the edge of the defect [68].

Recent studies focus on conjugation of the bioactive agents into-onto scaffolds for delaying their release and presenting them for a longer period to the bone microenvironment [65]. In one such study, FGF-2 was coated to the surface of hydroxyapaptite ceramics to enhance bone healing.

2.1.4 PDGF

Platelet derived growth factor, (PDGF), has been shown to have strong potential in promoting alveolar and gingival bone cementum regeneration in various studies [69]. It was also shown to promote proliferation and recruitment of both periodontal ligament and bone cells in vitro [70]. In non-human primates, the role of PDGF-BB for enhancing periodontal regeneration was also documented [71]. It was also used in bone defect fill in human clinical trials [72, 73]. Yet, it has been approved by FDA only for use in diabetic foot ulcers. Despite its potential on bone regeneration, due to very short half life in biological systems (2 min) and requirement of high or repeated doses, it has to be delivered by controlled release systems and related approaches. In order to achieve local high concentration of PDGF, Zhang et al. [74] have loaded PDGF gene rather than protein itself into the chitosan/coral carrier to be used in periodontal ligament repair. They showed the efficiency of this approach by significantly higher amount of PDGF protein product and proliferation of periodontal ligament cells in PDGF gene activated scaffolds compared with cell seeded coral scaffolds free of PDGF gene up to 18 days.

Dual release of VEGF and PDGF from brushite–chitosan systems was obtained with different rates for the growth factors to mimic natural regeneration process in bone tissue [47]. To achive this outcome, VEGF loaded alginate carriers were prepared and added to chitosan scaffolds. This complex was then mixed with the brushite paste (either involving PDGF or not) before setting to final form. By this system, PDGF which is suggested to be required for the initial phase of healing (first 3 days of bone repair) could be released faster (70% in 1st week) compared to VEGF (60% in 2 weeks). In case of VEGF normal physiological release was given to peak at 5–10 days (in rats). This novel delivery system was shown to increase bone formation in only PDGF containing scaffolds. However, the combined use also augmented the appearance of new bone tissue and fast vessel maturation in comparison to the PDGF alone.

2.2 Statins

Statins are cholesterol-lowering drugs that inhibit 3-hydroxy-3-methylglutaryl-coenzyme A (HMG-CoA) reductase in the mevalonate pathway [75]. Mundy et al. [76] first reported that statins induce mRNA expression of BMP-2 in osteoblasts in vitro. Since then, there are many in vitro and in vivo studies reporting that statins promote osteoblast differentiation and bone formation [77, 78]. The findings about the positive effect of statins on bone formation after administering orally [79, 80] or subcutaneously [81] have also generated interest among researchers in their possible use for developing new strategies in effective bone healing. Administration of statins locally to bone sites were reported as an alternative to growth factor treatment of bone defects [82]. The group injected different doses of fluvastatin (3–300 μg) in propylene glycol alginate vehicle gel into the tibia of rats

just before insertion of titanium implants. Their hypothesis was that fluvastatin administered locally would enhance peri-implant osteogenesis and improve implant osteointegration in the rat model. Delay in calcification of peri-implant bone at week 1 was observed only for the highest dose of fluvastatin. However, at weeks 2 and 4 no significant dose dependent differences were observed among treatment groups. The medullary canal was filled with abundant trabeculae in all these groups. The push test results supported the histomorphometric findings. The study showed that topical application of fluvastatin improved the initial fixation of the implants by promoting the formation of mineralized tissue around the implant. There are also researchers thinking that the prolonged bioavability of these factors at treatment sites is necessary to allow sufficient time to migrate to the defect site, populate and differentiate to form a new tissue. The prolonged bioavability can be achieved with the design of slow releasing delivery systems for statins. There are many studies focusing on the design of controlled delivery systems for statins. The burst release of the drug is not also desired for possible cytotoxicity of high doses since it has lowering effect on cholesterol synthesis. Benoit et al. [83] synthesized a fluvastatin-releasing macromer to prepare a sustained delivery system. They grafted hydrolytically degradable lactic acid linkages from PEG macromers and then conjugated fluvastatin covalently onto the synthesized macromer to obtain fluvastatin releasing hydrogel. The hydrolysis of lactic acid esters resulted with the release of fluvastatin from the macromer. The control over the fluvastatin release was achieved by changing the length of lactic acid linkers. In vitro studies showed that the released fluvastatin induced osteogenic differentiation of human mesenchymal stem cells (hMSC) and modulated their function (an increase BMP-2 production and mineralization).

Tanigo et al. [84] prepared a gelatin hydrogel delivery system for another hydrophobic statin, namely simvastatin. The group discussed that the choice of gelatin hydrogel as delivery system was based on the biodegradability and biocompatibility issues related with the other polymeric carrier. They first water solubilized simvastatin by entrapping in L-lactic acid oligomer-grafted gelatin micelles which were then immobilized in the matrix of gelatin hydrogels. The release of simvastatin from the delivery system depended on the degradation of the hydrogel which in turn was related with the degree of gelatin crosslinking with glutaraldehyde. In vitro studies showed that simvastatin release from micelles induced BMP-2 production of MC3T3-E1 cells. A rabbit model of tooth extraction was also used to evaluate the bone regeneration potential of gelatin hydrogels with incorporated statin micelles. Radiological and histological results showed that among the simvastatin doses (0, 1, 10 and 67 μg/site) very little bone regeneration was observed for highest simvastain dose 5 weeks after treatment. On the other hand, hydrogels with 1 and 10 μg simvastatin micelles augmented bone regeneration.

In a recent study by Monjo et al. [85] collagen sponges were evaluated as carrier for a hydrophilic statin named rosuvastatin in critical size cortical bone defects in rabbit tibia. Collagen sponges were soaked in different doses of rosuvastatin (0, 0.1, 0.5 and 2.5 mg/ml). As expected, the collagen hydrogels released their contents within 24 h in vitro. They placed collagen sponges with or without

rosuvastatin into bone marrow and fixed with coin shaped titanium implants. In the study, they reported that released rosuvastatin from collagen carriers increased mRNA levels of BMP-2 and ALP activity in the cortical tissue attached to the implant in a dose-dependent manner. The group observed a slight delay in bone formation at the highest rosuvastation dose in agreement with the work of Tanigo et al. [84]. On the other hand, an increased BMP-2 expression was reported for the highest statin dose.

Masuzaki et al. [86] used an injectable system with fluvastatin loaded PLGA microspheres administrated to the back of rats with single subcutaneous injection to enhance osteointegration of titanium implants in the tibia. Their argument point was that by this way they minimized the possibility of implant surface contamination and the risk of losing microspheres from the defect site due to blood flow by this approach. A sustained in vitro release was observed from PLGA microspheres (Fig. 3). The bone contact ratio and bone volume in the marrow of statin groups were higher than those of the nonstatin groups at weeks 2 and 4. The differences observed between statin and nonstatin groups at week 4 was nonsignificant suggesting that bone regeneration reaches a plateau at this time period. However, at week 4, it was observed that statin containing groups (Fig. 4c, d) had larger occupation of medullary canal with trabeculae than non-statin groups (Fig. 4a, b). Similarly, the bending tests revealed that single percutanous injection of the microspheres increased the static bone strength. These results suggest that an easily administered microsphere delivery system might be used as a stimulator for improved osteointegration of bone implants.

Statins hold promise for the bone regeneration. However, like growth factors, their dose to be used, best release profile, ideal carrier materials for local delivery still need to be investigated before these bioactive agents can be used solely for bone regeneration.

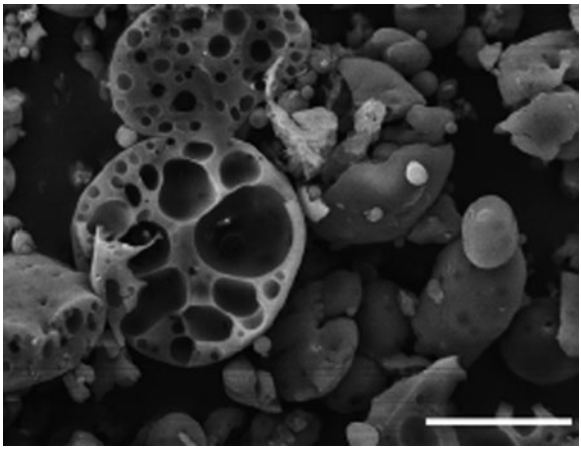

Fig. 3 Scanning electron microscopy ımage of fluvastatin impregnated PLGA microspheres. Bar = 20 μm. [86] (with the permission from Elsevier)

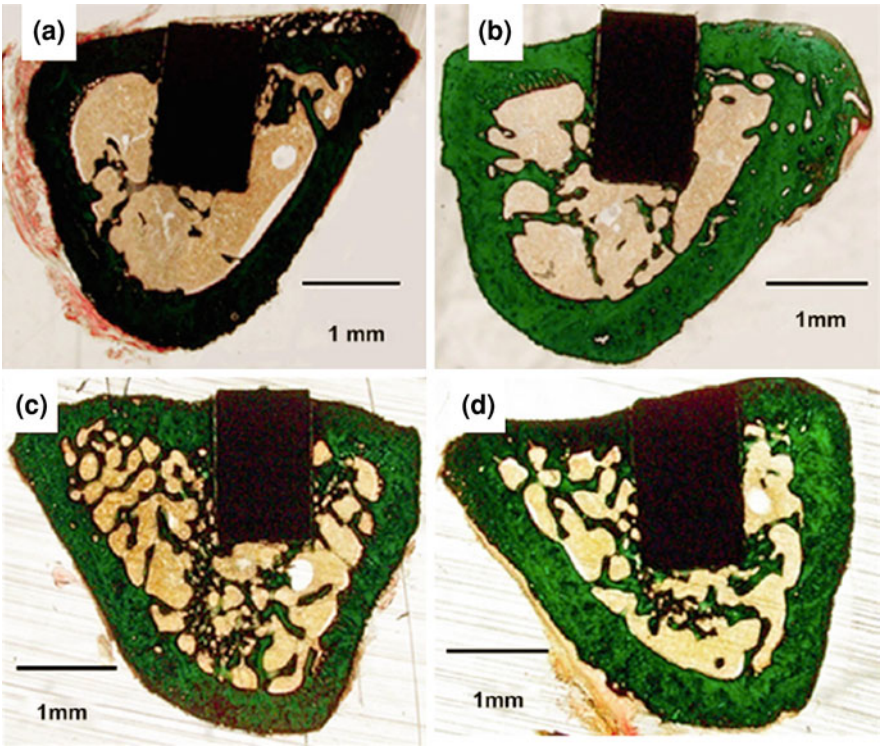

Fig. 4 Histological appearances of bone sections at 4 weeks after implantation with titanium. **a** Control group: percutaneous injection of saline, **b** PLGA microspheres only group, **c** PLGA microspheres carrying 0.5 mg/kg fluvastatin group, **d** PLGA microspheres carrying 1.0 mg/kg fluvastatin group. Statin containg groups, groups **c** and **d**, had larger occupation of medullary canal with trabeculae than non-statin groups (**a**, **b**) (Masson–Goldner staining) [86]. (with the permission from Elsevier)

2.3 Antibiotics

A scaffold with local antibiotic delivery property is an ideal approach for successive results in implant application to bone defects. Antibiotic use is necessary for preventing infection during orthopaedic operations related with osteoctomy for carcinogenic diseases and for treatment of an already occuring osteomyelitis or for relapses. Although systemic antibiotic treatments for long periods (4–6 weeks) may be applicable, especially in the case of osteomyelitis, mostly they result with inefficient treatment owing to bacterial bio-film at the site which creates a barrier against blood route defenses (cellular or therapeutic). In addition to these handicaps, long term systemic antibiotic may also cause unwanted side effects in susceptible tissues and organs like liver and kidneys. Another reason for failure of such long term systemic treatment might be related with the development of resistance against antibiotics. In some cases, increases in

the minimum inhibitory concentrations (MIC) of the bacteria to many hundreds folds of their normal values have been reported owing to reduced metabolic activity of the bacteria [87]. Besides these, even after a successive treatment, chronic osteomyelitis can show relapse after very longer times. Therefore, a local sustained antibiotic delivery system would be favourable for long term control of the disease at the site of infection. Such a delivery system can provide higher doses of antibiotic for longer terms than systemic routes without causing side effects.

One major step in treatment of osteomyelitis is the surgical debridement of the necrotic tissue [88]. Removal of the sequestrum (dead and infected bone that has detached from the bone and surrounded by avascular soft tissue) thus generate a dead space at the site of infection with remaining microorganisms still invading the surrounding healthy bone. As a result of the clinical outcomes, local antibiotic treatment strategies have been investigated and started with application of gentamycin loaded PMMA (polymethyl methacrylate) cements and beads [87, 89]. The PMMA based systems, however, are nondegradable in vivo, thereby requiring second surgery after delivering the antibiotic [90]. Recent approaches aim to combine treatment of osteomyelitis with antibiotic delivery and regeneration of the surgical site by providing biodegradable-bioresorbable scaffolds. These types of bone scaffolds generaly involve calcium phosphates, natural or synthetic biodegradable polymers and their composites. Despite advantageous properties of the calcium phosphates like osteoconductivity and biocompatibility, they often fail in complete regeneration of the bone due to their slow absorption in vivo and incomplete conversion to the natural bone minerals. HA carriers usually exhibit low initial drug loading and show fast antibiotic release profiles. Antibiotic loaded bone cements as well as fillers, films and coatings were reviewed by Zilberman and Elsner [91].

In a recent study, Chai et al. [92] have addressed this problem and provided a solution by cold plasma treatment of the carrier to enhance attachment and retention of antibiotic within HA. They presented efficient binding of vancomycin to microporous HA treated with He/NH_3 (100%) or He/NH_3-oxygen (50%). They have also concluded that this method could extent the bioactive agent release period (up to 5 days). This new way of increasing loading efficiency and bioeffectiveness period of antibiotic loaded to microporous HA carriers might be developed or applied to other bioactive agents to increase success of the implants.

Natural polymers used for local delivery of antibiotics to bone involve collagen, gelatin, chitosan, etc. [93]. Collagen sheets carrying gentamycin were prepared and used in clinic with successive infection control rates in osteomyelitis treatment. Unfortunately, these carriers were able to sustain the antibiotic release up to weeks. Chitosan microspheres loaded with vancomycin have been shown to be more effective in decreasing the local number of colony forming units of bacteria than intramuscular injection of the antibiotic upon 3-week treatment of experimental osteomyelitis (Fig. 5) [93].

Synthetic biodegradable polymers, on the other hand, can control the antibiotic release for extended periods up to months. They are more pliable and more resistant in harsh preparation conditions compared to natural ones. They do not

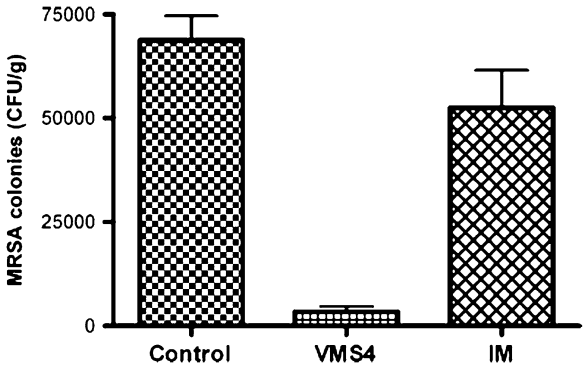

Fig. 5 Average methicillin-resistant *Staphylococcus aureus* (MRSA) colonies per gram of bone sample after 21-day treatment ($n = 8$) following experimental osteomyelitis in rats. Control group had sterile blank microspheres, VMS4 group had vancomycin loaded chitosan microspheres, IM group had daily intramuscular injection of vancomycin [93] (with the permission from Elsevier)

require second surgery after treatment [90] and are versatile to give required properties for a bone scaffold. Polyurethane is an example for such biodegradable polymers used in vancomycin delivery system for treatment of experimental osteomyelitis. This sytem has been shown to be comparable with current clinical standard, PMMA-gentamycin beads, for in vivo drug (vancomycin-base form) delivery [94]. However, other than inhibiting infection, this new system has not aimed to regenerate the segmental bone defect in the study model. Pillai et al. [95] also used a synthetic polymer for a penicillin type (nafcillin) antibiotic. These PLGA carrier system, however, was different from the carriers studied for osteomyelitis so far with being in nanoparticle form to target bacteria within the osteoblast cells. This interesting study was notable for pointing a reason for unsuccessive outcomes of osteomyelitis despite antibiotic treatments (local or systemic) and its recuring after long periods. The nanoparticles were succesful in killing or reducing intracellular bacteria within short periods. This important study has demonstrated that, an intracellular bacteria targeting sytem together with long term antibiotic delivery strategy should be developed to eliminate recurrence potential of osteomyelitis.

Liu et al. [13] have investigated the in vitro release properties of cylindrical (8 mm diameter) in PLGA capsules loaded with antibiotic within the capsule part and involving the growth factor (rhBPM-2) in the core of the capsule. The delivery system was designed to provide simultaneous antibiotic and growth factor release for osteomyelitis treatment besides supplying bioactive agnets to debrided bone tissue for regeneration. Their carrier system was effective for extending the release of both bioactive agents while retaining their activity throughout this period under in vitro conditions.

Other than these, materials like bioactive glasses have been studied for antibiotic delivery by many researchers. Xie et al. [96] have investigated the efficacy of vancomycin carrying borate glass implants. When they compared this system

with vancomycin-calcium sulfate implants, they have found superior results in borate glass groups compared to untreated and calcium sulfate carrier groups. Both antibiotic loaded implants were found successive in treating chronic osteomyelitis at the end of 8 weeks. While most of the borate glass implants have been reabsorbed, almost all calcium sulfate implants were found to be reabsorbed by radiological and histological studies. However, histological examination of the implant sites showed that vancomycin loaded borate glass group was either surrounded or replaced with the new bone tissue comparably more than vancomycin carrying calcium sulfates. Borate glass was also suggested as more biocompatible than calcium sulfate according to presence of foam cells around the implants [96]. One important observation in this study was that initial vancomycin release from calcium sulfate carriers was faster compared to borate glass in in vivo. However, the in vitro release of drug from calcium sulfate carriers was slower than that from borate glass. It was suggested that borate glass was better in bone regeneration compared to commonly used silicate bioactive glasses [97, 98].

In many studies for combining favoured properties like osteoconductivity, biocompatibility, biodegradability/bioabsorbability and control over release of bioactive agents scientists have used composites mostly of a polymer and bioceramic/bioglass. Borate glass-chitosan pellets with the antibiotic teicoplanin is a recent example of these composites. The composites could provide a sustained release of the effective local antibiotic concentration over 3–4 weeks while supporting new bone formation on the surface and within the implants via conversion of borate glass to HA-like structures in in vivo conditions (Fig. 6) [99].

Polymers, inspite of all preferable material charactistics, are not good as bone conductors, and therefore, mostly applied together with an osteoconductive material. Gatifloxacine loaded PCL (polycaprolactone, 10 kDa)-βTCP (tricalciumphosphate) implants were shown to be effective in controlling infection and supporting bone reconstruction in an experimental osteomyelitis study [88].

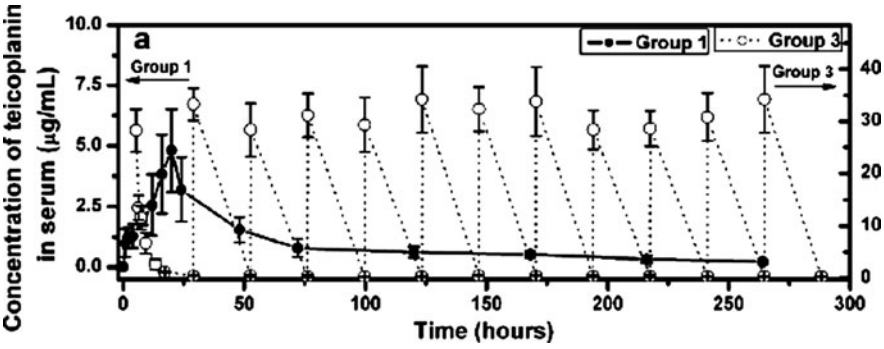

Fig. 6 Serum concentration of teicoplanin in rabbits treated by implantation teicoplanin loaded borate bioactive glass and chitosan (TBGC) (8 wt% teicoplanin) pellets (Group 1), and by intravenous injection of teicoplanin (Group 3) [99] (with the permission from Elsevier)

In another study, gentamycin sulfate carrying PLA-TCP(25%)-HA(75%) composites were prepared and investigated for antibiotic release properties either without coating or by coating with polymer (PLGA or PLA). Their results showed fast in vivo release of the antibiotic (95% in 1 week) for uncoated and PLGA coated implants. The third group (PLA coated), however, could extend the antibiotic release up to 4 weeks. This group was also found to provide ten times of the concentration of MIC for gentamycin against the most common microorganism causing osteomyelitis. They have suggested that this would be important as it gives approximately the minimum bactericidal concentration (MBC) value, thus suggesting potential of total elimination of these bacteria at the site of infection rather than inhibition of their growth. PLA coated group was also found succesful in terms of bone integration and presented with high bone repair outcomes. PLGA coated and uncoated groups have fragmented and could not be observed for total period of the study (20 weeks) [90].

Other major drawbacks for the use of polymers alone as bone implant are their low mechanical strength and stability especially in the physiological environment. Although a similar problem has also been suggested with calcium phospate ceramics, it is possible to overcome with low porosity formulations of these materials. Mesoporous (2–50 nm pore sized) silica-HA composites have been studied as carrier of antibiotics and components of polymer matrix for bone repair [100]. These composite scaffolds were found to be effective in slowing down the antibiotic release (up to 30 days), enhancing bioactivity, and compensating with the pH change that occur due to PLGA degradation. These scaffolds also enhanced mechanical properties and provided suitable surface for attachment and proliferation of mesenchymal stem cells. However, this sytem has not been evaluated for in vivo performance. Although presence of small pores are required for controlling the drug release and degradation rate of the system (besides improving mechanical properties) many researchers also focus on the importance of interconnected macroporous networks for enabling bone cell growth and vascularization within the implant [45, 101]. However, pores are known to make the materials sensitive to tensile forces and macroporous scaffolds are expected to yield easier under tension rather than compression. Therefore, composites with polymeric matrices might provide a solution for these types of forces.

For osteomyelitis treatment involving debridement of the infected bone tissue, bone regeneration aim has been mostly addressed by using osteoconductive and/or osteoinductive materials like CaPs or collagens scaffold. So far, a few researchers [13] have studied and suggested using dual loading and release of an osteoinductive agent (like growth factor) together with antibiotics. In accordance with this approach, Zilberman [102] has designed and investigated a novel bioresorbable composite fiber that can carry the dual release function for a drug (located in the shell) and protein (located in the core) combination. These fibers were also shown to have good mechanical properties making them usable for engineering new scaffolds. Hence, these types of implants could achieve better treatment plus regeneration in bone tissue.

3 Conclusion and Future Directions

Bone, as a natural composite structure, is a complex, dynamic tissue that responds to environmental (physical), hormonal and growth related changes of the body via structural modifications. As the rate of anabolic events decrease with age regeneration of the bone tissue becomes more difficult in trauma or disease conditions. Therefore, to help with the restoration of the bone, local, external supports as medications, growth factors, cells and scaffolds are needed.

Scientists are after developing multifunctional scaffolds (serving dual purposes as cell support and bioactive delivery system) for treatment of severe bone losses due to trauma, infectitious or other bone related diseases. Although current clinical collagen-based BMP delivery systems have promising results, optimization of new biomaterial designs for prolonged delivery with a predicted in vivo release profile that matches the natural bone regeneration as well as efficient loading of this growth factor family still remain challenge. Recent findings all agree that the prolonged bioavailability of the single or multiple bioactive molecule(s) with sustained release together with osteoconductive carrier and/or stem cells is the key factor affecting the outcome. For multiple factor delivery systems, new methods are being developed to control the release rate and order of release of these biomolecules for mimicking the physiological environment of the cells. Recent progresses in the research towards all of these goals hold promise. Moreover, the positive effects of alendronate and statins have been documented on bone regeneration. Yet, there is still need for further investigations to develop other carrier systems for BMPs and/or other candidate bioactive agents that can be used clinically.

The scaffolds studied for treatment of osteomyelitis disease compared with conventional systemic antibiotic therapies are definetely more sucessful but they are not that succesful in restoring mineralized, vascularized, organic, composite bone arhitecture. Therefore, more novel methodologies with combination of growth factors should be developed considering the repair/regeneration rate of bone tissue.

Here, a part of the route to bone regeneration has been evaluated with the question still remaining: how far are we from the end of the route?

References

1. Cancedda, R., Giannoni, P., Mastrogiacomo, M.: A tissue engineering approach to bone repair in large animal models and in clinical practice. Biomaterials **28**, 4240–4250 (2007). doi:10.016/j.biomaterials.2007.06.023
2. Wang, C.Z., Chen, S.M., Chen, C.H., Wang, C.K., Wang, G.J., Chang, J.K., Ho, M.L.: The effect of the local delivery of alendronate on human adipose derived stem cell-based bone regeneration. Biomaterials (in press) 1–10 (2010). doi:10.1016/J.biomaterials.2010.07.096

3. Damien, C.J., Parsons, J.R.: Bone graft and bone graft substitutes: A review of current technology and applications. J. Appl. Biomater. **2**, 187–208 (1991). doi:10.1002/jab.770020307
4. Kanczler, J.M., Ginty, P.J., Barry, J.J.A., Clarke, N.M.P., Howdle, S.M., Shakesheff, K.M., Oreffo, R.O.C.: The effect of mesenchymal populations and vascular endothelial growth factor delivered from biodegradable polymer scaffolds on bone formation. Biomaterials **29**, 1892–1900 (2008). doi:10.1016/j.biomaterials.2007.12.031
5. Tan, H., Yang, B., Duan, X., Wang, F., Zhang, Y., Jin, X., Dai, G., Yang, L.: The promotion of the vascularization of decalcified bone matrix in vivo by rabbit bone marrow monunuclear cell-derived endothelial cells. Biomaterials **30**, 3560–3566 (2009). doi:10.1016/j.biomaterials.2009.03.029
6. McKay, W.F., Peckham, S.M., Badura, J.M.: A comprehensive clinical review of recombinant human bone morphogenetic protein-2 (INFUSE_bone graft). Int. Orthop. **31**, 729–734 (2007). doi:10.1007/s00264-007-0418-6
7. Kanczler, J.M., Oreffo, R.O.: Osteogenesis and angiogenesis: the potential for engineering bone. Eur. Cell. Mater. 15, 100–114 (2008). http://www.ecmjournal.org/journal/papers/vol015/pdf/v015a08.pdf. Accessed 2 May 2008
8. Wang, C.K., Ho, M.L., Wang, G.J., Chang, J.K., Chen, C.H., Fu, Y.C., Fu, H.H.: Controlled release of rhBMP-2 carriers in the regeneration of osteonecrotic bone. Biomaterials **30**, 4178–4186 (2009). doi:10.1016/j.biomaterials.2009.04.029
9. Burastero, G., Scarfi, S., Ferrais, C., Fresia, C., Sessarego, N., Fruscione, F., Monetti, F., Scarfo, F., Schupbach, P., Podesta, M., Grappiolo, G., Zocchi, E.: The association of human mesenchymal stem cells with BMP-7 improves bone regeneration of critical-size segmental bone defects in athymic rats. Bone **47**, 117–126 (2010)
10. Kempen, D.H.R., Lu, L., Hefferan, T.E., Creemers, L.B., Maran, A., Classic, K.L., Dhert, W.J.A., Yaszemski, M.J.: Retention of in vitro and in vivo BMP-2 bioactivities in sustained delivery vehicles for bone tissue engineering. Biomaterials **29**, 3245–3252 (2008). doi:10.1016/j.biomaterials.2008.04.031
11. Duel, T.F., Chang, Y.: Growth factors. In: Lanzo, R., Langer, R., Vacanti, J.P. (eds.) Principles of Tissue Engineering, 3rd edn. Elsevier Academic Press, Burlington (2007)
12. Chen, F.M., Zhang, M., Wu, Z.F.: Toward delivery of multiple growth factors in tissue engineering. Biomaterials **31**, 6279–6308 (2010). doi:10.1016/j.biomaterials.2010.04.053
13. Liu, S.J., Chi, P.S., Lin, S.S., Ueng, S.W.N., Chan, E.C., Chen, J.K.: Novel solvent-free fabrication of biodegradable poly-lactic-glycolic acid (PLGA) capsules for antibiotics and rhBMP-2 delivery. Int. J. Pharm. **330**, 45–53 (2007). doi:10.1016/j.ijpharm.2006.08.036
14. Zhao, Y., Zhang, J., Wang, X., Chen, B., Xiao, Z., Shi, C., Wei, Z., Hou, X., Wang, Q., Dai, J.: The osteogenic effect of bone morphogenetic protein-2 on the collagen scaffold conjugated with antibodies. J. Cont. Rel. **141**, 30–37 (2010). doi:10.1016/j.conrel.2009.06.032
15. Luginbuehl, V., Meinel, L., Merkle, H.P., Gander, B.: Localized delivery of growth factors for bone repair. Eur. J. Pharm. Biopharm. **58**, 197–208 (2004). doi:10.1016/j.ejpb.2004.03.004
16. Basmanav, F.B., Kose, G.T., Hasirci, V.: Sequential growth factor delivery from complexed microspheres for bone tissue engineering. Biomaterials **29**, 4195–4204 (2008). doi:10.1016/j.biomaterials.2008.07.017
17. Jeon, O., Song, S.J., Yang, H.S., Bhang, S.H., Kang, S.W., Sung, M.A., Lee, J.H., Kim, B.S.: Long-term delivery enhances in vivo osteogenic efficacy of bone morphogenetic protein-2 compared to short-term delivery. Biochim. Biophys. Res. Commun. **369**, 774–780 (2008). doi:10.1016/j.bbrc.2008.02.099
18. Zhang, S., Doschak, M.R., Uludağ, H.: Pharmokinetics and bone formation by BMP-2 entrapped in polyethylimine-coated albumin nanoparticles. Biomaterials **3**, 5143–5155 (2009). doi:10.1016/j.biomaterials.2009.05.060
19. Wang, X., Wenk, E., Zhang, X., Meinel, L., Vunjak-Novakovic, G., Kaplan, D.L.: Growth factor gradients via microsphere delivery in bioplymer scaffolds for ostechondral tissue engineering. J. Cont. Rel. **134**, 81–90 (2009). doi:10.1016/jconrel.2008.10.021

20. Lan Levengood, S.K., Polak, S.J., Poellmann, M.J., Hoelzle, D.J., Maki, A.J., Clark, S.G., Wheeler, M.B., Johnson, A.J.W.: The effect of BMP-2 on micro- and macroscale osteointegration of biphasic calcium phosphate scaffolds with multiscale porosity. Acta Biomater. **6**, 3283–3291 (2010). doi:10.016/j.actbio.2010.02.026
21. Reddi, A.H.: Role of morphogenetic proteins in skeletal tissue engineering and regeneration. Nat. Biotech. **16**, 247–252 (1998). doi:10.1038/nbt0398-247
22. Reddi, A.H.: BMPs: from bone morphogenetic proteins to body morphogenetic proteins. Cytokine Growth Factor Rev. **16**, 249–250 (2005). doi:10.1016/j.cytogfr.2005.04.003
23. Chen, B., Lin, H., Wang, J., Zhao, Y., Wang, B., Zhao, W., Sun, W., Dai, J.: Homogenous osteogenesis and bone regeneration by demineralized bone matrix loading with collagen-targetting bone morphogenetic protein-2. Biomaterials **28**, 1027–1035 (2007). doi:10.1016/j.biomaterials.2006.10.013
24. Jones, A.L., Bucholz, R.W., Bosse, M.J., Mırza, S.K., Lyon, T.R., Webb, L.X., Pollak, A.N., Golden, J.D., Valentın-Opran, A.: Recombinant human BMP-2 and allograft compared with autogenous bone graft for reconstruction of diaphyseal tibial fractures with cortical defects: a randomized, controlled trial. J. Bone Joint Surg. **88A**, 1431–1441 (2006). doi:10.2106/JBJS.E.00381
25. Calori, G.M., Tagliabue, L., Gala, L., d'Imporzano, M., Peretti, G., Albisetti, W.: Injured application of rhBMP-7 and platelet-rich plasma in the treatment of long bone non-unions: A prospective randomised clinical study on 120 patients. Injury **39**, 1391–1402 (2008). doi:10.1016/j.injury.2008.08.011
26. Keskin, D.S., Tezcaner, A., Korkusuz, P., Korkusuz, F., Hasırcı, V.: Collagen–chondroitin sulfate-based PLLA–SAIB-coated rhBMP-2 delivery system for bone repair. Biomaterials **26**, 4023–4034 (2005). doi:10.1016/j.biomaterials.2004.09.063
27. Patel, Z.S., Yamamoto, M., Ueda, H., Tabata, Y., Mikos, A.G.: Biodegradable gelatin microparticles as delivery systems for the controlled release of bone morphogenetic protein-2. Acta. Biomater. **4**, 1126–1138 (2008). doi:10.1016/j.actbio.2008.04.002
28. Li, B., Yoshii, T., Hafeman, A.E., Nyman, J.S., Wenke, J.C., Guelcher, S.A.: The effects of rhBMP-2 released from biodegradable poyurethane/microsphere composite scaffolds on new bone formation in rat femora. Biomaterials **30**, 6768–6779 (2009). doi:10.1016/j.biomaterials.2009.08.038
29. Shen, H., Hu, X., Yang, F., Bei, J., Wang, S.: An injectable scaffold: rhBMP-2-loaded poly(lactide-co-glycolide)/hydroxyapatite composite microspheres. Acta. Biomater. **6**, 455–465 (2010). doi:10.1016/j.biomaterials.2009.02.004
30. Choi, D.H., Park, C.H., Kim, I.H., Chun, H.J., Park, K., Han, D.K.: Fabrication of core-shell microcapsules using PLGA and alginate for dual growth factor delivery system. J. Cont. Rel. (2010). doi: 10.1016/j.conrel.2010.0.103
31. Cook, S.D., Salkeld, S.L., Patron, L.P., Barrack, R.L.: The effect of demineralized bone matrix gel on bone ingrowth and fixation of porous implants. J. Arthroplasty **17**, 402–408 (2002). doi:10.1054/arth.2002.32169
32. Chakkalakal, D.A., Strates, B.S., Mashoof, A.A., Garvin, K.L., Novak, J.R., Fritz, E.D., Mollner, T.J., McGuire, M.H.: Repair of segmental bone defects in the rat: an experimental model of human fracture healing. Bone **25**, 321–332 (1999). doi:10.1016/S8756-3282(99)00167-2
33. Erdemli, O., Captuğ, O., Bilgili, H., Orhan, D., Tezcaner, A., Keskin, D.: In vitro and in vivo evaluation of the effects of demineralized bone matrix or calcium sulfate addition to polycaprolactone-bioglass composites. J. Mater. Sci. Mater. Med. **21**, 295–308 (2010). doi:10.1007/s10856-009-3862-6
34. Leach, K.L., Kaigler, D., Wang, Z., Krebsbach, P.H., Mooney, D.J.: Coating of VEGF-releasing scaffolds with bioactive glass for angiogenesis and bone regeneration. Biomaterials **27**, 3249–3255 (2006). doi:10.1016/j.biomaterials.2006.01.033
35. Liu, Y., Tian, X., Cui, G., Zhao, Y., Yang, Q., Yu, S., Xing, G., Zhang, B.: Segmental bone regeneration using an rhBMP-2-loaded gelatin/nanohydroxyapatite/fibrin scaffold in a rabbit model. Biomaterials **30**, 6276–6285 (2009). doi:10.1016/j.biomaterials.2009.08.003

36. Sawyer, A.A., Song, S.J., Susanto, E., Chuan, P., Lam, C.X.F., Woodruff, M.A., Hutchmaker, D.W., Cool, S.M.: The stimulation of of healing within a rat calvarial defect by mPCL-TCP/collagen scaffolds loaded with rhBMP-2. Biomaterials **30**, 2479–2488 (2009). doi:10.1016/j.biomaterials.2008.12.055
37. Simmons, C.A., Alsberg, E., Hsiong, S., Kim, W.J., Mooney, D.J.: Dual growth factor delivery and controlled scaffold degradation enhance in vivo bone formation by transplanted bone marrow stromal cells. Bone **35**, 562–569 (2004). doi:10.1016/j.bone.2004.02.027
38. Shen, H., Hu, X., Yang, F., Bei, J., Wang, S.: The bioactivity of rhBMP-2 immobilized poly(lactide-co-glycolide) scaffolds. Biomaterials **30**, 3150–3157 (2009). doi:10.1016/j.biomaterials.2009.02.004
39. Verron, E., Khairoun, I., Guicheux, J., Bouler, J.M.: Calcium phosphate biomaterials as bone drug delivery systems: a review. Drug. Discov. Today. 1–5 (2010). doi: 10.1016/j.drudis.2010.05.003
40. Quinten Ruhe, P., Kroeses-Deutman, H.C., Wolke, J.G.C., Spauwen, P.H.M., Jansen, J.A.: Bone inductive properties of rhBMP-2 loaded porous calcium phosphate cement implants in cranial defects in rabbits. Biomaterials **25**, 2123–2132 (2004). doi:10.1016/j.biomaterials.2003.09.007
41. Ionescu, L.C., Lee, G.C., Sennett, B.J., Burdick, J.A., Mauck, R.L.: An anisotropic nanofiber/microsphere composite with controlled release of biomolecules for fibrous tissue engineering. Biomaterials **31**, 4113–4120 (2010). doi:10.1016/j.biomaterials.2010.01.098
42. Patel, Z.S., Young, S., Tabata, Y., Jansen, J.A., Wong, M.E.K., Mikos, A.G.: Dual delivery of an angiogenic and osteogenic growth factor for bone regeneration in a critical size defect model. Bone **43**, 931–940 (2008). doi:10.1016/j.actabio.2008.04.002
43. Yılgör, P., Tuzlakoğlu, K., Reis, R.L., Hasirci, N., Hasirci, V.: Incorporation of a sequential BMP-2/BMP-7 delivery system into chitosan-based scaffolds for bone tissue engineering. Biomaterials **30**, 3551–3559 (2009). doi:10.1016/j.biomaterials.2009.03.024
44. Harper, J., Klagsbrun, M.: Cartilage to bone–angiogenesis leads the way. Nat. Med. **5**, 617–618 (1999). doi:10.1038/9460
45. Peng, H., Wright, V., Usas, A., Gearhart, B., Shen, H.C., Cummins, J., Huard, J.: Synergistic enhancement of bone formation and healing by stem cell-expressed VEGF and bone morphogenetic protein-4. J. Clin. Invest. **110**, 751–759 (2002). doi:10.1172/JCI26772
46. Street, J., Bao, M., deGuzman, L., Bunting, S., Peale, F.V., Ferrara Jr., N., Steinmetz, H., Hoeffel, J., Cleland, J., Daugherty, A., van Bruggen, N., Redmond, H.P., Carano, R.A., Filvaroff, E.H.: Vascular endothelial growth factor stimulates bone repair by promoting angiogenesis and bone turnover. Proc. Natl. Acad. Sci. U S A **99**, 9656–9661 (2002). doi:10.1073/pnas.152324099
47. De la Riva, B., Sanchez, E., Hernandez, A., Reyes, R., Tamimi, F., Lopez-Cabarcos, E., Delgado, A., Evora, C.: Local controlled release of VEGF and PDGF from a combined brushite-chitosan system enhances bone regeneration. J. Cont. Rel. **143**, 45–52 (2010). doi:10.1016/j.conrel.2009.11.026
48. Wang, D.S., Miura, M., Demura, H., Sato, K.: Anabolic effects of 1, 25-dihydroxyvitamin D3 on osteoblasts are enhanced by vascular endothelial growth factor produced by osteoblasts and by growth factors produced by endothelial cells. Endocrinology **138**, 2953–2962 (1997). doi:10.1210/en.138.7.2953
49. Mayr-Wohlfart, U., Waltenberger, J., Hausser, H., Kessler, S., Gunther, K.P., Dehio, C., Puhl, W., Brenner, R.E.: Vascular endothelial growth factor stimulates chemotactic migration of primary human osteoblasts. Bone **30**, 472–477 (2002). doi:10.1016/S8756-3282(01)00690-1
50. Colton, C.K.: Implantable biohybrid artificial organs. Cell Transplant **4**, 415–436 (1995). doi:10.1016/0963-6897(95)00025-S
51. Geiger, F., Lorenz, H., Xu, W., Szalay, K., Kasten, P., Claes, L., Augat, P., Richter, W.: VEGF producing bone marrow stromal cells (BMSC) enhance vascularization and resorption of a natural coral bone substitute. Bone **41**, 516–522 (2007). doi:10.1016/j.bone.2007.06.018

52. Kaigler, D., Wang, Z., Horger, K., Mooney, D.J., Krebsbach, P.H.: VEGF scaffolds enhance angiogenesis and bone regeneration in irradiated osseous defects. J. Bone Miner. Res. **21**, 735–744 (2006). doi:10.1359/JBMR.060120
53. Drake, C.J., Little, C.D.: Exogenous vascular endothelial growth factor induces malformed and hyperfused vessels during embryonic neovascularization. Proc. Natl. Acad. Sci. U S A 92, 7657–7661 (1995). http://www.pnas.org/content/92/17/7657.full.pdf+html. Accessed 15 May 1999
54. Wernike, E., Montjovent, M.O., Liu, Y., Wismeijer, D., Hunziker, E.B., Siebenrock, K.A., Hofstetter, W., Klenke, F.M.: VEGF incorporated into calcium phosphate ceramics promotes vascularisation and bone formation in vivo. Eur. Cells Mater. 19, 30–40 (2010). www.ecmjournal.org/journal/papers/vol019/pdf/v019a04.pdf. Accessed 22 February 2010
55. Heliotis, M., Lavery, K.M., Ripamonti, U., Tsiridis, E., di Silvio, I.: Transformation of a prefabricated hydroxyapatite/osteogenic protein-1 implant into a vascularised pedicled bone flap in the human chest. Int. J. Oral Maxillofac. Surg. **35**, 265–269 (2006). doi:10.1016/j.ijom.2005.07.013
56. Zhou, M., Peng, X., Mao, C., Xu, F., Hu, M., Yu, G.: Primate mandibular reconstruction with prefabricated, vascularized tissue engineered bone flaps and recombinant human bone morphogenetic protein-2 implanted in situ. Biomaterials **31**, 4935–4943 (2010). doi:10.1016/j.biomaterials.2010.02.072
57. Cho, T.J., Gerstenfeld, L.C., Einhorn, T.A.: Differential temporal expression of members of the transforming growth factor beta superfamily during murine fracture healing. J. Bone Miner. Res. **17**, 513–520 (2002). doi:10.1359/jbmr.2002.17.3.513
58. Uchida, S., Sakai, A., Kudo, H., Otomo, H., Watanuki, M., Tanaka, M.: Vascular endothelial factor is expressed along with its receptors during the healing process of bone and bone marrow after drill-hole injury in rats. Bone **32**, 491–501 (2003). doi: 0.1016/S8756-3282(03)00053-X
59. Niikura, T., Hak, D.J., Reddi, A.H.: Global gene profiling reveals a downregulation of BMP gene expression in experimental atrophic nonunions compared to standard healing fractures. J. Orthop. Res. **24**, 1463–1471 (2006). doi:10.1002/jor.20182
60. Bikfalvi, A., Klein, S., Pintucci, G., Rifkin, D.B.: Biological roles of fibroblast growth factor-2. Endocr. Rev. **18**, 26–45 (1997). doi:10.1210/er.18.1.26
61. Li, C.F., Hughes-Fulford, M.: Fibroblast growth factor-2 is an immediate-early gene induced by mechanical stress in osteogenic cells. J. Bone Miner. Res. **21**, 946–955 (2006). doi:10.1359/jbmr.060309
62. Hu, J., Zou, S., Li, J., Chen, Y., Wang, D., Gao, Z.: Temporospatial expression of vascular endothelial growth factor and basic fibroblast growth factor during mandibular distraction osteogenesis. J. Craniofac. Surg. **31**, 238–243 (2003). doi:10.1016/S1010-5182(03)00034-9
63. Marie, P.J.: Fibroblast growth factor signalling controlling osteoblast differentiation. Gene **316**, 23–32 (2003). doi:10.1016/S0378-1119(03)00748-0
64. Nakamura, Y., Tensho, K., Nakaya, H., Nawata, M., Okab, T., Wakitani, S.: Low dose fibroblast growth factor-2 (FGF-2) enhances bone morphogenetic protein-2 (BMP-2)-induced ectopic bone formation in mice. Bone **36**, 399–407 (2005). doi:10.1016/j.bone.2004.11.010
65. Tsurushima, H., Marushima, A., Suzuki, K., Oyane, A., Sogo, Y., Nakamura, K., Matsumara, A., Ito, A.: Enhanced bone formation using hydroxyapatite ceramic coated with fibroblast growth factor-2. Acta Biomater. **6**, 2751–2759 (2010). doi:10.1016/j.actbio.2009.12.045
66. Jiang, X., Zou, S., Ye, B., Zhu, S., Liu, Y., Hu, J.: bFGF-Modified BMMSCs enhance bone regeneration following distraction osteogenesis in rabbits. Bone **46**, 1156–1161 (2010). doi: 10.1016/j.bone.2009.12.017
67. Yuan, Q., Kubo, T., Doi, K., Morita, K., Takeshita, R., Katoh, S., Shiba, T., Gong, P., Akagawa, Y.: effect of combined application of bFGF and inorganic polyphosphate on bioactivities of osteoblasts and initial bone regeneration. Acta Biomater. **5**, 1716–1724 (2009). doi:10.1016/j.actbio.2009.01.034

68. Mabilleau, G., Aguado, E., Stancu, I.C., Cincu, C., Basle, M.F., Chappard, D.: Effects of FGF-2 release from a hydrogel polymer on bone mass and microarchitecture. Biomaterials **29**, 1593–1600 (2008). doi:10.1016/j.biomaterials.2007.12.018
69. Taba, M., Jin, Q., Sugai, V.J., Giannobile, W.V.: Current concepts in periodontal bioengineering. Orthod. Craniofac. Res. **8**, 292–302 (2005). doi:10.1111/j.1601-6343.2005.00352.x
70. Wei, G., Jin, Q., Giannobile, W.V., Ma, P.: Nano-fibrous scaffold for controlled delivery of recombinant human PDGF-BB. J. Cont. Rel. **112**, 103–110 (2006). doi:10.1016/j.conrel.2006.01.011
71. Giannobile, W.V., Hernandez, R.A., Finkelman, R.D., Ryan, S., Kiritsy, C.P., Dandrea, M., Lynch, S.E.: Comparative effects of platelet-drived growth factor-BB and insulin like growth factor-I, individually and in combination, on periodontal regeneration in Macca fascicularis. J. Periodont. Res. **31**, 301–312 (1996). doi:10.1111/j.1600-0765.1996.tb00497.x
72. Howell, T.H., Fiorellini, J.P., Paquette, D.W., Offenbacher, S., Giannobile, W.V., Lynch, S.E.: A phase I/II clinical trial to evaluate a combination of recombinant human platelet-derived growth factor-BB and recombinant human insulin like growth factor-I in patients with periodontal disease. J. Periodont. **68**, 1186–1193 (1997)
73. Nevins, M., Giannobile, W.V., McGuire, M.K., Kao, R.T., Mellonig, J.E., Hinrichs, B.S., McAllister, B.S., Murphy, K.S., McClain, P.K., Nevins, M.L., Paquette, D.W., Han, T.J., Reddy, M.S., Lavin, P.T., Genco, R.J., Lynch, S.E.: Platelet derived growth factor (rhPDGF-BB) stimulate bone fill and rate of attachment level gain: results of a large multi-center randomized controlled trial. J. Periodont. **76**, 2205–2215 (2005). doi:10.1902jop.2005.76.12.2205
74. Zhang, Y., Wang, Y., Shi, B., Cheng, X.: A platelet-derived growth factor releasing chitosan/coral composite scaffold for periodontal tissue engineering. Biomaterials **28**, 1515–1522 (2007). doi:10.1016/j.biomaterials.2006.11.040
75. Endo, A., Monacolin, K.: A new hypocholesterolemic agent that specifically inhibits 3-hydroxy-3-methylglutaryl coenzyme A reductase. J. Antibiot. **33**, 334–336 (1980)
76. Mundy, G.R., Garrett, R., Harris, S., Chan, J., Chen, D., Rossini, G., Boyce, B., Zhao, M., Gutierrez, G.: Stimulation of bone formation in vitro and in rodents by statins. Science **286**, 1946–1949 (1999). doi:10.1126/science.286.5446.1946
77. Sugiyama, M., Kodama, T., Konishi, K., Abe, K., Asami, S., Oikawa, S.: Compactin and simvastatin, but not pravastatin, induce bone morphogenetic protein-2 in human osteosarcoma cells. Biochem. Biophys. Res. Com. **271**, 688–692 (2000). doi:10.1006/bbrc.2000.2697
78. Song, C., Guo, Z., Ma, Q., Chen, Z., Liu, Z., Jia, H., Dang, G.: Simvastatin induces osteoblastic differentiation and inhibits adipocytic differentiation in mouse bone marrow stromal cells. Biochem. Biophys. Res. Com. **308**, 458–462 (2003). doi:10.1016/S0006-291X(03)01408-6
79. Skoglund, B., Forslund, C., Aspenberg, P.: Simvastatin improves fracture healing in mice. J. Bone Miner. Res. **17**, 2004–2008 (2002). doi:10.1359/jbmr.2002.17.11.2004
80. Ayukawa, Y., Okamura, A., Koyano, K.: Simvastatin promotes osteogenesis around titanium implants. Clin. Oral Implants Res. **15**, 346–350 (2004). doi:10.1046/j.1600-0501.2003.01015.x
81. Gutierrez, G.E., Lalka, D., Garret, I.R., Rossini, G., Mundy, G.R.: Transdermal application of lovastatin to rats causes profound increases in bone formation and plasma concentrations. Osteoporos. Int. **17**, 267–273 (2006). doi:10.1007/s00198-006-0079-0
82. Moriyama, Y., Ayukawa, Y., Ogino, Y., Atsuta, I., Todo, M., Takao, Y., Koyano, K.: Local application of fluvastatin improves peri-implant bone quantity and mechanical properties. Acta. Biomater. **6**, 1610–1618 (2010). doi:10.1016/j.actbio.2009.10.045
83. Benoit, D.S.W., Nuttelman, C.R., Collins, S.D., Anseth, K.S.: Synthesis and characterization of a fluvastatin-releasing hydrogel delivery system to modulate hMSC

differentiation and function for bone regeneration. Biomaterials (2006). doi: 10.1016/j.biomaterials.2006.06.031
84. Tanigo, T., Takaoka, R., Tabata, Y.: Sustained release of water-insoluble simvastatin from biodegradable hydrogel augments bone regeneration. J. Cont. Rel. **143**, 201–206 (2010). doi:10.1016/j.jconrel.2009.12.027
85. Monjo, M., Rubert, M., Wohlfahrt, J.C., Ronold, H.J., Ellingsen, J.E., Lyngstadaas: In vivo performance of absorbable collagen sponges with rosuvastatin in critical-size cortical bone defects. Acta Biomater. 6, 1405–1412 (2010). doi:10.1016/j.actbio.2009.09.027
86. Masuzaki, T., Ayukawa, Y., Moriyama, Y., Jinno, Y., Atsuta, I., Ogino, Y., Koyano, K.: The effect of a single remote injection of statin impregnated poly(lactic-co-glycolic acid) microspheres on osteogenesis around titanium implants. Biomaterials **31**, 3327–3334 (2010). doi:10.1016/j.biomaterials.2010.01.016
87. Diefenbeck, M., Muckley, T., Hofmann, G.O.: Prophylaxis and treatment of implant-related infections by local application of antibiotics. Injury **37**, S95–S104 (2006). doi:10.1016/j.injury.2006.04.015
88. Miyai, T., Ito, A., Tamazawa, G., Matsuno, T., Sogo, Y., Nakamura, C., Yamazaki, A., Satoh, T.: Antibiotic-loaded poly-ε-caprolactone and porous β-tricalcium phosphate composite for treating osteomyelitis. Biomaterials **29**, 350–358 (2008). doi:10.1016/j.biomaterials.2007.09.040
89. Hanssen, A.D.: Local antibiotic delivery vehicles in the treatment of musculoskeletal infection. Clin. Orthop. Relat. Res. **437**, 91–96 (2005). doi:10.1097/01.blo.0000175713.30506.77
90. Sanchez, E., Baro, M., Soriano, I., Perera, A., Evora, C.: In vivo-in vitro study of biodegradable and osteointegrable gentamycin bone implants. Eur. J. Pharm. Biopharm. **52**, 151–158 (2001). doi:10.1016/S0939-6411(01)00169-2
91. Zilberman, M., Elsner, J.J.: Antibiotic-eluting medical devices for various applications. J. Cont. Rel. **13**, 202–215 (2008). doi:10.1016/j.jconrel.2008.05.020
92. Chai, F., Hornez, J.C., Blanchemain, N., Neut, C., Descamps, M., Hildebrand, H.F.: Antibacterial activation of hydroxyapatite (HA) with controlled porosity by different antibiotics. Biomol. Eng. **24**, 510–514 (2007). doi:10.1016/j.bioeng.2007.08.001
93. Cevher, E., Orhan, Z., Mulazımoglu, L., Sensoy, D., Alper, M., Yıldız, A., Ozsoy, Y.: Characterization of biodegradable chitosan microspheres containing vancomycin and treatment of experimental osteomyelitis caused by methicillin-resistant Staphylococcus aureus with prepared microspheres. Int. J. Pharm. **317**, 127–135 (2006). doi:10.1016/j.jpharm.2006.03.014
94. Li, B., Brown, K.V., Wenke, J.C., Guelcher, S.A.: Sustained release of vancomycin from polyurethane scaffolds inhibits infection of bone wounds in a rat femoral segmental defect model. J. Cont. Rel. **145**, 221–230 (2010). doi:10.1016/j.jconrel.2010.04.002
95. Pillai, R.R., Somayaji, S.N., Rabinovich, M., Hudson, M.C., Gonsalves, K.E.: Nafcillin-loaded PLGA nanoparticles for treatment of osteomyelitis. Biomed. Mat. **3**, 1–7 (2008). doi: 10.1088/1748-6041/3/3/034114
96. Xie, Z., Liu, X., Jia, W., Zhang, C., Huang, W., Wang, J.: Treatment of osteomyelitis and repair of bone defect by degradable bioactive borate glass releasing vancomycin. J. Cont. Rel. **139**, 118–126 (2009). doi:10.1016/j.jconrel.2009.06.012
97. Huang, W., Day, E., Kittiratanapiboon, K., Rahaman, M.N.: Kinetics and mechanisms of the conversion of silicate (45S5), borate, and borosilicate glasses to hydroxyapatite in dilute phosphate solutions. J. Mater. Sci. Mater. Med. **17**, 583–596 (2006). doi:10.1007/S10856-006-9220
98. Yao, A., Wang, D., Huang, W., Fu, Q., Rahaman, M.N., Day, D.E.: In vitro bioactive characteristics of borate-based glasses with controllable degradation behaviour. J. Am. Ceram. Soc. **90**, 303–306 (2007). doi:10.1111/j.1551-2916.2006.01358
99. Jia, W.T., Zhang, X., Luo, S.H., Liu, X., Huang, W.H., Rahaman, M.N., Day, D.E., Zhang, C.Q., Xie, Z.P., Wang, J.Q.: Novel borate glass/chitosan composite as a delivery

vehicle for teicoplanin in the treatment of chronic osteomyelitis. Acta-Biomater. **6**, 812–819 (2010). doi:10.1016/j.actbio2009.09.011
100. Shi, X., Wang, Y., Ren, L., Zhao, N., Gong, Y., Wang, D.A.: Novel mesoporous silica-based antibiotic releasing scaffold for bone repair. Acta Biomater. **5**, 1697–1707 (2009). doi:10.1016/j.actbio.2009.01.010
101. Hutmacher, D.W.: Scaffolds in tissue engineering bone and cartilage. Biomaterials **21**, 2529–2543 (2000). doi:10.1016/S0142-9612(00)00121-6
102. Zilberman, M.: Novel composite fiber structures to provide drug/protein delivery for medical implants and tissue regeneration. Acta Biomater. **3**, 51–57 (2007). doi: 10.1016/j.actbio.2006.06.008
103. Khan, Y., Yaszemski, M., Mikos, A.G., Laurencin, C.T.: Tissue engineering of bone: material and matrix considerations. J. Bone Joint Surg. **90**, 36–42 (2008). doi: 10.2106/JBJS.G.01260
104. Spoerke, E.D., Murray, N.G., Li, H., Brinson, L.C., Dunand, D.C., Stupp, S.I.: A bioactive titanium foam scaffold for bone repair. Acta Biomaterialia. **1**, 523–533 (2005) doi: 10.1016/j.actbio.2005.04.005
105. Guarino, V., Ambrosio, L.: The synergic effect of polylactide fiber and calcium phosphate particle reinforcement in poly e-caprolactone-based composite scaffolds. Acta Biomater. **4**, 1778–1787 (2008). doi:10.1016/j.actbio.2008.05.013
106. Karageorgiou, V., Kaplan, D.: Porosity of 3D biomaterial scaffolds and osteogenesis. Biomaterials **26**, 5474–5491 (2005). doi:10.1016/j.biomaterials.2005.02.002
107. Frutos, G., Pastor, J.Y., Martínez, N., Virto, M.R., Torrado, S.: Influence of lactose addition to gentamicin-loaded acrylic bone cement on the kinetics of release of the antibiotic and the cement properties. Acta Biomater. **6**, 804–811 (2010). doi:10.1016/j.avtbio.2009.08.028
108. Petrone, C., Hall, G., Langman, M., Filiaggi, M.J.: Compaction strategies for modifying the drug delivery capabilities of gelled calcium phosphate matrices. Acta Biomater. **4**, 403–413 (2008). doi:10.1016/j.actbio.2007.09.007
109. Kim, H.W., Knowles, J.C., Kim, H.E.: Hydroxyapatite/poly(ε-caprolactone) composite coatings on hydroxyapatite porous bone scaffold for drug delivery. Biomaterials **25**, 1279–1287 (2004). doi:10.1016/j.biomaterials.2003.07.003
110. Xu, H.H.K., Weir, M.D., Simon, C.G.: Injectable and strong nano-apatite scaffolds for cell/growth factor delivery and bone regeneration. Dent. Mat. **24**, 1212–1222 (2008). doi: 10.1016/j.dental.2008.02.001
111. Shi, M., Kretlow, J.D., Nguyen, A., Young, S., Baggett, L.S., Wong, M.E., Kasper, F.K., Mikos, A.G.: Antibiotic-releasing porous methylmethacrylate constructs for osseous space maintenance and infection control. Biomaterials **31**, 4146–4156 (2010). doi:10.1016/j.biomaterials.2010.01.112
112. Mauduit, J., Bukh, N., Vert, M.: Gentamycin/poly (lactic acid) blends aimed at sustained release local antibiotic therapy administered per-operatively. III. The case of gentamycin sulfate in films prepared from high and low molecular weight poly (DL-lactic acids). J. Cont. Rel. **25**, 43–49 (1993). doi:10.1016/0168-3659(93)90093-K
113. Schmidt, C., Wenz, R., Nies, B., Moll, F.: Antibiotic in vivo/in vitro release, histocompatibility and biodegradation of gentamicin implants based on lactic acid polymers and copolymers. J. Cont. Rel. **37**, 83–94 (1995). doi:10.1016/0168-3659(95)00067-I
114. Kempen, D.H.R., Lu, L., Heijink, A., Hefferan, T.E., Creemers, L.B., Maran, A., Yaszemski, M.J., Dhert, W.J.A.: Effect of local sequential VEGF and BMP-2 delivery on ectopic and orthopic bone regeneration. Biomaterials **30**, 2816–2825 (2010). doi:10.016/j.biomaterials.2009.01.031

Bio-inspired Resorbable Calcium Phosphate-Polymer Nanocomposites for Bone Healing Devices with Controlled Drug Release

Irena Gotman and Sabine Fuchs

Abstract In orthopedic research, increasing attention is being paid to bioresorbable composite materials as an attractive alternative to permanent metal bone healing devices. Typical composites consist of a biodegradable polyester matrix loaded with bioactive calcium phosphate ceramic particles (tricalcium phosphate, TCP or hydroxyapatite, HA) added to improve the biological response and mechanical properties of the neat polymer. The mechanical behavior of such particle-reinforced composites, however, falls far short of the expected performance in high-load bearing situations. Replicating some features of nacre—a strong and tough natural nanocomposite with a very high content of brittle inorganic phase, can pave the way for a new generation of high-strength resorbable bone implants. This chapter will concentrate on the processing of such "bio-inspired" nanocomposites with high calcium phosphate content where the strong ceramic skeleton is toughened by a small amount of continuously dispersed polymer component. To further improve the mechanical properties, manipulating the adhesion at the interface between the ceramic and polymeric nanoscale components was attempted. An original high pressure consolidation method was employed to fabricate dense bulk nanocomposites without exposing them to high processing temperatures. This allows for incorporation of biomolecules that can then be released from the implanted device to enhance bone regeneration (growth factors) or prevent infection (antibacterial drugs). Finally, it is important to evaluate how polymer addition to calcium phosphate influences cell-material or

I. Gotman (✉)
Department of Materials Engineering, Technion-Israel Institute of Technology, 32000 Haifa, Israel
e-mail: gotman@tx.technion.ac.il

S. Fuchs
Institute of Pathology, Universitätsmedizin der Johannes Gutenberg-Universität, Langenbeckstrasse 1, Mainz, Germany

Stud Mechanobiol Tissue Eng Biomater (2011) 8: 225–258
DOI: 10.1007/8415_2010_63

Published Online: 26 March 2011

cell–cell interactions because of potential consequences for bone regeneration and vascularization. Towards this goal, CaP-polymer nanocomposites were assessed in monocultures of endothelial cells and osteoblasts and in co-culture thereof as an example of a more complex test system.

1 Introduction

Bioresorbable implants for bone repair are increasingly used in orthopedics as an attractive alternative to traditional metal instrumentation. The advantages of osteosynthesis devices that slowly degrade over time include elimination of the need for further surgical intervention and substantially reduced stress-shielding due to gradual transfer of mechanical loads to the newly forming bone as the material degrades [2, 75, 83, 84]. The current generation of biodegradable implants for bone repair are made of synthetic polymers, mostly poly(α-hydroxyester)s-polylactic and polyglycolic acids (PLA and PGA), their copolymers (PLGA) and polycaprolactone (PCL). These pure polymeric devices for osteosynthesis have shown some success in low or mild load bearing applications however they are not sufficiently strong to be used in highly loaded long bones such as the femur [18, 63]. Other limitations of degradable polymers include delayed inflammatory response to the acidic products of their hydrolytic degradation and lack of bioactivity [2, 63]. This latter attribute could be undesirable for traditional fixation devices where direct bone apposition on the implant surface would interfere with the removal procedure. For bioresorbable devices, however, ease of removal is not an issue and the use of bioactive materials that enhance osteoblastic activity is expected to support bone regeneration more effectively [18].

Combining degradable polymers and bioactive calcium phosphate ceramics (e.g., hydroxyapatite, HA and beta-tricalcium phosphate, β-TCP) into composite materials has been proposed as a means of creating bioactive implants with improved mechanical properties and tailored degradation behavior [15, 40, 67, 72, 73, 81]. A further advantage of such composites is that the alkaline resorption products of calcium phosphate will buffer the acidic degradation products of polyesters. A common feature of most polymer-ceramic systems studied as materials for bone healing materials is the low volume fraction of the ceramic phase. In such a design, the main contribution of the ceramic particles is increased stiffness and enhanced bioactivity. On the other hand, the strength of such polymer-matrix composites does not increase and actually decreases with increasing calcium phosphate volume fraction [90]. It seems, therefore, that today's approach to increasing strength by including CaP particles into polymer matrices is a dead end and the research should focus on other ways of developing high strength bioresorbable composites. One alternative strategy is to toughen calcium phosphate ceramics by incorporating a small amount of continuously dispersed polymer component. This can yield strong and tough composite materials whereby the ceramic skeleton provides structural consistency and strength while the polymeric

phase acts as glue and transfers stresses across phases thereby enhancing ductility and fracture resistance. Creating calcium phosphate matrix composites with uniformly distributed nanoscale ceramic and polymer features will allow for further toughness enhancement. In a way, such CaP-polymer nanocomposites will resemble nacre—an exceptionally tough biogenic material comprised of a high volume percent of brittle ceramic crystals (aragonite) separated by organic layers several tens of nanometers thick [46, 56, 60].

In has been argued by many authors that the unusual mechanical response of nacre is partly due to molecular interactions and adhesion forces at the organic–inorganic interfaces [62, 64, 89]. This suggests that the overall strength and toughness of bio-inspired calcium phosphate-based nanocomposites can also be enhanced by manipulating the adhesion at the CaP-polymer interfaces, e.g., by chemical grafting of organic moieties. Such approach resulted in increased mechanical properties of PLA-HA and PLGA-HA biocomposites reinforced with low fractions ($\leq$20 vol.%) of HA particles [35, 85, 96]. The effect is expected to be even more pronounced for CaP-polymer nanocomposites having a significantly larger amount of interfaces.

The standard approach to the processing of bulk ceramic-polymer composites involves the mixing of a pre-synthesized CaP powder with a polymer followed by densification. Ceramic nanoparticles, however, have a strong tendency to aggregate because of the relatively strong interparticle forces between them. It is therefore quite challenging to achieve homogeneous calcium phosphate dispersion while mixing with polymer, even using solution-mixing. To obtain CaP-polymer composites with more uniform phase distribution, an "in situ" processing approach has been recently advocated [3, 10, 33, 70]. In this approach, CaP nanocrystals are not pre-synthesized but are formed "in situ" in the presence of polymer. Thus, extensive ceramic particle agglomeration is avoided and higher degree of interaction and bonding between the organic and inorganic components of the composite is achieved, potentially resulting in better mechanical properties.

Despite improvements in operating techniques and advances in bone-healing devices, there is still a too high number of complications in fracture treatment like delayed healing or nonunion [91]. For better clinical outcome, biological stimulation of bone regeneration process by combining growth factors (e.g., bone morphogenetic proteins, BMPs) with biodegradable devices is of great interest. High incidence of implant-related infections is another issue in surgical treatment of bone fractures and defects [12, 80]. Implant infections are extremely resistant to antibiotic therapy and host defenses, and frequently persist until the implant is removed. Local antibiotic delivery systems are considered advantageous for treatment and prevention of implant-related infections because they may deliver high drug concentrations to the infected bone while avoiding systemic side-effects [25, 43, 68, 88]. Incorporation of BMPs or antimicrobial agents into bioresorbable bone healing devices seems especially attractive as this can produce mechanically reliable multifunctional implants combining load-bearing capacity with sustained drug release. Promising results were obtained for bioresorbable ciprofloxacin-releasing osteofixation screws for non-load-bearing applications made of pure

polymer and bioglass-reinforced PLGA and PLDLA [1, 59], however incorporation of drugs into dense bioresorbable CaP-polymer composite implants has not been reported. In principle, active ingredients can be admixed already to the loose composite powder, provided the biological activity is not lost during subsequent densification procedure. Unfortunately, most processing methods of dense calcium phosphate-bioresorbable polymer composites employ relatively high temperatures that may compromise the bioactivity of incorporated drugs. The goal of developing high-strength bone healing devices that can also release therapeutic agents should be achievable with further research into unconventional manufacturing processes. More specifically, high pressure consolidation of powders (cold sintering [31, 32]) could allow one to fabricate high density CaP-polymer nanocomposites at low temperatures that are less likely to be harmful for biomolecules.

Including polymers such as PLA and PCL will modify not only the mechanical but also physical and chemical properties of calcium phosphates thus potentially exerting effects on cell–material and cell–cell interactions. In complex tissues such as bone the material properties influence a variety of different cell types and may have consequences on osteogenic differentiation or endothelial cell growth, or may influence the formation of angiogenic structures. To analyze those effects, complex cell culture systems, such as co-cultures consisting of endothelial cells and primary osteoblasts, seem to be useful to simulate the dynamic processes during vascularization as it would occur in the physiological situation in vivo [23, 78, 87].

Recently co-culture systems based on outgrowth endothelial cells (OEC) [20, 29, 36], derived from so-called endothelial progenitor cell cultures and primary osteoblasts [21] have been established. This approach leads to promotion of a pro-angiogenic effect in OEC at both levels of investigation, that is, in vitro [23] and in vivo, resulting in perfused vascular structures after implantation of the constructs [22]. As well as being used to improve the vascularization of tissue-engineered constructs, co-cultures possess a significant potential as advanced in vitro test systems for biomaterial design.

This chapter describes our efforts to create strong bio-inspired calcium phosphate-biodegrdable polymer nanocomposites for bone healing devices using the above fabrication strategies [5, 57, 58, 71] and to test their biological performance in vitro [24].

2 Two-Step Processing of Resorbable *β*-TCP-Polymer Nanocomposites with High Ceramic Content

2.1 Synthesis and Properties

β-TCP nanopowder was prepared by a previously reported reaction [7]:

$$3Ca(OOCCH_3)_2 + 2H_3PO_4 \rightarrow Ca_3(PO_4)_2 + 6CH_3COOH \quad (1)$$

using ethanol (instead of methanol) as a solvent [5]. As can be seen from XRD spectrum in Fig. 1, the reaction did not produce the desired single-phase β-TCP; instead, the synthesized powder consisted of β-TCP, hydroxyapatite (HA) and dicalcium phosphate (DCP). DCP was previously proposed as an intermediate phase in the reaction between calcium acetate and phosphoric acid [7] and its presence in the product powder suggests that the synthesis reaction was incomplete. The formation of some HA along with β-TCP must be due to the small amounts of water contained in the reagents. The considerable peak width indicates nanoscale structure and/or presence of an amorphous phase. The IR spectrum of the powder, Fig. 2, presents the characteristic phosphate bands of calcium phosphates in the 1,000–1,200 and 500–700 cm^{-1} domains. In addition, the bands of unreacted calcium acetate are observed at 1,573, 1,463, 1,444 and 675 cm^{-1} [65].

Calcination treatments are usually employed after wet chemical synthesis of calcium phosphates to achieve full transformation to β-TCP [86, 95]. To prevent excessive coarsening of the nanoscale synthesized powder, calcination temperature should be kept as low as possible. Pure β-TCP with the smallest particle size ($\leq$100 nm, Fig. 3a) could be obtained after 1 day calcination at 650°C. Both the XRD pattern, Fig. 1, and FTIR spectrum, Fig. 2, of thus treated powder correspond to the single-phase β-TCP [42]. When the powder was calcined at lower temperatures, the reaction between DCP and the remaining calcium acetate was complete already at 500°C, however the peaks of hydroxyapatite in the XRD pattern persisted till 650°C. The complete transformation of the HA component into β-TCP at $T \geq 650$°C indicates that this HA was a Ca-deficient compound with Ca/P ratio close to that of TCP (1.5) [41]. At higher calcinations temperatures (700–750°C), the formation of the single-phase β-TCP could be achieved in much less than 1 day (1–2 h). Such treatments, however, led to considerable grain growth of the CaP powder. Therefore, the powder calcined at 650°C, 1 day was used for further experiments.

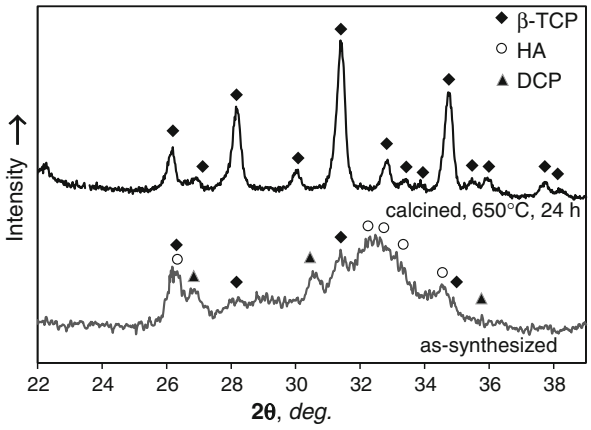

Fig. 1 XRD patterns of as-synthesized and calcined β-TCP powder [5]. Reprinted from [5] with kind permission from Wiley-VCH VerlagGmbH & Co. KGaA

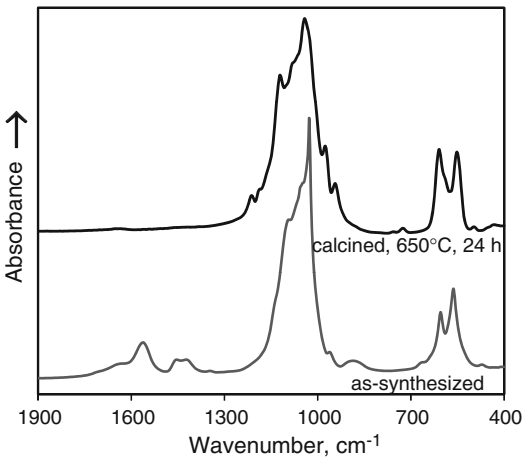

Fig. 2 FTIR spectra of the as-synthesized and calcined β-TCP powder [5]. Reprinted from [5] with kind permission from Wiley-VCH VerlagGmbH & Co. KGaA

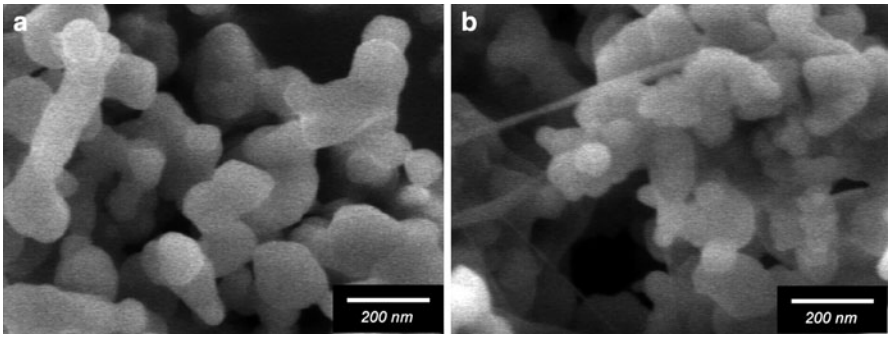

Fig. 3 HRSEM micrographs of calcined β-TCP powder [5] (**a**) and β-TCP-15 vol.% PCL blend (**b**). Reprinted from [5] with kind permission from Wiley-VCH VerlagGmbH & Co. KGaA

β-TCP-PCL and β-TCP-PLA composite nanopowders were prepared by solvent evaporation method as described in Bernstein et al. [5]. When the polymer was dissolved in chloroform and added to the β-TCP powder, it became uniformly distributed between the ceramic nanoparticles (presumably as very thin surface films) occasionally forming tiny polymer fibers, Fig. 3b. The results of TGA analysis confirmed that polymer contents of the β-TCP-PCL and β-TCP-PLA composite powders corresponded to the nominal composition, i.e. all the polymer dissolved in chloroform was fully incorporated in the composite powder.

Pure β-TCP and β-TCP-PCL composite powders were high pressure consolidated at room temperature—cold sintered [31, 32] at pressures up to 3 GPa. Figure 4a shows the density of cold sintered specimens as a function of applied pressure. As expected, the density of pure β-TCP as well as of β-TCP-PCL compositions increased with consolidation pressure. At 2.5 GPa, the density of

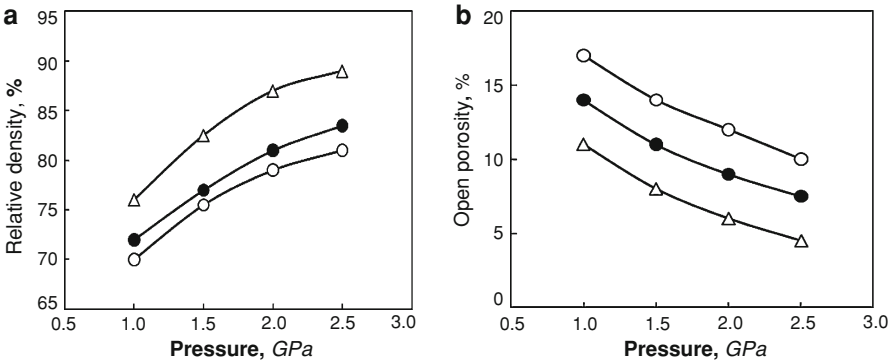

Fig. 4 Relative density (**a**) and open porosity (**b**) of pure β-TCP (*open circles*), β-TCP-5% PCL (*filled circles*) and β-TCP-15% PCL (*triangles*) composites as a function of consolidation pressure [5]. Reprinted from [5] with kind permission from Wiley-VCH VerlagGmbH & Co. KGaA

β-TCP, β-TCP-5PCL and β-TCP-15PCL composites was, correspondingly, ~80, 83 and 88%. Further pressure increase to 3 GPa resulted in only marginal density increase. The higher densities obtained in PCL-containing specimens was apparently due to the plastic flow of the soft polymer component under pressure. Similarly to the total porosity, the open porosity also decreased with increasing pressure, Fig. 4b.

The compressive strength of cold sintered β-TCP and β-TCP/PCL nanocomposites increased with increasing consolidation pressure, Fig. 5a, apparently due to the decreasing porosity. The pure β-TCP and β-TCP-5 vol.% PCL composite cold sintered at 2.5 GPa exhibited comparable strength and brittle behavior, Fig. 5b.

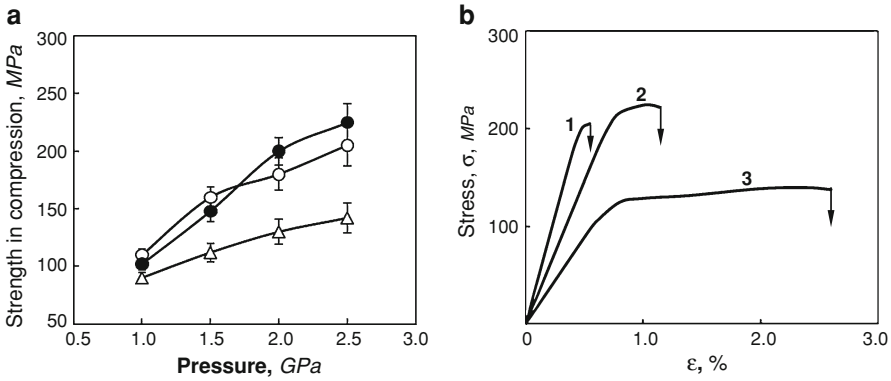

Fig. 5 **a** Compressive strength as a function of consolidation pressure of β-TCP (*open circles*), β-TCP-5% PCL (*filled circles*) and β-TCP-15% PCL (*triangles*) composites; **b** stress–strain curves of β-TCP (*curve 1*), β-TCP-5% PCL (*curve 2*) and β-TCP-15% PCL (*curve 3*) composites cold sintered at 2.5 GPa [5]. Reprinted from [5] with kind permission from Wiley-VCH VerlagGmbH & Co. KGaA

The addition of 15 vol.% PCL resulted in a more ductile behavior (~3% plastic deformation) albeit at the expense of strength. Even so, the compressive strength of this material (~140 MPa) is significantly higher than the corresponding value—27 MPa—reported for cast PCL-matrix composites containing 30 wt% hydroxyapatite [4]. It is believed that higher strength values can be achieved by substituting the weak PCL with the stronger PLA polymer. Still, even with the weak polymer phase, the compressive strength of cold sintered β-TCP-15 vol.% PCL composite is on a par with the strongest literature reported hot-forged PLA-HA composites with low volume fractions of the ceramic phase [37, 81].

2.2 Dissolution Behavior

Dissolution behavior pure β-TCP and β-TCP-PCL composites cold sintered at 2.5 GPa was studied in 0.05 M Tris buffer (pH 7.4) at 37°C [5]. The dissolution data are shown in Fig. 6. There was a time-dependent increase in the phosphate concentrations in Tris solution for all materials until the steady state conditions of dissolution-precipitation were reached. The dissolution curves of β-TCP/PCL composites with up to 15 vol.% PCL are not significantly different from that of PCL-free β-TCP. These results suggest that the dissolution of the β-TCP component is not strongly affected by the presence of PCL, at least not at short immersion times. The presence of β-TCP, on the other hand, may enhance the hydrolytic degradation of PCL by virtue of improved hydrophilicity. Also, faster degradation of the nanometric PCL phase may take place due to the high surface area-to-volume ratio and thus a greater water uptake. Given the fact that PCL is a slow degrading polymer, longer immersion times are needed to test the overall degradation kinetics of β-TCP-PCL composites. Such long-term experiments are currently underway. In the meantime β-TCP-15% PCL composites retained ≥85% of their compressive strength after 2 weeks immersion in TRIS buffer solution. The retention of mechanical properties for a sufficiently long period of time is important if the material is intended for load bearing bone healing applications.

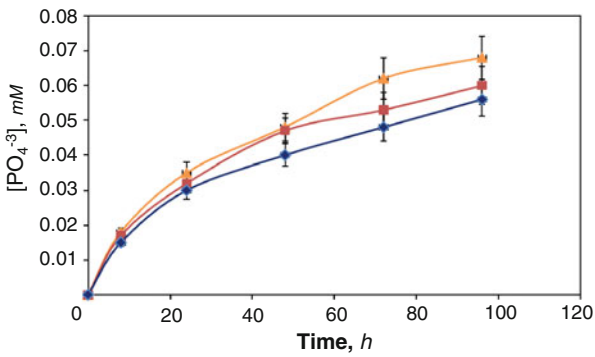

Fig. 6 Dissolution behavior (phosphate concentration in Tris buffer vs. immersion time) of pure β-TCP (*orange line*), β-TCP-5% PCL (*red line*) and β-TCP-15% PCL (*blue line*) composites cold sintered at 2.5 GPa [5]. Reprinted from [5] with kind permission from Wiley-VCH VerlagGmbH & Co. KGaA

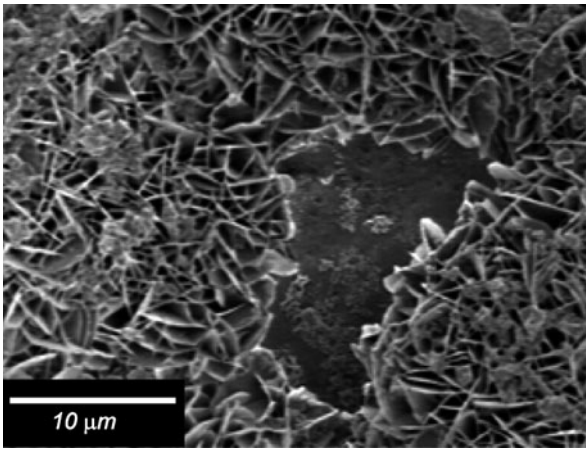

Fig. 7 Apatite layer formed on the surface of β-TCP-15 vol.% PCL composite after 7 days immersion in SBF solution. SEM [5]. Reprinted from [5] with kind permission from Wiley-VCH VerlagGmbH & Co. KGaA

Upon immersion of β-TCP-PCL disks in SBF, an uptake of both Ca and PO_4 ions was measured suggesting precipitation and growth of a new CaP phase on the surface of the composites. The formation of this CaP layer was observed in SEM, Fig. 7. FTIR surface analysis revealed that after immersion in SBF, the doublet of sharp peaks observed in the orthophosphate band at 1,030–1,130 cm^{-1} before immersion was replaced by one broad P–O band typical of hydroxyapatite [51, 52]. This formation of bone-like apatite on the surface of β-TCP-PCL composites suggests that the material is bioactive [16].

2.3 Vancomycin Release

Dry β-TCP-PLA and β-TCP-PCL composite powders were mixed with water solution of vancomycin (a representative antibiotic drug) and consolidated at 2.5 GPa to yield nanocomposite materials containing 3–10 wt% antibiotic (see Table 1) [58]. Fig. 8 shows drug release from β-TCP-15% PCL disks containing different amounts of vancomycin. Specimens with 10 wt% vancomycin ($\sim$24 mg) released the drug very rapidly and disintegrated completely after 2 days immersion. In contrast to this, disks with 3 and 5 wt% vancomycin (6 and 13 mg, respectively) released much more slowly and remained intact after 14 days immersion. 5 wt% vancomycin was chosen for further experiments as the largest antibiotic load that does not cause material disintegration upon immersion. As can be seen in Fig. 8, β-TCP-15% PCL disks containing 5 wt% vancomycin released $\sim$30% of the total drug load in an initial burst, and the remaining 70%—over the period of $\sim$10–12 days. The weight loss of the β-TCP-15% PCL disks measured after 14 days immersion, constituted only 3% of the initial weight. This suggests that the drug is released from the β-TCP-15% PCL composite by a diffusion mechanism rather than as the result of material dissolution. In the context of

Table 1 Density and compression strength of β-TCP-polymer nanocomposites used for vancomycin release studies [58]

Material	Density (% TD)	Porosity (%)	Compressive strength (MPa)
β-TCP-15% PCL	89 ± 2	11 ± 2	137 ± 13
β-TCP-15% PLA	87 ± 2	13 ± 2	118 ± 21
β-TCP-30% PLA	94 ± 1	6 ± 1	197 ± 12

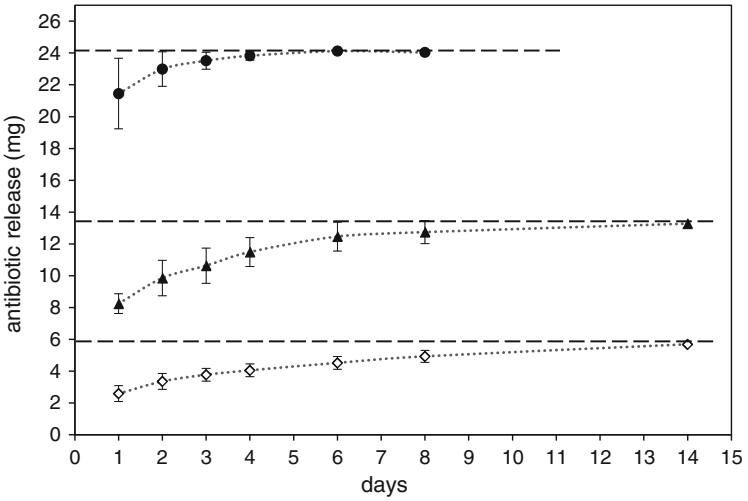

Fig. 8 Cumulative antibiotic release from β-TCP-15% PCL disks containing 3 wt% (*diamonds*), 5 wt% (*triangles*) and 10 wt% (*circles*) of vancomycin as a function of immersion time in TRIS buffer solution at 37°C. *Horizontal lines* indicate the corresponding initial vancomycin load [58]. Reprinted from [58] with kind permission from Springer Science+BusinessMedia

bone-healing applications, such a release-dissolution pattern will allow local prophylaxis against implant-related infection at the early stages after implantation followed by a much more slow dissolution of the load-carrying device.

As shown in Table 2, the incorporation of 5 wt% vancomycin did not strongly affect the compressive strength of β-TCP-15% PCL. Moreover, no significant strength deterioration was measured following 2 weeks immersion of the vancomycin-containing as well as vancomycin-free material. This must be due to the negligible material dissolution of 3%, see above. Figure 9 compares drug release profiles from β-TCP-polymer composites with 5 wt% vancomycin for different types (PCL and PLA) and fractions (15 and 30 vol.%) of the polymer. It can be seen that for the same polymer (PLA), drug release is slower from the composite

Table 2 Compression strength of β-TCP-15 vol.% PCL composites before and after 2 weeks immersion in TRIS buffer solution at 37°C [58]

Vancomycin content in β-TCP-15% PCL		No vancomycin	5 wt%
Compressive strength (MPa)	Before immersion	137 ± 13	120 ± 30
	After 2 weeks immersion in TRIS	110 ± 26	123 ± 24

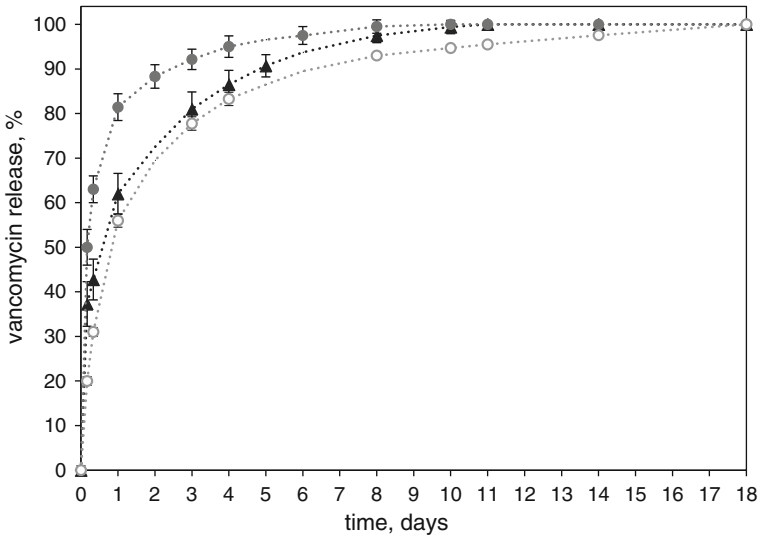

Fig. 9 Cumulative antibiotic release from β-TCP-15% PCL (*triangles*), β-TCP-15% PLA (*filled circles*) and β-TCP-30% PLA (*open circles*) composite disks containing 5 wt% vancomycin as a function of immersion time in TRIS buffer solution at 37°C [58]. Reprinted from [58] with kind permission from Springer Science+BusinessMedia

with the higher (30 vol.%) polymer fraction. This must be due to the significantly lower porosity of the latter material (6 vs. 13%, Table 1). Given our earlier assumption that vancomycin is released via a diffusion mechanism, higher porosity should favor faster drug release. Among the two composites with the same polymer volume fraction (15%), the material with PLA as the polymer phase releases vancomycin faster than the one with PCL. The small difference in the general porosity of these two composites (11 vs. 13%, Table 1) can hardly have such a pronounced effect on drug release. The slower vancomycin release from the PCL- versus PLA-containing material could be due to the smaller water uptake of the more hydrophobic PCL polymer which makes diffusion of the drug more difficult. So far, a β-TCP-30 vol.% PLA composite has exhibited the most attractive gently-sloping drug release profile and the highest compression strength ($\sim$200 MPa, Table 1).

3 Two-Step Processing of CDHA-PLA Nanocomposites: Effect of CDHA Surface Modification

3.1 CDHA Nanopowder Synthesis

Calcium deficient hydroxyapatite, (CDHA) $Ca_{10-x}(HPO_4)_x(PO_4)_{6-x}(OH)_{2-x}$ nanopowder with Ca/P ratio $\sim$1.5 was prepared by microwave accelerated wet method [82] according to the following reaction:

$$9Ca(NO_3) + 6H_3PO_4 \rightarrow Ca_9(HPO_4)(PO_4)_5(OH)_{\downarrow} \quad (2)$$

XRD analysis confirmed that the synthesized CaP powder was a single-phase hydroxyapatite, HA [71]. FTIR spectrum of the powder (Fig. 10a) is also typical for hydroxyapatite [82]. The presence of the P–O–H band at 873 cm^{-1} corresponding to bivalent phosphate ion, HPO_4^{2-}, suggests that the HA formed is a Ca-deficient compound, $Ca_{10-x}(HPO_4)_x(PO_4)_{6-x}(OH)_{2-x}$ (CDHA). CDHA is indistinguishable from stoichiometric HA by XRD, however, unlike stoichiometric HA, it will decompose upon heating to 750°C to β-tricalcium phosphate, $Ca_3(PO_4)_2$ (β-TCP), and stoichiometric HA [41]. Indeed, following a 2 h anneal at 750°C, the only phase detected by XRD in our synthesized powder was β-TCP. Full conversion into β-TCP was also supported by FTIR analysis: the bands of structural OH^- (at 635 and 3,569 cm^{-1}) and HPO_4^{2-} (at 873 cm^{-1}) characteristic of hydroxyapatite disappear from the spectrum of the annealed powder (Fig. 10c).

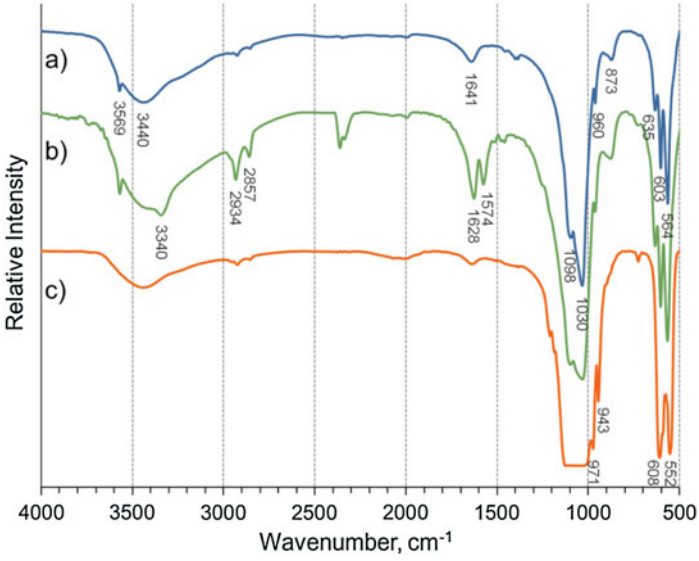

Fig. 10 FTIR spectra of: *a*—as-synthesized CDHA powder; *b*—HDI-modified CDHA powder; *c*—CDHA powder annealed at 750°C for 2 h [71]. Reprinted from [71] with kind permission from SpringerScience+Business Media

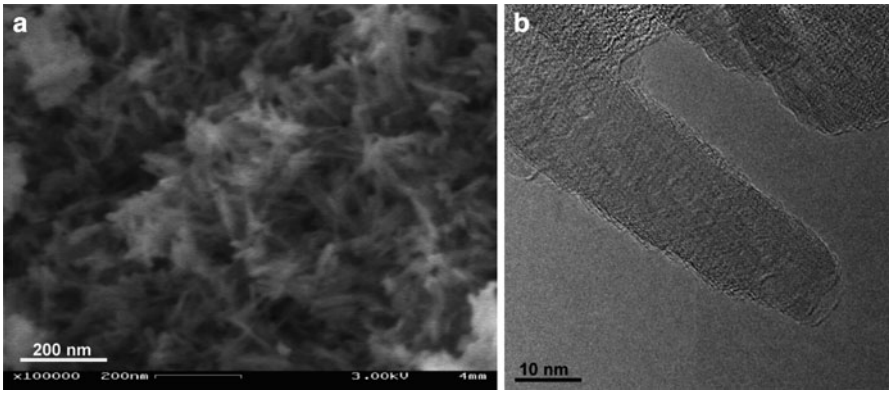

Fig. 11 Representative images of as-synthesized CDHA powder: **a** HRSEM; **b** TEM [71]. Reprinted from [71] with kind permission from SpringerScience+Business Media

These results confirm that the powder synthesized was indeed a Ca-deficient HA with x close to unity: $Ca_9(HPO_4)(PO_4)_5(OH)$. The Ca/P ratio of such CDHA is $\sim$1.5, and its solubility is comparable to that of β-TCP [6]. HRSEM and TEM micrographs (Fig. 11) demonstrate the needle-like morphology of the obtained CDHA particles and their nanoscale dimensions ($\sim$15 nm diameter and 50–150 nm length).

The specific surface area of the synthesized CDHA powder, as determined by BET, was $\sim$95 m^2/g. For needle-like (cylindrical) powder morphology, the relation between particle's dimensions and the specific surface area [SSA, (m^2/g)] is given by Chen et al. [9]:

$$\mathrm{SSA} = \frac{2 + 4L/d}{L\rho} \cdot 1,000 \tag{3}$$

where L and d are particle length and diameter in nm, respectively, and ρ is the density (3.156 g/cm^3 for CDHA). Basing on the above equation, the surface area of 95 m^2/g corresponds to a very fine nanoscale powder with the particle diameter of $\sim$15 nm, which is in a good agreement with the micrographs in Fig. 11.

3.2 CDHA Surface Modification with Isocyanate

The surface of CDHA nanopowder was covalently modified with hexamethylene diisocyanate (HDI) according to a method reported in Liu et al. [54]. As shown in Scheme 1, the surface hydroxyl groups of hydroxyapatite can react with isocyanates to form a covalent urethane bond. A typical FTIR spectrum of the synthesized CDHA powder treated with hexamethylene diisocyanate (CDHA-HDI) (Fig. 10b) contains new peaks in addition to those of CDHA: 1,574 and 1,628 cm^{-1} (amide bands); 2,857 and 2,934 cm^{-1} (–CH_2– bands); 3,340 cm^{-1}

Scheme 1 Reaction of hexamethylene diisocyanate (HDI) with HA powder

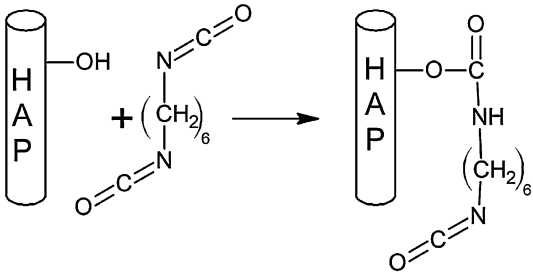

(–NH– band). This shows formation of covalent urethane bonds during the modification reaction. The details of such attachment, however, require further exploration. In earlier solid state ^{1}H-NMR [54, 55] and ^{13}C- and ^{31}P-NMR [14] studies, two different attachment paths were suggested: one through covalent bonding between isocyanate and structural hydroxyl groups, and the other—through the formation of PO–C(O)NH– bonds between isocyanate and P–O–H moieties of HPO_4^{2-} groups.

The mixing of unmodified and HDI-modified CDHA powder with the chloroform solution of PLA [71] resulted in complete incorporation of the dissolved polymer in CDHA-PLA composite powder.

3.3 Mechanical Properties

High pressure consolidation of CDHA-PLA composite nanopowder at 2.5 GPa at room temperature produced 82–90% dense specimens depending on the extent of modification and overall organics content. The highest density of 90% was obtained for the material with 40% total organics and 10% modification (CDHA-10H-40). Typical stress–strain curves of specimens tested in compression are presented in Fig. 12. It can be seen that both strength and ductility increase with increasing total organic content. At 40 vol.% organics, the plastic strain reaches $\sim$2% which is comparable with the plastic strain of pure PLA at room temperature [81]. Even without HDI modification, cold sintered CDHA-40 vol.% PLA nanocomposites have a high compression strength, σ_c, of 225 MPa. This is 1.5 times stronger than the hot pressed (194°C, 98 MPa) composites having a practically identical composition (HA-41 vol.% PLA, σ_c = 140 MPa) [38–40]. The high strength values obtained in our work may be the result of a more homogeneous phase distribution achieved through the use of the much finer CaP nanopowder (specific surface area SA = 95 m^2/g in our work vs. SA = 5 m^2/g in Ignjatović et al. [38]).

As shown in Fig. 13, the modification of CDHA with HDI further increased the compressive strength of CDHA-based composites with organic content $\geq$20 vol.%. The improvement of mechanical properties is especially obvious for the composites containing 40 vol.% organics. Compressive strengths of $\sim$265 and

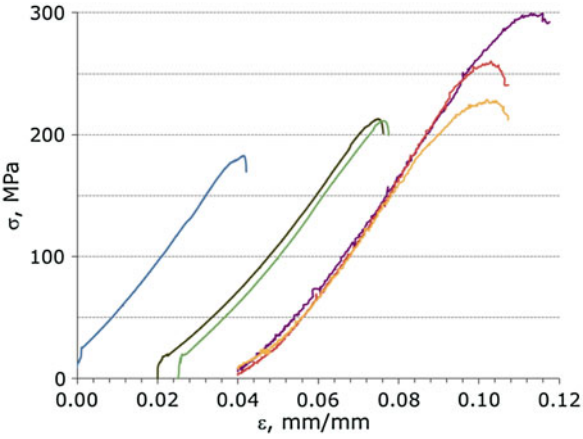

Fig. 12 Stress–strain curves in compression of CDHA-PLA nanocomposites with different total organic contents: 20% (*blue*—7% modification extent) 30% (*green*—no modification, *black*—10% modification extent) and 40% (*yellow*—no modification, *red*—7% modification extent, *purple*—10% modification extent) [71]. Reprinted from [71] with kind permission from SpringerScience+Business Media

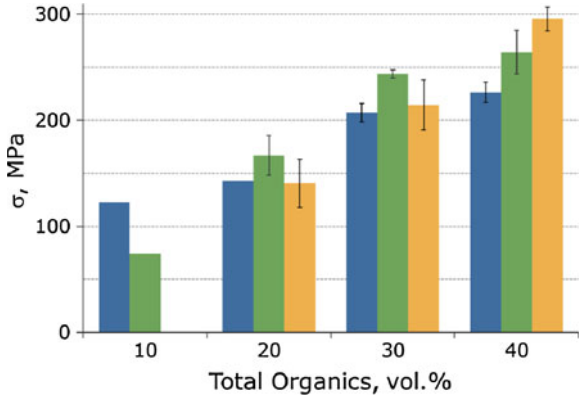

Fig. 13 Compressive strength as a function of total organic fraction and HDI surface modification: *blue*—no modification; *green*—7% modification extent; *yellow*—10% modification extent [71]. Reprinted from [71] with kind permission from SpringerScience+Business Media

∼295 MPa were obtained for 7 and 10% modification, respectively, which constitutes 15 and 25% improvement compared to the unmodified CDHA-40 vol.% PLA composite. This improvement is believed to be due to the better bonding integrity between the HDI-modified CDHA surface and PLA molecules.

4 One-Pot Synthesis of Ca Phosphate-PCL Composite Powder

4.1 Synthesis by Direct Reaction Between Phosphoric Acid and Ca Acetate

A single-step processing route was developed with goal to obtain a more intimate intermixing of the CaP ceramic and polymer nanocomponents. Reaction (1) [7] was the starting point for the one-pot synthesis of Ca phosphate-PCL composite

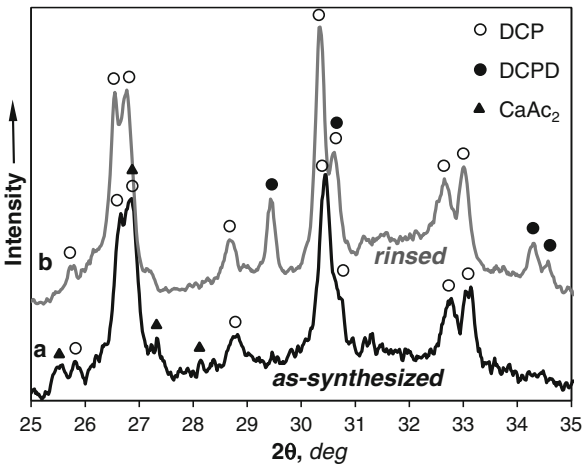

Fig. 14 XRD patterns of the powder synthesized by reaction between phosphoric acid and calcium acetate in THF with dissolved PCL: *a*—as synthesized; *b*—water rinsed [57]. Reprinted from [57] with kind permission from SpringerScience+Business Media

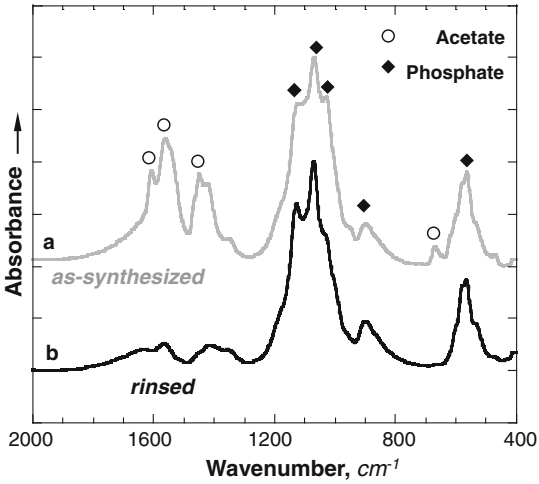

Fig. 15 FTIR spectra of the powder synthesized by reaction between phosphoric acid and calcium acetate in THF with dissolved PCL: *a*—as synthesized; *b*—water rinsed [57]. Reprinted from [57] with kind permission from SpringerScience+Business Media

powder. Since PCL is practically insoluble in methanol, Tetrahydrofurane (THF) was used as the reaction medium capable of dissolving the PCL polymer. In brief, H_3PO_4 was dissolved in THF after which $CaAc_2$ was added while stirring [57]. The XRD pattern of the powder obtained either in pure THF or in THF with dissolved PCL is shown in Fig. 14a. It can be seen that, instead of the expected β-TCP, the calcium phosphate product is dicalcium phosphate, $CaHPO_4$ (DCP). Small peak of unreacted calcium acetate can be detected, too. Strong bands of acetate (at 1,400–1,600 cm^{-1}) are also present in the FTIR spectrum, Fig. 15a. This means that the synthesis reaction does not proceed to the completion and can be described as:

$$3Ca(OOCCH_3)_2 + 2H_3PO_4 \leftrightarrow 2CaHPO_4 + 2CH_3COOH + Ca(OOCCH_3)_2 \quad (4)$$

The unreacted Ca acetate could be easily removed by water rinsing, leaving behind a mixture of DCP and dicalcium phosphate hydrate (DCPD), Figs. 14b and 15b.

No visible polymer agglomeration or deposition on the reaction vessel walls was observed when synthesis was performed in THF with dissolved PCL suggesting that all the PCL was incorporated in the product powder. The presence of predetermined amounts of polymer in the DCP/DCPD-15 PCL composite powders was further confirmed by the results of double extraction in dichloromethane and ethyl acetate. Such DCP/DCPD-PCL composite powders could become a useful material for fabrication of bioresorbable implants. The dissolution rate of such implants, however, could be too high for bone healing applications due to the rapid dissolution of the DCP/DCPD component. Therefore, the synthesis route of CaP-PCL composites by direct reaction between Ca acetate and phosphoric acid was not further pursued.

4.2 Synthesis by Reaction Between Phosphoric Acid, Sodium Methoxide and Ca Acetate

Once the difficulty of obtaining β-TCP by the direct reaction between Ca acetate and phosphoric acid had been established, several process modifications were attempted. The procedure that was finally decided upon involved the addition of an organic sodium base, sodium methoxide, $NaOCH_3$ as an intermediate step, the planned reaction sequence being:

$$H_3PO_4 + 3NaOCH_3 \leftrightarrow Na_3PO_4 + 3CH_3COH \tag{5a}$$

$$2Na_3PO_4 + 3Ca(OOCCH_3)_2 \leftrightarrow Ca_3(PO_4)_2 + 6NaCOOH \tag{5b}$$

Reaction (5a) was used to produce a homogeneous suspension of very fine Na_3PO_4 salt particles to be further transformed into β-TCP by reaction with $CaAc_2$ (5b) [57].

According to XRD analysis, the reaction between sodium methoxide, phosphoric acid and calcium acetate (Eqs. 5a, b) in THF, with or without dissolved PCL, produced, after 1–24 h stirring, an increasing amount of sodium acetate hydrate ($NaAc*3H_2O$) and decreasing amounts of sodium phosphate and calcium acetate hydrate ($CaAc_2*0.5H_2O$). No evidence of polymer phase separation was observed during processing. After 2 days of stirring, calcium acetate reagent was no longer detected in the XRD pattern, Fig. 16a. On the other hand, the peaks of the sodium acetate product were so strong that they concealed almost completely the shallow peaks of Ca phosphate. Removing the water-soluble components left behind a very fine white powder being, according to XRD, a pure calcium phosphate (Fig. 16b). The peak positions in the XRD pattern in Fig. 16b, however, do not correspond to the expected β-TCP but fit rather closely those of hydroxyapatite

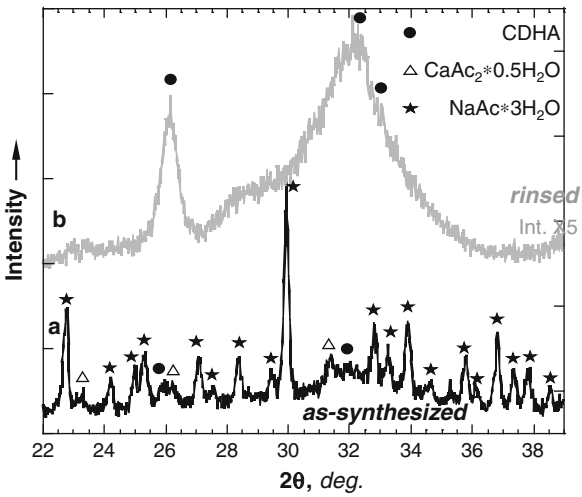

Fig. 16 XRD patterns of as-synthesized (*a*) and water rinsed (*b*) CaP-11PCL powder obtained by reaction between phosphoric acid, sodium methoxide and Ca acetate. Similar patterns were obtained for CaP-24PCL and pure CaP powders synthesized in the same way [57]. Reprinted from [57] with kind permission from SpringerScience+Business Media

(HA), $Ca_{10-x}(HPO_4)_x(PO_4)_{6-x}(OH)_{2-x}$. The peaks are broad and shallow suggesting a very fine nanocrystalline structure of the synthesized HA.

The stoichiometry of hydroxyapatite (the value of x) is important as it strongly affects the material's solubility. Stoichiometric HA, $Ca_{10}(PO_4)_6(OH)_2$ ($x = 0$) is practically insoluble in the body fluids, whereas the solubility of Ca-deficient HA (CDHA) increases with increasing x approaching that of β-TCP at $x = 1$ [6]. Although XRD patterns of HA and CDHA are very similar, the two compounds can be easily distinguished if heated above 700°C: the stoichiometric HA will remain unchanged whereas CDHA will transform into a mixture of HA and β-TCP for ($0 < x < 1$) or pure β-TCP (for $x = 1$) [41]. Our synthesized powder, when annealed at 700°C, 30 min, transformed almost completely in β-TCP, implying that the materials is a Ca-deficient HA with x slightly less than unity. It is believed that the formation of CDHA instead of the planned β-TCP occurs due to some water absorption by the strongly hygroscopic sodium methoxide and can be described by the following reaction:

$$\begin{aligned} &H_3PO_4 + NaOCH_3 + Ca(OOCCH_3)_2 + H_2O \\ &\quad \leftrightarrow Ca_{10-x}(HPO_4)_x(PO_4)_{6-x}(OH)_{2-x} + NaCOOH + CH_3COH \end{aligned} \tag{6}$$

The yield of synthesized CDHA powder increased with stirring time leveling off after approximately 2 days. Assuming $x = 1$, the amount of CDHA obtained in pure THF (without dissolved PCL) corresponded to near 100% conversion of the reagents according to Eq. 6.

The amount of PCL in the CHDA/PCL composite powders (extracted by double extraction in dichloromethane and ethyl acetate) was found to be lower than the amount initially dissolved in THF, see Table 3. It is assumed that the addition of a strongly basic sodium methoxide to THF causes chain scission of dissolved PCL and the resulting low molecular weight fragments are removed during subsequent water rinsing.

Table 3 Properties of one-pot synthesized CDHA-PCL nanocomposites [24]

Designation	Nominal PCL fraction (vol.%)	Measured PCL fraction (vol.%)	Density (% TD)	Compressive strength (MPa)
CDHA-11PCL	11	5	88 ± 2	128 ± 4
CDHA-24PCL	24	14	91 ± 2	142 ± 5

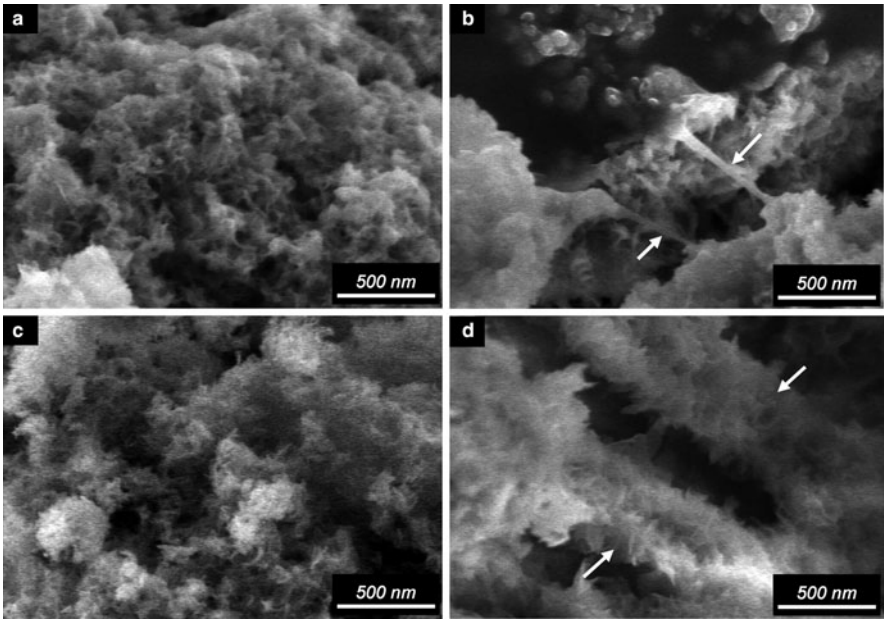

Fig. 17 Representative HR-SEM micrographs of the synthesized CDHA-11PCL (**a**, **b**) and CDHA-24PCL (**c**, **d**) composite powders [57]. Reprinted from [57] with kind permission from SpringerScience+Business Media

In Fig. 17, high resolution SEM images of the synthesized CDHA-PCL powder are presented. The powder has a very fine nanoscale needle-like morphology typical of CDHA [53]. The polymer phase is difficult to detect suggesting its homogeneous distribution. Occasionally, thin polymer fibers, Fig. 17b (arrows) or thin polymer strips decorated with CaP nanocrystals, Fig. 17d (arrows) can be observed.

Room temperature consolidation of CDHA-11PCL and CDHA-24PCL powders at 2.5 GPa yielded relatively dense composite materials with porosity not exceeding 12%, Table 3. The surface of consolidated disks was smooth, with no visible pores detected in HRSEM, Fig. 18, suggesting that either the pores are extremely fine (nanometers) or that polymer flow during high-pressure consolidation results in pore closure on the tablet surface. The compression strength, $\boldsymbol{\sigma_c}$, of the CDHA-11PCL and CDHA-24PCL specimens was about 130 and 145 MPa, respectively, Table 3.

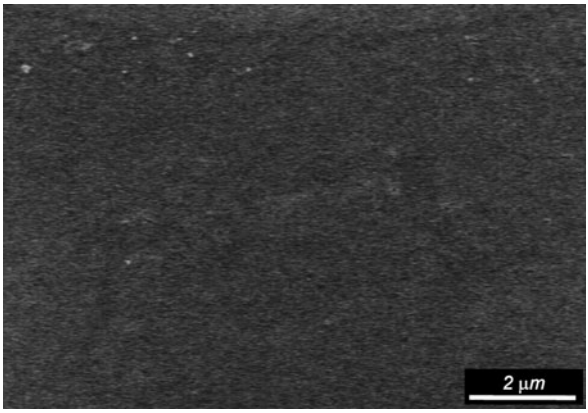

Fig. 18 Surface of high pressure consolidated CDHA-24PCL nanocomposite as seen in HRSEM [24]. Reprinted from [24] with kind permission from Elsevier

4.3 Effect of Polymer Content on Cell Interaction with CDHA-PCL Nanocomposites

Cell studies were conducted in monocultures of primary osteoblasts (pOB) and human umbilical vein endothelial cells (HUVEC), as well as in co-cultures of pOB and human outgrowth endothelial cells (OEC) [24].

4.3.1 Biocompatibility of CDHA-PCL Disks to Endothelial Cells and pOB

An essential feature of the biomaterials used in the construction of bio-engineered tissues is the biocompatibility of such materials. In this study, we used HUVECs to test the biocompatibility of CDHA-11PCL and CDHA-24PCL disks to endothelial cells. HUVECs cultured on CDHA-PCL disks for 1 and 2 weeks were assessed by confocal microscopy (Fig. 19a–d). Samples were stained for the endothelial marker CD31 (green) and cell nuclei (blue) for CLSM. HUVECs were found to form an interconnected endothelial monolayer with intercellular contacts. Comparing the HUVECs cultured on CDHA-PCL disks with different polymer content, after both 1 week (Fig. 19a, b) and 2 weeks (Fig. 19c, d), the HUVECs on the CDHA-24PCL disks (Fig. 19b, d) formed a more homogeneous endothelial monolayer than those on the CDHA-11PCL disks (Fig. 19a, c). To assess the influence of the two CDHA-PCL variants on endothelial cell growth we performed quantitative realtime PCR for two endothelial markers, CD31 (PECAM) and vWF (Fig. 19e), after 2 weeks of culture. Relative gene expression of CD31 did not change, whereas VWF seems to be increased on the CDHA variant prepared with 24% PCL.

Primary osteoblasts grown in monoculture on CDHA-PCL disks for 1 and 2 weeks were stained with Calcein-AM and imaged by CLSM (Fig. 20a–d). In all

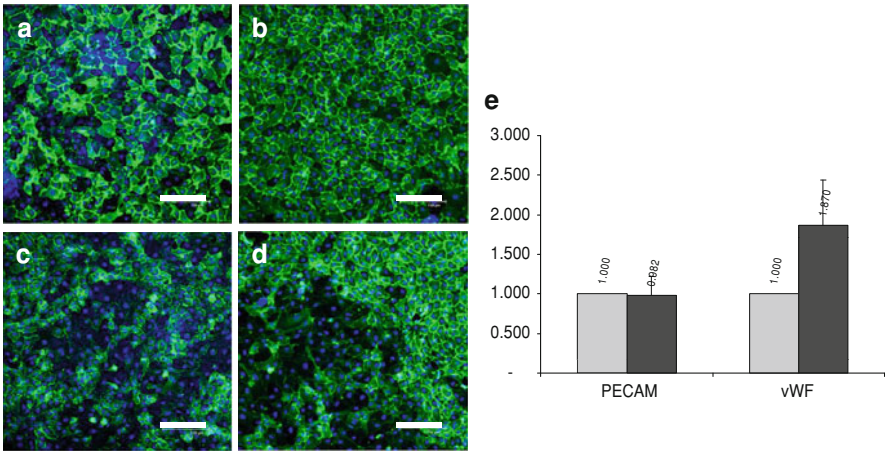

Fig. 19 Cell growth of HUVECs on CDHA-PCL disks. HUVECs were cultured on CDHA-11PCL (**a**, **c**) and CDHA-24PCL disks (**b**, **d**) for 1 week (**a**, **b**) and 2 weeks (**c**, **d**). Samples were imaged by CLSM after staining for CD31 (*green*) and cell nuclei (*blue*) (**a**–**d**). qRT-PCR analysis (**e**) suggested a similar relative expression level of CD31 (PECAM) and a higher expression level of vWF on CDHA-24PCL disks (*black bar*) compared with CDHA-11PCL disks (*gray bar*) investigated after 2 weeks. Bar = 150 μm [24]). Reprinted from [24] with kind permission from Elsevier

cases, viable cells were observed over the entire surface of the scaffolds, and these cells formed a compact cell layer with no obvious differences in the general cell growth influenced by the material composition (A, C: CDHA-11PCL; B, D: CDHA-24PCL) or culture time (A, B: 1 week; C, D: 2 weeks). In real-time PCR both material variants supported the increase in a series of osteogenic differentiation markers with progressing culture time. These were ALP, osteocalcin (OC), osteonectin (ON), osteopontin (OP) and runt-related transcription factor (Runx-2). Differences were statistically significant in the case of the CDHA-11PCL for some of the markers as indicated in Fig. 20e. The direct comparison of osteogenic differentiation after 4 weeks on the material variants showed a slightly better trend for the CDHA material variant containing 11% PCL, which was only found to be significant in the case of OC.

4.3.2 Expression of Osteoblastic Markers and Endothelial Markers in Cocultures

To gain insight into the expression of endothelial and osteogenic markers in the co-cultures grown on CDHA with either 11 or 24% polycaprolactone, qRT-PCR studies were performed. The total mRNAs were isolated from OEC-pOB co-culture samples after 1 and 4 weeks, and the relative expression of osteoblastic markers such as ALP, OC, OP and ON and the typical endothelial markers CD31

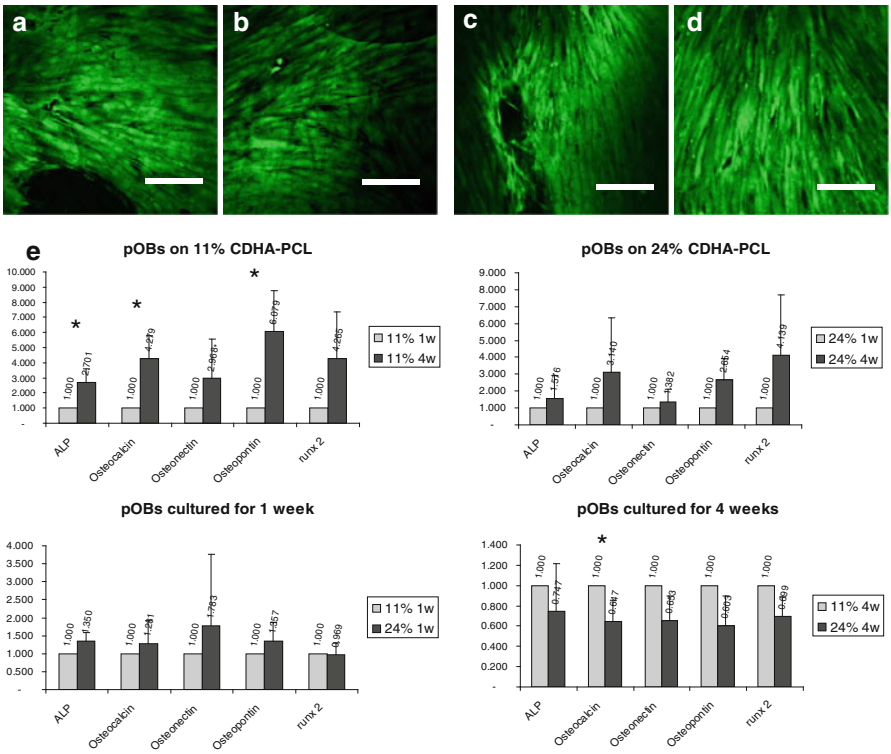

Fig. 20 Cell growth of pOB on CDHA-PCL disks. pOB were cultured on CDHA-11PCL (**a**, **c**) and CDHA-24PCL disks (**b**, **d**) for 1 week (**a**, **c**), 2 weeks (**c**, **d**). Samples were stained with Calcein-AM (*green*) and assessed by confocal microscopy. Relative expression of the osteogenic markers OC, ALP, OP, ON and Runx-2 were investigated by qRTPCR (**e**). Bar = 200 lm, $*p < 0.05$ [24]. Reprinted from [24] with kind permission from Elsevier

(PECAM) and vWF were quantified by being normalized to the house-keeping gene GAPDH. Samples were compared in four groups according either to culture time or to the material substrate (Fig. 21). On the CDHA-11PCL disks (Fig. 21a), ALP (significantly, $p < 0.05$), vWF and CD31 were less expressed after 4 weeks than after 1 week, whereas the relative expression of OC, OP and ON was similar after both time points. On the CDHA-24PCL disks (Fig. 21b), OC, OP, CD31 and vWF were up-regulated, whereas ALP and ON were down-regulated after 4 weeks compared to 1 week of cultivation. Comparing the expression of markers on CDHA with 11 and 24% PCL after 1 week (Fig. 21c), ON was expressed to a greater extent on CDHA-24PCL disks than on the 11% variant, whereas the other markers were expressed at similar levels. At the later stages of the culture after 4 weeks of cultivation (Fig. 21d), OC, ON and vWF (significantly, $p < 0.05$) were up-regulated. At the same time, ALP was significantly less expressed on the

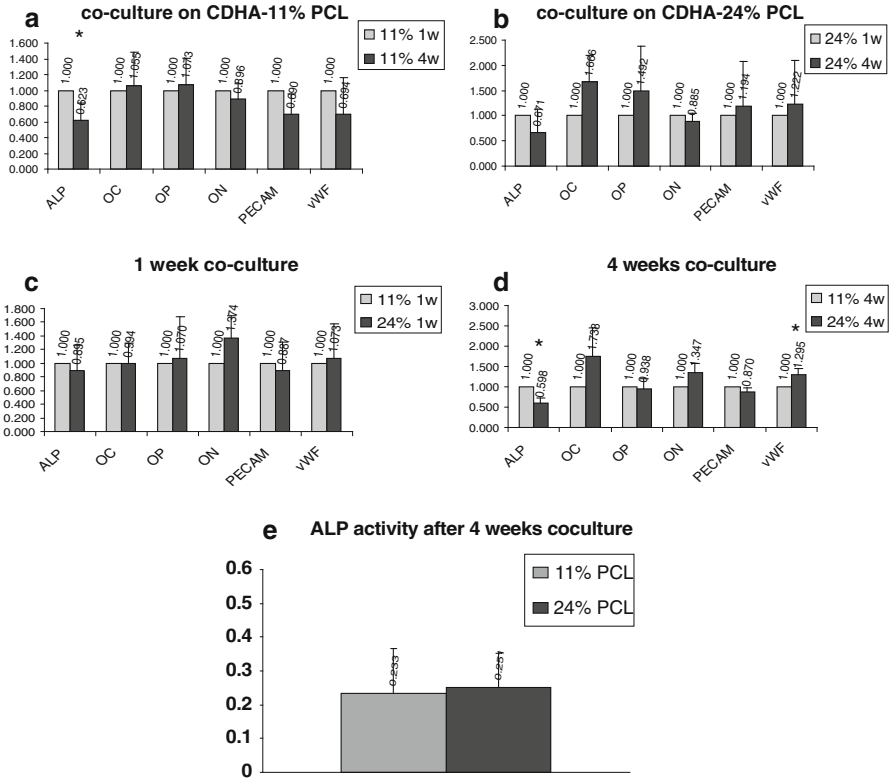

Fig. 21 Real-time PCR analysis and ALP activity test of OECs and pOBs co-cultured on CDHA-PCL disks. OECs and pOBs were co-cultured on CDHA-PCL disks for 1 and 4 weeks, and the relative expression of the endothelial markers PECAM (CD31) and vWF and the osteoblastic markers OC, ALP, OP, ON and Runx-2 was compared according to either polymer content (**a** CDHA-11PCL; **b** CDHA-24PCL) or incubation time (**c** 1 week; **d** 4 weeks). The ALP activity of the co-culture samples were assessed after 4 weeks of cultivation (**e**). $n = 3$, $^*p < 0.05$ [24]. Reprinted from [24] with kind permission from Elsevier

CDHA-24PCL disks compared to those with 11% PCL, whereas OP and CD31 were expressed similarly on both material variants.

4.3.3 ALP Activity in Co-Cultures

To further assess the osteogenic differentiation in the co-cultures depending on the PCL content of CDHA-PCL, we determined the ALP activity after 4 weeks of co-culturing. In total, three donors of OEC and pOB were co-cultured on CDHA-PCL disks for the ALP activity test. As indicated in the diagram (Fig. 21e), the ALP activity of co-cultures was similar on both material variants.

4.3.4 Microvessel Formation of OEC Co-Cultured with pOB on Different CDHA-PCL Variants

In order to study the effect of polymer content in the CDHA-PCL disks on the formation of pre-vascular structures, three donors of OEC and pOB were co-cultured on CDHA-PCL disks for 1 and 4 weeks before being assessed by CLSM (Fig. 22; donor 1: a–d; donor 2: e–h; donor 3: i–l). Samples were stained for CD31 (green), specifically detecting endothelial cells in the co-cultures. After 1 week of co-culture on the CDHA-11PCL disks (Fig. 22a, e, i), mainly monolayers and elongated OEC were detected, whereas microvessel-like structures dominated on the 24% CDHA-PCL disks after 1 week (Fig. 22c, g, k). This effect was reproducible for all tested donors, although the temporal dynamics in the formation of vascular structures was slightly different due to inter-donor variation. After 4 weeks, endothelial cells reacted very similarly on both the CDHA-11PCL (Fig. 22b, f, j) and CDHA-24PCL disks (Fig. 22d, h, l), and formed networks of pre-vascular structures (Fig. 22b, d). In some areas endothelial cells also formed larger aggregates of endothelial cell patches.

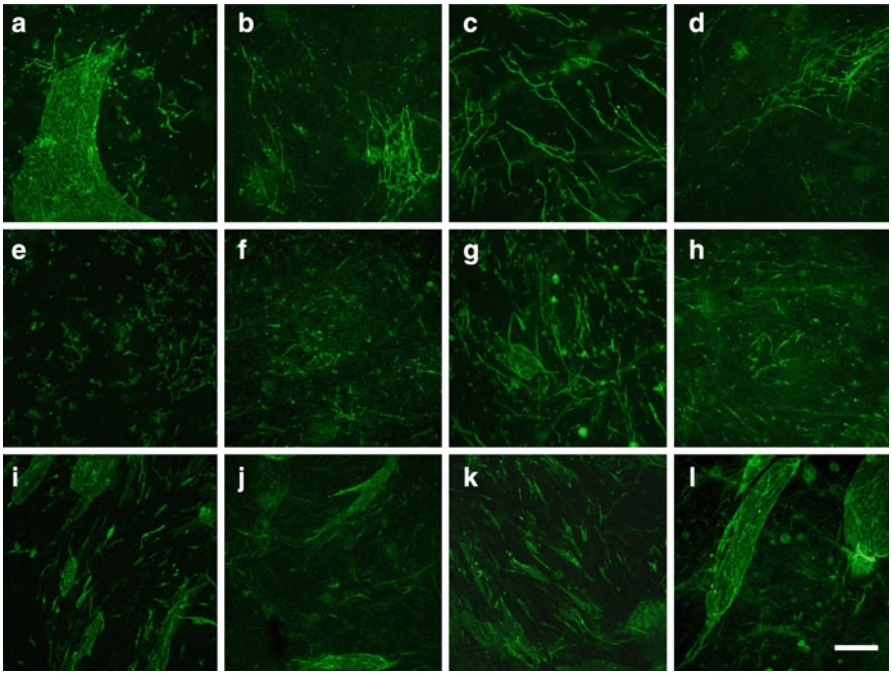

Fig. 22 Formation of microvessel-like structures in co-culture samples. Three donors of both OEC and pOB (donor 1, **a–d**; donor 2, **e–h**; donor 3, **i–l**) were co-cultured on CDHA-11PCL disks (**a**, **b**, **e**, **f**, **i**, **j**) and CDHA-24PCL disks (**c**, **d**, **g**, **h**, **k**, **l**) for 1 week (**a**, **c**, **e**, **g**, **i**, **k**) and 4 weeks (**b**, **d**, **f**, **h**, **j**, **l**). Samples were stained for CD31 (*green*) and imaged by CLSM. Bar = 150 μm [24]. Reprinted from [24] with kind permission from Elsevier

4.3.5 Quantitative Evaluation of Microvessel Formation on CDHA-PCL Variants

In order to quantify the development of the pre-vascular network on CDHA with 11 or 24% PCL, morphometric analysis of the vascular structures for different donors of OEC was performed after 1 and 4 weeks of culture (Fig. 23). Elongated vascular structures or structures with so-called vascular sprouts were included in the analysis, whereas continuous endothelial cell layers or single cells were not considered as vascular structures. In accordance with the morphological observations in Fig. 22, the extent of vascular structures was significantly increased on CDHA with 24% PCL after 1 week in comparison to CDHA with 11% PCL. This was documented by using several parameters for vascular structures, such as tube area and tube length, as well as number of nodes and meshes. After 4 weeks of culture the vascular structures on CDHA-24PCL regressed significantly,

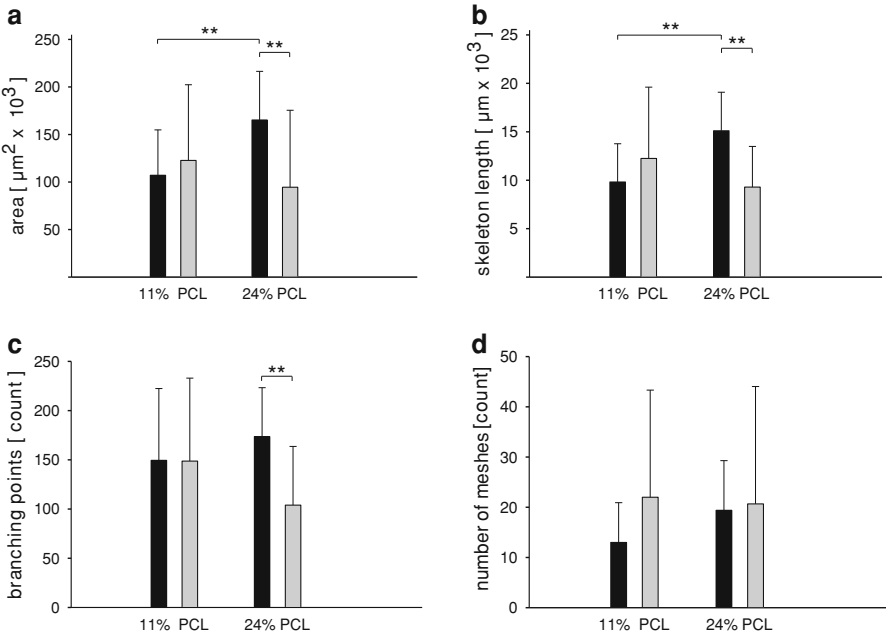

Fig. 23 Image quantification of vascular structures in co-cultures of OEC and pOB after 1 and 4 weeks of culture. The total area (**a**) and length (**b**) of vessel-like structures was quantified after 1 week (*black bars*) and 4 weeks (*gray bars*) of incubation on 11 and 24% PCL, respectively. After 1 week, both parameters are significantly increased on 24% PCL ($p < 0.01$). However, prolonged incubation on 24% PCL results in reduced vessel formation, indicated by a significant decrease in area (**a**), length (**b**), branching points (**c**) and number of meshes (**d**). This reduced vessel formation with long-term incubation is not observed on 11% PCL (values are given as means ± SD, $n = 15$; asterisks indicate significant difference ($^{**}p < 0.01$) between means tagged by the *horizontal bars*) [24]. Reprinted from [24] with kind permission from Elsevier

suggesting different dynamics in the formation of these structures on CDHA with 24 or 11% PCL.

4.3.6 Discussion

In this study we evaluated CDHA-PCL nanocomposite disks containing nominally 11 or 24% polymer as scaffolding materials for bone tissue engineering. We investigated the general biocompatibility of the two material variants to EC and pOB, as well as the influence of polymer content on the cell growth and functionality of individual cell types. Furthermore, the effect of polymer content on the formation of microvessel-like structures in a complex co-culture system consisting of OEC and pOB was evaluated by confocal microscopy and image quantification.

In recent years, co-culture systems have become of scientific interest as advanced in vitro models aiming to analyse mechanisms of vascularization in close approximation to complex physiological processes, as reviewed in Grellier et al. [26], Kirkpatrick et al. [49], Rivron et al. [74], and Santos and Reis [77]. Several studies applied co-cultures to analyse the cellular interaction of endothelial cells with other cell types [19, 22, 27, 28], either to mimic the neovascularization of tissue-engineered constructs [23, 76] or to assess the biocompatibility of biomaterials [11, 78, 87]. In addition, such co-cultures seem to be of therapeutical interest due to their positive effect on the vascularization of tissue constructs in vivo [34, 47, 48, 92]. Nevertheless, due to the complexity of such systems and the need to distinguish between the reactions of the individual cell types, it is necessary to compare the reaction of co-cultures with the relevant monocultures. In this study we compared the reaction of HUVECs as an endothelial cell reference cell type towards CDHA-PCL containing nominally 11 or 24% PCL. Larger interconnected patches of endothelial cells in confocal microscopy and a tentatively higher expression of the endothelial marker vWF on CDHA with 24% PCL suggest a beneficial influence of the polymer content on endothelial cell growth. In the co-cultures consisting of OEC and pOB, the beneficial influence of the higher PCL content seems to be reflected by a more extensive formation of angiogenic structures on CDHA with 24% in comparison to 11% PCL. This was only observed at the first time point of investigation, i.e. after 1 week of co-culture, whereas at a later time point (4 weeks) the CDHA-PCL with 11% seems to be superior for the formation of angiogenic structures. Angiogenesis is a highly dynamic process showing an increase in vascular structures over a certain time frame. The process is regulated by several factors, depending also on the interaction with other cell types that produce matrix components and angiogenic factors. This was also recently documented for the co-cultures of OEC and pOB, revealing that pOB produce angiopoietin 1 and VEGF [13]. Furthermore, the formation of angiogenic structures varies amongst the individual donors showing differences in the extent or the velocity of the angiogenic process. Nevertheless, the beneficial influence of the higher polymer content in the present study was consistent in all tested donors. Although the reason for this observation remains to

be further elucidated, the more equal distribution of endothelial cells on CDHA-PCL with higher polymer content, as indicated by confocal microscopy, might facilitate the arrangement of endothelial cells towards vascular structures. Intercellular interaction and molecular signaling within endothelial layers play a significant role in the assembly of vascular structures. Inter-endothelial contacts harboring adherens junctions and the corresponding molecules, known as cadherins, mediate the intercellular signal exchange and control the formation of angiogenic structures [8]. Promotion of the formation of larger inter-endothelial cell patches on CDHA with 24% PCL and the more equal distribution of endothelial cells on this CDHA-PCL variant might well favor inter-endothelial communication.

In contrast to cells grown on CDHA-24PCL, the endothelial cells grown on the CDHA-11PCL seem to be slower in forming such structures, resulting in the improved formation of vascular structures on CDHA with 11% PCL at the later time point (4 weeks). Thus, the polymer content seems to influence the temporal dynamics of angiogenesis. According to the real-time PCR data, it seems that CDHA with 24% PCL is beneficial for endothelial cell growth after longer periods of cultivation (2 weeks). Takinginto account the need for a fast connection to the vascular supply, including a high biocompatibility to endothelial cells, the current data suggest that CDHA-PCL with the higher polymer content should be preferred for vascularization strategies.

In terms of the general biocompatibility towards osteogenic cells grown on CDHA-PCL, calcein-AM staining showed an equal distribution of human primary osteoblasts on both variants of CDHA with PCL. In addition, we investigated the influence of the PCL content on the differentiation of osteoblasts in monocultures with time. On both variants of CDHA-PCL primary osteoblasts showed the up-regulation of several osteogenic markers with culture time, although this finding was only statistically significant in the case of CDHA with 11% PCL. Up-regulation over a time frame of 4 weeks of cultivation was observed for several osteogenic markers, such as ALP, OC, ON, OP and Runx-2. According to the literature, the expression of ALP is associated with the state of differentiation in osteoblasts and decreases during mineralization. Increased expression of OP [47, 61] and OC [69] correlates with the formation of mineralized bone tissue, while ON is associated with collagen type I, hydroxyapatite and calcium, involved in the bone mineralization process [66, 79]. In addition, up-regulation of the transcription factor Runx-2, which plays a significant role in osteoblast differentiation [17, 50], suggests an ongoing differentiation of primary osteoblasts on both CDHA-PCL variants. In the co-cultures, no obvious influence of the PCL content on the marker expression could be detected by real-time PCR or on the functional level by ALP activity assessment. In the real-time PCR the expression of alkaline was tentatively lower on the 24% variant of CDHA-PCL at the later time point, but was statistically significant only in case of the co-cultures. On the functional level, no influence of the PCL content on the ALP activity could be confirmed, thus there is a lack a clear evidence for the influence of the PCL content on osteogenic differentiation. Based on the current observations from mono- and co-culture

experiments, we conclude that there is no significant influence of the PCL content on osteogenic differentiation.

Several reports from the literature have reported good biocompatibility and osteoconductivity of CDHA in combination with mesenchymal stem cells [30, 44, 45]. A series of studies used CaP based materials in combination with PCL as potential materials in bone tissue engineering with a high biocompatibility and functionality towards osteogenic cells [94] or endothelial cells [92, 93]. However, it is important to evaluate how the material composition influences the individual cell types, as well as the interaction of different cell types involved in tissue formation and angiogenesis, such as endothelial cells and osteoblasts in the bone. This study indicates that co-culture models can be used to analyze how such material variations affect cellular function, resulting in potential consequences for biomaterial design. Further studies will have to reveal how such approaches can be adapted for three-dimensional scaffolds with different PCL contents, which will have to be evaluated in vitro and in vivo in terms of the properties needed to support both bone formation and appropriate vascularization of such tissue constructs.

In conclusion, in this study we provide evidence that the PCL content in CDHA-PCL nanocomposites influences more than just the material properties, such as compression strength. We demonstrate that the PCL also influences the formation of pre-vascular structures by OEC, a process which seems to be controlled by inter-endothelial communication as well as by the close interaction of endothelial cells with osteogenic cells, as presented in this and many other studies. In addition, this study further highlights the potential of co-culture models as in vitro models to study cell–material interaction especially with regard to complex processes such as angiogenesis.

5 Summary

The results reported herein demonstrate that the fabrication of calcium phosphate-polymer nanocomposites with high ceramic content and high mechanical properties is possible. Such nanocomposites are reminiscent of materials found in nature (e.g., nacre) and have a potential for both high strength and toughness due to the large interface area between the soft and hard nano-constituents. So far, β-TCP and Ca deficient HA-based nanocomposites toughened with no more than 40 vol.% (<20 wt%) biodegradable (PLA or PCL) polymer were produced. The materials exhibited compressive strengths up to 300 MPa and sustained a few percent plastic strain which compares favorably with results reported for more conventional biodegradable polymer-based composites reinforced with small volume fractions of CaP particles. These attractive properties were achieved through a combination of several original processing approaches including in situ synthesis of calcium phosphate to ensure uniform dispersion of large volume fractions of nanoparticles, manipulating the adhesion at the interfaces to realize an effective load transfer between the ceramic and polymeric nanoscale components,

and near-full density consolidation of the nanocomposite powders via application of high pressure. Furthermore, high pressure consolidation at room temperature has been shown useful for incorporating biomolecules (drugs, growth factors) that can then be slowly released from the implanted nanocomposite device. Sustained vancomycin release measured in test β-TCP-polymer specimens over the period of 2 weeks implies that even longer release time spans may be expected for larger real-world implantable devices. It has also been demonstrated, for one type of bio-inspired CaP-degradable polymer nanocomposites, that they support the attachment and proliferation of endothelial and osteoblastic cell lines, and that even the small content of polymer influences the formation of pre-vascular structures.

The results are encouraging however much progress has yet to be made in order to develop bioresorbable calcium phosphate-polymer nanocomposites with controlled nanostructure that could be used for bone healing devices in load-bearing body locations.

References

1. Ashammakhi, N., Veiranto, M., Suokas, E., Tiainen, J., Niemelä, S.M., Törmälä, P.: Innovation in multifunctional bioabsorbable osteoconductive drug-releasing hard tissue fixation devices. J. Mater. Sci. Mater. Med. **17**, 1275–1282 (2006)
2. Ambrose, C.G., Clanton, T.O.: Bioabsorbable implants: review of clinical experience in orthopedic surgery. Ann. Biomed. Eng. **32**, 171–177 (2004)
3. Ambrosio, A.M.A., Sahota, J.S., Khan, Y., Laurencin, C.T.: A novel amorphous calcium phosphate polymer ceramic for bone repair: I. Synthesis and characterization. J. Biomed. Mater. Res. **B58**, 295–301 (2001)
4. Ang, K.C., Leong, K.F., Chua, C.K., Chandrasekaran, M.: Compressive properties and degradability of poly(ε-caprolatone)/hydroxyapatite composites under accelerated hydrolytic degradation. J. Biomed. Mater. Res. **80A**, 655–660 (2007)
5. Bernstein, M., Gotman, I., Makarov, C., Phadke, A., Radin, S., Ducheyne, P., Gutmanas, E.Y.: Low temperature fabrication of β-TCP-PCL nanocomposites for bone implants. Adv. Biomater. **12**, B341–B347 (2010)
6. Bohner, M.: Calcium orthophosphates in medicine: from ceramics to calcium phosphate cements. Injury **31**, S-D37–S-D47 (2000)
7. Bow, J.S., Liou, S.C., Chen, S.Y.: Structural characterization of room-temperature synthesized nano-sized β-tricalcium phosphate. Biomaterials **25**, 3155–3161 (2004)
8. Cavallaro, U., Liebner, S., Dejana, E.: Endothelial cadherins and tumor angiogenesis. Exp. Cell Res. **312**, 659–667 (2006)
9. Chen, C.W., Riman, R.E., TenHuisen, K.S., Brown, K.: Mechanochemical–hydrothermal synthesis of hydroxyapatite from nonionic surfactant emulsion precursors. J. Cryst. Growth **270**, 615–623 (2004)
10. Choi, D., Marra, K.G., Kumta, P.N.: Chemical synthesis of hydroxyapatite/poly(ε-caprolactone) composites. Mater. Res. Bull. **39**, 417–432 (2004)
11. Choong, C.S., Hutmacher, D.W., Triffitt, J.T.: Co-culture of bone marrow fibroblasts and endothelial cells on modified polycaprolactone substrates for enhanced potentials in bone tissue engineering. Tissue Eng. **12**, 2521–2531 (2006)
12. Collins, I., Wilson-MacDonald, J., Chami, G., Burgoyne, W., Vineyakam, P., Berendt, T., Fairbank, J.: The diagnosis and management of infection following instrumented spinal fusion. Eur. Spine J. **17**, 445–450 (2008)

13. Dohle, E., Fuchs, S., Kolbe, M., Hofmann, S., Schmidt, H., Kirkpatrick, C.J.: Sonic Hedgehog promotes angiogenesis and osteogenesis in a co-culture system consisting of primary osteoblasts and outgrowth endothelial cells. Tissue Eng. A **16**, 1235–1237 (2010)
14. Dong, G.C., Sun, J.S., Yao, C.H., Jiang, J.G., Huang, C.W., Lin, F.H.: A study on grafting and characterization of HMDI-modified calcium hydrogenphosphate. Biomaterials **22**, 3179–3189 (2001)
15. Dorozhkin, S.V.: Calcium orthophosphate-based biocomposites and hybrid biomaterials. J. Mater. Sci. **44**, 2343–2387 (2009)
16. Ducheyne, P., Cuckler, J.M.: Bioactive ceramic prosthetic coatings. Clin. Orthop. Relat. Res. **276**, 102–114 (1992)
17. Ducy, P., Zhang, R., Geoffroy, V., Ridall, A.L., Karsenty, G.: Osf2/Cbfa1: a transcriptional activator of osteoblast differentiation. Cell **89**, 747–754 (1997)
18. Eglin, D., Alini, M.: Degradable polymeric materials for osteosnthesis: tutorial. Eur. Cell Mater. **16**, 80–91 (2008)
19. Elbjeirami, W.M., West, J.L.: Angiogenesis-like activity of endothelial cells cocultured with VEGF-producing smooth muscle cells. Tissue Eng. **12**, 381–390 (2006)
20. Fuchs, S., Hermanns, M.I., Kirkpatrick, C.J.: Retention of a differentiated endothelial phenotype by outgrowth endothelial cells isolated from human peripheral blood and expanded in long-term cultures. Cell Tissue Res. **326**, 79–92 (2006)
21. Fuchs, S., Hofmann, A., Kirkpatrick, C.J.: Microvessel-like structures from outgrowth endothelial cells from human peripheral blood in 2-dimensional and 3-dimensional co-cultures with osteoblastic lineage cells. Tissue Eng. **13**, 2577–2588 (2007)
22. Fuchs, S., Ghanaati, S., Orth, C., Barbeck, M., Kolbe, M., Hofmann, A., et al.: Contribution of outgrowth endothelial cells from human peripheral blood on in vivo vascularization of bone tissue engineered constructs based on starch polycaprolactone scaffolds. Biomaterials **30**, 526–534 (2009)
23. Fuchs, S., Jiang, X., Schmidt, H., Dohle, E., Ghanaati, S., Orth, C., et al.: Dynamic processes involved in the pre-vascularization of silk fibroin constructs for bone regeneration using outgrowth endothelial cells. Biomaterials **30**, 1329–1338 (2009)
24. Fuchs, S., Jiang, X., Gotman, I., Makarov, C., Schmidt, H., Gutmanas, E.Y., Kirkpatrick, C.J.: Influence of polymer content in Ca-deficient hydroxyapatite-polycaprolactone (CDHA-PCL) nanocomposites on the formation of microvessel-like structures. Acta Biomater. **6**, 3169–3177 (2010)
25. Garvin, K., Feschuk, C.: Polylactide-polyglycolide antibiotic implants. Clin. Orhtop. Relat. Res. **437**, 105–110 (2006)
26. Grellier, M., Bordenave, L., Amedee, J.: Cell-to-cell communication between osteogenic and endothelial lineages: implications for tissue engineering. Trends Biotechnol. **27**, 562–571 (2009)
27. Guillotin, B., Bourget, C., Remy-Zolgadri, M., Bareille, R., Fernandez, P., Conrad, V., et al.: Human primary endothelial cells stimulate human osteoprogenitor cell differentiation. Cell Physiol. Biochem. **14**, 325–332 (2004)
28. Guillotin, B., Bareille, R., Bourget, C., Bordenave, L., Amedee, J.: Interaction between human umbilical vein endothelial cells and human osteoprogenitors triggers pleiotropic effect that may support osteoblastic function. Bone **42**, 1080–1091 (2008)
29. Gulati, R., Jevremovic, D., Peterson, T.E., Chatterjee, S., Shah, V., Vile, R.G., et al.: Diverse origin and function of cells with endothelial phenotype obtained from adult human blood. Circ. Res. **93**, 1023–1025 (2003)
30. Guo, H., Su, J., Wei, J., Kong, H., Liu, C.: Biocompatibility and osteogenicity of degradable Ca-deficient hydroxyapatite scaffolds from calcium phosphate cement for bone tissue engineering. Acta Biomater. **5**, 268–278 (2009)
31. Gutmanas, E.Y.: Cold sintering under high pressure—mechanisms and application. Powder Metal. Int. **15**, 129–132 (1983)

32. Gutmanas, E.Y.: Cold-sintering—high pressure consolidation. In: Eisen, W.B. et al. (eds.) ASM Handbook, vol. 7, Powder Metal Technologies and Applications, p. 574. ASM International, Materials Park (1998)
33. Hakimimehr, D., Liu, D.M., Troczynski, T.: In situ preparation of poly(propylene fumarate)-hydroxyapatite composite. Biomaterials **26**, 7297–7303 (2005)
34. Henrich, D., Seebach, C., Kaehling, C., Scherzed, A., Wilhelm, K., Tewksbury, R., Powerski, M., Marzi, I.: Simultaneous cultivation of human endothelial like differentiated precursor cells and human marrow stromal cells on beta-Tricalciumphosphate. Tissue Eng. Part C Methods **15**, 551–560 (2009)
35. Hong, Z., Zhang, P., Liu, A., Chen, L., Chen, X., Jing, H.: Composites of poly(lactide-*co*-glycolide) and the surface modified carbonated hydroxyapatite nanoparticles. J. Biomed. Mater. Res. **81A**, 515–522 (2007)
36. Hur, J., Yoon, C.H., Kim, H.S., Choi, J.H., Kang, H.J., Hwang, K.K., et al.: Characterization of two types of endothelial progenitor cells and their different contributions to neovasculogenesis. Arterioscler. Thromb. Vasc. Biol. **24**, 288–293 (2004)
37. Ignjatović, N., Uskokovic, D.: Synthesis and application of composite biomaterial hydroxyapatite/polylactide. Appl. Surf. Sci. **238**, 314–319 (2004)
38. Ignjatović, N., Tomic, S., Dakić, M., Miljković, M., Plavšić, M., Uskoković, D.: Synthesis and properties of hydroxyapatite/poly-L-lactide composite biomaterials. Biomaterials **20**, 809–816 (1999)
39. Ignjatović, N., Delijić, K., Vukčević, M., Uskoković, D.: The designing of properties of hydroxyapatite/poly-L-lactide composite biomaterials by hot pressing. Z Metallkd **92**, 145–149 (2001)
40. Ignjatović, N., Suljovrujić, E., Budinski-Simendić, J., Krakovsky, I., Uskoković, D.: Evaluation of hot pressed hydroxyapatite/poly-L-lactide composite biomaterial. J. Biomed. Mater. Res. B Appl. Biomater. **71B**, 284–294 (2004)
41. Ishikawa, K., Ducheyne, P., Radin, S.: Determination of Ca/P ratio in calcium-deficient hydroxyapatite using X-ray diffraction analysis. J. Mater. Sci. Mater. Med. **4**, 165–168 (1993)
42. Jalota, S., Bhaduri, S.B., Tas, A.C.: In vitro testing of calcium phosphate (HA, TCP and biphasic HA-TCP) whiskers. J. Biomed. Mater. Res. **78A**, 481–490 (2006)
43. Jiang, P.J., Patel, S., Gbureck, U., Caley, R., Grover, L.M.: Comparing the efficacy of three bioceramic matrices for the release of vancomycin hydrochloride. J. Biomed. Mater. Res. **93B**, 51–58 (2010)
44. Kasten, P., Luginbühl, R., van Griensven, M., Barkhausen, T., Krettek, C., Bohner, M., et al.: Comparison of human bone marrow stromal cells seeded on calcium deficient hydroxyapatite, (beta)-tricalcium phosphate and demineralized bone matrix. Biomaterials **24**, 2593–2603 (2003)
45. Kasten, P., Vogel, J., Luginbühl, R., Niemeyer, P., Tonak, M., Lorenz, H., et al.: Ectopic bone formation associated with mesenchymal stem cells in a resorbable calcium deficient hydroxyapatite carrier. Biomaterials **26**, 5879–5889 (2005)
46. Katti, K.S., Katti, D.R., Mohanty, B.: Biomimetic lessons learnt from nacre. In: Mukherjee, A. (ed.) Biomimetics Learning from Nature, p. 193. INTECH, Vienna (2010)
47. Kim, H.J., Kim, U.J., Vunjak-Novakovic, G., Min, B.H., Kaplan, D.L.: Influence of macroporous protein scaffolds on bone tissue engineering from bone marrow stem cells. Biomaterials **26**, 4442–4452 (2005)
48. Kim, S.S., Park, M.S., Cho, S.W., Kang, S.W., Ahn, K.M., Lee, J.H., Kim, B.S.: Enhanced bone formation by marrow-derived endothelial and osteogenic cell transplantation. J. Biomed. Mater. Res. **92A**, 246–253 (2010)
49. Kirkpatrick, C.J., Fuchs, S., Hermanns, M.I., Peters, K., Unger, R.E.: Cell culture models of higher complexity in tissue engineering and regenerative medicine. Biomaterials **28**, 5193–5198 (2007)
50. Komori, T.: Requisite roles of Runx-2 and Cbfb in skeletal development. J. Bone Miner. Metab. **21**, 193–197 (2003)

51. LeGeros, R.Z., LeGeros, J.P.: Phosphate minerals in human tissues. In: Nriagu, J.O., Moore, P.B. (eds.) Phosphate Minerals, p. 351. Springer, New York (1984)
52. LeGeros, R.Z., Daculsi, G., Orly, I., Abergas, T., Torres, W.: Solution-mediated transformation of octacalcium phosphate (OCP) to apatite. Scanning Microsc. **3**, 129–137 (1989)
53. Liou, S.C., Chen, S.Y., Liu, D.M.: Phase development and structural characterization of calcium phosphate ceramics-polyacrylic acid nanocomposites at room temperature in water–methanol mixtures. J. Mater. Sci. **15**, 1261–1266 (2004)
54. Liu, Q., de Wijn, J.R., van Blitterswijk, C.A.: A study on the grafting reaction of isocyanates with hydroxyapatite particles. J. Biomed. Mater. Res. **40**, 358–364 (1998)
55. Liu, Q., de Wijn, J.R., de Groot, K., van Blitterswijk, C.A.: Surface modification of nano-apatite by grafting organic polymer. Biomaterials **19**, 1067–1072 (1998)
56. Luz, G.M., Mano, J.F.: Biomimetic design of materials and biomaterials inspired by the structure of nacre. Philos. Trans. R. Soc. A **367**, 1587–1605 (2009)
57. Makarov, C., Gotman, I., Jiang, X., Fuchs, S., Kirkpatrick, C.J., Gutmanas, E.Y.: In situ synthesis of calcium phosphate-polycaprolactone nanocomposites with high ceramic volume fractions. J. Mater. Sci. Mater. Med. **21**, 1771–1779 (2010)
58. Makarov, C., Gotman, I., Radin, S., Ducheyne, P., Gutmanas, E.Y.: Vancomycin release from bioresorbable calcium phosphate-polymer composites with high ceramic volume fractions. J. Mater. Sci. **45**, 6320–6324 (2010)
59. Mäkinen, T.J., Veiranto, M., Knuuti, J., Jalava, J.P., Törmälä, P., Aro, H.T.: Efficacy of bioabsorbable antibiotic containing bone screw in the prevention of biomaterial-related infection due to *Staphylococcus aureus*. Bone **36**, 292–299 (2006)
60. Mayer, G.: Rigid biological systems as models for synthetic composites. Science **310**, 1144–1147 (2005)
61. Meinel, L., Karageorgiou, V., Hofmann, S., Fajardo, R., Snyder, B., Li, C., et al.: Engineering bone-like tissue in vitro using human bone marrow stem cells and silk scaffolds. J. Biomed. Mater. Res. A **71**, 25–34 (2004)
62. Meyers, M.A., Lin, A.Y.M., Chen, P.Y., Muyco, J.: Mechanical strength of abalone nacre: role of the soft organic layer. J. Mech. Behav. Biomed. Mater. **I**, 76–85 (2008)
63. Middleton, J.C., Tipton, A.J.: Synthetic biodegradable polymers as orthopedic devices. Biomaterials **21**, 2335–2346 (2000)
64. Mohanty, B., Katti, K., Katti, D.: Experimental investigation of nanomechanics of the mineral–protein interface in nacre. Mech. Res. Commun. **35**, 17–23 (2008)
65. Musumeci, A.W., Frost, R.L., Waclawik, E.R.: A spectroscopic study of the mineral paceite (calcium acetate). Spectrochim. Acta A **A67**, 649–661 (2007)
66. Nakase, T., Takaoka, K., Hirakawa, K., Hirota, S., Takemura, T., Onoue, H., et al.: Alterations in the expression of osteonectin, osteopontin and osteocalcin mRNAs during the development of skeletal tissues in vivo. Bone Miner. **26**, 109–122 (1994)
67. Neumann, M., Epple, M.: Composites of calcium phosphate and polymers as bone substitution materials. Eur. J. Trauma **2**, 125–131 (2006)
68. Nikkola, L., Viitanen, P., Ashammakhi, N.: Temporal control of drug release from biodegradable polymer: multicomponent diclofenac sodium releasing PLGA 80/20 rod. J. Biomed. Mater. Res. **89B**, 518–526 (2009)
69. Owen, T.A., Aronow, M., Shalhoub, V., Barone, L.M., Wilming, L., Tassinari, M.S., et al.: Progressive development of the rat osteoblast phenotype in vitro: reciprocal relationships in expression of genes associated with osteoblast proliferation and differentiation during formation of the bone extracellular matrix. J. Cell. Physiol. **143**, 420–430 (1990)
70. Petricca, S.E., Marra, K.G., Kumta, P.N.: Chemical synthesis of poly(lactic-*co*-glycolic acid)/hydroxyapatite composites for orthopaedic applications. Acta Biomater. **2**, 277–286 (2006)
71. Rakovsky, A., Gotman, I., Gutmanas, E.Y.: Ca-deficient hydroxyapatite/polylactide nanocomposites with chemically modified interfaces by high pressure consolidation at room temperature. J. Mater. Sci. **45**, 6339–6344 (2010)

72. Ramakrishna, S., Mayer, J., Wintermantel, E., Leong, K.: Biomedical applications of polymer-composite materials: a review. Compos. Sci. Technol. **61**, 1189–1224 (2001)
73. Rezwan, K., Chen, Q.Z., Blaker, J.J., Boccaccini, A.R.: Biodegradable and bioactive porous polymer/inorganic composite scaffolds for bone tissue engineering. Biomaterials **27**, 3413–3431 (2006)
74. Rivron, N.C., Liu, J.J., Rouwkema, J., de Boer, J., van Blitterswijk, C.A.: Engineering vascularised tissues in vitro. Eur. Cell Mater. **15**, 27–40 (2008)
75. Rokkanen, P.U., Bostman, O., Hirvensalo, E., Makela, E.A., Partio, E.K., Patiala, H., Vainionpaa, S.I., Vihtonen, K., Tormala, P.: Bioabsorbable fixation in orthopaedic surgery and traumatology. Biomaterials **21**, 2607–2613 (2000)
76. Rouwkema, J., de Boer, J., Van Blitterswijk, C.A.: Endothelial cells assemble into a 3-dimensional prevascular network in a bone tissue engineering construct. Tissue Eng. **12**, 2685–2693 (2006)
77. Santos, M.I., Reis, R.L.: Vascularization in bone tissue engineering: physiology, current strategies, major hurdles and future challenges. Macromol. Biosci. **10**, 12–27 (2009)
78. Santos, M.I., Unger, R.E., Sousa, R.A., Reis, R.L., Kirkpatrick, C.J.: Crosstalk between osteoblasts and endothelial cells co-cultured on a polycaprolactone-starch scaffold and the in vitro development of vascularization. Biomaterials **30**, 4407–4415 (2009)
79. Sato, M., Yasui, N., Nakase, T., Kawahata, H., Sugimoto, M., Hirota, S., et al.: Expression of bone matrix proteins mRNA during distraction osteogenesis. J. Bone Miner. Res. **13**, 1221–1231 (1998)
80. Schmidt, A.H., Swiontkowski, M.F.: Pathophysiology of infections after internal fixation of fractures. J. Am. Acad. Orthop. Surg. **8**, 285–291 (2000)
81. Shikinami, Y., Okuno, M.: Bioresorbable devices made of forged composites of hydroxyapatite (HA) particles and poly-L-lactide (PLLA): part I. Basic characteristics. Biomaterials **20**, 859–877 (1999)
82. Siddharthan, A., Seshadri, S.K., Sampath Kumar, T.S.: Microwave accelerated synthesis of nanosized calcium deficient hydroxyapatite. J. Mater. Sci. Mater. Med. **15**, 1279–1284 (2004)
83. Simon, J.A., Ricci, J.L., Di Cesare, P.E.: Bioresorbable fracture fixation in orthopedics: a comprehensive review. Part I. Basic science and preclinical studies. Am. J. Orthop. **26**, 665–671 (1997)
84. Simon, J.A., Ricci, J.L., Di Cesare, P.E.: Bioresorbable fracture fixation in orthopedics: a comprehensive review. Part II. Clinical studies. Am. J. Orthop. **26**, 754–762 (1997)
85. Takayama, T., Todo, M.: Improvement of mechanical properties of hydroxyapatite particle filled poly(L-lactide) biocomposites using lysine tri-isocyanate. J. Mater. Sci. **44**, 5017–5020 (2009)
86. Tas, A.C., Korkusuz, F., Timicin, M., Akkas, N.: An investigation of the chemical synthesis and high-temperature sintering behavior of calcium hydroxyapatite (HA) and tricalcium phosphate (TCP) bioceramics. J. Mater. Sci. Mater. Med. **8**, 91–96 (1997)
87. Unger, R.E., Sartoris, A., Peters, K., Motta, A., Migliaresi, C., Kunkel, M., et al.: Tissue-like self-assembly in cocultures of endothelial cells and osteoblasts and the formation of microcapillary-like structures on three-dimensional porous biomaterials. Biomaterials **28**, 3965–3976 (2007)
88. Vogt, S., Schnabelrauch, M., Weisser, J., Kautz, A.R., Büchner, H., Kühn, K.D.: Design of an antibiotic delivery system based on a bioresorbable bone substitute. Adv. Eng. Mater. **9**, 1135–1140 (2007)
89. Wagner, H.D.: Paving the way to stronger materials. Nat. Nanotechnol. **2**, 742–744 (2007)
90. Wagoner Johnson, A.J., Herschler, B.A.: A review of the mechanical behavior of CaP and CaP/polymer composites for applications in bone replacement and repair. Acta Biomater. **7**(1), 16–30 (2010)
91. Wildemann, B., Bamdad, P., Holmer, Ch., Haas, N.P., Raschke, M., Schmidmaier, G.: Local delivery of growth factors from coated titanium plates increases osteotomy healing in rats. Bone **34**, 862–868 (2004)

92. Yu, H., VandeVord, P.J., Mao, L., Matthew, H.W., Wooley, P.H., Yang, S.Y.: Improved tissue-engineered bone regeneration by endothelial cell mediated vascularization. Biomaterials **30**, 508–517 (2009)
93. Yu, H., Wooley, P.H., Yang, S.Y.: Biocompatibility of poly-epsilon-caprolactone-hydroxyapatite composite on mouse bone marrow-derived osteoblasts and endothelial cells. J. Orthop. Surg. Res. **4**, 5 (2009)
94. Yu, H.S., Jang, J.H., Kim, T.I., Lee, H.H., Kim, H.W.: Apatite-mineralized polycaprolactone nanofibrous web as a bone tissue regeneration substrate. J. Biomed. Mater. Res. **88A**, 747–754 (2009)
95. Yubao, L., Klein, C.P.A.T., De Wijn, J., Van De Meer, S., de Groot, K.: Shape change and phase transition of needle-like non-stoichiometric apatite crystals. J. Mater. Sci. Mater. Med. **5**, 263–268 (1994)
96. Zhang, S.M., Liu, J., Zhou, W., Cheng, L., Guo, X.D.: Interfacial fabrication and property of hydroxyapatite/polylactide resorbable bone fixation composites. Curr. Appl. Phys. **5**, 516–518 (2005)

Polymer Scaffolds for Bone Tissue Regeneration

Rossella Dorati, Claudia Colonna, Ida Genta and Bice Conti

Abstract The term "tissue engineering" refers to methods and techniques used to improve the regeneration of human cells and tissues, including the manipulation of natural and synthetic materials which provide both the structural integrity and the biochemical information to young cells when they are growing into a specific kind of tissue. This chapter deals with the application of tissue engineering to bone tissue regeneration and is focused to the polymer structures studied and used as temporary templates to promote bone reconstruction. After a brief introduction about the general principle of regenerative medicine, the scaffold design criteria and their applications, attention will be focused to scaffold for bones. A scaffold classification is reported based on the type of constituent polymers and a detailed discussion is provided about these materials highlighting advantages and drawbacks for each of them. Moreover, polymer scaffold preparation and characterization techniques are described and discussed with some examples. Finally clinical aspects and criticisms are also presented to show the state of art of the topic.

1 Introduction

The regenerative medicine is a new way of treating injuries and diseases and it uses three different approaches: (i) cells, (ii) bioartificial tissues and (iii) specifically growth tissues. Independently from the approach used, the main goal of the

R. Dorati · C. Colonna · I. Genta · B. Conti (✉)
Department of Drug Sciences, University of Pavia,
Via Taramelli 12, 27100 Pavia, Italy
e-mail: bice.conti@unipv.it

Stud Mechanobiol Tissue Eng Biomater (2011) 8: 259–285
DOI: 10.1007/8415_2010_59

Published Online: 25 January 2011

regenerative medicine is to replace or to regenerate human cells, tissues and organs and to restore or establish the normal and original function of the damaged or compromised tissue [53]. In this context, the term "tissue engineering" refers to methods and techniques used to improve the regeneration of human cells and tissues, including the manipulation of natural and synthetic materials which provide both the structural integrity and the biochemical information to young cells when they are growing into a specific kind of tissue. Tissue engineering typically involves three main elements which provide the essential factors for the physiological regeneration process. The first component is a substrate (membranes, foams, meshes, gels and 3D-scaffolds) for the osteoconduction properties. These properties are defined as the ability to support the cell migration into the defect site from the host tissue and to promote the cell proliferation and growth. The second element is represented by signals, as growth factors (BMPs, TGF-βs and IGFs), that provide the osteoinductive properties, the ability to induce the proliferation of a specific kind of cells and to drive them to produce the new tissue. The last component are stem cells (somatic, adult and embryonic stem cells) for the osteogenic properties. These properties are defined as the capability to induce local mesenchymal cells to proliferate and differentiate into specific cells [35, 63]. In the regeneration process, the substrate plays a few roles as framework supporting the migration of cells from the surrounding tissue into the damaged tissue and as delivery system for the controlled or prolonged release of cells, genes, and growth factors. The substrate can work as matrix for the cell adhesion and controlling and regulating the in vivo or in vitro cell processes, mytosis, synthesis and migration. The scaffold can act as a matrix using biomaterials with ligands for cell receptor (integrines) or biomaterials that may selectively adsorb adhesion proteins which cells can bind. Moreover, the scaffold can be a reinforced structure which maintains the shape of the defect site preventing any distortion of host tissues and also it can be a barrier to prevent the infiltration of the tissues that are not involved in the reconstruction process and that may limit the regeneration process [7, 63].

1.1 Scaffold Design Criteria

To achieve and complete all the roles reported in the previous Sect. 1, the scaffold has to be consistent with several requirements.

Table 1 summarizes scaffold design criteria and the related resulting functions in the engineered tissues.

The scaffold and raw materials used for the preparation of the substrate must be biocompatible and not inducing inflammatory and immunogenic reactions. The scaffold has to present a tridimensional matrix architecture with highly porous structure, to allow the infiltration of cells, the diffusion of nutrients into the matrix and the exchanges of the waste products. The surface of the scaffold has to be bioactive to improve the cell attachment and the interactions between the surrounding tissue and the synthetic matrix. Depending to the intended application,

Table 1 Scaffold design criteria

Scaffold design criteria	Resulting function in engineered tissue
Biologic compatibility	Non-toxic/minimal inflammatory response
3D matrix architecture	Physiologically relevant environment for cell function
Void space	Highly porous and interconnected pores to allow cell infiltration, transport of nutrients, humoral factors and waste products
Surface chemistry and topography	Cell attachment and cell-matrix interactions
Appropriate mechanical behavior	Seamless integration with surrounding tissue(s) able to withstand in vivo forces and avoid stress shielding
Degradation rate	Scaffold lead to the formation of a functionalized matrix
Structural anisotropy	Anisotropic mechanical behaviour
	Influence orientation of cells and ECM deposition

the scaffold has to show appropriate mechanical properties and singular degradation rate to lead to the formation of a functionalized matrix. The last design criterium is defined as the structural anisotropy which can affect, as function of the direction, the mechanical behaviour, the orientation of cells into the support and potentially the deposition of extra cellular matrix (ECM) [35, 71].

1.2 Engineered Scaffold Type

The scaffold are divided into two main groups: three-dimensional scaffolds or preformed matrix, and injectable matrix. The preformed matrix could be further splitted into non-fibrous and fibrous synthetic scaffolds which can be developed by several different techniques. Figure 1 reports the scanning electron micrographs of non-fibrous (Fig. 1a) and fibrous matrix (Fig. 1b) prepared by thermal induced phase separation gas foaming and electron spinning.

The second type of scaffold is defined injectable matrix. The candidates used for the production of injectable matrix include those materials that are liquid at room temperature and become gelly under different stimula. The solidification processes may be: (i) thermal gelation, (ii) photocrosslinking, (iii) ionic gelation, (iv) radical polymerization and (v) self-assembly. Table 2 reports some of the materials and the solidification mechanisms used for the preparation of injectable scaffold intended for tissue regeneration.

Recently a new type of scaffold has been developed whose characteristics are both of the preformed and the injectable. It can be defined an injectable 3D composite matrix [54]. The system contains β-TCP beads and alginate polymer solution. The beads are treated with calcium chloride solution, when the alginate solution is pushed out by a syringe into the treated β-TCP the presence of $CaCl_2$ on the bead surface induces instantaneously crosslinking of the alginate chains forming the 3D composite matrix. Figure 2 shows the scanning electron

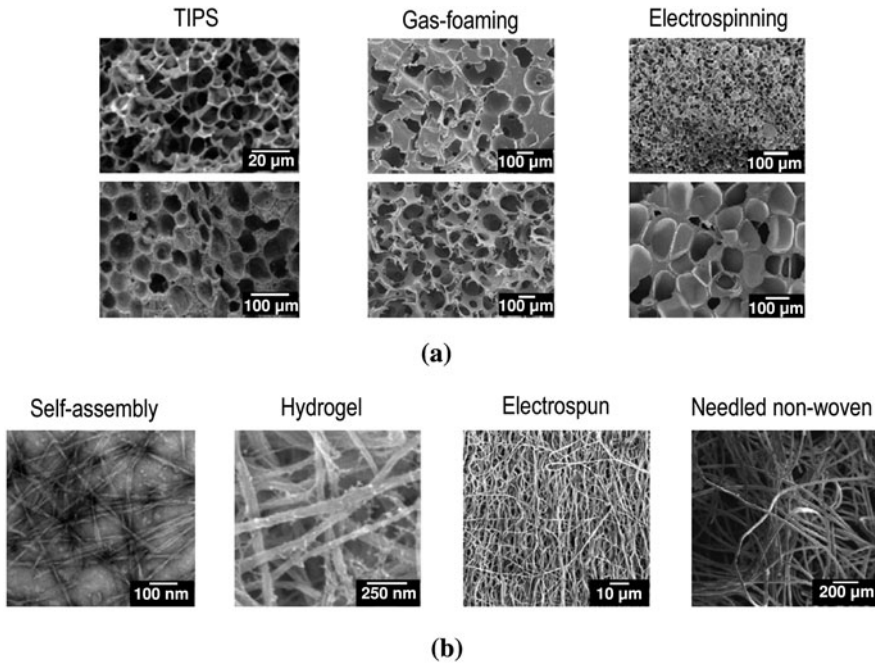

Fig. 1 Cross-sectional SEM micrographs of: **a** non-fibrous methods to manipulate micro-morphology, **b** methods commonly employed to create 3D scaffolds exhibiting fibrous structures with diameters on the order of native ECM (From [71])

Table 2 Injectable scaffolds reported for tissue regeneration

	Injectable scaffold	Solidification mechanism
Inorganic materials	Calcium phosphate	Ceramics setting
Natural polymers	Chitosan	Thermal gelation
	Methylcellulose	Thermal gelation
	Alginate	Photo cross-linking or Ionic gelation
Synthetic polymers	PEO–PPO–PEO	Thermal gelation
	PEO–PLLA	Thermal gelation
	PEO–PLLA–PEO	Photo cross-linking
	PLLA–PEG	Photo cross-linking
	PPF	Photo cross-linking or radical polymerization
	Polyanhydrides	Photo cross-linking
	P(CL/TMC)	Photo cross-linking
	PNIPAAm–PEG	Thermal gelation
	PLA–PEG-biotin	Self-assembly

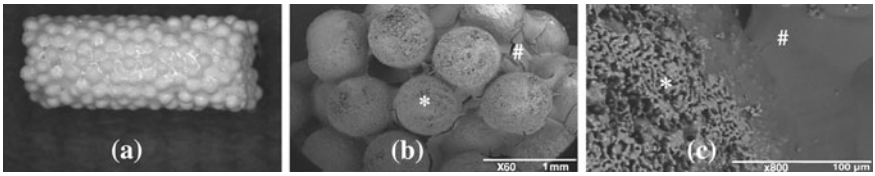

Fig. 2 Injectable 3D-formed composite of β-TCP beads and alginate: **a** light microscope photograph of the composite, **b** SEM photograph of the composite, **c** SEM photograph of the composite surface. Bar is 1,000 µm in (**b**) and 100 µm in (**c**). (From [54])

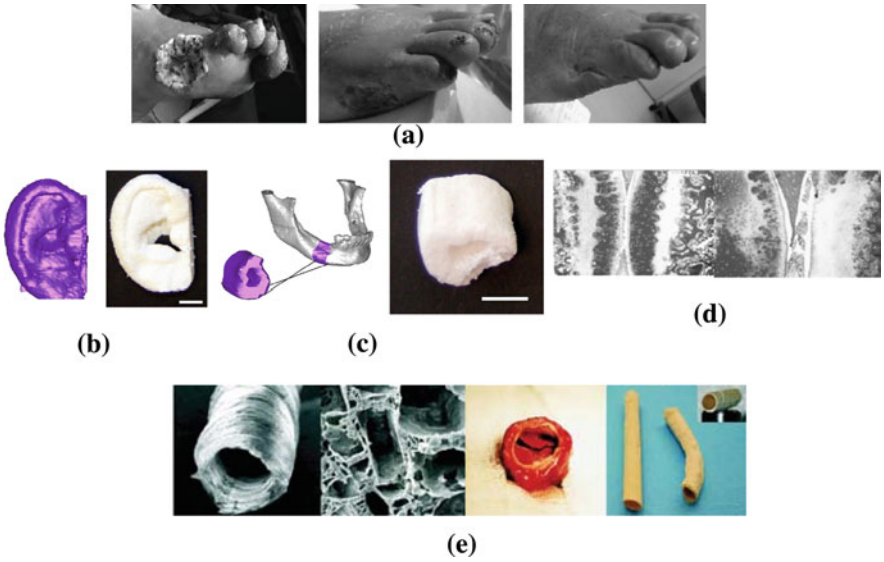

Fig. 3 Few examples of tissue engineered scaffolds used in the clinical tissue regeneration for: **a** diabetic foot ulcer, **b** ear reconstruction, **c** human mandibular reconstruction, **d** articular cartilage regeneration; **e** coronary artery regeneration. (From [50, 73])

microscope (Fig. 2a) and light microscope photographs (Fig. 2b) of the hybrid system.

1.3 The Tissue Engineered Scaffold Applications

The polymer scaffolds combined with growth factors or cells can be used for different final applications as the regeneration of coronary artheries, bone, articular cartilage, for the reconstruction of human mandible, ear and blood vessels. Moreover the tissue engineered scaffolds have been used in the clinical tissue regeneration for the therapeutic treatment of diabetic foot ulcers or intractable diseases (Fig. 3).

2 Scaffolds for Bone Regeneration

Bone tissue has high regenerative capacities and the majority of fractures heal without the need of major intervention. Nevertheless in presence of severe non-union fractures or after bone tumor resection, a template for the natural self-organizing regeneration is lacking, and surgical intervention is needed.

In these cases it is possible to proceed with: transplanting of autologous bone (autografting bone of the same patient), transplanting of allogenic bone (bone from a human cadaver) or of xenogenic bone (bone from animal source). Among these, bone autograft is the preferred procedure because of the good compatibility of the transplanted bone with the patient. Nevertheless, this is a painful treatment involving bone withdrawn from a site of the patient and its transplant in the lacking site with the risk of possible complications such as morbility at the site of action, pain, infections, inflammation and slow rehabilitation. Allograft implantation is an FDA approved technique; it is used since long time, with the advantages due to the similarity of the allogenic bone tissue to the bone tissue to be repaired. The main drawback of this technique is the potential transmission of pathologies expressed by the donor to the host. The same drawback is evident in the xenograft transplantation that has been almost abandoned.

The design and development of polymeric scaffold is addressed to eliminate the problems described and derived from xenograft, allograft and autograft transplantations. This chapter treats of polymeric scaffolds for bone regeneration, their morphological and functional characteristics, the advantages, disadvantages, and the preparation techniques. Attention is focused to the biomaterials in use and in study and the recent trends in this field.

2.1 Bone Structure

The knowledge of the bone cellular and molecular organization, biomechanics, remodeling, and biomimetics is a fundamental background for an intelligent design of bone polymeric scaffolds.

Bone is a complex, highly organized and specialized connective tissue. It plays several key-functions in the human physiology, such as movement and support of other critical organs, blood production, mineral storage and homeostasis, blood pH regulation, multiple progenitor cell (mesenchymal and hemopoietic) housing, etc. Moreover, the bone tissue has unique remodeling properties in response to external mechanical loads. Bones are composed of mineralized osseous tissue, marrow, endosteum and periosteum, nerves, blood vessels, and cartilage. Bones macroscopic structure is characterized of being a rigid and strong physical structure, while the tissue presents microscopically relatively few cells (bone cellular components) and abundant intercellular substance formed of collagen fibers and stiffening substances (bone a-cellular components).

Macroscopically there are two types of bone structures: (i) cortical or compact bone with a dense outer layer, the cortex, this structure is bending resistant; (ii) Cancellous (spongy or trabecular) bone, this structure is more porous than the compact one and it is compression resistant in such a way that bone elements place or displace themselves in the direction of functional pression.

From the histological standpoint two main types of bones are recognized: (i) primary bone tissue (non-lamellar bone), and (ii) secondary bone tissue (lamellar bone). Primary bone tissue is present in bones of faetuses and young children and is the first tissue to appear in the bone repair process. It is characterized by the presence of randomly oriented coarse collagen fibers. Secondary bone tissue is the mature bone characterized by the presence of collagen fibers arranged in parallel layers or sheet (lamellae). Lamellar bone is present both in cortical and cancellous adult bones.

2.1.1 A-cellular Components of Bones

The inorganic components of bones are primarily hydroxyapatite (HAP), that is a specific type of calcium–phosphate mineral ($Ca_{10}(PO_4)_6(OH)_2$). The organic component of bones is mostly type I collagen, but also an abundance of other proteins such as osteonectin, osteocalcin, osteopontin, proteoglycans (decorin and biglycan), and glycoproteins. The complex hierarchical physical structure, the constituent material properties of the constituents, the cellular organization and molecular cues work in concert to perform the function of bone.

2.1.2 Cellular Component of Bones

Cellular component of bone include three different cells types: osteoblasts, osteocytes and osteoclasts.

Osteoblasts differentiate from mesenchimal stem cells (MSCs) and they are not terminally differentiated cells. This type of cells are defined as bone forming cells located on the surfaces in a structure resembling a cuboid epithelium. The primary function of osteoblasts is to produce and secrete organic and inorganic bone ECM. Their activity is highlighted by alkaline phosphatase activity. They are responsible for skeletal architecture either through deposition of bone matrix and regulation of osteoclast activity [51, 64]. Osteoblasts can have two fates: after being embedded in their own bone matrix they become osteocytes, or they undergo programmed cell death, namely apoptosis.

Osteocytes occupy the lacunae in the bone and eventually stop generating osteoid, they have a key role in mechanical transduction.

Osteoclasts are large, multinucleated cell formed by the fusion of mononuclear hemopoietic precursors. They are located in shallow depressions on the bone surface, the Howship's lacunae. The primary function of osteoclasts is to secrete acids and proteolytic enzymes, which erode bone ECM under the influence of chemical cues.

Bone remodeling is the physiologic key process involved in the production and resorption of bone ECM by osteoblasts and osteoclasts [24, 51, 64].

2.1.3 Bone Remodeling

Bone remodeling is a complex and critical process by which the old bone is continuously replaced by the new one. This process is responsible for adjusting the architecture and hence the mechanical properties of bone and controlling the mechanical and chemical signaling function, keeping skeletal integrity, healing and blood calcium regulation. The bone remodeling process is regulated by a complicated biochemical cascade driven by several hormones such as parathyroid hormone, calcitrol, glucocorticoids, sex hormones, and growth factors such as insulin growth factor (IGF), prostaglandins, transforming growth factors (TGF-bs), bone morphogenetic proteins (BMPs). The process is still not completely understood, anyway good descriptions and hypothesis can be found in the literature [24, 32, 51].

2.1.4 Bone Classification

Bones are generally classified by their shape as: long, short, flat, and irregular. The bone shape affects the structural organization of bone: long or tubular bones have three primary regions: the diaphysis, epiphysis and epiphyseal plates. The diaphysis is the long portion of the bone made of compact, or cortical, bone surrounding a central cavity containing cancellous bone together with marrow and fat. The cortical bone is thickest in the mid-portion of the shaft, while the cancellous bone is more dense towards the end of the bones where cortical bone is less thick (Fig. 4). Short bones are spongy bones covered with a thin layer of compact tissue; these bones are less resistant than the long ones. Irregular bones, such as vertebrae, consist of a vertebral body anteriorly resembling a tubular bone with a superior and inferior central portion surrounded by a thin cortical shell with cartilaginous end plates in continuity with the intervertebral discs. The posterior vertebral arch consists of the pedicles with dense cortices and relatively little intervening spongy bone and laminae which are typically flat bones with relatively dense cortex and less, dense cancellous bone.

2.1.5 Mechanical Properties of Bones

Bone tissue undergoes mechanical stimuli of compression, elongation, torsion, depending on bone position in the organism, and on individual movements. Even if bone cells answer to mechanical stimuli is not completely known, there are two possible recognized mechanisms: (i) Cellular answer induced by direct mechanical

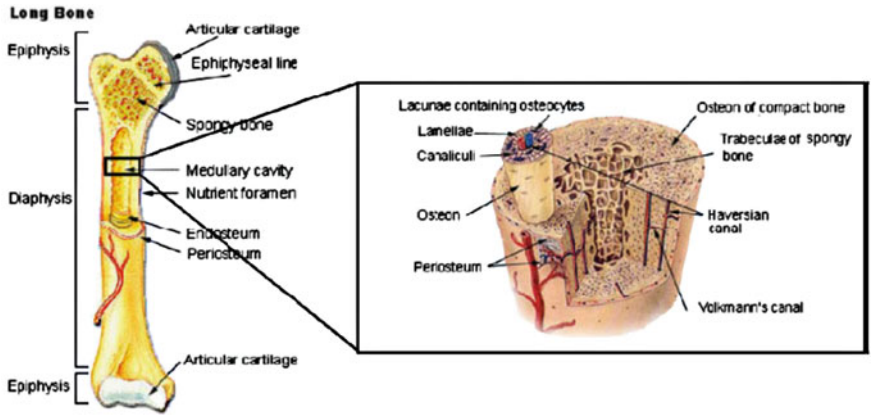

Fig. 4 General scheme of long bone illustrating the basic anatomy: cortical bone, cancellous bone and micro-structural features in bone (from [60])

stimulation; (ii) tissue answer induced by biochemical signalling on bone sensorial cells.

The knowledge of bone mechanical properties is important in designing scaffold for bone tissue engineering in such a way that scaffold mechanical properties should resemble the corresponding properties of bone. These properties are usually sized as compression and tensile resistance (flexural strength): different values can be found depending on the type of bone. For example, Young's modulus value for long bones is between 17 and 30 GPa on the longitudinal axis and between 7 and 13 GPa on the transversal axis, whereas for spongious bone the same parameter has values between 50–100 MPa [60]. The bone tissue is a two phase composite in which the mineral and organic components are bound in a complex manner. For this reason a broad range of values are obtained in testing the mechanical properties. Recent studies on the nanoscale structure analysis using atomic force microscopy (AFM), have highlighted that also the organic matrix plays an important role in bone mechanics [25].

2.2 Scaffold Classification

Depending on the constituent material, scaffolds can be classified as natural scaffolds, hydrogels, synthetic scaffolds, ceramic scaffolds and composite scaffold. The polymer choice selection is determinant for scaffold structural and functional properties. Upon accurate consideration of the intended application and final purpose, as structural support or barrier for delivery system, different candidates can be selected, combined and matched to the final structure.

The raw materials used for the preparation of scaffolds for regenerative medicine are essentially polymers and ceramics. The desired longevity of the

polymeric scaffold dictates the use of biostable or biodegradable polymers, whereas the desired cellular interactions guide the choice of naturally derived or synthetic polymers. Materials to be used in tissue engineering should present some fundamental properties, namely they should be biocompatible, non-toxic and non-inflammatory. The following definition of biocompatibility has been recently proposed [81]: *"The biocompatibility of a scaffold or a matrix for a tissue engineering product refers to the ability to perform as a substrate that will support the appropriate cellular activity including the facilitation of molecular and mechanical signalling systems, in order to optimize tissue regeneration, without eliciting any undesirable local or systemic responses in the eventual host"*. This definition includes some of the characteristics that are specific of those materials defined either biomimetics or biomaterials. These are materials that mimic one or multiple characteristics of the natural ECM, promoting cell adhesion and regeneration. Moreover, biomaterials can act as drug delivery systems (DDS) for biosignalling molecules stabilizing them and enhancing their biological activity.

Biodegradability and/or bioresorption are essential properties to get scaffolds that can act as temporary extracellular matrix. Biodegradability should happen in such a way the biodegradation rate matches the neo-tissue formation rate. When talking about biodegradable polymers, it is fundamental also that their degradation products meet biodegradability and bioresorption criteria. The last but not the least, for effective tissue integration, it is important that the polymer and its degradation products show only minimal inflammatory response. Inflammatory response is influenced by the polymer composition and its degradation rate, which depends also on scaffold structure: faster degradation rates can promote higher local concentration of potentially inflammatory degradation products.

Table 3 lists few natural and synthetic polymers used for the preparation of functional substrates for the regeneration of bone tissue [35].

Each biomaterial shows peculiar physico-chemical properties and therefore singular degradation time, specific mechanical properties and different mechanisms of degradation. The selection of the most suitable polymer has to be performed considering the final application and also the type of scaffold. For instance, matrix intended as structural support should be prepared with polymers that are in the solid state and not in the rubbery phase when they are at 37°C and in contact with biological fluids.

In the following subchapters a selection of the natural and synthetic polymers most used to make polymeric scaffolds is presented.

2.2.1 Natural Polymers and Hydrogels

Natural polymers are usually biocompatible, easy to be modified and to be processed into various structures. Some of them, as hyaluronic acid or collagen, possess a peculiar composition that is able to stimulate cell response.

Nevertheless there are concerns over the use of natural polymers in tissue engineering, because of the risks of pathogen transmission and immune-rejection

Table 3 Some natural, synthetic polymers and ceramic materials used for the preparation of functional substrates for bone tissue regeneration

Material	Mechanical properties	Degradation time	Degradation
Natural polymers			
Type-I collagen	High mechanical properties, tunable through varied cross-linking	Dependent to crosslinking degree	Enzymatic
Chitosan	Below trabecular bone as a hydrogel	Dependent to cross-linking degree and environmental pH	Hydrolysis, enzymatic
Hyaluronic acid	Viscoelastic in nature, lower than trabecular bone	Related to molecular weight	Enzymatic
Synthetic polymers			
Poly-alpha-hydroxyacids	Similar to trabecular bone, depending on 3D structure	6 weeks–1 year, depending on polymer composition and molecular weight	Hydrolysis
Polycaprolactones	Slightly higher than trabecular bone	6 months–2 years, depending on molecular weight	Hydrolysis
Polypropylene fumarate	Similar to trabecular bone	Related to molecular weight and cross-linking density	Hydrolysis
Polyanhydrides	Lower range of trabecular bone	Related to degree of polimerization, molecular weight	Hydrolysis
Polyphosphazenes	From far below to far above trabecular bone	>1 year	Hydrolysis
Ceramics			
Calcium phosphate	Variable based on 3D structure, generally above trabecular bone	6 months–1 year	Dissolution, osteoclastic resorption
Calcium sulphate	Similar to trabecular bone	4–12 weeks	Dissolution
Bioactive glass	Similar to trabecular bone, but dependent on 3D structure	>1 year	Dissolution, osteoclastic resorption

associated with natural materials that arise from animal and cadaver sources. One more drawback for the use of natural polymers in bone tissue engineering is their weak mechanical strength to give the sufficient structural support and the appropriate protection for the seeded osteoblasts.

The most studied naturally derived degradable polymers for tissue engineering applications are collagen, chitosan and hyaluronic acid.

Collagen is a fibrous protein and the main component of ECM of mammalian tissue such as bone, cartilage, tendon, ligament and skin [4]. About 25 types of collagen differing in their chemical composition and molecular structure have been identified. Type I collagen is the most abundant in nature: it is naturally cell-adhesive and provides conductive environment for cell viability. The polymer is

already commercialized as injectable product, thus it has been recognized as safe material by the regulatory agencies [40, 59]. Two mainly collagen-based products containing BMP-2 or BMP-7 have been approved by Food and Drug Administration (FDA) in recent years for human clinical use: Infuse Bone Graft (Medtronik, US; Wyeth, UK), containing rhBMP-2, and Osigraft (Stryker Biotech), containing rhBMP-7. The last one has been approved for long bone fractures and as an alternative to autografts in patients requiring posterolateral lumbar spinal fusion.

Crosslinked porous scaffold with the appropriate properties for cell penetration have been designed [68]. Due to the above mentioned poor mechanical properties, collagen alone is more used for cartilage regeneration than for bone tissue engineering. Indeed, when combined with other polymers, collagen mechanical features can be better exploited for bone regeneration (see Sect. 2.2.4).

Chitosan is a biodegradable polycationic polymer made of D-glucosamine and *N*-acetyl-D-glucosamine linked by $\beta(1,4)$ glycosidic bonds. Due to its positive charge, it can ionically interact with negatively charged polymers and/or molecules. Chitosan is an abundant polymer in nature: it derives from the deacetylation of chitin that forms the crustaceous exoskeleton. Its properties such as degree of water solubility, degradation rate and cytotoxicity vary depending on its molecular weight and deacetylation degree [29, 47, 61]. Generally, the polymer is soluble in water at acidic pH, but it can be chemically modified and/or salified to make it soluble at physiologic pH. It undergoes enzymatic degradation promoted by chitosanases, lysozyme and some non-specific neutral proteases [47]. Chitosan finds several applications as food integrator and it has been widely investigated as polymer for drug delivery [1, 13, 42, 66]. It seems to be promising also for tissue engineering applications [38]. For example chitosan glycerophosphate has been investigated as injectable in situ forming gel for cartilage repair [28], or it has been processed to form coil-reinforced hydrogel tubes to be used as nerve guidance channels [34]. Moreover, to obtain more resistant structures chitosan can be crosslinked with chemical reagent such as genepin [84].

Hyaluronic acid (HAP, hyaluronan), [a-1,4-D-glucuronic acid-b-1,3-*N*-acetyl-D-glucosamine]$_n$, is a natural, hydrophilic, non-immunogenic and biodegradable glycosaminoglycan. It accumulates during morphogenesis and may contribute to fetal scarless healing and wound healing. HAP has been found in high concentrations in the early bone fracture callus, in lacunae surrounding hypertrophic chondrocytes in the growth plate and in the cytoplasm of osteoprogenitor cells. In the human body, HAP biodegradation occurs through enzymatic pathway performed by hyaluronidase. HAP supports bone growth in combination with other osteoconductive molecules, such as collagen, and is able to increase some markers of differentiation in cultured osteoblasts, with dose and size dependent effects. Moreover, it has been shown that HAP modulates the inflammatory response [22, 33] and prevents tissue adhesion [17, 29]. Due to the above cited advantages HAP is usefully used in commercial products, such as Viscoseal®, Hyalart®, Synvisc®, Hyalubrix®, Durolane®, to be injected to knee for cartilage regeneration purposes. For bone repairing applications HAP can be copolymerized with other polymers

(see Sect. 2.2.4), or it can be derivatized through esterification, to improve its mechanical properties.

Hyaff® is a well stated semisynthetic derivative of HAP that has been exploited for skin repair, wound dressings for burns and ulcers, and for nerve-regeneration applications, for bone repair and as carrier for BMPs [36]. It is a benzyl ester derivative (100% esterified) of HAP, and is commercially available from Fidia Biopolymer in different esterification degrees and molecular weights. The benzyl esterification of the guluronic acid residues of hyaluronic acid makes the polymer water insoluble and significantly decreases the in vivo degradation rate by hydrolysis and hyaluronidases. Its biocompatibility has been well established [6, 8] and Hyaff® degradation can be controlled by the esterification degree.

Glycidyl methacrylate modified HAP (HAP-GMA) has been prepared through reaction of HAP with glycidyl methacrylate (GMA) in mild conditions. The derivative can be prepared with different methods and different degree of substitution; polymer degradation rate can be controlled through this parameters. This HAP derivative seems to have suitable mechanical properties to be used in bone regeneration. [57].

2.2.2 Synthetic Polymers

The synthetic polymers are particularly advantageous in tissue engineering applications because they are very versatile and their properties, such as the mechanical strength or biodegradation rate, can be modified and tailored by chemical reaction. They can be easily functionalized to enhance the biological response. Obviously, they should be atoxic and approved for human use. The last requirement represents the main block found by researchers trying to place a new synthetic biomaterial on the market. Biodegradable synthetic polymers have been extensively studied in DDS technology and from this area applied to tissue engineering, several reviews regarding the topic are available in the literature [43, 73].

A disadvantage that can be found in some synthetic polymers, with respect to natural polymers, is the lack of the biological cues typical of many natural polymers and of promoting cell responses.

Table 3 reports some of the more used synthetic polymers.

Poly-alpha-hydroxyacids and their related copolymers are certainly the synthetic polymers most widely studied to make scaffolds, even for bone regeneration, because of their favourable properties such as: (i) no potential risks of disease transmission and immunologic reactions, (ii) approved by FDA and (iii) high biocompatibility [15, 50]. The poor mechanical properties are a limit for the use of these polymers in high loading bearing bones. These polymers biodegrade by hydrolysis through random chain scission generating monomers as lactic and glycolic acid which are eliminated through the metabolic pathways. The degradation rate of poly-alpha-hydroxyacids depends on their molecular weight and their composition. Poly-D,L-lactic acid and poly-L,L-lactic acid (PLA) are highly

hydrophobic linear polymers. The copolymers poly-lactide-co-glycolides (PLGA) are more hydrophilic than the corresponding omopolymers, because of the presence of glycolic acid. So biodegradation rate can be tailored depending on the amount of glycolic acid in the copolymer, and on its molecular weight. The polymer composition results to be an important parameter affecting the interaction of cell with the scaffold. It has been proven that scaffolds made of PLGA 75/25 promote cell induction and conduction better than PLGA 50/50 or PLGA 85/15. 3D scaffolds have been prepared with these polymers using different preparation methods (see Sect. 2.4) in order to achieve suitable porosity and mechanical resistance. Cells are seeded on the 3D solid scaffold, they migrate throughout the porous scaffold network and grow. Due to the biodegradable nature of the polymer, these are temporary scaffolds: the polymer biodegradation rate should be in sink with tissue growing rate. Examples of scaffold based on PLLA and PLGA can be found in the literature [15, 16, 37, 48, 65, 69,]. Maenpaa et al. proposed bilayer biodegradable polylactide (PLA) discs comprising a non-woven mat of poly(L/D)lactide (P(L/D)LA) 96/4 and a P(L/DL)LA 70/30 membrane plate to be applied for tissue engineering of the fibrocartilaginous temporomandibular joint disc. The PLA discs resulted to be suitable platforms for chondrogenic differentiation of adipose stem cells (ASCs) in vitro [52]. Moreover PLA is suitable as coating of bone implants, improving cell proliferation [2].

Polycaprolactone (PCL) is a bioresorbable, biocompatible polymer that has been well studied in these years for bone and cartilage repair. With respect to polylactic acid, this polymer is more stable at room conditions, less expensive and readily available in large amounts [62, 82]. It has been frequently studied in combination with other polymers or materials (see Sect. 2.2.4). The polymer is approved by the FDA for implantation in human body as drug delivery device, suture material (e.g. commercial Monocryl®), it is used in dentistry as root canal filling (e.g. Resilon™) and it has been approved recently as dermal filler product to be used in cosmetic treatments (Ellansé, AQTIS Medical, Netherlands).

Poly(propylene fumarate) (PPF) is an attractive biocompatible, biodegradable, osteoconductive biomaterial recently proposed for bone regeneration. It is an unsaturated linear polyester whose properties, such as glass transition temperature (*Tg*), can be varied depending on the polymer molecular weight. PPF can be crosslinked, through its fumarate double bonds, via radical polymerization by itself or with crosslinkers such as methylmethacrylate, *N*-vinyl pyrrolidinone (*N*-VP). The polymer can be used in preformed and injectable applications. It degrades to fumaric acid by hydrolysis of the ester bonds; the degradation time depends on polymer characteristics such as its molecular weight and, in case of crosslinked PPF, the type of crosslinker, and crosslinking degree [79].

Polyanhydrides and polyphosphazens are surface eroding polymers, unlike polyesters that are bulk eroding polymers. This means that their degradation is spatially controlled through their surface, with controlled release of degradation byproducts. Surface eroding polymers do not facilitate cell adhesion, but keep their structure and strength for longer periods than bulk eroding polymers.

Polyanhydrides are a hydrolytically unstable class of polymers that display poor mechanical properties (Young's modulus close to 1.3 MPa). They can be either aromatic, aliphatic, or a mixture of the two components and are synthesized by dehydration of the diacid or mixture of diacids by melt polycondensation. Since polyanhydrides demonstrated to be biodegradable and biocompatible polymers, they have been investigated as DDS.

Synthetic polyanhydrides derivatives, such as poly-[trimellitylimidoglycinr-co-bis(carboxyphenoxy)hexane] and polypyromellitylimidoalanine-co-1,6-bis(carboph-enoxy)hexane] resulted in considerable improved mechanical properties, with compressive strength up to 50–60 MPa; the osteocompatibility of these materials have been demonstrated [19]. Photocrosslinkable polyanhydrides have been also developed for orthopaedic applications, as injectable material to be in situ cross-linked [31]. Polyanhydrides degradation happen through hydrolysis, of firstly anhydride bonds, and subsequently of imides copolymer bonds, leading to non-toxic byproducts. Even if these polymers have several advantages in orthopaedic applications, such as good biocompatibility and atoxicity, their use is limited by their hydrolytical unstability.

Polyphosphazenes are polymers with high molecular weight, they present a phosphorous nitrogen backbone, the addition of imidazoyl or aminoacid alkyl ester side chains make them hydrolytically degradable. Degradation rate and cell attachment can be easily controlled by the nature of side chain and the percent of substitution. Polyphosphazene exhibits high blood compatibility and it is studied as a material for blood connecting devices. Also the degradation byproducts of the polymer are non-toxic. Derivatives of polyphosphazene that seems interesting for tissue engineering applications are: poly (ethyl glycinate)(p-methyl phenoxy) phosphazene, polyphosphazenes with amino acid pendat groups [10, 44, 45]

2.2.3 Ceramics

Ceramics are materials made from inorganic and non-metallic compounds with crystalline structure. This type of material shows good compressive strength and low ductility providing high resistance to the deformation and distortion, but they all fail for the brittle and the fragile nature. For this reason it is possible to overcome the drawbacks of this materials maintaining their advantages combining ceramics with polymeric materials (see Sect. 2.2.4). The materials that can be defined ceramics are reported in Table 3. The most common types of calcium phosphates used in bone engineering applications are hydroxyapatite (HAPP), β-tricalcium phosphate (β-TCP), biphasic calcium phosphate (BCP). These materials have good biocompatibility and osteoconductive properties, they have the capability to integrate into bone structures and support bone in-growth, without breaking down or dissolving. Hydroxyapatite ($Ca_{10}(PO_4)_6(OH)_2$) is a naturally occurring mineral form of calcium apatite crystallized in the hexagonal crystal system whose structure is similar to the mineral component of bones and hard tissues in mammals. HAP coming from teeth or bones as long as HAP from coral skeleton has been used in

bone tissue engineering. Nowadays a synthetic calcium based ceramic chemically similar to hydroxyapatite is available for bone engineering purposes. It has been used in orthopaedic, dental and maxillofacial applications as filler and to coat bone implants (e.g., in hip replacement) and dental implants. The dissolution rate of synthetic HAP depends on environmental parameters such as pH and ionic concentration of the soaking solution and on HAP composition and crystallinity.

β-TCP is the beta crystal form of tribasic calcium phosphate ($Ca_3(PO_4)_2$), it can be defined a bioceramic with bioresorbable properties. The degradation rate of β-TCP is 3–12 times higher than that of crystalline HAP. Partial degradation of β-TCP promotes bone bonding to the ceramic. Biodegradable composite scaffolds made of TCP and polyglycolic acid have been proposed [9]

BCP is a mixture of β-TCP and HAP (60%HAP, 40% β-TCP) that combines the reactivity of β-TCP and the stability of HAP; it results in a very bioactive compound.

Bioactive glasses (bioglass) are composed basically of SiO_2, Na_2O, CaO and P_2O_5. These materials are able to form a biological interface with surrounding tissue, they support enzyme activity, vascularization, osteoblast adhesion, growth, differentiation, inducing also mesenchimal cell differentiation into osteoblasts [14, 27, 49]. Several bioglasses are available on the market and are successfully used in clinical treatment of periodontal diseases (45S5 Bioglass®, Perioglass™) and as bone filler material (Novabone™). These materials have been extensively studied [26, 27] and it has been proved that they osteoinductives and osteoconductive properties depend on the composition. For example the commercial 45S5 Bioglass ® with SiO_2–Na_2O–CaO–P_2O_5 composition and less than 55% of SiO_2 has high bioactivity index and bond to soft and hard connective tissue. In general, it has been found that bioglass surface, whenever in contact with biological fluids, reacts and releases soluble ions such as Si, Ca, P, Na in critical concentrations that can induce intracellular and extracellular responses [14, 83]. As all ceramic materials, also bioglasses have poor mechanical properties in terms of low fracture toughness and mechanical strength, above all when formulated in porous structures.

2.2.4 Composite Materials

The term composite material generally refers to the combination, on a macroscopic scale, of two or more materials with different compositions, in order to achieve specific chemical, physical and mechanical properties. The different types of composites materials studied can be differentiated in two main categories: (i) the combination of one or more polymers with ceramic material, (ii) the combination of two different polymers. In all cases the purpose is to improve the physicochemical and biological performances of the final scaffold. In the case of composite materials obtained by combination of one or more polymers with ceramic materials there are several experimentals in the literature, and few of these composite materials are already on the market. For example hydroxyapatite has been combined to natural polymers such as chitosan [11] or synthetic polymers as PCL,

PLA, PLGA. Also a three phase combination of PCL and PLA with α-tricalciumphosphate (α-TCP), and a biphasic combination of polyglycolic acid (PGA) and β-TCP have been experimented achieving significant improvement of scaffold mechanical properties and osteoconductivity [9, 20, 21, 56, 63].

Polymeric blends of PLA and PEG, or PDLLA and PCL have also been studied in order to modulate the release kinetic of proteins loaded into the scaffolds [18].

The combination of two or more different polymers can be achieved through polymer copolymerization and/or polymer crosslinking.

For example in order to control HA degradation rate, and to make the polymer more tough, thus more suitable for bone applications, the polymer can be photocrosslinked with polyethylene glycol (PEG), or injected and in situ crosslinked with other polymers such as methylcellulose [22].

An example of composite material obtained by the combination of two different polymers is the multiblock copolymer containing poly-alpha-hydroxyacids and PEG, or polyethylene oxide at high molecular weight. These are extremely hydrophilic polymers with excellent solubility in a range of solvents and high solution mobility. The combination with poly-alpha-hydroxyacids can confer more elasticity and hydrophilicity to these last polymers. These properties can be useful in some tissue engineering applications [58].

The combination of two polymers can be achieved also by blending the polymers in order to form scaffolds. This has been experimented by combining PLA and calcium alginate, PLA and PCL or PLA and PEG. Each polymer combination can be useful to get specific and suitable scaffold properties. For example addition of PEG to PLA leads to polymer plasticisation, depending on the PEG amount added and its molecular weight, while addition of PCL to PLA makes the final composite more though and with lower degradation rate than the starting PLA. These combinations are able to modulate the release kinetic of a biomolecule such as a growth factor, from the scaffold [18, 30]

2.3 Structural and Functional Characteristics of Polymer Scaffold for Bone Regeneration

Apart from the scaffold characteristics strictly related to the polymer, there are some structural and functional characteristics typical of the scaffold. Thus, the scaffold should comply the structural design criteria highlighted in Sect. 1.1.

More details about porosity requirements and mechanical properties are here reported.

A macroscopic pore network in the scaffold is a necessary tool to promote cell seeding distribution, cell migration throughout the 3D space, exchange of waste products and neovascularisation after in vivo implantation of the scaffold. Pore size should be bigger than 100 μm, and the pores should be interconnected: this parameter can be thoroughly characterized. Scanning electron microscopy (SEM)

allows the examination either of the whole scaffold or of its sections in order to evaluate whether the porosity is homogeneously distributed and if pores are interconnected (Fig. 5). Sometimes, depending on the scaffold preparation method

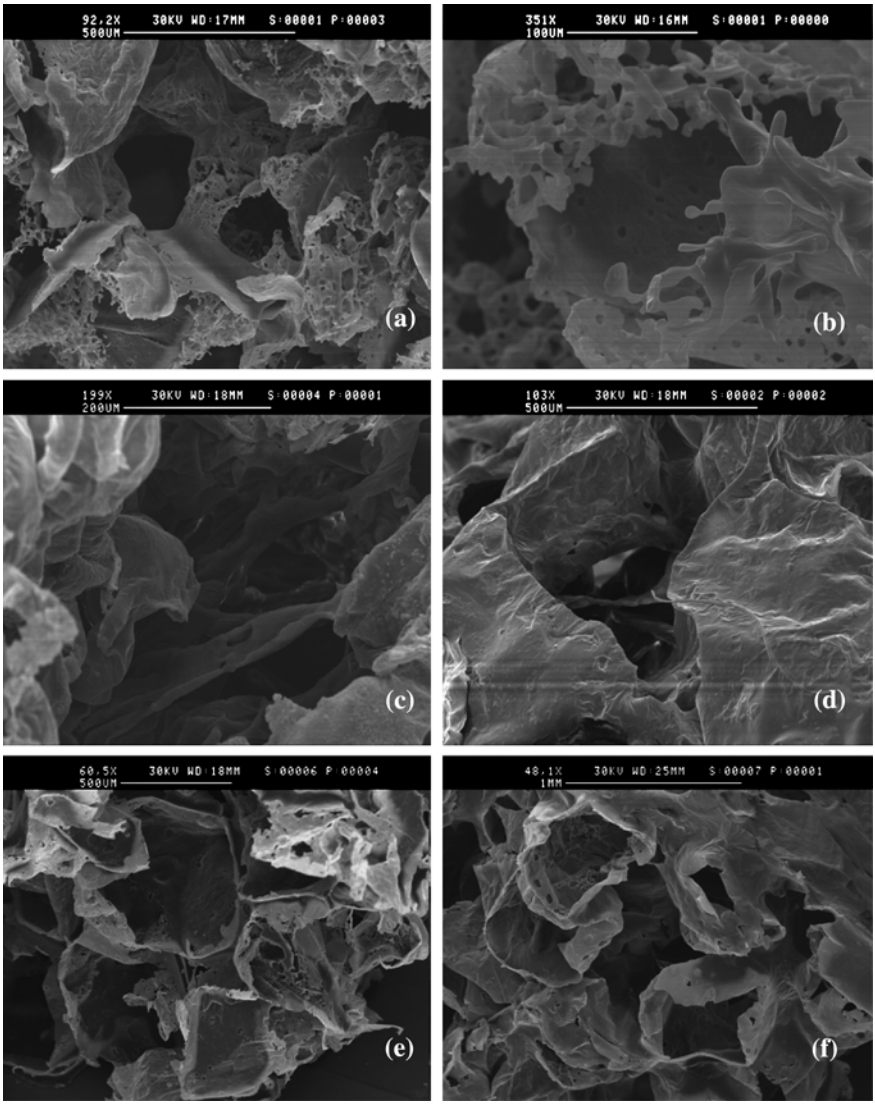

Fig. 5 Scanning electron photomicrographs of PLGA scaffolds prepared using salt as porogen: **a** view transverse section at low magnification (92.2×), **b** wall pore structure (magnification 351×), **c** interconnected scaffold network (magnification 199), **d** interconnected scaffold network (magnification 103), **e** view transverse section at low magnification (60.5), **f** porous structure details (magnification 48.1). (From [15])

used, the outer surface is significantly different in morphology with respect to the inner surface.

AFM is another important tool to examine the outer scaffold surface, highlighting porosity and nanostructurations [25].

Total scaffold macroporosity can be measured by techniques such as liquid displacement and surface area analyzer. The data that can be obtained by these techniques are: porosity reported as a percentage value and density. Suitable porosities values should be >80%; these techniques do not give information about pore size.

Porosity and pore size can affect also scaffold mechanical properties: that is the two parameters must match.

In recent years attention has been addressed to scaffold nanostructure mimicking the nanoscale size of bone constituents such as collagen fibers that are between 50–500 nm. In order to better promote cell interaction, nanofibrous porewall structures have been prepared by thermally induced phase separation method combined to solvent casting particle leaching. Another example of scaffold nanostructuration is achieved by growing apatite crystals onto the polymeric scaffold [25, 70, 76].

As mentioned above, the mechanical properties of scaffolds are an important functional parameter. A polymer scaffold for bone regeneration should have compressive and tensile resistance similar to bone. Hard and brittle materials such as hydroxyapatite have excellent compressive strength but poor tensile properties, while a lot of polymers, above all natural polymers, have poor compressive strength. The combination of two or more materials is a good strategy in order to modulate scaffold mechanical properties. It must be considered that also the scaffold porosity can affect its mechanical properties.

In a work performed by the research group [3] the compressive, tensile and flexural strengths have been determined on PLGA and PLGA/HAPP scaffold using the electromagnetic machine Enduratec Elf3200 (Bose Corporation, Eden Prairie, MN, USA). In this example compression stress–strain curves of PLGA scaffolds showed three linear regions and compression stress–strain curves of PLGA/HAP scaffolds showed two linear regions (Fig. 6). All tension tests showed one linear region before yield and failure. Compression and tensile moduli as derived from all the linear regions are reported in Table 4. The presence of HAP in the composite scaffolds did not seem to improve the compression properties of polymeric scaffolds, while tensile properties are improved by addition of HAP to the polymeric structure.

2.4 Tissue Engineered Scaffold Preparation Techniques

Several preparation techniques have been proposed for scaffolds in the last years. Some of them have been adapted from other research areas or they have been achieved through modification of traditional techniques. A suitable preparation

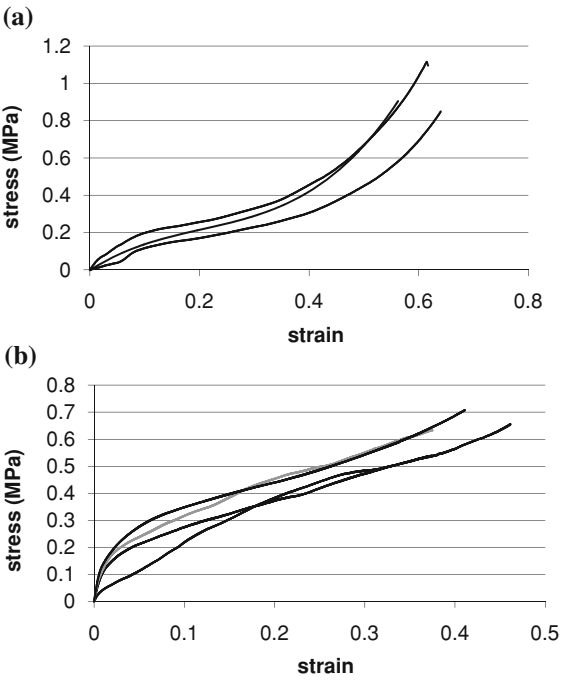

Fig. 6 Stress–strain curves of: **a** PLGA scaffold, **b** PLGA/HAP scaffold

Table 4 Compression and tensile properties of PLGA and PLGA/HAP scaffolds (From [3])

	Compression test			Tensile test		
Scaffold type	Ec1 (Mpa)	Ec2 (Mpa)	Ec3 (Mpa)	Et (Mpa)	Ts (Mpa)	UTS (Mpa)
PLGA	1.66 ± 0.76	0.88 ± 0.17	3.07 ± 0.28	2.88 ± 1.44	0.13 ± 0.03	0.15 ± 0.03
PLGA/HAP	4.76 ± 2.32	1.07 ± 0.16	–	15.68 ± 4.41	0.17 ± 0.04	0.35 ± 0.12

technique should allow: (i) the manufacturing of scaffolds whose characteristics match their design requirements and, (ii) the reproducibility of the preparation process and of scaffold properties. The most common conventional techniques are: solvent casting particulate (porogen) leaching, non-solvent induced phase separation, thermally induced phase separation, foaming process, microsphere sintering and electrospinning. Among these, solvent casting particulate leaching is one the first applied scaffold preparation methods suitable for synthetic hydrophobic, biodegradable polymers such as PLA, PLGA. In this method the polymer is dissolved in an organic solvent (e.g. chloroform, methylene chloride), the polymeric solution is mixed with a particulate material (porogen) such as NaCl or sugar, the suspension is placed in a mould. The solid 3D-scaffold is achieved by evaporation of polymer solvent, that can take place under vacuum (freezedrying) or at room temperature, and subsequent elimination of the porogen material through prolonged soaking in deionized water. The parameter most affecting scaffold

properties by this preparation technique is porogen granulometry that should be enough large to obtain interconnected pores bigger than 300–350 μm. In a study performed by Dorati [15], scaffolds with high porosity (83.8 and 89.4%) and an interconnected network were obtained by solvent casting particulate leaching (Fig. 5). It was found that the choice of the porogen type (sodium chloride or sucrose) was responsible for the three-dimensional structure (pore size, porosity, apparent density), the mechanical properties of the scaffold and for physico-chemical PLGA polymer modifications such as polymer degradation reactions, polymer chain rearrangement, T_g changes [15]. Paraffin microspheres have also been used as porogen in alternative to salt or sucrose. The advantage of using paraffin microsphere is their regular spherical shape and size that acts as template for the scaffold, leading to scaffolds with very high porosity whose pore size is tailored by the paraffin microsphere size. The drawback is the use of organic solvents such as exane and cycloexan to dissolve the paraffin particles, that should be accurately eliminated through subsequent freeze-drying cycles.

In general, the main drawbacks of the technique of solvent casting particle (porogen) leaching are the long processing times, the use of organic solvents, the differences in the morphology of the outer scaffold surface with respect to the inner scaffold surface. The combination of this technique with other methods as injection or compression molding, gas foaming process, are useful to overcome the drawbacks highlighted [80].

Gas foaming technique is an interesting method to produce highly porous scaffold avoiding the use of cytotoxic organic solvents. The method has been frequently applied to thermoplastic polymers such as PLGA, PLA, PCL. The technique is assessed depending of the different foaming agents used: water, fluoroform, CO_2 and nitrogen. CO_2 as foaming agent has the advantage that the solvent is cheap, non-toxic and does not need to be removed before seeding the scaffold. The gas can be dissolved in the solid polymer or in the polymer melt at high temperature and pressure. For example suitable process conditions for PLGA can be 35–40°C, 10–20 MPa, for PCL 70–90°C and 7–32 MPa [37, 48, 65, 69].

Electrospinning is one of the most versatile conventional techniques since it allows the formation of nanosized fibers that can be assembled together to form non-woven sheets with 2D profiles, non-woven 3D fibrous meshes or multilayered structures of different polymers solutions. The scaffolds obtained by an electrospinning process are nanofiber-based scaffold with favourable properties such as wide range of pore size distribution, high porosity and surface area/volume ratio [23, 46, 68, 78, 80].

Some of the recently proposed preparation techniques are: rapid prototyping (RP), solid free-form (SFF), shape deposition manufacturing, fused deposition modelling, 3D printing, selective laser sintering, stereolithographic technique, molecular self-assembly.

Among these, RP is an emerging technique for biomaterials based scaffold that can be used with different materials [5, 12, 55, 75]. Moreover, scaffold is manufactured directly from a computer-aided design data set, thus it is built up in a specific body shape by the selective material addition guided by a computer

program. This technique has been expanded through the computer-aided tissue engineering techniques that represent a valid supporting utility.

Molecular self-assembly is an attractive approach for scaffold preparation even if it has the disadvantage of being quite elaborate. It is based on hierarchical structures formation by self-association of molecules, and it allows the realization of different constructs such as peptide nanotubes, ordered nanofiber scaffolds, segmented surface assembling peptides, dipolar molecules [39, 41].

An attractive aspect of scaffold preparation technology is the loading of bioactive agents. The presence of growth factors inside a scaffolds should improve bone regeneration, being an important aid for those patients with low tissue regeneration potential, e.g. old and sick patients. Nevertheless some problems are highlighted: (i) growth factors are instable molecules with short half-life in vivo; (ii) the amount of growth factor should be set very attentively, because of their cancerogenic potential. The bioactive agents most studied for bone regeneration are: BMPs, TGF, basic fibroblast growth factor (bFGF). Growth factor instability can be overcome through loading into a carrier that protect the protein and promotes its controlled release hence prolongs its activity whenever administered into the body. Hydrogel polymers such as gelatine, dextran, alginate have been successfully studied on this purpose. Microspheres and sponges can be suitable carriers; the protein should physically interact with the hydrogel, and it should be released upon its biodegradation. In this way growth factor release can be controlled by the delivery system characteristics [72, 74, 77].

2.5 Clinical Aspects

The goal of bone regeneration through polymer scaffold application can be achieved by different ways: (i) in vivo application of the polymer scaffold; (ii) in vitro tissue reconstruction by cell culture and in vivo application of the grown tissue; (iii) in vivo application of cells combined to an immunoisolation membrane or biomaterial.

The In vivo application of polymeric scaffold has the advantage that all the components necessary for tissue regeneration, such as growth factors, are provided by the biological environment. For this reason this approach is the most pursued. However, different answer to the regenerative therapy have been highlighted in young healthy patients with respect to old sick patients, suffering for example of diabetes or hyperlipidemiae, and presenting lower regeneration potential.

For the latter type of patients the use of polymer scaffold loaded with growth factors and/or already available differentiated cells should be advantageous. In vitro tissue reconstruction involves large scale cell culture methods to achieve bioartificial hybrid organs. The big problem in developing in vitro tissue reconstruction is to induce artificial arrangement of a biological environment and its successful implantation in vivo. This promising approach can involve also in vitro differentiation of mesenchymal stem cells.

3 Conclusion

The goal of the chapter was to introduce polymer scaffold for bone regeneration. Polymeric scaffolds are not only plain implants for bone regeneration, but they can be also delivery systems for bioactive agents. Moreover when speaking about biodegradable polymers their goal is to act as temporary support promoting cell adhesion and proliferation in vivo or in vitro, also in order to create artificial tissues.

It is important to underline that tissue engineering technology is an expanding area where different disciplines are involved in order to achieve tissue regeneration.

Collaborative research between material, pharmaceutical, biological and clinical scientists is needed and work is still to be done.

In the field of polymer scaffold an important effort should be done to investigate newly synthesized biodegradable polymers with suitable properties for bone regeneration.

References

1. Amidi, M., Romeijn, S.G., Verhoef, J.C., Junginger, H.E., Bungener, L., Huckriede, A., Crommelin, D.J.A., Jiskoot, W.: N-Trimethyl chitosan (TMC) nanoparticles loaded with influenza subunit antigen for intranasal vaccination: biological properties, immunogenicity in a mouse model. Vaccine **25**, 144–155 (2007)
2. Asti, A., Visai, L., Dorati, R., Conti, B., Saino, E., Sbarra, S., Gastaldi, G., Benazzo, F.: Improved cell growth by Bio-Oss/PLA scaffolds for use as a bone substitute. Technol. Health Care **16**, 401–413 (2008)
3. Asti, A., Gastaldi, G., Dorati, R., Saino, E., Conti B., Visai, L., Benazzo, F.: Human adipose-derived stem cells (hASCs) grown on PLGA, PLGA/HAP and titanium scaffolds for surgical applications. Bioinorg. Chem. Appl. Article ID 831031,12 (2010)
4. Badylak, S.F.: Modification of natural polymers: collagen. In: Atala, A., Lanza, R. P. (eds.) Methods of Tissue Engineering. pp. 505–514. Academic Press, San Diego (2002)
5. Bartolo, P.J.S., Almeida, H., Laoui, T.: Rapid prototyping and manufacturing for tissue engineering scaffolds. Int. J. Comput. Appl. Technol. **36**(1), 1–9 (2009)
6. Benedetti, L., Cortivo, R., Berti, T., Berti, A., Pea, F., Mazzo, M., Moras, M., Abatangelo, G.: Biocompatibility and biodegradation of different hyaluronan derivatives (Hyaff) implanted in rats. Biomaterials **14**, 1154–1160 (1994)
7. Cai, X., Tong, H., Shen, X., Chen, W., Yan, J., Hu, J.: Preparation and characterization of homogeneous chitosan–polylactic acid/hydroxyapatite nanocomposite for bone tissue engineering and evaluation of its mechanical properties. Acta Biomater. **5**(7), 2693–2703 (2009)
8. Campoccia, D., Hunt, J.A., Doherty, P.J., Zhong, S.P., O'Regan, M., Benedetti, L.: Quantitative assessment of the tissue response to films of hyaluronan derivatives. Biomaterials **17**, 963–975 (1996)
9. Cao, H., Kuboyama, N.: A biodegradable porous composite scaffold of PGA/β-TCP for bone tissue engineering. Bone **46**, 386–395 (2010)
10. Chang, Y., Bender, J.D., Phelps, M.V.B., Allcock, H.R.: Synthesis and self-association behavior of biodegradable amphiphilic poly[bis(ethyl glycinat-N-y)phosphazene]-PEO block copolymers. Biomacromolecules **3**, 1364–1369 (2002)

11. Chesnutt, B.M., Yuan, Y., Buddington, K., Haggard, W.O., Bumgardner, J.D.: Composite chitosan/nano-hydroxyapatite scaffolds induce osteocalcin production by osteoblasts in vitro and support bone formation in vivo. Tissue Eng. Part A **15**(9), 2571–2579 (2009)
12. Chua, C.K., Feng, C., Lee, C.W., Ang, G.Q.: Rapid investment casting: direct and indirect approaches via model maker II. Int. J. Adv. Manuf. Technol. **25**(1), 26–32 (2005)
13. Colonna, C., Conti, B., Perugini, P., Pavanetto, F., Modena, T., Dorati, R., Iadarola, P., Genta, I.: Ex vivo evaluation of prolidase loaded chitosan nanoparticles for the enzyme replacement therapy. Eur. J. Pharm. Biopharm. **70**, 58–65 (2008)
14. Day, R.M., Boccaccini, A.R., Shurey, S., Roether, J.A., Forbes, A., Hench, L.L.: Assessment of polyglycolic acid mesh and bioactive glass for soft tissue engineering scaffolds. Biomaterials **25**, 5857–5866 (2004)
15. Dorati, R., Colonna, C., Genta, I., Modena, T., Conti, B.: Effect of porogen on the physico-chemical properties and degradation performance of PLGA scaffolds. Polym. Degrad. Stab. **94**, 694–701 (2010)
16. Ghosh, S., Viana, J.C., Reis, R.L., Mano, J.F.: The double porogen approach as a new technique for the fabrication of interconnected poly(L-lactic acid) and starch based biodegradable scaffolds. J. Mater. Sci. Mater. Med. **18**, 185–193 (2007)
17. Gianolio, D.A., Philbrook, M., Avila, L.Z., Young, L.E., Plate, L., Santos, M.R., Bernasconi, R., Liu, H., Ahn, S., Sun, W., Jarrett, P.K., Miller, R.J.: Hyaluronan-tethered opioid depots: synthetic strategies and release kinetics in vitro and in vivo. Bioconjugate Chem. **19**(9), 1767–1774 (2008)
18. Ginty, P.J., Barry, J.J.A., White, L.J., Howdle, S.M., Shakesheff, K.M.: Controlling protein release from scaffold using polymer blends and composites. Eur. J. Pharm. Biopharm. **68**, 82–89 (2008)
19. Gopferich, A., Tessmar, J.: Polyanhydrides degradation and erosion. Adv. Drug Deliv. Rev. **54**, 911 (2002)
20. Guarino, V., Ambrosio, L.: The synergic effect of polylactide fiber and calcium phosphate particle reinforcement in poly-epsilon-caprolactone based composite scaffolds. Acta Biomater. **4**, 1778–1787 (2008)
21. Guarino, V., Taddei, D., DiFoggia, M.: The influence of hydroxyapatite particles on in vitro degradation behaviour of poly epsilon caprolactone based composite scaffolds. Tissue Eng. Part A **15**, 3655–3668 (2009)
22. Gupta, D., Tator, C.H., Shoichet, M.S.: Fast-gelling injectable blend of hyaluronan and methylcellulose for intrathecal, localized delivery to the injured spinal cord. Biomaterials **27**(11), 2370–2379 (2006)
23. Gupta, D., Venugopal, J., Mitra, S., GiriDev, V.R., Ramakrishna, S.: Nanostructured biocomposite substrates by electrospinning and electrospraying for the mineralization of osteoblasts. Biomaterials **30**(11), 2085–2094 (2009)
24. Hadjidakis, D.J., Androulakis, I.I.: Bone remodeling. Ann. N. Y. Acad. Sci. **1092**, 385–396 (2006)
25. Hassenkam, T., Fantner, G.E., Cutroni, J.A., Weaver, J.C., Morse, D.E., Hansma, P.K.: High resolution AFM imaging of intact and fractured trabecular bone. Bone **35**(1), 4–10 (2004)
26. Hench, L.L.: Bioceramics: from concept to clinic. J. Am. Ceram. Soc. **74**, 1487–1510 (1991)
27. Hench, L.L.: Bioceramics. J. Am. Ceram. Soc **81**(7), 1705–1728 (1998)
28. Hoeman, C.D., Sun, J., Legare, A., McKee, M.D., Buschmann, M.D.: Tissue engineering of cartilage using an injectable and adhesive chitosan-based cell-delivery vehicle. Osteoarthritis Cartilage **13**(4), 318–329 (2005)
29. Homma, A., Sato, H., Okamachi, A., Emura, T., Ishizawa, T., Kato, T., Matsuura, T., Sato, S., Tamura, T., Higuchi, Y., Watanabe, T., Kitamura, H., Asanuma, K., Yamazaki, T., Ikemi, M., Kitagawa, H., Morikawa, T., Ikeya, H., Maeda, K., Takahashi, K., Nohmi, K., Izutani, N., Huang, M., Khor, E., Lim, L.Y.: Uptake and cytotoxicity of chitosan molecules, nanoparticles: effects of molecular weight, degree odf deacetylation. Pharm. Res. **21**(2), 344–353 (2004)

30. Hou, Q.P., Walsh, M.C., Freeman, J.J.A., Barry, S.M., Howdle, K.M.: Incorporation of protein within fibre-based scaffolds using a post-fabrication entrapment method. J. Pharm. Pharmacol. **58**, 895–902 (2006)
31. Ifkovits, J.L., Burdick, J.A.: Photopolymerizable and degradable biomaterials for tissue engineering applications. Tissue Eng. **13**(10), 2369–2385 (2007)
32. Jacobs, C.R.: The mechanobiology of cancellous bone structural adaptation. J. Rehabil. Res. Dev. **37**, 209–216 (2000)
33. Kanda, M., Suzuki, R.: Novel hyaluronic acid-methotrexate conjugates for osteoarthritis treatment. Bioorg. Med. Chem. **17**(13), 4647–4656 (2009)
34. Katayama, Y., Montenegro, R., Freier, T., Midha, R., Belkas, J.S., Shoichet, M.S.: Coil-reinforced hydrogel tubes promote nerve regeneration equivalent to that of nerve autografts. Biomaterials **27**(3), 505–518 (2006)
35. Khan, Y., Yaszemski, M.J., Mikos, A.G., Laurencin, C.T.: Tissue engineering of bone: material and matrix considerations. J. Bone Joint Surg. **90**, 36–42 (2008)
36. Kim, H.D., Valentini, R.F.: Retention and activity of BMP-2 in hyaluronic acid-based scaffolds in vitro. J. Biomed. Mater. Res. Part A **59**(3), 573–584 (2002)
37. Kim, T.K., Yoon J.J., Lee, D.S., Park, T.G.: Gas foamed open porous biodegradable polymeric microspheres. Biomaterials **27**(2), 152–159 (2006)
38. Kim, I.Y., Seo, S.J., Moon, H.S., Yoo, M.K., Park, I.Y., Kim, B.C., Cho, C.S.: Chitosan and its derivatives for tissue engineering applications. Biotechnol. Adv. **26**(1), 1–21 (2008)
39. Kisiday, J.D., Jim, M., DiMicco, M.A., Kurz, B., Grodzinsky, A.J.: Effects of dynamic compressive loading on chondrocyte biosynthesis in self assembling peptide scaffolds. J. Biomech. **37**(5), 595–604 (2004)
40. Klein, A.W.: Collagen substances. Facial Plast. Surg. Clin. North. Am. **9**(2), 205–218 (2001)
41. Klok, H.-A., Hwang, J.J., Hartgerink, J.D., Stupp, S.I.: Self assembling biomaterials: L-lysine-dendron-substitute cholesterylg(L-lactic acid). Macromolecules **35**(16), 6101–6111 (2002)
42. Krauland, A.H., Alonso, M.J.: Chitosan/cyclodextrin nanoparticles as macromolecular drug delivery system. Int. J. Pharm. **340**, 134–142 (2007)
43. Lakshmi, N.S., Laurencin, C.T.: Polymers as biomaterials for tissue engineering and controlled drug delivery. Adv. Biochem. Eng./Biotechnol. **102**, 47–90 (2006)
44. Lakshmi, S., Katti, D.S., Laurencin, C.T.: Biodegradable polyphosphazenes for drug delivery applications. Adv. Drug Deliv. Rev. **25;55**(4), 467–482 (2003)
45. Lakshmi, S., Lee, D., Bender, J.D., Barrett, E.W., Greish, Y.E., Brown, P.W., Allcock, H.R., Laurencin, C.T.: Synthesis, characterization and in vitro osteocompatibility evaluation of novel biodegradable [poly(ethylalanato)(alkyloxybenzoate)phosphazenes]. J. Biomater. Res. **76A**, 206–213 (2006)
46. Li, M., Mondrinos, M.J., Chen, X., Gandhi, M.R., Ko, F.K., Lelkes, P.I.: Co-electrospun poly(lactide-co-glycolide), gelatin, and elastin blends for tissue engineering scaffolds. J. Biomed. Mater. Res. A **79**(4), 963 (2006)
47. Li, J., Du, Y., Liang, H.: Influence of molecular parameters on the degradation of chitosan by a commercial enzyme. Polym. Degrad. Stab. **92**(3), 515–524 (2007)
48. Lim, Y.M., Gwon, H.J., Shin, J., Jeun, J.P., Nho, Y.C.: Preparation of porous poly (ε-caprolactone) scaffolds by gas foaming process and in vitro/in vivo degradation behavior using γ-ray irradiation. J. Ind. Eng. Chem. **14**(4), 436–441 (2008)
49. Lu, H.H., Tang, A., Oh, S.C., Spalazzi, J.P., Dionisio, K.: Compositional effects on the formation of a calcium phosphate layer and the response of osteoblast-like cells on polymer-bioactivecomposites. Biomaterials **26**, 2281–2288 (2005)
50. Ma, P.X.: Biomimetic materials for tissue engineering. Adv. Drug Del. Rev. **60**, 184–198 (2008)
51. Mackie, E.J.: Osteoblasts: novel roles in orchestration of skeletal architecture. Int. J. Biochem. Cell Biol. **35**, 1301–1305 (2003)
52. Mäenpää, K., Ellä, V., Mauno, J., Kellomäki, M., Suuronen, R., Ylikomi, T., Miettinen, S.: Use of adipose stem cells and polylactide discs for tissue engineering of the temporomandibular joint disc. J. R. Soc. Interface (2009). doi:10.1098/rsif.2009.0117

53. Mason, C., Dunnill, P.: A brief definition of regenerative medicine. Regen. Med. **3**(1), 1–5 (2008)
54. Matsuno, T., Hashimoto, Y., Adachi, S., Omata, K., Yoshitaka, Y., Ozeki, Y., Umezu, Y., Tabata, Y., Nakamura, M., Satoh, T.: Preparation of injectable 3D-formed beta-tricalcium phosphate bead/alginate composite for bone tissue engineering. Dent Mater J**27** (6), 827–834 (2008).
55. Mironov, V., Boland, T., Trusk, T., Forgacs, G., Markwald, R.R.: Organ printing: computer-aided jet-based 3D tissue engineering. Trends Biotech. **21**(4), 157–161 (2003)
56. Nie, H., Wang, C.-H.: Fabrication and characterization of PLGA/HAP composite scaffolds for delivery of BMP-2 plasmid DNA. J Control Release. **120**(1–2), 111–121 (2007)
57. Patterson, J., Siew, R., Herring, S.W., Lin, A.S.P., Guldberg, R., Stayton, P.S.: Hyaluronic acid hydrogels with controlled degradation properties for oriented bone regeneration. Biomaterials **31**(26), 6772–6781 (2010)
58. Place, E.S., George, J.H., Williams, C.K., Stevens, M.M.: Synthetic polymer scaffolds for tissue engineering. Chem. Soc. Rev. **38**, 1139–1151 (2009)
59. Porpiglia, F., Renard, J., Billia, M., Morra, I., Terone, C., Scarpa, R.M.: Biological glues and collagen fleece for hemostasis during laparoscopic partial nephrectomy: technique and results of perspective study. J. Endourol. **21**(4), 423–428 (2007)
60. Porter, J.R., Ruckh, T.T., Popat, K.C.: Bone tissue engineering: a review in bone biomimetics and drug delivery strategies. Biotechnol. Prog. **25**, 1539–1560 (2009)
61. Portero, A., Remunan-Lopez, C., Criado, M.T., Alonso, M.J.: Reacetylated chitosan microspheres for controlled delivery of antimicrobial agents to the gastric mucosa. J. Microencapsul. **19**(6), 797–809 (2002)
62. Reichert, J.C., Heymer, A., Berner, A., Eulert, J., Nöth, U.: Fabrication of polycaprolactone collagen hydrogel constructs seeded with mesenchymal stem cells for bone regeneration. Biomed. Mater. **4**(6), 5001 (2009)
63. Rezwan, K., Chen, Q.Z., Blaker, J.J., Boccaccini, A.R.: Biodegradable and bioactive porous polymer/inorganic composite scaffolds for bone tissue engineering. Biomaterials **27**, 3413–3431 (2006)
64. Safadi, F.F., Xu, J., Smock, S.L., Kanaan, R.A., Selim, A.H., Odgren, P.R., Marks Jr, S.C., Owen, T.A., Popoff, S.N.: Expression of connective tissue growth factor in bone: its role in osteoblast proliferation and differentiation in vitro and bone formation in vivo. J. Cell. Physiol. **196**, 51–62 (2003)
65. Salerno, A., Di Maio, E., Iannace, S., Netti, P.A.: Engineering of foamed structures for biomedical application. J. Cell. Plast. **45**, 103–117 (2009)
66. Sayin, B., Somavarapu, S., Li, X.W., Thanou, M., Sesardic, D., Alpar, H.O., Senel, S.: Mono-N-carboxymethyl chitosan (MCC) and N-trimethyl chitosan (TMC) nanoparticles for non-invasive vaccine delivery. Int. J.Pharm. **363**, 139–148 (2008)
67. Sell, S.A., Francis, M.P., Garg, K., McClure, M.J., Simpson, D.G., Bowlin, G.L.: Cross-linking methods of electrospun fibrinogen scaffolds for tissue engineering applications. Biomed. Mater. **3**(4), 450–501 (2008)
68. Shen, Y.H., Shoichet, M.S., Radisic, M.: Vascular endothelial growth factor immobilized in collagen scaffold promotes penetration and proliferation of endothelial cells. Acta Biomater. **4**(3), 477–489 (2008)
69. Singh, I., Kumar, V., Ratner, B.D.: Generation of porous microcellular 85/15 poly(DL)-lactide-co-glycolide foams for biomedical applications. Biomaterials **25**(3), 2611–2617 (2004)
70. Smith, I.O., Liu, X.H., Smith, L.A., Ma, P.X.: Nanostructured polymer scaffolds for tissue engineering and regenerative medicine. Adav. Rev. **1**, 226–236 (2009)
71. Stella, J.A., D'Amore, A., Wagner, W.R., Sacks, M.S.: On the biomechanical function of scaffolds for scaffolds for engineering load-bearing soft tissues. Acta Biomater. **6**(7), 2365–2381 (2010)
72. Tabata, Y.: Tissue regeneration based on growth factor release. Tissue Eng. **9**(S1), 5–15 (2004)

73. Tabata, Y.: Biomaterial technology for tissue engineering aplications. J. R. Soc. Interface **6**, S311–S324 (2009)
74. Tessmar, J.K., Gopferich, A.M.: Matrices and scaffolds for protein delivery in tissue engineering. Adv. Drug Del. Rev. **59**, 274–291 (2007)
75. Thushari, H.M., Herath, U., DiSilvio, L., Evans, J.R.G.: Biological evaluation of solid freeformed, hard tissue scaffold for orthopedic applications. J. Appl. Biomater. Biomech. **8**(2), 89–96 (2010)
76. Tran, N., Webster, T.J.: Nanotechnology for bone materials. WIREs Nanomed. Nanobiotechnol. **1**, 336–351 (2009)
77. Van Tomme, S.R., Hennink, W.E.: Biodegradable dextran hydrogels for protein delivery applications. Expert Res. Med. Dev. **4**, 147–164 (2007)
78. Wan, L.S., Xu, Z.K.: Polymer surfaces structured with random or aligned electrospun nanofibers to promote the adhesion of blood platelets. J. Biomed. Mater. Res. Part A **89**(1), 168–175 (2009)
79. Wang, S., Lu, L., Yaszemski, M.J.: Bone tissue-engineering material poly(propylene fumarate): correlation between molecular weight, chain dimensions, and physical properties. Biomacromolecules **7**(6), 1976–1982 (2006)
80. Weigel, T., Schinkel, G., Lendlein, A.: Design and preparation of polymeric scaffolds for tissue engineering. Future Drugs **6**, 835–851 (2006)
81. Williams, D.F.: On the mechanisms of biocompatibility. Biomaterials **29**(20), 2941–2953 (2008)
82. Williams, J.M., Adewunmib, A., Scheka, R.M., Flanagan, C.L., Krebsbacha, P.H., Feinberg, S.E., Hollister, S.J., Das, S.: Bone tissue engineering using polycaprolactone scaffolds fabricated via selective laser sintering. Biomaterials **26**, 4817–4827 (2005)
83. Xynos, I.D., Edgar, A.J., Buttery, L.D.K., Hench, L.L., Polak, M.: Gene expression profiling of human osteoblests following treatment with the ionic production of Bioglass 45S5 dissolution. J. Biomed. Mater. Res. **55**, 151–157 (2001)
84. Yuan, Y., Chesnutt, B.M., Utturkar, G., Haggard, W.O., Yang, Y., Ong, J.L., Bumgardner, J.D.: The effect of cross-linking of chitosan microspheres with genipin on protein release. Carbohydr. Polym. **68**(3), 561–567 (2007)

Part III
Scaffolds Based on Natural Polymers

Instructive Biomaterials for Myocardial Regeneration and Repair

Emil Ruvinov and Smadar Cohen

Abstract Tissue regeneration following myocardial infarction (MI) represents a major challenge in cardiovascular therapy, as current clinical approaches are limited in their ability to regenerate or replace damaged myocardium. The lack of clinically-relevant cell sources, and the growing importance of paracrine effects of cell therapy, mediated by soluble growth factors and cytokines, favors the use of acellular biomaterials for myocardial tissue engineering. While the efficacy of acellular scaffold-based approaches have already been shown, applying the biomaterial in an injectable form represents a more clinically-appealing strategy, where only minimally invasive interventions are required to deliver the biopolymer solution. However, in order to enhance the passive effects mediated by the injected biomaterial on infarct stabilization and mechanical support, and achieve long-term functional improvement and regeneration of the cardiac muscle, the combination with controlled spatio-temporal delivery of bioactive molecules is required. Biomaterial-based growth factor delivery has already been shown to improve therapeutic outcome after MI. Affinity-binding alginate represents an example of such a system. This strategy has promising potential for myocardial repair and regeneration, as it provides mechanical support conferred by in situ hydrogel formation, and can affect multiple processes of myocardial regeneration by controlled delivery of multiple proteins. In conclusion, as the development of novel polymer schemes and approaches continues, the application of biomaterials that can instruct a favorable tissue reconstruction, facilitate self-repair, tissue salvage and regeneration, represents a platform for future modifications and combinations (for instance, with cell therapy). Hopefully, such efforts will have major clinical consequences on the treatment of MI and improve long-term outcome in heart failure patients.

E. Ruvinov (✉) and S. Cohen
The Avram and Stella Goldstein-Goren Department of Biotechnology Engineering,
Ben-Gurion University of the Negev, 84105 Beer-Sheva, Israel
e-mail: ruvinovemil@gmail.com

Stud Mechanobiol Tissue Eng Biomater (2011) 8: 289–328
DOI: 10.1007/8415_2010_53

Published Online: 20 January 2011

1 Myocardial Infarction, Heart Failure and Current Therapies

Coronary heart disease (CHD) is now the leading cause of death worldwide [126]. Death rates from CHD have decreased in North America and in many countries in Western Europe [71]. This decline has been due to improved prevention, diagnosis, and treatment, in particular reduced cigarette smoking among adults, and lower average levels of blood pressure and blood cholesterol. However, the burden of CHD is increasing in developing and transitional countries, partly as a result of increasing longevity, urbanization, and lifestyle changes. It is expected that 82% of the future increase in coronary heart disease mortality will occur in developing countries.

One of the major causes of CHD is acute myocardial infarction (MI). MI results from temporary or permanent occlusion of the main coronary arteries, causing significant blood supply reduction to the beating heart muscle. Five partially overlapping phases can be distinguished in the progression from healthy to infarcted myocardium: (1) cardiomyocyte loss due to an initial ischemic event, (2) acute inflammatory response, (3) extracellular matrix (ECM) remodeling, (4) granulation tissue formation, and (5) scar formation and left ventricular (LV) remodeling. The structural remodeling of the heart (i.e. infarct wall thinning, scar formation and noninfarcted myocardium hypertrophy) leads to LV functional remodeling; a progressive deterioration in heart muscle function that eventually leads to congestive heart failure (CHF) [74].

Over recent decades, major improvements have been realized in the management of patients with acute MI [10]. These include in-hospital treatments (e.g. pharmacological lysis, anti-platelet and anti-thrombin therapies), interventional therapies and surgery (e.g. cardiac catheterization, percutaneous coronary intervention, coronary artery bypass surgery, and heart transplantation) and drug regimens for prevention and long-term treatment (e.g. aspirin, ACE inhibitors, β-blockers, and statins). Improved management of acute coronary events, however, has led to a significant increase in the number of patients that suffer from chronic conditions, namely CHF.

The major disadvantage of current therapies is their inability to replace, at least partially, cardiac muscle loss after infarction. Thus, there is a need for alternative approaches able to overcome the limitations of standard therapies. The ultimate goal of such novel therapies is the induction of myocardial tissue regeneration (therapeutic, endogenous or combined) in situ or ex vivo.

2 Myocardial Regeneration

2.1 Regeneration by Endogenous Sources

Recent data have challenged the view of the heart as a terminally differentiated organ and provided convincing evidence that new cardiomyocytes can be formed

in the adult heart. To date, two main studies have evaluated the degree of myocyte renewal in the adult human heart. Bergmann et al. performed a virtual pulse-chase experiment by measuring the incorporation of carbon-14, which was released during above-ground nuclear-bomb tests, into genomic DNA of human cardiomyocytes, to calculate rates of turnover in these cells. The researchers found that at the age of 25 years, approximately 1% of cardiomyocytes turn over annually, and the turn-over rate decreases to 0.45% at the age of 75 years [7]. Kajstura et al. used another approach, where they examined the incorporation of iododeoxyuridine in postmortem samples obtained from cancer patients who received this thymidine analog for therapeutic purposes. The authors report the average of 22% turnover of cardiomyocytes per year [56]. Despite the conflicting results, both reports point to the intrinsic regeneration ability of the adult human heart. Endogenous regeneration of the myocardium after injury such as MI or pressure overload, was reported in mice, where only 5–15% of remuscularization was detected [48]. The extremely low regeneration rates can explain the lack of significant restoration of cardiac muscle after severe ischemic injury, the formation of a fibrotic scar at the infarct and progressive deterioration in cardiac function, that eventually leads to CHF.

Two major mechanisms could account for the endogenous regeneration of the myocardium [85]. By the first, adult cardiomyocytes may re-enter cell cycle and divide. This type of myocyte regeneration represents an ancient regenerative program observed in the hearts of amphibians and fish. For instance, cardiomyocyte dedifferentiation and subsequent proliferation is the major mechanism of heart regeneration in zebrafish, rather than regeneration by progenitor or stem cells [55]. Importantly, cell cycle control in adult cardiomyocytes could be altered or reprogrammed in order to induce cell proliferation, either by genetic manipulation or by applying various bioactive molecules [3, 8, 14, 44, 82]. The second mechanism of endogenous regeneration is driven by resident populations of cardiac progenitor cells (CPCs). Numerous CPC pools within the adult heart have been characterized on the basis of stem cell marker expression and cardiomyogenic potential [11]. Despite the apparent existence of these subpopulations, the recruitment and/or activation of resident CPCs for cardiac repair is insufficient to significantly affect and prevent the deterioration in cardiac performance and adverse remodeling after a major ischemic event, due to the physical separation of CPC niches from the site of injury, the formation of fibrotic scar tissue or the lack of appropriate signaling.

2.2 Therapeutic Regeneration

Therapeutic regeneration aims to induce myocardial regeneration, improve tissue salvage, facilitate self-repair, reverse or attenuate adverse remodeling, and, ultimately, achieve long-term functional stabilization and improvement in heart function. Five major processes associated with MI are being targeted at present by various experimental regeneration strategies [94]:

- Cardioprotection—the prevention of progressive cardiomyocyte loss following MI by applying various apoptosis-inhibiting reagents or by inducing pro-survival signaling [1, 37].
- Inflammation—time-adjusted modulation of the post-MI pro/anti-inflammatory cytokine/chemokine profile or cellular responses (e.g. granulation tissue formation and macrophage infiltration) in an attempt to induce effective tissue healing and repair, and to avoid negative inflammatory effects (e.g. cell death, fibrosis etc.) [31, 81].
- ECM remodeling and cardiac fibrosis—time-adjusted positive modulation of the fibrotic response (i.e. ECM remodeling and scar formation), utilizing recent knowledge on pro-fibrotic signaling; matrix metalloproteinase (MMP) inhibition or modification; altering tissue inhibitors of MMPs (TIMPs)/MMPs ratio, which may lead to successful anti-fibrotic therapy [63, 117].
- Angiogenesis induction—effective tissue healing by increasing the blood supply to ischemic regions is an extensively used approach employed with a variety of strategies, proteins, genes or cells, aimed at inducing the formation of new vasculature at the infarct site [90, 109].
- Cardiomyogenesis—myocyte regeneration by activation and/or migration of distinct cell populations with stem- or progenitor-like properties in the adult myocardium which can contribute to de novo myocardium formation after MI. In addition, another novel mechanism for endogenous myocyte regeneration could be the induction of cardiomyocyte cell cycle re-entry by reprogramming of differentiated cardiomyocytes towards proliferation (see previous section).

All these targets and goals can be translated into various therapy strategies aimed at inducing myocardial regeneration (Fig. 1).

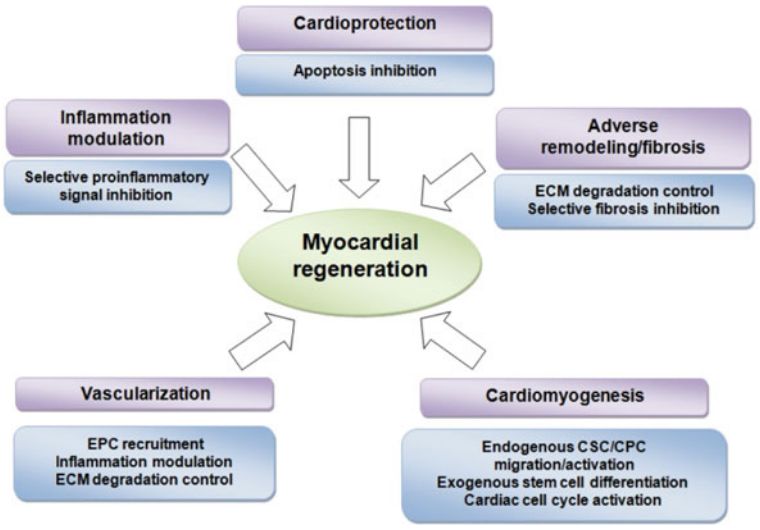

Fig. 1 Targets and goals of therapeutic myocardial regeneration [94]

2.3 Regeneration by Exogenous Sources and Stem Cell Therapy

In pathological situations where large numbers of cardiomyocytes are lost, e.g. following severe ischemic injury after MI or chronic stress, the endogenous regeneration capacity is insufficient to form adequate cardiac contractile mass to maintain heart contractility. Cardiac cell therapy, therefore, ideally aims at actively replacing the damaged and non-functional cardiomyocytes with a new and viable transplantable tissue. Stem cell therapy could also have the potential to introduce new functional cardiomyocytes, by applying differentiation protocols ex vivo or inducing differentiation in situ. Major stem cell types used for myocardial regeneration are bone-marrow-derived different cell subsets (mononuclear cells, hematopoietic progenitors, mesenchymal stem cells), endothelial progenitor cells and skeletal myoblasts [16, 25, 99].The success in preclinical animal studies, in terms of infarct reduction, angiogenesis and functional improvement, has powered the fast translation of stem cell transplantation to human trials.

However, despite the big promise in stem cell therapy for acute MI, the randomized controlled clinical trials in patients, beyond showing an apparent safety of the treatment, have resulted in only modest improvements, and some relatively large trials even failed to show any functional benefit (e.g. LV ejection fraction (EF) increase) [75]. Although the several trials performed differ greatly in cell preparation protocols, timing of the treatment, routes of delivery and patient characteristics, several major conclusions could be drawn based on the observed results. First, the efficacy of stem cell therapy is suboptimal due to extremely low engraftment rates of the transplanted cells [99]. In addition, transient improvements in cardiac function cannot be treated as direct evidence of cardiac regeneration per se, and the transplanted cells have no true cardiomyogenic differentiation potential. Moreover, a portion of the positive effect of cell transplantation may relate to effects of decreasing wall stress by increasing tissue mass in a thinning myocardial wall, an anatomic and mechanistic effect that is independent of real regenerative effect [16, 25, 41].

The mixed results of stem cell transplantation trials in humans enforce rethinking and a more detailed analysis of the positive effects and mechanisms of action of cell transplantation. In this context, emerging evidence suggests that paracrine effects significantly contribute to the positive effect of cell therapy. The so-called “paracrine effect hypothesis” has already been confirmed in various stem cell types, and also deduced from the analysis of data from preclinical and clinical studies. These data show that the expression and secretion of various soluble factors from transplanted cells (cytokines, chemokines, growth factors and others) could be responsible for the major mechanisms involved in myocardial repair, such as cell survival, improved contractility, neovascularization, differentiation and/or induction of endogenous regeneration, and more favorable remodeling [39, 61, 76]. Although the identification of such a “cocktail” of components secreted from the transplanted cells is difficult, attempts have already been made to use known cardioprotective molecules to influence these mechanisms.

Local intramyocardial delivery of such molecules could be more reproducible, less time consuming and more technically appealing than the injection of heterogeneous populations of stem or progenitor cells.

3 Bioactive Molecules for Myocardial Regeneration and Repair

The use of bioactive molecules (growth factors, cytokines, and stem cell mobilizing factors) is of a continuous interest in the field of therapeutic myocardial regeneration. The variable effects exerted by these molecules cover almost every target in the regeneration strategies mentioned in Sect. 2.2 [6, 45, 116].

The type of bioactive molecules investigated for therapeutic myocardial regeneration and their respective activities are summarized in Table 1. Many of these molecules have pleiotropic functions, emphasizing the need for careful, local and time-adjusted interventions.

The systemic delivery of various growth factors was found to be beneficial for the restoration of cardiac function in animal models. However, data emerging from clinical studies is less conclusive, as in the case of using granulocyte colony-stimulating factor (G-CSF) [2, 130]. The mixed results obtained with systemic cytokine or growth factor administration are also accompanied by numerous safety concerns and side effects. These include an increased incidence of restenosis, elevated blood pressure and viscosity, thrombolytic events, arrhythmogenesis and other potential detrimental effects [6, 64, 116]. In addition, systemic administration

Table 1 Bioactive molecules to enhance self-repair, angiogenesis and myocardial regeneration

Factor	Stem cell recruitment or mobilizaiton	Myogenesis	Angiogenesis	Anti-apoptosis	References
Erythropoietin	Yes	No	Yes	Yes	[86, 115]
Insulin-like growth factor-1	Yes	Yes	Yes	Yes	[20, 111]
Fibroblast growth factor	Yes	Yes	Yes	Yes	[12, 68]
Granulocyte–colony stimulating factor	Yes	No	Yes	No	[43, 107]
Hepatocyte growth factor	Yes	Yes	Yes	Yes	[53, 59]
Periostin	No	Yes	Yes	Yes	[27, 60]
Platelet-derived growth factor	Yes	No	Yes	Yes	[49, 50]
Stromal cell-derived growth factor	Yes	No	Yes	Yes	[46, 51]
Thymosin-β4	Yes	Yes	Yes	Yes	[9, 104]
Vascular endothelial growth factor	Yes	Yes	Yes	Yes	[30, 118]

requires higher doses of the drug due to unspecific delivery, fast elimination and extremely low protein stability in the blood. Thus, significant efforts are being invested in the development of strategies for achieving effective local and temporary delivery of various bioactive molecules by employing biomaterial-based polymeric delivery systems.

4 Biomaterials for Cardiac Tissue Engineering and Regeneration

Cardiac tissue engineering aims to restore tissue loss after MI. This can be done by introducing tissue grafts prepared in vitro or by enhancing self-repair and preventing tissue loss in situ. In both cases, the restoration of cardiac tissue microenvironment is required. Thus, ideally, biomaterials used for cardiac tissue engineering, must mimic in their final structure and function, the native cardiac ECM. Cardiac ECM plays a critical role in maintenance, integrity and function of the heart tissue. Dynamic changes and alterations in cardiac ECM composition following MI have a detrimental effect on both systolic and diastolic function [4, 26]. Cardiac ECM composition is complex and hard to recreate, but various types of natural and synthetic polymers are able to mimic (to various degrees) several important ECM properties and provide temporary tissue support, preserve cardiac function and facilitate self-repair.

The paradigm of cardiac tissue engineering is depicted in Fig. 2. The concept allows for the use of biomaterials, cells and bioactive molecules in different combinations. Different stages and components in future-implanted construct creation (e.g. cell or biomolecule integration) can be omitted and/or reintroduced later, in vitro or in vivo.

4.1 Biomaterials—Basic Design Criteria

There are several criteria in biomaterial design, properties and preparation, which are critical for its successful application in each of the strategies employed for myocardial repair and regeneration:

- *Biocompatibility*—this property depends on the material chemistry and morphology. The materials should be tolerated in vivo, be non-immunogenic, non-inflammatory and non-toxic.
- *Mechanical strength*—The matrix should be strong enough to protect the seeded or recruited cells and maintain its structure under mechanical perturbations existing at the implant site. Yet, it should be flexible and compatible with the host tissue.
- *Material erosion or degradation*—Ideally, the material should disappear when it is no longer needed, to allow to integration of the new tissue with the host.

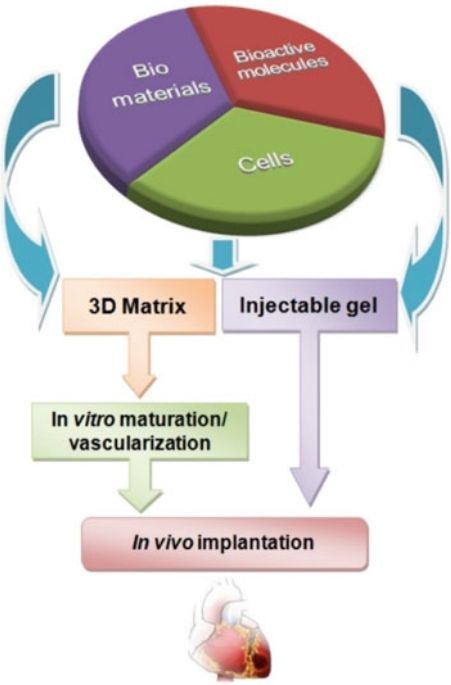

Fig. 2 Cardiac tissue engineering paradigm [94]

The desired kinetics for this process depends on the rate of tissue formation. Scaffold or hydrogel degradation and erosion may occur via polymer backbone degradation (e.g. hydrolysis, enzymatic cleavage) or dissolution of the matrix. The products of this process should be non-toxic and non-immunogenic.

- *Internal morphology*—The matrix should be porous, with interconnecting pores and pore size larger than 50 μm, to allow cell–cell interactions, vascularization of the scaffold after implantation and mass transport.
- *Cross-linking*—The formation of stable matrices or gels often requires cross-linking between the polymer chains. Cross-linking can be physical, where the polymer chains self-assemble due to secondary forces, like electrostatic interactions, temperature change or irradiation. The second type of cross-linking is chemical, where covalent bonds are introduced between the polymer chains. Chemical cross-linking allows more precise control over the properties of the resulting construct, e.g. degradation rate, mechanical stiffness etc. However, this can raise biocompatibility issues, because of the use of chemical agents and/or the possible adverse effects of degradation products.
- *The chemical nature* of the material may have a detrimental effect on cell–matrix interactions. Generally, if the materials carry specific biological moieties, these interactions will prevail, while in their absence, non-specific interactions between cells and matrix, such as van der Waals, hydrogen and electrostatic interactions, may be important. The latter interactions depend on

material chemistry and whether it is hydrophilic or hydrophobic. Hydrophilic materials are preferred since they allow better cell/host integration, handling, and provide hydrated space for the nutrient and metabolite diffusion and can sustain release of various cytokines, growth factors and other hydrophilic bioactive molecules.

4.2 Commonly Used Polymers and Construct Types

Polymers commonly used for cardiac tissue engineering can be categorized by their origin (natural or synthetic) and by their chemical structure (peptides/proteins or polysaccharides). Next, we briefly review the major groups of ECM biomimetic materials, which are in use in acellular forms for myocardial repair [4].

Collagen, a natural protein and the important constituent of native cardiac ECM, is widely used in myocardial tissue engineering. Biocompatibility, biodegradability and cell-adhesive properties of collagen make it an attractive candidate for tissue growth and support. The fibrillar Type I collagen is extensively used for scaffold preparations for subsequent implantation into infarcted hearts. Gelatin (irreversibly hydrolyzed form of collagen) is also used in myocardial tissue engineering, especially for hydrogel preparations (by chemical cross-linking). Gelatin is also a biodegradable material, but under various conditions can provoke an unspecific inflammatory response [4].

Fibrin is another natural protein that is used for myocardial tissue engineering. It is FDA-approved, and is routinely used as a surgical adhesive sealant. The preparation of fibrin utilizes a natural mechanism where fibrinogen is converted to fibrin through a thrombin-mediated reaction. Fibrin is used mainly in injectable form, where its components (fibrinogen and thrombin) are mixed during injection.

Among naturally-occurring polysaccharides, alginate (produced from brown seaweed) is widely used for tissue engineering applications, either as 3D scaffolds or injectable hydrogel. Alginate is FDA approved as a food additive and in various medical applications. The cross-linking process of alginate is physical in nature, and is based on electrostatic non-covalent interactions in the presence of divalent cations, such as calcium. This represents a significant advantage, as the use of various chemical agents is eliminated. Alginate is non degradable in mammals, but its hydrogel is readily erodable with time due to reduction in local cation concentration, polymer chain dissolution and subsequent excretion through kidneys. The disadvantage of alginate is the lack of cell-adhesive properties, but this can be overcome by surface modification with cell adhesive peptides.

Among the synthetic biomaterials, of special interest is the use of self-assembling peptides. These peptides are 8–16 amino acids long and composed of alternating hydrophobic and hydrophilic residues. They form stable β-sheets in water, and upon exposure to physiological salt concentration or pH they form a stable hydrogel of flexible nanofibers. These peptide nanofibers can create a specific microenvironment upon injection into the infarct, and also can be readily applied for growth factor delivery [98].

At present, due to the lack of clinically-relevant cell sources for in vitro creation of cardiac patches, many efforts are focused on the employment of acellular constructs, which can instruct tissue restoration in situ and/or deliver various therapeutic molecules. Acellular forms of polymeric biomaterial applications for myocardial tissue engineering include three main types:

- *Implantable macroporous scaffolds*—prepared by cross-linking (chemical or physical) of biomaterial solution in the desired shape, with a subsequent solidification step and/or drying/freeze-drying. Such porous structures allow tissue growth in vitro or in-growth in situ [13, 35, 36, 58].
- *Implantable hydrogel sheets*—relatively solid 2D sheet-like structures prepared by cross-linking of biomaterial hydrogel and subsequent molding. These sheets allow incorporation of cells or various bioactive molecules [57, 73, 108].
- *Injectable hydrogels*—3D polymer solid networks swollen by water, prepared by physical or covalent cross-linking of the polymer. Due to their aqueous nature, some of these hydrogels can be relatively easily delivered to infarcted heart by catheter-based techniques, which require only a minimally-invasive surgical procedure [17, 19, 21, 62, 65, 122].

4.3 Implantable Scaffolds for In Situ Tissue Support

Implantable scaffolds represent a unique type of construct, ideally capable of completely recreating the 3D microenvironment of the infarcted tissue. The porosity, pore interconnectivity and 3D nature of the biomaterial-based scaffolds strongly favor their use for cell seeding prior to implantation for the creation of tissue-like 3D grafts. However, acellular scaffolds were also found to contribute to myocardial repair, further suggesting their promising potential use in acellular biomaterial-based strategies.

Callegari et al. evaluated the effect of type I collagen porous scaffolds on vascularization in cryoinjured rat hearts. The scaffolds were implanted immediately after cryoinjury and the degree of vascularization and tissue infiltration were analyzed up to 60 days. The collagen cardiac patches induced angiogenic and arteriogenic responses. Interestingly, the absence of myofibroblasts and significantly elevated macrophage infiltration were observed in the patch-treated animals. This can explain the strong angiogenic response observed. The effect of this treatment on cardiac function was not tested [13]. Goldman and co-workers used collagen type I scaffold to repair non-transmural, not-ST-elevation MI induced by cryoinjury in rats. Three weeks after grafting, the scaffold that was integrated into the myocardium, prevented adverse remodeling by reducing LV dilatation, and increased angiogenesis [36].

In another study, Wagner and co-workers used elastomeric biodegradable microporous polyester urethane urea (PEUU) patch for infarct repair in rats. The patch was placed and affixed on the infarct area 2 weeks after coronary artery

ligation, and the outcome was analyzed after additional 8 weeks. The patch region in the infarct was infiltrated with smooth muscle bundles with increased capillary density compared to control. This approach also prevented LV dilatation and improved cardiac function. These benefits were attributed to LV dilatation prevention, increased scar thickness and reduced wall stress [35].

An emerging approach to myocardial repair after MI is the use of decellularized natural extracellular matrices from various animal sources. In such a way, the native structure and ECM composition is preserved, and the matrix can be used for in vitro cell seeding or for instructive tissue restoration and support in situ. This approach is already intensively investigated in the field of heart valve engineering [119]. Decellularization is generally carried out by perfusion of the tissue with various detergents, aiming at removal of the cells without compromising the integrity and structure of the remaining ECM. The main type of naturally-derived decellularized ECM scaffold used for infarct or myocardial defects repair is prepared from porcine urinary bladder (UB). The ECM of this tissue represents a biologically latent membrane, which is already applied for various tissue engineering applications. Kochupura et al. used this matrix for repair of full thickness defect in the right ventricle. Eight weeks after implantation, UB matrix improved regional systolic and diastolic function, compared to Dacron implantation. Importantly, cardiomyocytes were found in the ECM implant region, in contrast to Dacron implantation [58]. In another report, Badylak and co-workers evaluated the effect of UB matrix on infarcted hearts. At 6–8 weeks after the infarct, the matrix was placed as a full thickness LV wall replacement. Three months after implantation, myofibroblast infiltration associated with α-sarcomeric actin-positive cells was observed in the UB matrix group, compared to synthetic expanded polytetrafluoroethylene (ePTFE) patch. Cardiac function was not evaluated [93].

Ideally, the best source of decellularized matrix for myocardial repair should be the matrix derived from the myocardium, which will have a composition and structure required for specific needs of the heart. The potential of such cardiac matrix for successful myocardial tissue engineering and bioartificial heart creation was proven in a proof-of-concept study performed by Ott et al., where whole rat hearts were decellularized and re-seeded with cardiac or endothelial cells. These hearts generated modest but detectable contractions and pump function [84]. Wainwright et al. prepared intact cardiac ECM from whole porcine heart decellalurization. This matrix supported the formation of organized chicken cardiomyocyte sarcomere structure in vitro [120]. Eitan et al. prepared cardiac ECM from LVs of porcine hearts, and showed the biocompatibility of the resulted scaffold for successful cell seeding, including cardiomyocytes, that showed functional phenotype and organization [29].

Collectively, the use of decellularized matrices from natural ECM sources represents an attractive approach, as in this way the properties of the resulting scaffold can be directly matched to the target tissue, including the heart. However, several technical issues are still to be resolved, such as the need for effective decellularization protocols, possible immunogenicity, preservation/storage etc.

5 In Situ Tissue Reconstruction by Injectable Biomaterials

Various natural or synthetic polymers can form hydrogels, namely solid networks of physically or chemically-cross-linked polymer chains with varying water content, which can be directly injected into the infarcted heart. There, the hydrogels form the microenvironment for inducing effective tissue repair, providing temporary support and instructing tissue restoration. The application of injectable biopolymers is less invasive than implanting macroporous scaffolds, and is, therefore, more clinically appealing. Various natural or synthetic acellular injectable biomaterials have been found to improve the outcome after MI.

Dai et al. examined injection of collagen (95% type I, 5% type III) gel into the infarcted rat hearts. This improved LV stroke volume and ejection fraction, and limited paradoxical systolic bulging, compared to saline injection [21]. In another study, Christman et al. used fibrin injection for treatment of 1-week old rat infarcts. Fibrin injection reduced infarct size, increased angiogenesis and preserved cardiac function [17, 19]. Wang et al. used a synthetic polymer based on the thermoresponsive poly(N-isopropylacrylamide) (PNIPAAm) for injection into infarcted rabbit hearts. This polymer solution gels rapidly at physiological body temperature in situ, thus creating a scaffold for tissue repair [73, 102]. The injection of this hydrogel prevented infarct expansion, increased LV ejection fraction and attenuated LV systolic and diastolic dilatation [122]. In a comparative study by Yu et al., fibrin or alginate injection effects were evaluated in a chronic rat model of ischemic cardiomyopathy. Both biopolymer injections increased blood vessel density and scar thickness, and there was a trend towards improved cardiac function in the alginate-treated group, compared to fibrin-treated animals. Alginate also showed higher tissue persistence 5 weeks after injection, compared to fibrin, which was completely reabsorbed [127]. Mukherjee et al. utilized a different approach by creating a fibrin-alginate biocomposite injectable material for MI treatment in pigs. The injection reduced infarct expansion and attenuated LV wall thickness decrease [77].

All of the above treatments were biomaterial injections directly into the myocardium, into or near the infarct. Our group developed an injectable alginate biomaterial which can be delivered by intracoronary injection as a solution. Then, and only at the infarct, due to the high calcium concentration, does this solution undergo gelation forming a hydrogel [62, 65].

6 Alginate as an Instructive Biomaterial for Infarct Repair

Among the naturally-occurring polysaccharides, alginate (produced from brown seaweed) is widely used for tissue engineering applications, either in the form of 3D scaffolds or injectable hydrogel.

Alginate is an anionic water-soluble polysaccharide, composed of 1→4 linked β-D-mannuronic acid (M) and α-L-guluronic acid (G) (Fig. 3). It is approved by

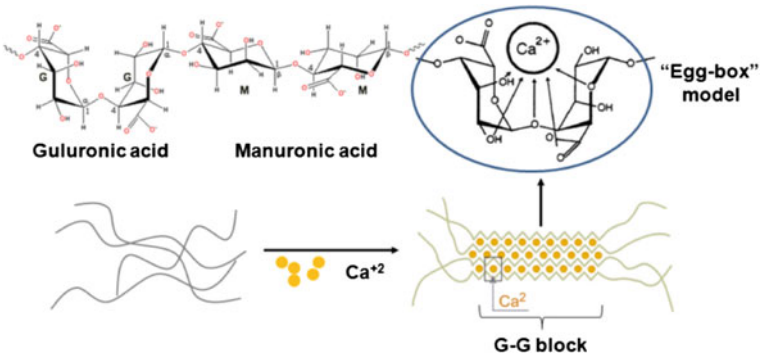

Fig. 3 Alginate structure and "egg box" model of hydrogel formation

the FDA as a food additive and for various medical applications, such as dental impression materials, injury dressings, wound management and more.

Divalent cations, such as calcium ions, interact with high affinity with blocks of G monomers to form ionic bridges between different polymer chains ("egg box" model) (Fig. 3). This physical cross-linking of alginate represents a significant advantage, as the use of various chemical agents is eliminated. Since there is no known mammalian enzyme which degrades the alginate backbone, it is assumed that alginate is not degradable in mammals. However, the calcium-cross-linked hydrogel is readily erodable with time due to exchange of calcium ions by sodium ions, leading to hydrogel dissolution. The water-soluble alginate chains are excreted through the kidney if their molecular weight is below 50 kDa [5].

Injection of a partially cross-linked alginate solution was found to have a beneficial effect on heart function in recent and chronic models of MI [62]. This solution is composed of a 1% (w/v) solution of ~30 kDa alginate and 0.3% (w/v) D-gluconic acid/hemicalcium salt, and is capable of flowing due to its relatively low apparent viscosities (10–50 cP) [112]. At the infarct, the partially cross-linked alginate solution undergoes gelation and phase transition into a hydrogel due to enhanced cross-linking, in response to the elevated concentrations of calcium ions at the infarct after MI and due to water diffusion from the injectable solution to the surrounding tissue [62, 65, 112]. The unique properties of the partially cross-linked alginate solution were exemplified by rheology; the mechanical spectra revealing that the storage (G') and loss (G'') moduli of the solution are closely related or share a cross-point. This type of physical behavior is usually characteristic of cross-linked material in the verge of phase transition from its liquid state into a hydrogel, and such transition can occur by increasing local cation concentration [112].

In recent and older infarcts, intramyocardial injection of the partially cross-linked alginate solution post-MI resulted in significant functional improvement and scar thickening. In recent infarct, the effect of alginate was comparable to fetal cardiomyocyte transplantation. Intracoronary alginate injection in pigs prevented and even reversed LV enlargement and increased scar thickness, assessed 2 months after the injection [65]. The in situ forming alginate hydrogel was shown

to undergo slow erosion and dissolution over a period of 1 month, probably due to the decrease in local calcium concentration during healing.

7 Passive Versus Active Regeneration in Myocardial Repair

The possible mechanisms behind the beneficial effects of biopolymer injection are most likely related to the increase in scar thickness, early infarct stabilization, scaffolding, and critical physical support to the healing of the LV, as well as replacement for the damaged ECM. All these effects are significant for reducing wall stress, prevention of LV dilatation, effective healing and repair. By thickening the scar, wall stress is reduced (by Laplace law) and the degree of outward motion of the infarct that occurs during systole (paradoxical systolic bulging) is also reduced. This is a significant effect, since one of the most important predictors of mortality in patients with MI is the degree of LV systolic dilatation.

The functional improvement observed after acellular biomaterial injections or scaffold implantation implies that these types of treatment have a positive impact without inducing actual tissue regeneration, meaning without addition of new contractile units. This passive type of mechanical regeneration was confirmed by utilizing computational simulation models analyzing the impact of any material injection into infarcted myocardium [121]. However, to achieve long-term function restoration and/or diminish adverse LV remodeling, the therapy should have added value, inducing active myocardial regeneration, e.g. to introduce viable beating tissue [38]. This goal can be achieved by inducing resident myocyte proliferation, migration and activation of resident stem/progenitor cells and/or effective salvaging of existing viable functional tissue after initial infarct. Various cytokines, growth factors and other bioactive molecules could contribute significantly to these desired effects. To maximize the efficiency of this bioactive approach, the combination of bioactive molecules with biomaterials seems to be a very attractive option. In such way, the biomaterial will provide structural temporary matrix support and direct the formation of functional tissue. Simultaneously, it will provide a temporary depot for sustained delivery of bioactive molecules with spatial and controlled distribution of the desired agent [18, 23].

8 Biomaterial Delivery of Bioactive Molecules

8.1 Growth Factor Delivery by Implantable Matrices

Various scaffolds or sheet-like structures are also applicable for growth factor delivery to infarcted myocardium or for repair of cardiac defects. Ota et al. used a decellularized porcine urinary bladder to create a scaffold that was used for the repair of a surgically created defect in right ventricular wall. The scaffold was

loaded with fibronectin collagen binding domain (CBD) -HGF fusion protein. The presence of CBD significantly improved HGF retention in the scaffold, probably due to specific interactions with the scaffold collagen. The implantation of this scaffold increased contractility and electrical activity, and was associated with homogenous repopulation by host cells and increased angiogenesis [83].

The second type of implantable cell- or growth factor-containing biomaterial constructs, hydrogel sheets, is extensively used in cardiovascular tissue engineering [73, 106]. Takehara et al. evaluated the effect of controlled delivery of bFGF from gelatin hydrogel sheets in a chronic MI model in pigs [108]. At 4 weeks after implantation, the local sustained delivery of bFGF stimulated myocardial perfusion and increased left ventricular ejection fraction. However, these effects were not compared to empty hydrogel controls. Fujiwara and co-workers used the same concept of gelatin hydrogel sheets for erythropoietin (EPO) delivery for infarct repair in rabbits. The patch was placed on the surface risk area immediately after infarct induction. Two months later, the EPO-containing hydrogel sheet improved cardiac function and reduced infarct size, compared to empty sheets or systemic EPO administration [57].

Zhang and coworkers created SDF-1α-containing PEGylated fibrin patch and tested the effect of this delivery system in murine MI model. The patch increased c-kit$^+$ stem cell homing to myocardium and improved cardiac function [128].

8.2 Injectable Biomaterial-Based Growth Factor Delivery

The delivery of various bioactive compounds by injectable biomaterials significantly expands the use of biomaterials for induction of active myocardial regeneration. In addition, local and controlled delivery of bioactive molecules can significantly maximize the efficacy of the treatment and simultaneously avoid possible adverse effects associated with systemic delivery. And finally, the biomaterial vehicle can confer protection from proteolysis or other types of degradation, increase stability, prolong tissue retention and provide a more favorable microenvironment for tissue repair and/or regeneration. Several polymeric systems have been used for the delivery of various therapeutic proteins into infarcted hearts.

Gelatin hydrogel is widely used as a carrier for growth factor delivery in various settings, including into the infarcted heart. For instance, Iwakura et al. used gelatin hydrogel microspheres for controlled delivery of bFGF into infarcted myocardium of rats. The treatment resulted in increased angiogenesis and improved systolic and diastolic function [52, 78]. In a similar approach, Deng and coworkers injected bFGF-containing gelatin hydrogel microspheres into infarcted hearts of dogs. MRI showed improved LV function and angiogenesis [70].

One of the best characterized systems of protein delivery to the infarcted heart is the self-assembling peptide nanofiber system developed by the group of Richard Lee [98]. Self-assembling peptides typically are 8–16 amino acids long and are

composed of alternating hydrophilic and hydrophobic residues. They form stable β-sheets in water, and upon exposure to physiological salt concentration or pH they form a stable hydrogel of flexible nanofibers (7–20 nm in diameter) consisting of more than 99% water. Slow release of the proteins (e.g. PDGF-BB) from this system can be achieved by the physical entrapment of the protein in the hydrogel and possibly by its adsorption on the self-assembling peptides by non-covalent interactions [47]. To improve protein retention in hydrogel, biotinylation of the self-assembling peptides can be performed. By this method, for example, IGF-1 was tethered to biotinylated self-assembling peptides [24]. To improve protein stability and confer protection from proteolysis, Segers et al. genetically engineered a protease-resistant form of SDF-1 that was subsequently delivered by self-assembling nanofibers into the infarcted heart by intramyocardial injection [100].

Multiple and/or sequential factor delivery have been described by other groups, applying different delivery systems or different combination of polymers [72, 91]. For example, Hao et al. used a combination of partially oxidized alginates with low and high molecular weights to produce a hydrogel system that can sequentially deliver VEGF and PDGF-BB into the infarcted myocardium [42]. The sequential factor delivery was achieved due to the different degradation rates of the partially oxidized alginates constituting the hydrogel. This protocol of alginate preparation was applied in order to overcome the disadvantage of unmodified alginate, that only poorly controls the release of various entrapped proteins.

9 Affinity-Binding Alginate Biomaterial

9.1 Alginate-sulfate

To enable precise control over factor release and to allow the release of combinations of growth factors, we recently developed an alginate biomaterial with affinity binding sites for heparin-binding proteins, by sulfation of the uronic acid monomers in alginate [34] (Fig. 4a). The binding to alginate-sulfate mimics an example from nature, where many growth factors, chemokines, and cell adhesion molecules, collectively known as heparin-binding proteins, bind the proteoglycans heparin and heparan sulfate via high affinity, specific electrostatic interactions with the low- and high-sulfated sequences in these glycosaminoglycans (GAG) [103]. In this aspect, heparan sulfate GAGs play an important role in sequestering and storage of the proteins, and also participate in the formation of active signaling complex with a respective cell surface receptor. Surface Plasmon Resonance (SPR) analysis revealed strong binding of various heparin-binding proteins to alginate-sulfate [33, 34] (Table 2).

We found the release rate from bioconjugates of alginate-sulfate/growth factors to be dependent on the growth factor binding constants (K_A) and the initial concentrations of individual components forming the bioconjugate (Fig. 4b).

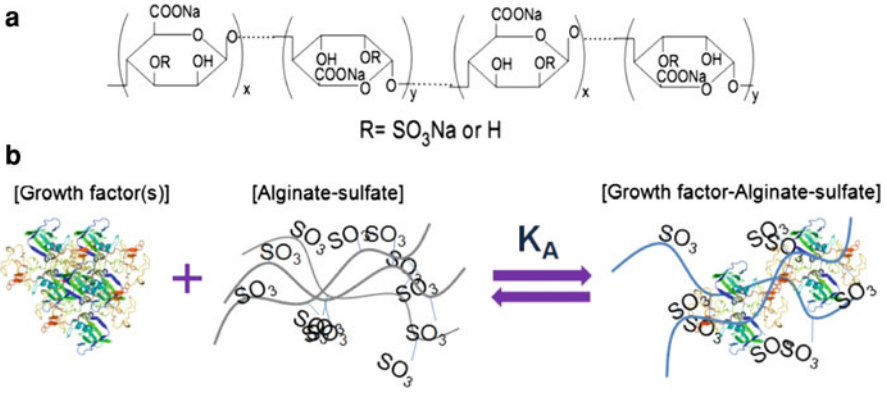

Fig. 4 Alginate-sulfate (**a**) and the model of reversible binding (**b**)

Table 2 Equilibrium binding constants (K_A) calculated from the interactions of alginate-sulfate with proteins (SPR analysis) [33, 34]

K_A (M^{-1})	Protein
2.80×10^7	Acidic fibroblast growth factor
2.57×10^6	Basic fibroblast growth factor
9.93×10^6	Epidermal growth factor
5.36×10^7	Hepatocyte growth factor
1.01×10^8	Insulin-like growth factor-1
1.38×10^7	Interleukin-6
3.53×10^7	Platelet-derived growth factor-BB
2.06×10^8	Stromal cell derived factor-1
6.63×10^7	Transforming growth factor- β1
1.81×10^6	Thrombopoietin
6.98×10^6	Vascular endothelial growth factor

9.2 Bioconjugation with Alginate-sulfate Protects the Protein from Enzymatic Degradation

The bioconjugation of proteins with alginate-sulfate was found to enhance their stability by protecting the protein from enzymatic proteolysis induced by trypsin. This was shown by the reduction in the number of digestion fragments in the mass spectra of the bioconjugated IGF-1 and HGF obtained by Matrix-Assisted Laser Desorption/Ionization—Time of Flight (MALDI-TOF) [95, 96] (Fig. 5). The bioconjugation of alginate-sulfate with these growth factors provides physical masking, protecting the protein from the activity of the proteolytic enzyme. The existence of such masking due to physical complexation of the proteins with alginate-sulfate was further strengthened by the demonstration of nanoparticle formation by different high-resolution microscopy techniques, such as Atomic Force Microscopy (AFM), Transmission Electron Microscopy (TEM) and cryo-TEM, and also by Dynamic Light Scattering (DLS) (unpublished data).

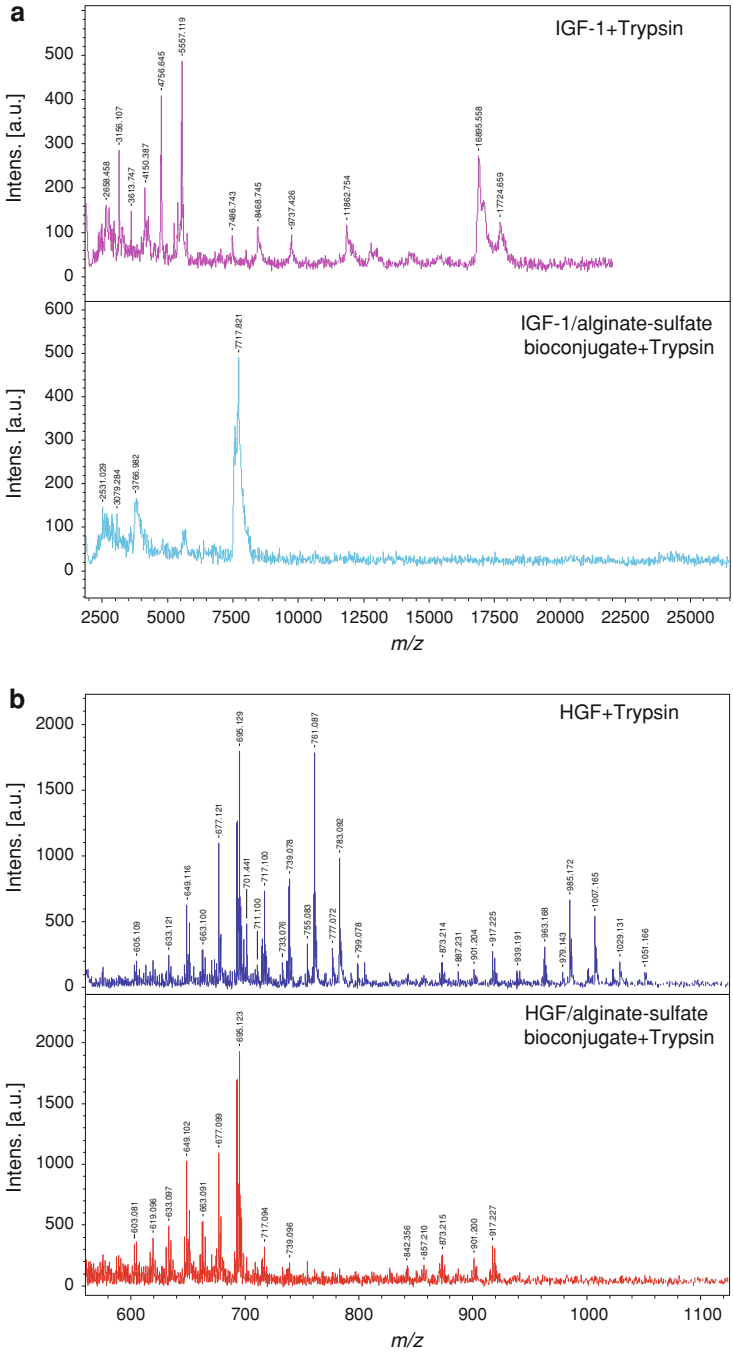

Fig. 5 Bioconjugation with alginate-sulfate protects IGF-1 and HGF from enzymatic proteolysis. **a** MALDI-TOF spectra of IGF-1, soluble or in the bioconjugate form. **b** MALDI-TOF spectra of HGF, soluble or in the bioconjugate form [95, 96]

The effect of protein protection from proteolysis is of great importance, if the delivered proteins are to remain active for prolonged periods of time in harsh environments, where extensive protein degradation takes place, such as the infarct area during the first few weeks after the initial ischemic event.

9.3 The Concept of Affinity-Binding Alginate

Combination of alginate-sulfate with unmodified alginate represents a unique type of a novel *affinity-binding* alginate biomaterial, which is capable of controlled delivery of multiple proteins, while retaining the already mentioned properties and characteristics of the alginate, in scaffold or hydrogel forms. In the following sections we describe the applications of affinity-binding alginate in these formulation types.

10 Affinity-Binding Alginate: The Scaffold-Based Approach

Macroporous alginate scaffolds were fabricated by a freeze-dry technique [101, 129]. In order to produce affinity-binding alginate scaffolds, alginate-sulfate was mixed with unmodified alginate before the cross-linking step and then scaffolds were fabricated [33] (Fig. 6). As revealed by Scanning Electron Microscopy (SEM) analysis, incorporation of 10% (dry weight polymer) of alginate-sulfate into the alginate scaffold did not affect scaffold porosity or mechanical stability in culture [33].

The ability of the affinity-binding alginate scaffolds to control the release of multiple growth factors was tested using the combination of three known angiogenic factors: platelet-derived growth factor-BB (PDGF-BB), transforming growth factor-β1 (TGF-β1) and vascular endothelial growth factor (VEGF). Initial loading and binding of the factors was achieved by the addition of protein solutions to the

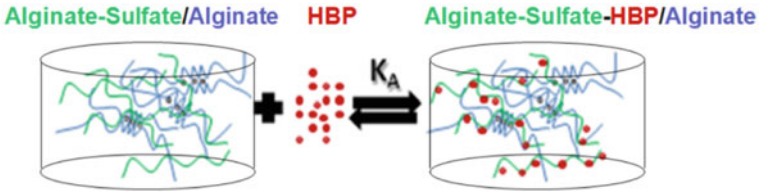

Fig. 6 The concept of affinity-binding alginate scaffolds for controlled delivery of heparin-binding proteins. The scaffold fabricated from alginate-sulfate/alginate can bind multiple heparin-binding proteins (HBP) via specific affinity sites on alginate-sulfate. The release rate from such scaffolds is correlated with the equilibrium binding constants (K_A) of the factors (Table 2)

dry scaffolds and subsequent incubation for 1 h at 37°C. In vitro release studies revealed a sequential order of protein release from the scaffold: VEGF was released first, followed by PDGF-BB and TGF-β1. Importantly, the observed release order coincided with the predicted order of the release based on the values of the equilibrium binding constants to alginate-sulfate (see Table 2). By contrast, factor release from the scaffolds lacking alginate-sulfate was rapid and was governed mainly by burst effect.

The sequential delivery of VEGF, PDGF-BB and TGF-β1 from the scaffold mimics the signal cascade acting in angiogenesis, namely the initiation of the process by VEGF, followed by vessel stabilization by PDGF-BB-mediated smooth muscle cell and pericyte recruitment, and finally, vessel remodeling with ECM induced by TGF-β1 [15, 92]. In order to test the effect of affinity-binding alginate scaffolds containing the three above-mentioned proteins on angiogenesis, the scaffolds were implanted subcutaneously in the dorsal area in rats, and the tissues were assessed for blood vessel number and maturation 1 and 3 months after implantation by immunohistochemistry for α-lectin (a marker of endothelial cells) and α-smooth muscle actin (SMA, a marker of smooth muscle cells) (Fig. 7). Consistent with the pattern of sequential factor delivery, vessel density increase was observed at 1 month after implantation, while effects on vessel maturation were observed after 3 months, as revealed by the density of α-SMA-immunostained vessels, which increased by two-fold compared to the situation after 1 month. By contrast, the instantaneous delivery of the three factors from alginate scaffolds resulted in two-fold lower blood vessel density, smaller sized vessels and a similar percentage of mature vessels at 1 and 3 months, indicating the short-term effect of the adsorbed factors on scaffold vascularization [33].

The affinity-binding alginate scaffolds were used for the creation of a vascularized cardiac patch [28] (Fig. 8). Such scaffolds containing a cocktail of pro-survival and angiogenic factors (insulin-like growth factor-1 (IGF-1), stromal cell-derived factor-1 (SDF-1) and VEGF) were seeded with rat neonatal cardiomyocytes, and then transplanted onto the omentum to achieve host-induced vascularization of the patch. Seven days post-implantation on the omentum, the patches were harvested and after detecting the formation of proper and mature networks of blood vessels, the omentum-generated patches were re-transplanted to replace the scar tissue of the infarcted heart. Four weeks post-transplantation onto an infarcted heart, the omentum-generated patches had structurally and electrically integrated into the scar tissue. Most importantly, by echocardiography and electrophysiology, the pre-vascularized cardiac patch in affinity-binding alginate scaffolds was able to attenuate the deterioration of cardiac function 1 month after implantation in recent acute MI model. Interestingly, similar beneficial results were obtained when the omentum-generated patch was constructed from an affinity-binding scaffold that was supplemented with only the mixture of pro-survival and angiogenic factors and without seeded cardiac cells.

In summary, the affinity-binding alginate scaffolds were proven to provide an improved cell microenviroment and improve the therapeutic outcome in vivo, either in cellular or acellular forms. Using this tool with specific combinations of

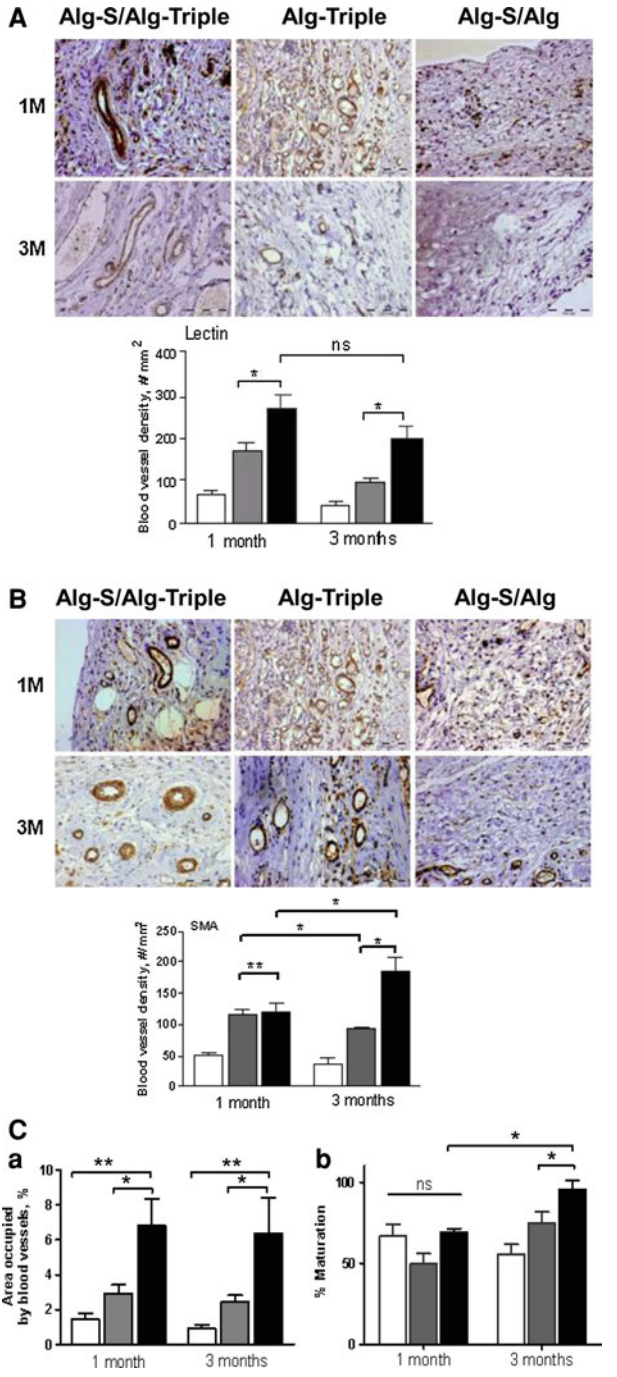
A
Alg-S/Alg-Triple
Alg-Triple
Alg-S/Alg
1M
3M
Lectin
Blood vessel density, #/mm2
ns
1 month
3 months
B
Alg-S/Alg-Triple
Alg-Triple
Alg-S/Alg
1M
3M
SMA
Blood vessel density, #/mm2
1 month
3 months
C
a
Area occupied by blood vessels, %
1 month
3 months
b
% Maturation
ns
1 month
3 months

◀ **Fig. 7** Affinity-binding alginate scaffolds loaded with PDGF-BB, TGF-β1 and VEGF induce angiogenesis and vessel maturation. Quantification of blood vessel densities by counting (**A**) lectin-positive vessels or (**B**) SMC-positive vessels in sections from implanted scaffolds retrieved after 1 and 3 months. Scale bar 100 μm. **C**. Blood vessel size and maturation in the implanted scaffolds as judged by (**a**) percentage of area occupied by blood vessels determined on lectin-stained sections, and (**b**) percentage of matured vessels. i.e. the ratio of α-SMA-positive vessel density to lectin-positive vessel density × 100. Alg-S/Alg-Triple and Alg-Triple are alginate-sulfate/alginate and alginate scaffolds, respectively, loaded with triple factors (PDGF-BB, TGF-β1 and VEGF). Alg-S/Alg is alginate-sulfate/alginate scaffold with no supplemental factors. Empty bars—Alg-S/Alg; grey bars—Alg-Triple; black bars—Alg-S/Alg-Triple. (*) $p < 0.05$, (**) $p < 0.01$. Values represent the mean and standard deviation [33]

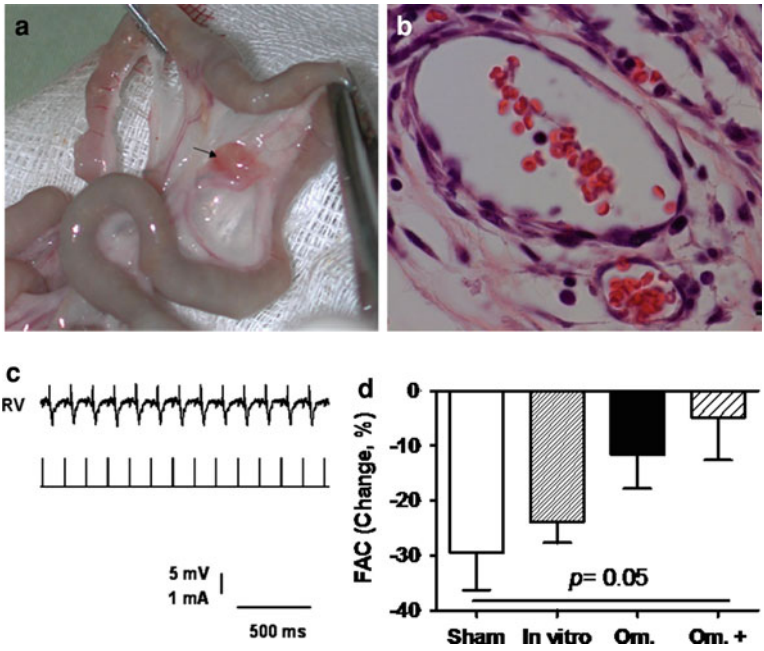

Fig. 8 Prevascularization of a cardiac patch created in affinity-binding alginate scaffolds on the omentum improves its therapeutic outcome. **a** The cardiac patch is transplanted on the omentum for 7 days to promote its vasculogenesis. **b** Functional blood vessels within the patch. **c** Twenty-eight days post transplantation of the vascularized patch on the infarcted heart, stimulation of the patch was able to trigger synchronized beating of the healthy right ventricle. **d** Fractional area change (FAC) of infarcted hearts after treatment with a stitch (sham), implantation of in vitro-grown patch, empty patch grown on the omentum (Om), or omentum-generated cardiac patch (Om+) [28]

growth factors and other bioactive molecules, cell fate and/or tissue reconstruction and reparative processes could be affected to meet different and specific needs, such as improved vascularization, cell survival, regeneration, and guided stem cell differentiation.

11 Injectable Affinity-Binding Alginate

11.1 The Concept and Preparation of Injectable Affinity-Binding Alginate

The collected data suggests that alginate-sulfate can serve as an effective platform for multiple growth factor delivery systems. Yet, for greater clinical applicability of this concept for myocardial repair, the system should be produced in an injectable form. This has been achieved by mixing the alginate-sulfate/growth factor bioconjugates with partially-cross-linked alginate solution (Fig. 9). The preparation of the system is simple and rapid (~2 h), compared to far more elaborative processes of preparation of partially oxidized polymers, peptide synthesis, biotinylation, genetic engineering, that are employed in preparation of other single or multiple growth factor delivery systems.

The injectable affinity-binding alginate system can be easily delivered into the infarcted heart and create a hydrogel in situ capable of sustained delivery of growth factors. This affinity-binding alginate hydrogel has dual functions: (1) it may confer temporary tissue support and replace damaged ECM, together with temporary mechanical stabilization of the infarct, as previously shown for this unique alginate biomaterial; (2) it should control the release and presentation of multiple growth factors.

11.2 Dual Growth Factor Release and Tissue Retention at Infarct

Among the known available bioactive molecules, insulin-like growth factor-1 (IGF-1) and hepatocyte growth factor (HGF) are well known as potent cardiovascular-

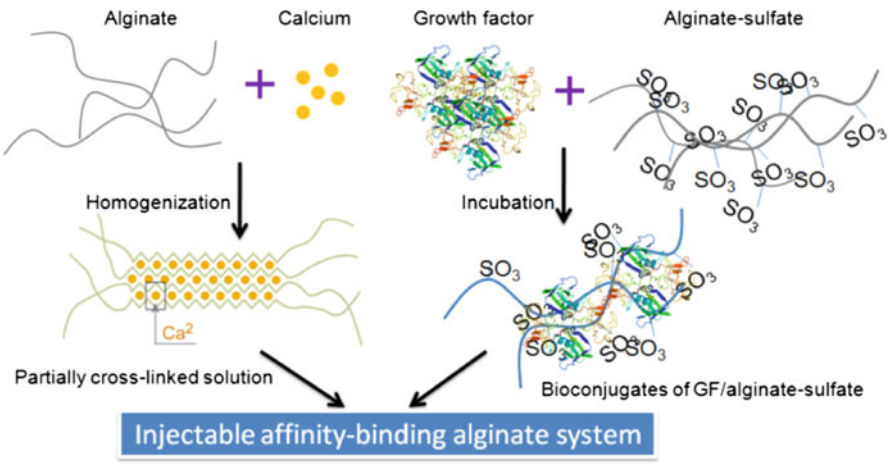

Fig. 9 Schematic representation of the preparation of injectable affinity-binding alginate system

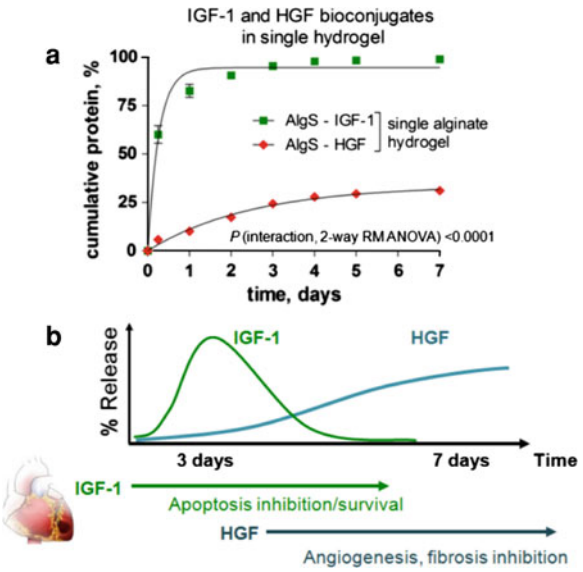

Fig. 10 Growth factor release pattern from affinity-binding alginate hydrogel. **a** In vitro release from dual factor-loaded system containing both protein bioconjugates [96]. **b** Correlation of growth factor release profile from affinity-binding alginate hydrogel with required reparative processes after MI. Faster released IGF-1 could provide strong pro-survival signal at early stages, while slower released HGF could reduce fibrosis and induce angiogenesis at later stages

protective proteins, affecting several major aspects of myocardial regeneration. IGF-1 is a strong antiapoptotic factor in different cell types, including cardiomyocytes [20, 22, 66, 89]. Due to its marked cardioprotection effect, IGF-1 administration can improve cardiac function after MI [45]. HGF is a strong proangiogenic and antifibrotic factor [54, 80, 113, 116, 123]. In addition, HGF, together with IGF-1, induced resident cardiac stem cell migration and activation, that led to new myocardium formation in dogs [69, 114]. Due to their established and complimentary beneficial effects on infarcted myocardium, these proteins were chosen as bioactive components of the injectable delivery system. Strong affinity binding of both proteins to alginate-sulfate was previously confirmed (Table 2) [34].

The release profile of the proteins from affinity-binding alginate hydrogel revealed a sequential factor delivery pattern with a greater amount of IGF-1 initially being released to the external medium until cessation on day 3, while HGF continued to be released and accumulated in the medium (Fig. 10a) [96]. The sequential delivery of IGF-1 and HGF is suited for the proper execution of the reparative processes in the infarcted myocardium, to achieve a more favorable course of repair (Fig. 10b). The faster released IGF-1 could provide an immediate strong pro-survival signal to rescue the functional myocardium and reduce cell apoptosis and loss after the initial ischemic event [67, 105, 125]. Processes required at later phases of repair, such as angiogenesis induction, more favorable ECM remodeling and fibrosis reduction, can be mediated by the slower, yet continuous, release of HGF [79, 110, 124].

The released IGF-1 and HGF maintained their biological activities. Both proteins were shown to activate their respective intracellular signaling pathways (phosphorylation of AKT and ERK1/2 protein kinases for IGF-1 and HGF, respectively) and prevent cardiac cell apoptosis in an oxidative stress model [95, 96].

a

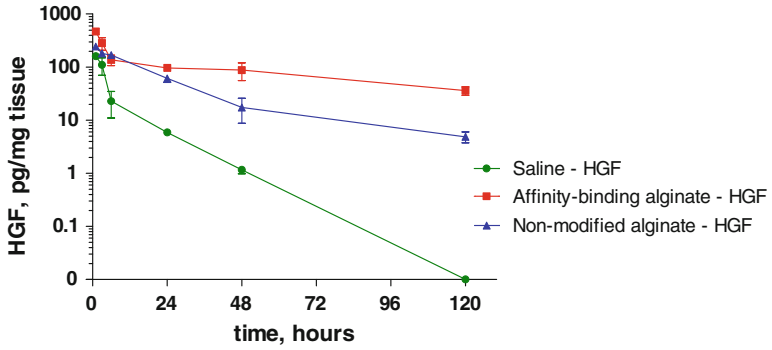

b

Parameter	Saline - HGF	Affinity-binding alg - HGF	Non-modified alg - HGF
AUC – measure of bioavailability, pg×h/mg tissue	1002	10322	4532

Fig. 11 Myocardial tissue retention of HGF in a rat acute MI model. **a** HGF retention profile when injected in various formulations. **b** Nonlinear regression of data obtained from HGF retention studies in infarcted myocardium. AUC—area under the curve [95]

Increased retention of therapeutic proteins over time is one of the main attributes of a successful therapy. As mentioned, the infarct after the initial ischemic event represents a very hostile environment, where extensive protein degradation takes place as part of inflammation and ECM remodeling-induced enzymatic responses [26, 32]. Thus, we chose an acute MI and immediate post-MI injection as a model for testing the efficacy and impact of our delivery system on protein retention. HGF delivery from the affinity-binding alginate solution resulted in much greater retention and bioavailability of the factor in myocardial tissue after acute MI, as measured using anti-human HGF-specific ELISA assay. In contrast, soluble HGF administered by bolus injection was rapidly eliminated from the infarct [95] (Fig. 11). The greater retention of HGF when delivered from the affinity-binding system is attributed to the strong, yet reversible, binding of the factor to alginate-sulfate. The in situ gelation of alginate forms a reservoir for the HGF/alginate-sulfate bioconjugates, thus providing an additional barrier for HGF diffusion and release.

Based on the collected data (bioconjugation and growth factor protection, sustained release and increased protein retention in vivo), the activity of the growth factors delivered by the in situ formed hydrogel with the affinity module could be the manifestation of three main processes and their combinations: (1) the proteins are released at a rate determined by their equilibrium binding constants to alginate-sulfate and the concentration of the individual components (affinity-binding mechanism); (2) the bioconjugates of alginate-sulfate and the factors are presented

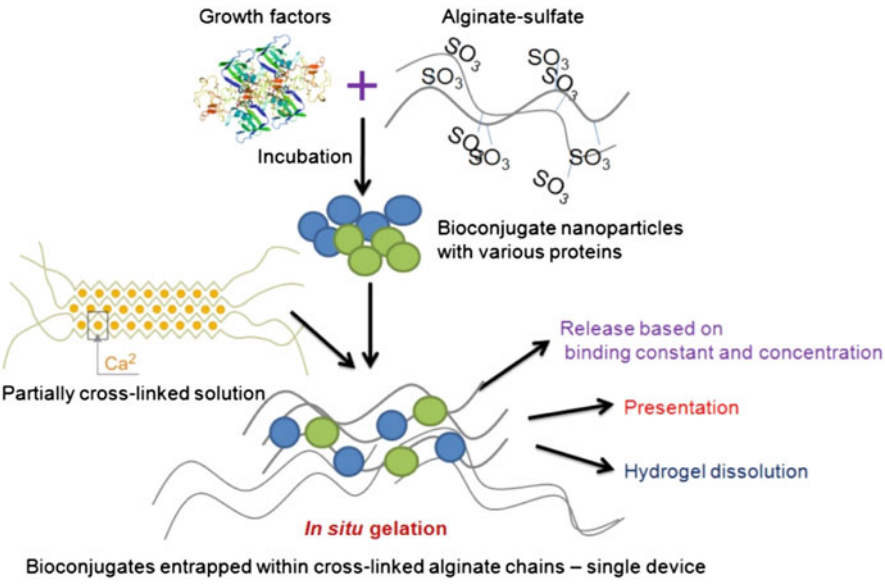

Fig. 12 The concept of injectable affinity-binding alginate biomaterial, and mode of protein release and action

in a natural way to their respective cellular receptors, thus improving their activation and signaling, similar to their native interaction with heparan sulfate [103]; and (3) bioconjugates are released with time due to hydrogel dissolution, due to a decrease in calcium concentration (Fig. 12).

12 Therapeutic Efficacy of Growth Factor Delivery by Injectable Affinity-Binding Alginate

The therapeutic outcome of a single or multiple growth factor delivery by injectable affinity-binding alginate was evaluated in two ischemic disease models: (1) severe hindlimb ischemia in mice; and (2) rat model of acute MI.

12.1 Therapeutic Angiogenesis in Hindlimb Ischemia

Therapeutic angiogenesis is one of the key constituents for successful therapy of ischemic heart disease, peripheral artery disease and other disorders. Induction of re-vascularization can salvage damaged ischemic tissues and facilitate self-repair [40]. As HGF is a potent angiogenic factor, we tested whether its controlled delivery by an affinity-binding alginate system would prolong and maximize its therapeutic action in a murine disease model of hindlimb ischemia [116, 124].

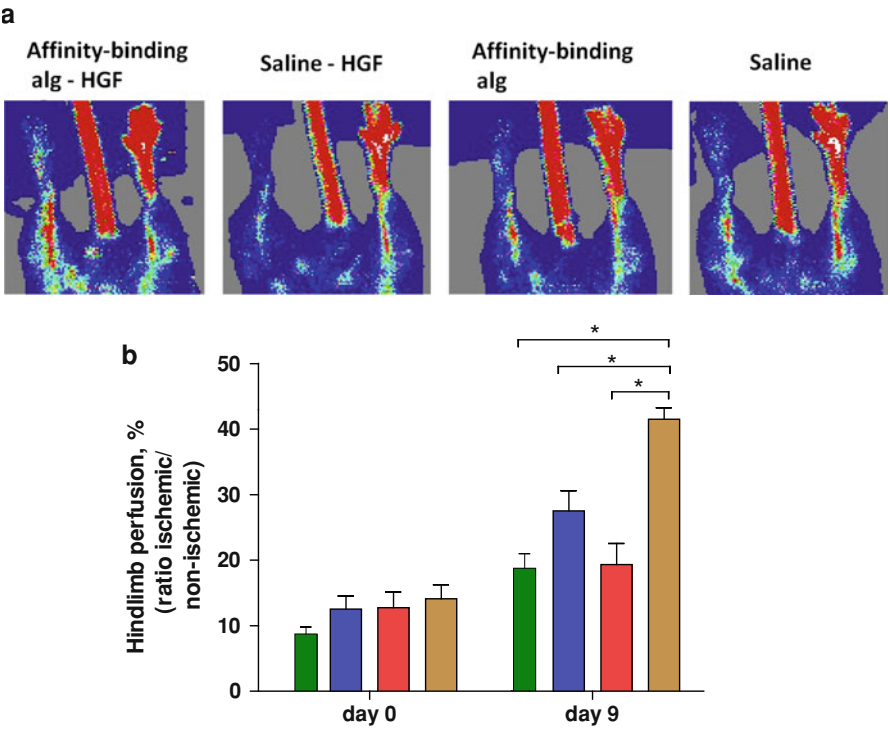

Fig. 13 The delivery of HGF from affinity-binding alginate improves limb perfusion. **a** Representative laser Doppler scans, 9 days after ischemia induction. **b** Calculated perfusion percentage in different treatment groups at baseline and 9 days after operation. *Green bars*—saline; *blue bars*—affinity-binding alginate; *red bars*—saline-soluble HGF; *brown bars*—HGF-affinity-binding alginate. *P* (interaction, two-way repeated measures ANOVA) <0.0001. *-$p < 0.05$ (Bonferroni's post-hoc test), n = 10/group [95]

This strategy resulted in improved tissue perfusion, as judged by laser Doppler analysis 9 days after the operation, compared to other treatment groups (Fig. 13). Moreover, the treatment with HGF delivered by the affinity-binding alginate system resulted in a greater density of mature blood vessels [95].

The affinity-binding alginate was able to translate the known angiogenic effect of HGF into an improved therapeutic outcome, due to creation of a temporary favorable microenvironment for self-repair on one hand, and successful controlled delivery of the protein together with protection from enzymatic degradation and fast elimination in ischemic tissue, on the other hand.

12.2 Acute MI Model

Short (1 week) and long-(4 weeks) term effects of dual (IGF-1 and HGF) growth factor delivery from the injectable affinity-binding alginate were tested in a rat

model of acute MI. We focused on various parameters and aspects in myocardial tissue regeneration and repair, in order to examine the efficacy of the delivery system to translate known effects of the growth factors into a significant therapeutic outcome.

12.2.1 The Effects on Infarct Expansion, Fibrosis, Angiogenesis and Cell Apoptosis

The sequential delivery of IGF-1/HGF reduced scar fibrosis, increased scar thickness and prevented infarct expansion. It also induced angiogenesis at the infarct; the vessels were mature, judging by their coverage by smooth muscle cells (stained positive for α-SMA). Finally, this treatment reduced cell apoptosis, as evaluated by staining for the active form of caspase-3 [96] (Fig. 14).

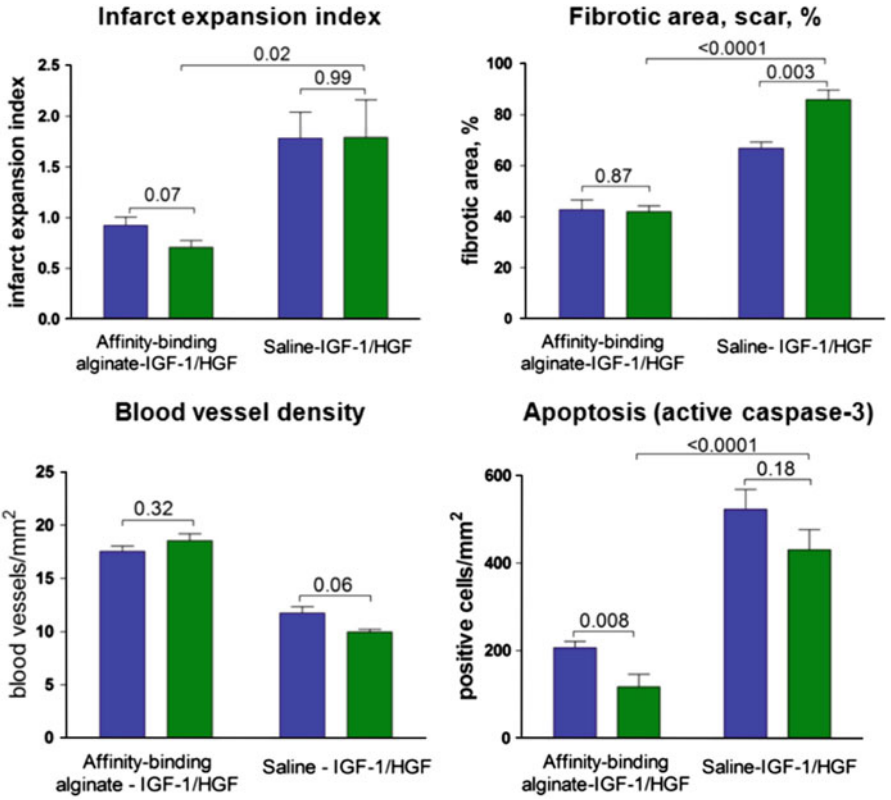

Fig. 14 The effects of sequential delivery of IGF-1/HGF by injectable affinity-binding alginate biomaterial on various aspects of tissue regeneration. Infarct expansion index was evaluated by Masson's trichrome staining. Blood vessels were identified by α-SMA staining. Apoptotic cells were identified by active caspase-3 staining. *Blue bars*—1 week follow-up; *green bars*—4-week follow-up. *—$p < 0.05$ [96]

All these long-term effects were shown to be specifically mediated by the active components of the system, i.e. IGF-1 and HGF. The effect of the biomaterial, if found, was limited to only short-term effects which were not seen after 4 weeks. This initial effect is possibly due to the sequestering and increased local retention of various endogenous cardioprotective and angiogenic factors by the affinity-binding system.

The results observed after the treatment with the sequentially-delivered proteins from the affinity-binding alginate system collectively suggest that marked salvage of the functional tissue occurs already at early stages after infarction. Increased retention and prolonged release of the growth factors, due to affinity-binding mechanism and in situ gelation of the system, facilitate a more favorable course of repair, by supplying the required protective signals for longer periods of time. As a result, prolonged growth factor activity leads to more favorable remodeling at later stages (4 weeks after MI). These effects could also be accompanied by passive tissue support and mechanical stabilization of the infarct conferred by the alginate hydrogel itself [62, 65].

12.2.2 Induction of Endogenous Regeneration

We evaluated the contribution of endogenous regeneration to increased tissue salvage. We focused on two processes that can be responsible for endogenous regeneration of cardiac muscle: adult cardiomyocyte proliferation (shown by staining for mitotic marker Ki-67) and the existence of cardiac stem/progenitor cells (identified by staining for transcription factor GATA-4, generally associated with cardiomyogenic differentiation) (Fig. 15).

Ki-67-positive cardiomyocytes were identified at the infarct border of all animal groups, 1 week after treatment (Fig. 15a). Due to the high ultrastructural fiber organization of Ki-67-positve cells, the likely explanation for this phenomenon is cell cycle re-entry that can occur at higher incidence after MI [87]. Strikingly, the sequential delivery of IGF-1/HGF from the affinity-binding alginate biomaterial in the infarct increased the incidence of Ki-67-positive cardiomyocytes [96]. Cell cycle re-entry could point to actual cell proliferation, an important constituent of myocardial regeneration, especially in light of recent data suggesting that endogenous myocardial regeneration could be driven by the induction of cell cycle re-entry and proliferation of existing cardiomyocytes rather than by stem or progenitor cells [55].

As an additional aspect of possible myocardial regeneration, we examined GATA-4 expression in the infarcts (Fig. 15b). Recent data show that along with its established critical role in early and late heart development and morphogenesis, GATA-4 also acts as a pro-angiogenic, anti-apoptotic and stem cell-recruiting factor post-MI [88, 97]. The GATA-4-positive cell clusters were found only in the peri-infarct areas of animals treated with the factors, with the highest incidence detected 4 weeks post-MI in the animals treated with the sequentially-delivered

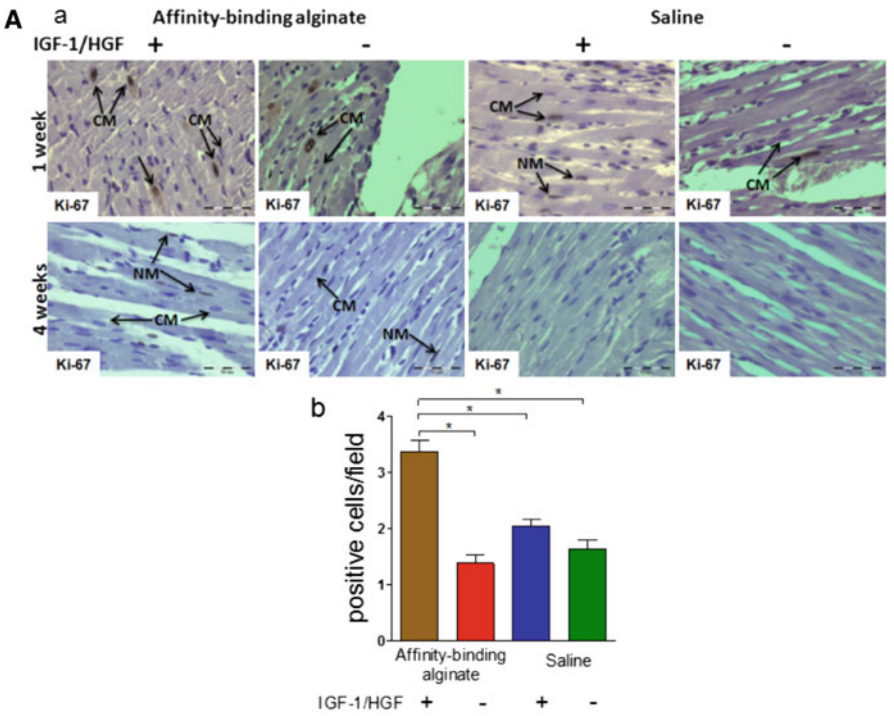

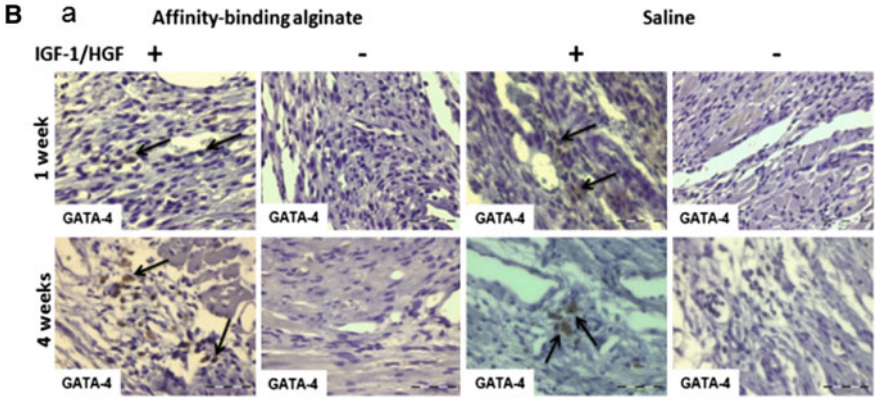

b

	Affinity-binding alg-IGF-1+HGF	Affinity-binding alg	Saline-IGF-1+HGF	Saline
1 week	1/5 (20%)	0/5 (0%)	1/5 (20%)	0/5 (0%)
4 weeks	4/5 (80%)	0/4 (0%)	2/5 (40%)	0/4 (0%)

Fig. 15 The effect of sequential IGF-1/HGF delivery on endogenous myocardial regeneration. **A-a** Representative photomicrographs of Ki-67 (*brown*) in infarcted hearts (healthy/infarct border region). *Arrows* show nuclear localization or unstained nuclei. Bar = 50 μm. **A-b** Quantitative analysis of Ki-67-positive cardiomyocytes in short-term experiment. *P* (one-way ANOVA, 1 week; n = 5/group) < 0.0001; *—$p < 0.001$. *NM* non-myocytes, *CM* cardiomyocytes. **B-a** Representative photomicrographs of GATA-4 (*brown*) in infarcted hearts (peri-infarct region). *Arrows* show nuclear localization. Bar=50 μm; **B-b** Incidence of GATA-4-positive cell clusters in different treatment groups. Incidence = (number of animals with positive staining/total number of animals in each group) × 100 [96]

factors [96]. From the cell cluster organization, we propose that these cells could be stem- or progenitor cells of unknown origin. IGF-1 and HGF were previously shown to activate distinct sub-sets of cardiac stem cells [114]. The long-term delivery of both factors could induce the migration of these cells to the infarct region and their subsequent activation, which in turn, can partially contribute to myocardial tissue salvage.

The extent of endogenous regeneration after the treatment with sequentially-delivered proteins in affinity-binding alginate hydrogel was significantly reduced after a longer period of time (4 weeks) [96]. This can be explained by the sub-optimal concentration of the growth factors due to cessation of growth factor release and action, and also by the lack of additional endogenous signals, that could act synergistically with the delivered proteins, and are present only for a limited period of time after initial infarct.

13 Conclusions and Future Aspects

Biomaterials, despite their current relatively limited use compared to stem cell transplantation, have great potential in cardiac repair. First, biomaterial-based constructs can serve as the platform for the integration of various therapies (cell-, gene-, or bioactive molecule-based). Biomaterial-provided mechanical support can drive tissue restoration, either engrafted or created in situ. Second, self-repair processes such as improved remodeling, endogenous stem cell recruitment, or positive inflammation modulation, can be induced and monitored by biomaterial-based delivery of various bioactive molecules, providing a favourable local microenvironment for tissue repair and regeneration. The development of "smart" biomaterial systems able to respond to post-MI changes by sequential and controlled release of various substances, will add additional value to this concept.

The in vitro creation of cardiac patches for MI treatment or cardiac defect repair represents an ideal strategy for effective tissue restoration and replacement. However, along with several technical hurdles, such as low cell survival, lack of proper vascularization etc., the major "bottleneck" of successful cardiac patch creation is the lack of a clinically relevant cell source. Most current stem cell types

being studied are unable to efficiently differentiate and generate functional cardiac tissue. Pioneering work by Yamanaka in creating induced pluripotent stem (iPS) cells from human somatic cells allows the production of autologous stem cells in adults. These iPS cells can serve as a platform for autologous cardiomyocyte production, and, thus, represent a clinically suitable cell source for cardiac tissue engineering.

Concurrently, the identification and characterization of paracrine factors responsible for the beneficial effects of cell transplantation will continue. A variety of cytokines, growth factors and other bioactive molecules have been (re)discovered, and have been found to positively affect various aspects of myocardial regeneration. These efforts may lead to the transition from cell- to protein-based therapy, which can be more easily translated into clinical benefits than can cell-based therapy.

In this regard, acellular biomaterial-based delivery of bioactive molecules represents a promising strategy for myocardial repair. The effective spatio-temporal deliveries, together with protein protection and tissue support, have been already proven to significantly improve the therapeutic outcome in various animal models. However, as there is a need to simultaneously address multiple aspects and processes in heart failure progression and myocardial repair in order to achieve long-term improvement, the delivery of multiple proteins from a single device is required. Affinity-binding alginate biomaterial can serve as a platform for such device. This system shows results comparable to other growth factor delivery systems, in terms of facilitated self-repair, more favorable remodeling, reduced infarct expansion, angiogenesis and apoptosis inhibition. In addition, affinity-binding alginate system provides numerous advantages over the existing systems from several aspects. First, the preparation of the system is simple and rapid ($\sim$2 h). Second, the affinity-binding mechanism allows high affinity-binding of multiple proteins, and their release is controlled by equilibrium-binding constants and components concentration. In addition, bioconjugation between the growth factor and alginate-sulfate results in the masking of the protein from enzymatic proteolysis. And finally, due to the physical properties of partially cross-linked alginate solution, the affinity-binding alginate-based release system can be delivered to the infarcted heart by minimally-invasive catheter-based techniques via coronary arteries. The developed platform of “smart” injectable alginate biomaterial also enables future modifications to better control multiple protein delivery and retention, and also allows combination of this approach with cell therapy to improve transplanted cell survival and function.

In conclusion, the field of instructive biomaterials for myocardial repair is continuously growing. Along with the use and refinement of already known polymer schemes and approaches, novel types are being developed. There is still a long way to go for the clinical implementation of most of these strategies. However, better understanding of “how nature works”, together with major recent developments and breakthroughs in cardiac and general biology fields make these efforts and goals not only more achievable, but also far more ambitious.

References

1. Abbate, A., Bussani, R., Amin, M.S., Vetrovec, G.W., Baldi, A.: Acute myocardial infarction and heart failure: role of apoptosis. Int. J. Biochem. Cell Biol. **38**(11), 1834–1840 (2006)
2. Abdel-Latif, A., Bolli, R., Zuba-Surma, E.K., Tleyjeh, I.M., Hornung, C.A., Dawn, B.: Granulocyte colony-stimulating factor therapy for cardiac repair after acute myocardial infarction: a systematic review and meta-analysis of randomized controlled trials. Am. Heart J. **156**(2), 216–226 (2008)
3. Ahuja, P., Sdek, P., MacLellan, W.R.: Cardiac myocyte cell cycle control in development, disease, and regeneration. Physiol. Rev. **87**(2), 521–544 (2007)
4. Akhyari, P., Kamiya, H., Haverich, A., Karck, M., Lichtenberg, A.: Myocardial tissue engineering: the extracellular matrix. Eur. J. Cardiothorac. Surg. **34**(2), 229–241 (2008)
5. Al-Shamkhani, A., Duncan, R.: Radioiodination of alginate via covalently-bound tyrosinamide allows monitoring of its fate in vivo. J. Bioactive Compat. Polym. **10**(1), 4–13 (1995)
6. Beohar, N., Rapp, J., Pandya, S., Losordo, D.W.: Rebuilding the damaged heart the potential of cytokines and growth factors in the treatment of ischemic heart disease. J. Am. Coll. Cardiol. **56**(16), 1287–1297 (2010)
7. Bergmann, O., Bhardwaj, R.D., Bernard, S., Zdunek, S., Barnabe-Heider, F., Walsh, S., Zupicich, J., Alkass, K., Buchholz, B.A., Druid, H., Jovinge, S., Frisen, J.: Evidence for cardiomyocyte renewal in humans. Science **324**(5923), 98–102 (2009)
8. Bersell, K., Arab, S., Haring, B., Kuhn, B.: Neuregulin1/ErbB4 signaling induces cardiomyocyte proliferation and repair of heart injury. Cell **138**(2), 257–270 (2009)
9. Bock-Marquette, I., Saxena, A., White, M.D., Michael DiMaio, J., Srivastava, D.: Thymosin [beta]4 activates integrin-linked kinase and promotes cardiac cell migration, survival and cardiac repair. Nature **432**(7016), 466–472 (2004)
10. Boersma, E., Mercado, N., Poldermans, D., Gardien, M., Vos, J., Simoons, M.L.: Acute myocardial infarction. Lancet **361**(9360), 847–858 (2003)
11. Bollini, S., Smart, N., Riley, P.R.: Resident cardiac progenitor cells: at the heart of regeneration. J. Mol. Cell. Cardiol. (2010). doi:10.1016/j.yjmcc.2010.07.006
12. Bougioukas, I., Didilis, V., Ypsilantis, P., Giatromanolaki, A., Sivridis, E., Lialiaris, T., Mikroulis, D., Simopoulos, C., Bougioukas, G.: Intramyocardial injection of low-dose basic fibroblast growth factor or vascular endothelial growth factor induces angiogenesis in the infarcted rabbit myocardium. Cardiovasc. Pathol. **16**(2), 63–68 (2007)
13. Callegari, A., Bollini, S., Iop, L., Chiavegato, A., Torregrossa, G., Pozzobon, M., Gerosa, G., De Coppi, P., Elvassore, N., Sartore, S.: Neovascularization induced by porous collagen scaffold implanted on intact and cryoinjured rat hearts. Biomaterials **28**(36), 5449–5461 (2007)
14. Campa, V.M., Gutierrez-Lanza, R., Cerignoli, F., Diaz-Trelles, R., Nelson, B., Tsuji, T., Barcova, M., Jiang, W., Mercola, M.: Notch activates cell cycle reentry and progression in quiescent cardiomyocytes. J. Cell Biol. **183**(1), 129–141 (2008)
15. Carmeliet, P.: Mechanisms of angiogenesis and arteriogenesis. Nat. Med. **6**(4), 389–395 (2000)
16. Chavakis, E., Koyanagi, M., Dimmeler, S.: Enhancing the outcome of cell therapy for cardiac repair: progress from bench to bedside and back. Circulation **121**(2), 325–335 (2010)
17. Christman, K.L., Fok, H.H., Sievers, R.E., Fang, Q., Lee, R.J.: Fibrin glue alone and skeletal myoblasts in a fibrin scaffold preserve cardiac function after myocardial infarction. Tissue Eng. **10**(3–4), 403–409 (2004)
18. Christman, K.L., Lee, R.J.: Biomaterials for the treatment of myocardial infarction. J. Am. Coll. Cardiol. **48**(5), 907–913 (2006)

19. Christman, K.L., Vardanian, A.J., Fang, Q., Sievers, R.E., Fok, H.H., Lee, R.J.: Injectable fibrin scaffold improves cell transplant survival, reduces infarct expansion, and induces neovasculature formation in ischemic myocardium. J. Am. Coll. Cardiol. **44**(3), 654–660 (2004)
20. Conti, E., Carrozza, C., Capoluongo, E., Volpe, M., Crea, F., Zuppi, C., Andreotti, F.: Insulin-like growth factor-1 as a vascular protective factor. Circulation **110**, 2260–2265 (2004)
21. Dai, W., Wold, L.E., Dow, J.S., Kloner, R.A.: Thickening of the infarcted wall by collagen injection improves left ventricular function in rats: a novel approach to preserve cardiac function after myocardial infarction. J. Am. Coll. Cardiol. **46**(4), 714–719 (2005)
22. Davani, E.Y., Brumme, Z., Singhera, G.K., Cote, H.C.F., Harrigan, P.R., Dorscheid, D.R.: Insulin-like growth factor-1 protects ischemic murine myocardium from ischemia/reperfusion associated injury. Critical Care **7**, 176–183 (2003)
23. Davis, M.E., Hsieh, P.C., Grodzinsky, A.J., Lee, R.T.: Custom design of the cardiac microenvironment with biomaterials. Circ. Res. **97**(1), 8–15 (2005)
24. Davis, M.E., Hsieh, P.C., Takahashi, T., Song, Q., Zhang, S., Kamm, R.D., Grodzinsky, A.J., Anversa, P., Lee, R.T.: Local myocardial insulin-like growth factor 1 (IGF-1) delivery with biotinylated peptide nanofibers improves cell therapy for myocardial infarction. Proc. Natl. Acad. Sci. USA **103**(21), 8155–8160 (2006)
25. Dimmeler, S., Burchfield, J., Zeiher, A.M.: Cell-based therapy of myocardial infarction. Arterioscler. Thromb. Vasc. Biol. **28**(2), 208–216 (2008)
26. Dobaczewski, M., Gonzalez-Quesada, C., Frangogiannis, N.G.: The extracellular matrix as a modulator of the inflammatory and reparative response following myocardial infarction. J. Mol. Cell. Cardiol. **48**(3), 504–511 (2010)
27. Dorn 2nd, G.W.: Periostin and myocardial repair, regeneration, and recovery. N. Engl. J. Med. **357**(15), 1552–1554 (2007)
28. Dvir, T., Kedem, A., Ruvinov, E., Levy, O., Freeman, I., Landa, N., Holbova, R., Feinberg, M.S., Dror, S., Etzion, Y., Leor, J., Cohen, S.: Prevascularization of cardiac patch on the omentum improves its therapeutic outcome. Proc. Natl. Acad. Sci. USA **106**(35), 14990–14995 (2009)
29. Eitan, Y., Sarig, U., Dahan, N., Machluf, M.: Acellular cardiac extracellular matrix as a scaffold for tissue engineering: in vitro cell support, remodeling and biocompatibility. Tissue Eng. C Methods **16**(4), 671–683 (2009)
30. Ferrarini, M., Arsic, N., Recchia, F.A., Zentilin, L., Zacchigna, S., Xu, X., Linke, A., Giacca, M., Hintze, T.H.: Adeno-associated virus-mediated transduction of VEGF165 improves cardiac tissue viability and functional recovery after permanent coronary occlusion in conscious dogs. Circ. Res. **98**(7), 954–961 (2006)
31. Frangogiannis, N.G., Smith, C.W., Entman, M.L.: The inflammatory response in myocardial infarction. Cardiovasc. Res. **53**(1), 31–47 (2002)
32. Frantz, S., Bauersachs, J., Ertl, G.: Post-infarct remodelling: contribution of wound healing and inflammation. Cardiovasc. Res. **81**(3), 474–481 (2009)
33. Freeman, I., Cohen, S.: The influence of the sequential delivery of angiogenic factors from affinity-binding alginate scaffolds on vascularization. Biomaterials **30**(11), 2122–2131 (2009)
34. Freeman, I., Kedem, A., Cohen, S.: The effect of sulfation of alginate hydrogels on the specific binding and controlled release of heparin-binding proteins. Biomaterials **29**(22), 3260–3268 (2008)
35. Fujimoto, K.L., Tobita, K., Merryman, W.D., Guan, J., Momoi, N., Stolz, D.B., Sacks, M.S., Keller, B.B., Wagner, W.R.: An elastic, biodegradable cardiac patch induces contractile smooth muscle and improves cardiac remodeling and function in subacute myocardial infarction. J. Am. Coll. Cardiol. **49**(23), 2292–2300 (2007)
36. Gaballa, M.A., Sunkomat, J.N., Thai, H., Morkin, E., Ewy, G., Goldman, S.: Grafting an acellular 3-dimensional collagen scaffold onto a non-transmural infarcted myocardium

induces neo-angiogenesis and reduces cardiac remodeling. J. Heart Lung Transplant. **25**(8), 946–954 (2006)
37. Garg, S., Narula, J., Chandrashekhar, Y.: Apoptosis and heart failure: clinical relevance and therapeutic target. J. Mol. Cell. Cardiol. **38**(1), 73–79 (2005)
38. Gaudette, G.R., Cohen, I.S.: Cardiac regeneration: materials can improve the passive properties of myocardium, but cell therapy must do more. Circulation **114**(24), 2575–2577 (2006)
39. Gnecchi, M., Zhang, Z., Ni, A., Dzau, V.J.: Paracrine mechanisms in adult stem cell signaling and therapy. Circ. Res. **103**(11), 1204–1219 (2008)
40. Haider, H., Akbar, S.A., Ashraf, M.: Angiomyogenesis for myocardial repair. Antioxid. Redox Signal. **11**(8), 1929–1944 (2009)
41. Hansson, E.M., Lindsay, M.E., Chien, K.R.: Regeneration next: toward heart stem cell therapeutics. Cell Stem Cell **5**(4), 364–377 (2009)
42. Hao, X., Silva, E.A., Mansson-Broberg, A., Grinnemo, K.H., Siddiqui, A.J., Dellgren, G., Wardell, E., Brodin, L.A., Mooney, D.J., Sylven, C.: Angiogenic effects of sequential release of VEGF-A(165) and PDGF-BB with alginate hydrogels after myocardial infarction. Cardiovasc. Res. **75**(1), 178–185 (2007)
43. Harada, M., Qin, Y., Takano, H., Minamino, T., Zou, Y., Toko, H., Ohtsuka, M., Matsuura, K., Sano, M., Nishi, J., Iwanaga, K., Akazawa, H., Kunieda, T., Zhu, W., Hasegawa, H., Kunisada, K., Nagai, T., Nakaya, H., Yamauchi-Takihara, K., Komuro, I.: G-CSF prevents cardiac remodeling after myocardial infarction by activating the Jak-Stat pathway in cardiomyocytes. Nat. Med. **11**(3), 305–311 (2005)
44. Hassink, R.J., Pasumarthi, K.B., Nakajima, H., Rubart, M., Soonpaa, M.H., de la Riviere, A.B., Doevendans, P.A., Field, L.J.: Cardiomyocyte cell cycle activation improves cardiac function after myocardial infarction. Cardiovasc. Res. **78**(1), 18–25 (2008)
45. Hausenloy, D.J., Yellon, D.M.: Cardioprotective growth factors. Cardiovasc. Res. **83**(2), 179–194 (2009)
46. Hiasa, K., Ishibashi, M., Ohtani, K., Inoue, S., Zhao, Q., Kitamoto, S., Sata, M., Ichiki, T., Takeshita, A., Egashira, K.: Gene transfer of stromal cell-derived factor-1alpha enhances ischemic vasculogenesis and angiogenesis via vascular endothelial growth factor/endothelial nitric oxide synthase-related pathway: next-generation chemokine therapy for therapeutic neovascularization. Circulation **109**(20), 2454–2461 (2004)
47. Hsieh, P.C., Davis, M.E., Gannon, J., MacGillivray, C., Lee, R.T.: Controlled delivery of PDGF-BB for myocardial protection using injectable self-assembling peptide nanofibers. J. Clin. Invest. **116**(1), 237–248 (2006)
48. Hsieh, P.C., Segers, V.F., Davis, M.E., MacGillivray, C., Gannon, J., Molkentin, J.D., Robbins, J., Lee, R.T.: Evidence from a genetic fate-mapping study that stem cells refresh adult mammalian cardiomyocytes after injury. Nat. Med. **13**(8), 970–974 (2007)
49. Hsieh, P.C.H., Davis, M.E., Gannon, J., MacGillivray, C., Lee, R.T.: Controlled delivery of PDGF-BB for myocardial protection using injectable self-assembling peptide nanofibers. J. Clin. Invest. **116**, 237–248 (2006)
50. Hsieh, P.C.H., MacGillivray, C., Gannon, J., Cruz, F.U., Lee, R.T.: Local controlled intramyocardial delivery of platelet-derived growth factor improves postinfarction ventricular function without pulmonary toxicity. Circulation **114**, 637–644 (2006)
51. Hu, X., Dai, S., Wu, W.J., Tan, W., Zhu, X., Mu, J., Guo, Y., Bolli, R., Rokosh, G.: Stromal cell derived factor-1 alpha confers protection against myocardial ischemia/reperfusion injury: role of the cardiac stromal cell derived factor-1 alpha CXCR4 axis. Circulation **116**(6), 654–663 (2007)
52. Iwakura, A., Fujita, M., Kataoka, K., Tambara, K., Sakakibara, Y., Komeda, M., Tabata, Y.: Intramyocardial sustained delivery of basic fibroblast growth factor improves angiogenesis and ventricular function in a rat infarct model. Heart Vessels **18**(2), 93–99 (2003)
53. Jayasankar, V., Woo, Y.J., Bish, L.T., Pirolli, T.J., Chatterjee, S., Berry, MF., Burdick, J., Gardner, T.J., Sweeney, H.L.: Gene transfer of hepatocyte growth factor attenuates postinfarction heart failure. Circulation **108**(Suppl 1), II230–II236 (2003)

54. Jayasankar, V., Woo, Y.J., Pirolli, T.J., Bish, L.T., Berry, M.F., Burdick, J., Gardner, T.J., Sweeney, H.L.: Induction of angiogenesis and inhibition of apoptosis by hepatocyte growth factor effectively treats postischemic heart failure. J. Card. Surg. **20**, 93–101 (2005)
55. Jopling, C., Sleep, E., Raya, M., Marti, M., Raya, A., Belmonte, J.C.: Zebrafish heart regeneration occurs by cardiomyocyte dedifferentiation and proliferation. Nature **464**(7288), 606–609 (2010)
56. Kajstura, J., Urbanek, K., Perl, S., Hosoda, T., Zheng, H., Ogorek, B., Ferreira-Martins, J., Goichberg, P., Rondon-Clavo, C., Sanada, F., D'Amario, D., Rota, M., Del Monte, F., Orlic, D., Tisdale, J., Leri, A., Anversa, P.: Cardiomyogenesis in the adult human heart. Circ. Res. **107**(2), 305–315 (2010)
57. Kobayashi, H., Minatoguchi, S., Yasuda, S., Bao, N., Kawamura, I., Iwasa, M., Yamaki, T., Sumi, S., Misao, Y., Ushikoshi, H., Nishigaki, K., Takemura, G., Fujiwara, T., Tabata, Y., Fujiwara, H.: Post-infarct treatment with an erythropoietin-gelatin hydrogel drug delivery system for cardiac repair. Cardiovasc. Res. **79**(4), 611–620 (2008)
58. Kochupura, P.V., Azeloglu, E.U., Kelly, D.J., Doronin, S.V., Badylak, S.F., Krukenkamp, I.B., Cohen, I.S., Gaudette, G.R.: Tissue-engineered myocardial patch derived from extracellular matrix provides regional mechanical function. Circulation **112**(9 Suppl), I144–I149 (2005)
59. Kondo, I., Ohmori, K., Oshita, A., Takeuchi, H., Fuke, S., Shinomiya, K., Noma, T., Namba, T., Kohno, M.: Treatment of acute myocardial infarction by hepatocyte growth factor gene transfer: the first demonstration of myocardial transfer of a "functional" gene using ultrasonic microbubble destruction. J. Am. Coll. Cardiol. **44**(3), 644–653 (2004)
60. Kuhn, B., del Monte, F., Hajjar, R.J., Chang, Y.S., Lebeche, D., Arab, S., Keating, M.T.: Periostin induces proliferation of differentiated cardiomyocytes and promotes cardiac repair. Nat. Med. **13**(8), 962–969 (2007)
61. Laflamme, M.A., Zbinden, S., Epstein, S.E., Murry, C.E.: Cell-based therapy for myocardial ischemia and infarction: pathophysiological mechanisms. Annu Rev Pathol **2**, 307–339 (2007)
62. Landa, N., Miller, L., Feinberg, M.S., Holbova, R., Shachar, M., Freeman, I., Cohen, S., Leor, J.: Effect of injectable alginate implant on cardiac remodeling and function after recent and old infarcts in rat. Circulation **117**(11), 1388–1396 (2008)
63. Leask, A.: TGFbeta, cardiac fibroblasts, and the fibrotic response. Cardiovasc. Res. **74**(2), 207–212 (2007)
64. Lee, T.M., Chen, C.C., Chang, N.C.: Granulocyte colony-stimulating factor increases sympathetic reinnervation and the arrhythmogenic response to programmed electrical stimulation after myocardial infarction in rats. Am. J. Physiol. **297**(2), H512–H522 (2009)
65. Leor, J., Tuvia, S., Guetta, V., Manczur, F., Castel, D., Willenz, U., Petnehazy, O., Landa, N., Feinberg, M.S., Konen, E., Goitein, O., Tsur-Gang, O., Shaul, M., Klapper, L., Cohen, S.: Intracoronary injection of in situ forming alginate hydrogel reverses left ventricular remodeling after myocardial infarction in Swine. J. Am. Coll. Cardiol. **54**(11), 1014–1023 (2009)
66. Li, Q., Li, B., Wang, X., Leri, A., Jana, K.P., Liu, y., Kajstura, J., Baserga, R., Anversa, P.: Overexpression of insulin-like growth factor-1 in mice protects from myocyte death after infarction, attenuating ventricular dilation, wall stress, and cardiac hypertrophy. J. Clin. Invest. **100**, 1991–1999 (1997)
67. Li, Q., Li, B., Wang, X., Leri, A., Jana, K.P., Liu, Y., Kajstura, J., Baserga, R., Anversa, P.: Overexpression of insulin-like growth factor-1 in mice protects from myocyte death after infarction, attenuating ventricular dilation, wall stress, and cardiac hypertrophy. J. Clin. Invest. **100**(8), 1991–1999 (1997)
68. Liao, S., Porter, D., Scott, A., Newman, G., Doetschman, T., Schultz Jel, J.: The cardioprotective effect of the low molecular weight isoform of fibroblast growth factor-2: the role of JNK signaling. J. Mol. Cell. Cardiol. **42**(1), 106–120 (2007)
69. Linke, A., Muller, P., Nurzynska, D., Casarsa, C., Torella, D., Nasclimbene, A., Castaldo, C., Cascapera, S., Bohm, M., Quaini, F., Urbanek, K., Leri, A., Hintze, T.H., Kajstura, J.,

Anversa, P.: Stem cells in the dog heart are self-renewing, clonogenic, and multipotent and regenerate infarcted myocardium, improving cardiac function. PNAS **102**, 8966–8971 (2005)
70. Liu, Y., Sun, L., Huan, Y., Zhao, H., Deng, J.: Effects of basic fibroblast growth factor microspheres on angiogenesis in ischemic myocardium and cardiac function: analysis with dobutamine cardiovascular magnetic resonance tagging. Eur. J. Cardiothorac. Surg. **30**(1), 103–107 (2006)
71. Lloyd-Jones, D., Adams, R.J., Brown, T.M., Carnethon, M., Dai, S., De Simone, G., Ferguson, T.B., Ford, E., Furie, K., Gillespie, C., Go, A., Greenlund, K., Haase, N., Hailpern, S., Ho, P.M., Howard, V., Kissela, B., Kittner, S., Lackland, D., Lisabeth, L., Marelli, A., McDermott, M.M., Meigs, J., Mozaffarian, D., Mussolino, M., Nichol, G., Roger, V.L., Rosamond, W., Sacco, R., Sorlie, P., Thom, T., Wasserthiel-Smoller, S., Wong, N.D., Wylie-Rosett, J.: Heart disease and stroke statistics–2010 update: a report from the American Heart Association. Circulation **121**(7), e46–e215 (2010)
72. Lu, H., Xu, X., Zhang, M., Cao, R., Brakenhielm, E., Li, C., Lin, H., Yao, G., Sun, H., Qi, L., Tang, M., Dai, H., Zhang, Y., Su, R., Bi, Y., Cao, Y.: Combinatorial protein therapy of angiogenic and arteriogenic factors remarkably improves collaterogenesis and cardiac function in pigs. Proc. Natl. Acad. Sci. USA **104**(29), 12140–12145 (2007)
73. Masuda, S., Shimizu, T., Yamato, M., Okano, T.: Cell sheet engineering for heart tissue repair. Adv. Drug Deliv. Rev. **60**(2), 277–285 (2008)
74. McMurray, J.J.: Clinical practice. Systolic heart failure. N. Engl. J. Med. **362**(3), 228–238 (2010)
75. Menasche, P.: Cardiac cell therapy: lessons from clinical trials. J. Mol. Cell. Cardiol. (2010) doi:10.1016/j.yjmcc.2010.06.010
76. Mirotsou, M., Jayawardena, T.M., Schmeckpeper, J., Gnecchi, M., Dzau, V.J.: Paracrine mechanisms of stem cell reparative and regenerative actions in the heart. J. Mo.l Cell. Cardiol. (2010). doi:10.1016/j.yjmcc.2010.08.005
77. Mukherjee, R., Zavadzkas, J.A., Saunders, S.M., McLean, J.E., Jeffords, L.B., Beck, C., Stroud, R.E., Leone, A.M., Koval, C.N., Rivers, W.T., Basu, S., Sheehy, A., Michal, G., Spinale, F.G.: Targeted myocardial microinjections of a biocomposite material reduces infarct expansion in pigs. Ann. Thorac. Surg. **86**(4), 1268–1276 (2008)
78. Nakajima, H., Sakakibara, Y., Tambara, K., Iwakura, A., Doi, K., Marui, A., Ueyama, K., Ikeda, T., Tabata, Y., Komeda, M.: Therapeutic angiogenesis by the controlled release of basic fibroblast growth factor for ischemic limb and heart injury: toward safety and minimal invasiveness. J. Artif. Organs. **7**(2), 58–61 (2004)
79. Nakamura, T., Matsumoto, K., Mizuno, S., Sawa, Y., Matsuda, H.: Hepatocyte growth factor prevents tissue fibrosis, remodeling, and dysfunction in cardiomyopathic hamster hearts. Am. J. Physiol. **288**(5), H2131–H2139 (2005)
80. Nakamura, T., Mizuno, S., Matsumoto, K., Sawa, Y., Matsuda, H., Nakamura, T.: Myoardial protection from ischemia/reperfusion injury by endogenous and exogenous. HGF J. Clin. Invest. **106**, 1511–1519 (2000)
81. Nian, M., Lee, P., Khaper, N., Liu, P.: Inflammatory cytokines and postmyocardial infarction remodeling. Circ. Res. **94**(12), 1543–1553 (2004)
82. Novoyatleva, T., Diehl, F., van Amerongen, M.J., Patra, C., Ferrazzi, F., Bellazzi, R., Engel, F.B.: TWEAK is a positive regulator of cardiomyocyte proliferation. Cardiovasc. Res. **85**(4), 681–690 (2010)
83. Ota, T., Gilbert, T.W., Schwartzman, D., McTiernan, C.F., Kitajima, T., Ito, Y., Sawa, Y., Badylak, S.F., Zenati, M.A.: A fusion protein of hepatocyte growth factor enhances reconstruction of myocardium in a cardiac patch derived from porcine urinary bladder matrix. J. Thorac. Cardiovasc. Surg. **136**(5), 1309–1317 (2008)
84. Ott, H.C., Matthiesen, T.S., Goh, S.K., Black, L.D., Kren, S.M., Netoff, T.I., Taylor, D.A.: Perfusion-decellularized matrix: using nature's platform to engineer a bioartificial heart. Nat. Med. **14**(2), 213–221 (2008)

85. Parmacek, M.S., Epstein, J.A.: Cardiomyocyte renewal. N. Engl. J. Med. **361**(1), 86–88 (2009)
86. Parsa, C.J., Matsumoto, A., Kim, J., Riel, R.U., Pascal, L.S., Walton, G.B., Thompson, R.B., Petrofski, J.A., Annex, B.H., Stamler, J.S., Koch, W.J.: A novel protective effect of erythropoietin in the infarcted heart. J. Clin. Invest. **112**(7), 999–1007 (2003)
87. Pasumarthi, K.B., Field, L.J.: Cardiomyocyte cell cycle regulation. Circ. Res. **90**(10), 1044–1054 (2002)
88. Pikkarainen, S., Tokola, H., Kerkela, R., Ruskoaho, H.: GATA transcription factors in the developing and adult heart. Cardiovasc. Res. **63**(2), 196–207 (2004)
89. Ren, J., Samson, W.K., Sowers, J.R.: Insulin-like growth factor I as a cardiac hormone: physiological and pathophysiological implications in heart disease. J. Mol. Cell. Cardiol. **31**, 2049–2061 (1999)
90. Renault, M.A., Losordo, D.W.: Therapeutic myocardial angiogenesis. Microvasc. Res. **74**(2–3), 159–171 (2007)
91. Richardson, T.P., Peters, M.C., Ennett, A.B., Mooney, D.J.: Polymeric system for dual growth factor delivery. Nat. Biotechnol. **19**(11), 1029–1034 (2001)
92. Risau, W.: Mechanisms of angiogenesis. Nature **386**(6626), 671–674 (1997)
93. Robinson, K.A., Li, J., Mathison, M., Redkar, A., Cui, J., Chronos, N.A., Matheny, R.G., Badylak, S.F.: Extracellular matrix scaffold for cardiac repair. Circulation **112**(9 Suppl), I135–I143 (2005)
94. Ruvinov, E., Dvir, T., Leor, J., Cohen, S.: Myocardial repair: from salvage to tissue reconstruction. Expert Rev. Cardiovasc. Ther. **6**(5), 669–686 (2008)
95. Ruvinov, E., Leor, J., Cohen, S.: The effects of controlled HGF delivery from an affinity-binding alginate biomaterial on angiogenesis and blood perfusion in a hindlimb ischemia model. Biomaterials **31**(16), 4573–4582 (2010)
96. Ruvinov, E., Leor, J., Cohen, S.: The promotion of myocardial repair by the sequential delivery of IGF-1 and HGF from an injectable alginate biomaterial in a model of acute myocardial infarction. Biomaterials **32**(2), 565–578 (2011)
97. Rysa, J., Tenhunen, O., Serpi, R., Soini, Y., Nemer, M., Leskinen, H., Ruskoaho, H.: GATA-4 is an angiogenic survival factor of the infarcted heart. Circ. Heart Fail **3**(3), 440–450 (2010)
98. Segers, V.F., Lee, R.T.: Local delivery of proteins and the use of self-assembling peptides. Drug discovery today **12**(13–14), 561–568 (2007)
99. Segers, V.F., Lee, R.T.: Stem-cell therapy for cardiac disease. Nature **451**(7181), 937–942 (2008)
100. Segers, V.F., Tokunou, T., Higgins, L.J., MacGillivray, C., Gannon, J., Lee, R.T.: Local delivery of protease-resistant stromal cell derived factor-1 for stem cell recruitment after myocardial infarction. Circulation **116**(15), 1683–1692 (2007)
101. Shapiro, L., Cohen, S.: Novel alginate sponges for cell culture and transplantation. Biomaterials **18**(8), 583–590 (1997)
102. Shimizu, T., Yamato, M., Kikuchi, A., Okano, T.: Cell sheet engineering for myocardial tissue reconstruction. Biomaterials **24**(13), 2309–2316 (2003)
103. Shriver, Z., Liu, D., Sasisekharan, R.: Emerging views of heparan sulfate glycosaminoglycan structure/activity relationships modulating dynamic biological functions. Trends Cardiovasc. Med. **12**(2), 71–77 (2002)
104. Smart, N., Risebro, C.A., Melville, A.A., Moses, K., Schwartz, R.J., Chien, K.R., Riley, P.R.: Thymosin beta4 induces adult epicardial progenitor mobilization and neovascularization. Nature **445**(7124), 177–182 (2007)
105. Suleiman, M.S., Singh, R.J., Stewart, C.E.: Apoptosis and the cardiac action of insulin-like growth factor I. Pharmacol. Ther. **114**(3), 278–294 (2007)
106. Tabata, Y., Ikada, Y.: Vascularization effect of basic fibroblast growth factor released from gelatin hydrogels with different biodegradabilities. Biomaterials **20**(22), 2169–2175 (1999)
107. Takano, H., Ueda, K., Hasegawa, H., Komuro, I.: G-CSF therapy for acute myocardial infarction. Trends Pharmacol. Sci. **28**(10), 512–517 (2007)

108. Takehara, N., Tsutsumi, Y., Tateishi, K., Ogata, T., Tanaka, H., Ueyama, T., Takahashi, T., Takamatsu, T., Fukushima, M., Komeda, M., Yamagishi, M., Yaku, H., Tabata, Y., Matsubara, H., Oh, H.: Controlled delivery of basic fibroblast growth factor promotes human cardiosphere-derived cell engraftment to enhance cardiac repair for chronic myocardial infarction. J. Am. Coll. Cardiol. **52**(23), 1858–1865 (2008)
109. Tomanek, R.J., Zheng, W., Yue, X.: Growth factor activation in myocardial vascularization: therapeutic implications. Mol. Cell. Biochem. **264**(1–2), 3–11 (2004)
110. Tomita, N., Morishita, R., Taniyama, Y., Koike, H., Aoki, M., Shimizu, H., Matsumoto, K., Nakamura, T., Kaneda, Y., Ogihara, T.: Angiogenic property of hepatocyte growth factor is dependent on upregulation of essential transcription factor for angiogenesis, ets-1. Circulation **107**(10), 1411–1417 (2003)
111. Torella, D., Rota, M., Nurzinska, D., Musso, E., Monsen, A., Shiraishi, I., Zias, E., Walsh, K., Rozenzweig, A., Sussman, M.A., Urbanek, K., Nadal-Ginard, B., Kajstura, J., Anversa, P., Leri, A.: Cardiac stem cell and myocyte aging, heart failure, and insulin-like growth factor-1 overexpression. Circ. Res. **94**, 514–524 (2004)
112. Tsur-Gang, O., Ruvinov, E., Landa, N., Holbova, R., Feinberg, M.S., Leor, J., Cohen, S.: The effects of peptide-based modification of alginate on left ventricular remodeling and function after myocardial infarction. Biomaterials **30**(2), 189–195 (2009)
113. Ueda, H., Nakamura, T., Matsumoto, K., Sawa, Y., Matsuda, H., Nakamura, T.: A potential cardioprotective role of hepatocyte growth factor in myocardial infarction in rats. Cardiovasc. Res. **51**, 41–50 (2001)
114. Urbanek, K., Rota, M., Cascapera, S., Bearzi, C., Nascimbene, A., De Angelis, A., Hosoda, T., Chimenti, S., Baker, M., Limana, F., Nurzynska, D., Torella, D., Rotatori, F., Rastaldo, R., Musso, E., Quaini, F., Leri, A., Kajstura, J., Anversa, P.: Cardiac stem cells possess growth factor-receptor systems that after activation regenerate the infarcted myocardium, improving ventricular function and long-term survival. Circ. Res. **97**(7), 663–673 (2005)
115. van der Meer, P., Lipsic, E., Henning, R.H., Boddeus, K., van der Velden, J., Voors, A.A., van Veldhuisen, D.J., van Gilst, W.H., Schoemaker, R.G.: Erythropoietin induces neovascularization and improves cardiac function in rats with heart failure after myocardial infarction. J. Am. Coll. Cardiol. **46**(1), 125–133 (2005)
116. Vandervelde, S., van Luyn, M.J., Tio, R.A., Harmsen, M.C.: Signaling factors in stem cell-mediated repair of infarcted myocardium. J. Mol. Cell. Cardiol. **39**(2), 363–376 (2005)
117. Vanhoutte, D., Schellings, M., Pinto, Y., Heymans, S.: Relevance of matrix metalloproteinases and their inhibitors after myocardial infarction: a temporal and spatial window. Cardiovasc. Res. **69**(3), 604–613 (2006)
118. Vera Janavel, G., Crottogini, A., Cabeza Meckert, P., Cuniberti, L., Mele, A., Papouchado, M., Fernandez, N., Bercovich, A., Criscuolo, M., Melo, C., Laguens, R.: Plasmid-mediated VEGF gene transfer induces cardiomyogenesis and reduces myocardial infarct size in sheep. Gene Ther. **13**(15), 1133–1142 (2006)
119. Vesely, I.: Heart valve tissue engineering. Circ. Res. **97**(8), 743–755 (2005)
120. Wainwright, J.M., Czajka, C.A., Patel, U.B., Freytes, D.O., Tobita, K., Gilbert, T.W., Badylak, S.F.: Preparation of cardiac extracellular matrix from an intact porcine heart. Tissue Eng. C Methods **16**(3), 525–532 (2009)
121. Wall, S.T., Walker, J.C., Healy, K.E., Ratcliffe, M.B., Guccione, J.M.: Theoretical impact of the injection of material into the myocardium: a finite element model simulation. Circulation **114**(24), 2627–2635 (2006)
122. Wang, T., Wu, D.Q., Jiang, X.J., Zhang, X.Z., Li, X.Y., Zhang, J.F., Zheng, Z.B., Zhuo, R., Jiang, H., Huang, C.: Novel thermosensitive hydrogel injection inhibits post-infarct ventricle remodelling. Eur. J. Heart Fail. **11**(1), 14–19 (2009)
123. Wang, Y., Ahmad, N., Wani, M.A., Ashraf, M.: Hepatocyte growth factor prevents ventricular remodeling and dysfunction in mice via Akt pathway and angiogenesis. J. Mol. Cell. Cardiol. **37**, 1041–1052 (2004)

124. Wang, Y., Ahmad, N., Wani, M.A., Ashraf, M.: Hepatocyte growth factor prevents ventricular remodeling and dysfunction in mice via Akt pathway and angiogenesis. J. Mol. Cell. Cardiol. **37**(5), 1041–1052 (2004)
125. Webster, K.A.: Programmed death as a therapeutic target to reduce myocardial infarction. Trends Pharmacol. Sci. **28**(9), 492–499 (2007)
126. World Health Organization: The atlas of heart disease and stroke. http://wwwwhoint/cardiovascular_diseases/resources/atlas/en/
127. Yu, J., Christman, K.L., Chin, E., Sievers, R.E., Saeed, M., Lee, R.J.: Restoration of left ventricular geometry and improvement of left ventricular function in a rodent model of chronic ischemic cardiomyopathy. J. Thorac. Cardiovasc. Surg. **137**(1), 180–187 (2009)
128. Zhang, G., Nakamura, Y., Wang, X., Hu, Q., Suggs, L.J., Zhang, J.: Controlled release of stromal cell-derived factor-1 alpha in situ increases c-kit+ cell homing to the infarcted heart. Tissue Eng. **13**(8), 2063–2071 (2007)
129. Zmora, S., Glicklis, R., Cohen, S.: Tailoring the pore architecture in 3-D alginate scaffolds by controlling the freezing regime during fabrication. Biomaterials **23**(20), 4087–4094 (2002)
130. Zohlnhofer, D., Dibra, A., Koppara, T., de Waha, A., Ripa, R.S., Kastrup, J., Valgimigli, M., Schomig, A., Kastrati, A.: Stem cell mobilization by granulocyte colony-stimulating factor for myocardial recovery after acute myocardial infarction: a meta-analysis. J. Am. Coll. Cardiol. **51**(15), 1429–1437 (2008)

Three-Dimensional Porous Scaffold of Hyaluronic Acid for Cartilage Tissue Engineering

Dae-Duk Kim, Dong-Hwan Kim and Yun-Jeong Son

Abstract Reconstitution of the articular cartilage tissue can be achieved by cell delivery techniques. However, an optimal procedure exhibiting minimal toxicity and maximum therapeutic efficacy is still to be developed. The two most common cell types that are being investigated for the treatment of osteoarthritis are chondrocytes and mesenchymal stem cells which need to be formulated with the proper signaling molecules and biomaterial scaffolds. So far, derivatized hyaluronic acid (HA) in porous three-dimensional scaffolds is considered the most promising means for delivering and culturing chondrocytes. HA is an attractive framework among the numerous biomaterial scaffolds for its good biocompatibility, biodegradability, as well as excellent gel-forming properties. This section describes the concept of articular cartilage engineering and how far the HA scaffolds have been developed.

1 Introduction

Articular cartilage is a smooth and white tissue that covers the joint surfaces. It plays essential roles in absorbing compressive stress, distributing load which enables smooth frictionless movement. However, the cartilage undergoes a slowly progressive change due to joint injuries and pathogenic mechanisms which can be restored spontaneously only when the defect is minor. In serious cases, cartilage destruction and degeneration may lead to osteoarthritis (OA) [34].

D.-D. Kim (✉), D.-H. Kim and Y.-J. Son
College of Pharmacy, Seoul National University, Seoul 151-742, Korea
e-mail: ddkim@snu.ac.kr

Stud Mechanobiol Tissue Eng Biomater (2011) 8: 329–349
DOI: 10.1007/8415_2010_51

Published Online: 6 January 2011

OA is characterized by a loss of elasticity and erosion of the cartilage, bone thickening, fibrillation and change of the synovial fluid composition [68]. The principal problem in treating OA is the limitation of self-regeneration. Because cartilage is short of innervations and blood supply, normal repairing system requiring humoral factors and progenitor cells to the damaged site does not apply [41]. Furthermore, low cell density limits the ability to self-repair [87].

Autologous chondrocyte implantation (ACI) is a method that has been proposed for the regeneration of articular cartilage, which is based on the transplanting of isolated cells with chondrogenic traits within the damaged cartilage [9]. However, in spite of some encouraging results, ACI has limitations. The cells are eliminated easily before initiating extracellular matrix production because of difficult in adhering to the lesion [95]. Moreover, when isolated cells are grown in monolayer culture (i.e., two dimensions) in order to get adequate quantity of cells to fill the damaged cartilage, they lose expression of the essential chondrogenic markers and dedifferentiate to a fibrocartilage state [83]. This is why attention has been given to the development of three-dimensional (3D) scaffolds which have the advantage of anchoring the cells in the recipient site enabling the synthesis of a particular extracellular matrix and bioactive molecules like cytokines and morphogenic factors [20].

Hyaluronic acid (HA) is an attractive framework among the numerous biomaterial scaffolds for application to the defective cartilage. HA is one of the major components within synovial fluids, and is composed of repeating disaccharides of glucuronic acid and *N*-acetylglucosamine [6]. Properties including biocompatibility, immunogenicity, biodegradability, viscoelasicity make HA useful in medical, pharmaceutical and cosmetic areas [28]. In addition, it is able to anchor to the cell surface via cell surface receptors such as CD44 and RHAMM [21]. Yet, although HA is an ideal candidate for cartilage repair, it requires modification because of its poor mechanical properties, fast degradation and clearance in vivo by enzymatic or hydrolytic reactions [7].

The concept of articular cartilage engineering with emphasis on the HA scaffolds will be introduced in this section.

2 Articular Cartilage Engineering

Tissue engineering is described as the reconstitution of tissues both structurally and functionally [62]. Although Heabler et al. [40] first acknowledged the chondrogenic possibility of perichondrial tissue, it took about 30 years to establish auto-transplantation in the domain of defected cartilage therapy [15]. Since then, a great deal of attention has been paid to the articular cartilage tissue engineering.

Three key constituents usually form the foundation of a tissue engineering approach, namely, cells, signaling molecules, and biomaterial scaffolds [29]. The main concepts of scaffolds and cells in each area of articular cartilage engineering are described as follows.

2.1 Cell Sources

The chondrocytes are predominant due to having the properties of their original tissue. On the other hand, adult mesenchymal stem cells which can be accessed easily have also attracted the attention of researchers. All cell types that have been used are similar in that controlling the differentiation need to be mainly considered. Among the various cells that have been applied in cartilage tissue engineering, the two major cell types will be discussed.

2.1.1 Chondrocytes

Chondrocytes, the resident cells of cartilage, are characterized by the potential candidate for current articular tissue engineering. They produce the constituents of the extracellular matrix such as collagen and sulfated glycosaminoglycan (s-GAG) [93]. Chondrocytes can be isolated from a number of sources, including articular, auricular, septal, nasal and coastal cartilage [71]. According to the cell sources, they exhibit the characteristics of their original tissue and different functions [51]. These cartilages are sorted into three types; hyaline, elastic and fibrocartilage. For the repair of articular cartilage, the hyaline type nasal chondrocytes may be the most appropriate candidate because of the quantity of cartilage that can be produced after transplantation [55, 89]. Moreover, rabbit chondrocytes and human chondrocyte cell lines have been used in numerous studies to investigate chondrocyte-specific tissue repair [47, 84, 92]. The human chondrocyte cell lines including C-20/A4, T/C-28a2, T/C-28a4 and C-28/I2, are characterized molecular phenotypes which could be served as useful models for studying chondrocyte functions [24, 25].

However, whereas chondrocytes are the potential candidate for recent ACI procedures, their instable phenotype called ‘dedifferentiation’ in vitro limits their utility [29]. During the proliferation process in monolayer culture to reach abundant number of cells for transplantation, they easily lose their chondrocytic character and change to fibroblastic character. This change is accompanied by the loss of the expression of type II collagen and aggrecan and increased expression of type I collagen. Their morphology also shifts from round shape to fusiform like fibroblasts. Fortunately, this process of dedifferentiation is reversible. When the dedifferentiated cells are put in the 3D system or taken appropriate signaling molecules, they could redifferentiate and return to their original phenotype [66]. A study by Bonaventure et al. showed that dedifferentiated chondrocytes cultured in 3D alginate bead recovered their property [8].

2.1.2 Mesenchymal Stem Cells

Mesenchymal stem cells (MSCs) are self-renewing progenitor cells isolated from many adult tissues and retain potential to differentiate into chondrocytes,

adipocytes, fibroblasts, osteoblasts, and various lineages of mesenchymal origin under controlled conditions [33]. They have been isolated from a number of tissues including bone marrow, adipose, synovium, periosteum, umbilical cord vein or placenta [13].

Cell sources between bone marrow and adipose tissue have been compared in various studies. Bone marrow has extensive capacity to differentiate into a variety of cell types. In early studies, the focus was on the osteogenesis of bone marrow derived mesenchymal stem cells (BM-MSCs). Recently, however, the bone marrow cells have been mainly used as an alternative source of chondrocyte. Therefore, although the capacity for differentiation to the chondrogenic cells is higher at the bone marrow cells, mesenchymal stem cells (AD-MSCs) are derived from the adipose tissues since the process is less invasive, providing larger quantities compared to those derived from the bone marrow [58]. The AD-MSCs isolated from the human adipose tissue are purified through several processes for selecting multi-potent MSCs-like cells. A simple liposuction procedure from subcutaneous adipose tissue can be used, and its donor site damage and pain are almost negligible compared to the donating procedure of BM-MSCs. It was reported that AD-MSCs were comparable to BM-MSCs with respect to the multi-lineage potential, growth kinetics and cells senescence [18]. However, under conventional culture conditions including the two-dimensional (2D) plate culture system and serum-supplemented medium, AD-MSCs tend to be committed into the adipogenic or osteogenic lineage rather than the chondrogenic lineage [44]. Therefore, developing a suitable culture technique to direct AD-MSCs into the chondrogenic lineage is a crucial prerequisite for the cartilage defect repair application of AD-MSCs. Fortunately, 3D culture systems and chondrogenic media have been well established for in vitro chondrogenic culture of AD-MSCs [39, 44].

One of the scaffolds that has been reported to be effective for obtaining AD-MSCs is HA which is known to enhance cell–cell contact by modulating pericellular matrix in cell condensation process, the initial stage of chondrogenesis [60]. Moreover, interactions between HA and various cell-surface receptors including CD44 are known to play an important role in maintaining differentiated characteristics of the chondrocytes [60, 79]. Wu et al. investigated the enhancing effect of HA-enriched microenvironment on human adipose derived stem cell (hADSC) chondrogenesis for articular cartilage tissue engineering [99]. They examined the use of HA coated well for its effect on hADSC differentiation during chondrogenesis, as well as the effect of HA modified PLGA scaffolds on cell adherence and viability. The results indicated that HA-enriched microenvironment enhanced cell adherence and aggregation, promoted chondrogenesis, and increased matrix synthesis. Moreover, a more recent study reported that the chondrogenic differentiation of AD-MSCs was induced successfully in the porous 3D HA scaffold (unpublished data). Furthermore, better proliferation and chondrogenic differentiation of AD-MSCs were obtained in the 3D HA scaffold culture as compared to the micromass culture, a standard 3D culture system.

2.2 Signaling Molecules

Commonly investigated signaling molecules include the Transforming Growth Factor-β (TGF-β) family, Bone Morphogenetic Proteins (BMPs), Insulin like Growth Factor-1 (IGF-1), and Fibroblast Growth Factor (FGF) [29]. These growth factors enhance chondrocyte proliferation, differentiation and formation of cartilage. Because MSCs have multipotent differentiation capacity, under appropriate conditions they differentiate into the chondrogenic lineage. The ideal conditions to promote the chondrogenic differentiation include the supplementation of specific signaling molecules, appropriate oxygen tension and 3D culture [44]. A number of signaling molecules such as cytokines, growth factors, nonproteinaceous chemical compounds are investigated in chondrogenesis. The exposure of MSCs to TGF-β1 induces chondrogenesis of MSCs and increases the expression of collagen II [98]. Likewise BMPs, FGF and IGF have expressed similar effects to MSC [71]. In a recent study, BMP-2 in 3D culture system markedly increased the level of chondrogenic differentiation of AD-MSCs, which showed the feasibility of BMP-2 as an effective chondrogenic supplement for AD-MSCs. However, Platelet-Derived Growth Factor (PDGF) inhibited the chondrogenic differentiation of AD-MSCs, being inappropriate as a chondrogenic supplement for AD-MSCs (unpublished data).

2.3 Materials for Scaffold Preparation

The scaffolds, which mimic the 3D environment of the extracellular matrix, provide the necessary support for cells to proliferate and differentiate while keeping their inherent phenotype [81]. Much attention has been paid to the development of many different types of scaffold. They can be classified according to their chemical nature; synthetic, protein-based or carbohydrate based (Table 1). The necessary requirements for the scaffolds are biocompatibility and being biodegradable with non-toxic byproducts. They also need to show controllable degradation and resorption rate to match cell growth in vitro and in vivo [49]. When the scaffolds are not biocompatible, inflammatory and immunological responses could occur [16]. Moreover, suitable surface chemistry for cell attachment, proliferation and differentiation should be considered as well [14]. One must also remember that the pore size and interconnectivity are significant factors for cell growth, migration, and transport of nutrients and waste products [74].

2.3.1 Synthetic Scaffolds

Diverse synthetic materials used for the fabrication of scaffolds in articular cartilage repair include polylactic acid (PLA), polyglycolic acid (PGA), carbon fiber, polyesterurethane, polybutyric acid, polyethylmethacrylatem hydrozyapatite, Dacron (polyethyleneterephthalates), and Teflon (polytetrafluoroethylene) [12].

Table 1 Materials used for scaffold preparation in articular cartilage tissue engineering

Synthetic materials
Polylactic acid (PLA)
Polyglycolic acid (PGA)
Carbon fibre
Calcium phosphate
Polyesterurethane
Polybutyric acid
Polyethylmethacrylate
Hydrozyapatite
Dacron(Polyethyleneterephthalates)
Teflon (Polytetrafluorothylene)
Protein-based materials
Collagen
Fibrin
Gelatin
Carbohydrate-based materials
Cellulose
Alginate
Chitosan
Agarose
Hyaluronic acid

There are advantages and disadvantages for these polymers as carrier for cells. Advantages of using synthetic scaffolds include easiness to mold into specific shapes, unlimited supply, and possibility to regulate exact mechanical properties including dissolution and degradation [29]. However, their poor biocompatibility limits popular use of these competent materials. Sometimes hydrolysis produces acidic by-products and particulates [37], which induce inflammation or giant cell reaction bringing about cell death [38]. Since synthetic materials lack natural sites for cell attachment, they need to be modified by coating or adding adhesion of peptides or proteins onto the surface [12]. In several studies, effects of these synthetic scaffolds on chondrocytes were evaluated, but biocompatibility and toxicity are always major concerns to be overcome [96].

2.3.2 Protein-Based Scaffolds

Collagen is a major connective tissue protein in animals. Tropocollagen, the basic subunit of collagen, is composed of three polypeptide chains and binds together very tightly [86]. The degradation products of collagen are non-toxic. Collagen has ligands to enhance cell growth and cell adhesion while influencing cell migration, differentiation and phenotype [59]. The ligands also interact with other molecules such as growth factors. Reconstituted collagen matrix is found to be easily acceptable to the host and enhance the spontaneous healing in osteochondral defects [85]. In the area of the cartilage tissue repair, collagen has been utilized not only as a naked

scaffolding material but also as a carrier for transferring the cells or growth factors. In in vitro studies, collagen matrix is reported to be particularly useful as it promotes chondrocyte proliferation and differentiation [48]. Thus, despite its problem of biocompatibility, it is still a promising building block of tissue engineering.

Fibrin is produced by polymerization of fibrinogen with thrombin, which is the natural component of the intravascular area [78]. This natural 3D solid matrix functions as facilitating and promoting tissue healing within the extra-vascular space [46]. It plays an essential role in facilitating spontaneous repair activities within full-thickness articular cartilage defects, and alternating the defected cartilage to the hyaline-like tissue which includes abundant type II collagen and sulfate GAGs [43]. Several researchers have used fibrin glues as 3D matrices to support chondrocytes and mesenchymal stem cells in vitro and in vivo [26, 73]. However, in spite of the many researches, application of this type of matrix is limited because of its lack in mechanical stability [78].

Gelatin is fundamentally denatured collagen and has not been investigated widely as a scaffold for articular tissue engineering. Yet a few studies did show that chondrocytes growth in vitro and in vivo have been markedly influenced by the cartilage gelatin [77, 80]. Gelfoam® is a promising candidate for delivery of mesenchymal stem cells (MSCs), and is known to support proliferation and differentiation of hMSCs in vitro [80].

2.3.3 Carbohydrate-Based Polymers

Alginate is a gelatinous polysaccharide composed of linear chains of L-guluronic and D-mannuronic acid residues derived from brown algae. In the presence of divalent ions such as calcium and strontium, it forms a unique meshwork, cross-linked through ionic bonding, which is called alginate "beads" [97]. The beads promote chondrogenesis and maintain chondrocytic phenotype in 3D cultured environments [48]. An in vitro study showed that the alginate beads are useful for the re-differentiation of dedifferentiated chondrocytes which have lost their own expression during monolayer culture [8]. Similarly, marrow stromal cells obtained chondrogenic phenotype in the alginate vehicle [19]. In addition, adult human chondrocytes cultured in alginate beads showed that the majority of synthesized aggrecan was rapidly incorporated into aggregates which are present in the native tissue [42]. However, in spite of its ideal properties, concerns over biocompatibility hinders its use in human patients [76].

Chitosan is a copolymer of glucosamine and *N*-acetylglucosamine found in arthropod exoskeletons [48]. Its cationic property and high charge density in acidic solution enables it to cross link with a variety of polyanionic substances like chondroitin-sulfate [57]. In several in vitro studies, chondrocytes cultured on the chitosan scaffold maintained their morphological and functional properties like normal cartilage [27]. Also, chitosan supports the expression of cartilage extracellular matrix proteins by chondrocytes in vitro [61]. It not only acts as a chondrogenic promotor, but also as a carrier of growth factors [67]. However,

despite its articular cartilage repair ability, it has not been approved as a matrix for clinical study.

Hyaluronic acid is a linear high-molecular weight polysaccharide, composed of repeating disaccharide units of *N*-acetyl-D-glucosamine and D-glucuronic acid [4, 22]. HA is a component of synovial fluid and many other extracellular matrices (ECM). In ECM, HA is the backbone of GAG superstructure complexes, mostly associated with other polysaccharides such as chondroitin sulfate [10]. Its viscoelasticity is responsible for conferring lubrication and mechanical support to joints. In clinical practice, intra-articular HA injection has been used to relieve arthritic pain relief and functional improvements for osteoarthritis. Moreover, it interacts with cell surfaces through CD44 and receptor for hyaluronic-acid-mediated motility (RHAMM), and thus the loaded cells could be fixed at the HA matrix [21]. HA has been a valuable carrier for chondrocytes or mesenchymal stem cells in tissue engineering [100]. Since it consists of linear disaccharide chains, it is required to cross-link by esterfication or other chemical processes in order to achieve a construct for supporting articular cartilage repair [32]. Due to its good biocompatibility, biodegradability, as well as excellent gel-forming properties, HA shows potential in biomedically-relevant hydrogel systems. However, although HA is used as therapeutic aids in the treatment of OA, it has not been proven effective enough because of its poor mechanical properties, rapid degradation and clearance in vivo [5, 7]. Therefore, a modified structure of HA has been attempted for the chondrocyte culture in cartilage repair. Other studies utilizing the 3D scaffold of HA include those where HA is chemical modified and/or cross-linked with glutaraldehyde [90] or carbodiimide [91], although toxicity problems still need to be solved.

3 HA Scaffolds for Cartilage Tissue Repair

3.1 Three-dimensional Scaffold

As mentioned previously, HA has the merit of providing optimal environment for chondrocytes. Although HA itself is used as therapeutic aids in the treatment of OA to improve the lubrication of articulating surfaces and to reduce joint pain [5], direct injection of un-crosslinked soluble HA is not effective enough because of its poor mechanical properties, rapid degradation and clearance in vivo [7]. Thus, when the HA is used as a cell-carrier scaffold for chondrocyte culture, one can expect better effectiveness in the chondrocyte implantation resulting in better cartilage repair. Moreover, it is known that chondrocytes grown in monolayer culture (i.e., two dimensions) undergo characteristic processes of dedifferentiation, marked by loss of collagen type II and aggrecan core protein as well as induction of collagen type I expression [45, 63, 88] while when grown in a porous three-dimensional scaffold, chondrocytes are able to maintain their differentiated phenotype and function. The pore size in the scaffold is crucial for retaining the cells

[36] and retaining macromolecules of the cell in the scaffold is critical in cell-based strategies, which can be controlled by the size of pores in the scaffold. Too large a pore size could cause insufficient initial attachment of cells; enlargement of the pore size might decrease the proportion of cells that adhere to the scaffold. Even though chondrocytes are metabolically active, they seem to lack the appropriate environment or proper stimuli to produce extracellular matrix in large pore size scaffolds [36]. In contrast, when the pore size in the scaffold is too small, it may potentially limit the access of nutrients [3] and impede the permeation of cell waste that need to be secreted and eliminated. When pores are too small, they may interfere with a homogeneous cell distribution within the scaffold and increase the edge effect [36].

Since scaffolds can encourage the proliferation of chondrocytes without losing important functions of differentiation, 3D scaffold and chondrocyte-based strategies in cartilage tissue engineering are currently regarded as one of the most promising approaches for the treatment of OA. Although there have been many studies in the past decades that used HA matrix and chondrocyte culture for cartilage repair, all of them utilized the HA matrix with chemical modification and/or cross-linkage using glutaraldehyde [90] or carbodiimide [91]. Recently, a porous 3D scaffold of chondrocyte culture using chemically unmodified HA which was minimally cross-linked using polyethyleneglycol diglycidylether (PEGDG) was prepared [56]. This was because the conventional cross-linkers glutaraldehyde and carbodiimde have demonstrated high toxicity that could be the cause of side effects [35]. In order to minimize the possible risk of toxicity, PEGDG has been introduced since diepoxy crosslinkers had been reported to exhibit lower cytotoxicity than formaldehyde, glutaraldehyde, and a water-soluble carbodiimide [72]. The pore size of the matrix is being controlled by fabrication conditions, including swelling time and composition of the scaffold [56]. The viability, proliferation and differentiation of rabbit primary articular chondrocytes and human chondrocytic cell lines (C-20/A4) in porous HA scaffold have been systematically investigated. Studies showed that the chondrocytes retained chondrocytic spherical morphology in this HA matrix. Moreover, results from the MTT assay showed good cellular viability within the HA matrix; optical density increased for up to 28 days, demonstrating that the cells continued to proliferate inside the HA matrix. Phenotypic analysis (RT-PCR, Alcian blue staining and quantification of s-GAG) showed that chondrocytes, when three-dimensionally cultured within the HA matrix, expressed transcripts encoding collagen type II and aggrecan, and produced sulfated glycosaminoglycans (s-GAG), indicating chondrogenic differentiation.

However, the key disadvantage of a “rigid” 3D scaffold is that it is needed to fit the matrix into the cartilage lesion site during an implant surgery, which may further damage the cartilage due to its rigid structure. Thus, a “flexible” gel is in great need to fill the cartilage site to reduce the morbidity of the damaged site and to enhance the cell bioadhesion at the cartilage lesion site for better results [64]. A gel-like flexible 3D scaffold of HA was thus developed by carefully controlling the composition, cross-linking time and the amount of cross linker (PEGDG) (unpublished data). This scaffold permitted the growth of phenotypically stable

chondrocytes, and enabled the synthesis of cartilage-like ECM. Moreover, as this modified scaffold is "flexible", this would make the application, handling and treatment much easier than implanting solid-gel matrices by fitting on the defect site in the OA treatment.

3.2 Injectable Scaffolds

Even though the three-dimensional scaffolds have been widely studied for cartilage regeneration for the last decade, the problem of surgical implantation of the solid shaped scaffolds generally causing cartilage defects still need to be solved. To fit the matrix into the cartilage lesion sign, an implant surgery is inevitable, but this process may further damage the cartilage due to the rigid structure [64]. This is why "injectable" scaffolds or hydrogels needed to be developed.

Jin et al. designed hybrids of HA grafted with a dextran-tyramine conjugate (Dex-TA) and investigated this injectable biomimetic hydrogels for cartilage tissue engineering [53]. HA-g-Dextran-Tyramine copolymers were prepared by the conjugation of dextran-tyramine conjugates with HA using EDAC/NHS activation. The characterization of hybrid structure was determined using ^{1}H-NMR, and was determined to resemble the molecular structure of proteoglycans present in the extracellular matrix of native cartilage (Fig. 1). Then, hydrogels were prepared in PBS by the horseradish peroxidase (HRP) as a catalyst and H_2O_2 as an oxidant mediated coupling reaction. This enzymatic cross-linking of hybrid structure led to fast gelation within 2 min. Hydrogel degradation was observed in the presence of hyaluronidase and exhibited good biocompatibility. Rheological experiments on injectable properties of hydrogels were carried out with a rheometer.

3.3 Scaffolds Consisting of Hyaluronic Acid Derivatives

Fabricating scaffolds with HA only is very difficult because of its hydrophilic physicochemical properties. Derivative of HA and cross-linker is therefore

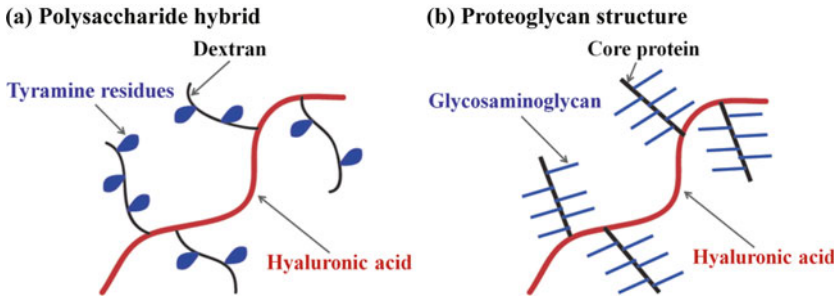

Fig. 1 Chemical structure of **a** polysaccharide hybrids based on hyaluronic acid and dextran–tyramine conjugates and **b** structure of a proteoglycan

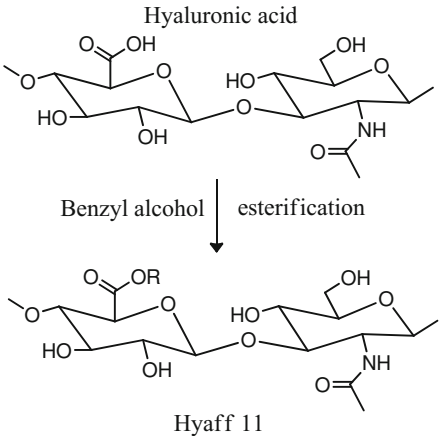

Fig. 2 The structure of hyaluronic acid and Hyaff 11. Hyaff 11 is the structure of hyaluronic acid esters. *R* is a benzyl group

preferred for manufacturing scaffolds as in the case of Hyaff-11 which was developed as a semi-synthetic resorbable material from Fidia Advanced Biopolymers (FAB, Abano Terme, Italy) [11]. The HA in Hyaff-11 was esterified with benzyl alcohol on the free carboxyl groups of glucuronic acid along the polymeric chain, leading to an increase in the hydrophobic component of the polymer chain (Fig. 2). The possibility of using nonwoven structured samples of Hyaff-11 as a potentially valuable scaffold for cartilage-tissue engineering was systematically studied [1]. The re-differentiation capacity of cultured chondrocytes on two bioresorbable nonwoven biomaterials composed of Hyaff-11, and its sulphated derivative, Hyaff-11S [30] was also investigated.

HA modified biodegradable scaffolds for cartilage tissue engineering has been prepared by using HA and PLGA-PEG di-block copolymer [100], and compared with the PLGA scaffold. The PLGA scaffolds were fabricated by a gas forming/salt leaching method by chemically conjugation with PLGA and amine-terminated PLGA-PEG di-block copolymer. The HA modified scaffolds were fabricated by chemical surface modification of the exposed amino group of the PLGA scaffold. HA modification led to enhanced cellular attachment and proliferation as well as dedifferentiation of chondrocytes.

3.4 Interpenetrating Polymer Network Scaffold of HA

Interpenetrating polymeric network (IPN) is a 3D network which comprises of two or more networks which are fully or partially interlaced on a molecular scale but not covalently bonded to each other and not being separated unless chemical bonds are broken [69]. The most widely investigated IPN is composed of two

independent polymers with different chemical compositions. It is believed that the formation of an IPN structure can conserve the properties of both polymers, and the interlocked structure in the cross-linked networks enhance the stability of the materials, thereby ensuring the mechanical strength [70]. Despite its general acceptance as a tissue biocompatible material, the fabricated HA scaffolds show poor mechanical properties, rapid degradation and clearance in vivo, which restricts the possibility of its exploitation in the medical field. Hence, it was has been proposed to modify the natural polymers physically or chemically [56, 75, 100]. In a recent study, porous sodium hyaluronic acid/sodium alginate (HA/SA) scaffold based on IPN technique has been fabricated, where HA and SA were cross-linked with PEGDG and calcium chloride, respectively (unpublished data). The results showed that a porous IPN scaffold was successfully prepared from naturally derived sodium hyaluronic acid (HA) and sodium alginate (SA) polymers with significantly improved mechanical and biological properties as compared to its hyaluronic acid counterpart. Also, rabbit chondrocytes readily attached to the HA/SA scaffold, and maintained a chondrocyte-specific phenotype and the addition of SA in HA slightly up-regulated chondrogenic differentiation. Thus, it could serve as an effective cell delivery system for the three-dimensional culture of chondrocytes.

3.5 Peptide Surface Modification of Scaffolds for Promoting Cell Attachment and Proliferation

Although HA provides apposite environment for cell attachment and proliferation, its negative charge can bring repulsive force with cells. Moreover, HA does not provide the perfect configuration of the ECM environment by itself. Therefore, surface modification by peptide/protein that can promote cell-scaffolds interactions has been emerged in the development of scaffolds. The arginine-glycine-aspartic acid (RGD) sequence is a typical adhesion motif in ECM proteins (i.e., fibronectin, fibrin, laminin and collagen) and also directly binds to several integrin receptors (i.e., $\alpha 5\beta 1$ and $\alpha v\beta 3$) [31, 52]. Members of the integrin receptor family are known to be linked directly to intracellular signaling events, including growth factor responsiveness [94], tyrosine kinase activation and alterations in gene expression [54]. The configuration of the ECM environment is important for the conservation of cell function. Other study also demonstrated the potential use of the laminin-derived peptide sequences IKVAV, YIGSR and RGD to promote the attachment of ADSCs to scaffolds [82]. Another study demonstrated the inhibition effect of chondrogenesis in RGD-modified alginate gels [17]. In RGD-modified 3D alginate gels, the proliferation and attachment of bone marrow stem cells (BMSCs) to the gel was increased, but initial chondrogenesis was inhibited. This effect was owing to interaction of RGD peptide with $\alpha 5$ integrin family. They claimed that cell-scaffold interaction can regulate

chondrogenesis, and thus it is important to design appropriate biomaterials for cartilage tissue engineering.

4 How to Characterize Cell Functions on Scaffolds

The fact that 3D scaffold culture is advantageous for cells to maintain their chondrocyte-specific phenotype and chondrogenic differentiation can be concluded once the scaffolds as well as the cells are properly characterized. When the 3D scaffolds are developed and cells are seeded on them, the scaffolds as well as cells in terms of their viability, proliferation and differentiation are investigated by various means which are described below.

4.1 Morphological Observation

The morphological observation of scaffolds and cells can be performed by using scanning electron microscope (SEM). After 21 days of cell seeding on the HA scaffold, the typical morphology of chondrocytes are as shown in Fig. 3. Once the cells are attached on the HA scaffold structure, they maintain the roundness characteristic and acquire predominantly spherical or some fusiform shape. Some cells are attached on the polymer by filapodia, but most of the cells are connected to each other by forming cell aggregations.

The SEM images are also useful to observe the porous morphology of the HA scaffolds and to measure the pore size. Pore size in the scaffold is known to be critical for the growth of cells [3, 36] and that between 50 and 300 μm is known to be optimum for cell growth. Figure 4 shows an example of SEM images of the cross-section of the HA scaffold.

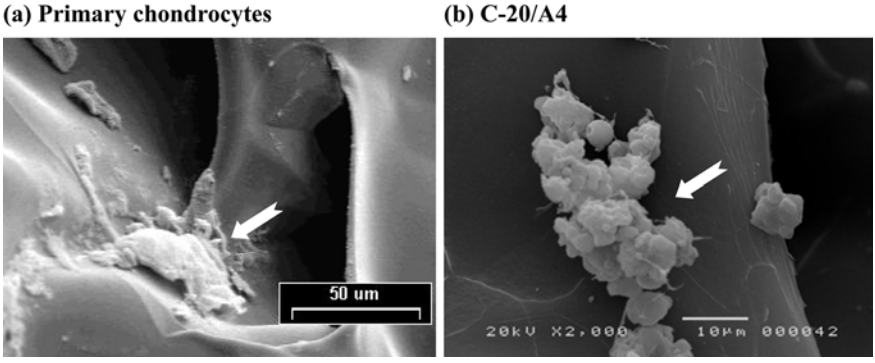

Fig. 3 Scanning electron micrographs of the **a** primary chondrocytes and **b** C-20/A4 (human chondrocytic cell line) cultured in the HA scaffold for 21 days. The characteristic round morphology of the chondrocytes (*white arrows*) and the dense fibers of the extracellular matrix can be found around the chondrocytes. Data from Kang et al. [56])

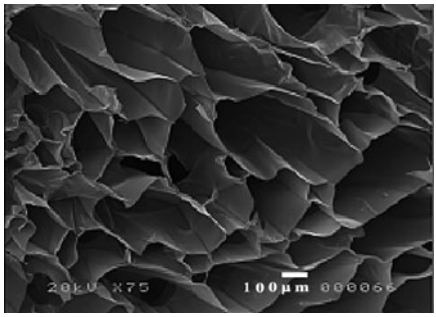

Fig. 4 Scanning electron microscopic images of the cross-section of a porous HA scaffold (Data from [56])

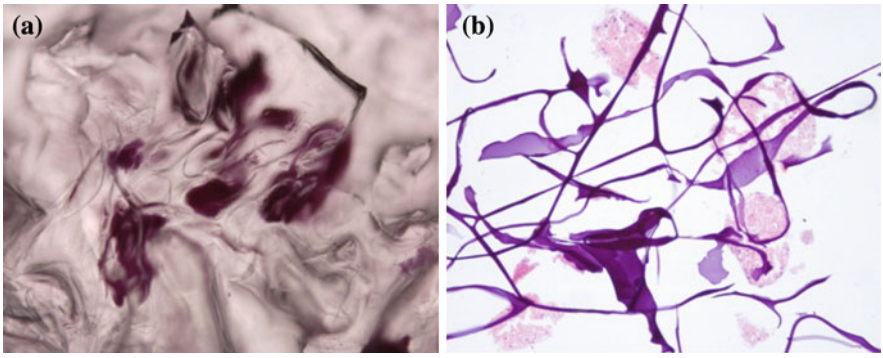

Fig. 5 **a** MTT staining of AD-MSCs and **b** H&E staining of rabbit chondrocytes in 3D HA scaffold after culturing for 14 and 28 days, respectively

4.2 Cell Viability

Cell viability and morphology during the culture in the scaffolds can be determined by MTT [3-(4, 5-dimethythiazol-2-yl)-2, 5-diphenyl tetrazolium bromide] mitochondrial reduction. After washing the stained construct with PBS, observation can be made with naked eyes or under microscopy ($\times 100$) (Fig. 5a). Cells in the scaffold can also be embedded in paraffin, and small section can be stained with hematoxylin–eosin (H&E) after removing paraffin after which they are rehydrated. In the H&E staining, the basic dye hematoxylin colors basophilic structures (usually the one containing nucleic acids) with blue-purple hue, and the alcohol-based acidic eosin colors eosinophilic structures (generally composed of intracellular or extracellular protein) with bright pink (Fig. 5b).

4.3 Cell Proliferation

Proliferation of cells in 3D chondrogenic culture systems can be evaluated by the quantification of genomic DNA. The isolation of the genomic DNA can be

performed by using commercial kits (ex., DNeasy tissue kit, QIAGEN) according to the protocol provided by the company. The measurement of absorbance at 260 nm by ELISA can be used to quantitatively determine the proliferation of cells in the scaffold. Moreover, the cell proliferation can also be quantitatively determined by measuring optical density at 560 nm after dissolving MTT formazan crystal by using DMSO.

4.4 Chondrogenic Differentiation of Cells

The chondrogenic differentiation of chondrocytes can be visualized by staining the sulfated glycosaminoglycan (s-GAG), which is a differentiation marker of chondrocytes and a major component of cartilage tissue. The production of s-GAG from the cells in the scaffold can be observed colorimetrically using an Alcian blue staining and dimethylmethylene blue (DMMB) staining methods. Alcian blue staining is a useful method to visualize the cell viability in 3D culture system. The dark blue staining of the s-GAG can be observed with naked eyes and under light microscopy (Fig. 6a). Quantification of s-GAG is also possible by measuring the absorbance at 560 nm after DMMB staining method using shark chondroitin sulfate C as a standard [23]. Synthesis of s-GAG is one of the important functions of chondrocytes and plays a significant role in regulating the chondrocyte phenotype. Increase in the staining implies the accumulation of s-GAG in the extracellular matrix of chondrocytes cultured in the scaffold. When cells are embedded in paraffin for hematoxylin–eosin (H&E) staining, they also can be stained with 0.1% safranin O, which highly stains negatively charged s-GAG (Fig. 6b).

The RT-PCR (polymeric chain reaction) technique made it possible to amplify a specific DNA sequence, and thus confirm the mRNA expression of type II collagen and aggrecan, the main chondrogenic differentiation markers, during the cell cultures in the scaffold. In the cartilage, chondrocytes and proteoglycan are entrapped in collagen fibrillar network. Type II collagen and aggrecan are the

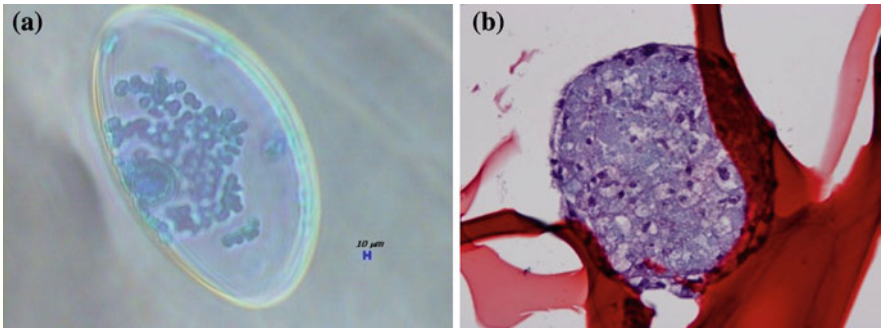

Fig. 6 **a** Alcian blue staining of C-20/A4 cells and **b** Safarin-O staining in the 3D HA scaffold after culturing for 7 days and 28 days, respectively

predominant collagen fiber and proteoglycan, respectively, in the cartilage. AGGRECAN and COL2A1 encode the core protein of aggrecan and α1 chain of type 2 collagen, respectively. Thus, these two genes are generally considered the primary marker gene for chondrogenic differentiation [65, 101]. Sox9 protein is the transcription factor of COL2A1 gene, and functions as an important transcriptional regulator of early chondrogenic differentiation [2, 50, 63]. Since SOX9 encodes sox9 protein, it can be also a marker gene for chondrogenic differentiation. Increase in the expression of these markers indicates the maintenance of chondrocyte phenotype and chondrogenic differentiation of cells.

Generally, it is know that the chondrogenic differentiation of AD-MSCs and chondrocytes in the HA scaffold is significantly higher than that in the micromass culture, which is the standard 3D culture system. HA is known to enhance cell–cell contact by modulating the pericellular matrix in the cell condensation process, which is the initial stage of chondrogenesis [60]. Moreover, interactions between HA and various cell-surface receptors including CD44 are known to play an important role in maintaining differentiated characteristics of chondrocytes [60, 79]. Thus, the culture in HA scaffold seems to be better for both proliferation and chondrogenic differentiation compared to the micromass culture system.

5 Conclusions

The demand for articular cartilage engineering is expected to increase with the advancement of biotechnology. In particular, for the treatment of osteoarthritis, various means of chondrocyte or mesenchymal stem cell delivery is being investigated. Studies have progressed to show that the porous 3D scaffolds of hyaluronic acid derivatives are promising in maintaining the cell-specific phenotype and differentiation. However, despite its biocompatibility and biodegradability, hyaluronic acid system as cell-carrier and scaffold still needs further improvement to be modified into a more flexible cell delivery system with improved mechanical and biological properties.

References

1. Aigner, J., Tegeler, J., Hutzler, P., Campoccia, D., Pavesio, A., Hammer, C., Kastenbauer, E., Naumann, A.: Cartilage tissue engineering with novel nonwoven structured biomaterial based on hyaluronic acid benzyl ester. J. Biomed. Mater. Res. Part. A **42**(2), 172–181 (1998)
2. Akiyama, H., Chaboissier, M., Martin, J., Schedl, A., De Crombrugghe, B.: The transcription factor Sox9 has essential roles in successive steps of the chondrocyte differentiation pathway and is required for expression of Sox5 and Sox6. Genes Dev. **16**(21), 2813–2828 (2002)
3. Allemann, F., Mizuno, S., Eid, K., Yates, K., Zaleske, D., Glowacki, J.: Effects of hyaluronan on engineered articular cartilage extracellular matrix gene expression in 3-dimensional collagen scaffolds. J. Biomed. Mater. Res. Part A **55**(1), 13–19 (2001)

4. Ameer, G., Mahmood, T., Langer, R.: A biodegradable composite scaffold for cell transplantation. J. Orthop. Res. **20**(1), 16–19 (2002)
5. Balazs, E., Bland, P., Denlinger, J., Goldman, A., Larsen, N., Leshchiner, E., Leshchiner, A., Morales, B.: Matrix engineering. Blood Coagul. Fibrinolysis **2**(1), 173 (1991)
6. Balazs, E., Watson, D., Duff, I., Roseman, S.: Hyaluronic acid in synovial fluid. I. Molecular parameters of hyaluronic acid in normal and arthritic human fluids. Arthritis Rheum. **10**(4), 357–376 (1967)
7. Barbucci, R., Lamponi, S., Borzacchiello, A., Ambrosio, L., Fini, M., Torricelli, P., Giardino, R.: Hyaluronic acid hydrogel in the treatment of osteoarthritis. Biomaterials **23**(23), 4503–4513 (2002)
8. Bonaventure, J., Kadhom, N., Cohen-Solal, L., Ng, K., Bourguignon, J., Lasselin, C., Freisinger, P.: Reexpression of cartilage-specific genes by dedifferentiated human articular chondrocytes cultured in alginate beads. Exp. Cell Res. **212**(1), 97–104 (1994)
9. Brittberg, M., Lindahl, A., Nilsson, A., Ohlsson, C., Isaksson, O., Peterson, L.: Treatment of deep cartilage defects in the knee with autologous chondrocyte transplantation. N. Engl. J. Med. **331**(14), 889–895 (1994)
10. Bulpitt, P., Aeschlimann, D.: New strategy for chemical modification of hyaluronic acid: preparation of functionalized derivatives and their use in the formation of novel biocompatible hydrogels. J. Biomed. Mater. Res. Part A **47**(2), 152–169 (1999)
11. Campoccia, D., Hunt, J., Doherty, P., Zhong, S., O'Regan, M., Benedetti, L., Williams, D.: Quantitative assessment of the tissue response to films of hyaluronan derivatives. Biomaterials **17**(10), 963–975 (1996)
12. Capito, R., Spector, M.: Scaffold-based articular cartilage repair. IEEE Eng. Med. Biol. Mag. **22**(5), 42–50 (2003)
13. Chen, Y., Shao, J., Xiang, L., Dong, X., Zhang, G.: Mesenchymal stem cells: a promising candidate in regenerative medicine. Int. J. Biochem. Cell Biol. **40**(5), 815–820 (2008)
14. Clouet, J., Vinatier, C., Merceron, C., Pot-vaucel, M., Maugars, Y., Weiss, P., Grimandi, G., Guicheux, J.: From osteoarthritis treatments to future regenerative therapies for cartilage. Drug Dis Today 14, 913–925 (2009)
15. Cohen, J., Lacroix, P.: Bone and cartilage formation by periosteum: assay of experimental autogenous grafts. J. Bone Joint Surg. **37**(4), 717–730 (1955)
16. Cohen, S., Bano, M., Cima, L., Allcock, H., Vacanti, J., Vacanti, C., Langer, R.: Design of synthetic polymeric structures for cell transplantation and tissue engineering. Clin. Mater. **13**(1–4), 3–10 (1993)
17. Connelly, J., Garcia, A., Levenston, M.: Inhibition of in vitro chondrogenesis in RGD-modified three-dimensional alginate gels. Biomaterials **28**(6), 1071–1083 (2007)
18. De Ugarte, D., Morizono, K., Elbarbary, A., Alfonso, Z., Zuk, P., Zhu, M., Dragoo, J., Ashjian, P., Thomas, B., Benhaim, P.: Comparison of multi-lineage cells from human adipose tissue and bone marrow. Cells Tissues Organs **174**(3), 101–109 (2000)
19. Diduch, D., Jordan, L., Mierisch, C., Balian, G.: Marrow stromal cells embedded in alginate for repair of osteochondral defects. Arthroscopy: J. Arthrosc. Relat. Surg. **16**(6), 571–577 (2000)
20. Dutta, R., Dutta, A.: Cell-interactive 3D-scaffold; advances and applications. Biotechnol. Adv. **27**(4), 334–339 (2009)
21. Evanko, S., Tammi, M., Tammi, R., Wight, T.: Hyaluronan-dependent pericellular matrix. Adv. Drug Deliv. Rev. **59**(13), 1351–1365 (2007)
22. Fan, H., Hu, Y., Qin, L., Li, X., Wu, H., Lv, R.: Porous gelatin-chondroitin-hyaluronate tri copolymer scaffold containing microspheres loaded with TGF β1 induces differentiation of mesenchymal stem cells in vivo for enhancing cartilage repair. J. Biomed. Mater. Res. Part A **77**(4), 785–794 (2006)
23. Farndale, R., Buttle, D., Barrett, A.: Improved quantitation and discrimination of sulphated glycosaminoglycans by use of dimethylmethylene blue. Biochim. Biophys. Acta (BBA) Gen Sub **883**(2), 173–177 (1986)

24. Finger, F., Schoerle, C., Zien, A., Gebhard, P., Goldring, M., Aigner, T.: Molecular phenotyping of human chondrocyte cell lines T/C 28a2, T/C 28a4, and C 28/I2. Arthritis Rheum. **48**(12), 3395–3403 (2003)
25. Finger, F., Schorle, C., Soder, S., Zien, A., Goldring, M., Aigner, T.: Phenotypic characterization of human chondrocyte cell line C-20/A4: a comparison between monolayer and alginate suspension culture. Cells Tissues Organs **178**(2), 65–77 (2004)
26. Fortier, L., Lust, G., Mohammed, H., Nixon, A.: Coordinate upregulation of cartilage matrix synthesis in fibrin cultures supplemented with exogenous insulin-like growth factor-I. J. Orthop. Res. **17**(4), 467–474 (1999)
27. Francis Suh, J.K., Matthew, H.W.T.: Application of chitosan-based polysaccharide biomaterials in cartilage tissue engineering: a review. Biomaterials **21**(24), 2589–2598 (2000)
28. Gaffney, J., Matou-Nasri, S., Grau-Olivares, M., Slevin, M.: Therapeutic applications of hyaluronan. Mol. Biosyst. **6**(3), 437–443 (2010)
29. Getgood, A., Brooks, R., Fortier, L., Rushton, N.: Articular cartilage tissue engineering: today's research, tomorrow's practice? J. Bone Joint Surg. Br. Vol. **91**(5), 565 (2009)
30. Girotto, D.: Tissue-specific gene expression in chondrocytes grown on three-dimensional hyaluronic acid scaffolds. Biomaterials **24**(19), 3265–3275 (2003)
31. Glass, J., Dickerson, K., Stecker, K., Polarek, J.: Characterization of a hyaluronic acid-Arg-Gly-Asp peptide cell attachment matrix. Biomaterials **17**(11), 1101–1108 (1996)
32. Goa, K., Benfield, P.: Hyaluronic acid: a review of its pharmacology and use as a surgical aid in ophthalmology, and its therapeutic potential in joint disease and wound healing. Drugs **47**(3), 536–566 (1994)
33. Goepfert, C., Slobodianski, A., Schilling, A., Adamietz, P., Pörtner, R.: Cartilage engineering from mesenchymal stem cells. Adv. Biochem. Eng./Biotechnol. **123**, 163–200 (2010)
34. Goldring, M.: The role of the chondrocyte in osteoarthritis. Arthritis Rheum. **43**(9), 1916–1926 (2000)
35. Gough, J., Scotchford, C., Downes, S.: Cytotoxicity of glutaraldehyde crosslinked collagen/poly (vinyl alcohol) films is by the mechanism of apoptosis. J. Biomed. Mater. Res. Part A **61**(1), 121–130 (2002)
36. Grad, S., Kupcsik, L., Gorna, K., Gogolewski, S., Alini, M.: The use of biodegradable polyurethane scaffolds for cartilage tissue engineering: potential and limitations. Biomaterials **24**(28), 5163–5171 (2003)
37. Grande, D., Halberstadt, C., Naughton, G., Schwartz, R., Manji, R.: Evaluation of matrix scaffolds for tissue engineering of articular cartilage grafts. J. Biomed. Mater. Res. Part A **34**(2), 211–220 (1997)
38. Gray, M., Pizzanelli, A., Grodzinsky, A., Lee, R.: Mechanical and physicochemical determinants of the chondrocyte biosynthetic response. J. Orthop. Res. **6**(6), 777–792 (1988)
39. Guilaka, F., Awada, H., Fermora, B., Leddy, H., Gimbleb, J.: Adipose-derived adult stem cells for cartilage tissue engineering. Biorheology **41**(3), 389–399 (2004)
40. Haebler, C.: Experimentelle untersuchungen uber die regeneration des gelenkknorpels. Klin Chir **134**, 602–640 (1925)
41. Hardingham, T., Tew, S., Murdoch, A.: Tissue engineering: chondrocytes and cartilage. Arthritis Res. **4**(suppl 3), S63–S68 (2002)
42. Hauselmann, H., Aydelotte, M., Schumacher, B., Kuettner, K., Gitelis, S., Thonar, E.: Synthesis and turnover of proteoglycans by human and bovine adult articular chondrocytes cultured in alginate beads. Matrix (Stuttgart, Germany) **12**(2), 116 (1992)
43. Hendrickson, D., Nixon, A., Grande, D., Todhunter, R., Minor, R., Erb, H., Lust, G.: Chondrocyte-fibrin matrix transplants for resurfacing extensive articular cartilage defects. J. Orthop. Res. **12**(4), 485–497 (1994)
44. Heng, B., Cao, T., Lee, E.: Directing stem cell differentiation into the chondrogenic lineage in vitro. Stem cells **22**(7), 1152–1167 (2004)
45. Hering, T., Kollar, J., Huynh, T.D., Varelas, J.B., Sandell, L.J.: Modulation of extracellular matrix gene expression in bone high-density chondrocyte cultures by ascorbic acid and enzymatic resuspension. Arch. Biochem. Biophys. **314**, 90–98 (1994)

46. Hinsbergh, V., Collen, A., Koolwijk, P.: Role of fibrin matrix in angiogenesis. Ann. NY Acad. Sci. **936** (Fibrinogen: XVIth International Fibrinogen Workshop), 426–437 (2001)
47. Hiraki, Y., Inoue, H., Shigeno, C., Sanma, Y., Bentz, H., Rosen, D., Asada, A., Suzuki, F.: Bone morphogenetic proteins (BMP 2 and BMP 3) promote growth and expression of the differentiated phenotype of rabbit chondrocytes and osteoblastic MC3T3 E1 cells in vitro. J. Bone Miner Res. **6**(12), 1373–1385 (1991)
48. Hunziker, E.: Articular cartilage repair: basic science and clinical progress. A review of the current status and prospects. Osteoarthr. Cartil. **10**(6), 432–463 (2002)
49. Hutmacher, D.W.: Scaffolds in tissue engineering bone and cartilage. Biomaterials **21**(24), 2529–2543 (2000)
50. Ikeda, T., Kamekura, S., Mabuchi, A., Kou, I., Seki, S., Takato, T., Nakamura, K., Kawaguchi, H., Ikegawa, S., Chung, U.: The combination of SOX5, SOX6, and SOX9 (the SOX trio) provides signals sufficient for induction of permanent cartilage. Arthritis Rheum. **50**(11), 3561–3573 (2004)
51. Isogai, N., Kusuhara, H., Ikada, Y., Ohtani, H., Jacquet, R., Hillyer, J., Lowder, E., Landis, W.: Comparison of different chondrocytes for use in tissue engineering of cartilage model structures. Tissue Eng. **12**(4), 691–703 (2006)
52. Jeschke, B., Meyer, J., Jonczyk, A., Kessler, H., Adamietz, P., Meenen, N., Kantlehner, M., Goepfert, C., Nies, B.: RGD-peptides for tissue engineering of articular cartilage. Biomaterials **23**(16), 3455–3463 (2002)
53. Jin, R., Moreira Teixeira, L.S., Dijkstra, P.J., van Blitterswijk, C.A., Karperien, M., Feijen, J.: Enzymatically-crosslinked injectable hydrogels based on biomimetic dextran–hyaluronic acid conjugates for cartilage tissue engineering. Biomaterials **31**(11), 3103–3113 (2010)
54. Juliano, R., Haskill, S.: Signal transduction from the extracellular matrix. J. Cell Biol. **120**(3), 577 (1993)
55. Kafienah, W., Jakob, M., Demarteau, O., Frazer, A., Barker, M., Martin, I., Hollander, A.: Three-dimensional tissue engineering of hyaline cartilage: comparison of adult nasal and articular chondrocytes. Tissue Eng. **8**(5), 817–826 (2002)
56. Kang, J.Y., Chung, C.W., Sung, J.-H., Park, B.-S., Choi, J.-Y., Lee, S.J., Choi, B.-C., Shim, C.-K., Chung, S.-J., Kim, D.-D.: Novel porous matrix of hyaluronic acid for the three-dimensional culture of chondrocytes. Int. J. Pharm. **369**(1–2), 114–120 (2009)
57. Kim, S., Park, J., Cho, Y., Chung, H., Jeong, S., Lee, E., Kwon, I.: Porous chitosan scaffold containing microspheres loaded with transforming growth factor-[beta] 1: implications for cartilage tissue engineering. J. Control. Rel. **91**(3), 365–374 (2003)
58. Kisiday, J., Kopesky, P., Evans, C., Grodzinsky, A., McIlwraith, C., Frisbie, D.: Evaluation of adult equine bone marrow-and adipose-derived progenitor cell chondrogenesis in hydrogel cultures. J. Orthop. Res. **26**(3), 322–331 (2008)
59. Kleinman, H., Klebe, R., Martin, G.: Role of collagenous matrices in the adhesion and growth of cells. J. Cell Biol. **88**(3), 473–485 (1981)
60. Knudson, C.: Hyaluronan and CD44: strategic players for cell–matrix interactions during chondrogenesis and matrix assembly. Birth Defects Res Part C: Embryo Today Rev. **69**(2), 174–196 (2003)
61. Lahiji, A., Sohrabi, A., Hungerford, D., Frondoza, C.: Chitosan supports the expression of extracellular matrix proteins in human osteoblasts and chondrocytes. J. Biomed. Mater. Res. Part A **51**(4), 586–595 (2000)
62. Langer, R., Vacanti, J.P.: Tissue engineering. Science **260**, 920–926 (1993)
63. Lefebvre, V., Garofalo, S., Zhou, G., Metsaranta, M., Vuorio, E., De Crombrugghe, B.: Characterization of primary cultures of chondrocytes from type II collagen/[beta]-galactosidase transgenic mice. Matrix Biol. **14**(4), 329–335 (1994)
64. Lima, E., Bian, L., Ng, K., Mauck, R., Byers, B., Tuan, R., Ateshian, G., Hung, C.: The beneficial effect of delayed compressive loading on tissue-engineered cartilage constructs cultured with TGF-[beta] 3. Osteoarthr. Cartil. **15**(9), 1025–1033 (2007)
65. Lin, Y., Luo, E., Chen, X., Liu, L., Qiao, J., Yan, Z., Li, Z., Tang, W., Zheng, X., Tian, W.: Molecular and cellular characterization during chondrogenic differentiation of adipose

tissue derived stromal cells in vitro and cartilage formation in vivo. J. Cell. Mol. Med. **9**(4), 929–939 (2005)
66. Malda, J., Van Blitterswijk, C., Grojec, M., Martens, D., Tramper, J., Riesle, J.: Expansion of bovine chondrocytes on microcarriers enhances redifferentiation. Tissue Eng. **9**(5), 939–948 (2003)
67. Mattioli-Belmonte, M., Gigante, A., Muzzarelli, R., Politano, R., De Benedittis, A., Specchia, N., Buffa, A., Biagini, G., Greco, F.: *N*, *N*-dicarboxymethyl chitosan as delivery agent for bone morphogenetic protein in the repair of articular cartilage. Med. Biol. Eng. Comput. **37**(1), 130–134 (1999)
68. McDevitt, C.: Biochemistry of articular cartilage. Nature of proteoglycans and collagen of articular cartilage and their role in ageing and in osteoarthrosis. Ann. Rheum. Dis. **32**(4), 364–378 (1973)
69. McNaught, A., Wilkinson, A.: International Union of Pure and Applied Chemistry. Compendium of Chemical Terminology: IUPAC Recommendations. Blackwell Science, Oxford, England (1997)
70. Myung, D., Koh, W., Ko, J., Hu, Y., Carrasco, M., Noolandi, J., Ta, C., Frank, C.: Biomimetic strain hardening in interpenetrating polymer network hydrogels. Polymer **48**(18), 5376–5387 (2007)
71. Nesic, D., Whiteside, R., Brittberg, M., Wendt, D., Martin, I., Mainil-Varlet, P.: Cartilage tissue engineering for degenerative joint disease. Adv. Drug Deliv. Rev. **58**(2), 300–322 (2006)
72. Nishi, C., Nakajima, N., Ikada, Y.: In vitro evaluation of cytotoxicity of diepoxy compounds used for biomaterial modification. J. Biomed. Mater. Res. **29**(7), 829–834 (1995)
73. Nixon, A., Fortier, L., Williams, J., Mohammed, H.: Enhanced repair of extensive articular defects by insulin-like growth factor-I-laden fibrin composites. J. Orthop. Res. **17**(4), 475–487 (1999)
74. O'brien, F., Harley, B., Yannas, I., Gibson, L.: The effect of pore size on cell adhesion in collagen-GAG scaffolds. Biomaterials **26**(4), 433–441 (2005)
75. Oerther, S., Payan, E., Lapicque, F., Presle, N., Hubert, P., Muller, S., Netter, P.: Hyaluronate–alginate combination for the preparation of new biomaterials: investigation of the behaviour in aqueous solutions. Biochim. Biophys. Acta (BBA)-Gen. Sub. **1426**(1), 185–194 (1999)
76. Paige, K., Cima, L., Yaremchuk, M., Schloo, B., Vacanti, J., Vacanti, C.: De novo cartilage generation using calcium alginate–chondrocyte constructs. Plast. Reconstr. Surg. **97**(1), 168–178 (1996)
77. Pesakov, V., Stol, M., Adam, M.: Comparison of the influence of gelatine and collagen substrates on growth of chondrocytes. Folia Biol. **36**(5), 264–270 (1990)
78. Petersen, B., Barkun, A., Carpenter, S., Chotiprasidhi, P., Chuttani, R., Silverman, W., Hussain, N., Liu, J., Taitelbaum, G., Ginsberg, G.: Tissue adhesives and fibrin glues. Gastrointest. Endosc. **60**(3), 327–333 (2004)
79. Ponta, H., Sherman, L., Herrlich, P.: CD44: from adhesion molecules to signalling regulators. Nat. Rev. Mol. Cell Biol. **4**(1), 33–45 (2003)
80. Ponticiello, M., Schinagl, R., Kadiyala, S., Barry, F.: Gelatin-based resorbable sponge as a carrier matrix for human mesenchymal stem cells in cartilage regeneration therapy. J. Biomed. Mater Res Part A **52**(2), 246–255 (2000)
81. Risbud, M.V., Sittinger, M.: Tissue engineering: advances in in vitro cartilage generation. Trends Biotechnol. **20**(8), 351–356 (2002)
82. Santiago, L., Nowak, R., Peter Rubin, J., Marra, K.: Peptide-surface modification of poly (caprolactone) with laminin-derived sequences for adipose-derived stem cell applications. Biomaterials **27**(15), 2962–2969 (2006)
83. Schnabel, M., Marlovits, S., Eckhoff, G., Fichtel, I., Gotzen, L., Vecsei, V., Schlegel, J.: Dedifferentiation-associated changes in morphology and gene expression in primary human articular chondrocytes in cell culture. Osteoarthr. Cart. **10**(1), 62–70 (2002)

84. Shimazu, A., Jikko, A., Iwamoto, M., Koike, T., Yan, W., Okada, Y., Shinmei, M., Nakamura, S., Kato, Y.: Effects of hyaluronic acid on the release of proteoglycan from the cell matrix in rabbit chondrocyte cultures in the presence and absence of cytokines. Arthritis Rheum. **36**(2), 247–253 (1993)
85. Speer, D., Chvapil, M., Vorz, R., Holmes, M.: Enhancement of healing in osteochondral defects by collagen sponge implants. Clin. Orthop. Rel. Res. **144**, 326–335 (1979)
86. Stenzel, K., Miyata, T., Rubin, A.: Collagen as a biomaterial. Ann. Rev. Biophys. Bioeng. **3**, 231–253 (1974)
87. Stockwell, R.: The interrelationship of cell density and cartilage thickness in mammalian articular cartilage. J. Anat. **109**(Pt 3), 411–421 (1971)
88. Takigawa, M., Shirai, E., Fukuo, K., Tajima, K., Mori, Y., Suzuki, F.: Chondrocytes dedifferentiated by serial monolayer culture form cartilage nodules in nude mice. Bone Miner. **2**(6), 449–462 (1987)
89. Tay, A., Farhadi, J., Suetterlin, R., Pierer, G., Heberer, M., Martin, I.: Cell yield, proliferation, and postexpansion differentiation capacity of human ear, nasal, and rib chondrocytes. Tissue Eng. **10**(5–6), 762–770 (2004)
90. Tomihata, K., Ikada, Y.: Crosslinking of hyaluronic acid with glutaraldehyde. J. Polym. Sci. Part A Polym. Chem. **35**(16), 3553–3559 (1997)
91. Tomihata, K., Ikada, Y.: Crosslinking of hyaluronic acid with water-soluble carbodiimide. J. Biomed. Mater. Res. Part A **37**(2), 243–251 (1997)
92. Van Osch, G., van der Veen, S., Verwoerd-Verhoef, H.: In vitro redifferentiation of culture-expanded rabbit and human auricular chondrocytes for cartilage reconstruction. Plast. Reconstr. Surg. **107**(2), 433–440 (2001)
93. Vinatier, C., Bouffi, C., Merceron, C., Gordeladze, J., Brondello, J.M., Jorgensen, C., Weiss, P., Guicheux, J., Noel, D.: Cartilage tissue engineering: towards a biomaterial-assisted mesenchymal stem cell therapy. Curr. Stem Cell Res. Ther. **4**(4), 318–329 (2009)
94. Vuori, K., Ruoslahti, E.: Association of insulin receptor substrate-1 with integrins. Science **266**(5190), 1576 (1994)
95. Wakitani, S., Goto, T., Young, R., Mansour, J., Goldberg, V., Caplan, A.: Repair of large full-thickness articular cartilage defects with allograft articular chondrocytes embedded in a collagen gel. Tissue Eng. **4**(4), 429–444 (1998)
96. Williams, R., Gamradt, S.: Articular cartilage repair using a resorbable matrix scaffold. Instr. Course Lect. **57**, 563–571 (2008)
97. Wong, M., Siegrist, M., Wang, X., Hunziker, E.: Development of mechanically stable alginate/chondrocyte constructs: effects of guluronic acid content and matrix synthesis. J. Orthop. Res. **19**(3), 493–499 (2001)
98. Worster, A., Nixon, A., Brower-Toland, B., Williams, J.: Effect of transforming growth factor α1 on chondrogenic differentiation of cultured equine mesenchymal stem cells. Am. J. Vet. Res. **61**(9), 1003–1010 (2000)
99. Wu, S.-C., Chang, J.-K., Wang, C.-K., Wang, G.-J., Ho, M.-L.: Enhancement of chondrogenesis of human adipose derived stem cells in a hyaluronan-enriched microenvironment. Biomaterials **31**(4), 631–640 (2010)
100. Yoo, H., Lee, E., Yoon, J., Park, T.: Hyaluronic acid modified biodegradable scaffolds for cartilage tissue engineering. Biomaterials **26**(14), 1925–1933 (2005)
101. Zuk, P., Zhu, M., Ashjian, P., De Ugarte, D., Huang, J., Mizuno, H., Alfonso, Z., Fraser, J., Benhaim, P., Hedrick, M.: Human adipose tissue is a source of multipotent stem cells. Mol. Biol. Cell **13**(12), 4279–4295 (2002)

Chitosan Derivative Based Hydrogels: Applications in Drug Delivery and Tissue Engineering

Marta Roldo and Dimitrios G. Fatouros

Abstract Chitosan is a biodegradable, biocompatible and non-irritant polymer that exhibits good mechanical strength and adhesion. These characteristics make it suitable for applications in controlled delivery systems and tissue engineering. Chitosan gels may be easily obtained by a cross-linking reaction. These hydrogels exhibit good swelling properties and are widely used as a temporary extracellular matrix in tissue engineering and regenerative medicine as well as controlled drug delivery matrices. Considerable advances have been made in this area throughout the past decade, including the development of novel formulations containing chitosan derivatives with improved properties. This area of research is providing the fundamental knowledge required to rationally develop new strategies for biomedical engineering to tackle problems related with regenerative therapy. This survey presents different biologically active chitosan systems designed for drug delivery and tissue engineering applications and assesses the parameters needed for these formulations to achieve improved properties.

1 Introduction

Recent developments in controlled and targeted drug delivery are calling for the development of novel materials with enhanced biocompatibility and

M. Roldo (✉)
School of Pharmacy and Biomedical Science, University of Portsmouth, St Michael's Building, White Swan Road, Portsmouth PO1 2DT, UK
e-mail: marta.roldo@port.ac.uk

D. G. Fatouros
School of Pharmacy, Aristotle University of Thessaloniki, 54124 Thessaloniki, Greece

Stud Mechanobiol Tissue Eng Biomater (2011) 8: 351–376
DOI: 10.1007/8415_2010_55

Published Online: 21 January 2011

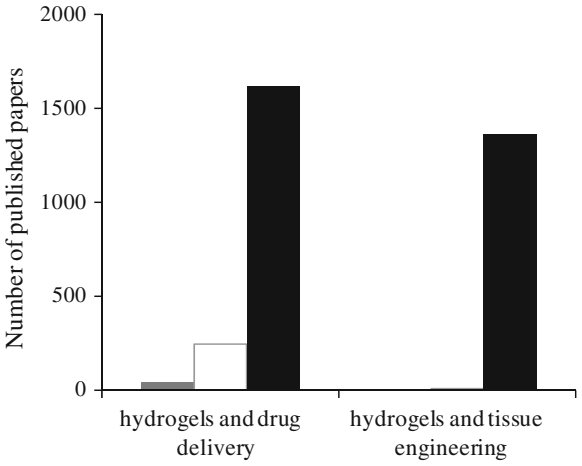

Fig. 1 Number of papers published in the 80s (*grey*), 90s (*white*) and 2000s (*black*) according to a PubMed search carried out with "hydrogels and drug delivery" and "hydrogels and tissue engineering" as keywords

biodegradability [68]. Since the 1960 ground-breaking work by Witchrerle and Lim, hydrogel formulations have been attracting a lot of interest (Fig. 1) as the type of drug delivery platforms that can provide these properties and be suitable for several different applications [26].

Their use in drug delivery applications is stimulated by the unique physical properties presented by hydrogels. The polymeric network forms a highly porous structure which properties can be tuned by adjustments to the crossliking density of the hydrogels or its affinity for the external environment; hydrogels that change porosity in response to modified pH, temperature or ionic strength can also be engineered [23]. The pores are suitable for loading of drugs that will be subsequently released according to their diffusion coefficient [25]. Degradation of the hydrogel is another property that can be designed according to the required application, the process can occur by hydrolysis, enzymatic degradation or dissolution [25]. Hydrogels are generally classified into two categories: physical or reversible and chemical or permanent. In physical hydrogels the crosslinking is given by physical entanglement and/or weak interactions; while in chemical gels crosslinking occurs by covalent bonding [24]. Both classes of hydrogels possess advantages and disadvantages depending on the desired application, these have been comprehensively reviewed in a recent paper [25]. Hydrogels are an extremely flexible drug delivery platform as they can be formulated as films, nano- and micro-particles and in situ-forming gels; they can also be used for coatings, pressed powder matrices [26, 68], or as scaffolds for tissue engineering.

Polymers of different nature have been used in the formulation of hydrogels [68], however, natural macromolecules, such as polysaccharides, have demonstrated superior properties. Their use is highly sustainable as they are generally abundant and readily available. Furthermore, polysaccharides come in a variety of compositions that are difficult to reproduce synthetically [14]. Amongst other polysaccharides, such as alginate, carrageenan, dextran, gellan, guar gum, hyaluronic acid, pullulan, scleroglucan, xanthan, xyloglucan and pectin, chitosan has

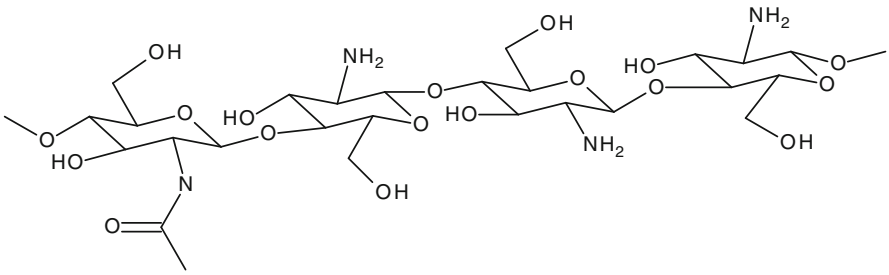

Fig. 2 Structure of chitosan

been the focus of many investigations; the most recent advances in chitosan applications have been reported in several reviews [1, 3, 5, 6, 10, 31, 40, 44, 53, 57, 63, 70, 78, 79]. Chitosan is an aminoglucopyran composed of N-acetylglucosamine (GlcNAC) and glucosamine (GlcN) residues (Fig. 2) and obtained by deacetylation of chitin in harsh alkali environment. Chitosan is soluble only in acidic aqueous environment, characteristic that somewhat limits its applications in vivo. However, this hurdle can be easily overcome as chitosan is amenable to chemical modification by simple reactions, thanks to its primary amino group as well as primary and secondary hydroxyl groups (Fig. 2) [56]. Several derivatives of chitosan with enhanced solubility and diverse physicochemical and biological properties have been prepared as summarized in recent reviews [2, 56].

Despite successful formulation of chitosan-based hydrogels for tissue engineering, wound healing and subcutaneous, oral, ophthalmic, nasal and transdermal drug delivery [6, 10, 51] there is a great interest in the development of hydrogels based on chitosan derivatives as these might lead to the next generation of delivery systems able to adapt to different loading and release requirements specific to the type of application. This chapter will provide a summary of recent progress on how different types of chitosan derivatives have been formulated into hydrogels for drug delivery and tissue engineering and what advantages these show when compared to chitosan.

2 Positively Charged Chitosan Derivatives

The pH dependence of chitosan properties such as mucoadhesion and absorption enhancement has prompted investigation into the synthesis of positively charged derivatives that show high solubility and maintain their properties in a wider pH range [56]. Quaternized chitosan derivatives have been prepared mainly by using two methods [66]. The first involves the methylation of the amino group in position C2 achieved by reaction of the polymer with methyl iodide in solution of sodium hydroxide and *N*-methyl pyrrolidinone (NMP) to obtain trimethylchitosan chloride (TMC) (Fig. 3) [69, 77]. The second one involves the modification of the

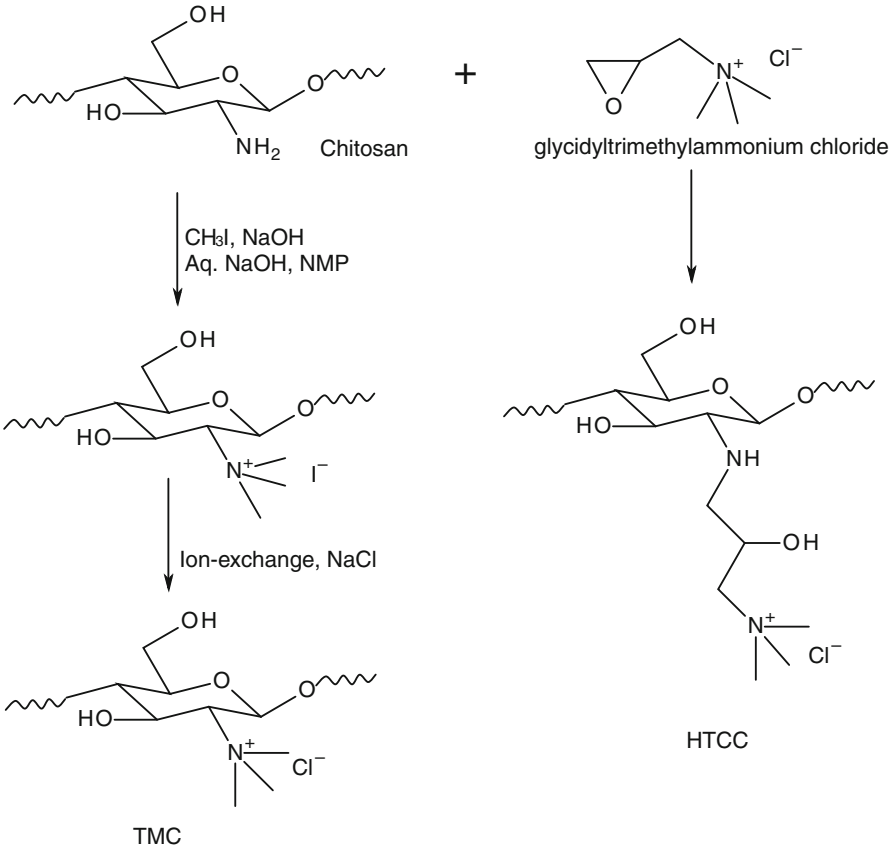

Fig. 3 Synthesis of TMC and HTCC

amino group with a pendant chain carrying the positive charge, e.g. glycidyltrimethylammonium chloride in the synthesis of *N*-[(2-hydroxy-3-trimethylammomium)propyl]chitosan (HTTC) (Fig. 3) [89, 90].

TMC has been used in the formation of different types of hydrogels. Polyelectrolyte complexes (PECs) have been for example formulated by crossliking TMC with insulin [52]. The interactions involved in the formation of PECs are mainly electrostatic and highly dependent on pH and charge density. The substitution of TMC to chitosan in the formulation of the hydrogels allowed preparation and use at physiological pH, which would otherwise cause precipitation of the complex. The PEC guarantees the stability of insulin in the pH range 6.5–8. A further development to the PECs formulation was the introduction of poly(ethylene) glycol (PEG) chains grafted onto TMC. The use of pegylated-TMC produced complexes with smaller particle size compared to those obtained with TMC alone. Pegylation also enhanced the mucoadhesion due to the synergistic effects of the interpenetration between PEG chains and the mucus and the

electrostatic interactions formed between the quaternized groups on the polysaccharide and the negative charges of the glycoproteins on the mucus [35]. However, the higher mucoadhesion did not translate in better insulin absorption, in fact the TMC-insulin complexes resulted more effective than the PEG-TMC-insulin complexes in favoring the peptide uptake by E12 cells monolayers. This was due to the fact that the pegylated complexes released the whole payload as soon as mucodhesion occurred [35].

PECs were also prepared by mixing TMC with enoxaparin (or low molecular weight heparin), an anticoagulant drug used for the prevention of venous thrombosis and pulmonary embolism in patients undergoing surgery [73]. This drug is generally characterized by poor absorption through the intestinal mucosa and for this reason it has been formulated with TMC as an absorption enhancer. The formation of these complexes was found to be dependent on both electrostatic and hydrophobic interactions; soluble PECs with particle size of 200–500 nm were obtained in the 3.0–6.5 pH range and drug encapsulation efficiency was as high as 90%. In terms of bioadhesion, drug delivery and absorption, these complexes demonstrated similar characteristics to those obtained between TMC and insulin; TMC-enoxaparin systems were more effective in enhancing drug uptake even if pegylated systems had a higher impact on the mucoadhesive properties [74].

Furthermore, PECs can be formed by the self assembling of TMC with a negatively charged polymer such as poly(γ-glutamic acid) (γ-PGA). These systems have been studied for the delivery of insulin by the oral route [55]. Insulin was loaded with an efficiency of more than 70% to obtain a final insulin load of around 23%. The stability of the formulation was superior compared to formulations employing chitosan instead of TMC, and the stability was extended to a broader pH range. The use of TMC prevented the disintegration of the hydrogel particles at physiological pH, nevertheless maintaining pH dependent swelling (Fig. 4) and a

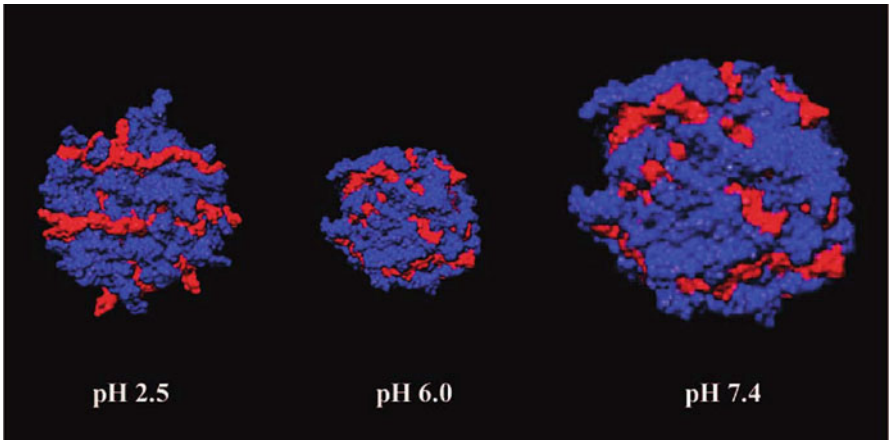

Fig. 4 Structural changes of the self-assembled TMC/γ-PGA complex at distinct pH values obtained by molecular dynamic simulations. TMC in *blue*; γ-PGA in *red* [55]

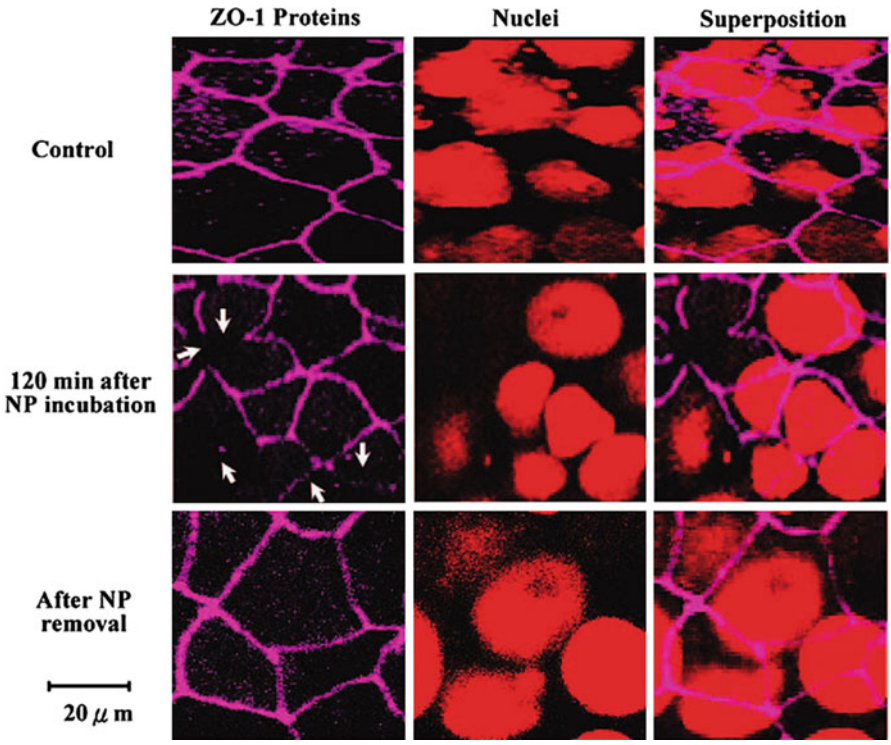

Fig. 5 Fluorescence images of Caco-2 cell monolayers immunofluorescently stained for ZO-1 proteins after incubation with TMC/γ-PGA nonoparticles (NPs) for 120 min [55]

sustained release of the drug. The presence of TMC in the system also favored insulin absorption by inducing opening of tight junctions (Fig. 5). The formulation has been demonstrated to be a suitable vehicle for transmucosal delivery of peptide drugs by the oral route.

HTCC is obtained by a simple reaction between chitosan and glycidyltrimethylammonium chloride (GTMAC) in aqueous environment (Fig. 2) [83]. Selective modification of the amino group in position C2 is obtained as the nucleophilicity of the hydroxyl groups compared to that of the amino groups of chitosan is not sufficient to open the epoxy ring on the GTMAC molecule [84]. The degree of quaternization of the polymer can be controlled by changing the ratio of reagents in the reaction medium. Crosslinking of HTCC with α-β-glycerophosphate (α-β-GP) in the presence of poly(ethylene glycol) (PEG) [84] affords thermosesitive hydrogels. GP promotes the hydration of the quaternized chitosan molecules maintaining them free in solution at low temperatures. An increase in temperature provides increased internal energy and therefore entropy of the system promoting formation of hydrophobic interactions between the chains, aimed at reducing this entropy. PEG provides extra crosslinking points and favors gelation, for this reason its molecular weight and concentration can affect the kinetics of gel formation and

drug release [84]. HTCC-PEG-GP hydrogels were loaded with insulin as a model peptide drug, its release was initially quick and then sustained for several hours; in rats this gave rise to a sustained effect with reduced blood glucose levels for 4–5 h. The gels have been shown to have an effect on the permeability of the nasal mucosa, with HTCC inducing opening of tight junctions, and GP increasing the biocompatibility of the formulation [84]. Application of these gels in the periodontal delivery of chlorexidine has also been investigated [33]. Thermosenstive hydrogels based on the same principle were also obtained using TMC instead of HTCC. A detailed rheological study showed that the time and temperature of gelation can be finely tuned by modifying formulation parameters such as components ratio and molecular weight and degree of quaterinization of TMC [11, 60]. Hydrogels formulated with TMC obtained from medium molecular weigh chitosan, with low degree of quaternization and crosslinked with 2.5% GP showed the best properties for nasal application: sol-to-gel transition at 32.5°C, within 7 min, and viscoelastic properties after gelation that should guarantee reduction of mucociliary clearance and prolonged residence [61].

2.1 Positively Charged Chitosans for Tissue Engineering

One of the most important issues in tissue engineering and regenerative medicine is the angiogenesis of an implanted construct; Mao et al. addressed this problem by applying DNA encoding vascular endothelial growth factor (VEGF) into a collagen scaffold [54]. TMC/DNA complexes were incorporated into the collagen scaffolds to control the release of the DNA, following studies on the in vivo angiogenesis ability of the scaffold. VEGF expression level in vitro was assessed with a 3-D static culture model (HEK293 cells). TMC/DNA complexes incorporated scaffold increased the VEGF expression level by a factor of 3.5 over the DNA-free scaffold at day 4. Moreover, an increase in the dose of the loaded TMC/DNA complexes resulted in increased levels of VEGF expression (Fig. 6).

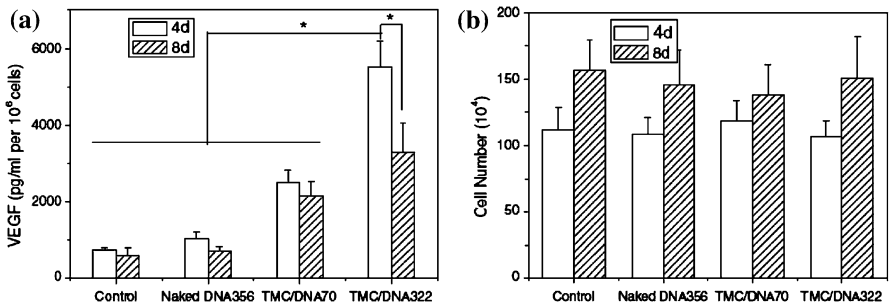

Fig. 6 **a** VEGF expression by HEK293 cells and **b** number of HEK293 cells in different samples after transfection at day 4 and 8. $*p < 0.01$ [54]

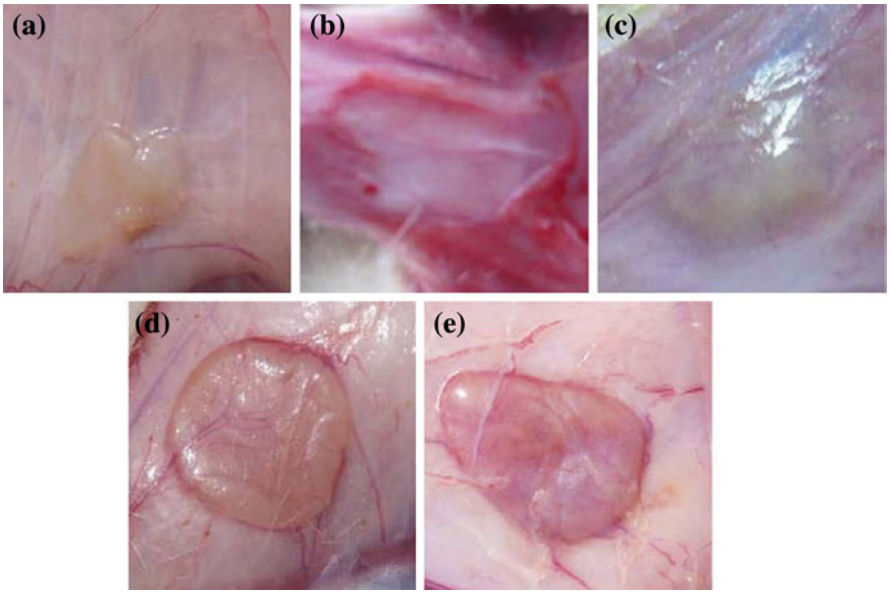

Fig. 7 Gross views of the scaffolds 2 weeks after implantation. **a** DNA-free scaffold, **b** naked DNA356 scaffold, **c** TMC/DNA-EGFP scaffold, **d** TMC/DNA70 scaffold, and **e** TMC/DNA322 scaffold [54]

In vivo studies with Sprague–Dawley mice demonstrated that the implanted scaffolds containing TMC/DNA complexes enhanced the VEGF expression and thereby the angiogenesis of implanted scaffolds.

The gross views of the implanted scaffolds 2 weeks after implantation are illustrated at Fig. 7. No blood vessels on the surface were present on the DNA-free (Fig. 7a) and the TMC/DNA-EGFP (enhanced green fluorescence protein) scaffolds (Fig. 7c). Blood vessels could be seen surrounding the naked DNA356 (containing 356 μg of DNA) scaffold (Fig. 7b). On the contrary a lot of blood vessels were on the surface of the TMC/DNA70 scaffold (Fig. 7d). Even more blood vessels were present on the TMC/DNA322 scaffold as more DNA was present (Fig. 7e) demonstrating the enhanced ability of the scaffolds to promote angiogenesis.

In another study, TMC/DNA complexes were incorporated in a composite designed to repair articular cartilage defects [80]. The composite was comprised of bone marrow mesenchymal stem cells (BMSCs), plasmid DNA encoding transforming growth factor-b1 (pDNA-TGF-b1), fibrin gel and poly (lactide-co-glycolide) (PLGA) sponge. The gene complexes had a transfection efficiency of 9% to BMSCs in vitro, which was enough to express the TGF-b1 protein. Transplantation of the composites into cartilage defects of rabbit knees resulted in hyaline cartilage, better chondrogenesis of BMSCs and subchondral bone connection.

3 Ampholytic Chitosan Derivatives for pH Sensitive Hydrogels

3.1 N-*Succinyl Chitosan*

N-succinyl chitosan (NSC) is obtained by ring opening reaction of succinic anhydride in the presence of the polysaccharide (Fig. 8).

Different degrees of substitution can be achieved by varying the amount of succinic anhydride employed in the reaction or by modifying reaction time. The derivative obtained has ampholytic properties and therefore it is soluble both at acidic and alkaline pH, being insoluble in the pH range 4.8–6.8 [87]. The presence of negative charges on the polymer favors its prolonged systemic circulation [38, 39] which has been exploited for tumor drug targeting [71, 72]. Crosslinking of NSC with other polymers has been used as a mean of formulating hydrogels. NSC was co-formulated with sodium alginate into pH sensitive hydrogel beads by ionic gelation in the presence of $CaCl_2$ [15]. The presence of Ca^{2+} ions induced both gelation of the chitosan derivative and the alginate causing the formation of interpenetrating polymer networks. Nifedipine drug loading and release studies demonstrated that as the pH increases both swelling and drug release are improved. Furthermore, these properties could be fine tuned by modifying the weight ratio of drug to polymer.

Polymer–polymer covalent crosslinking was also used in the preparation of NSC hydrogels. Mixtures of oxidized carboxymethyl-cellulose (OCMC) and NSC formed gels by electrostatic interaction and hydrogen bonding; these gels were finally stabilized by the formation of a Schiff base between the aldehyde groups on OCMC and the amine groups on NSC [50]. Thanks to the susceptibility of Schiff bonds in aqueous environment, all gels completely degraded within 12 days. The extent of oxidation of OCMC determined the degree of crosslinking within the gel and consequently the pore size (Fig. 9), and the drug diffusion coefficient. These gels have potential in the release of macromolecular drugs as it was shown that the structure and activity of BSA was not affected by the encapsulation within

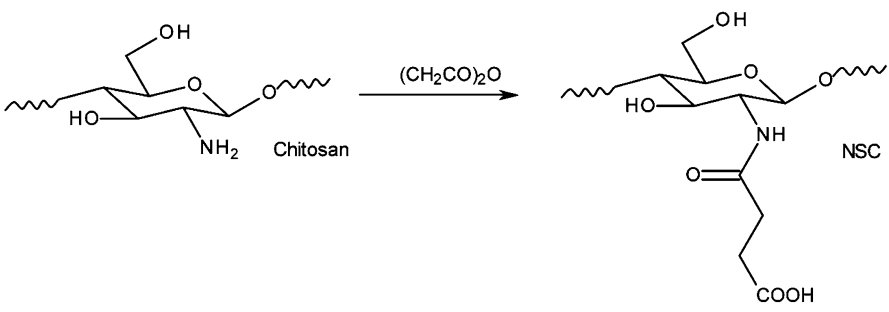

Fig. 8 Synthesis of *N*-succinyl chitosan

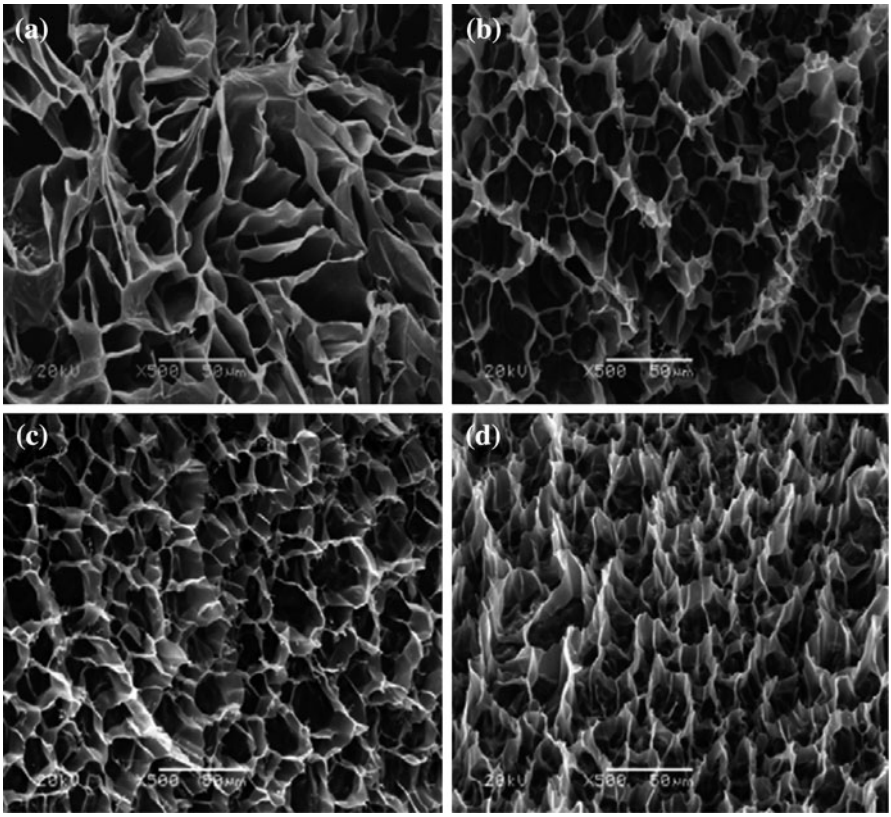

Fig. 9 SEM images of hydrogels formed with decreasing NSC/OCMC ratios from a to d (amine groups/aldehyde groups ratio 1:0.5, 1:1.1, 1:1.6 and 1:2.2, respectively). As the average pore diameter decreases (from a to d), the gelling time, the equilibrium swelling ratio and the water diffusion coefficient also decrease [50]

the polymeric network. Drug release studies showed that the release follows Fick's first law of diffusion in the first 90 min when the release is thought to be mainly affected by swelling and not by degradation. As degradation starts to take place the release profile changes and a constant rate is obtained. The cumulative release increases with the decrease in the degree of crosslinking but complete release is not obtained for any of the hydrogels in the 12 days observed.

A similar derivative, namely *N*-maleolyl-chitosan has been employed in the formation of thermosensitive hydrogels [19]. The *N*-maleolyl-chitosan was prepared by recation of the polysaccharide with maleic anhydride, this was subsequently grafted with poly(*N*-isopropylacrylamide) by electon beam irradiation. The polymer obtained had a LCST (lower critical solution temperature) of 32°C and presented limited swelling in the 4–5 pH region.

3.2 Carboxyalkyl Chitosans

The introduction of carboxylic groups along the polymeric backbone can be achieved by carboxyalkylation of the amino group of chitosan. The derivatives obtained have been shown to have favorable properties such as non-toxicity, biodegradability, biocompatibility, antibacterial and antifungal activity, water solubility (which can be controlled by the degree of substitution), high viscosity, large hydrodynamic volume and ability to form pH sensitive hydrogels [42]. The synthesis of these derivatives has been described in depth in a recent review [32]. Both *N*- and *O*-carboxymethyl chitosan have been synthesized and studied (Fig. 10); two main synthetic pathways can be used to achieve selective *N*-modification, namely reaction with monohalocaboxylic acids [20] or with carboxyaldehydes [59]. Other derivatives of this kind are *N*-(2-carboxyethyl) chitosan, *N*-carboxybenzyl chitosan, derivatives obtained with hydroxyethyl acrylate, hydroxypropyl acrylate, acrylamide, acrylonitrile, PEG-acrylate, pyruvic acid and its derivatives, α-ketoglutaric acid, levulonic acid and hydroxybenzaldehydes [56].

Carboxymethylated chitosan (CMC, Fig. 10) has been used for the preparation of both chemical and physical gels. Ionic gelation in the presence of Ca^{2+} is a well known process for the formation of alginate hydrogels; due to the presence of carboxylate groups, CMC is also a good candidate for the formation of Ca^{2+} crosslinked gels [16]. However, it was found that the molecular weight of CMC constitutes a limiting factor in the preparation of gels with good mechanical strength, in fact only low molecular weight CMC affords stable formulations [49]. The swelling ratios of these hydrogels were highest at neutral pH with limited swelling at acidic pH; an ideal behavior for oral drug delivery of proteins where the drug delivery system must protect the drug from the harsh environment of the stomach. Even though beads prepared with these hydrogels present a high BSA (bovine serum albumin) entrapment efficiency they do not prevent early release of the drug, phenomenon commonly observed in physical gels. However, the release profile of 5-fluorouracil from $CaCl_2$ crosslinked CMC nanoparticles (Fig. 11) has been shown to be ideal for delivery of cancer drugs [16].

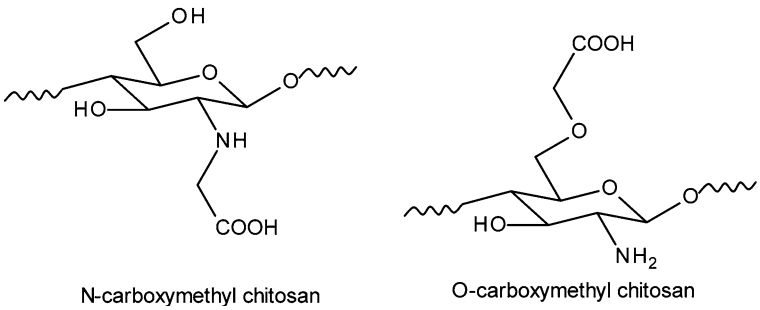

Fig. 10 Structure of carboxymethyl chitosan

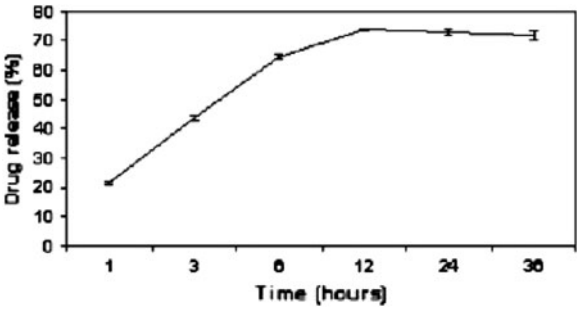

Fig. 11 Release rate of 5-FU drug from CMC nanoparticles[16]

CMC with nitrocinnamate as pendant group was used in the preparation of chemical gels by photoinitiated crosslinking [29]. Gelation is carried out in the absence of potentially toxic initiators due to the cinnamate ability to undergo *trans–cis* isomerisation and [2 + 2] cycloaddition when irradiated with UV light at more than 290 nm. The gelling efficiency was found to be dependent on irradiation time and degree of substitution of the carboxymethylated chitosan. An increasing degree of crosslinking was obtained when the gel was irradiated for longer and when a derivative with a higher number of nitrocinnamate molecules attached was used. The gel was biodegradable in the presence of lysozyme, with quicker degradation obtained for the derivative with a lower degree of crosslinking. The gels obtained were capable of controlling the release of doxorubicin over a period of 2 days at physiological pH. Chemical gels based on CMC were also obtained by the more conventional method of crosslinking with glutaraldehyde [12]. This procedure leads to the formation of hydrogels which pH sensitivity can be tailored by changing the degree of deacetylation and substitution. Polymer swelling was highest below and above the isoelectric point (IEP) that was found to be in the region 2.0–4.0, depending on the degree of deacetylation, that decreased the IEP value, and the degree of substitution, that increased it. The controllable pH dependent behavior of these hydrogels, together with the fact that they undergo complete degradation in vivo and present high biocompatibility, justify their suggested use as protein delivery carriers for oral administration. BSA loaded hydrogels released the unbound protein by Fickian diffusion during the first 4 h; bound BSA was released later with a rate maintained constant by the degradation of the hydrogel.

Glutaraldehyde crosslinked gels were also obtained with *N*-(2-carboxybenzyl) chitosan. These gels were studied for uses such as buccal application for delivery of antifungal drugs i.e. fluconazole [42] and colon specific drug delivery of fluorouracil [47]. *N*-(2-carboxybenzyl) chitosan was synthesised by reaction with carboxybenzaldehyde which leads to the formation of a Schiff base, followed by reduction with sodium borohydride. The hydrogel was successively obtained by crosslinking the polymer in the presence of glutaraldahyde. The reaction gave water soluble derivatives when it was carried out at low temperature (50°C) and for a prolonged period of time (5 h). These gels gave sustained release of fluconazole. The drug release from the formulations decreased with the increase in

the amount of drug loaded due to the modification from amorphous to crystalline state of the drug within the gel [42]. The release was determined to be pH dependent, with higher release rate obtained at pH values above 5.

Glutaraldehyde capacity to produce undesirable reactive species has initiated research into safer crosslinkers such as the natural occurring genepin [58]. *N,O*-carboxymethyl chitosan and alginate crosslinked by genipin have also been shown to produce pH-sensitive hydrogels, these release up to 80% of the loaded albumin at pH 7.4 compared to 20% release obtained at pH 1.2 [13].

A polymer–polymer covalent complex formation has been employed in the preparation of *N*-carboxyethyl chitosan and quartenised chitosan (HTCC) hydrogels [28]. Both polymers were modified with methacrylamide pendant groups which formed covalent crosslinking undergoing a redox reaction at room temperature. The hydrogels were loaded with BSA as a model drug; this was released from the hydrogels by diffusion after an initial burst release. Polymer swelling and drug release were found to be pH dependent; almost complete release was achieved after 12 h at pH 7.4, after 7 h at pH 2.2 and a very limited release was observed at pH 5.0.

Amphyphilic derivatives of carboxyalkyl chitosan have also been used in the formation of hydrogels for drug delivery. Carboxymethyl-hexanoyl-chitosan (CHC) and carboxymethyl-palmitoyl-chitosan (CPC) were gelled by crosslinking with genipin [48]. These materials were employed in the formulation of antiadhesion implants for release of ibuprofen. The swelling, drug loading and release properties as well as the antiadhesion behavior were affected by the degree of carboxymethylation of the derivatives and more importantly by the degree of modification with the hydrophobic chain. This study demonstrates that by engineering the degree of modification, a specific drug release profile can be obtained for these formulations.

3.3 Ampholytic Chitosan Derivatives for Tissue Engineering

Biodegradable and biocompatible polymers have been attractive candidates for scaffolding materials in tissue engineering because they degrade as the new tissues are formed, without any toxic product. Natural polymers such as collagen, chitosan and *N*-succinyl-chitosan were used as a coating material for PLGA scaffolds for bone-repair with the aim of increasing osteoblast adhesion [85]. Chitosan and collagen improved the hydrophilic properties of the PLGA scaffold surface. The degradation rate was increased in collagen- and NSC-coated scaffolds, whilst it was decreased in chitosan-coated scaffolds. This was attributed to the fact that water molecules play the role of a plasticizer which attack the amorphous regions of PLGA and degrade it into lactic acid and glycolic acid. As a result the pH value of the medium is decreased inducing the degradation process. However, even if the chitosan-treated scaffolds had the highest water absorption, they showed the lowest degradation rate amongst the tested scaffolds, probably due to the capacity of

the amino groups to neutralize the acid molecules produced during the degradation process. Seeded osteoblasts proliferated over 14 days in all constructs in vitro. However, in collagen-coated scaffolds the cells grew faster, this might be explained by the fact that collagen is the main extracellular matrix of the bone promoting cellular proliferation. This study demonstrated that charged chitosan, whether positively or negatively charged, does not favor cell adhesion, nevertheless its ability to stimulate expression of extracellular matrix proteins in human osteoblasts indicate its potential as a microenviroment that can trigger osteoblasts differentiation [45].

NSC was also employed to prepare composite hydrogels together with aldehyde hyaluronic acid; different polymers ratios were used [75]. The composite hydrogels with higher NSC content showed a slower degradation rate than hydrogels with less NSC. The amount of NSC and aldehyde hyaluronic acid used in the hydrogel synthesis significantly affected the swelling properties of the hydrogels resulting in an increase in the crosslinking density and a decrease in the water content and mass weight loss. The biocompatibility of the composite hydrogels was assessed in vitro by encapsulating bovine articular chondrocytes into the hydrogels. SEM images revealed the existence of small "bumps" on the top surface of the hydrogel supporting the encapsulation of the cells (Fig. 12).

Another ampholityc water-soluble chitosan derivative was obtained by sequentially grafting of methacrylic acid and lactic acid on the polymer backbone using carbodiimide [27]. A chemical hydrogel was formed at neutral pH and body temperature upon initiation of a redox reaction by ammonium persulfate (APS)/*N,N,N′,N′*- tetramethylethylenediamine. At a low concentration of the initiator, the gel was degraded rapidly when lysozyme was present in the medium; on the contrary no degradation occurred in PBS during an incubation of 18 days. The hydrogel formed did not degrade in either media when increasing amounts of the initiator were used due to the higher crosslinking degree. Chondrocytes showed

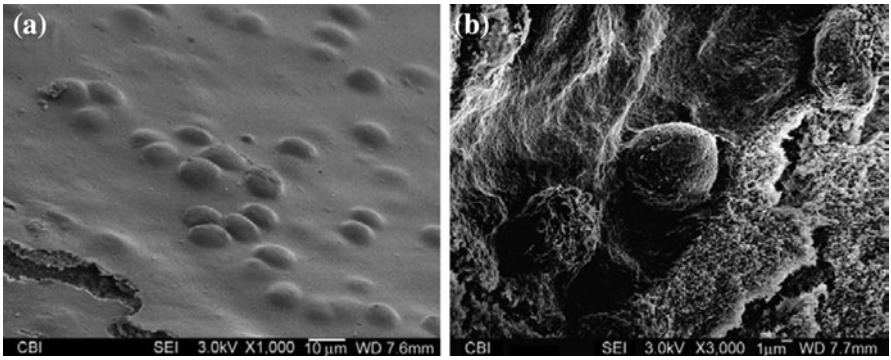

Fig. 12 **a** SEM image depicting surface morphology of the 5/5 ratio composite hydrogel encapsulated with chondrocytes after 24 h culture. **b** SEM image depicting the morphology of encapsulated chondrocytes after 24 h culture. Cell seeding density: 5×10^6/mL [75]

increased viability up to 6 days. The DNA content in the gel, which is proportional to the total cell amount including viable and dead cells, remained unchanged between 3 and 6 days and then decreased. This was attributed to the fast metabolism of the chondrocytes rather than to an increase of the cell population. Electron microscopy studies revealed that elliptical or round shaped chondrocytes were present in the hydrogel possessing normal morphology.

An in situ forming hydrogel was synthesized by mixing oxidized dextran and *N*-carboxyethyl chitosan in PBS at room temperature [81]. The gelation time decreased rapidly with an increase in the theoretical oxidation degree of the oxidized dextran from 5 to 25%, which was attributed to the fact that gelation is correlated to the aldehyde groups content in the mixture. The relative amounts of the oxidized dextran and *N*-carboxyethyl chitosan modulated their swelling behavior and degradation. More specifically, the crosslinking density increased with an increase in the oxidized dextran, leading to a decrease in the swelling ratio. Cell viability studies of mouse dermal fibroblasts in the hydrogels revealed no toxicity. Notably, after 30 days the cells started to proliferate in the same manner comparable to that of the controls, offering further evidence of the non-cytotoxic nature of the hydrogels. Furthermore, the gels were tested for their potential wound healing properties. A mouse full-thickness transcutaneous wound model was used to form hydrogels in situ and the healing patterns were investigated. The biodegradation of the implanted hydrogel was confirmed, as histological studies revealed lack of the initial gel integrity. Application of the hydrogel resulted in 100% re-epithelialization advocating that this formulation might be used as wound dressing for promoting wound healing.

4 Thiolated Chitosans: In Situ Forming Gels

Citosan-cysteine, chitosan-thioglycolic acid, chitosan-4-thiobutylamidine and chitosan-thioethylamidine are examples of derivatives of chitosan bearing a thiol group (Fig. 13) [56]. The first two derivatives are obtained by formation of amide bonds between cysteine [7] or thioglycolic acid [36] and the free amino group of chitosan. Thiol groups are maintained free during the reaction by using an inert atmosphere or by carrying out the reaction at pH lower than 5. Thiolated chitosans possess several properties that make them ideal for the delivery of hydrophilic macromeolcular drugs. They present an enhanced mucoadhesive behavior due to the formation of disulfide bonds between the polymer and cysteine rich subdomains of mucus glycoproteins. Mucoadhesion can be adjusted by changing the degree of modification of the chitosan derivative [65]. Through the enhanced immobilization of the drug delivery system on the mucus layer lining the mucosa, thiolated chitosans are also able to enhance 1.6–3 fold the permeation of macromolecular drugs through the intestinal mucosa, compared to unmodified chitosan [7, 8]. Furthermore, their ability to chelate ions, such as zinc, enables the inhibition of enzymes such as aminopetidases and carboxypeptidases [9]. Thiolated chitosans also show in situ

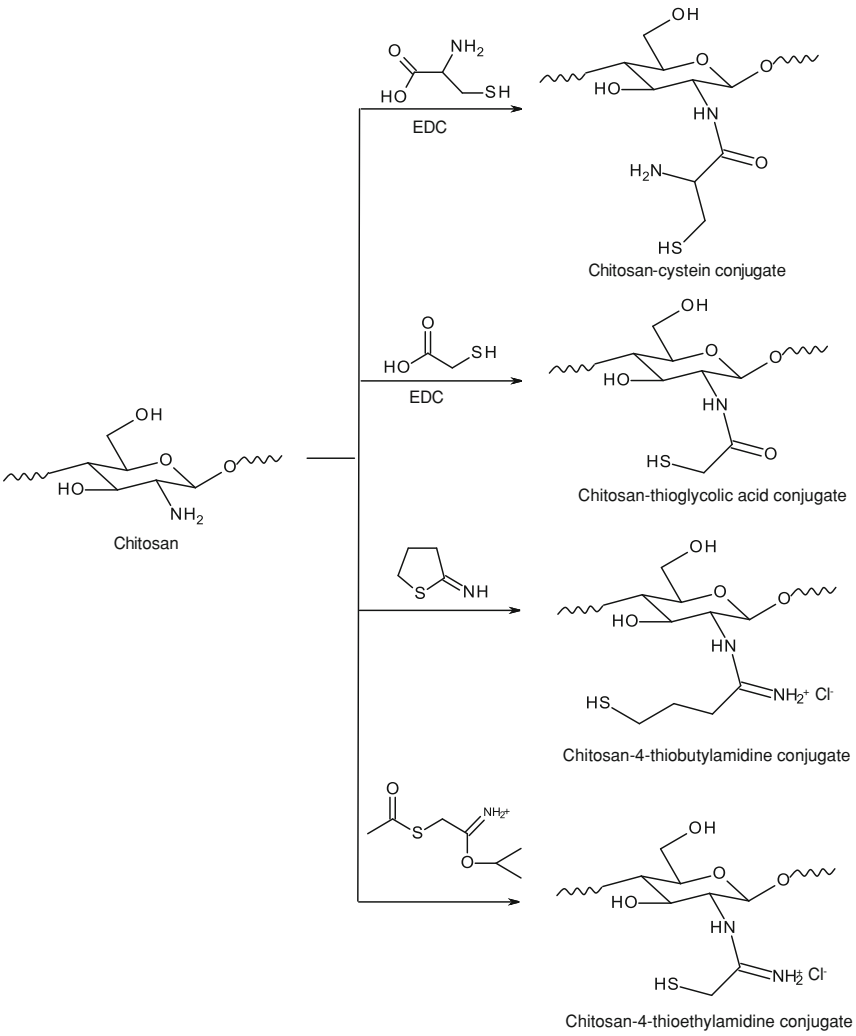

Fig. 13 Synthesis of thiolated chitosans

gelling properties due to the presence of reduced thiol groups able to establish both intra- and inter-molecular crosslinking bonds by oxidation at physiological pH, leading to the formation of polymeric matrices ideal for controlled release of drugs to the vaginal, nasal, buccal and ocular mucosa [2, 82]. The length of the sol–gel transition phase as well as the viscosity of the formed gel depend on the number of thiol groups present on the chitosan molecule, the higher the degree of modification the quicker the transition and the higher the viscosity of the gel.

The number of crosslinks formed consequently affects the degree and rate of biodegradation of the formulation with slower degradation taking place in gels

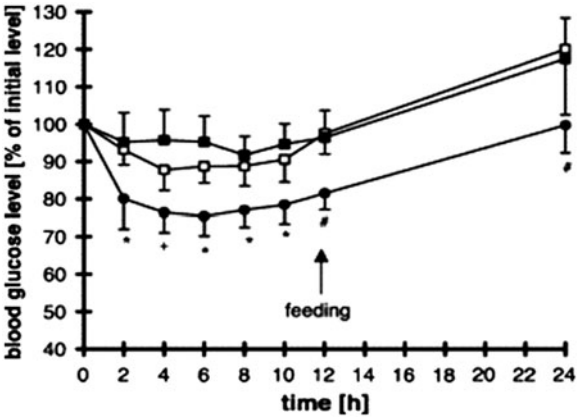

Fig. 14 Decrease of the blood glucose level as a biological response to insulin administration to fasted rats after oral application of chitosan–TBA–insulin tablets (*filled circle*), control tablets (*open square*) and the control solution (insulin in ascorbic acid solution) (*filled square*). Rats were fed after 12 h. Indicated values are the means of 6 rats (chitosan–TBA–insulin tablets) and of 7 rats (control tablets and control solution, respectively) ± S.D.; *differs from control $p < 0.005$; +differs from control $p < 0.01$; #differs from control $p < 0.05$ [43]

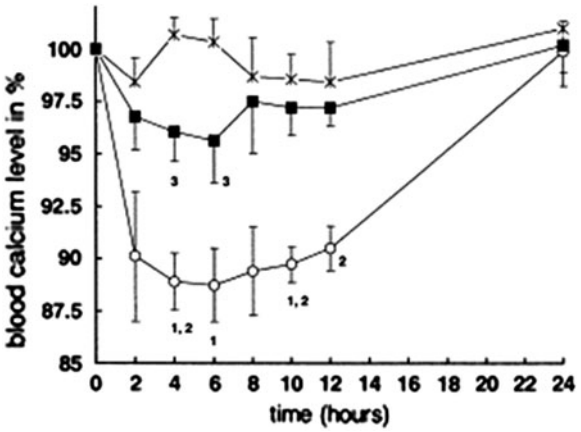

Fig. 15 Decrease in plasma calcium level as a biological response for the salmon calcitonin bioavailability in fasted rats after oral administration of dosage form A (*open circle*), containing thiolated chitosan and an enzyme inhibitor; dosage form B (*filled square*) containing chitosan and an enzyme inhibitor; and dosage form C (*filled star*), containing chitosan only. All formulations contain 50 μg of the peptide drug. Indicated values are the mean results from five rats ± S.D.; *1* different from dosage form C, $p < 2 \times 10^{-6}$; *2* different from dosage form B, $p < 0.0001$; *3* different from dosage form C, $p < 0.005$ [22]

presenting a higher number of crosslinks [67]. All of the properties described above make thiolated chitosan ideal excipients in the formulation of delivery systems for drugs such as proteins and peptides; several studies have demonstrated their potential using insulin (Fig. 14, [43]) and salmon calcitonin (Fig. 15, [22]) as model drugs.

4.1 Thiolated Chitosans for Tissue Engineering

Chitosan-thioglycolic acid conjugates were also evaluated as scaffold material in tissue engineering. The effect of the thiol groups on the viability of L-929 mouse fibroblasts was evaluated showing that this material could induce cell proliferation [37]. Composites of chitosan and hydroxyapatite were used to immobilize laminin peptides on their surface and further assessed as scaffolds for tissue engineering [30]. Laminin-1 is one of the most common cell adhesion molecules [18]. Tendon chitosan tubes were prepared from crab tendons; hydroxyapatite was bound to the chitosan tube surface and finally thiolated. The biocompatibility of CDPGYIGSR (YIGSR) peptide (a recognition sequence for laminin-1 67-kDa receptor) [21], conjugated to thiolated and non-thiolated hydroxyapatite-coated crab tendon chitosan as nerve conduits was further assessed. Bridge grafting into the nerve gap of rats was carried out with the implantation of these tubes. The results showed that transplantation of YIGSR-conjugated tubes gave rise to regenerated nerve tissue attached to thin layers of epineurium-like structure formed on the inner-tube surface.

Another scaffold composed from thiolated chitosan derivatives was proposed to promote nerve regeneration [88]. A methacrylated chitosan derivative was synthesized upon addition of methacrylic anhydride to an acetic solution of chitosan. The thiolated methacrylated chitosan composite was prepared by covalently coupling of thioglycolic acid. Two maleimide-terminated cell adhesive peptides, namely—mi-GDPGYIGSR and mi-GQASSIKVAV—were coupled to the scaffold to promote neural cell adhesion. These cell adhesive peptides, containing the YIGSR and IKVAV peptide sequences derived from laminin, have been shown to promote cell adhesion and neurite outgrowth, respectively [64, 76].The degradation characteristics of the scaffold were studied over a period of 28 days at 37°C using the concentration of lysozyme found in serum. The results showed that increased concentration of the crosslinking agent decreased the biodegradation rate of the scaffold. Cell adhesion studies with SCG ganglia showed that the peptide modified surfaces resulted in higher average neurite length compared to methacrylated chitosan alone. Moreover when the combined GQAASIKVAV/GDPGYIGSR peptide-modified methacrylated chitosan was tested they produced the longest neurites amongst the materials studied. This was attributed to the synergistic effect of the two peptides.

A thiol-modified chitosan crosslinked to form hydrogels was evaluated as a 3-D scaffold for cell proliferation; the release kinetics (in vitro) of model proteins

(insulin and bovine serum albumin) encapsulated in the hydrogels was also assessed. As seen in other studies, the gelation of the formulation was highly depended on the content of thiol groups, the polymer concentration and its molecular weight. Morphological studies revealed a 3-D structure with pores ranging from 5 to 30 μm. Studies of the hydrogels on cultured NIH 3T3 cells were carried out to further assess their toxicity. The results demonstrated that the hydrogels were biocompatible and the cells could migrate into the hydrogels preserving their viability and their morphology [86].

Also thiolated-chitosan/chitosan (TCS/CS) composites of different ratios, prepared via freeze-drying method, were proposed as scaffold material for tissue engineering. Their structural properties were optimized under different temperatures. Their morphology was visualized by scanning electron microscopy (SEM) and their mechanical properties by tensile strength analysis. Scaffolds obtained from the TCS/CS complex (7:3 ratio) and at freezing temperature of −20°C had the maximum tensile strength with a pore distribution ranging from a few to several hundred micrometers (Fig. 16). The preferential growth of fibroblasts on this composite was also demonstrated [46].

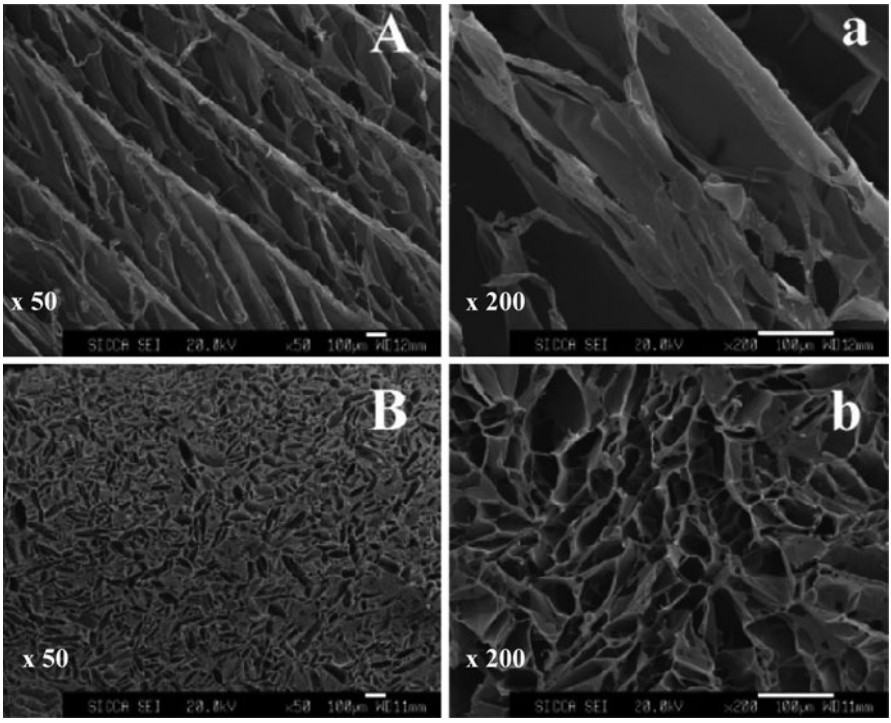

Fig. 16 SEM images of the TCS/CS (7:3 ratio) scaffolds at different freezing temperatures. Scaffolds obtained at a freezing temperatures of −80°C at original magnifications x50 (**A**) and x200 (**a**), and of −196°C at original magnifications x50 (**B**) and x 200 (**b**). *Scale Bars*: 100 μm for all images [46]

5 Glycol Chitosan

Glycol-chitosan (GC) is a chitosan derivative bearing glycol groups in position C6; (Fig. 17) it is characterized by high aqueous solubility at all pH values and good cytocompatibility [4]. Different crosslinking agents have been used to obtain GC physical gels. A polymer–polymer covalent crossliking method was used to crosslink GC with benzaldehyde-capped poly(ethylene glycol)-block-poly(propylene glycol)-block-poly(ethylene glycol) (PEO-PPO-PEO) [17]. Benzaldehyde end groups react with chitosan free amino groups at physiological pH, the bond is reversible if the pH decreases, i.e. in tumor or inflamed tissue, making these hydrogels potential targeted drug delivery systems. The porosity of the gel depends on the crosslinker content, the lower the amount of crosslinker the larger the pores. Drug release occurs partially through the swollen polymer matrix and partially through hydrolysis of the matrix and it can be increased by a decrease in pH or an increase in temperature [17].

The use of GC physical hydrogels as both drug delivery platforms and scaffold material in the regeneration of articular cartilage has been recently proposed [4]. A photopolymerizable prepolymer was obtained by grafting GC with glycidyl methacrylate in aqueous media at pH 9.0. Selective *N*-methacrylation was guaranteed by the pH of the reaction media as the opening of the epoxy ring by hydroxyl groups would occur only at pH 11–12. Furthermore, the degree of *N*-methacrylation could be controlled by changing reaction conditions such as reagents ratios and time; degrees of modification between 1.5 and 25% were obtained. The hydrogels were then prepared by UV induced polymersiation, factors such as light intensity and time of polymerization controlled the degree of crosslinking of the final material. Gels were found to slowly degrade in the presence of lysozyme, with degradation kinetics related to the degree of crosslinking.

GC hydrogels were also produced by transesterification reaction between its hydroxyl groups and the highly reactive vinylester groups of divinyladipate (DVA) [41]. The slow reaction carried out in mild conditions afforded biodegradable gels able to provide pH dependent sustained release.

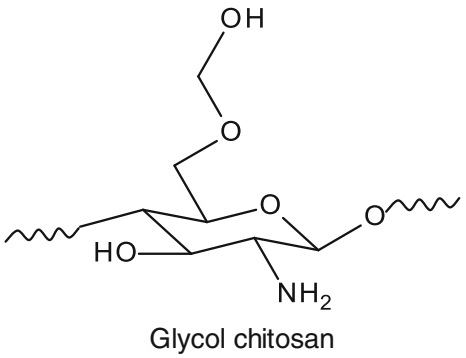

Fig. 17 Structure of glycol chitosan

Superporous GC hydrogels were tested as gastroretentive drug carriers for the eradication of *Helicobacter Pylori* by sustained release of amoxicillin [62]. Chemical grafting of the drug to the polymer allowed for sustained release to be achieved. Gels were obtained by crosslinking with a dialdehyde (glyoxal) and the formation of pores was favored by the addition of $NaHCO_3$ in the gelation mixture.

5.1 Glycol Chitosan for Tissue Engineering

A water soluble chitosan derivative hydrogel for cartilage tissue engineering was developed in two steps by first reacting chitosan with glycolic acid followed by a reaction with phloretic acid [34]. Gelation was achieved within 10 s when the polymer concentration was increased from 1 to 3% w/w in the presence of horseradish peroxidase and H_2O_2. The water uptake of the hydrogel was highly dependent on the initial concentration of the polymer. An increase in the amount of polymer resulted in a decrease to the water uptake indicating that the network formed at higher concentrations had a higher crosslinking density. The enzymatic degradation of the hydrogel was controlled by the amount of the polymer present in the gel; as a result hydrogels prepared at higher polymer concentrations degraded more slowly. The mechanical analysis of the gels showed that higher storage moduli were obtained at higher concentration of the polymer. The biocompatibility of the gel was further assessed by incorporating chondrocytes into the hydrogel, these were cultured in medium without differentiation factors up to 2 weeks. The results showed that viable cells (>90%) were found within the hydrogel, advocating that the formulation exhibits good biocompatibility.

6 Conclusion

There has been growing interest by scientists in understanding and controlling the properties of novel hydrogel-based formulations towards the development of improved scaffolds and drug delivery systems. Chitosan, a natural based-polymer obtained by alkaline deacetylation of chitin, is non-toxic, biocompatible, and biodegradable; however the need for acidic environments to ensure solubility prompted researchers to synthesize chitosan derivatives. Such derivatives are promising platforms as controlled drug delivery systems and biomaterials in tissue engineering. Owing to their properties, such systems can offer prolongation of the contact time between the drug and the absorptive sites in the mucosa and slow and continuous drug release. Moreover, these hydrogles can also absorb large quantities of water, without the dissolution of the polymer, because of their hydrophilic but crosslinked structure, thus giving them physical characteristics similar to soft tissues. Because of their physicochemical properties, they find applications in tissue engineering as scaffolds. There is a body of literature giving evidence that

chitosan and its derivatives can create cell environments suitable for tissue regeneration. These scaffolds can promote both the cell proliferation and differentiation and the controlled release of active compounds. However, there are still questions to be tackled like the degradability of the scaffolds, their mechanical properties and their sterility. The degradability of a scaffold plays a crucial role on the long-term performance of tissue-engineered cell/material construct because it affects cellular processes, including cell growth, tissue regeneration, and host response. Degradability is also closely related with the mechanical properties and the strength of the scaffold which in turn will affect the regeneration process. Therefore, a careful design of these biomaterials is needed to balance these two opposite properties.

References

1. Agnihotri, S.A., Mallikarjuna, N.N., Aminabhavi, T.M.: Recent advances on chitosan-based micro- and nanoparticles in drug delivery. J. Control. Release **100**(1), 5–28 (2004)
2. Alves, N.M., Mano, J.F.: Chitosan derivatives obtained by chemical modifications for biomedical and environmental applications. Int. J. Biol. Macromol. **43**(5), 401–414 (2008)
3. Amidi, M., Mastrobattista, E., Jiskoot, W., Hennink, W.E.: Chitosan-based delivery systems for protein therapeutics and antigens. Adv. Drug Deliv. Rev. **62**(1), 59–82 (2010)
4. Amsden, B.G., Sukarto, A., Knight, D.K., Shapka, S.N.: Methacrylated glycol chitosan as a photopolymerizable biomaterial. Biomacromolecules **8**(12), 3758–3766 (2007)
5. Berger, J., Reist, M., Mayer, J.M., Felt, O., Gurny, R.: Structure and interactions in chitosan hydrogels formed by complexation or aggregation for biomedical applications. Eur. J. Pharm. Biopharm. **57**(1), 35–52 (2004)
6. Berger, J., Reist, M., Mayer, J.M., Felt, O., Peppas, N.A., Gurny, R.: Structure and interactions in covalently and ionically crosslinked chitosan hydrogels for biomedical applications. Eur. J. Pharm. Biopharm. **57**(1), 19–34 (2004)
7. Bernkop-Schnürch, A., Brandt, U.M., Clausen, A.E.: Synthesis and in vitro evaluation of chitosan-cysteine conjugates. Sci. Pharm. **67**, 197–208 (1999)
8. Bernkop-Schnürch, A., Hornof, M., Zoidl, T.: Thiolated polymers–thiomers: synthesis and in vitro evaluation of chitosan-2-iminothiolane conjugates. Int. J. Pharm. **260**(2), 229–237 (2003)
9. Bernkop-Schnürch, A., Kast, C.E.: Chemically modified chitosans as enzyme inhibitors. Adv. Drug Deliv. Rev. **52**(2), 127–137 (2001)
10. Bhattarai, N., Gunn, J., Zhang, M.: Chitosan-based hydrogels for controlled, localized drug delivery. Adv. Drug Deliv. Rev. **62**(1), 83–99 (2010)
11. Chang, Y., Xiao, L., Du, Y.: Preparation and properties of a novel thermosensitive n-trimethyl chitosan hydrogel. Polym. Bull. **63**, 531–545 (2009)
12. Chen, L., Tian, Z., Du, Y.: Synthesis and ph sensitivity of carboxymethyl chitosan-based polyampholyte hydrogels for protein carrier matrices. Biomaterials **25**(17), 3725–3732 (2004)
13. Chen, S.-C., Wu, Y.-C., Mi, F.-L., Lin, Y.-H., Yu, L.-C., Sung, H.-W.: A novel pH-sensitive hydrogel composed of n, o-carboxymethyl chitosan and alginate cross-linked by genipin for protein drug delivery. J. Control. Release **96**(2), 285–300 (2004)
14. Coviello, T., Matricardi, P., Marianecci, C., Alhaique, F.: Polysaccharide hydrogels for modified release formulations. J. Control. Release **119**(1), 5–24 (2007)
15. Dai, Y.N., Li, P., Zhang, J.P., Wang, A.Q., Wei, Q.: A novel pH sensitive N-succinyl chitosan/alginate hydrogel bead for nifedipine delivery. Biopharm. Drug Dispos. **29**, 173–184 (2008)

16. Dev, A., Mohan, J.C., Sreeja, V., Tamura, H., Patzke, G.R., Hussain, F., Weyeneth, S., Nair, S.V., Jayakumar, R.: Novel carboxymethyl chitin nanoparticles for cancer drug delivery applications. Carbohydr. Polym. **79**(4), 1073–1079 (2010)
17. Ding, C., Zhao, L., Liu, F., Cheng, J., Gu, J., Dan, S., Liu, C., Qu, X., Yang, Z.: Dually responsive injectable hydrogel prepared by in situ cross-linking of glycol chitosan and benzaldehyde-capped peo-ppo-peo. Biomacromolecules **11**(4), 1043–1051 (2010)
18. Engel, J.: Laminins and other strange proteins. Biochemistry **31**, 10643–10651 (1992)
19. Fan, J., Chen, J., Yang, L., Lin, H., Cao, F.: Preparation of dual-sensitive graft copolymer hydrogel based on N-maleoyl-chitosan and poly(N-isopropylacrylamide) by electron beam radiation. Bull. Mater. Sci. **32**, 521–526 (2009)
20. Fei Liu, X., Lin Guan, Y., Zhi Yang, D., Li, Z., De Yao, K.: Antibacterial action of chitosan and carboxymethylated chitosan. J. Appl. Polym. Sci. **79**(7), 1324–1335 (2001)
21. Graf, J., Ogle, R.C., Robey, F.A., Sasaki, M., Martin, G.R., Yamada, Y., Kleinman, H.K.: A pentapeptide from the laminin b1 chain mediates cell adhesion and binds to 67000 laminin receptor. Biochemistry **26**(22), 6896–6900 (1987)
22. Guggi, D., Krauland, A.H., Bernkop-Schnürch, A.: Systemic peptide delivery via the stomach: In vivo evaluation of an oral dosage form for salmon calcitonin. J. Control. Release **92**(1–2), 125–135 (2003)
23. Gupta, P., Vermani, K., Garg, S.: Hydrogels: from controlled release to pH-responsive drug delivery. Drug Discov. Today **7**(10), 569–579 (2002)
24. Hennink, W.E., van Nostrum, C.F.: Novel crosslinking methods to design hydrogels. Adv. Drug Deliv. Rev. **54**(1), 13–36 (2002)
25. Hoare, T.R., Kohane, D.S.: Hydrogels in drug delivery: progress and challenges. Polymer **49**(8), 1993–2007 (2008)
26. Hoffman, A.S.: Hydrogels for biomedical applications. Adv. Drug Deliv. Rev. **54**(1), 3–12 (2002)
27. Hong, Y., Song, H., Gong, Y., Mao, Z., Gao, C., Shen, J.: Covalently crosslinked chitosan hydrogel: Properties of in vitro degradation and chondrocyte encapsulation. Acta Biomater. **3**, 23–31 (2007)
28. Hu, H., Yu, L., Tan, S., Tu, K., Wang, L.-Q.: Novel complex hydrogels based on N-carboxyethyl chitosan and quaternized chitosan and their controlled in vitro protein release property. Carbohydr. Res. **345**(4), 462–468 (2010)
29. Hu, R., Chen, Y.-Y., Zhang, L.-M.: Synthesis and characterization of in situ photogelable polysaccharide derivative for drug delivery. Int. J. Pharm. **393**(1–2), 97–104 (2010)
30. Itoh, S., Matsuda, A., Kobayashi, H., Ichinose, S., Shinomiya, K., Tanaka, J.: Effects of a laminin peptide (YIGSR) immobilized on crab-tendon chitosan tubes on nerve regeneration. J. Biomed. Mater. Res. B Appl. Biomater. **73B**(2), 375–382 (2005)
31. Jayakumar, R., Prabaharan, M., Nair, S.V., Tamura, H.: Novel chitin and chitosan nanofibers in biomedical applications. Biotechnol. Adv. **28**(1), 142–150 (2010)
32. Jayakumar, R., Prabaharan, M., Nair, S.V., Tokura, S., Tamura, H., Selvamurugan, N.: Novel carboxymethyl derivatives of chitin and chitosan materials and their biomedical applications. Prog. Mater. Sci. **55**(7), 675–709 (2010)
33. Ji, Q.X., Zhao, Q.S., Deng, J., Lu, R.: A novel injectable chlorhexidine thermosensitive hydrogel for periodontal application: preparation, antibacterial activity and toxicity evaluation. J. Mater. Sci. Mater. Medicine **21**(8), 2435–2442 (2010)
34. Jin, R., Moreira Teixeira, L.S., Dijkstra, P.J., Karperien, M., van Blitterswijk, C.A., Zhong, Z.Y., Feijen, J.: Injectable chitosan-based hydrogels for cartilage tissue engineering. Biomaterials **30**, 2544–2551 (2009)
35. Jintapattanakit, A., Junyaprasert, V.B., Kissel, T.: The role of mucoadhesion of trimethyl chitosan and pegylated trimethyl chitosan nanocomplexes in insulin uptake. J. Pharm. Sci. **98**(12), 4818–4830 (2009). doi:10.1002/jps.21783
36. Kast, C.E., Bernkop-Schnürch, A.: Thiolated polymers–thiomers: development and in vitro evaluation of chitosan-thioglycolic acid conjugates. Biomaterials **22**(17), 2345–2352 (2001)

37. Kast, C.E., Frick, W., Losert, U., Bernkop-Schnürch, A.: Chitosan-thioglycolic acid conjugate: A new scaffold material for tissue engineering? Int. J. Pharm. **256**(1–2), 183–189 (2003)
38. Kato, Y., Onishi, H., Machida, Y.: Evaluation of N-succinyl-chitosan as a systemic long-circulating polymer. Biomaterials **21**, 1579–1585 (2000)
39. Kato, Y., Onishi, H., Machida, Y.: N-succinyl-chitosan as a drug carrier: water-insoluble and water-soluble conjugates. Biomaterials **25**(5), 907–915 (2004)
40. Kean, T., Thanou, M.: Biodegradation, biodistribution and toxicity of chitosan. Adv. Drug Deliv. Rev. **62**(1), 3–11 (2010)
41. Kim, B.S., Yeo, T.Y., Yun, Y.H., Lee, B.K., Cho, Y.W., Han, S.S.: Facile preparation of biodegradable glycol chitosan hydrogels using divinyladipate as a crosslinker. Macromol. Res. **17**, 734–738 (2009)
42. Koutroumanis, K.P., Avgoustakis, K., Bikiaris, D.: Synthesis of cross-linked N-(2-carboxybenzyl)chitosan pH sensitive polyelectrolyte and its use for drug controlled delivery. Carbohydr. Polym. **82**(1), 181–188 (2010)
43. Krauland, A.H., Guggi, D., Bernkop-Schnürch, A.: Oral insulin delivery: the potential of thiolated chitosan-insulin tablets on non-diabetic rats. J. Control. Release **95**(3), 547–555 (2004)
44. Kumar, M.N.V.R., Muzzarelli, R.A.A., Muzzarelli, C., Sashiwa, H., Domb, A.J.: Chitosan chemistry and pharmaceutical perspectives. Chem. Rev. **104**(12), 6017–6084 (2004)
45. Lahiji, A., Sohrabi, A., Hungerford, D.S., Frondoza, C.G.: Chitosan supports the expression of extracellular matrix proteins in human osteoblasts and chondrocytes. J. Biomed. Mater. Res. A **51**, 586–595 (2000)
46. Li, Z., Cen, L., Zhao, L., Cui, L., Liu, W., Cao, Y.: Preparation and evaluation of thiolated chitosan scaffolds for tissue engineering. J. Biomed. Mater. Res. A **92A**(3), 973–978 (2010)
47. Lin, Y., Chen, Q., Luo, H.: Preparation and characterization of N-(2-carboxybenzyl)chitosan as a potential pH-sensitive hydrogel for drug delivery. Carbohydr. Res. **342**(1), 87–95 (2007)
48. Liu, T.-Y., Lin, Y.-L.: Novel pH-sensitive chitosan-based hydrogel for encapsulating poorly water-soluble drugs. Acta Biomater. **6**(4), 1423–1429 (2010)
49. Liu, Z., Jiao, Y., Zhang, Z.: Calcium-carboxymethyl chitosan hydrogel beads for protein drug delivery system. J. Appl. Polym. Sci. **103**(5), 3164–3168 (2007)
50. Lü, S., Liu, M., Ni, B.: An injectable oxidized carboxymethylcellulose/N-succinyl-chitosan hydrogel system for protein delivery. Chem. Eng. J. **160**(2), 779–787 (2010)
51. Luppi, B., Bigucci, F., Cerchiara, T., Zecchi, V.: Chitosan-based hydrogels for nasal drug delivery: Fron inserts to nanoparticles. Expert Opin. Drug Deliv. **7**(7), 811–828 (2010)
52. Mao, S., Bakowsky, U., Jintapattanakit, A., Kissel, T.: Self-assembled polyelectrolyte nanocomplexes between chitosan derivatives and insulin. J. Pharm. Sci. **95**(5), 1035–1048 (2006)
53. Mao, S., Sun, W., Kissel, T.: Chitosan-based formulations for delivery of DNA and siRNA. Adv. Drug Deliv. Rev. **62**(1), 12–27 (2010)
54. Mao, Z., Shi, H., Guo, R., Ma, L., Gao, C., Han, C., Shen, J.: Enhanced angiogenesis of porous collagen scaffolds by incorporation of TMC/DNA complexes encoding vascular endothelial growth factor. Acta Biomater. **5**(8), 2983–2994 (2009)
55. Mi, F.-L., Wu, Y.-Y., Lin, Y.-H., Sonaje, K., Ho, Y.-C., Chen, C.-T., Juang, J.-H., Sung, H.-W.: Oral delivery of peptide drugs using nanoparticles self-assembled by poly(γ-glutamic acid) and a chitosan derivative functionalized by trimethylation. Bioconj. Chem. **19**(6), 1248–1255 (2008)
56. Mourya, V.K., Inamdar, N.N.: Chitosan-modifications and applications: opportunities galore. React. Funct. Polym. **68**(6), 1013–1051 (2008)
57. Muzzarelli, R., Muzzarelli, C.: Chitosan chemistry: relevance to the biomedical sciences. In: Heinze, T. (ed.) Polysaccharides I, vol. 186. Advances in Polymer Sciencepp, pp. 151–209. Springer, Berlin, Heidelberg (2005)
58. Muzzarelli, R.A.A.: Genipin-crosslinked chitosan hydrogels as biomedical and pharmaceutical aids. Carbohydr. Polym. **77**(1), 1–9 (2009)

59. Muzzarelli, R.A.A., Tanfani, F., Emanuelli, M., Mariotti, S.: N-(carboxymethylidene)chitosans and N-(carboxymethyl)chitosans: novel chelating polyampholytes obtained from chitosan glyoxylate. Carbohydr. Res. **107**(2), 199–214 (1982)
60. Nazar, H., Fatouros, D., van der Merwe, S., Roldo, M.: Thermosensitive hydrogel formulations containing N-trimethylchitosan chloride (tmc) for nasal drug delivery. In: 36th Annual Meeting and Exposition of the Controlled Release Society, Copenhagen, Denmark (2009)
61. Nazar, H., Fatouros, D.G., van der Merwe, S.M., Bouropoulos, N., Avgouropoulos, G., Tsibouklis, J., Roldo, M. Thermosensitive hydrogels for nasal drug delivery: The formulation and characterisation of systems based on N-trimethyl chitosan chloride, Euro J Pharma Biopharma, doi:10.1016/j.ejpb.2010.11.022.
62. Park, J., Kim, D.: Release behavior of amoxicillin from glycol chitosan superporous hydrogels. J. Biomater. Sci. **20**, 853–862 (2009)
63. Park, J.H., Saravanakumar, G., Kim, K., Kwon, I.C.: Targeted delivery of low molecular drugs using chitosan and its derivatives. Adv. Drug Deliv. Rev. **62**(1), 28–41 (2010)
64. Pierschbacher, M.D., Ruoslahti, E.: Cell attachment activity of fibronectin can be duplicated by small synthetic fragments of the molecule. Nature **309**, 30–33 (1984)
65. Roldo, M., Hornof, M., Caliceti, P., Bernkop-Schnurch, A.: Mucoadhesive thiolated chitosans as platforms for oral controlled drug delivery: synthesis and in vitro evaluation. Eur. J. Pharm. Biopharm. **57**(1), 115–121 (2004)
66. Sajomsang, W.: Synthetic methods and applications of chitosan containing pyridylmethyl moiety and its quaternized derivatives: a review. Carbohydr. Polym. **80**(3), 631–647 (2010)
67. Sakloetsakun, D., Hombach, J.M.R., Bernkop-Schnürch, A.: In situ gelling properties of chitosan-thioglycolic acid conjugate in the presence of oxidizing agents. Biomaterials **30**(31), 6151–6157 (2009)
68. Schwall, C.T., Banerjee, I.A.: Micro- and nanoscale hydrogel systems for drug delivery and tissue engineering. Materials **2**(2), 577–612 (2009)
69. Sieval, A.B., Thanou, M., Kotze, A.F., Verhoef, J.E., Brussee, J., Junginger, H.E.: Preparation and nmr characterization of highly substituted n-trimethyl chitosan chloride. Carbohydr. Polym. **36**, 157–165 (1998)
70. Sinha, V.R., Singla, A.K., Wadhawan, S., Kaushik, R., Kumria, R., Bansal, K., Dhawan, S.: Chitosan microspheres as a potential carrier for drugs. Int. J. Pharm. **274**(1–2), 1–33 (2004)
71. Song, Y., Onishi, H., Machida, Y., Nagai, T.: Drug release and antitumor characteristics of n-succynil-chitosan-mitomycin c as an implant. J. Control Release **42**, 93–100 (1996)
72. Song, Y., Onishi, H., Nagai, T.: Synthesis and drug-release characteristics of the conjugates of mitomycin c with N-succinyl-chitosan and carboxymethyl-chitin. Chem. Pharm. Bull. **40**(10), 2822–2825 (1992)
73. Sun, W., Mao, S., Mei, D., Kissel, T.: Self-assembled polyelectrolyte nanocomplexes between chitosan derivatives and enoxaparin. Eur. J. Pharm. Biopharm. **69**(2), 417–425 (2008)
74. Sun, W., Mao, S., Wang, Y., Junyaprasert, V.B., Zhang, T., Na, L., Wang, J.: Bioadhesion and oral absorption of enoxaparin nanocomplexes. Int. J. Pharm. **386**(1–2), 275–281 (2010)
75. Tan, H., Chu, C.R., Payne, K.A., Marra, K.G.: Injectable in situ forming biodegradable chitosan-hyaluronic acid based hydrogels for cartilage tissue engineering. Biomaterials **30**(13), 2499–2506 (2009)
76. Tashiro, K., Sephel, G.C., Weeks, B., Sasaki, M., Martin, G.R., Kleinman, H.K., Yamada, Y.A.: A synthetic peptide containing the ikvav sequence from the a chain of laminin mediates cell attachment, migration, and neurite outgrowth. J. Biol. Chem. **264**(27), 16174–16182 (1989)
77. Thanou, M., Kotze, A.F., Scharringhausen, T., Luessen, H.L., de Boer, A.G., Verhoef, J.C., Junginger, H.E.: Effect of degree of quaternization of N-trimethyl chitosan chloride for enhanced transport of hydrophilic compounds across intestinal caco-2 cell monolayers. J. Control. Release **64**, 15–25 (2000)

78. Thanou, M., Verhoef, J.C., Junginger, H.E.: Chitosan and its derivatives as intestinal absorption enhancers. Adv. Drug Deliv. Rev. **50**(Supplement 1), S91–S101 (2001)
79. Thanou, M., Verhoef, J.C., Junginger, H.E.: Oral drug absorption enhancement by chitosan and its derivatives. Adv. Drug Deliv. Rev. **52**(2), 117–126 (2001)
80. Wang, W., Li, B., Li, Y., Jiang, Y., Ouyang, H., Gao, C.: In vivo restoration of full-thickness cartilage defects by poly(lactide-co-glycolide) sponges filled with fibrin gel, bone marrow mesenchymal stem cells and DNA complexes. Biomaterials **31**(23), 5953–5965 (2010)
81. Weng, L., Romanov, A., Rooney, J,C.C.: Non-cytotoxic, in situ gelable hydrogels composed of n-carboxyethyl chitosan and oxidized dextran. Biomaterials **29**, 3905–3913 (2008)
82. Werle, M., Bernkop-Schnürch, A.: Thiolated chitosans: useful excipients for oral drug delivery. J. Pharm. Pharmacol. **60**(3), 273–281 (2008)
83. Wu, J., Su, Z.G., Ma, G.H.: A thermo- and pH-sensitive hydrogel composed of quaternized chitosan/glycerophosphate. Int. J. Pharm. **315**, 1–11 (2006)
84. Wu, J., Wei, W., Wang, L.-Y., Su, Z.-G., Ma, G.-H.: A thermosensitive hydrogel based on quaternized chitosan and poly(ethylene glycol) for nasal drug delivery system. Biomaterials **28**(13), 2220–2232 (2007)
85. Wu, Y.-C., Shaw, S.-Y., Lin, H.-R., Lee, T.-M., Yang, C.-Y.: Bone tissue engineering evaluation based on rat calvaria stromal cells cultured on modified plga scaffolds. Biomaterials **27**(6), 896–904 (2006)
86. Wu, Z.M., Zhang, X.G., Zheng, C., Li, C.X., Zhang, S.M., Dong, R.N., Yu, D.M.: Disulfide-crosslinked chitosan hydrogel for cell viability and controlled protein release. Eur. J. Pharm. Sci. **37**(3–4), 198–206 (2009)
87. Yan, C., Chen, D., Gu, J., Hu, H., Zhao, X., Qiao, M.: Preparation of N-succinyl chitosan and their physical-chemical propoerties as novel excipient. J. Pharm. Soc. Jpn. **126**(9), 789–793 (2006)
88. Yu, L.M., Kazazian, K., Shoichet, M.S.: Peptide surface modification of methacrylamide chitosan for neural tissue engineering applications. J. Biomed. Mater. Res. A **82**(1), 243–255 (2007)
89. Zambito, Y., Uccello-Barretta, G., Zaino, C., Balzano, F., Di Colo, G.: Novel transmucosal absorption enhancers obtained by aminoalkylation of chitosan. Eur. J. Pharm. Sci. **29**(5), 460–469 (2006)
90. Zambito, Y., Zaino, C., Uccello-Barretta, G., Balzano, F., Di Colo, G.: Improved synthesis of quaternary ammonium-chitosan conjugates (N+ -Ch) for enhanced intestinal drug permeation. Eur. J. Pharm. Sci. **33**(4–5), 343–350 (2008)

Fucoidan: A Versatile Biopolymer for Biomedical Applications

Ali Demir Sezer and Erdal Cevher

Abstract Fucoidan is a natural, anionic sulfated polysaccharide extracted from brown marine algae with a wide variety of pharmacological features like anti-inflammatory, anti-oxidative, anticoagulant and antithrombotic effects. Fucoidan has been extensively studied for last decade due to its numerous interesting biological activities. In recent years, the research on drug and gene delivery systems, diagnostic microparticles and wound and burn healing formulations of fucoidan has been increasing in course of time. This review gives an overview about the research of concerning structural characterization and biological activity of fucoidan; application of fucoidan-based systems in pharmaceutical field for drug and DNA delivery and in biomedical area for wound and burn treatment.

1 Structure and Extraction of Fucoidan

Fucoidan, which was first isolated and termed by Kylin [57, 86], is also referred to as fucoidin in the literature. Fucoidan is abundant in intracellular sections and in the mucilaginous matrix of brown algae. Studies after the 1950s revealed that the algae such as *Laminaria digitata*, *Ascophyllum nodosum* and *Macrocystis pyrifera* contained fucoidan in addition to alginic acid and it was reported that the amount

A. D. Sezer (✉)
Department of Pharmaceutical Biotechnology, Faculty of Pharmacy, Marmara University, 34668 Haydarpaşa, Istanbul, Turkey
e-mail: adsezer@marmara.edu.tr

E. Cevher
Department of Pharmaceutical Technology, Faculty of Pharmacy, Istanbul University, 34116 Universite, Istanbul, Turkey

Stud Mechanobiol Tissue Eng Biomater (2011) 8: 377–406
DOI: 10.1007/8415_2011_67

Published Online: 11 March 2011

of fucoidan varied according to algae species [57, 86]. Fucoidan is a hygroscopic polysaccharide that is found in the form of a viscous solution in algae and prevents dehydration of the algae. Figure 1 shows the chemical structure of fucoidan.

Fucose was separated by hydrolyzing of fucoidan isolated from algae such as *L. digitata*, *Fucus vesiculosus* and *A. nodosum* and the presence of pentoses in fucoidan structure was proved [86]. Further studies reported that fucoidan was comprised of L-fucose nucleus bonded with 1,4-*O*-bridges and sulfate groups. In addition to L-fucose, the fucan nucleus contains galactose, xylose or uronic acid, depending on the algae species [55, 57, 83, 93].

Fucoidan is isolated from crude polysaccharide obtained from algae by extracting with water or dilute acids using following methods.

1.1 Purification in the form of Lead Hydroxide Complex

The algae are extracted with hot water. The extract is treated with lead acetate and barium hydroxide to obtain the fucoidan-lead hydroxide complex. After decomposing the complex with sulfuric acid, the obtained crude fucoidan is purified using a dialysis method [57, 86].

1.2 Purification Using Formaldehyde and Alcohol

The algae are extracted with dilute acid. The neutralized extract, is precipitated by treating with ethanol. The residue is treated with formaldehyde and is then evaporated.

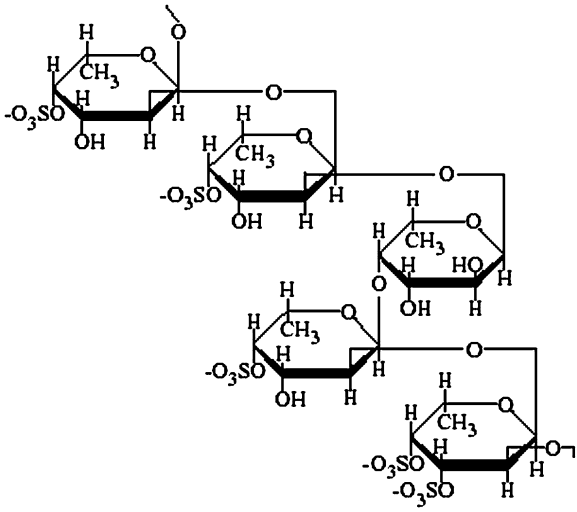

Fig. 1 Chemical structure of fucoidan [98]

When this residue is extracted with water again, the impurities remain in the sediment, while fucoidan passes to the solution. Pure fucoidan is isolated by adding ethanol to the solution [85, 86].

1.3 Purification Using Cetylpyridinium Chloride

The aqueous extract of algae is dialyzed against water and treated with calcium chloride to precipitate the alginic acid. Supernatant is separated and precipitated with cetylpyridinium chloride. The sediment is dissolved with calcium chloride and is re-precipitated using ethanol. The sediment is dissolved in water and dialyzed to obtain the pure fucoidan in soluble form [23].

2 Physicochemical Properties of Fucoidan

Fucoidan which is a yellow-brown colored powder, dissolves easily in water, but does not in organic solvents [8, 13, 83, 93]. Depending on the molecular weight of fucoidan, the viscosity of the aqueous solution varies significantly [57, 83, 86, 93]. It was reported that low concentration fucoidan solution exhibited the dilatant flow characteristics [86]. Strong acids and alkalines degrade fucoidan [57, 83, 93]. High-concentration calcium, potassium or aluminum salts of fucoidan obtained via acid extraction from algae do not dissolve in water [57, 86].

The structure and physicochemical properties of fucoidan vary according to the algae species. It was reported that even polysaccharides isolated from the same species showed variations [57, 86, 93]. Molecular weights of fucoidan fractions obtained from various algae species vary between 10 and 788 kDa; even the same algae contains fucoidan fractions with different molecular weight [24, 61, 76, 83, 93]. O'Neill [83] reported that identification of polysaccharide obtained from algae using osmometric methods showed that the molecular weight of fucoidan was 133 ± 20 kDa. Different fucoidan fractions obtained from *F. vesiculosus* were identified using gel permeation chromatography and it was found that the algae contained fucoidans with three different molecular weights (50, 100 and 150 kDa). Furthermore, it was reported that the sulfate content in fucoidan fractions varied between 7.6 and 10.8% [24]. Nardella et al. [76] identified the molecular weight of fucoidan fractions, which they isolated from *A. nodosum,* using high performance steric exclusion chromatography and found that the algae contains many fucoidan fractions with high and low molecular weights. It was reported that the fractions with high molecular weight varied between 156 and 600 kDa, while those fractions with low molecular weight varied between 11 and 40 kDa.

3 Biological Properties of Fucoidan

Fucoidan is the source of L-fucose, which is a pentose important for the metabolism of organisms, and which can rarely be synthesized in nature. Fucoidan is one of the few substances that is used to obtain this sugar [12, 57, 86]. On the studies that were carried out on different algae species, many fucoidan fractions with anticoagulant activity were obtained [12, 53, 65, 68, 79, 80, 116]. Soeda et al. [116] showed that fucoidan and its sulfated derivatives which were obtained from *Fucus vesiculosus* stimulated t-PA-catalyzed Glu- or Lys-plasminogen activation according to the degree of sulfation. When calculated on a molar basis, the abilities of native and highly sulfated fucoidans were found to be 9.4 and 20.8 times higher than that of heparin, respectively.

Nishino et al. [81] reported that fucoidan with 19 kDa molecular weight isolated from *Eclonia kurome* increased the plasminogen activity of high-molecular-weight urokinase-type plasminogen activator and tissue-type plasminogen activator and had fibrinolytic activity. Analyses of the anticoagulant effects of the fucoidans isolated from three species (*E. kurome*, *A. nodosum* and *F. vesiculosus*) showed similar results [45, 78, 131]. Similarly, studies analyzing the anticoagulant effect on the fucoidans obtained from various algae species indicated that anticoagulant effect showed variations due to the structural difference of polysaccharides and sulfate content [15, 16, 18, 65, 67, 70, 87, 114, 131]. Mauray et al. [66] showed that fucoidan catalyses thrombin inhibition by antithrombin and by heparin cofactor II, with a preferential effect on the latter and the anticoagulant activity depends on the molecular weight and the chemical composition of fucoidan, particularly the fucose and sulfate contents.

The effect of fucoidan on leukocyte increase was analyzed in experimentally induced pneumococcal meningitis in rats; 3 mg/kg dose of fucoidan solution was injected intracisternally at 0, 2 and 4 h. Treatment with fucoidan increased the number of leukocytes by approximately 50%, resulting in significantly reduced inflammation [3].

Another pharmacological property of fucoidan is its affinity to various growth hormones and leukocytes. Various researchers investigated the bonding properties of sulfated glucan and glycolipids, including fucoidan, to different growth hormones [4, 47, 59, 111, 115, 126]. Aria et al. [4] investigated the effects of heparin, highly sulfated heparin, dermatan sulfate and fucoidan on insulin-like growth factor (IGF) and found that *O*-bonded sulfate group amount of polysaccharides was the most important factor in bonding to IGF. The study reported that highly sulfated heparin, dermatan sulfate and fucoidan had an inhibitory effect on IGF, which emerged from *O*-sulfate groups in two or three positions of the polysaccharides. It was also reported that no inhibitory effect was found in heparin, which might have stemmed from the absence of the sulfate group.

The literature contains studies on the interaction of fucoidan with interleukins (ILs) [71, 73, 92]. Ramsden and Rider [92] investigated the bonding properties of heparin, chondroitin sulfate, hyaluronic acid and fucoidan on ^{125}I labeled

recombinant IL-1α, IL-1β, IL-2 and IL-6, using affinity chromatography. It was reported that heparin was sensitive to four ILs and that it quickly bonded; the bonding time of chondroitin sulfate was longer; hyalunoric acid showed affinity only to IL-1α, IL-1β; and fucoidan only bonded to IL-2 much more strongly than other polysaccharides, and that it significantly increased the activity of IL-2. As reported in the literature, these differences might be caused by the bonding of the polysaccharides to different receptors Ramsden and Rider [92]. The bonding properties of fucoidan to surface antigens and thus the elimination of pathogenic viruses were also investigated. Furthermore, the literature contains information suggesting that fucoidan inhibits the activity of the virus, such as Hepatitis B and HIV, by bonding to different epitope regions of the viruses [95, 122].

The literature contains only a limited number of in vivo studies on the effect of fucoidan in wound treatment and most of the studies were generally carried out using cell culture models [17, 20, 27, 29, 56, 124]. Therefore, comprehensive studies should be conducted on this subject. Fujimura et al. [27] used a fibroblast-collagen cell culture model to investigate the effect of fucoidan on wound-healing process in dermal injuries. They obtained 12 fucoidan fractions with different molecular weights by extracting from *F. vesiculosus*. The effectiveness of the fractions with molecular weights above 10 kDa was determined in a fibroblast cell culture. The results indicated that the fractions with molecular weight of 30 kDa or higher accelerated collagen gel construction; significantly increased fibroblast migration; and accelerated the expression of integrin $\alpha 2\beta 1$, which is crucial for wound healing. It was also reported that the fucose that constitutes the nucleus of fucoidan and the sulfate groups had a role in this effect.

In dermal fibroblast cell culture, the effect of fucoidan and transforming growth factor β_1 (TGF-β_1) combinations on fibroblast proliferation was investigated. It was reported that when used at doses of 1 mg/ml and higher, fucoidan modulated the anti-proliferative effect of TGF-β_1 on dermal fibroblasts and caused a rapid growth in fibroblast population [56].

In a study that investigated the effect of fucoidan on corneal cell proliferation of rabbits with experimentally induced eye-burns, the presence of fucoidan prevented leukocyte infiltration of the limbus and cornea after the formation of the burn [29].

The effect of fucoidan on tissue injury in rats was investigated in an epigastric wound model that was formed after arterial ischemic reperfusion. The rats were treated with 10 and 25 mg/kg doses of fucoidan with perfusion and the results were evaluated by considering tissue neutrophil count, tissue malondialdehyde content and tissue myeloperoxidase activity. In rats that were treated with 25 mg/kg dose of fucoidan, neutrophil amount and myeloperoxidase activity significantly decreased; however, fucoidan had no effect on tissue malondialdehyde content [17].

In a study on the proliferative effects of fucoidan and heparin on arterial soft muscle cells (ASMC), fucoidan or heparin solutions with concentrations between 80 and 100 μg/ml were added to ASMC cell culture and it was observed that heparin had a lower inhibitory effect on proliferation than fucoidan. This inhibitory effect of fucoidan varied according to time and that it produced the strongest effect in the first 6 h. Polysaccharide had no effect on cell proteins and glycoconjugates;

however, it indirectly increased fibronectin and thrombospondin synthesis and secretion [124].

4 Toxicity of Fucoidan

Ning et al. [77] investigated acute and sub-chronic toxicity of the purified fucoidan isolated from *Laminaria japonica.* In acute toxicity studies, 10 male and 10 female Wistar rats were treated with 4000 mg/kg/day dose of fucoidan with oral gavage for 7 days. No toxicity symptoms or behavioral changes were observed in the animals within 7 days. In sub-chronic toxicity tests, a total of 120 Wistar rats were given 300, 900 and 2500 mg/kg/day dose of fucoidan solution with oral gavage 6 days a week for 6 months. At the end of each month, some subjects were killed and their blood and organs were analyzed toxicologically. In terms of hematology, fucoidan treatment at all doses extended the clotting time. A decrease on aspartate aminotransferase amount was observed in female rats that were treated with fucoidan. Serum glucose amount significantly decreased in rats that were treated with 2500 mg/kg/day dose. Macroscopic observations conducted on the organs of the animals for 6 months indicated that gross necropsy and pathological examination of treated rats did not reveal any abnormality in morphology of brain, thymus, lungs, heart, spleen, liver, adrenals, kidneys, thyroids, testes, prostate gland, uterus or ovaries. The study showed that when fucoidan from *L. japonica* was administered to rats at a dose of 300 mg/kg/day, no significant toxicological changes were observed. However, when the dose was increased to 900 and 2500 mg/kg/day, it was thought the anticoagulant effect of fucoidan might be a problem.

The genotoxicity of fucoidan isolated from *Undaria pinnatifida* was examined using a test battery of three different methods [50]. In a reverse mutation assay using four *Salmonella typhimurium* strains and *Escherichia coli*, fucoidan did not increase the number of revertant colonies in any tester strain, regardless of metabolic activation by S9 mix, and did not cause chromosomal aberration in short tests with S9 mix or in the continuous test. A bone marrow micronucleus test in ICR mice dosed by oral gavage at doses up to 2000 mg/kg/day showed no significant or dose-dependent increases in the frequency of micronucleated polychromatic erythrocytes, and the high dose suppressed the ratio of polychromatic erythrocytes to total erythrocytes (Table 1). The authors concluded that fucoidan presented no significant genotoxic risk under the anticipated conditions of use.

5 Applications of Fucoidan in Biomedicine

5.1 Pharmaceutical Usage

In pharmaceutical and biomedical applications, it is important to use non-toxic and biocompatible materials with tissue [62, 120]. Many polymers and biopolymers

Table 1 Bone marrow micronucleus test, clinical sign and mortality in male ICR mice ($n = 5$) with fucoidan from sporophyll of *Undaria pinnatifida* [50]

Treatment	Dose (mg/kg w/day)	Body weights (Mean ± SD g)		MNPCE/2000PCF.'s (mean ± SD, %)	PEC/(PCE + NCE) (mean ± SD, %)	Clinical signs	Mortality (dead/total)
		Administration	Kill				
Vehicle (corn oil)	0	31.08 ± 1.48	31.31 ± 0.66	0.09 ± 0.04	51.87 ± 1.78	N	0% (0/5)[a]
Fucoidan	500	31.77 ± 1.10	31.69 ± 0.69	0.14 ± 0.04	50.69 ± 0.97	N	0% (0/5)
Fucoidan	1,000	31.51 ± 1.57	31.51 ± 1.22	0.12 ± 0.03	50.53 ± 0.46	N	0% (0/5)
Fucoidan	2,000	31.32 ± 1.06	31.13 ± 0.91	0.09 ± 0.04	51.38 ± 0.55	N	0% (0/5)
CPA	70	31.46 ± 1.06	30.87 ± 1.44	6.31 ± 0.83	48.47 ± 0.95	N	0% (0/5)

MNPC PCE with one or more micronucleus, *PCE* polychromatic erythrocyte, *NCE* normochromatic erythrocyte, *CPA* cyclophosphamide (positive control), *N* normal

* $P < 0.01$

[a] Number of dead animals/no. of tested animals

with these properties are also used in the drug industry. Many institutes continue to conduct research on the development of new polymers [2, 11, 28, 30, 98, 105]. Since biopolymers are generally natural, biodegradable and their degradation products are non-toxic, they are among the commonly used polymers in biomedicine [82]. For example, alginic acid, which is an anionic polymer, is used in tissue engineering and new generation multiparticulate drug and gene delivery systems [19, 64]. Similarly, chitosan which is a polycationic biopolymer is commonly used for preparation of nano- and micro-drug delivery systems, artificial tissue production in bioengineering, developing gene and vaccine delivery systems, and wound and burn treatment in pharmaceutical and biomedical area [51, 84, 99, 107, 123]. Curdlan and xanthan gums, which are microbial polysaccharides, are among the biopolymers used in drug industry in recent years [113].

Fucoidan is a negatively charged biopolymer that contains a sulfate group in its structure. It has been a source of interest for many researchers in recent years due to its pharmacological activity and non-toxicity [35, 52, 58, 88]. Although the number of biomedical studies on fucoidan increases in course of time, there is only a limited literature on developing fucoidan-based drug delivery systems. The first study on this subject was carried out by Sezer and Akbuğa [98]. The researchers prepared negatively charged fucoidan and positively charged chitosan microparticles, based on the principle of forming polyion complex in optimum conditions and termed the resulting particle structure a "fucosphere". Figure 2 shows scanning electron microscopy image of fucospheres.

It was reported that fucospheres loaded with bovine serum albumin (BSA) had a particle size range between 0.61 and 1.28 μm. Among the fucospheres which had an encapsulation activity of approximately 90%, BSA release lasted for 60–90 days, depending on the polyanion/polycation ratio. Table 2 presents the findings on in vitro characterization of the content of fucospheres.

In another study, fucosphere formulations were prepared containing granulocyte–macrophage colony-stimulating factor (GM-CSF), which is a cytokine,

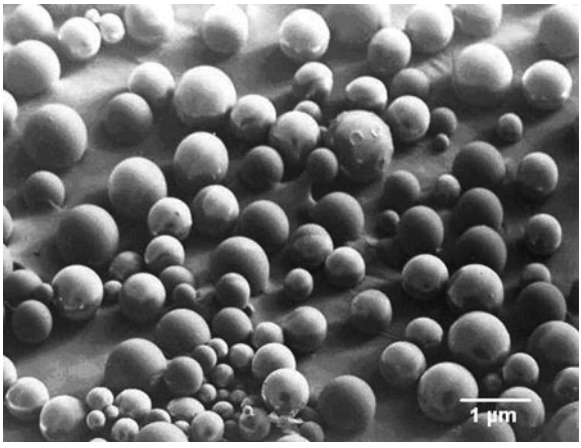

Fig. 2 Scanning electron micrograph showing of BSA-encapsulated fucospheres composed of 1.5% fucoidan and 0.5% chitosan [98]

Table 2 Codes, size, drug encapsulation capacity and zeta potential values of fucospheres [98]

Codes	Preparation method	Fucoidan conc. (%)	Chitosan conc. (%)	BSA conc. (%)	Chitosan origin	Mean particle size (μm ± SD)	Encapsulation capacity (% ± SD)	Zeta values (mV ± SD)
A1	Microencapsulation	1.50	0.50	0.25	Fluka	0.87 ± 0.03	68.8 ± 2.5	22.7 ± 0.4
A2	Microencapsulation	1.75	0.50	0.25	Fluka	0.96 ± 0.02	75.7 ± 0.4	14.3 ± 0.2
A3	Microencapsulation	2.00	0.50	0.25	Fluka	1.07 ± 0.11	82.0 ± 1.4	12.4 ± 0.2
A4	Microencapsulation	2.50	0.50	0.25	Fluka	1.23 ± 0.05	89.5 ± 1.4	6.9 ± 0.1
B1	Microencapsulation	1.50	0.25	0.25	Fluka	0.61 ± 0.02	51.8 ± 2.5	I6.3 ± 0.3
B2	Microencapsulation	1.50	0.75	0.25	Fluka	1.16 ± 0.10	82.2 ± 2.3	26.1 ± 0.3
C1	Microencapsulation	1.50	0.50	0.50	Fluka	1.02 ± 0.09	75.9 ± 1.1	25.2 ± 0.3
C2	Microencapsulation	1.50	0.50	0.75	Fluka	1.13 ± 0.11	82.9 ± 1.9	28.9 ± 0.4
D1	Microencapsulation	1.50	0.50	0.25	Sigma	0.89 ± 0.04	59.1 ± 1.9	17.6 ± 0.2
D2	Microencapsulation	1.50	0.50	0.25	Pronova 243	1.11 ± 0.02	53.1 ± 1.4	8.7 ± 0.1
E	Adsorption	1.50	0.50	0.25	Fluka	1.28 ± 0.26	50.3 ± 4.3	32.3 ± 0.5

within its glycoprotein structure [97]. GM-CSF regulates the viability, proliferation, differentiation and function of hematopoietic progenitor cells while increasing the viability, function of dendritic cells, the differentiation and growth of dermal Langerhans cells and the ability of antigen-presenting cells to capture foreign antigens [33]. It is used in the treatment of serious conditions resulting from chemotherapy and bone marrow transplantation, such as neutropenia and aplastic anemia [36]. Despite these pharmacological properties, GM-CSF has a very short biological half-life in physiological conditions, due to its short-term serum stability causing destruction and inactivation of protein; it, therefore, requires frequent injection throughout the treatment [22, 54]. In recent years studies have investigated the efficacy of systems providing long duration of action in treatment with plasmid DNA coding GM-CSF [9, 40, 41, 44, 96]. The authors have encapsulated GM-CSF in fucospheres and evaluated their characteristics, such as influence of formulation parameters, on the physiochemical properties, encapsulation capacity, plasmid release and stability studies. Plasmid DNA was successfully encapsulated into fucospheres with high encapsulation efficiency. DNA release from fucospheres continued for 80–140 days and no burst effect was observed during the release studies (Fig. 3).

Agarose gel electrophoresis method indicated that GM-CSF that was encapsulated within fucospheres remained stable for 140 days in a PBS (pH 7.4) buffer in which release studies were carry on [97].

In recent years, many techniques were developed for the preparation of silver nanoparticles, which are used in biomedicine and targeted drug delivery systems. However, the use of agents that are toxic for human health and the environment, such as sodium borohydride and dimethylformamide, which accelerate the reactions in intermediate phases of the preparation, is a serious disadvantage. Yiu Leung et al. [129] prepared silver nanoparticles using carboxymethylated-curdlan and fucoidan. The nanoparticle fabrication method is based on adding silver nitrate to aqueous solution of carboxymethylated-curdlan and fucoidan at 100°C. Using this relatively simple method, non-toxic nanoparticles with a particle size of 40–80 nm were obtained. Authors reported that these nanoparticles could be used in pharmaceutical and biomedical applications and are suitable for industrial production due to the easy preparation method.

5.2 Application in Wound Healing

Fucoidan has potential for use in wound and burn treatment; it has heparin-like activity triggers transforming growth factor (TGF-β_1) while providing fibroblast migration and activation in damaged tissue [17, 27, 56]. Second-degree dermal burns are one of the most common pathologic conditions. These kinds of burns involve the loss of deep dermis; healing starts at damaged dermal areas, beginning with significant scar formation (epidermal thickening) and functional losses and generally show aesthetic deterioration and pigmentation changes by the end of

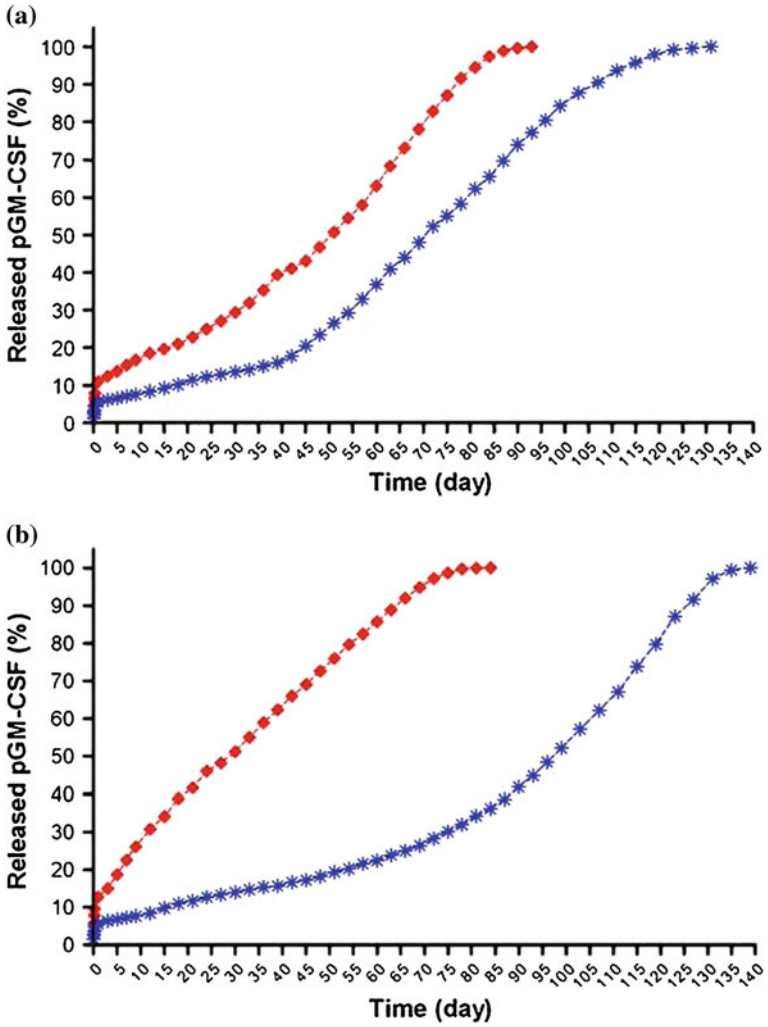

Fig. 3 Effect of **a** initial plasmid amount, **b** chitosan molecular weight on release behavior of plasmid pGM-CSF encapsulated fucospheres. Formulation compositions: **a** (*open square*) 336 μg pDNA + 0.25% chitosan + 0.5% fucoidan + 400 kDa chitosan molecular weight + 20,000 rpm stirring rate; **a** (*asterisk*) 673 μg pDNA + 0.25% chitosan + 0.5% fucoidan + 400 kDa chitosan molecular weight + 20,000 rpm stirring rate; **b** (*open square*) 336 μg pDNA + 0.25% chitosan + 0.5% fucoidan + 150 kDa chitosan molecular weight + 20,000 rpm stirring rate; **b** (*asterisk*) 336 μg pDNA + 0.25% chitosan + 0.5% fucoidan + 600 kDa chitosan molecular weight + 20,000 rpm stirring rate [97]

treatment. For this reason, if accurate diagnosis is made and there is no donor problem, considering the size of the burn at an early stage, these kinds of wounds generally require surgical intervention [130].

There is ongoing research into alternative materials and methods that might provide alternatives to surgical intervention in the treatment of second-degree dermal burns. The literature suggests that many of the existing treatment methods are not successful in deep dermal wound and burn treatment [90, 91]. In clinical applications, gauze bandage and composites are among the most widely used materials [117]. Gauze bandage and composites, which have a high absorption capability, are economical and can be sterilized easily. The most serious complications associated with gauze bandage and composites include trauma caused by the removal of the bandage from the wound surface, infection and irritation caused by foreign bodies. Although autografts give positive results and are the most widely used materials in large wounds and burns, the most important drawback of this technique is insufficient donor area [1].

These limitations of conventional and biological dressing materials led researchers to investigate the development of artificial ones with different properties and structures for use in the treatment of wounds and burns [42, 117]. Artificial dressing materials are available in the form of film, gel, spray, foam, micro-/nanoparticles, microsponges, etc. and are prepared using different polymers [1, 42, 94]. However, none of the existing technological products and artificially-prepared dressings has the properties of an ideal wound and burn dressing material. Therefore, clinical use of these materials, which are undergoing testing, is also limited [106].

Almost all of the factors that adversely affect wound and burn healing are caused by the loss of skin integrity. Wound and burn healing would be much faster using a dressing material that can replace the skin [63, 75]. Therefore, the use of biomaterials as dressing materials began to be given priority in tissue engineering and biotechnology, due to their treatment-accelerating effect [5, 42, 118]. Natural polymers like fibrin, fibrinogen, collagen, hyaluronic acid, alginate derivatives, chitin and chitosan are important biopolymers. These natural dressing materials have many advantages over other topically-applied systems in wound and burn treatment, including their biological adaptation, minimal toxicity and immunogenicity and co-applicability with different active agents [38, 106].

In addition to biopolymers, skin and similar dressing materials or semi-synthetic polymers have been considered for use in covering burn and open wound surfaces on the skin. However, due to problems such as biological adaptation, immune response and histoincompatibility, the use of these kinds of skin-like materials or polymers was limited [110, 125]. It was reported that systems which have a design that does not fully prevent contact of the surface with air and water provides better and faster healing, and that the micropore structure of the biomaterials used is important in burn and wound treatment [5, 118].

In addition, an ideal wound material should also have some important properties such as stability, non-antigenicity, flexibility prevention of water loss and bacterial transmission and ease of use. Chitosan performed well in these criteria and positive results were obtained with these polymers [37, 108, 121]. Burn dressings prepared with chitosan and alginate derivatives are available as commercial product. While the tissue-repair and re-epithelialization increasing effects of glycosaminoglycans (GAG) gained importance in wound treatment, the literature also contained

information on positive results obtained from heparin. It is known that chitosan–heparin complexes provide epithelialization and improve healing. In some studies on wound and burn treatment, fucoidan, which has GAG structure and heparinic activity, was used for this purpose [31]. It is also known that fucoidan accelerates fibroblast migration and provides re-epithelialization in wound treatment [17, 27].

In different studies, film [102], hydrogel [100] and microparticle [101] formulations were prepared using fucoidan and chitosan which are two biopolymers. The treatment efficacy of the formulations was investigated in experimentally induced second-degree dermal burns on rabbits.

As shown in Fig. 4, fucoidan–chitosan films prepared by the solvent casting method for use in burn treatment have a microporous structure and a thickness of 29.7–269.0 μm (Table 3).

Depending on the increase of film thickness, water vapor permeability decreased from 16.6/0.1 to 3.3/0.1 g film. Furthermore, the drying technique affected water vapor permeability of the films. Although the films that were dried using lyophilization method had a more porous structure than those dried in an incubator, due to their greater thickness, their water vapor permeability was found to be lower. It was reported that these findings were similar to those of previous studies [43, 60, 109, 127]. In addition to air and vapor permeability, sufficient absorption by the membrane of the exudate which forms on the wound is also important in wound/burn dressing materials. The liquid absorption capacities of the films prepared using different proportions of fucoidan and chitosan were found to be quite high (0.67–1.77 g water/g film). The films prepared using lyophilization absorbed a higher proportion of water due to their high porosity.

Films for use in wound/burn treatment should remain on the inflammation area for a long time and protect the area from external factors. Therefore, such films should have sufficient mechanical strength and elasticity, and high bioadhesion to the application site. Mechanical strength and elasticity values of the prepared films were found to be 7.1–45.8 N and 5.5–49.8%, respectively. While the mechanical strength of the films increased in line with chitosan concentration, increasing of

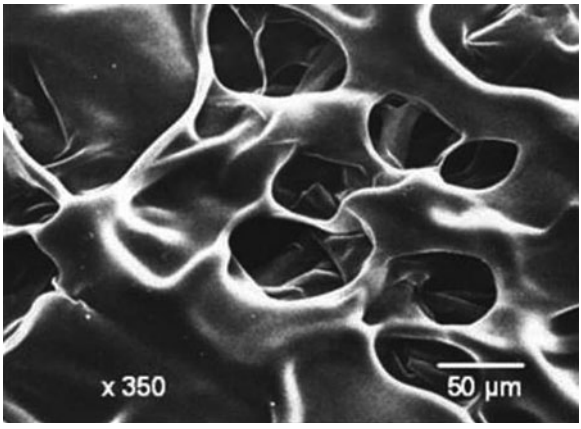

Fig. 4 Scanning electron micrographs of fucoidan–chitosan film composed of 0.5% fucoidan and 2% chitosan [102]

Table 3 Physical, mechanical and bioadhesive properties of fucoidan–chitosan films [102]

Codes	Film thickness (μm ± SD)	Water vapor permeability[a] (g ± SD)	Water absorption capacity[b] (g ± SD)	Tensile strength (N ± SD)	Film elongation (% ± SD)	Work of bioadhesion (mJ/cm^2 ± SD)	Peak detachment force (mN/cm^2)
A1	29.7 ± 0.6	16.6 ± 0.8	0.67 ± 0.02	7.1 ± 0.7	36.3 ± 0.7	0.076 ± 0.006	405.0 ± 13.2
A2	41.3 ± 0.6	10.6 ± 0.5	0.83 ± 0.06	21.6 ± 0.3	6.7 ± 0.2	0.120 ± 0.007	605.0 ± 10.7
A3	51.7 ± 0.6	6.2 ± 0.2	1.03 ± 0.02	36.5 ± 1.9	8.0 ± 0.2	0.731 ± 0.010	2968.0 ± 17.3
A4	50.3 ± 0.2	6.3 ± 0.1	1.03 ± 0.02	20.7 ± 1.3	5.6 ± 0.1	0.722 ± 0.010	722.0 ± 20.1
Bl	44.0 ± 0.1	5.7 ± 0.2	0.98 ± 0.01	45.8 ± 4.0	7.4 ± 0.3	0.181 ± 0.009	2521.0 ± 22.5
B2	58.3 ± 1.1	6.2 ± 0.1	1.09 ± 0.02	30.9 ± 1.0	9.5 ± 0.3	1.771 ± 0.030	5350.0 ± 17.3
CI	61.5 ± 0.8	6.3 ± 0.3	1.04 ± 0.04	14.6 ± 2.8	49.8 ± 2.1	1.158 ± 0.013	7162.0 ± 28.7
Dl	64.0 ± 1.0	5.6 ± 0.2	0.96 ± 0.02	35.6 ± 0.6	5.5 ± 0.2	0.587 ± 0.012	5525.0 ± 16.5
D2	269.0 ± 3.0	3.3 ± 0.1	1.77 ± 0.04	12.2 ± 1.7	9.8 ± 0.1	1.136 ± 0.013	2647.0 ± 19.3

Formulation compositions *A1* 1% chitosan + 0.5% fucoidan + 1% lactic acid, *A2* 1.5% chitosan + 0.5% fucoidan + 1% lactic acid, *A3*, *D1* and *D2* 2% chitosan + 0.5% fucoidan + 1% lactic acid, *A4* 2% chitosan + 1% lactic acid, *B1* 2% Sigma chitosan + 0.25% fucoidan + 1% lactic acid, *B2* 2% Sigma chitosan + 0.75% fucoidan + 1% lactic acid, *C1* 2% Fluka chitosan + 0.5% fucoidan + 2% lactic acid. Drying conditions *A*, *B*, *C* in oven at 40°C, *D1* at room temperature, *D2* by lyophilization

[a] Water vapour permeability values of 0.1 g of the films

[b] Water absorption capacity values of 1.0 g of the films

fucoidan and lactic acid concentrations led to reduced mechanical strength. The mechanical strength of the membranes was generally inversely proportional to their elasticity. Bangyekan et al. [6], Khan et al. [43], and Wong et al. [128] reported that, depending on the increase of chitosan concentrations in the film formulations, mechanical strength increased, which decreased the elasticity of the films. The solvent used in the preparation of fucoidan–chitosan films also affected mechanical properties. When lactic acid was used, the elasticity of the films increased and mechanical strength decreased compared with films prepared using other acids [102].

Bioadhesion values of fucoidan–chitosan films were found to be between 0.076 and 1.771 mJ/cm^2, and the highest bioadhesion was observed in films which had the highest fucoidan content. With the increase of polymer concentration, free ionic groups (amine and sulfate) in the formulation also increased. This enhanced the bioadhesion of the films in the inflammation area due to their ionic interactions with the negatively charged wound tissue proteins [39, 112].

Treatment effectiveness of fucoidan–chitosan films with optimum properties was investigated in rabbits with experimentally induced superficial burns with partial thickness. At the end of day 7, no edema was observed on the burns that were treated with film (Fig. 5). Polymorphonuclear leukocytes, which indicate edema and inflammation occurrence, increased only in the control group by day 14. At the end of day 14 and day 21, it was found that wound contraction areas of the groups treated with fucoidan–chitosan films were higher than those that were treated with fucoidan solution and chitosan films. Evaluation of all macroscopic findings revealed that the healing levels of the wounds were as follows: fucoidan films > chitosan films > fucoidan solution. Histopathological analysis at the end of day 14 and day 21 indicated that the length of the new epithelia in the samples which were treated with fucoidan–chitosan films increased when compared to those which were treated with chitosan film.

In treatment groups, epithelium thickness increased slightly between day 7 and day 21, depending on fibroblast and collagen increase in the wound area. On day 21, epithelial thickness of the wounds that were treated with fucoidan–chitosan film decreased and healing ratio was found to be higher than those of other groups. The healing phase of partial thickness superficial dermal burns was accelerated between day 7 and day 14 and, after 7 days, fibroblast migration to the wound area increased and thus collagen amount increased between days 7 and 14. These results are consistent with the re-epithelialization findings in similar studies [25, 89]. As indicated in Fig. 5, while healing continued in groups treated with fucoidan solution and chitosan film; a large area of the scar in the group of fucoidan–chitosan film was replaced by epithelia and all of the wounds treated with fucoidan–chitosan film was completely healed at day 21.

In addition to damaged epidermis, papillary nicks connecting epidermis to dermis are also damaged in wounds and burns. Therefore, one of the proofs of the healing of the wounded area is the re-formation of papillary projections. In the group that was treated with fucoidan–chitosan film, the papillary nicks in the wound area increased by approximately 2.5 times and reached the highest level

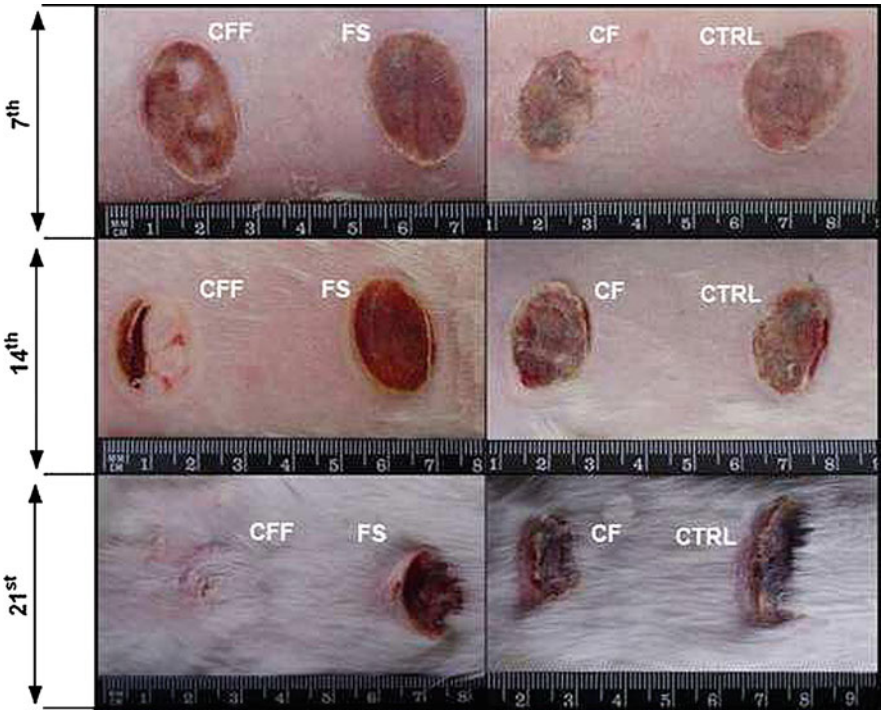

Fig. 5 The photographs of the wounds area treated with fucoidan solution (*FS*), chitosan film (*CF*), chitosan film containing fucoidan (*CFF*), and control group (*CTRL*) at *7th*, *14*th, and *21st* days [102]

after day 14 when compared to the group treated with chitosan film. Similar findings were reported by Erdağ and Sheridan [26].

When the wounds were compared in terms of nucleolar organizing region (NOR) values, which are an indication of cell division activity [21, 119], it was observed that NOR values increased in line with the healing process in fucoidan solution and chitosan film treated groups; among the experimental groups, NOR values reached the highest level within the fucoidan–chitosan film treated groups on day 14 of the treatment process and then declined. It was suggested that this change resulted from the excessive propagation of epithelial cells during the treatment process between days 7 and 14 in fucoidan–chitosan film treated group.

In another study, chitosan-based hydrogels containing fucoidan were prepared and the effect of polymer concentration on water absorption capacity, textural properties and ex vivo bioadhesion of the gels were investigated [100]. Increase in molecular weight and concentration of chitosan enhanced the water absorption capacity of fucoidan–chitosan gels; however, fucoidan concentration did not significantly increase the water absorption capacity of the gels. Knapczyk [46] obtained similar results in a study that used chitosan gels.

The textural properties of hydrogels used in wound healing are important criteria that affect treatment efficacy. Gels that are applied to the wound should have suitable hardness value for properly spreading on the wound; they should have suitable adhesion to remain on the wound for a long time and should have suitable cohesion to hold the gel together on the application site. Figure 6 shows findings on the mechanical properties of fucoidan–chitosan gels.

Chitosan and fucoidan concentration changed the textural properties of hydrogels. The highest adhesion value was obtained from gels prepared with fucoidan and chitosan at highest concentration.

The adhesion of chitosan with high molecular weight and high deacetylation degree (MW: 750, deacetylation degree: ≥85, Sigma) was approximately 7–14 times higher than that of the formulations prepared with medium molecular weight chitosan (MW: 400, deacetylation degree: ≥75, Fluka) and low molecular weight

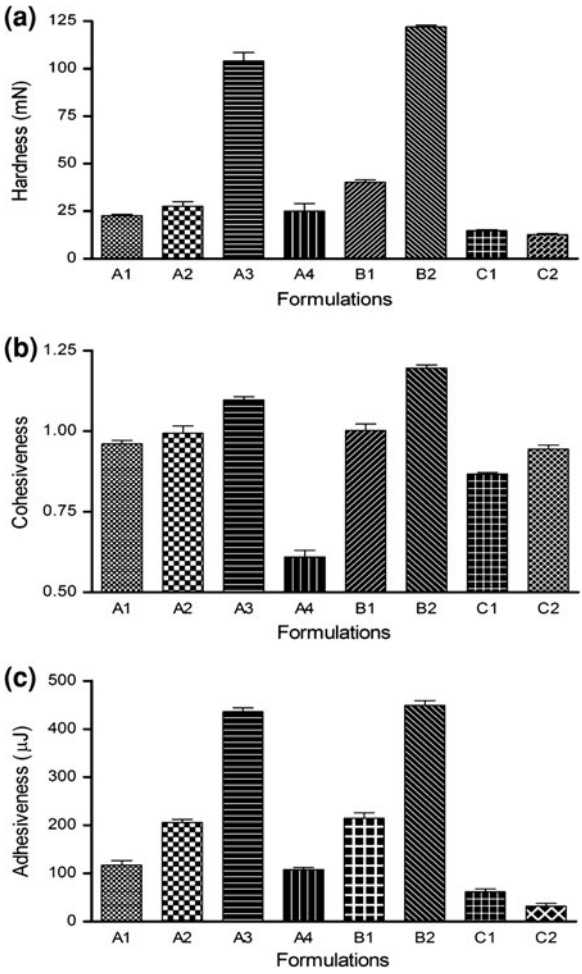

Fig. 6 The mechanical properties of hydrogel formulations. **a** hardness, **b** cohesiveness and **c** adhesiveness ($n = 6$). Formulation compositions: *A1* 1.5% Sigma chitosan + 0.5% fucoidan, *A2* 1.75% Sigma chitosan + 0.5% fucoidan, *A3* 2% Sigma chitosan + 0.5% fucoidan, *A4* 2% Sigma chitosan, *B1* 2% Sigma chitosan + 0.25% fucoidan, *B2* 2% Sigma chitosan + 0.75% fucoidan, *C1* 2% Fluka chitosan + 0.5% fucoidan, and *C2* 2% Protan 243 chitosan + 0.5% fucoidan [100]

chitosan (MW: 250, deacetylation degree: ≥60, Protan 243). The presence of fucoidan increased the adhesion of the hydrogels and optimal textural properties were achieved.

Gels prepared with high molecular weight chitosan had much greater bioadhesion than those prepared using chitosan with medium and low molecular weight. One of the reasons for this was that high molecular weight chitosan with long chain attracts more exudates in the wound area and forms a more stable gel film [34, 69]; the second reason is that the structure of the same chitosan with high deacetylation degree contains more free amine groups than other chitosans and thus it has greater interaction with the negatively charged proteins in the wound area [7, 112].

The treatment effectiveness of fucoidan–chitosan hydrogels was investigated in comparison with chitosan gel and fucoidan solution in an experimental burn model using optimized hydrogel formulation [100]. Macroscopic analyses in the first 7 days showed that edema was observed only in control groups, while no similar contraction was observed in the groups which were treated with fucoidan solution, chitosan gel and fucoidan–chitosan gel. On day 14, the highest contraction was observed in the subjects that were treated with fucoidan–chitosan gel, followed by chitosan gel and fucoidan solution treated groups. In addition to contraction, hairing was observed to increase in the wound areas that were treated with fucoidan–chitosan gel and chitosan gel. On day 21, fucoidan gel treated groups were completely healed and hairing reached to maximum levels. During the healing stage, the epithelial length of a wound generally increases. Epithelial cells and collagen migration significantly increase, particularly during the healing phase of second-degree burns. When wound epithelium lengths of the groups that were treated with fucoidan solution, chitosan gel and fucoidan–chitosan gel were compared on day 7, no significant difference was found. On days 14 and 21, epithelial length in the fucoidan–chitosan gel treated group was significantly more increased then those of other treatment groups. On the other hand, epithelial thickness and scarring decreased in the same group between days 14 and 21 (Fig. 7). In parallel to the increase in epithelial length, papillary nicks, which promote the integration of the newly formed epithelial tissue, showed a greater increase in the fucoidan–chitosan gel treated group between days 14 and 21.

Histopathological analyses revealed that fucoidan–chitosan gels were more effective in burn treatment when compared to other treatment groups. On day 14, NOR values in fucoidan–chitosan gel treated wounds increased significantly; however, the rate of increase slowed down between days 14 and 21. NOR values of fucoidan solution and chitosan gel treatment groups were lower than those treated with fucoidan–chitosan gel. This increase in fucoidan–chitosan gel treated group was related to the epithelial cell propagation in the wound area between days 7 and 14 and increased the thickness of the epithelial layer.

Microparticles were prepared through the formation of polyion complex between the amine groups of chitosan (cationic) and carboxyl groups of fucoidan (anionic) and their effectiveness in wound and burn treatment were investigated in vivo [101]. The size of the particles varied between 367 and 1017 nm depending

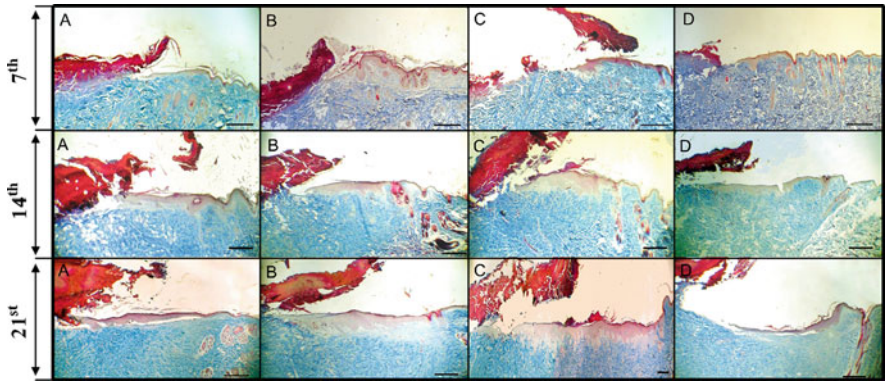

Fig. 7 The histopathological photographs of the burn epithelial tissues stained with haematoxylin and eosin on days 7, 14, and 21 (**A** control wounds, **B** treated with chitosan hydrogel, **C** treated with fucoidan–chitosan hydrogel, and **D** treated with fucoidan solution, the bars are 500 μm) [100]

on formulation parameters. Fucoidan and chitosan concentrations, the source, molecular weight and deacetylation degree of chitosan significantly affected the particle size. A decrease in fucoidan concentration in the formulation caused a decrease in particle size. Zeta potentials of the microparticles increased directly proportionally with the increase in chitosan/fucoidan ratio. With the increase of electronegative fucoidan amount, free sulfate groups also increased in the formulation and zeta potential of microparticles decreased. On the contrary, increasing amounts of electropositive chitosan which contains free amine groups caused an increase in zeta potential of microparticles. Similar findings were obtained in multiparticulate systems fabricated with different negatively charged polymers and chitosan [32, 49].

Bioadhesion values which were varied between 81 and 191 $\mu J/cm^2$, enhanced with increased concentrations of both chitosan and fucoidan used in preparation of fucospheres. For example, when chitosan concentration was increased from 0.25 to 0.75%, bioadhesion values increased by approximately 2.5 times. Kockisch et al. [48] and Chowdary and Rao [14] indicated that, due to free amine groups in the structure of chitosan, the microparticles possess bioadhesive properties. With the increase of fucoidan, bioadhesion of the microparticles also increased. The reason for this increase was that negatively charged sulfate groups in the structure of fucoidan had an ionic interaction with the proteins in the wound area [86, 103, 104].

The treatment effectiveness of fucosphere formulation was investigated on superficial burns. It was found that at the end of days 14 and 21, the fucosphere treated group had the highest contraction area and thus the highest healing level, and that treatment effectiveness of fucospheres was higher than those of chitosan microparticles and fucoidan solution.

In groups that were treated with fucospheres, chitosan microparticles and fucoidan solution, wound epithelial length increased with time. However, between days 7 and 14, the epithelial length in the fucosphere treated group was found to be much higher than those in other groups (Table 4).

Similarly, epithelial thickness in the fucosphere treated group was found to be higher than the values for groups that were treated with fucoidan solution and chitosan microparticles (Table 5).

These differences in epithelial length and thickness are thought to vary according to the increase in fibroblast, collagen and epithelial cells between days 7 and 14 (Table 4). Fibroblast and collagen amounts in fucosphere treated group were higher on day 14 compared to day 7; however, they decreased on day 21. The number of papillary nicks in the fucosphere treated group was higher than in the groups treated with other formulations. The number of papillary nicks was highest on day 14 (Table 5). Similarly, the highest NOR value was observed in the fucosphere treated group on day 14. The increase in number of papillary nicks and NOR value is evidence of accelerated re-epithelialization between days 7 and 14.

These results indicated that fucoidan–chitosan formulations improved burn healing. Today, chitosan and alginate films are commercially available in the form of wound and burn dressing materials. However, recent studies indicated that the treatment effectiveness of combined fucoidan–chitosan formulations (microsphere, hydrogel and film) was higher than those of formulations containing only chitosan.

Murakami et al. [72] prepared composite hydrogel sheets containing 60:20:2.4 (w/w) sodium alginate, chitin/chitosan and fucoidan with a method given in Fig. 8 and applied the formulations prepared to experimentally induced wounds in rats.

It was found that the composite protected the wound area, possessed optimal adhesion and accelerated healing by providing a good moist healing environment with exudates. Histological examination on day 7 demonstrated significantly advanced granulation tissue and capillary formation in the healing-impaired wounds treated with composites, compared to those treated with commercially-available calcium alginate fiber (Kaltostat; Convatec Ltd., Tokyo, Japan) and those left untreated (Fig. 9).

These findings indicated that the composites containing fucoidan provided more effective treatment than the commercial preparations available on the market.

In a study that analyzed potential toxicological properties of fucoidan films used in surgical operations, a cecal-sidewall model of surgical adhesions were formed in male Sprague–Dawley rats and the treatment effectiveness of surgically-placed fucoidan films on this area was investigated [10]. In vivo studies revealed that fucoidan loaded films reduced adhesion scores by approximately 90% compared with control films.

A total of 50–100% of animals were adhesion-free at fucoidan film loadings of 0.33–33% compared with the adhesions observed in animals treated with control film. No adverse effects were observed from 33% fucoidan films, which were equivalent to approximately 30 mg fucoidan/kg body weight. Local administration of fucoidan film during rat cecal-sidewall surgery safely reduced

Table 4 Wound epithelial elongation and thickness values at days 7, 14 and 21 after treatment with fucospheres [101]

Days	Wound epithelial elongation values (μm ± SE)				Wound epithelial thickness values (μm ± SE)			
	Fucosphere group	Fucoidan solution group	Chitosan microsphere group	Control group	Fucosphere group	Fucoidan solution group	Chitosan microsphere group	Control group
7	1366 ± 44	1455 ± 64	1358 ± 57	1302 ± 90	193 ± I5	121 ± 8	118 ± 6	111 ± 10
14	2733 ± 213	2086 ± 134	2316 ± 244	1950 ± 82	220 ± 27	187 ± 9	119 ± 14	154 ± 5
21	3275 ± 730	3586 ± 149	3250 ± 319	3533 ± 196	157 ± 13	146 ± 10	123 ± 15	134 ± 8

Table 5 The number of rete pegs and NORs at days 7, 14 and 21 after treatment with fucospheres [101]

Days	Number of rete pegs ± SE				Number of NORs ± SE			
	Fucosphere group	Fucoidan solution group	Chitosan microsphere group	Control group	Fucosphere group	Fucoidan solution group	Chitosan microsphere group	Control group
7	4.8 ± 0.4	3.1 ± 0.4	3.0 ± 0.3	3.4 ± 0.5	3.3 ± 0.1	2.9 ± 0.2	2.9 ± 0.1	2.7 ± 0.2
14	6.8 ± 0.5	6.1 ± 0.2	5.0 ± 0.5	3.9 ± 0.2	5.5 ± 0.1	3.6 ± 0.5	4.2 ± 0.1	2.6 ± 0.2
21	5.3 ± 1.0	4.6 ± 0.7	2.3 ± 0.3	3.8 ± 0.4	2.6 ± 0.1	3.5 ± 0.8	4.3 ± 0.1	2.6 ± 0.3

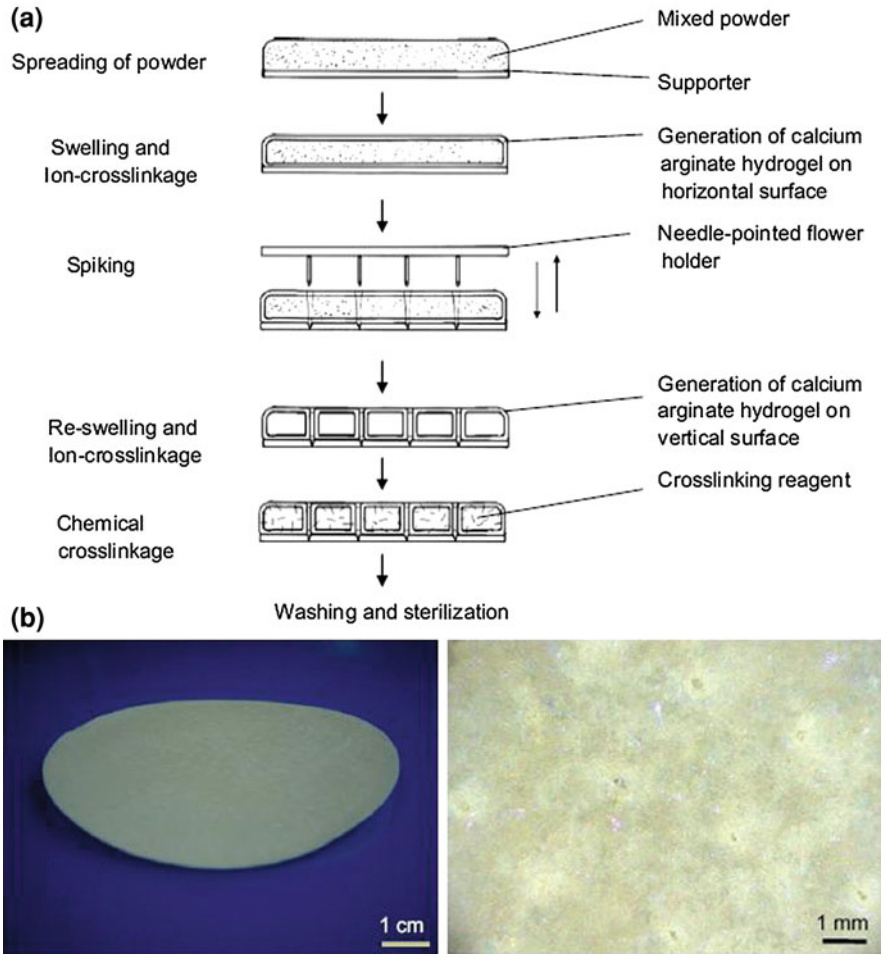

Fig. 8 **a** Preparative procedures for ACF-HS, **b** Photographic appearance of ACF-HS [72]

adhesion scores by approximately 90% and resulted in 50–100% of animals being adhesion-free [10].

Chitosan/fucoidan micro complex-hydrogel as a carrier for controlled release of heparin binding growth factors was fabricated and evaluated the ability of chitosan/fucoidan micro complex-hydrogel to immobilize fibroblast growth factor (FGF-2) and protect its activity [74]. The chitosan/fucoidan complex-hydrogel had high affinity for FGF-2. The interaction of FGF-2 with chitosan/fucoidan complex-hydrogel substantially prolonged the biological half-life of FGF-2. One week after FGF-2 containing complex-hydrogel was subcutaneously injected to mice, neovascularization and fibrous tissue formation were induced, while no significant vascularization was observed after the injection of FGF-2 alone (Fig. 10).

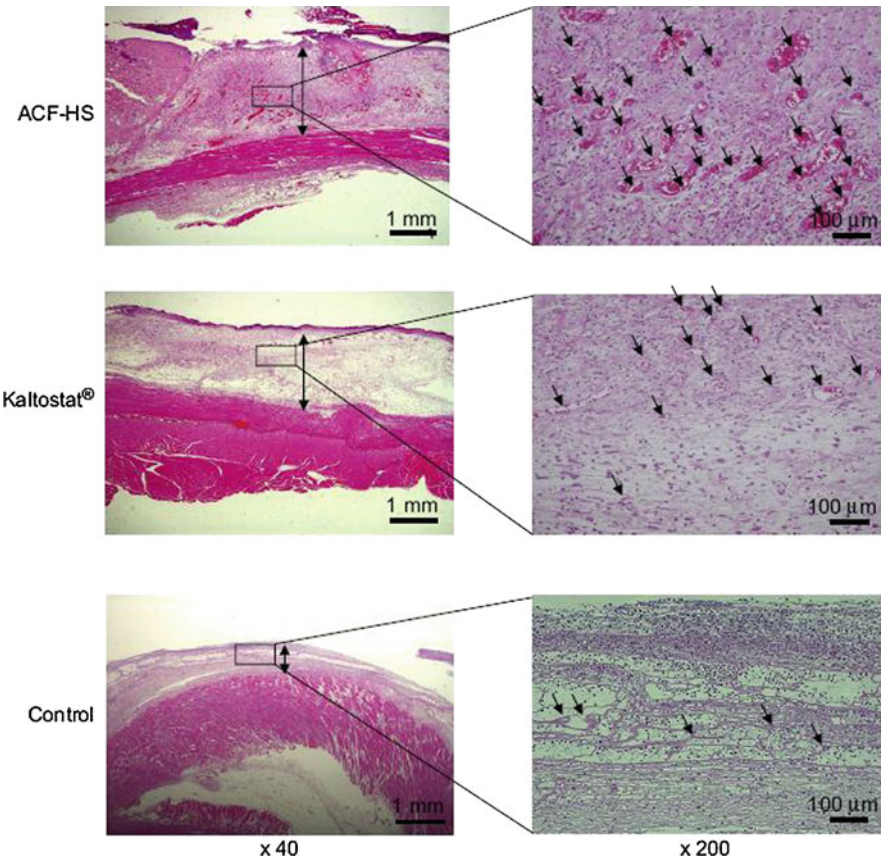

Fig. 9 Histological examination of wounds covered with ACF-HS or Kaltostat®, and controls. Each wound on day 7 is representative of eight wounds (four rats) covered with ACF-HS or Kaltostat®, or not covered (control). In the left panel, *black arrows* show formed granulation tissues, and *squares* show the sites for microphotographs (*right panels*). In the *right panels*, *black arrows* show blood vessels containing erythrocytes [72]

Injection of FGF-2 without a hydrogel carrier caused excessively rapid diffusion of FGF-2 molecules from the injected site to induce any vascularization effect. The researchers suggested that FGF-2 containing chitosan–fucoidan complex-hydrogel might be a promising new biomaterial for induction of vascularization and fibrous tissue formation in ischemic limbs.

6 Conclusion

Although there is limited available literature, research on the use of fucoidan in drug delivery systems and as a biomaterial has been increasing. Toxicity studies

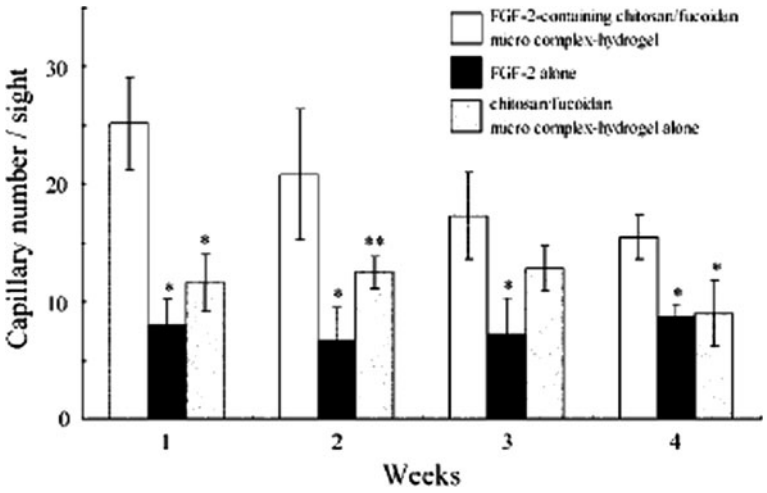

Fig. 10 Effect of injection of FGF-2-containing chitosan/fucoidan micro complex-hydrogel on vascularization in vivo. The number of capillaries was counted using a microphotograph of each section (n ¼ 6) exhibiting the highest mature capillary density. All values are means ±SD. For comparison of experimental and control groups, the unpaired t-test was used, with findings of $p < 0.001$ marked with an *asterisk* and of $p < 0.01$ with a *double asterisk* [74]

indicated that the use of fucoidan in these systems was quite reliable. Polyion complexes that form with fucoidan and positively charged chitosan were investigated in terms of drug and gene delivery and positive results were obtained. The results of various studies suggest that fucoidan-containing film, microparticle and hydrogel formulations have a promising future as dressing materials in wound and burn treatment. Previous studies found that fucoidan formulations were more effective in wound treatment than typical wound dressings such as chitosan. It is believed that the reasons for this increased effectiveness are as follows: antiseptic property of fucoidan, early phase microvascularization, capillarization and angiogenesis effect, bonding to leukocytes and accelerating infiltration in wound area. In addition, by bonding to high ratio fibroblasts, fucoidan increases fibroblast migration in the wound area and activates some cytokines which is important in wound healing. In light of these findings, fucoidan is a promising biopolymer. Recent research has expanded the range of uses of fucoidans.

References

1. Alsbjörn, B.: In search of an ideal skin substitute. Scand. J. Plast. Reconstr. Surg. **18**, 127–133 (1984)
2. Akbuğa, J., Özbaş-Turan, S., Erdoğan, N.: Plasmid-DNA loaded chitosan microspheres for in vitro IL-2 expression. Eur. J. Pharm. Biopharm. **58**, 501–507 (2004)

3. Angstwurm, K., Weber, J.R., Segert, A., Bürger, W., Weih, M., Freyer, D., Einhaupl, K.M., Dirnagl, U.: Fucoidin, a polysaccharide inhibiting leukocyte rolling, attenuates inflammatory responses in experimental pneumococcal meningitis in rats. Neurosci. Lett. **191**, 1–4 (1995)
4. Arai, T., Parker, A., Busby, W., Clemmons, D.R.: Heparin, heparan sulfate, and dermatan sulfate regulate formation of the insulin-like growth factor-I and insulin-like growth factor-binding protein complex. J. Biol. Chem. **269**, 20388–20393 (1994)
5. Balasubramani, M., Kumar, T.R., Babu, M.: Skin substitutes: a review. Burns **27**, 534–544 (2001)
6. Bangyekan, C., Aht-Ong, D., Srikulkit, K.: Preparation and properties evaluation of chitosan-coated cassava starch films. Carbohydr. Polym. **63**, 61–71 (2006)
7. Bertram, U., Bodmeier, R.: In situ gelling, bioadhesive nasal inserts for extended drug delivery: in vitro characterization of a new nasal dosage form. Eur. J. Pharm. Sci. **27**, 62–71 (2006)
8. Bilan, M.I., Grachev, A.A., Ustuzhanina, N.E., Shashkov, A.S., Nifantiev, E.N., Usov, A.I.: Structure of a fucoidan from the brown seaweed *Fucus evanescens* C.Ag. Carbohydr. Res. **337**, 719–730 (2002)
9. Borrello, I., Pardoll, D.: GM-CSF-based cellular vaccines: a review of the clinical experience. Cytokine Growth Factor Rev. **13**, 185–193 (2002)
10. Cashman, J.D., Kennah, E., Shuto, A., Winternitz, C., Springate, C.M.: Fucoidan film safely inhibits surgical adhesions in a rat model. J. Surg. Res. (2010)
11. Cheung, R.Y., Ying, Y., Rauth, A.M., Marcon, N., Wu, X.Y.: Biodegradable dextran-based microspheres for delivery of anticancer drug mitomycin C. Biomaterials **26**, 5375–5385 (2005)
12. Chevolot, L., Foucault, A., Chaubet, F., Kervarec, N., Sinquin, C., Fisher, A.M., Vidal, C.B.: Further data on the structure of brown seaweed fucans: relationships with anticoagulant activity. Carbohyd. Res. **319**, 154–165 (1999)
13. Chizhov, A.O., Dell, A., Morris, H.R., Halsam, S.M., McDowell, R.A., Shashkov, A.S., Nifat'ev, N.E., Khatuntseva, E.A., Usov, A.I.: A study of fucoidan from the brown seaweed *Chorda filum*. Carbohyd. Res. **320**, 108–119 (1999)
14. Chowdary, K.P.R., Rao, Y.S.: Mucoadhesive microspheres for controlled drug delivery. Biol. Pharm. Bull. **27**, 1717–1724 (2004)
15. Church, F.C., Meade, J.B., Treanor, R.E., Whinna, H.C.: Antithrombin activity of fucoidan. J. Biol. Chem. **264**, 3618–3623 (1989)
16. Colwell, N.S., Grupe, M.J., Tollefsen, M.: Amino acid residues of heparin cofactor II required for stimulation of thrombin inhibition by sulphated polyanions. BBA **1431**, 148–156 (1999)
17. Çetin, C., Köse, A.A., Aral, E., Çolak, Ö., Erçel, C., Karabağlı, Y., Özyılmaz, M., Alataş, Ö., Eker, A.: Protective effect of fucoidin (a neutrophil rolling inhibitor) on ischemia reperfusion injury: experimental study in rat epigastric island flaps. Ann. Plast. Surg. **47**, 540–546 (2001)
18. Dace, R., Mcbride, E., Brooks, K., Gander, J., Buszko, M., Doctor, V.M.: Comparison of the anticoagulant action of sulfated and phosphorylated polysaccharides. Thromb. Res. **87**, 113–121 (1997)
19. D'Ayala, G.G., Malinconico, M., Laurienzo, P.: Marine derived polysaccharides for biomedical applications: chemical modification approaches. Molecules **13**(9), 2069–2106 (2008)
20. Del Bigio, M.R., Yan, H.J., Campbell, T.M., Peeling, J.: Effect of fucoidan treatment on collagenase-induced intracerebral hemorrhage in rats. Neurol. Res. **21**, 415–419 (1999)
21. Derenzini, M.: The AgNORs. Micron **31**, 117–120 (2000)
22. Desire, L., Mysiakine, E., Bonnafous, D., Couvreur, P.: Sustained delivery of growth factors from methylidene malonate 2.1.2-based polymers. Biomaterials **27**, 2609–2620 (2006)
23. Duarte, M.E., Cardoso, M.A., Noseda, M.D., Cerezo, A.S.: Structural studies on fucoidans from the brown seaweed *Sargassum stenophyllum*. Carbohydr. Res. **333**(4), 281–293 (2001)

24. Dürig, J., Bruhn, T., Zurborn, K.H., Gutensohn, K., Bruhn, H.D., Beress, L.: Anticoagulant fucoidan fraction from *Fucus vesiculosus* induce platelet activation in vitro. Thromb. Res. **85**, 479–491 (1997)
25. Eichler, M.J., Carlson, M.A.: Modeling dermal granulation tissue with the linear fibroblast-populated collagen matrix: a comparison with the round matrix model. J. Dermatol. Sci. **41**, 97–108 (2006)
26. Erdağ, G., Sheridan, R.L.: Fibroblasts improve performance of cultured composite skin substitutes on athymic mice. Burns **30**, 322–328 (2004)
27. Fujimura, T., Shibuya, Y., Moriwaki, S., Tsukahara, K., Kitahara, T., Sano, T., Nishizawa, Y., Takema, Y.: Fucoidan is the active component of *Fucus vesiculosus* that promotes contraction of fibroblast-populated collagen gels. Biol. Pharm. Bull. **23**, 1180–1184 (2000)
28. Fundueanu, G., Constantin, M., Ascenzi, P.: Preparation and characterization of pH- and temperature-sensitive pullulan microspheres for controlled release of drugs. Biomaterials **29**, 2767–2775 (2008)
29. Gan, L., Fagerholm, P., Joon Kim, H.: Effect of leukocytes on corneal cellular proliferation and wound healing. Invest. Ophthalmol. Vis. Sci. **40**, 575–581 (1999)
30. George, M., Abraham, T.E.: Polyionic hydrocolloids for the intestinal delivery of protein drugs: alginate and chitosan—a review. J. Control Release **114**, 1–14 (2006)
31. Giraux, J.L., Bretaudiere, J., Matou, S., Fischer, A.M.: Fucoidan, as heparin, induces tissue factor pathway inhibitör release from cultured human endothelial cells. Thromb. Haemost. **80**, 692–695 (1998)
32. Grenha, A., Seijo, B., Remunan-Lopez, C.: Microencapsulated chitosan nanoparticules for lung protein delivery. Eur. J. Pharm. Sci. **25**, 427–437 (2005)
33. Hamilton, J.A.: Colony-stimulating factors in inflammation and autoimmunity. Nat. Rev. Immunol. **8**(7), 533–544 (2008)
34. Henriksen, I., Green, K.L., Smart, J.D., Smistad, G., Karlsen, J.: Bioadhesion of hydrated chitosans: an in vitro and in vivo study. Int. J. Pharm. **145**, 231–240 (1996)
35. Holtkamp, A.D., Kelly, S., Ulber, R., Lang, S.: Fucoidans and fucoidanases—focus on techniques for molecular structure elucidation and modification of marine polysaccharides. Appl. Microbiol. Biotechnol. **82**(1), 1–11 (2009)
36. Holt, G.E., Disis, M.L.: Immune modulation as a therapeutic strategy for non-small-cell lung cancer. Clin. Lung Cancer **9**, 13–19 (2008)
37. Howling, G.I., Dettmar, P.W., Goddard, P.A., Hampson, F.C., Dornish, M., Wood, E.J.: The effect of chitin and chitosan on the proliferation of human skin fibroblast and keratinocytes in vitro. Biomaterials **22**, 2959–2966 (2001)
38. Ho, W.S., Ying, S.Y., Choi, P.C.L., Wong, T.W.: A prospective controlled clinical study of skin donor sites treated with a 1–4, 2-acetamide-deoxy-B-D-glucan polymer: a preliminary report. Burns **27**, 759–761 (2001)
39. Ishihara, M., Nakanishi, K., Ono, K., Sato, M., Kikuchi, M., Saito, Y., Yura, H., Matsui, T., Hattori, H., Uenoyama, M., Kurita, A.: Photocrosslinkable chitosan as a dressing for wound occlusion and accelerator in healing process. Biomaterials **23**, 833–840 (2002)
40. Jakobsen, U., Simonsen, A.C., Vogal, S.: DNA controlled assembly of soft nanoparticles. Nucleic Acids Symp. Ser. **52**, 225–226 (2008)
41. Kawakami, S., Higuchi, Y., Hashida, M.: Nonviral approaches for targeted delivery of plasmid DNA and oligonucleotide. J. Pharm. Sci. **97**, 726–745 (2008)
42. Kearney, J.N.: Clinical evaluation of skin substitutes. Burns **27**, 545–551 (2001)
43. Khan, T.A., Peh, K.K., Chng, H.S.: Mechanical, bioadhesive strength and biological evaluations of chitosan films for wound dressing. J. Pharm. Pharmaceut. Sci. **3**, 303–311 (2000)
44. Kim, T.H., Jiang, H.L., Nah, J.W., Cho, M.H., Akaike, T., Cho, C.S.: Receptor-mediated gene delivery using chemically modified chitosan. Biomed. Mater. **2**(3), 95–100 (2007)
45. Kim, W.J., Koo, Y.K., Jung, M.K., Moon, H.R., Kim, S.M., Synytsya, A., Yun-Choi, H.S., Kim, Y.S., Park, J.K., Park, Y.I.: Anticoagulating activities of low-molecular weight fuco-

oligosaccharides prepared by enzymatic digestion of fucoidan from the sporophyll of Korean *Undaria pinnatifida*. Arch. Pharm. Res. **33**(1), 125–131 (2010)
46. Knapczyk, J.: Chitosan hydrogels as a base for semisolid drug forms. Int. J. Pharm. **93**, 233–237 (1993)
47. Kobayashi, T., Honke, K., Miyazaki, T., Matsumoto, K., Nakamura, T., Ishizuka, I., Makita, A.: Hepatocyte growth factor specifically binds to sulfoglycolipids. J. Biol. Chem. **269**, 9817–9821 (1994)
48. Kockisch, S., Rees, G.D., Young, S.A., Tsibouklis, J., Smart, J.D.: Polymeric microspheres for drug delivery to the oral cavity: an in vitro evaluation of mucoadhesive potential. J. Pharm. Sci. **92**, 1614–1623 (2003)
49. Kubota, N., Kikuchi, Y.: Macromolecular complexes of chitosan. In: Dumitriu, S. (ed.) Polysaccharides, pp. 595–628. Marcel Dekker, New York (1998)
50. Kui-Jin, K., Ok-hwan, L., Boo-yong, L.: Genotoxicity studies on fucoidan from Sporophyll of *Undaria pinnatifida*. Food Chem. Toxicol. **48**, 1101–1104 (2010)
51. Kumar, M.N., Muzzarelli, R.A., Muzzarelli, C., Sashiwa, H., Domb, A.J.: Chitosan chemistry and pharmaceutical perspectives. Chem. Rev. **104**(12), 6017–6084 (2004)
52. Kusaykin, M., Bakunina, I., Sova, V., Ermakova, S., Kuznetsova, T., Besednova, N., Zaporozhets, T., Zvyagintseva, T.: Structure, biological activity, and enzymatic transformation of fucoidans from the brown seaweeds. Biotechnol. J. **3**(7), 904–915 (2008)
53. Kuznetsova, T.A., Besednova, N.N., Mamaev, A.N., Momot, A.P., Shevchenko, N.M., Zvyagintseva, T.N.: Anticoagulant activity of fucoidan from brown algae *Fucus evanescens* of the okhotsk sea. Bull. Exp. Biol. Med. **5**, 471–473 (2003)
54. Lambert, O., Nagele, O., Loux, V., Bonny, J.D., Marchal-Heussler, L.: Poly(ethylene carbonate) microsphere: manufacturing process and internal structure characterization. J. Control Release **67**, 89–99 (2000)
55. Larsen, B., Haug, A.: Free-boundary electrophoresis of acidic polysaccharides from marine alga *Ascophyllum nodosum* (L.). Le. Jol. **17**, 1646–1652 (1963)
56. Leary, R.O., Rerek, M., Wood, E.J.: Fucoidan modulates the effect of transforming growth factor (TGF)-β_1 on fibroblast proliferation and wound repopulation in in vitro models of dermal wound repair. Biol. Pharm. Bull. **27**, 266–270 (2004)
57. Fucoidan. In: Levring, T., Hoppe, H.A., Schmid, O.J., (eds.) Marine Algae, pp. 330–332, Cram, De Gruyter & Co., Hamburg, Germany (1969)
58. Li, B., Lu, F., Wei, X., Zhao, R.: Fucoidan: structure and bioactivity. Molecules. **13**(8), 1671–1695 (2008)
59. Linnemann, G., Reinhart, K., Parade, U., Philipp, A., Pfister, W., Straube, E., Karzai, W.: The effects of inhibiting leukocyte migration with fucoidin in a rat peritonitis model. Intensive. Care Med. **26**, 1540–1546 (2000)
60. Lopez, C.R., Bodmeier, R.: Mechanical, water uptake and permeability of crosslinked chitosan glutamate and alginate films. J. Control Release **44**, 215–225 (1997)
61. Mabeau, S., Kloareg, B., Joseleau, J.P.: Fraction and analysis of fucan from brown alage. Phytochemistry **29**, 2441–2445 (1990)
62. MacEwan, S.R., Chilkoti, A.: Elastin-like polypeptides: biomedical applications of tunable biopolymers. Biopolymers **94**(1), 60–77 (2010)
63. Madri, J.A.: Inflammation and healing. In: Kıssane, J.M. (ed.) Anderson's Pathology, vol. 1, pp. 67–110, the CV Mosby Company, St. Louis (1990)
64. Matricardi, P., Meo, C.D., Coviello, T., Alhaique, F.: Recent advances and perspectives on coated alginate microspheres for modified drug delivery. Expert. Opin. Drug Deliv. **5**(4), 417–425 (2008)
65. Mauray, S., Raucourt, E.D., Chaubet, F., Maiga-Revel, O., Sternberg, C., Fischer, A.M.: Comparative anticoagulant activity and influence on thrombin generation of dextran derivatives and of a fucoidan fraction. J. Biomater. Sci. Polymer Edn. **9**, 373–387 (1998)
66. Mauray, S., Raucourt, E., Talbot, J.C., Dachary-Prigent, J., Jozefowicz, M., Fischer, A.M.: Mechanism of factor IXa inhibition by antithrombin in the presence of unfractionated and low molecular weight heparins and fucoidan. BBA **1387**, 184–194 (1998)

67. Mauray, S., Sternberg, C., Theveniaux, J., Millet, J., Sinquin, C., Tapon-Bretaudiere, J., Fischer, A.M.: Venous antithrombotic and anticoagulant activities of a fucoidan fraction. Thromb. Haemostasis **74**, 1280–1285 (1995)
68. Minix, R., Doctor, V.M.: Interaction of fucoidan with proteases and inhibitors of coagulation and fibrinolysis. Thromb. Res. **87**, 419–429 (1997)
69. Montembault, A., Viton, C., Domard, A.: Physico-chemical studies of the gelation of chitosan in a hydroalcoholic medium. Biomaterials **26**, 933–943 (2005)
70. Mulloy, B., Mourao, P.A.S., Gray, E.: Structure/function studies of anticoagulant sulphated polysaccharides using NMR. J. Biotechnol. **77**, 123–135 (2000)
71. Mummery, R.S., Rider, C.C.: Characterization of the heparin-binding properties of IL-6. J. Immunol. **165**, 5671–5679 (2000)
72. Murakami, K., Aoki, H., Nakamura, S., Nakamura, S., Takikawa, M., Hanzawa, M., Kishimoto, S., Hattori, H., Tanaka, Y., Kiyosawa, T., Sato, Y., Ishihara, M.: Hydrogel blends of chitin/chitosan, fucoidan and alginate as healing-impaired wound dressings. Biomaterials **31**(1), 83–90 (2010)
73. Najjam, S., Mulloy, B., Theze, J., Gordon, M., Gibbs, R., Rider, C.C.: Further characterization of the binding of human recombinant interleukin 2 to heparin and identification of putative binding sites. Glycobiology **8**, 509–516 (1998)
74. Nakamura, S., Nambu, M., Ishizuka, T., Hattori, H., Kanatani, Y., Takase, B., Kishimoto, S., Amano, Y., Aoki, H., Kiyosawa, T., Ishihara, M., Maehara, T.: Effect of controlled release of fibroblast growth factor-2 from chitosan/fucoidan micro complex-hydrogel on in vitro and in vivo vascularization. J. Biomed. Mater. Res. **85**A, 619–627 (2008)
75. Nanchahal, J., Dover, R., Otto, W.R.: Allogeneic skin substitutes applied to burns patients. Burns **28**, 254–257 (2002)
76. Nardella, A., Chaubet, F., Boisson-Vidal, C., Blondin, C., Duran, P., Jozefonvicz, J.: Anticoagulant low molecular weight fucans produced by radical process and ion exchange chromatography of high molecular weight fucans extracted from the brown seaweed *Ascophyllum nodosum*. Carbohydr. Res. **289**, 201–208 (1996)
77. Ning, L., Quanbin, Z., Jinming, S.: Toxicological evaluation of fucoidan extracted from *Laminaria japonica* in Wistar rats. Food Chem. Toxicol. **43**, 421–426 (2005)
78. Nishino, T., Fukuda, A., Nagumo, T., Fujihara, M., Kaji, E.: Inhibition of the generation of thrombin and factor Xa by a fucoidan from the brown seaweed *Ecklonia kurome*. Thromb. Res. **96**, 37–49 (1999)
79. Nishino, T., Nagumo, T.: Anticoagulant and antithrombin activities of oversulfated fucans. Carbohydr. Res. **229**, 355–362 (1992)
80. Nishino, T., Nagumo, T.: Structural characterization of a new anticoagulant fucan sulfate from the brown seaweed *Ecklonia kurome*. Carbohydr. Res. **211**, 77–90 (1991)
81. Nishino, T., Yamauchi, T., Horie, M., Nagumo, T., Suzuki, H.: Effects of a fucoidan on the activation of plasminogen by u-PA and t-PA. Thromb. Res. **99**, 623–634 (2000)
82. Oh, J.K., Lee, D.I., Park, J.M.: Biopolymer-based microgels/nanogels for drug delivery applications. Prog. Polym. Sci. **34**(12), 1261–1282 (2009)
83. O'Neill, A.N.: Degradative studies on fucoidin. J. Am. Chem. Soc. **76**, 5074–5076 (1954)
84. Paños, I., Acosta, N., Heras, A.: New drug delivery systems based on chitosan. Curr. Drug. Discov. Technol. **5**(4), 333–341 (2008)
85. Passaquet, C., Thomas, J.C., Caron, L., Hauswirth, N., Puel, F., Berkaloff, C.: Light-harvesting complexes of brown alage: biochemical characterization and immunological relationships. FEBS **280**, 21–26 (1991)
86. Percival, E., McDowell, R.H.: Sulphated polysaccharides containing neutral sugars: fucoidan. In: Percival, E., McDowell, R.H. (eds.) Chemistry and Enzymology of Marine Algal Polysaccharides, pp. 157–175, Academic Press, London (1967)
87. Pereira, M.S., Mulloy, B., Mourao, P.A.S.: Structure and anticoagulant activity of sulfated fucans. J. Biol. Chem. **274**, 7656–7667 (1999)
88. Pomin, V.H., Mourão, P.A.: Structure, biology, evolution, and medical importance of sulfated fucans and galactans. Glycobiology **18**(12), 1016–1027 (2008)

89. Provenzano, P.P., Alejandro-Osorio, A.L., Valhmu, W.B., Jensen, K.T., Vanderby, R.: Intrinsic fibroblast-mediated remodeling of damaged collagenous matrices in vivo. Matrix Biol. **23**, 543–555 (2005)
90. Pruitt, B.A., Levine, N.S.: Characteristics and uses of biologic dressings and skin substitutes. Arch. Surg. **119**, 312–322 (1984)
91. Quinn, K.J., Courtney, J.M., Evans, J.H., Gaylor, J.D.S.: Principles of burn dressings. Biomaterials **6**, 369–377 (1985)
92. Ramsden, L., Rider, C.C.: Selective and differential binding of interleukin (IL)-1α, IL-1β, IL-2 and IL-6 to glycosaminoglycans. Eur. J. Immunol. **22**, 3027–3031 (1992)
93. Ruperez, P., Ahrazem, O., Leal, A.: Potential antioxidant capacity of sulfated polysaccharides from the edible marine brown seaweed *Fucus vesiculosus*. J. Agric. Food Chem. **50**, 840–845 (2002)
94. Sai, P., Babu, M.: Collagen based dressings—a review. Burns **26**, 54–62 (2000)
95. Schaeffer, D.J., Krylov, V.S.: Anti-HIV activity of extracts and compounds from algae and cyanobacteria. Ecotox. Environ. Safe. **45**, 208–227 (2000)
96. Scheerlinck, J.P.Y., Casey, G., Mcwaters, P., Kelly, J., Woollard, D., Lightowlers, M.W., Tennent, J.M., Chaplin, P.J.: The immune response to a DNA vaccine can be modulated by co-delivery of cytokine genes using a DNA prime-protein boost strategy. Vaccine **19**, 4053–4060 (2001)
97. Sezer, A.D., Akbuğa, J.: Comparison on in vitro characterization of fucospheres and chitosan microspheres encapsulated plasmid DNA (pGM-CSF): formulation design and release characteristics. AAPS PharmSciTech. **10**(4), 1193–1199 (2009)
98. Sezer, A.D., Akbuğa, J.: Fucosphere—new microsphere carriers for peptide and protein delivery: preparation and in vitro characterization. J. Microencapsul. **23**(5), 513–522 (2006)
99. Sezer, A.D.: Chitosan: properties and its pharmaceutical and biomedical aspects. In: Davis, S.P. (ed.) Chitosan: Manufacture, Properties, and Usage, 1st edn. Nova Science Publishers, New York (2011)
100. Sezer, A.D., Cevher, E., Hatipoğlu, F., Oğurtan, Z., Baş, A.L., Akbuğa, J.: Preparation of fucoidan–chitosan hydrogel and its application as burn healing accelerator on rabbits. Biol. Pharm. Bul. **31**(12), 2326–2333 (2008)
101. Sezer, A.D., Cevher, E., Hatipoğlu, F., Oğurtan, Z., Baş, A.L., Akbuğa, J.: The use of fucosphere in the treatment of dermal burns in rabbits. Eur. J. Pharm. Biopharm. **69**(1), 189–198 (2008)
102. Sezer, A.D., Hatipoğlu, F., Cevher, E., Oğurtan, Z., Baş, A.L., Akbuğa, J.: Chitosan film containing fucoidan as a wound dressing for dermal burn healing: preparation and in vitro/in vivo evaluation. AAPS PharmSciTech. **8**(2), Article 39 (2007)
103. Sezer, A.D., Hatipoğlu, F., Oğurtan, Z., Baş, A.L., Akbuğa, J.: Evaluation of fucoidan—chitosan hydrogels on superficial dermal burn healing in rabbit: an in vivo study. The 12th European Congress on Biotechnology, Copenhagen, 21–24 August 2005
104. Sezer, A.D., Hatipoğlu, F., Oğurtan, Z., Cevher, E., Baş, A.L., Akbuğa, J.: New nanosphere system for treatment of full-thickness burn on rabbit. The 31st FEBS Congress, Istanbul, 24–29 June 2006
105. Sezer, A.D., Kazak, H., Toksoy Öner, E., Akbuğa, J.: Levan as a promising biomaterial for protein delivery. 36th Annual Meeting and Exposition of the Controlled Release Society, Copenhagen, 18–22 July 2009
106. Shakespeare, P.: Burn wound healing and skin substitutes. Burns **27**, 517–522 (2001)
107. Shi, C., Zhu, Y., Ran, X., Wang, M., Su, Y., Cheng, T.: Therapeutic potential of chitosan and its derivatives in regenerative medicine. J. Surg. Res. **133**(2), 185–192 (2006)
108. Shigemasa, Y., Minami, S.: Applications of chitin and chitosan for biomaterials. Biotechnol. Genet. Eng. Rev. **13**, 383–420 (1995)
109. Shu, X.Z., Zhu, K.J., Song, W.: Novel pH-sensitive citrate cross-linked chitosan film for drug controlled release. Int. J. Pharm. **212**, 19–28 (2001)
110. Singer, A.J., Mohammad, M., Thode, H.C., Mcclain, S.A.: Octylcyanoacrylate versus polyurethane for treatment of burns in swine: a randomized trail. Burns **26**, 388–392 (2000)

111. Skinner, M.P., Lucas, C.M., Burns, G.F., Chesterman, C.N., Berndt, M.C.: GMP-140 binding to neutrophils is inhibited by sulfated glycans. J. Biol. Chem. **266**, 5371–5374 (1991)
112. Smart, J.D.: The basics and underlying mechanisms of mucoadhesion. Adv. Drug. Deliver. Rev. **57**, 1556–1568 (2005)
113. Smelcerovic, A., Knezevic-Jugovic, Z., Petronijevic, Z.: Microbial polysaccharides and their derivatives as current and prospective pharmaceuticals. Curr. Pharm. Des. **14**(29), 3168–3195 (2008)
114. Soeda, S., Fujii, N., Shimeno, H., Nagamatsu, A.: Oversulfated fucoidan and heparin suppress endotoxin induction of plasminogen activator inhibitor-1 in cultured human endothelial cells: their possible mechanism of action. BBA **1269**, 85–90 (1995)
115. Soeda, S., Kozako, T., Iwata, K., Shimeno, H.: Oversulfated fucoidan inhibits the basic fibroblast growth factor-induced tube formation by human umbilical vein endothelial cells: its possible mechanism of action. BBA **1497**, 127–134 (2000)
116. Soeda, S., Sakaguchi, S., Shimeno, H., Nagamatsu, A.: Fibrinolytic and anticoagulant activities of highly sulfated fucoidan. Biochem. Pharmacol. **43**, 1853–1858 (1992)
117. Stashak, T.S., Farstvedt, E., Othic, A.: Update on wound dressings: indications and best use. Clin. Tech. Equine Pract. **3**, 148–163 (2004)
118. Tan, W., Krishnaraj, R., Desai, T.A.: Evaluation of nanostructured composite collagen-chitosan matrices for tissue engineering. Tissue Eng. **7**, 203–210 (2001)
119. Trere, D.: AgNOR staining and quantification. Micron **31**, 127–131 (2000)
120. Uebersax, L., Merkle, H.P., Meinel, L.: Biopolymer-based growth factor delivery for tissue repair: from natural concepts to engineered systems. Tissue Eng. Part B Rev. **15**(3), 263–289 (2009)
121. Ueno, H., Mori, T., Fujinaga, T.: Topical formulation and wound healing applications of chitosan. Adv. Drug Delivery Rev. **52**, 105–115 (2001)
122. Venkateswaran, P.S., Millman, I., Blumberg, B.S.: Interaction of fucoidan from *Pelvetia fastigiata* with surface antigens of hepatitis B and woodchuck hepatitis viruses. Planta Med. **55**, 265–270 (1989)
123. Vinsova, J., Vavrikova, E.: Recent advances in drugs and prodrugs design of chitosan. Curr. Pharm. Des. **14**(13), 1311–1326 (2008)
124. Vischer, P., Buddecke, E.: Different action of heparin and fucoidan on arterial smooth muscle cell proliferation and thrombospondin and fibronectin metabolism. Eur. J. Cell Biol. **56**, 407–414 (1991)
125. Vloemans, A.F.P.M., Soesman, A.M., Kreis, R.W., Middelkoop, E.: A newly developed hydrofibre dressing, in the treatment of partial-thickness burns. Burns **27**, 167–173 (2001)
126. Willenborg, D.O., Parish, C.R.: Inhibition of allergic encephalomyelitis in rats by treatment with sulfated polysaccharides. J. Immunol. **140**, 3401–3405 (1988)
127. Wittaya-Areekul, S., Prahsarn, C.: Development and in vitro evaluation of chitosan-polysaccharides composite wound dressings. Int. J. Pharm. **313**, 123–128 (2006)
128. Wong, C.F., Yeun, K.H., Peh, K.K.: Formulation and evaluation of controlled release Eudragit buccal patches. Int. J. Pharm. **178**, 11–22 (1999)
129. Yiu Leung, T.C., Wong, C.K., Xie, Y.: Green synthesis of silver nanoparticles using biopolymers, carboxymethylated-curdlan and fucoidan. Mater. Chem. Phys. **121**, 402–405 (2010)
130. Yurt, R.M.: Burns. In: Norton, J.A. (ed.) Essential Practice of Surgery: Basic Science and Clinical Evidence, pp. 119–126, Springer-Verlag, New York (2003)
131. Zhu, Z., Zhang, Q., Chen, L., Ren, S., Xu, P., Tang, Y., Luo, D.: Higher specificity of the activity of low molecular weight fucoidan for thrombin-induced platelet aggregation. Thromb. Res. **125**, 419–426 (2010)

Part IV
Unique Polymeric Systems for Active Implants

Synthesis of Novel Chain Extended and Crosslinked Polylactones for Tissue Regeneration and Controlled Release Applications

Jukka Seppälä, Harri Korhonen, Risto Hakala and Minna Malin

Abstract In addition to ring opening homo- and co-polymerization, chain extension and crosslinking are attractive routes for synthesizing polylactones. Through manipulation of molecular composition and molecular architecture a wide range of mechanical, thermal and degradation properties can be achieved, and using different coupling chemistries, polylactones belonging to many kinds of linear and network-structured polymer families have been synthesized. The poly(ester-urethanes), poly(ester-amides), poly(ester-urethane-amides), polyphosphoesters, poly(ester-anhydrides) and methacrylated crosslinking polyesters polymer families have great potential in biomedical applications such as surgery, tissue-engineering, and controlled active agent release. Mechanical properties, degradation characteristics and rate, and release properties of these polymers can be adjusted within wide ranges. Biopolymers showing bone-like hardness or soft non-creeping elasticity have been synthesized. Poly(ester-anhydrides) in particular combine useful properties of polyesters and polyanhydrides, and have been shown to degrade by surface-erosion, enabling controlled macromolecular active agent release. Photocuring of liquid pre-polymers enables the use of biopolymers in high precision lithographic techniques like micromolding in capillaries, stereolithography and two-photon polymerization. This makes it possible to design and customize complicated scaffold structures, with desired drug release profiles for various biomedical applications.

J. Seppälä (✉), H. Korhonen, R. Hakala and M. Malin
Polymer Technology Research Group, Department of Biotechnology and Chemical Technology, School of Science and Technology, Aalto University,
P.O. Box 16100, 00076 Aalto, Finland
e-mail: jukka.seppala@tkk.fi

Stud Mechanobiol Tissue Eng Biomater (2011) 8: 409–438
DOI: 10.1007/8415_2010_52

Published Online: 11 January 2011

1 Introduction

Aliphatic polyesters are the best characterized and most widely-studied biodegradable polymers. The mechanism of degradation in polyester materials is classified as bulk degradation with random hydrolytic scission of the polymer backbone. Biodegradable polyesters have been used in a number of medical applications [1]. The major applications include resorbable sutures, drug delivery systems and orthopedic fixation devices such as pins, rods and screws. Of the various families of synthetic polymers, the polyesters are attractive for these applications because of their ease of degradation by hydrolysis, with the degradation products being resorbed through metabolic pathways, and the potential to tailor the structure to alter the degradation rate. Polyesters have also been considered for use in tissue engineering applications. In addition to medical applications, biodegradable polyesters are increasingly used in high-volume applications such as packaging, films and fibers [2, 3].

The most common way to obtain high molecular weight polyesters is through ring-opening polymerization (ROP) of cyclic esters. ROP can be used in the preparation of polyesters such as polyglycolide, polylactides with different stereo structures, poly(ε-caprolactone), poly(δ-valerolactone) and polycarbonates. Good control of the polymerization allows tailoring of the properties related to the microstructure and molecular architecture of the polymer [4].

The insertion mechanism has been shown to provide the most efficient method for ROP of cyclic esters. The most widely-used initiators for the insertion reaction are carboxylates and alkoxides of Sn, Ti, Zn, and Al. Among the initiators, Tin (II) 2-ethylhexanoate (SnOct2) is probably the most widely used in the polymerization of cyclic esters. When stannous octoate is used, it first reacts with compounds containing hydroxyl groups, forming tin alkoxide, which then acts as the initiator in the polymerization [5]. Polymerization yields hydroxyl-terminated polymers with the molecular weight depending on the ratio of monomer to co-initiator. The structure of the polymer depends on the alcohol used as co-initiator. Mono- and difunctional alcohols yield linear polymers, whereas alcohols with more than two hydroxyl functional groups give comb-shaped, star-shaped, hyper-branched, or dendritic polymers.

An additional approach is to take advantage of chain extending and crosslinking reactions, where functional telechelic oligomers are used as precursors. This reaction route enables synthesis of molecules belonging to novel linear and thermoplastic polyester families, such as poly(ester-urethanes), poly(ester-amides), poly(ester-urethane-amides), poly(ester-anhydrides) and polyphosphoesters, as well as crosslinked polyesters [6, 7].

Macromolecular engineering is increasingly important for polymers used in medical applications. It is highly desirable that properties such as glass transition temperature, crystallinity, and hydrophilicity are tailored to fulfill the requirements of specific applications. In this article we review the work carried out in our laboratory in the preparation of degradable polyesters by various chain linking and

crosslinking methods. These methods extend the possibilities for macromolecular engineering, and by controlling characteristics such as molecular architecture, block lengths, and copolymer composition, materials with a wide range of properties can be produced.

2 Synthesis of Pre-polymers for Chain Linking and Crosslinking

Chain linking and crosslinking techniques involve the use of telechelic pre-polymers. In our laboratory the pre-polymers used for chain linking or crosslinking have been either OH- or COOH-terminated low molecular weight polylactones. The properties of these pre-polymers have been modified using different monomers, co-initiators, and functionalization agents.

2.1 Hydroxyl Terminated Pre-polymers

In the preparation of chain linked or crosslinked polymers, the first step was to prepare hydroxyl-terminated pre-polymers. Poly(L-lactide), poly(D,L-lactide), and poly(ε-caprolactone) pre-polymers were synthesized by ring-opening polymerization of cyclic esters in the presence of a co-initiator containing the hydroxyl group. Different co-initiators used in the polymerization are shown in Fig. 1. Linear pre-polymers were prepared using 1,4-butanediol as a hydrophilic

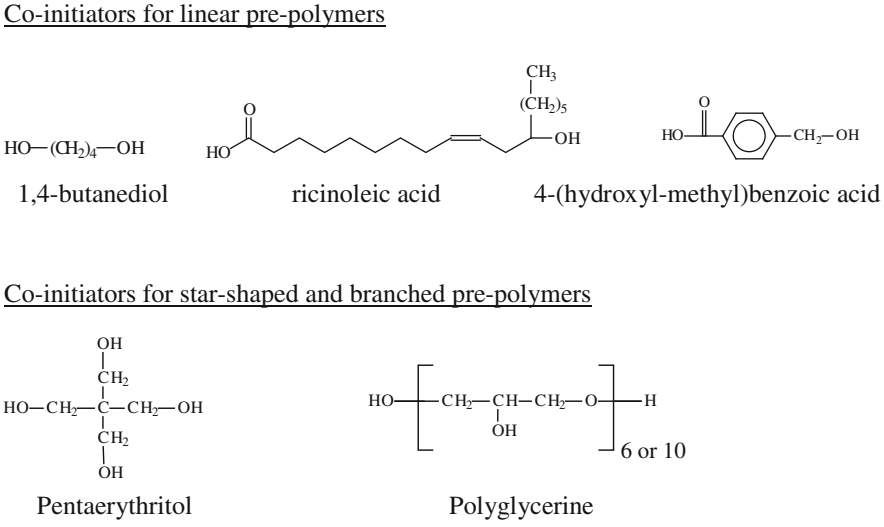

Fig. 1 Co-initiators used in the preparation of polyester precursors [8, 10]

co-initiator, whereas ricinoleic acid and 4-(hydroxyl-methyl)benzoic acid were used as hydrophobic co-initiators [8–10]. Based on ^{1}H NMR all these co-initiators yielded products with molecular weights that were near those expected by theory.

In addition to linear pre-polymers, star-shaped and branched polylactides were prepared using alcohols with different numbers of hydroxyl groups as co-initiators (Fig. 1). Pentaerythritol has four primary hydroxyl groups in equivalent positions and it was used to yield a four-arm star-shaped polymer structure. The co-initiators of primary interest were polyglycerine-06 (PGL-06) and polyglycerine-10 (PGL-10), which were used as novel co-initiators with the aim of achieving a more branched structure than that obtained with pentaerythritol. According to ^{1}H NMR, initiation activity (the number of hydroxyl groups initiating polymerization) was stoichiometric for 1,4-butanediol (2 OH groups) and near stoichiometric for pentaerythritol (4 OH groups). Similar initiation activity for pentaerythritol has been reported in other studies. Kim et al. [11] have reported that increasing the ratio of monomer to initiator increases initiation activity, and four-armed oligomers were formed when the ratio of monomer to pentaerythritol reached 32. Similarly, Lang and Chu [12]) have reported that PCL oligomers had one, two, three, or four arms when the ratio of monomer to pentaerythritol was 5:1, whereas a higher ratio (40:1) produced mainly three- or four-armed oligomers.

The initiation activities for polyglycerines were 4.0–6.2 for PGL-06 (8 OH-groups) and 8.3 for PGL-10 (12 OH-groups). It seems that secondary hydroxyl groups of PGL did not initiate polymerization as efficiently as primary hydroxyl groups, and thus measured values were somewhat lower than theoretical values. However, it can be concluded that a substantial proportion of secondary hydroxyl groups take part in the initiation, and that their participation increases as the co-initiator content decreases. This is in accordance with the behavior of hyperbranched polyglycerol as co-initiator in the polymerization of ε-caprolactone. Burgath et al. [13] have reported that in the case of a theoretical arm length of ten CL units, the initiation activity of hydroxyl groups was 75%. However, when the monomer/co-initiator ratio was higher and the theoretical arm length was 30 CL units, an initiation activity of 96% was measured.

2.2 Carboxylic Acid Terminated Pre-polymers

Carboxylic acid terminated pre-polymers were prepared by converting terminal hydroxyl groups of pre-polymers to carboxylic acid functional groups by allowing the hydroxyl groups to react with succinic [8, 10] or alkenylsuccinic anhydride [14, 15]. The reaction scheme for the functionalizations is presented in Fig. 2. Functionalization of hydroxyl groups to carboxylic acids was carried out in bulk without a catalyst. Comparing the two types of pre-polymer, there was a clear difference in the reactivities of the hydroxyl groups of PCL and PLA. According to ^{1}H NMR studies, hydroxyl groups of PCL reacted completely with succinic anhydride within 3 h at 160°C. For PLA, the degree of substitution was 85–93%

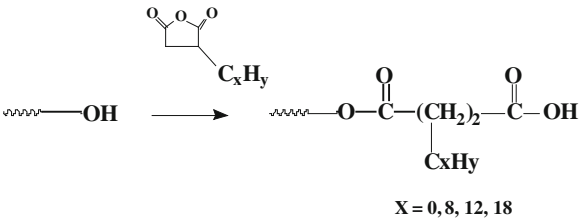

Fig. 2 Functionalization of hydroxyl terminated polyester to carboxylic acid functionality

despite a longer reaction time of 6 h. Lang and Chu [12] have suggested that the difference in the reactivity of cyclic anhydride with hydroxyl groups in PCL and PLA is mainly due to the different reactivities of anhydride with primary and secondary alcohols.

Of key significance in developing applications for poly(ester-anhydrides) was the finding that alkenyl groups can be used to adjust the degradation rate of these polymers [15]. Alkenylsuccinic anhydrides (ASAs) contain alkenyl chains of various lengths and have been found useful for tailoring the hydrophobicities of biomaterials. ASAs are reported to increase the hydrophobicity of soy protein and gelatin surfactants and to improve the hydrophobicity of chitosan and starch surfaces [16–18]. We have used ASAs to modify the degradation of thermoplastic and crosslinked poly(ester-anhydrides) based on polylactone oligomers [15]. The effect of alkenyl chains on hydrophobicity of pre-polymers was investigated in a study in which linear and star-shaped PCL oligomers were functionalized with succinic anhydride or with alkenylsuccinic anhydrides containing alkenyl chains of 8 or 18 carbons [14]. The increase in the hydrophobicity of pre-polymers is clearly seen in the contact angles: succinic anhydride-functionalized PCL-based pre-polymer clearly showed a lower contact angle than the two ASA-functionalized pre-polymers (Fig. 3). In comparison with ASA-functionalized polymers, lengthening of the alkenyl chain resulted in a considerable increase in the contact angle.

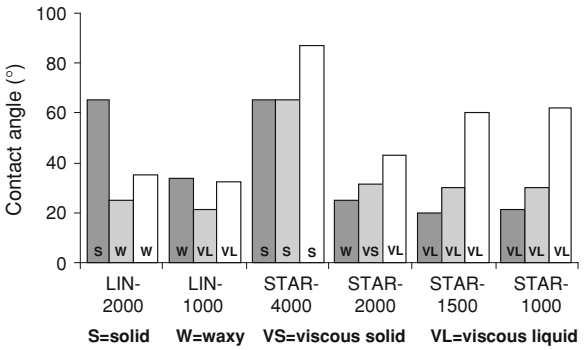

Fig. 3 Equilibrium contact angles of (*dark shaded*) SAH-, (*light shaded*) 8-ASA-, and (*unshaded*) 18-ASA-functionalized linear and star-shaped PCL oligomers in different physical states [14], reproduced with permission from Elsevier)

3 Chain Extended Polylactones

Chain extension of polyester oligomers offers an alternative route for obtaining high molecular weight polymers. Chain extenders such as diisocyanates, bis(2-oxazolines), bis(epoxides), and bis(ketene acetals) are bifunctional low-molecular weight monomers that in small amounts increase the molecular weight of polymers in rapid reactions. The chain extenders also introduce new functional groups, and increase flexibility in the manufacture of polymers, which can lead to improved physical and mechanical properties and biodegradability of the resulting polymers. In addition to the use of chain extenders, polyester precursors can be linked to each other by introducing suitable functionalities into the pre-polymers by end functionalization [4].

3.1 Poly(ester-urethanes)

As is well known in polyurethane chemistry, diisocyanates react rapidly with –OH functional oligomers, which are called polyols in polyurethane technology. In the synthesis of high molecular weight poly(ester-urethanes) the first stage is to synthesize aliphatic polyester-based telechelic oligolactones having –OH end functionalities. Typically these pre-polymers have molecular weights in the range of 5,000–50,000 g/mol. A high molecular weight polymer can then be obtained in the second stage through a chain linking reaction between the above-mentioned polyols and diisocyanate compounds. Different diisocyanates, such as 1,6-hexamethylene diisocyanate, isophorone diisocyanate, 4,4-dicyclohexylmethane diisocyanate, and 1,4-butane diisocyanate have been used in this type of chain linking. The chain linking typically yields thermoplastic poly(lactic acids) with a molecular weight of around 100,000–300,000 g/mol [19, 20].

The reaction between the hydroxyl end-functionalized pre-polymers with diisocyanate as chain extender forms a urethane bond. The pre-polymer chain length determines the urethane link concentration in the polymer chains. The ratio between reactive chain ends and isocyanate groups should be close to unity to produce high-molecular-weight linear polymers. In addition, the hydroxyl termination of the pre-polymers should be as complete as possible. If isocyanate is added in excess in chain linking, broadening of the molecular weight distribution, branching of the molecules and finally crosslinking will occur during the chain linking reactions. It has been proposed that this is due to the reaction between the isocyanate and the urethane bond leading to an allophanate bond. The reaction leading to allophanatesis is a competing side reaction in chain linking and it leads to branching of the polymer chains. This can be used in the preparation of poly(ester-urethanes) (PEUs) with modified rheological properties due to the formation of long-chain branches [19–22].

There are alternative synthesis routes for obtaining the end-functional aliphatic polyester pre-polymers, such as ring opening polymerization of lactones and direct polycondensation of diols and dicarboxylic acids or hydroxyacids. The chemical composition of the pre-polymers is the primary tool for adjusting polymer and product properties such as mechanical properties and degradation rate. Only lactic acid (LA)-based pre-polymers lead to rigid poly(ester-urethanes), whereas the use of caprolactone (CL) as co-monomer can confer some elastomeric properties on the product. Rubbery poly(ester-urethanes) can be produced by using CL as a co-monomer with lactic acid in the preparation of the telechelic pre-polymers and chain extending these pre-polymers [22]. On the other hand, the glass transition temperature and thus heat resistance of the poly(ester-urethanes) has been successfully increased by using DL-mandelic acid as a co-monomer [23]. In addition, the mechanical and thermal properties of the rigid PEUs have been modified by blending with more flexible copolymers in order to improve impact strength. Tough biodegradable composites have also been prepared with reinforcing fillers. Mechanical properties have been reported to depend heavily on compatibility and phase separation [24, 25]. We have reported toxic degradation products in connection with some poly(ester-urethanes) [26]. This aspect needs to be considered carefully when planning the uses of these polymers in biomedical applications.

3.2 Poly(ester-amides)

Aliphatic poly(ester-amides) have good potential for environmental and biomedical applications because of their biodegradability, biocompatibility, and favorable physical properties. The positive characteristics of poly(ester-amides) arise on one hand from the ability of amide groups to form intermolecular hydrogen bonds, enhancing the thermal and mechanical properties of the resulting polymers, and on the other hand from the well-known tendency of ester linkages to enhance hydrolytic degradation of polymers. Enzymatic degradation of copolymers synthesized by the ester-amide interchange reaction between polyamide and polycaprolactone was reported already in 1979 [27]. Since then, many types of poly(ester-amides) with random, multi-block, or alternating distributions of ester and amide groups have been prepared by various methods using aliphatic dicarboxylic acids, amino acids, hydroxyl acids, diols, and their derivatives. Polycondensation reactions have been carried out both in melt and in solution.

One possibility for synthesizing poly(ester-amides) is to use a bisoxazoline group as a chain-extender [28–30]. Bis-cyclic imino-ethers, such as bis-2-oxazolines, are an attractive class of chain extenders for linear polyesters and polyamides, especially for those that are mainly terminated by carboxylic groups. There are no significant side reactions during the chain extending reaction, and the ester-amides formed are reported to be thermally rather stable.

3.2.1 Poly(ester-amides) Based on Lactic Acid

2,2′-Bis(2-oxazoline) has been used as a coupling agent to link carboxyl-terminated lactic acid-based oligomers. The highest molecular weights for poly(ester-amides) (PEAs) were over 300,000 g/mol. These molecular weights were obtained in 10 min at 200°C. Optimally, the ratio of oxazoline functional groups to carboxylic end functionalities was 1.0–1.2. The mechanical properties of poly(ester-amides) polymerized in this way were very comparable with those of other biopolymers. A tensile strength of 67 MPa and impact strength of 34 kJ/m^2 was reported [29].

The addition to PLA of 2,2′-bis(2-oxazoline) as a chain extender increased the hydrolytic degradation rate of the polymer. The release profiles of all small model drugs from PDLLA films were biphasic or triphasic, while release profiles of small model drugs from corresponding poly(ester-amide) (PEA) films varied substantially. In particular, PEA enhanced the release of a macromolecule from microspheres due to its faster degradation rate [31, 32].

3.2.2 Poly(ester-amides) Based on ε-Caprolactone

Oxazoline-linked ε-caprolactone polymers have been successfully produced by a three-step synthesis [28]. The molecular weights of hydroxyl-terminated pre-polymers were controlled by varying the ratio of 1,4-butanediol to ε-caprolactone monomer (1/100, 2/100, 5/100 and 10/100) in ring-opening polymerization of ε-caprolactone at 160°C. The hydroxyl-terminated intermediates were further converted to low molecular-weight carboxyl-terminated pre-polymers by allowing them to react with a slight molar excess of succinic anhydride at 160°C for 1 h. Finally, these carboxyl-terminated CL-pre-polymers were linked with 2,2′-bis(2-oxazoline) as a chain extender at 200°C to get ε-caprolactone-based oxazoline linked poly(ester-amides)(PCL-O). The structure of these polymers is shown in Fig. 4, and their molecular weights and thermal characteristics are presented in Table 1.

Tarvainen et al. [33] showed in their studies that the in vitro degradation of polymer films in phosphate buffer solution (PBS) was enhanced by oxazoline modification. It was found to affect only the decrease in molecular weight, but not erosion behavior. The molecular weight (M_n) of polycaprolactone-based poly(ester-amide) film decreased to 55% of its original value during the half-year study while the corresponding molecular weight decrease of PCL film was only

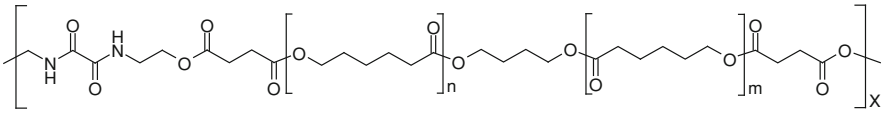

Fig. 4 Structure of oxazoline linked poly(ester-amides)

Table 1 Characteristics of synthesized poly(ester-amides) [35]

Polymer	CL-block (M_n)[a]	M_w^b (g/mol)	M_n^b (g/mol)	T_{m1}/T_{m2} (°C)	Cryst. (%)
PCL-O	1,500	37,100	20,300	39/25	24
	1,500	52,000	24,500	39/26	28
	3,900	88,300	46,200	62/52	47
	7,500	62,100	35,400	60/53	50
	7,500	88,100	46,100	63/52	49
	12,000	86,100	45,000	62/54	49
PCL	–	67,600	41,500	65/56	52

[a] The molecular weights of PCL pre-polymers measured by ^{13}C NMR
[b] Measured by SEC

18%. The oxamide groups in the polymer structure had no substantial effect on the release profiles of low molecular weight drugs, as their release was in all cases diffusion controlled and closely followed square-root-of-time kinetics. In contrast, macromolecule release (FITC-dextran, M_w 4,400 g/mol) from polymer microparticles was clearly enhanced by the modification due to faster polymer degradation.

Further in vitro studies indicated, however, that the erosion behavior of polycaprolactone-based poly(ester-amides) can be greatly affected by the chosen hydrolysis medium [34]. When solvent cast films and injection molded bars of poly(ester-amides) were incubated in simulated intestinal fluid (SIF), a clear weight loss was observed already after 5 days (Fig. 5). At the same time notable changes in surface morphology of polymer samples were seen (Fig. 6).

The enhanced erosion behavior was related to the pancreatin (1 wt%) present in SIF. Pancreatin contains enzymes, principally amylase, lipase and protease.

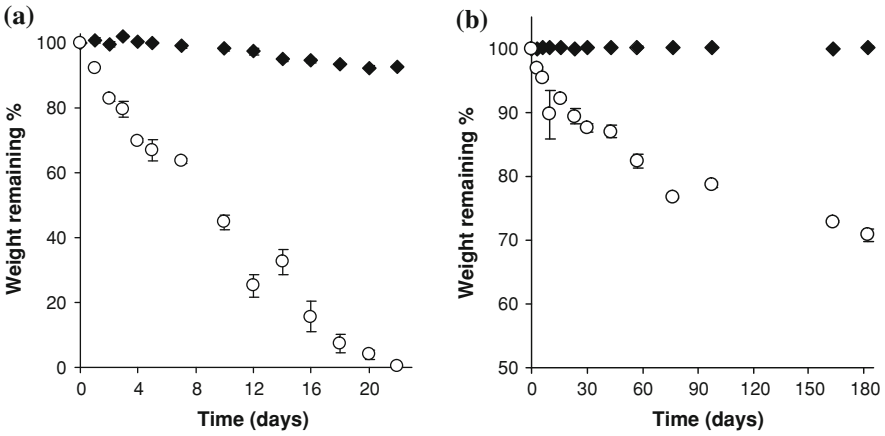

Fig. 5 Percentage of remaining weight of (*filled diamond*) PCL and (*open circle*) PLC-O **a** films and **b** bars incubated in simulated intestinal fluid at 37°C (Tarvainen et al. [34] reproduced with permission from Elsevier)

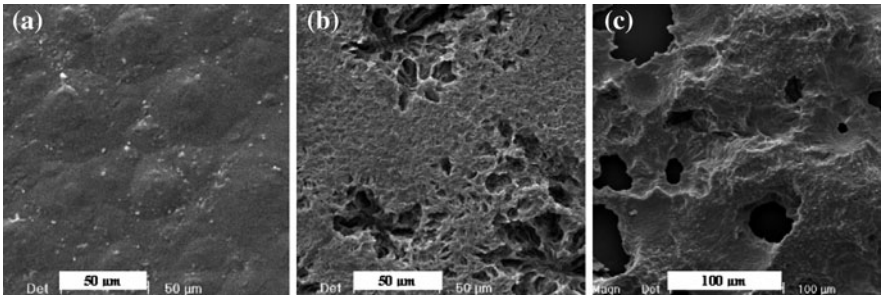

Fig. 6 SEM micrographs of PCL-O films **a** before incubation, **b** after 5 days and **c** after 18 days in simulated intestinal fluid at 37°C (Tarvainen et al. [34] reproduced with permission from Elsevier)

Pulkkinen et al. [35] concluded that the observed surface erosion is mainly due to the effect of lipase and that the erosion rate can be controlled by changes in the PCL block length. They also developed a straightforward mass spectrometric method for the analysis of enzymatic degradation products of poly(ester-amides). A wide variety of water-soluble oligomers have been separated and identified by high-performance liquid chromatography/electrospray ionization tandem mass spectrometry (HPLC/ESI-MS^n). According to these studies, pancreatic enzymes mainly cleaved ester bonds in the polymer chain, whereas amide bonds were left largely intact [36]. The enzyme sensitive surface erosion has also been confirmed in vivo (subcutaneous implantation of discs in rats for 12 weeks), and an evaluation based on hematology, clinical chemistry and histology of the implantation area and main organs demonstrated biocompatibility and safety of the studied poly(ester-amides) [37].

3.3 Polyphosphoesters

Polylactones based on phosphoester bonds in the main chain are hydrolytically degradable and have been claimed to be enzymatically resorbable in vivo. The phosphorus atoms in the polymeric chains are potential sites for ionic interactions and attachment of active agents. Polyphosphoesters have been investigated as potential polymers for use in tissue engineering, as well as drug and gene delivery. Properties like rate of degradation can be tailored during synthesis by modifying side chain hydrophobicity. Of special research interest is the hypothesis of improved biocompatibility of this class of the polymers due to enhanced tissue contact and the presence of phosphorus [38].

Studies have focused on the phosphoester derivatives of polylactides and their potential biomedical applications in drug delivery, as gene carrier substances, and as tissue engineering materials. The pentavalency of the phosphorous atom in the polyphosphoester backbone allows the conjugation of charged groups to the side

chain of the phosphate, producing cationic polyphosphates for use in non-viral gene delivery. The side chain of phosphate can also be varied to control hydrophobicity in order to tailor degradation properties of polymers.

Allcock et al. [39] reported synthesis methods for phosphorous-containing polymers. Polyphosphoesters can be produced synthetically through three different reaction mechanisms: ring-opening polymerization, polycondensation and transesterification (Fig. 7) [40, 41]. Of these methods, Puska et al. [42] applied polycondensation by using ethyldichlorophosphate as a coupling agent to chain extension of poly(ε-caprolactone). In vitro studies showed some indication of probable bioactivity of these polymers.

3.4 Poly(ester-anhydrides)

Polyesters and polyanhydrides differ significantly in the rate and mode of degradation. As a means of improving the degradation behavior and other properties of the two types of polymer, polyesters and polyanhydrides have been combined into various poly(ester-anhydrides) [10, 15, 43–45]. These polymers possess properties of individual polyesters and polyanhydrides and may therefore provide considerable advantages over either polymer alone. Besides having unique degradation profiles, poly(ester-anhydrides) have the potential for surface modification, making the delivery potential of poly(ester-anhydride) devices similar to that of polyanhydride devices [46, 47].

In our studies, the preparation of poly(ester-anhydrides) consisted of three steps. Hydroxyl-terminated pre-polymers were prepared by ring-opening polymerization of cyclic esters in the presence of a co-initiator containing the hydroxyl group. In the next step, terminal hydroxyl groups were converted to carboxylic

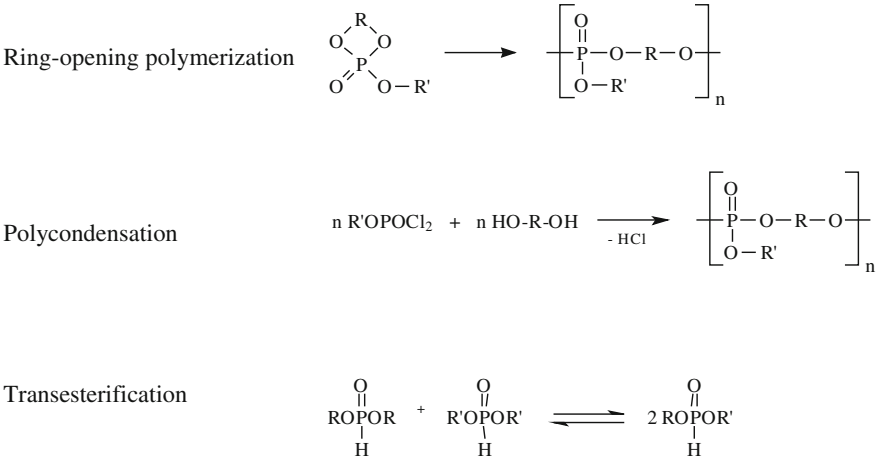

Fig. 7 Polyphosphoester synthesis routes

acid functionality by reaction of the hydroxyl groups with succinic or alkenylsuccinic anhydride. In the final step, carboxylic acid groups were converted to anhydrides with acetic anhydride, and these intermediates were coupled to poly(ester-anhydrides) by melt polycondensation. Upon coupling of PCL-based pre-polymer, size exclusion chromatography (SEC) analyses showed an increase from 3,600 to 70,000 g/mol in number average molecular weight.

Polyester precursors were prepared from L-lactide, DL-lactide and ε-caprolactone. In addition to the different monomers used, the structure of the pre-polymers was modified using ricinoleic acid and alkenylsuccinic anhydrides with different chain lengths as hydrophobic components in the syntheses of pre-polymers. The chemical structures of the different poly(ester-anhydrides) studied are shown in Fig. 8.

In dissolution, all the poly(ester-anhydrides) showed hydrolysis of anhydride linkages within a few days. A rapid disappearance of the anhydride peak was detected irrespective of the monomer used. In addition, the use of ricinoleic acid or alkenylsuccinic anhydride did not affect the rate of hydrolysis of anhydride linkages. It thus seems that an increase in the hydrophobicity of polymers was not sufficient to markedly slow the penetration of water into the specimen.

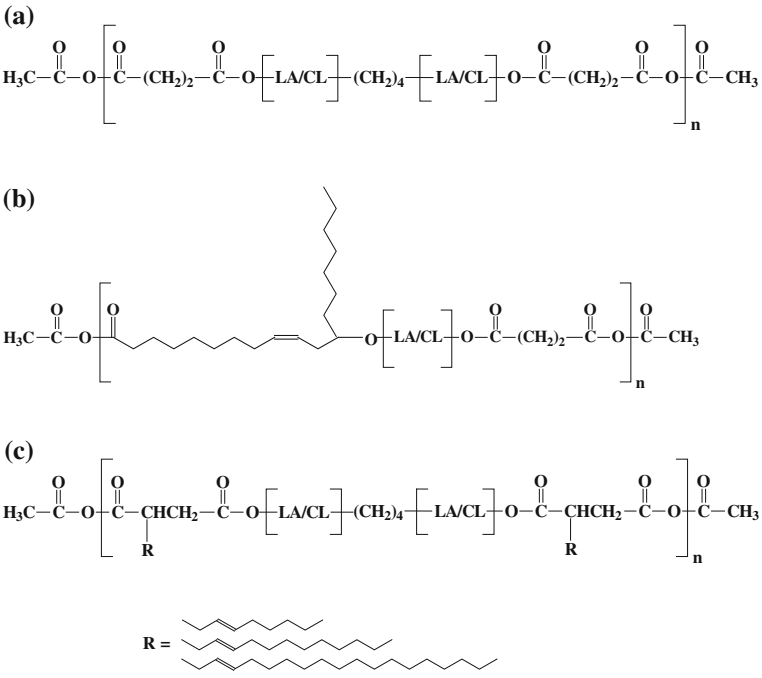

Fig. 8 Chemical structures of different poly(ester-anhydrides): **a** poly(ester-anhydrides) from different monomers, **b** ricinoleic acid initiated poly(ester-anhydrides), **c** alkenylsuccinic anhydride functionalized poly(ester-anhydrides)

After hydrolysis of the anhydride bonds, mass loss of the poly(ester-anhydrides) depended on the composition of the original polyester pre-polymer, and the mass loss was greatly affected by the molecular weight and thermal properties of the pre-polymers. The differences in loss of mass attributable to the monomer used are shown in Fig. 9. For poly(ester-anhydrides) prepared from pre-polymers with thermal transitions below 37°C, hydrolysis of anhydride linkages was accompanied by rapid mass loss caused by fast dissolution of the degradation products. When thermal transitions of pre-polymers were above the hydrolysis temperature, the poly(ester-anhydrides) showed a clear two-stage degradation: a rapid hydrolysis of anhydride linkages was followed by slower hydrolysis and mass loss of the remaining polyester oligomer.

In the case of ricinoleic acid-initiated poly(ester-anhydrides), mass loss in hydrolysis was greatest for the polymer with the highest ricinoleic acid content, although it would have been expected to be the most hydrophobic polymer. Since this polymer had the lowest melting temperature, it seems that for ricinoleic acid-initiated polymers, as for 1,4-butanediol-initiated (BD) polymers, chain length and thermal properties are the most critical factors affecting the solubility of polyester precursors and thus the rate of degradation.

The presence of an alkenyl chain in the polyester precursor had a marked effect on the thermal properties and hydrolysis behavior of the poly(ester-anhydrides). For poly(ester-anhydrides) prepared from low molecular weight pre-polymers (PDLLA-BD10-AHs) with thermal transitions below 37°C, the presence of hydrophobic alkenyl chains in the polyester precursors slowed the rate of mass loss. As seen in Fig. 8a, poly(ester-anhydrides) without an alkenyl chain showed rapid mass loss within a few days, while ASA-functionalized polymers exhibited a much lower rate of mass loss over 4 weeks of immersion. Differences in lengths of the alkenyl chain, as such, had little effect on the mass loss behavior of the ASA-functionalized poly(ester-anhydrides).

Poly(ester-anhydrides) prepared from higher molecular weight pre-polymers (PDLLA-BD5-AHs) showed a different mass loss behavior. Among the polyester

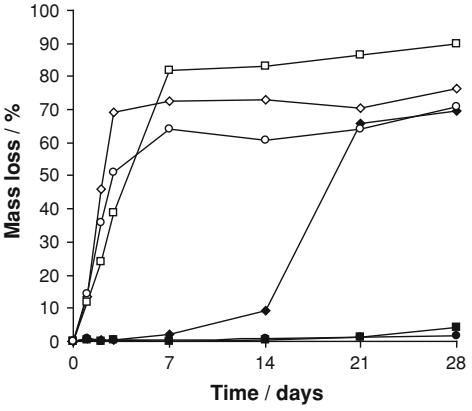

Fig. 9 Mass loss of 1,4-butanediol-initiated poly(ester-anhydrides) during immersion in PBS (pH 7.0) at 37°C (*filled diamond*, DLLA-BD5; *open diamond*, DLLA-BD10; *filled square*, LLA-BD5; *open square*, LLA-BD10; *filled circle*, CL-BD5; *open circle*, CL-BD10) (Korhonen et al. [10], reproduced with permission from Wiley–VCH)

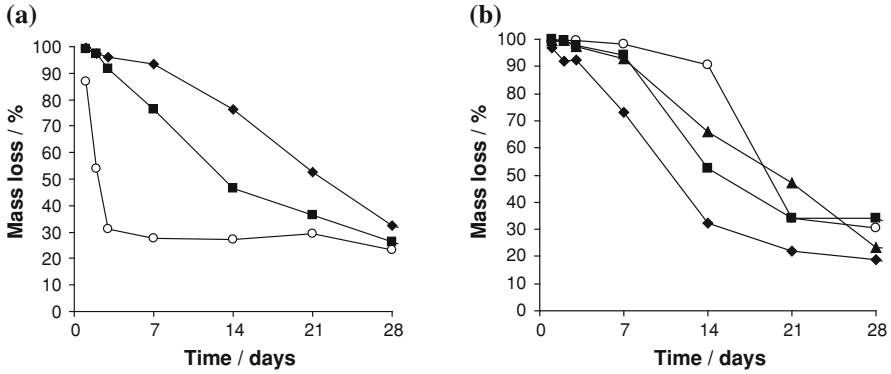

Fig. 10 Mass loss of **a** PDLLA-BD10-AHs and **b** PDLLA-BD5-AHs with different alkenyl chain lengths during immersion in PBS (pH 7.0) at 37°C: (*open circle*) 0, (*filled square*) 8, (*filled diamond*) 12, or (*filled triangle*) 18 carbons (Korhonen et al. [15] reproduced with permission from Wiley–VCH)

precursors and poly(ester-anhydrides), thermal transitions of alkenylsuccinic anhydride-functionalized polymers tended to be 10–15°C lower than those of the corresponding polymers without an alkenyl chain. Due to lower crystallinities and thermal transitions, alkenyl chain-containing poly(ester-anhydrides) showed a faster mass loss than poly(ester-anhydrides) without an alkenyl chain (Fig. 10b).

4 Crosslinked Polylactones

Another class of biopolymers besides thermoplastics is crosslinked degradable polymers. Crosslinking has been used to obtain polymers with high strength or with elastic properties [48, 49]. The preparation of the crosslinked polyesters usually comprises several steps. This more complicated synthesis, as compared to the preparation of thermoplastic polyesters, can be seen to provide opportunities not only for structural tailoring but also for processing. By using liquid polyester precursors with low viscosity, even in situ curing can be used in the formation of highly crosslinked networks [50–52].

Biodegradable crosslinked materials prepared from lactides and ε-caprolactone do not inherently contain groups that can form primary bonds between the polymer chains. Thus they have been made crosslinkable by functionalizing low molecular weight pre-polymers with suitable reactive end groups [12, 51, 53–55]. Due to the good reactivity of acrylic and methacrylic double bonds, they have been commonly used in the preparation of resorbable networks. Acrylated or methacrylated poly(α-hydroxy acid) precursors have often been synthesized by functionalizing hydroxyl-terminated oligomers with the corresponding acid chloride [56–59].

Our research (Fig. 11) has focused on the preparation of crosslinked resorbable polyesters and poly(ester-anhydrides) from oligomers based on lactides,

ε-caprolactone and their copolymers [53–55, 60]. In our studies, the methacrylation of the OH- and COOH-terminated oligomers has been mainly carried out with methacrylic anhydride (MAAH), similar to the preparation of crosslinked polyanhydrides and poly(ether-anhydrides) [50, 61, 62]. Crosslinking of the methacrylated precursors has been carried out mainly with thermal initiation. Dibenzoyl peroxide has been used to initiate the crosslinking at temperatures where all the functionalized precursors are in the liquid state and the peroxide can be added to the reaction mixture. However, our recent studies have focused on polymers that can be crosslinked by light curing [63–66].

4.1 Hard and Rigid Networks

The dependence of the properties of the networks on their structure was shown with hard and rigid PDLLA networks by Storey et al. [67]. The properties of networks are governed by the properties of the constituent monomers, but also by the crosslinking density, which is related to the distance between the crosslinking points. When the crosslinking density is high, i.e. the chain lengths between the crosslinks are short, the glass transition temperature and modulus are higher [67].

In our study, PDLLA-based networks were used to reveal the effects of precursor structure on the properties of crosslinked networks [53]. PDLLA-based networks retained the inherent mechanical properties of the thermoplastic PDLLA. As shown in Table 2, the crosslinked networks are hard and rigid, exhibiting

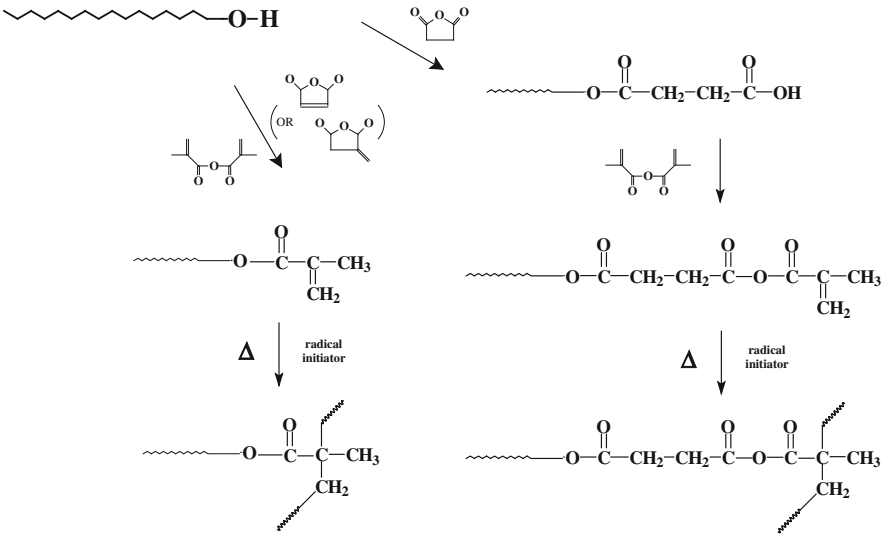

Fig. 11 Functionalization and crosslinking reactions of resorbable polyesters and poly(ester-anhydrides)

Table 2 Compressive and thermal properties of the crosslinked PDLLA prepared via methacrylic anhydride functionalization [53]

Sample	Composition	Yield strength (MPa)	Yield strain (%)	Modulus (GPa)	Gel-% (%)	Tg (°C)	ΔH (J/g)
P(DLLA/BD 100:5)	10/100	78 ± 2	6.5 ± 0.4	1.8 ± 0.3	85	42	0
P(DLLA/BD 100:10)	20/100	72 ± 3	5.2 ± 0.2	1.8 ± 0.1	85	40	0
P(DLLA/PERYT 100:5)	20/100	91 ± 5	6.7 ± 1.0	2.0 ± 0.1	95	46	0
P(DLLA/PERYT 100:8)	32/100	120 ± 4	5.0 ± 0.1	2.8 ± 0.1	99	49	0
P(DLLA/PERYT 100:12.5)	50/100	107 ± 14	5.5 ± 0.4	2.5 ± 0.2	99	51	4
P(DLLA/PGL-06 100:5)	40/100	101 ± 8	4.7 ± 0.3	2.6 ± 0.1	100	56	0
P(DLLA/PGL-10 100:5)	60/100	116 ± 3	5.8 ± 0.3	2.4 ± 0.2	97	54	0

compressive yield strains from 4 to 7%, compressive yield strengths of 70–120 MPa and moduli of 1,800–2,800 MPa, depending on the molecular structure. For thermoplastic PDLLA, Grijpma et al. [68] have described rather ductile behavior with a compressive strain of over 30% and a compressive stress over 100 MPa.

By comparing PDLLA networks prepared with equal amounts of co-initiator (100:5) but containing different numbers of hydroxyl groups (BD, PERYT, PGL-06 and PGL-10), the increase in branching of the precursor can be seen to lead to higher compressive strengths and moduli (Table 2). This is due to the increase in reactive double bonds in the precursors and the resultant higher crosslinking density of the networks. In addition, the T_g increased with branching due to the more restricted movement of chain segments. Overall, branched oligomers yielded networks with higher yield strengths and moduli than the linear precursors. Networks from linear precursors only have crosslinking points originating from crosslinking sites, whereas the branched oligomers already contain crosslinking points in their structures in addition to the final crosslinking bonds formed during curing.

4.2 Elastic Networks

In contrast to hard and rigid PDLLA polymer networks, properties of networks can be tailored using P(CL/DLLA) copolymer precursors [54, 69]. Amsden [70] has recently reviewed synthesis strategies for curable biodegradable elastomers. In our studies, the range of mechanical properties achievable by crosslinking has been extended to soft and elastic polymer networks, which were prepared from

star-shaped P(CL/DLLA) precursors differing from each other in their molecular weights and CL/DLLA ratios [54]. The swelling factor of the networks showed that lower molecular weight oligomers yielded networks with a higher crosslinking density, i.e. the distance between the crosslinks was smaller. The T_g values supported the swelling results by indicating a higher T_g for samples with a shorter distance between the crosslinks, even though the corresponding precursors exhibited lower T_g values. Higher crosslinking density was also found to increase tensile modulus and maximum strain.

The ratio of CL/DLLA was also found to have a pronounced effect on the properties of the networks, as shown in Fig. 12. In general, the properties followed the same trends as the thermoplastic P(CL/DLLA) copolymers. When the DLLA portion was increased to 50 mol.%, the networks showed higher strain values and decreased tensile strengths and moduli. With a further increase in DLLA content in the copolymer networks, the stiffness of the polylactide chains caused an increase in the modulus and strength. Similar effects of the CL/DLLA ratio on moduli in copolymer networks have also been shown by Storey et al. [71] and Davis et al. [57].

4.3 Poly(ester-anhydride) Networks

To increase the degradation rate of the crosslinked polyesters, we incorporated anhydride bonds into the polyester precursors [60, 64]. Crosslinkable poly(ester-anhydride) precursors were prepared by allowing carboxylic acid-terminated polyester oligomers to react with methacrylic anhydride, as shown in Fig. 13. Upon thermal crosslinking [60], the polymers changed from sticky or waxy oligomers into hard polymer specimens that showed considerable swelling in CH_2Cl_2. Like linear thermoplastic poly(ester-anhydrides), crosslinked lactide-based poly(ester-anhydrides) showed a two-stage degradation profile in which a rapid cleavage of anhydride bonds was followed by the degradation and dissolution of constituent oligomers [9, 60].

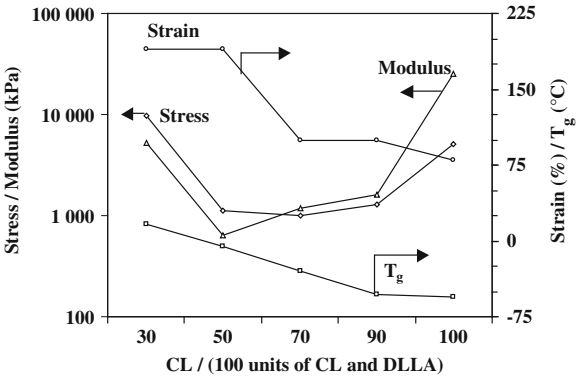

Fig. 12 Tensile stress, modulus, strain at break and T_g of the polymer networks as a function of the amount of CL per 100 monomer (CL + LA) units [54]

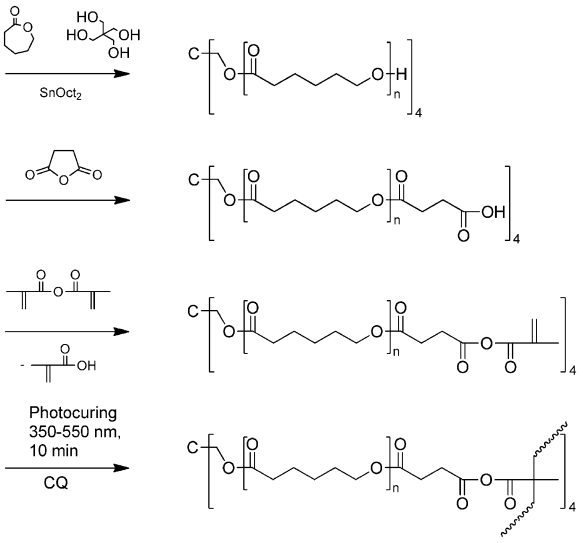

Fig. 13 Preparation of poly(ester-anhydride) networks [64]

In addition to thermal curing, the low melting point of star-shaped PCL-based poly(ester-anhydride) precursors enabled photocrosslinking with visible light (Fig. 13) [64]. The advantage of photocrosslinking is that a wide variety of drugs and heat-sensitive macromolecules can be entrapped as solid powders into the photocrosslinkable polymer network under mild reaction conditions without the need for heat or solvents [62, 72]. In addition, photocrosslinking is thought to be a suitable method for in situ administration as injectable oligomers can be polymerized in a rapid and controlled manner at physiological temperatures [50, 73].

As shown in Fig. 14, these photocrosslinked PCL-based poly(ester-anhydrides) degraded in a few days in vitro and in vivo. In addition, the dimensions of the specimen decreased steadily and showed clear signs of surface erosion, with a linear mass loss but a practically intact core (Fig. 14, bottom) [64].

The drug release and safety of the photocrosslinked poly(ester-anhydrides) in vitro and in vivo was also studied. A small water-soluble drug, propranolol HCl, was used as the model drug in an evaluation of the erosion-controlled release. Drug-free and drug-loaded (10–60% w/w) poly(ester-anhydride) discoids eroded in vitro linearly within 48 h (Fig. 15). A strong correlation between the polymer erosion and the linear drug release in vitro was observed, indicating that the release was controlled by the erosion of the polymer. Similarly, in vivo studies (subcutaneous implantation of discoids in rats) indicated that drug release from the discoids was controlled by surface erosion. In addition, oligomers did not decrease cell viability in vitro and the implanted discoids did not evoke any cytokine activity in vivo [64].

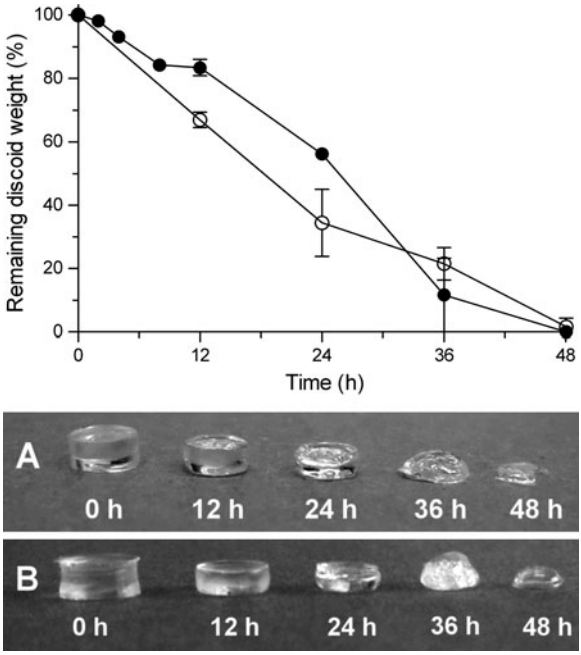

Fig. 14 Erosion of poly(ester-anhydride) discoids in vitro (*filled circle*) and in vivo (*open circle*) (*top*) and cores of drug-free poly(ester-anhydride) discoids in vitro (*A*) and in vivo (*B*) (*bottom*) (Mönkäre et al. [64, 65] reproduced with permission from Elsevier)

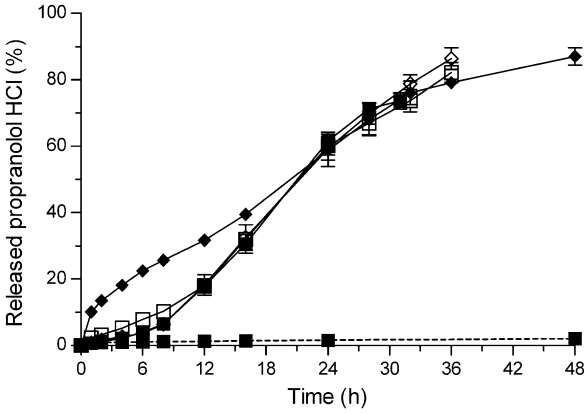

Fig. 15 Drug release from poly(ester-anhydride) discoids (*solid line*) and corresponding polyester discoids without anhydride bonds (*dashed line*) in vitro (pH 7.4, +37°C). Drug loading: *filled square*, 10%; *open diamond*, 20%; *open square*, 40% and *filled diamond*, 60% propranolol HCl (Mönkäre et al. [64, 65] reproduced with permission from Elsevier)

In a recent study, crosslinked poly(ester-anhydrides) have been used for sustained macromolecular drug delivery in vivo. The macromolecular drug used was peptide $YY_{3\text{-}36}$ ($PYY_{3\text{-}36}$, M_w 3,900 g/mol). $PYY_{3\text{-}36}$ loaded (1% w/w) discoids were implanted subcutaneously into rats. When compared with subcutaneous administration of $PYY_{3\text{-}36}$ solution, $PYY_{3\text{-}36}$-loaded poly(ester-anhydride) discoids resulted in sustained delivery of $PYY_{3\text{-}36}$. Results indicate that photocrosslinked poly(ester anhydrides) can be used for delivery of macromolecules [65].

5 Tissue Engineering Scaffolds

Bioresorbable polymers have received increasing attention in reconstructive medicine. Their role has expanded from traditional fixation devices to bone substitutes and scaffolds used for tissue engineering. Besides the chemistry and material properties of the scaffold and the local cell morphology, the function of the scaffold is dependent on its proper design. As the scaffold should act as a template to direct cell growth in three dimensions, porous 3D structures are preferred. Porosity, pore size, and pore structure are important factors to be considered with respect to oxygen and nutrient supplies to transplanted and regenerated cells. An interconnected pore network enhances the diffusion rates to and from the center of the scaffold and facilitates vascularization. By choosing appropriate processing techniques, scaffolds of specific architecture and structural characteristics may be fabricated. Our approach has focused on techniques available for crosslinking bioresorbable polymers.

5.1 Bioactive Composite Scaffolds Prepared by Salt Leaching

Bioresorbable polymers may be used to support cell growth in vitro, to direct tissue growth in vivo and to deliver bioactive molecules. Bioactive glasses are surface-active ceramic materials that bond chemically to bone minerals. Clinical use of bioactive ceramics has so far been restricted due to their limited handling properties and lack of a proper carrier material. To overcome these problems it has been of interest to us to produce composite scaffold structures with interconnective porosity.

Our first studies on preparing porous and elastic composite scaffolds (Fig. 16) for non-load-bearing tissue engineering applications utilized a simple and cheap particle leaching method. Porous matrices and composites with bioactive glass

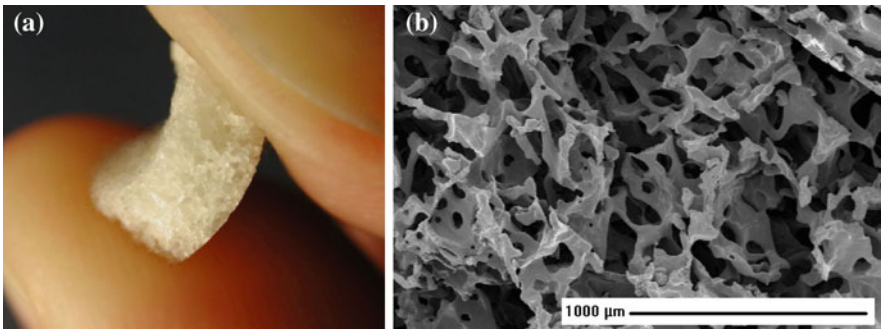

Fig. 16 Photograph of **a** elastic composite scaffold and **b** SEM picture of the structure

(BAG) S53P4 (Vivoxid Ltd., Finland) were prepared by mixing the crosslinkable copolyester P(CL/DLLA) with a crosslinking initiator together with BAG granules and sieved sodium chloride, NaCl crystals (size range 400–600 μm) [74]. The mixture was then thermally cured in a mold, and the salt crystals were leached with distilled water to obtain the final porous scaffold structure. The size of the pores corresponded well with the size of the NaCl crystals, and porosity volumes could be easily altered by changing the amount of salt. In vitro the composite showed silica solubility and calcium phosphate (CaP) precipitation ability in simulated body fluid (SBF), although the pre-treatment of the composite structure was found to inhibit BAG-solution interactions. The major drawback of this method was, however, that the desired interconnective porosity was not obtained.

A great success in applying the salt leaching technique was achieved when calcium chloride hexahydrate, $CaCl_2 \cdot 6H_2O$, was used as a porogen agent. These salt crystals contain high amounts of combined water and have a low decomposition temperature. A continuous porogen phase was formed during photocuring of the scaffolds. The bioactive glass filler remained essentially inert during the stage when the salt was leached with ethanol. As a result, scaffolds with 60–80 vol% continuous phase macroporosity (typically 100–300 μm) were obtained and composites with BAG showed high ceramic dissolution as well as calcium phosphate formation in vitro [75].

Meretoja et al. [76] compared osteogenic differentiation and scaffold colonization in rat bone marrow stromal cell cultures of porous polymer scaffolds with composites containing 30 wt% of bioactive glass filler. In these studies, composites enhanced proliferation, early osteogenic differentiation, and mineralization of cultured cells under static conditions. The cells grew on the surface of the scaffolds and a confluent cell layer was formed within 7 days. Use of a rotating wall bioreactor caused penetration of the cells into the scaffold interior, but at the same time decreased the number of cells and partly inhibited their differentiation process.

Preliminary in vivo tests [77] with cell-free scaffolds and cultured cell-scaffold constructs subcutaneously implanted in rats showed that well-vascularized soft connective tissue invaded the scaffolds during 4 weeks of implantation and 1 week of implantation, respectively. Both scaffold types were biocompatible, but bone formation occurred only within cell-scaffold constructs after 12 weeks of implantation. Further optimization of dynamic culture conditions in vitro and investigation of bone formation in vivo are essential and are currently underway.

5.2 Crosslinked Poly(ester-anhydrides) as Porogen Materials

Poly(ester-anhydrides) are expected to find use in tissue engineering and in controlled release applications. In order to demonstrate the potential of poly (ester-anhydrides) in these applications, the use of poly(ester-anhydride) fibers as

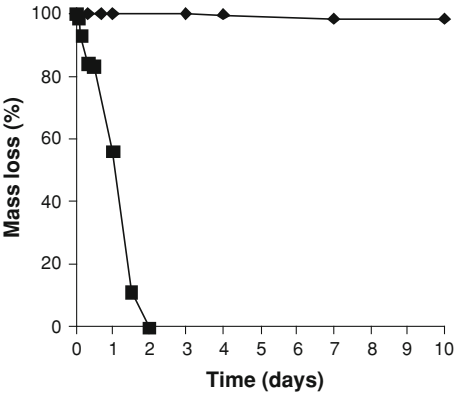

Fig. 17 Degradation of poly(ester-anhydride) fibers (*filled square*) and the polyester matrix (*filled diamond*) during immersion in PBS (pH 7.0) at 37°C (Rich et al. [66] reproduced with permission from Wiley–VCH)

porogen materials was investigated. Fast-eroding poly(ester-anhydride) fibers were selectively leached from a more slowly-degrading polyester matrix to form a predetermined pore structure within the matrix material [66]. The degradation rates for the poly(ester-anhydride) fibers and for the polyester matrix are shown in Fig. 17.

Porogen fibers were prepared by photo curing and they were used in the form of elastic fiber mats or mesh. The fibers were half-moon shaped with a thickness of 100 μm and diameters of 450–850 μm along the wider edge. During incubation, poly(ester-anhydride) porogens dissolved from the photo-cured polyester matrix within 1 week. The shapes and dimensions of the pores formed in hydrolysis closely corresponded to those of the original porogen fibres. Furthermore, micro-CT images showed that porosity mimicked the form and dimensions of the porogen mat or mesh throughout the matrix sample. The porosities estimated by micro-CT were 30–39%, while the amount of porogen added to the matrix was 30 wt%.

One of the main rationales for producing polymeric fiber porogens was the possibility of including bioactive agents in the porogen fibers. The bioactive agent would be readily available in the scaffold as pore formation proceeded and porogen fibers eroded. Bioactivity was introduced in the form of bioactive glass and different amounts of bioactive glass were mixed with the poly(ester-anhydride) resin when preparing the fiber mesh. Since bioactive glass increased viscosity of the resin, the highest BAG content that allowed fabrication of fibers was 40 wt%. The reactivity of BAG-containing composites was studied in vitro by carrying out a dissolution study in simulated body fluid. The overall reactivity of BAG in the composites was monitored by dissolution of silica. Calcium phosphate formation, indicating (bone) bioactivity of the material, was verified by the decrease in the phosphate concentration in SBF. Silica and phosphorus concentrations in SBF as a function of immersion time are shown in Fig. 18.

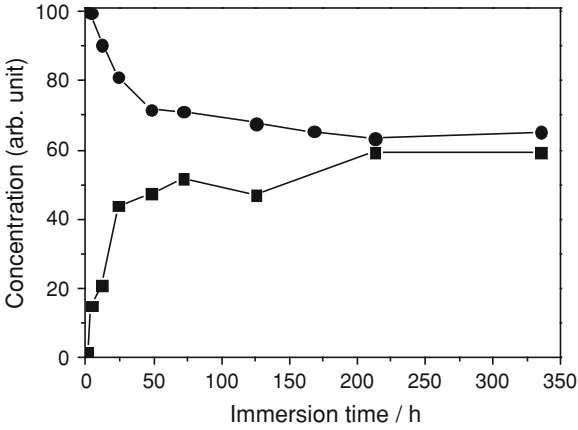

Fig. 18 Changes in silica (*filled square*) and phosphorus (*filled circle*) concentrations in SBF as a function of immersion time for scaffold containing 50% BAG fiber (BAG content 40% in the fiber) (Rich et al. [66], reproduced with permission from Wiley–VCH)

5.3 Micromolding in Capillaries

Micromolding in capillaries (MIMIC) is a method of fabricating patterned microstructures of polymeric materials by molding them in enclosed, continuous channels formed between a solid support and an elastomeric master with a patterned surface. When a low-viscosity liquid pre-polymer is placed at the open ends of the network of channels, the liquid spontaneously fills the channels by capillary action. After filling the channels, the pre-polymer is cured, resulting in microstructures in a pattern complementary to that present in the mold [78].

PCL-based low molecular weight photocurable oligomer was used for testing the applicability of MIMIC to the preparation of polymeric scaffolds. A lithographic master was used for fabrication of an elastomeric polysiloxane mold. In the preparation of scaffolds, individual PCL layers were prepared first by MIMIC. Partly cured layers were then manually stacked and a final curing was done. Figure 19 shows that well-organized structures with inter-connected porosity can be prepared by this method. Furthermore, composites with 30 wt% of bioactive glass (BAG) filler were successfully prepared, imparting bioactivity to the scaffold.

5.4 Stereolithography

To fabricate a porous 3D structure, a number of conventional methods such as salt leaching and gas foaming have been utilized. To build extremely complex and accurate 3D structures, rapid prototyping (RP) methods have been developed. Stereolithography (SLA) is one of the most important RP methods. By SLA, 3D structures can be built utilizing photopolymerization of liquid polymeric materials

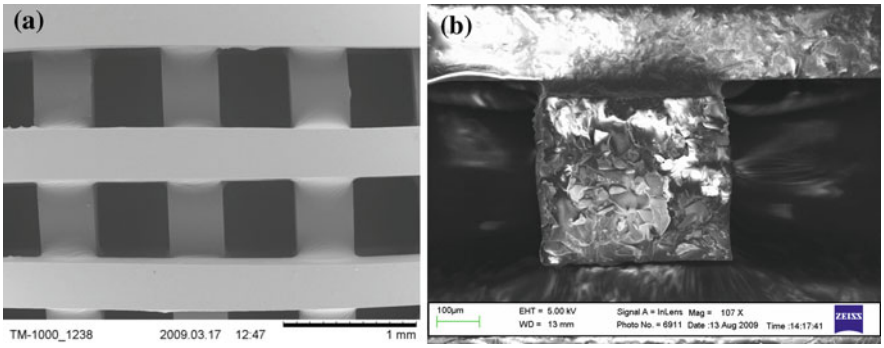

Fig. 19 SEM micrographs of **a** PCL-based scaffold, **b** PCL-based composite with 30 wt% of bioactive glass prepared by micromolding in capillaries

to produce solid crosslinked networks with the desired shape and microstructure. A variety of photopolymers are available for SLA but only a few of them are biodegradable. Promising results have been obtained by Jansen et al. [79] and Melchels et al. [80] who used LLA-based biodegradable resins.

In a recent study by us in co-operation with Twente University, a biodegradable polymer resin suitable for SLA was prepared [63]. Three-branched PCL oligomers were synthesized using trimethylolpropane as a co-initiator. Oligomers were then methacrylated with methacrylic anhydride to prepare a suitable photocrosslinkable macromer. The molecular weights of the oligomers were tailored by varying the amount of co-initiator: the smaller the amount of TMP, the longer the PCL chains. The melting temperatures of the oligomers were in the range of 23–54°C. Molten polyester macromers were photocrosslinked using Irgacure 2959 photoinitiator and 365 nm UV light. The macromer with the

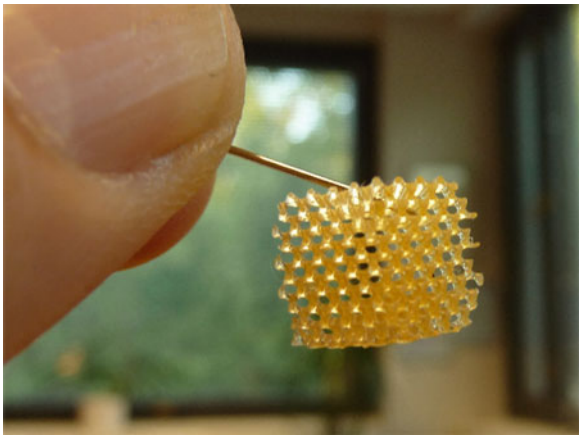

Fig. 20 Photograph of a PCL-based scaffold prepared by SLA [63]

lowest molecular weight, 1500-ohm, was the most densely crosslinked and its gel content was 98.2%. Cytotoxicity of the crosslinked networks was tested using skin cells. Cell experiments showed good biocompatibility, with the cells spread evenly onto the surface of the network samples, and good metabolic activity was detected.

Porous, three-dimensional tissue engineering scaffolds were built by SLA (Fig. 20). No solvent was used in SLA, but macromers were heated above the melting point to obtain a suitable viscosity for the resin. Characterization proved that the scaffolds had highly-defined micro- and macrostructure. The average porosity was found to be 70.5% when the designed porosity was 70%. More than 90% of the pores were in the range of 350–550 μm in diameter, and the average pore size was 465 μm. The scaffolds accurately adopted the structure modeled by computer-aided design.

5.5 Two-Photon Polymerization

The principle of two-photon polymerization (2PP) is somewhat similar to that of the stereolithography technique, but 2PP provides much better structural resolution and quality. Unique opportunity to reach micrometer or even sub-micrometer resolution is enabled by utilizing photocurable biopolymers for 2PP. Preliminary results [81] show that two-dimensional structures with high resolution can be prepared by two-photon polymerization from photocurable poly(ε-caprolactone) resin (Fig. 21). Currently, the process parameters and resin properties are being further optimized to prepare precise 3D structures. The challenge is to master viscosity-curing balance in the process.

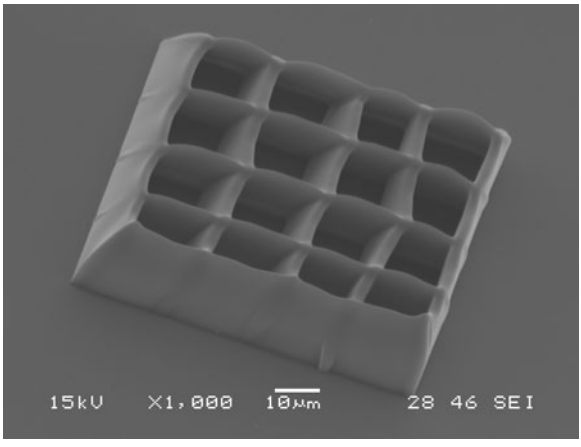

Fig. 21 SEM micrograph of a PCL lattice prepared by two-photon polymerization [81]

6 Conclusions

Chain extension, coupling and crosslinking offer practical alternatives to ring opening homo- and copolymerization for tailoring polymer properties and producing novel biomedical polymers. Telechelic, functional polymers can be based on various monomers, largely determining the nature of the final polymers. By using different coupling chemistries, several linear and network-structured polymer families have been synthesized. The biopolymer families with the most potential are poly(ester-urethanes), poly(ester-amides), poly(ester-urethane-amides), poly(phosphoesters) and poly(ester-anhydrides) and methacrylated crosslinked polyesters. These polymer families have shown a wide range of properties having potential in the biomedical field. Mechanical properties can be tailored, giving polymers ranging from those with bone-like hardness to soft non-creeping elastomers.

Degradation rates and mechanisms of biopolymers can be adjusted over a broad range. The degradation rates can vary from days to several months. Some poly(ester-amides) have shown an enzyme-activated, fast surface erosion degradation. Rapidly surface eroding poly(ester-anhydrides) enable degradation-based zero-order active agent release, including sustained and controlled release of macromolecular active agents like peptides. Controlled release of a high load of small molecular weight active agents in a time span of tens of hours has been demonstrated using poly(ester-anhydrides). This has a potential application in the oral administration of medications.

Control of the liquid to solid transition in biopolymers opens up new possible applications. Specific molecular architectures combined with controlled crosslinking chemistries enable synthesis of thermosetting or photocuring biopolymers. These polymers have great potential in bioactive composite manufacturing. The future is in the production of customized, highly precise bioactive scaffolds produced with methods that combine novel biomaterials, medical imaging, computer design and rapid manufacturing methods like stereolithography.

References

1. Nair, L.K., Laurencin, C.T.: Biodegradable polymers as biomaterials. Progress Polym. Sci. **32**, 762–798 (2007)
2. Auras, R., Harte, R., Selke, S.: An overview of polylactides as packaging materials. Macromol. Biosci. **4**, 835–864 (2004)
3. Van de Velde, K., Kiekens, P.: Polymer testing, biopolymers: overview of several properties and consequences on their applications. Polym. Test. **21**, 433–442 (2002)
4. Seppälä, J.V., Korhonen, H., Kylmä, J., Tuominen, J.: General methodology for chemical synthesis of polyester. In: Doi, Y., Steinbüchel, A. (eds.) Biopolymers vol 3b: polyesters II—properties and chemical synthesis, pp. 327–369. Wiley–VCH, Weinheim (2002)
5. Kowalski, A., Duda, A., Penczek, S.: Mechanism of cyclic ester polymerization initiated with tin(II) octoate. 2. Macromolecules fitted with tin(II) alkoxide species observed directly in MALDI-TOF spectra. Macromolecules **33**, 702–709 (2000)

6. Narayanan, N., Roychoudhury, P.K., Srivastava, A.: L(+) lactic acid fermentation and its product polymerization. Electron. J. Biotechnol. **7**, 167–179 (2004)
7. Seppälä, J.V., Helminen, A.O., Korhonen, H.: Degradable polyesters through chain linking for packaging and biomedical applications. Macromol. Biosci. **282**, 208–217 (2004)
8. Korhonen, H., Helminen, A., Seppälä, J.V.: Synthesis of polylactides in the presence of co-initiators with different numbers of hydroxyl groups. Polymer **42**, 7541–7549 (2001)
9. Korhonen, H., Seppälä, J.V.: Synthesis of poly(ester-anhydride)s based on poly(ε-caprolactone) prepolymer. J. Appl. Polym. Sci. **81**, 176–185 (2001)
10. Korhonen, H., Helminen, A., Seppälä, J.V.: Synthesis of poly(ester-anhydrides) based on different polyester precursors. Macromol. Chem. Phys. **205**, 937–945 (2004)
11. Kim, S.H., Han, Y.K., Kwang-Duk, A., Kim, Y.H., Taihyun, C.: Preparation of star-shaped polylactide with pentaerythritol and stannous octoate. Macromol. Chem. **194**, 3229–3236 (1993)
12. Lang, M., Chu, C.C.: Functionalized multiarm poly(ε-caprolactone)s: synthesis, structure analysis, and network formation. J. Appl. Polym. Sci. **86**, 2296–2306 (2002)
13. Burgath, A., Sunder, A., Neuner, A., Mülhaupt, R., Frey, H.: Multi-arm star block copolymers based on ε-caprolactone with hyperbranched polyglycerol core. Macromol. Chem. Phys. **201**, 792–797 (2000)
14. Hakala, R.A., Korhonen, H., Holappa, S., Seppälä, J.V.: Hydrophobicities of poly(ε-caprolactone) oligomers functionalized with different succinic anhydrides. Eur. Polym. J. **45**, 557–564 (2009)
15. Korhonen, H., Hakala, R.A., Helminen, A.O., Seppälä, J.V.: Synthesis and hydrolysis behaviour of poly(ester-anhydrides) from polyester precursors containing alkenyl moieties. Macromol. Biosci. **6**, 496–505 (2006)
16. Chi, H., Xu, K., Xue, D., Song, C., Zhang, W., Wang, P.: Synthesis of dodecenyl succinic anhydride (DDSA) corn starch. Food Res. Int. **40**, 232–238 (2007)
17. Lin, L.H., Chen, K.M.: Preparation and surface activity of modified soy protein. J. Appl. Polym. Sci. **102**, 3498–3503 (2006)
18. Tangpasuthadol, V., Pongchaisirikul, N., Hoven, V.P.: Surface modification of chitosan films. Effects of hydrophobicity on protein adsorption. Carbohydr. Res. **338**, 937–942 (2003)
19. Hiltunen, K., Seppälä, J., Härkönen, M.: Lactic acid based poly(ester-urethanes). Use of hydroxyl terminated pre-polymer in urethane synthesis. J. Appl. Polym. Sci. **63**, 1091–1100 (1997)
20. Hiltunen, K., Seppälä, J., Härkönen, M.: Lactic acid based poly(ester-urethanes). The effects of different polymerization conditions on the polymer structure and properties. J. Appl. Polym. Sci. **64**, 865–873 (1997)
21. Helminen, A., Kylmä, J., Tuominen, J., Seppälä, J.V.: Effect of structure modification on rheological properties of biodegradable poly(ester-urethane). Polym. Eng. Sci. **40**, 1655–1662 (2000)
22. Kylmä, J., Seppälä, J.: Synthesis and characterization of biodegradable thermoplastic Poly(ester-urethane) elastomer. Macromolecules **30**, 2876–2883 (1997)
23. Kylmä, J., Härkönen, M., Seppälä, J.: The modification of lactic acid based poly(ester-urethane) by copolymerization. J. Appl. Polym. Sci. **63**, 1865–1872 (1997)
24. Hiljanen-Vainio, M., Kylmä, J., Hiltunen, K., Seppälä, J.: Impact modification of lactic acid based poly(ester-urethanes) by blending. J. Appl. Polym. Sci. **63**, 1335–1343 (1997)
25. Kylmä, J., Hiljanen-Vainio, M., Seppälä, J.: Miscibility, morphology and mechanical properties of rubber-modified biodegradable poly(ester-urethanes). J. Appl. Polym. Sci. **76**, 1074–1084 (2000)
26. Tuominen, J., Kylmä, J., Seppälä, J., Kapanen, A., Venelampi, O., Itävaara, M.: Biodegradation of lactic acid based polymers under controlled composting conditions and evaluation of the ecotoxicological impact. Biomacromolecules **3**, 445–455 (2002)
27. Tokiwa, Y., Suzuki, T., Ando, T.: Synthesis of copolyamide-esters and some aspects involved in their hydrolysis by lipase. J. Appl. Polym. Sci. **24**, 1701–1711 (1979)

28. Tuominen, J., Korhonen, H., Seppälä, J.: The synthesis of lactic acid and ε-caprolactone based poly(ester-amides). In: International Symposium on Recent Advances in Ring Opening (Metathesis) Polymerization, Mons, Belgium, April 12–15 (1999)
29. Tuominen, J., Seppälä, J.: Synthesis and characterization of lactic acid based poly(ester-amide). Macromolecules **33**, 3530–3535 (2000)
30. Tuominen, J., Kylmä, J., Seppälä, J.: Chain extending of lactic acid oligomers. 2. Increase of molecular weight with 1, 6-hexamethylene diisocyanate and 2, 2′-bis(2-oxazoline). Polymer **43**, 3–10 (2002)
31. Tarvainen, T., Karjalainen, T., Malin, M., Pohjolainen, S., Tuominen, J., Seppälä, J., Järvinen, K.: Degradation of and drug release from a novel 2, 2-bis(2-oxazoline) linked poly(lactic acid) polymer. J. Control. Drug Release **81**, 251–261 (2002)
32. Tarvainen, T., Malin, M., Barragan, I., Tuominen, J., Seppälä, J., Järvinen, K.: Effects of incorporated drugs on degradation of novel 2, 2′-bi(2-oxazoline) linked poly(lactic acid) films. Int. J. Pharm. **310**, 162–167 (2006)
33. Tarvainen, T., Karjalainen, T., Malin, M., Peräkorpi, K., Tuominen, J., Seppälä, J., Järvinen, K.: Drug release profiles from and degradation of a novel biodegradable polymer, 2, 2-bis(2-oxazoline) linked poly(ε-caprolactone). Eur. J. Pharm. Sci. **16**, 323–331 (2002)
34. Tarvainen, T., Malin, M., Suutari, T., Pöllänen, M., Tuominen, J., Seppälä, J., Järvinen, K.: Pancreatin enhanced erosion of and macromolecule release from 2, 2-bis(2-oxazoline)-linked poly(ε-caprolactone). J. Control. Release **86**, 213–222 (2003)
35. Pulkkinen, M., Malin, M., Tarvainen, T., Saarimäki, T., Seppälä, J., Järvinen, K.: Effects of block length on the enzymatic degradation and erosion of oxazoline linked poly-ε-caprolactone. Eur. J. Pharm. Sci. **31**, 119–128 (2007)
36. Pulkkinen, M., Palmgrén, J.J., Auriola, S., Malin, M., Seppälä, J., Järvinen, K.: High-performance liquid chromatography/electrospray ionization tandem mass spectrometry for characterization of enzymatic degradation of 2, 2′-bis(2-oxazoline)-linked poly-ε-caprolactone. Rapid Commun. Mass Spectrom. **22**, 121–129 (2008)
37. Pulkkinen, M., Malin, M., Böhm, J., Tarvainen, T., Wirth, T., Seppälä, J., Järvinen, K.: In vivo implantation of 2, 2′-bis(oxazoline)-linked poly-ε-caprolactone: Proof for enzyme sensitive surface erosion and biocompatibility. Eur. J. Pharm. Sci. **36**, 310–319 (2009)
38. Zhao, Z., Wang, J., Mao, H.-Q., Leong, K.W.: Polyphosphoesters in drug and gene delivery. Adv. Drug Deliv. Rev. **55**, 483–499 (2003)
39. Allcock, H.R., O'Connor, S.J.M., Olmeijer, D.L., Napierala, M.E., Cameron, C.G.: Polyphosphazenes bearing branched and linear oligoethyleneoxy side groups as solid solvents for ionic conduction. Macromolecules **29**, 7544–7552 (1996)
40. Pretula, J., Kaluzynski, K., Szymanski, R., Penczek, S.: Transesterification of oligomeric dialkyl phosphonates leading to the high-molecular-weight poly-H-phosphonates. J. Polym. Sci. A Polym. Chem. **37**(9), 1365–1381 (1999)
41. Shimasaki, C., Kitano, H.: Phosphorus-containing polymers (overview). In: Salamone, J.C. (ed.) Polymeric materials encyclopedia. CRC Press, New York (1996)
42. Puska, M., Silva-Nykänen, V.R., Korventausta, J., Nykänen, A., Närhi, T., Ruokolainen, J., Seppälä, J.: Calcium phosphate formation on ethylphosphoester of poly(ε-caprolactone) and poly[bis(methacrylate)]phosphazene in vitro. Key Eng. Mater. (Bioceramics 21) **396–398**, 171–174 (2009)
43. Miao, H., Fan, Y., Liu, Y., Hao, J., Deng, X.: Biodegradable poly(sebacic anhydride-co-ε-caprolactone) multi-block copolymers: synthesis, characterization, crystallinity and crystalline morphology. Eur. Polym. J. **43**, 1055–1064 (2007)
44. Storey, R.F., Taylor, A.E.: Synthesis of novel biodegradable poly(ester-anhydride)s. J. Macromol. Sci. Pure Appl. Chem. **34**, 265–280 (1997)
45. Xiao, C., Zhu, K.J.: Synthesis and in vitro degradation properties of poly[(tetramethylene carbonate)-co-(sebacic anhydride)]. Polym. Int. **50**, 414–420 (2001)
46. Pfeifer, B.A., Burdick, J.A., Langer, R.: Formulation and surface modification of poly(ester-anhydride) micro- and nanosphres. Biomaterials **26**, 117–124 (2005)

47. Pfeifer, B.A., Burdick, J.A., Langer, R.: Poly(ester-anhydride): poly(β-amino ester) micro- and nanospheres: DNA encapsulation and cellular transfection. Int. J. Pharm. **34**, 210–219 (2005)
48. Domb, A.J., Manor, N., Elmalak, O.: Biodegradable bone cement compositions based on acrylate and epoxide terminated poly(propylene fumarate) oligomers and calcium salt compositions. Biomaterials **17**, 411–417 (1996)
49. Wang, Y., Ameer, G.A., Sheppard, B.J., Langer, R.: A tough biodegradable elastomer. Nat. Biotechnol. **20**, 602–606 (2002)
50. Anseth, K.S., Shastri, V.R., Langer, R.: Photopolymerizable degradable polyanhydrides with osteocompatibility. Nat. Biotechnol. **17**, 156–159 (1999)
51. Burdick, J.A., Philpott, L.M., Anseth, K.S.: Synthesis and characterization of tetrafunctional lactic acid oligomers: a potential in situ forming degradable orthopaedic biomaterial. J. Polym. Sci. A Polym. Chem. **39**, 683–692 (2001)
52. Peter, S.J., Miller, M.J., Yaszemski, M.J., Mikos, A.G.: Poly(propylene fumarate). In: Domb, A.J., Kost, J., Wiseman, D.M. (eds.) Handbook of Biodegradable Polymers. Harwood Academic Publishers, Amsterdam (1997)
53. Helminen, A., Korhonen, H., Seppälä, J.V.: Structure modification and crosslinking of methacrylated polylactide oligomers. J. Appl. Polym. Sci. **86**(14), 3616–3624 (2002)
54. Helminen, A., Korhonen, H., Seppälä, J.V.: Crosslinked poly(ε-caprolactone/D, L-lactide) copolymers with elastic properties. Macromol. Chem. Phys. **203**(18), 2630–2639 (2002)
55. Turunen, M.P.K., Korhonen, H., Tuominen, J., Seppälä, J.V.: Synthesis, characterization and crosslinking of functional star-shaped poly(ε-caprolactone). Polym. Int. **51**, 92–100 (2001)
56. Aoyagi, T., Miyata, F., Nagase, Y.: Preparation of cross-linked aliphatic polyester and application to thermo-responsive material. J. Control. Release **32**, 87–96 (1994)
57. Davis, K.A., Burdick, J.A., Anseth, K.S.: Photoinitiated crosslinked degradable copolymer networks for tissue engineering applications. Biomaterials **24**, 2485–2495 (2003)
58. Sawhney, A.S., Pathak, C.P., Hubbell, J.A.: Bioerodible hydrogels based on photopolymerized poly(ethylene glycol)-co-poly(α-hydroxy acid) diacrylate macromers. Macromolecules **26**, 581–587 (1993)
59. Storey, R.F., Warren, S.C., Allison, C.J., Puckett, A.D.: Methacrylate-endcapped poly(D, L-lactide-co-trimethylene carbonate) oligomers. Network formation by thermal free-radical curing. Polymer **38**, 6295–6301 (1997)
60. Helminen, A., Korhonen, H., Seppälä, J.V.: Crosslinked poly(ester-anhydrides) based on poly(ε-caprolactone) and polylactide oligomers. J. Polym. Sci. A Polym. Chem. **41**, 3788–3797 (2003)
61. Kim, B.S., Hrkach, J.S., Langer, R.: Synthesis and characterization of novel degradable photocrosslinked poly(ether-anhydride) networks. J. Polym. Sci. A Polym. Chem. **38**, 1277–1282 (2000)
62. Quick, D.J., Macdonald, K.K., Anseth, K.S.: Delivering DNA from crosslinked, surface eroding polyanhydrides. J. Control. Release **97**, 333–343 (2004)
63. Elomaa, L.: Preparation of polycaprolactone based tissue engineering scaffolds by stereolithography. Master's thesis, Helsinki University of Technology, Espoo (2009)
64. Mönkäre, J., Hakala, R.A., Vlasova, M.A., Huotari, A., Kilpeläinen, M., Kiviniemi, A., Meretoja, V., Herzig, K.H., Korhonen, H., Seppälä, J.V., Järvinen, K.: Biocompatible photocrosslinked poly(ester anhydride) based on functionalized poly(ε-caprolactone) prepolymer shows surface erosion controlled drug release in vitro and in vivo. J. Control. Release **146**, 349–355 (2010)
65. Mönkäre, J., Hakala, R.A., Kilpeläinen, M., Herzig, K.H., Korhonen, H., Seppälä, J.V., Järvinen, K.: Photocrosslinked poly(ester anhydride) for controlled delivery of peptide YY3-36. In: 23rd European Conference on Biomaterials, ESB2010, September 11–15, 2010 Tampere, Finland (2010)
66. Rich, J., Korhonen, H., Hakala, R., Korventausta, J., Elomaa, L., Seppälä, J.: Porous biodegradable scaffold: predetermined porosity by dissolution of poly(ester-anhydride) fibers from polyester matrix. Macromol. Biosci. **9**, 654–660 (2009)

67. Storey, R.F., Wiggins, J.S., Mauritz, K.A., Puckett, A.D.: Bioabsorbable composites. II: nontoxic, L-lysine-based poly(ester-urethane) matrix composites. Polym. Compos. **14**, 17–25 (1993)
68. Grijpma, D.W., Altpeter, H., Bevis, M.J., Feijen, J.: Improvement of the mechanical properties of poly(D, L-lactide) by orientation. Polym. Int. **51**, 845–851 (2002)
69. Amsden, B.G., Misra, G., Gu, F., Younes, H.M.: Synthesis and characterization of a photo-cross-linked biodegradable elastomer. Biomacromolecules **5**, 2479–2486 (2004)
70. Amsden, B.: Curable, biodegradable elastomers: emerging biomaterials for drug delivery and tissue engineering. Soft Matter **3**, 1335–1348 (2007)
71. Storey, R.F., Wiggins, J.S., Puckett, A.D.: Hydrolyzable poly(ester-urethane) networks from L-lysine diisocyanate and D, L-lactide/ε-caprolactone homo- and copolyester triols. J. Polym. Sci. A Polym. Chem. **32**, 2345–2363 (1994)
72. Baroli, B.: Photopolymerization of biomaterials: issues and potentialities in drug delivery, tissue engineering, and cell encapsulation applications. J. Chem. Technol. Biotechnol. **81**, 491–499 (2006)
73. Elisseeff, J., Anseth, K., Sims, D., Mcintosh, W., Randolph, M., Langer, R.: Transdermal photopolymerization for minimally invasive implantation. Proc. Natl Acad. Sci. USA **96**, 3104–3107 (1999)
74. Meretoja, V., Helminen, A., Korventausta, J., Haapa-aho, V., Seppälä, J., Närhi, T.: Crosslinked poly(ε-caprolactone/D,L-lactide) bioactive glass composite scaffolds for bone tissue engineering. J. Biomed. Mater. Res. A **77A**, 261–268 (2006)
75. Malin, M., Korventausta, J., Meretoja, V., Seppälä, J.: Elastic ceramic-polymer scaffold with interconnected pore structure: preparation and in vitro reactivity. Key Eng. Mater. **361–363** (Bioceramics 20), 395–398 (2008)
76. Meretoja, V.V., Malin, M., Seppälä, J.V., Närhi, T.O.: Osteoblast response to continuous phase macroporous scaffold under static and dynamic culture conditions. J. Biomed. Mater. Res. A **89A**, 317–325 (2008)
77. Meretoja, V., Tirri, T., Malin, M., Seppälä, J., Närhi, T.: Subcutaneous implantation of continuous phase macroporous scaffolds with and without cells. In: Word Biomaterials Conference, May 28-June 1, 2008 Amsterdam, The Netherlands (2008)
78. Xia, Y., Kim, E., Whitesides, G.M.: Micromolding of polymers in capillaries: applications in microfabrication. Chem. Mater. **8**, 1558–1567 (1996)
79. Jansen, J., Melchels, F.P.W., Feijen, J., Grjpma, D.W.: Fumaric acid monoethyl ester-functionalized poly(D, L-lactide/N-vinyl-2-pyrrolidone resins for the preparation of tissue engineering scaffolds by stereolithography. Biomacromolecules **10**, 214–220 (2009)
80. Melchels, F.P.W., Feijen, J., Grjpma, D.W.: A poly(D, L-lactide) resin for the preparation of tissue engineering scaffolds by stereolithography. Biomaterials **30**, 3801–3809 (2009)
81. Koskela, J.: Light-induced biomaterial microfabrication for advanced cell culturing—a comparative study. Master's thesis, Tampere University of Technology, Tampere (2010)

Drug Delivery Systems Based On Mucoadhesive Polymers

Maya Davidovich-Pinhas and Havazelet Bianco-Peled

Abstract Transmucosal delivery of therapeutic agents is a non-invasive approach that utilizes human entry paths such as the nasal, buccal, rectal and vaginal routs. Mucoadhesive polymers have the ability to adhere to the mucus layer covering those surfaces and by that promote drug release, targeting and absorption. Mucoadhesive polymers commonly interact with mucus through non-covalent bonds such as hydrogen bonds, ionic interactions and/or chain entanglement. This chapter reviews variety of mucoadhesive polymeric systems with a special emphasis on recent developments in the field. In particular, a new class of covalently interacting mucoadhesive polymers termed acrylated mucoadhesive polymers is described in detail. Acrylated mucoadhesive polymers are macromolecules which carry at least one double bond therefore are capable of forming covalent link with thiol groups on mucin type glycoproteins, the main component of mucus. To date, two acrylated mucoadhesive polymers were synthesized, and their ability to act as a mucoadhesive drug release vehicle was characterized and compare to other covalently binding mucoadhesive polymers. This approach opens a way to additional clinical applications that will benefit from the administration of drugs through the mucosa surface.

1 Introduction

Drug delivery methods are widely used for variety of drugs due to their onset, intensity, and duration of pharmacological action. The use of direct injection of drug into the blood is straightforward however it is clearly not convenient for the

M. Davidovich-Pinhas and H. Bianco-Peled (✉)
Department of Chemical Engineering, Technion, Haifa 32000, Israel
e-mail: bianco@tx.technion.ac.il

Stud Mechanobiol Tissue Eng Biomater (2011) 8: 439–456
DOI: 10.1007/8415_2010_39

Published Online: 28 December 2010

patients. Therefore development of more comfortable methods is obvious. Delivery through the oral rout is the most common approach being used primarily due to its simplicity, however it suffers from some limitation such as drug hydrolysis in the gastric track and lack of solubility of some drugs leading to low bioavailability. Another non-invasive method of drug delivery utilizes human entry paths such as the nasal, buccal, rectal and vaginal routs. These entry paths are covered with a hydrated layer termed mucus rather than with skin, thus often termed mucosal paths of delivery. The mucus-covered interfaces are characterized with a high blood flow and therefore have the potential for numerous sites for drug absorption [1].

The term bioadhesion refers to the adherence of two surfaces, where at least one of them is biological in nature. Bioadhesion is a useful phenomenon facilitating drug delivery processes by providing a prolong residence time and contact, thus leading to improvement of drug absorption at a given site. Most frequently, bioadhesion drug delivery systems operate in mucus covered environment where the mucus functions as a barrier between the adherent and the epithelial surface. Such three phase system is therefore a specific case of bioadhesion which can be referred to as mucoadhesion phenomenon [2].

Mucoadhesive polymers were first introduced in the early 1980's as a new approach to improve drug release, targeting and absorption. Mucoadhesion, defined as the ability to adhere to the mucus gel layer, is a key element in the design of these materials [3, 4]. Combining mucoadhesion with other advantages of polymeric drug carriers such as controlled drug release rate, protection of the drug from hydrolysis or other types of chemical degradation, protection from enzymatic degradation, reduction of drug toxicity, and improvement of drug solubility and availability [5], allows design of powerful drug delivery systems.

This chapter reviews variety of mucoadhesive polymeric systems with a special emphasis on recent developments in the field. In particular, a new class of covalently interacting mucoadhesive polymers termed acrylated mucoadhesive polymers is described in detail.

2 Mucoadhesive Polymers

Mucohadhesive polymers are known in their ability to adhere to the mucus gel layer [3]. The epithelial cells which cover the cavities of most organs that opens to the outside of the body, such as the alimentary canal, the respiratory tract and the genitourinary tract, are responsible for the mucus secretion. The mucus gel layer has a multiple functions such as absorption, lubrication, entrapment and antibacterial activity [1]. Mucus is composed primarily of water ($\sim$95%), but also contains small amounts of salts, lipids, and proteins. The main components responsible for the elastic gel-like structure of the mucus are glycoproteins termed mucins. Mucins are high molecular weight extracellular glycoproteins which share many common features. Due to the characteristics of these glycoproteins they can

form electrostatic, hydrophobic, sulfide and H-bonding interactions with other substances which lead to mucoadhesion [6]. The mucoadhesion process is believed to be a result of chain penetration, entanglement and molecular interaction (covalent or/and non-covalent). Therefore, it can be described using the diffusion and chemical bonding theories of adhesion. The diffusion theory of adhesion is based on the assumption that the adhesion strength of polymers to themselves (auto-adhesion) or to each other is due to mutual diffusion (inter-diffusion) of macromolecules across the inter-phase. The chemical bonding theory of adhesion invokes the formation of interaction such as covalent, ionic or hydrogen bonds across the adhesive surface inter-phase [7–9].

2.1 Classes of Mucoadhesive Polymers

Several types of polymers are known in their ability to interact physically and/or chemically with mucus [3]. Polymers which form non-covalent bonds such as hydrogen bonds, Van-Der Waals forces, ionic interactions and/or chain entanglements are the most common [10]. More recently, attempts have been made to improve the mucoadhesive properties through modification that enable formation of covalent bonds between the polymer and the mucin type glycoproteins. This family includes polymers capable of forming disulfide bonds [11–15], specific binding based on adhesive molecules that attach directly to the cell surface [16], or acrylate- sulfide linking [17, 18] .

2.1.1 Non-Covalently Binding Polymers

Due to the negative surface charge of the mucus, electrostatic interactions play an important role in the adhesion process. Therefore, non-covalently binding mucoadhesive polymers are commonly classified according to their molecular charge into anionic, cationic, nonionic and amphiphilic polymers [3].

Anionic polymers, carrying–COOH groups, can form hydrogen bonds with the hydroxyl groups of the glycoprotein's oligosaccharide side chain. This group includes polymers such as polyacrylates, alginate, and hyaluronuc acid. Cationic polymers carry a positively charged amine group and can therefore adhere to mucus due to ionic attraction to the sialic acid groups on the oligosaccharide side chain. Chitosan and poly-lysine are good examples for such mucoadhesive polymers. The interaction of nonionic polymers is based on interpenetration of the polymer chains followed by chain entanglement. Therefore their ability to adhere is not influenced by the surrounding pH. Recent studies showed that nonionic polymers are, in most cases, less adhesive than anionic or cationic mucoadhesives. In this group one can find hydroxypropyl-cellulose and polyvinyl-alcohol [3].

2.1.2 Covalently Binding Polymers

Covalently binding polymers can be classified into two groups based on their type of interaction, specific or non-specific. Specifically binding mucoadhesive systems take advantage from the ability of lectins and/or other adhesion molecules to bind directly to receptors on the cell surface rather than to the mucus gel layer. Since specific binding to the cell surface is often followed by uptake and intracellular transport, new chances for drug delivery are evolved [16]. The non-specific binding approach offers an easy, simple and multifunctional mucoadhesion technique which can adhere to several types of mucus tissues. The adhesion is due to bonds that can execute in physiology environment. The first generation of non-specifically binding polymers utilized known covalent biological interactions—disulfide bridges. This approach has lead to the development of thiolated polymers, also termed thiomers, in which a small molecule (ligand) consisting a thiol functional group is attached to the polymer chain [11–14]. The concept of thiolated polymers have been wildly explored in the last decay. Thiolation of many synthetic polymers such as poly(methacrylic acid) and poly(acrylic acid), and natural polymers such as chitosan, deacetylated gellan gum and alginate, is described in the literature [19]. In all those studies better adhesion ability of the thiomer compare to the native polymer was demonstrated. However, concerns related to the ability of thiomers to form disulfide bridges in hydrated environment have been recently raised [20]. Although dry carriers prepared from thiolated alginate demonstrated high adhesion to mucus [21], the hydrated alginate-thiol displayed similar adherence to that of the native alginate. It was suggested that the benefit achieved by adding thiol groups to the polymer was flawed in the hydrated cross-linked form due to the formation of inter-molecular di-sulfide junctions. This study highlighted the need for new mucoadhesive polymers that can create non-specific covalent bonds with mucin glycoproteins under mild physiology conditions, and has lead to the development of a new class polymers which bind to the thiol group via acrylate- sulfide linking [17, 18]. This approach will be described in details in the following section.

3 Acrylated Mucoadhesive Polymers

Acrylated mucoadhesive polymers are macromolecules which carry at least one double bond therefore are capable of forming covalent link with thiol groups on mucin type glycoproteins. Their design was inspired from the ability of molecules carrying electronegative vinyl end group to covalently attach to electronegative neighboring groups, in a reaction termed Michael type addition, which can take place in physiological environment. A form of this reaction have been developed by Hubbell et al. [22, 23] for conjugating sulfhydryl-containing bio-molecules such as peptides or proteins to vinyl-carrying polymers, see Fig. 1. This methodology was further developed for the modification of many hydrogel systems

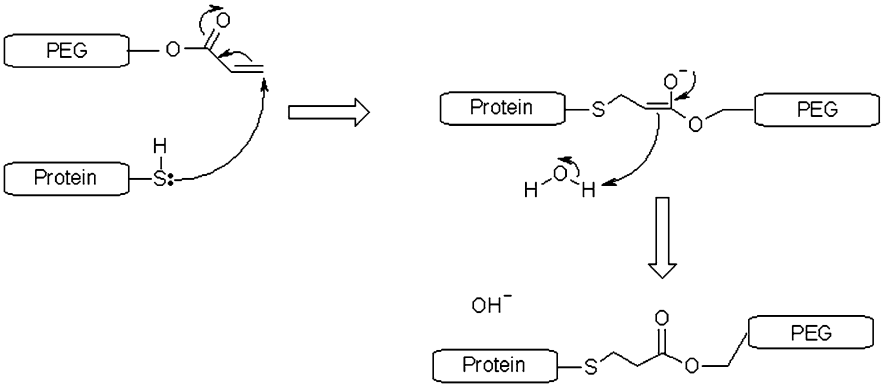

Fig. 1 Protein PEGylation using a Michael type addition reaction

such as poly(vinyl alcohol) [24], poly(ethylene glycol)-*b*-poly(lactic acid) [25], PEGylated fibrinogen [26] and other PEGylated proteins [26, 27].

3.1 Polyehtylene Glycol Di-Acrylate (PEG-DA)

A relatively simple example of acrylated mucoadhesive polymer is polyehtylene glycol di-acrylate (PEG-DA). PEG-DA can be synthesized from the linear hydrophilic polyether polyehtylene glycol (PEG) [22, 26]. In brief, PEG acrylation is carried out under Argon by activating a dichloromethane (DCM) solution of PEG with acryloyl chloride and triethylamine at a molar ratio of 1-OH to 1.5-acryloyl chloride to 1.5-triethylamine. The final product is precipitated in ice-cold diethyl ether and dried under vacuum [26]. The chemical structure of PEG-DA is shown is Fig. 2. Since each molecule carries two double bonds, linking one group to the thiol leaves an unsaturated group on each molecule which is capable of further crosslinking to form a hydrogel.

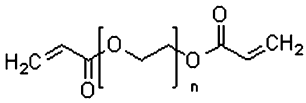

Fig. 2 The molecular structure of polyethylene glycol di-acrylate (PEG-DA)

3.2 Alginate-PEGAc

Acrylated polymers combine the inherent properties of the backbone with the acrylated side chains which enhances their mucoadhesiveness. An example for this approach is a biosynthetic molecule termed alginate- polyehtylene glycol acrylate (alginate-PEGAc) [18]. The use of alginate as a drug release carrier is well known

and extensively studied [28, 29]. Over the years several approaches have been developed in order to improve alginate characteristics by conjugating various molecules [30] such as acrylic acid [31, 32], Cystein [21] and PEG [33] to its backbone. Alginate was also used in combination with PEG molecules by physical blending of the polymers followed by alginate cross-linking. This approach lead to formation of alginate hydrogel with larger pore sized that can be used for cells encapsulation [34–36].

To further exploit the mucoadhesion properties of PEG and alginate, a biomaterial which consists of PEG-acrylate chains attached to an alginate backbone was developed [18]. Such a polymer combines the strength, simplicity, and gelation ability of alginate with the mucoadhesion properties arising from the PEG's characteristics and the acrylate functionality. Alginate-PEGAc has the potential to be used in many biotechnology applications due to its unique characteristics. In particular, the ability to induce both physical cross-linking of the alginate backbone using divalent ions, and/or chemical cross-linking of the PEG's acrylate end group using UV radiation, offers a new approach to control the polymer properties.

The synthesis of alginate-PEGAc was designed as a two step procedure where synthesis of alginate-thiol is performed first, followed by the conjugation of PEG-DA to the alginate backbone [18], see Fig. 3.

Synthesis of alginate-thiol [20, 21] was achieved by activating the alginate carboxylic groups by the carbodiimide functional group within the 1-ethyl-3-(3-dimethylaminopropyl)-carbodiimide hydrochloride (EDAC) intermediate reagent. Next, EDAC was replaced with L-Cystein molecule through its amine end group to form an amide bond. The molecular structure of alginate-thiol was verified using ^{1}H NMR experiments [18]. In addition, thiol presence in the final products was verified using ellmen's reagent reaction.

The resulting alginate-thiol was dissolved in Tris(2-carboxyethyl)phosphine hydrochloride (TCEP) solution in order to prevent intra-molecular disulfide interaction [20]. Finally, a Michael type addition reaction, involving a nucleophilic addition of the thiols on the thiolated alginate to the vinyl group on the acrylate functionalized polyethylene glycol, was performed. In order to lower the probability of multiple attachments of single PEG-DA molecule to the backbone, a large molar excess of PEG-DA was used. The resulted product consist PEG chains, still carrying one acrylate end group, connected to alginate backbone through the cystein spacer molecule.

Laurienzo et al. [33] conjugated PEG molecules to alginate through its hydroxyl end groups in order to maintain the gelation ability of alginate which involves the carboxylic end groups. The synthetic approach described above reduces the number of carboxylic groups on the alginate backbone. Yet, the product retained its gelation ability and gel microparticles could be formed by dropping 1% PEGAc solution into 1% $CaCl_2$ aqueous solution [18].

In vitro cell assays were conducted in order to evaluate the cytotoxicity of the new biomaterial [18]. Alginate-PEGAc samples prepared from two types of alginate were cultured with human foreskin fibroblasts (HFFs) cells for 24 h and

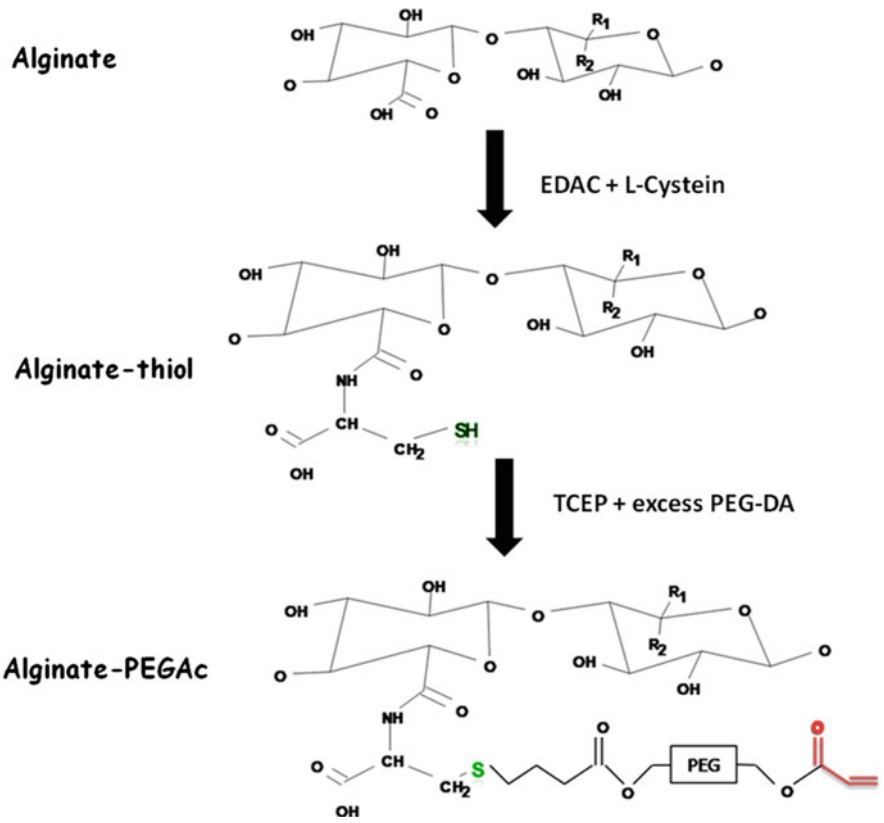

Fig. 3 Schematic illustration of the alginate-PEGAc synthesis

assayed for the live/dead cells using fluorescent calcien and ethidium homodimer labeling followed by fluorescent microscopy imaging. None of the alginate-PEGAc caused cytotoxic effect in HFFs cells.

4 Acrylate-Sulfide Interaction: Proof of Concept

An experimental evidence to support the hypothesis that acrylate end groups are able to covalently associate with mucin type glycoproteins was provided by mixing PEG-DA with mucin glycoproteins extracted from porcine's fresh small intestine [17]. The existence of sulfidryl-acrylate interactions was demonstrated based on nuclear magnetic resonance (NMR) and rheology measurements.

Michael type addition reaction involves coupling oxygen on vinyl end group with other electronegative end group such as sulfides. The reactive double bond is

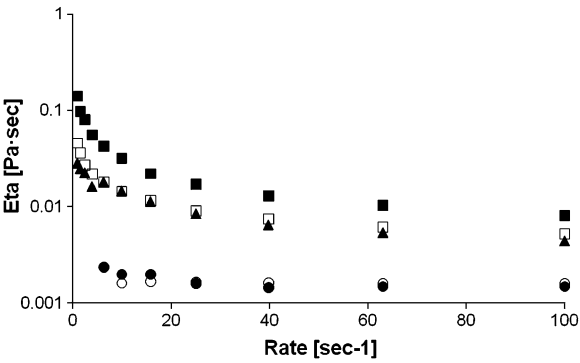

Fig. 4 Rate sweep experiment of (▲) mucin 20 mg/ml, (●) PEG-Da 10 kDa 20 mg/ml, (○) PEG-OH 10 kDa 20 mg/ml, (■) mucin 20 mg/ml + PEG-Da 10 kDa 20 mg/ml and (□) mucin 20 mg/ml + PEG-OH 10 kDa 20 mg/ml in distilled water at 25° C

opened to create a new covalent bond between the two components. Therefore the use of NMR in order to monitor acrylate-sulfide interaction on the molecular level is straightforward. The experiments were conducted by measuring the ^{1}H proton spectra of each components and comparing it to their mixture [17]. The spectrum obtained from native PEG-DA revealed several peaks ascribed to the vinyl end group protons ($\delta = 5.9$–6.5 ppm) and to the protons of the methylene repeating unit ($\delta = 4.3$ and $\delta = 3.6$). The vinyl protons were also detected in the spectrum obtained from the mucin/PEG-DA mixture however their intensity decreased. It is known that changes in electron environment due to double bond opening allude to peak disappearance therefore this finding suggested that some of the vinyl bonds disappear due to glycoprotein addition. Moreover, new protons were found in the low ppm region where -CH_2 groups are usually located, further supporting the hypothesis that PEG-DA created intermolecular interactions with mucin glycoproteins [17].

Additional analysis by rheology measurements verified the existence of acrylate-mucin glycoproteins in PEG-DA/mucin mixture. Figure 4 demonstrates that the addition of mucin to PEG-DA has led to a viscosity increase. This result supports the suggestion that PEG-DA interacts with the mucin glycoproteins, and is in line with previous works in the field of mucoadhesive polymers that attributed viscosity enhancement after mucin addition to molecular interaction between the polymer and glycoproteins [11, 37]. Importantly, a mixture of PEG-OH and mucin displays a lower viscosity than the mucin/PEG-DA mixture (Fig. 4). This observation overrules the possibility that the increased viscosity is caused from the addition of relatively high molecular weight glycoprotein to polymer solution which might induce formation of additional entanglements as a result of a concentration increase. Thus, the viscosity increase can be attributed to Michael type addition reaction between the PEG-DA's acrylate end group and glycoprotein's sulfide end group, since this is the only possible interactions which cannot occur when PEG-OH chains are mixed with the mucin. This result further strengthens the hypothesis that the PEG-DA's acrylate end groups can create molecular interaction with mucin glycoproteins.

5 Acrylated Polymers as Mucoadhesive Drug Delivery Vehicles

After verifying the ability of acrylate end group to covalently associate with mucin type glycoproteins, two different mucoadhesive drug delivery vehicles that possess both adhesion and drug release ability were suggested, as described below.

5.1 PEG-DA Based Mucoadhesive System

5.1.1 Mucoadhesion Ability

The mucoadhesion properties of PEG-DA were characterized using a methodology that was designed to allow evaluation of the adherence ability of cross-linked networks in wet environment [17]. This experimental setup allows the cross-linking reaction to occur on the adhesion surface, see Fig. 5 the results reveal that increasing the PEG-DA concentration enhances the adhesion to the mucus (Fig. 6). This finding could reflect increased chain entanglements which, according to the diffusion theory, is expected to improve the adhesion [7–9]. However, larger

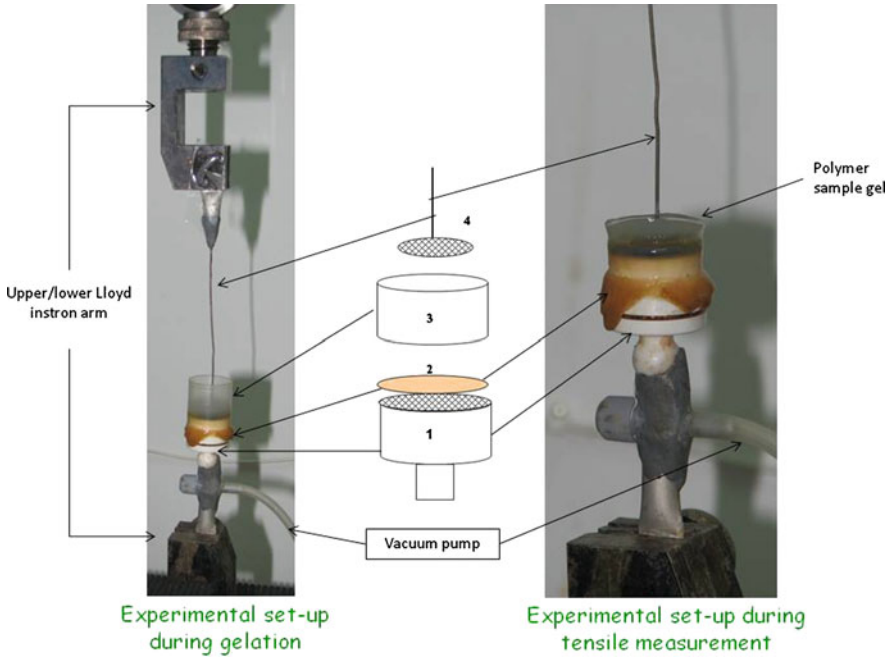

Fig. 5 Schematic illustration of the instrument for assessment of bioadhesion. 1-lower apparatus arm which connects to the vacuum system, 2-location of the mucus tissue, 3-polyethylene mold and 4- stainless steel grid connected to the upper instrument arm

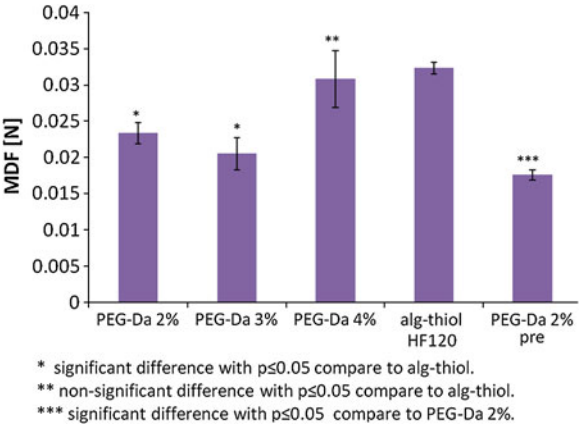

Fig. 6 Maximum detachment force (MDF) of various polymer samples from fresh mucus surface at 25°C

polymer concentration also leads to an increase in the concentration of acrylate group near the surface and higher probability of chemical bonds formation [17]. In order to demonstrate the influence of sample preparation conditions and these two possible mechanisms on the adhesion, macromer solutions containing 2 wt% PEG-DA were cross-linked on a hydrophobic surface prior to placing them on the mucus surface and measuring the adhesion strength. This has lead to a significant decrease in the adhesion strength compare to the same PEG-DA sample that was cross-linked on the mucosa surface, thus suggesting that by preventing cross-linking on the surface both the diffusion and penetration of PEG-DA chains beneath the surface and the ability to form covalent bonds, were harmed. This result is in a good agreement with previous published work done on the ability of PEG to penetrate and promote adhesion with other polymer surfaces [38–42].

A comparison between PEG-DA and alginate-thiol which is a known covalently binding mucoadhesive polymer is presented in Fig. 6. The maximum detachment force obtained for these two polymers is of the same order of magnitude. Moreover, a significant difference is observed between the results obtained from the 2% and 3% PEG-DA, whereas the difference between the 4% PEG-DA and the alginate-thiol was not significant. Previously studied mucoadhesive systems based on thiolated polymers also display comparable adhesion capability. For example, Bernkop-schnurch et al. [43] characterized the adhesion of alginate and alginate-thiol to a commercial-grade crude porcine mucin. Maximum detachment forces of approximately 0.01 N and 0.07 N were obtained for alginate and alginate-thiol, respectively. In another study by the same group [10] maximum detachment forces of 0.027 N, 0.256 N and 0.056 N were measured for low, medium and high molecular weight 2-iminothiolane conjugated chitosan (chitosan-TBA). It should be noted, however, that the exact setup used for the adhesion measurements have a vast influence on the measured force, as described in detail in a recently published review [44]. In particular, the detachment force of PEG-DA were performed using hydrated samples which were cross-linked on the mucus surface, whereas the above mentioned previous studies have utilized dry, compressed sample which did

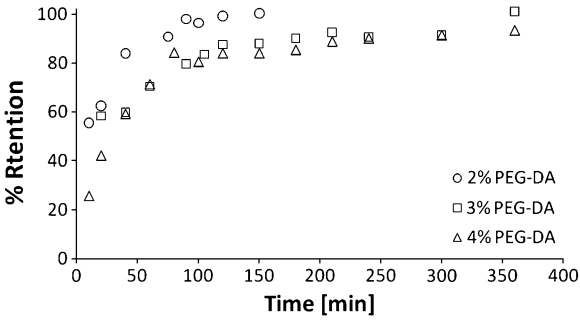

Fig. 7 Ibuprofen release profile from PEG-Da gel tablets having varied polymer concentration (○) 2%, (□) 3% and (Δ) 4% at room temperature

not contain any cross-linker. It is known that during the swelling process of dry sample the polymer chains tend to penetrate to the surface due to their swelling [45, 46]. This process probably leads to an increase in the adhesion ability according to the diffusion theory of adhesion. The acrylated mucoadhesion polymers displays similar adhesion ability in hydrated environment in spite of the lack of swelling.

5.1.2 PEG-DA as Drug Delivery Vehicle

Release profiles of the hydrophilic model drug Ibuprofen, a non-steroidal anti-inflammatory drug used in the commercial products Advil® (Wyeth Inc.) and Nurofen® (Reckitt Benckiser Inc.), are presented in Fig. 7. The kinetics of drug release is rapid, and 100% of the initial dose is released within the first few hours. A relatively rapid release and absorption of Ibuprofen is essential since it is used to treat pain and fever, and its half life time in the body is around two hours. Newa et al. [47] have demonstrated shorter release time scale of minutes using a solid dispersions of PEG and Ibuprofen. Drug release from PEG dispersions is expected to be fast due to fast dissolution of the polymer and the large surface area from which the drug diffuses. Therefore, cross-linked PEG-DA matrices offer longer Ibuprofen release time, with the additional benefit of the ability to adhere to mucus.

As expected, the release kinetics can be altered by changing the polymer concentration (Fig. 7). Increasing the polymer concentration has led to slower release kinetics due to denser hydrogel network formed at higher polymer concentration [48].

Ibuprofen release profiles were further analyzed in order to calculate the diffusion coefficients of the drug [17]. The analysis included fitting the early-time Eq. 1 and late-time Eq. 2 approximation equations developed by Ritger and Peppas [49, 50] to the experimental data,

$$\frac{M_t}{M_\infty} \cong 4\left(\frac{D_E \cdot t}{\pi \delta^2}\right)^{0.5} \tag{1}$$

Table 1 Diffusion coefficients obtained from fits of the early and the late time models to the release profiles shown in Fig. 7

PEG-DA concentration [mg/ml]	D_E [cm^2/sec]	D_L [cm^2/sec]
20	2.11E-06	1.93E-06
30	9.56E-07	6.83E-07
40	7.85E-07	4.68E-07

$$\frac{M_t}{M_\infty} \cong 1 - \frac{8}{\pi^2} \cdot \exp\left(-\frac{\pi^2 D_L \cdot t}{\delta^2}\right) \tag{2}$$

where M_t/M_∞ is the fractional drug release, t is the release time, D_E and D_L are the early and late diffusion coefficients respectively and δ is the diffusion distance. The diffusion distance δ was set to be half of the tablet width. A good fit was obtained using both the late and the early time models. The diffusion coefficients obtained from this analysis (Table 1) decrease when the polymer concentration is increased, due to a decrease in the matrix's mesh size leading to a slower solute diffusion.

The release profiles and the calculated diffusion coefficients suggest that PEG-DA limits the rate of drug release and thus can act as a vehicle for sustained drug delivery. Manipulating the drug release profile is possible by changing the polymer concentration and its molecular weight, parameters which affect the mesh size of the network.

5.2 Alginate-Polyethyleneglycol Acrylate (alg-PEGAc) Mucoadhesive System

5.2.1 Mucoadhesion Ability

The adherence of dry alginate-PEGAc tablets to fresh small intestine mucus surface was compared to that of native alginate and alginate-thiol, a known covalently binding mucoadhesive polymer [18]. The maximum detachment force (MDF) of two alginate-PEGAc samples was significantly higher ($p < 0.005$) compare to both native alginate and alginate-thiol (Fig. 8). No significant difference was observed between the adhesion ability of the two native alginate samples. In contradiction to the results reported by Bernkop-Schnurch et el. [21], the adhesion of the thiolated alginate was higher than that of the native alginate in the case of alginate HF120, but not in the case alginate LF200S. Moreover, MDF of the thiolated alginate HF120 was significantly higher compare that of the thiolated alginate LF200S. Thiolated alginate HF120 contains larger amount of thiol groups therefore the probability for di-sulfide interactions with mucin glycoproteins on the mucosa surface increases. An analogous behavior was also detected when comparing the two alginate-PEGAc samples. Alginate-PEGAc synthesized from HF120 demonstrated a significantly higher MDF compare to the alginate-PEGAc prepared by modifying LF200S. It stands for reason that the thiol content is

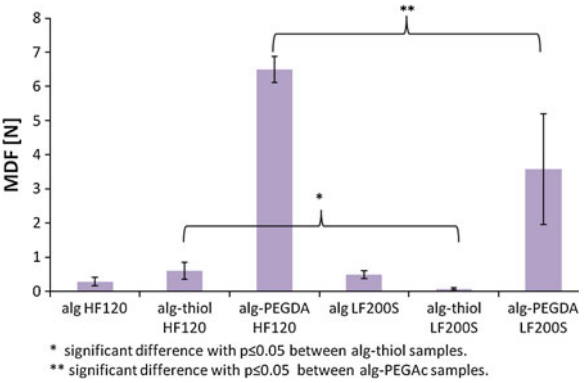

Fig. 8 Maximum detachment force (MDF) of 13 mm dry uncross-linked compressed polymer samples to fresh small intestine surface at room temperature (n = 4)

strongly correlated with the PEGylation degree, since larger thiol content increases the probability that a PEG-DA would attach to the alginate thus leads to a larger PEG content. An increase in PEG and acrylate content could be expected to increase the probability for chain entanglements, polymer non-covalent bonds such as hydrogen bonds and covalent bonds between the acrylate and sulfide with the mucosa surface.

5.2.2 Alginate-PEGAc as Drug Delivery Vehicle

Release of Ibuprofen from alginate-PEGAc dry tablets display typical release times of few hours [18] (Fig. 9).

The release patterns were fit to the semi-empirical equation known as the power law model [51–53]:

$$\frac{M_t}{M_\infty} = kt^n \tag{3}$$

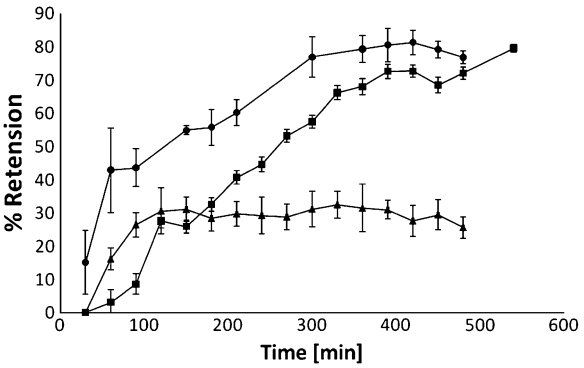

Fig. 9 Ibuprofen release profile from alginate (■), alginate-thiol (▲) and alg-PEGAc (●) tablets based on alginate LF200S using 1:2 drug:polymer content. Experiments were performed in PBS pH 7.4 at 37°C

Table 2 Fit parameter obtained from the power low model Eq. 3 for the different polymer samples

Polymer sample	k	n
Alginate LF200S	0.0019	1.00
Alginate-thiol	0.0089	0.76
Alginate-PEGAc	0.0233	0.60

Here, M_t and M_∞ are the absolute cumulative amount of drug released at time t and at infinite time, respectively, k is a constant incorporating structural and geometric characteristic of the device, and n is the release exponent, indicative of the drug release mechanism.

Generally speaking, the power law can be referred to as a superposition of two apparently independent mechanisms participating in drug transport, a Fickian diffusion observed in diffusion-controlled systems and a case-2 transport, describes in many cases of drug release from glassy polymers during polymer swelling. The power law equation has two distinct physical boundary meanings: $n = 0.5$, indicating a diffusion-controlled drug release mechanism (Fickian diffusion) and $n = 1.0$, indicating a swelling-controlled drug release mechanism (case-2 transport). Values of n between these two limiting values can be described as a superposition of both phenomena mentioned above and is often termed anomalous transport. The limiting values of n presented above are valid for slab geometry only [51–53]. The samples used in this study have similar physical characteristics as a thin slab since their surface cross section area is significantly larger than their width ($A \gg d$).

Fits of the experimental release data to Eq. 3 lead to exponent values in the range of 0.6 and 1.0 (Table 2). Dry polymer samples are characterized by a swelling driven phase transition from dried compressed state where the drug molecules entrapped in the tablet remain immobile until wetting and hydration is accomplished and the drug molecules are allowed to freely diffuse. Therefore, a swelling-controlled delivery mechanism (where $n = 1.0$) is expected, as indeed observed for the native alginate sample. However, modification of the alginate decreases the power law exponent. Furthermore, increasing the bulkiness of the side group decreased the power low exponent: Alginate-thiol consists a small side group of only one amino-acid (Cystein) while the final alginate-PEGAc has longer 10 kDa PEG side chain. The decrease in the power law exponent was attributed to two separate processes: (1) decrease in electrostatic repulsion between the polymer chains and (2) increase in steric effects due to the increased bulkiness of the side chain. Alginate is an anionic polyelectrolyte therefore one would expect that its volume will increase rapidly following sample hydration and swelling due to electrostatic repulsion. Modification of the alginate in which the carboxyl groups are replaced with the nonionic cystein or PEG groups decreases the electrostatic repulsion phenomena thus decreasing the degree of swelling and as a result the power exponent. Moreover, due to the chemical nature of the molecular modification, Cystein or PEGAc, the probability for physical and/or chemical chain intermolecular interactions such as hydrogen bonds and disulfide bond have increased. Thus, changing the polymer modification might increase the polymer self

interaction which leads to a decrease in the chains free volume which, in turn, prevents the drug molecules from diffusing freely. In addition, increase in bulkiness of the side group can hinder drug diffusion. The variation in the value n between the thiol and PEGAc branching could be therefore attributed to the length and chemical characteristics of the side group. The longer the chain length, its ability to create covalent and non-covalent bonds is higher, due to the presence of larger number of functional groups which are free to interact, thus reducing the polymer's swelling. At the same time, the larger side group obviously limits drug diffusion. Overall, an increase in bulkiness of the side group increases the diffusion controlled effect on the drug release mechanism which brings the power law exponent value closer to 0.5.

6 Summary

Drug delivery systems based on mucoadhesive polymers is a promising platform that offer benefits such as prolong residence time of pharmaceuticals localized in the vicinity of the mucosal surface, a rapid uptake of a drugs into the systemic circulation through the relatively permeable mucus membranes, and enhanced bioavailability of therapeutic agents that become possible due to avoidance of some to the natural defense mechanisms of the body. This chapter reviews some of the recent advances in the field of mucoadhesive polymers, with a special emphasis on covalently binding systems and in particular the new family of acrylated mucoadhesive polymers. Acrylated polymers covalently associate with mucin glycoproteins through a sulfidryl-acrylate Michael type addition reaction, as demonstrated using both NMR and rheometry measurements. To date, two acrylated mucoadhesive polymers—PEG-DA and alg-PEGAc—were synthesized, and their ability to act as a mucoadhesive drug release vehicle was characterized and compare to other covalently binding mucoadhesive polymers.

The combination of enhanced mucoadhesion properties and controlled drug release abilities opens a way to clinical applications that will benefit from the administration of drugs through the mucosa surface. As an example, administration of drugs with poor bioavailability is more efficient due to the substantially longer retention times. Additionally, drugs which are sensitive to the hostile environment in the GI track can be delivered systemically. Another obvious example is local drug delivery to the surroundings of the mucosa.

References

1. Worakul, N., Robinson, J.R.: Drug delivery via mucosal routes. In: Dumitriu, S. (ed.) Polymeric Biomaterials, 2nd edn. Marcel Dekker, Inc. (2002)
2. Woolfson, A.D., Malcolm, R.K., McCarron, P.A., Jones, D.S.: Bioadhesive drug delivery systems. In: Dumitriu, S. (ed.) Polymeric Biomaterials, 2nd edn. Marcel Dekker, Inc. (2002)

3. Bernkop-Schnurch, A.: Mucoadhesive polymers. In: Dumitriu, S. (ed.) Polymer Biomaterial, 2nd edn. Marcel Dekker, Inc. (2002)
4. Lee, J.W., Park, J.H., Robinson, J.R.: Bioadhesive-based dosage forms: the next generation. J. Pharm. Sci. **89**, 850–866 (2000)
5. Malmsten, M.: Soft drug delivery systems. Soft Matter **2**, 760–769 (2006)
6. Bansil, R., Turner, B.S.: Mucin structure, aggregation, physiological functions and biomedical applications. Curr. Opin. Colloid Interface Sci. **11**, 164–170 (2006)
7. Comyn, J.: Adhesion science. In: Comyn, J. (ed.) The Royal Society of Chemistry (1997)
8. Nardin, M.: Theories and mechanisms of adhesion. In: Mittal, K.L. (ed.) Handbook of Adhesive Technology, edn. Marcel Dekker, Inc. (1994)
9. Pocius, V: Adhesion and Adhesives Technology—an Introduction. Hanser-Gardner (1997)
10. Roldo, M., Hornof, M., Caliceti, P., Bernkop-Schnurch, A.: Mucoadhesive thiolated chitosans as platforms for oral controlled drug delivery: synthesis and in vitro evaluation. Eur. J. Pharm. Biopharm. **57**, 115–121 (2004)
11. Leitner, V.M., Walker, G.F., Bernkop-Schnurch, A: Thiolated polymers: evidence for the formation of disulfide bonds with mucus glycoproteins. Eur. J. Pharm. Biopharm. **56**, 207–214 (2003)
12. Bernkop-Schnuerch, A.: Thiomers: a new generation of mucoadhesive polymers. Adv. Drug Deliv. Rev. **57**, 1569–1582 (2005)
13. Kast, C.E., Bernkop-Schnurch, A: Thiolated polymers—thiomers: development and in vitro evaluation of chitosan-thioglycolic acid conjugates. Biomaterials **22**, 2345–2352 (2001)
14. Bernkop-Schnurch, A., Hornof, M., Zoidl, T.: Thiolated polymers-thiomers: synthesis and in vitro evaluation of chitosan-2-iminothiolane conjugates. Int. J. Pharm. **260**, 229–237 (2003)
15. Bernkop-Schnurch, A., Scholler, S., Biebel, R.G.: Development of controlled drug release systems based on thiolated polymers. J. Control. Release **66**, 39–48 (2000)
16. Haas, J., Lehr, C.-M.: Developments in the area of bioadhesive drug delivery systems. Expert Opin. Biol. Ther. **2**, 287–298 (2002)
17. Davidovich-Pinhas, M., Bianco-Peled, H.: Novel mucoadhesive system based on sulfhydryl-acrylate interactions. J. Mat. Sci. Mat. Med. **21**, 2027–2034 (2010)
18. Davidovich-Pinhas, M., Bianco-Peled, H.: Alginate-PEGAc: A new mucoadhesive polymer. Acta Biomaterialia (2010, in Press)
19. Bernkop-Schnuerch, A.: Thiomers: a new generation of mucoadhesive polymers. Adv. Drug Deliv. Rev. **57**, 1569–1582 (2005)
20. Davidovich-Pinhas, M., Harari, O., Bianco-Peled, H.: Evaluating the mucoadhesive properties of drug delivery systems based on hydrated thiolated alginate. J. Control. Release **136**, 38–44 (2009)
21. Bernkop-Schnurch, A., Kast, C.E., Richter, M.F.: Improvement in the mucoadhesive properties of alginate by the covalent attachment of cysteine. J. Control. Release **71**, 277–285 (2001)
22. Elbert, D.L., Pratt, A.B., Lutolf, M.P., Halstenberg, S., Hubbell, J.A.: Protein delivery from materials formed by self-selective conjugate addition reactions. J. Control. Release **76**, 11–25 (2001)
23. Lutolf, M.P., Hubbell, J.A.: Synthesis and Physicochemical Characterization of End-Linked Poly(ethylene glycol)-co-peptide Hydrogels Formed by Michael-Type Addition. Biomacromolecules **4**, 713–722 (2003)
24. Tortora, M., Cavalieri, F., Chiessi, E., Paradossi, G.: Michael-type addition reactions for the in situ formation of poly(vinyl alcohol)-based hydrogels. Biomacromolecules **8**, 209–214 (2007)
25. Rydholm, A.E., Bowman, C.N., Anseth, K.S.: Degradable thiol-acrylate photopolymers: polymerization and degradation behavior of an in situ forming biomaterial. Biomaterials **26**, 4495–4506 (2005)
26. Almany, L., Seliktar, D.: Biosynthetic hydrogel scaffolds made from fibrinogen and polyethylene glycol for 3D cell cultures. Biomaterials **26**, 2467–2477 (2005)

27. Seal, B.L., Panitch, A.: Viscoelastic behavior of environmentally sensitive biomimetic polymer matrices. Macromolecules **39**, 2268–2274 (2006)
28. Pandey, R., Khuller, G.K.: Alginate as a drug delivery carrier. In: Yarema, K.J. (ed.) Handbook of Carbohydrate Engineering, edn. CRC Press—Taylor and Francis Group, Boca Raton (2005)
29. Tonnesen, H.H., Karlsen, J.: Alginate in drug delivery systems. Drug Dev. Ind. Pharm. **28**, 621–630 (2002)
30. d'Ayala, G.G., Malinconico, M., Laurienzo, P.: Marine derived polysaccharides for biomedical applications: chemical modification approaches. Molecules **13**, 2069–2106 (2008)
31. Laurienzo, P., Malinconico, M., Mattia, G., Russo, R., Rotonda, M.I.L., Quaglia, F., Capitani, D., Mannina, L.: Novel alginate-acrylic polymers as a platform for drug delivery. J. Biomed. Mat. Res. Part A **78**, 523–531 (2006)
32. Hua, S., Wang, A.: Synthesis, characterization and swelling behaviors of sodium alginate-g-poly(acrylic acid)/sodium humate superabsorbent. Carbohydr. Polym. **75**, 79–84 (2009)
33. Laurienzo, P., Malinconico, M., Motta, A., Vicinanza, A.: Synthesis and characterization of a novel alginate-poly(ethylene glycol) graft copolymer. Carbohydr. Polym. **62**, 274–282 (2005)
34. Caykara, T., Demirci, S., Eroglu, M.S., Guven, O.: Poly(ethylene oxide) and its blends with sodium alginate. Polymer **46**, 10750–10757 (2005)
35. Seifert, D.B., Phillips, J.A.: Porous alginate-poly(ethylene glycol) entrapment system for the cultivation of mammalian cells. Biotechnol. Prog. **13**, 569–576 (1997)
36. Mahou, R., Wandrey, C.: Alginate-Poly(ethylene glycol) hybride microspheres with adjustable physical properties. Macromolecules **43**, 1371–1378 (2010)
37. Bromberg, L.E.: Interactions between hydrophobically modified polyelectrolytes and mucin. Polym. Prepr. **40**, 616–617 (1999)
38. Bures, P., Huang, Y., Oral, E., Peppas, N.A.: Surface modifications and molecular imprinting of polymers in medical and pharmaceutical applications. J. Control. Release **72**, 25–33 (2001)
39. Yoncheva, K., Gomez, S., Campanero Miguel, A., Gamazo, C., Irache Juan, M.: Bioadhesive properties of pegylated nanoparticles. Expert. Opin. Drug Deliv. **2**, 205–218 (2005)
40. Ascentiis, A.D., deGrazia, J.L., Bowman, C.N., Colombo, P., Peppas, N.A.: Mucoadhesion of poly(2-hydroxyethyl methacrylate) is improved when linear poly(ethylene oxide) chains are added to the polymer network. J. Control. Release **33**, 197–201 (1995)
41. Sahlin, J.J., Peppas, N.A.: Enhanced hydrogel adhesion by polymer interdiffusion: Use of linear poly(ethylene glycol) as an adhesion promoter. J. Biomater. Sci. Polym. Ed. **8**, 421–436 (1997)
42. Huang, Y., Leobandung, W., Foss, A., Peppas, N.A.: Molecular aspects of muco- and bioadhesion: tethered structures and site-specific surfaces. J. Controlled Release **65**, 63–71 (2000)
43. Bernkop-Schnurch, A., Kast, C.E., Richter, M.F.: Improvement in the mucoadhesive properties of alginate by the covalent attachment of cysteine. J. Control. Release **71**, 277–285 (2001)
44. Davidovich-Pinhas, M., Bianco-Peled, H.: Mucoadhesion: a review of characterization techniques. Expert Opin. Drug Deliv. **7**, 259–271 (2010)
45. Rubinstein, M., Colby H.: Polymer Physics. Oxford university press Inc. (2003)
46. Flory, J.: Principles of Polymer Chemistry. Cornell University (1953)
47. Newa, M., Bhandari, K.H., Li, D.X., Kim, J.O., Yoo, D.S., Kim, J.-A., Yoo, B.-K., Woo, J.-S., Choi, H.-G., Yong, C.-S.: Preparation and evaluation of immediate release ibuprofen solid dispersions using polyethylene glycol 4000. Biol. Pharm. Bull. **31**, 939–945 (2008)
48. Dhawan, S., Varma, M., Sinha, V.R.: High molecular weight poly(ethylene oxide)-based drug delivery systems. Part I: hydrogels and hydrophilic matrix systems. Pharm. Technol. **29**, 72–74, 76–80 (2005)

49. Ritger, P.L., Peppas, N.A.: A simple equation for description of solute release I. Fickian and non-fickian release from non-swellable devices in the form of slabs, spheres, cylinders or discs. J. Control. Release **5**, 23–36 (1987)
50. Ritger, P.L., Peppas, N.A.: A simple equation for description of solute release II. Fickian and anomalous release from swellable devices. J. Control. Release **5**, 37–42 (1987)
51. Brazel, C.S., Peppas, N.A. Mechanisms of solute and drug transport in relaxing, swelleble, hydrophilic glassy polymers. Polymer **40**, 3383–3398 (1999)
52. Lin, C.-C., Metters, A.T.: Hydrogels in controlled release formulation: network design and mathematical modeling. Adv. Drug Delivery Rev. **58**, 1379–1408 (2006)
53. Siepmann, J., Peppas, N.A.: Modeling of drug release from delivery systems based on hydroxypropyl methylcellulose (HPMC). Adv. Drug Delivery Rev. **48**, 139–157 (2001)

Thermosensitive Polymers for Controlled Delivery of Hormones

Yu Tang, Mayura Oak, Rhishikesh Mandke, Buddhadev Layek, Gitanjali Sharma and Jagdish Singh

Abstract Thermosensitive polymeric systems, which remain as solution at room temperature and transform into gel at body temperature, have been extensively investigated for biomedical and pharmaceutical applications. The gel depot formed at the site of injection after the administration of an aqueous polymeric solution provides several benefits over the conventional delivery systems. These thermosensitive drug delivery systems are easy to formulate by simple mixing of therapeutic agents with the aqueous polymeric solutions, easy to administer by single injection, remain stable at the physiological conditions for a definite period of time, provide excellent stability for labile biomolecules such as proteins and peptides, and maintain the controlled and sustained release profile of the incorporated agents. Most of these systems are biodegradable and biocompatible, thereby eliminating the need of surgical explantation. This chapter discusses the classification of temperature sensitive systems, their synthesis and characterization procedures and provides a survey of recent literature on the in vitro and in vivo applications of thermosensitive polymers for controlled delivery of hormones.

Y. Tang
Novartis Biologics, Process Sciences and Production, Novartis Institutes for BioMedical Research, Inc, Cambridge, MA 02139, USA
e-mail: yu.tang@novartis.com

M. Oak · R. Mandke · B. Layek · G. Sharma · J. Singh (✉)
Department of Pharmaceutical Sciences, College of Pharmacy, Nursing, and Allied Sciences Dept# 2665, North Dakota State University, PO Box 6050Sudro Hall Room 102A, Fargo, ND 58108-6050, USA
e-mail: Jagdish.singh@ndsu.edu

Stud Mechanobiol Tissue Eng Biomater (2011) 8: 457–479
DOI: 10.1007/8415_2011_65

Published Online: 12 February 2011

List of Abbreviations

AUC	Area under the curve
ATRP	Atomic transfer radical polymerization
BE	Butyl vinyl ether
BMA	Butyl methacrylate
CD	Circular dichroism
$CDCl_3$	Deuterated chloroform
C_{max}	Maximum plasma concentration
CMC	Critical micelle concentration
CMT	Critical micelle temperature
DLS	Dyanamic light scattering
DPH	1,6-diphenyl-1,3,5-hexatriene
D_2O	Deuterated water
DMSO-d_6	Deuterated dimethyl sulfoxide
DSC	Differential scanning calorimetery
EGVE	Ethylene glycol vinyl ether
FT-IR	Fourier transform infrared spectroscopy
G-CSF	Granulocyte colony stimulating factor
GLP	Glucagon-like peptide
GPC	Gel permeation chromatography
hGH	Human growth hormone
HP-β-CD	Hydroxypropyl-β-cyclodextrin
HPLC	High performance liquid chromatography
IGF	Insulin-like growth factor
ISO	International organization of standardization
LA/GA	Lactic acid/Glycolic acid
LCST	Lower critical solution temperature
LNG	Levonorgestrel
MALDI	Matrix-assisted laser desorption/ionization
ME	Methoxyestradiol
M_n	Number average molecular weight
MPA	Methyl prednisolone
MPEG	Methoxy poly(ethylene glycol)
MTT	3-(4,5-dimethylthiazol-2-yl)-2,5-diphenyltetrazolium bromide
M_w	Weight average molecular weight
NIPAAm	N-isopropyl acrylamide
NMR	Nuclear magnetic resonance
PAGE	Polyacrylamide gel electrophoresis
PDEAAM	Poly (N, N′-diethylacrylamide)
PDI	Polydispersity index
PEG	Poly(ethylene glycol)
PEO	Poly(ethylene oxide)
pGH	Porcine growth hormone
PLA	Poly(lactic acid)

PLGA	Poly(DL-lactic acid-co-glycolic acid)
PNIPAAm	Poly(N-isopropylacrylamide)
PPO	Poly(propylene oxide)
RAFT	Reversible addition-fragmentation chain transfer
sCT	Salmon calcitonin
SD	Sprague–Dawley
SEM	Scanning electron microscopy
SLS	Static light scattering
TEM	Transmission electron microscopy
TMS	Tetramethyl silane
TSN	Testosterone
UV	Ultraviolet

1 Introduction

Development of new protein/peptide therapeutics has increased exponentially due to the explosion of genomic information, final mapping of the human genome, and functional studies of proteins/peptides in the pathology of various diseases [3, 50, 70]. The total global market for protein/peptide drugs was $47.4 billion in 2006. The market is estimated to reach $53 billion by the end of 2010 with an average annual growth rate of ~7% [45]. These protein/peptide therapeutics include hormones, growth factor, enzymes, interferons, interleukins, modified and engineered antibodies. Unfortunately, upon oral administration these macromolecules can easily lose their biological activity in gastrointestinal tract (GI tract) with poor absorption into systemic circulation. As a result, oral administration of these macromolecules is usually avoided and parenteral delivery routes (such as intravenous, subcutaneous and intramuscular) are commonly adopted. Besides the limitations in administration route, protein/peptide therapeutics also require frequent dosing to achieve and maintain therapeutic effects, due to rapid clearance in vivo. The high frequency of injections often results in low patient compliance due to pain, stress and inconvenience.

In order to relieve the stress caused by frequent injections and increase patient compliance, various delivery routes such as intranasal, intra-pulmonary, transdermal, buccal, and vaginal have been investigated. However, low bioavailability which is caused by poor membrane permeability and enzymatic metabolism at absorption sites limits the application of protein/peptide therapeutics through these delivery routes. Currently, frequent administration via injection is still preferred over those delivery routes. This highlights the need of a suitable delivery system which can control the delivery of proteins and peptides over a long period to increase patient compliance and maintain therapeutic effects while showing comparable bioavailability to conventional injection administration. To achieve

these goals, polymer based parenteral controlled drug delivery systems attracted a great deal of research interest, because polymer matrix was found to be able to slow down the release rate of loaded therapeutics. Thermosensitive polymers based in situ gel forming controlled delivery systems have potential to resolve the difficulties in the delivery of protein/peptide therapeutics due to their larger loading capacity, ease of formulation, and smaller initial burst release [26].

1.1 Thermosensitive Polymers

Aqueous solutions of some polymers show abrupt changes in their solubility as a function of change in temperature. These polymeric systems exhibit sol to gel transition either by elevating or lowering the temperature. Depending upon the phase change behavior in response to temperature, they are classified as positive and negative (reverse) temperature sensitive systems. This reverse thermogelation property constitutes one of the most promising strategies for the development of injectable systems for biomedical application. The main components of this system are thermosensitive polymers and water. At lower critical solution temperature (LCST), the interaction (hydrogen bonding) between water molecules and polymer become unfavorable compared to polymer–polymer and water–water interaction and therefore phase separation occurs as the polymer dehydrates. Consequently, aqueous polymer solutions display low viscosity at ambient temperature but exhibit a sharp increase in viscosity following a small temperature rise, forming a semi-solid gel at body temperature [56]. Some amphiphilic copolymers can self assemble in an aqueous environment to form micelles. These micelles show polymer–polymer interactions at higher temperature, which leads to gel formation. Thus, the ideal thermosensitive delivery system should be liquid/free flowing at room temperature, and should quickly form gel at/near body temperature [56]. Therapeutic agents can be dispersed/dissolved in sol state and injected using a syringe into subcutaneous layers or at diseased site to form gel depots. The major advantages of these delivery systems are the absence of organic solvents, ease of formulation, less invasive administration by single bolus injection, less expensive and controlled release of incorporated agents to obtain sustained therapeutic action. It is also reported that the drugs incorporated in these delivery systems conserve their physical and chemical stability and biological activity during the release period.

The prototype of thermosensitive polymers is poly(N-isopropyl acrylamide) (poly-NIPAAM) [62]. An aqueous solution of poly-NIPAAM is liquid below 32°C, and turns into gel above 32°C. However, poly-NIPAAM cannot be used for biomedical application due to its well-known cytotoxicity and non-biodegradability. The first type of triblock thermosensitive copolymers is poly(ethylene oxide)–poly(propylene oxide)–poly(ethylene oxide) (PEO–PPO–PEO) known as poloxamers or Pluronics® [7, 54]. Aqueous solutions of these polymers show gelation at body temperature, at concentration higher than 15% w/w.

Unfortunately biocompatibility studies revealed that this concentration leads to notable cytotoxicity and increases plasma cholesterol and triglycerol levels in rats after intraperitoneal injection [48, 73]. Macromed Inc. further modified the triblock copolymers by using poly lactic acid (PLA) and poly D,L-lactic-co-glycolic acid (PLGA) to replace PPO as the hydrophobic block, producing copolymers such as PEG–PLA–PEG, PEG–PLGA–PEG, and PLGA–PEG–PLGA. These types of polymers have thermosensitive gel transition property, excellent biodegradability and promising controlled release for drugs [32, 33]. ReGel®, which contains 23% of ABA triblock copolymer (PLGA–PEG–PLGA) in phosphate buffer saline (pH 7.4), has been used for drug delivery. Variety of biodegradable components including poly (ε-caprolactone), poly (propylene fumarate), poly(R)-3-hydroxybutyrate have also been modified by hydrophilic PEG blocks or other materials to develop biodegradable thermogelling delivery systems [6, 24, 28, 37, 42, 74].

2 Synthesis and Characterization of Thermosensitive Polymer

2.1 Synthesis

Extensive research has been conducted towards the designing of amphiphilic copolymers having distinct and novel macromolecular architectures. Reversible addition-fragmentation chain transfer (RAFT) polymerization [21, 23, 47, 71, 81], ring opening polymerization [8, 79], atomic transfer radical polymerization (ATRP) [21, 41, 44, 63, 64], and Michael-type addition reaction [72] are the most commonly adopted synthetic routes for designing specific temperature sensitive block polymers. For example, poly(N-isopropyl acrylamide) can be synthesized by RAFT, ATRP, or Cerium (IV) redox initiated polymerization, while living anionic polymerization is reported to be a better choice for poly (N, N′-diethylacrylamide) (PDEAAM) synthesis. Living cationic polymerization is employed for the synthesis of a series of block copolymers containing vinyl ether moiety [21]. A new method of synthesis of thermosensitive cyclotriphosphazenes by stepwise nucleophilic substitution reactions has been reported [67]. Depending upon the property, performance and functional need, various polymeric architectures have been synthesized.

2.2 Characterization

Different properties of thermosensitive polymers are characterized using various analytical techniques presented in Table 1.

The details of the characterization techniques are presented below.

Table 1 Characterization of thermosensitive polymers

Polymer property	Analytical technique/method	References
Structural characterization, Completion of polymerization reaction	Nuclear Magnetic Resonance (NMR), Fourier Transform Infrared Spectroscopy (FT-IR)	Singh et al. [59], Tang and Singh [65], Cho et al. [16], Jeong et al. [33], Cui et al. [20], Du et al. [22]
Molecular weight and distribution	Gel permeation chromatography (GPC)	Singh et al. [59], Jeong et al. [35], Chen et al. [12]
Micelle formation/ visualization/micelle size	NMR (^{1}H and ^{13}C-NMR)	Jeong et al. [33]
	Transmission electron microscopy (TEM), dynamic light scattering (DLS)	Soga et al. [51, 53], Park et al. [60, 61]
Critical micelle concentration (CMC)	Dye solubilization method	Jeong et al. [33]
	Fluorescence spectroscopy	Basu et al. [5]
Critical micelle temperature (CMT)	Static light scattering (SLS)	Soga et al. [60]
Phase inversion/ temperature sensitivity and cloud point	Tube inversion method	Jeong et al. [34]
	Dynamic mechanical analysis	Jeong et al. [35]
	Differential scanning calorimetry (DSC)	
	Ultraviolet spectroscopy (UV)	Lutz et al. [44], Mori et al. [46]
Rheology/Viscosity	Viscometry	Vermonden et al. [68]
Hydrogel microstructure	Confocal microscopy	Vermonden et al. [69]
	Scanning electron microscopy (SEM)	
Hydrogel swelling, In vitro degradation	GPC	Hu et al. [24]
	FT-IR	
	DSC	
In vitro and in vivo biocompatibility	Cell viability assay	Chen and Singh [15], Tang and Singh [65]
	Histological evaluation of implanted site using microscopy	

2.2.1 Structural Characterization

The structure/composition of the synthesized polymer, completion of the polymerization reaction, degradation residues, and presence of impurities can be elucidated by NMR and FT-IR Spectroscopy [16, 33, 59, 65]. Deuterated solvents such as $CDCl_3$, D_2O, DMSO-d_6 are used to dissolve the copolymers and tetramethylsilane (TMS) signal is taken as the zero chemical shift (δ). Signals originating from different protons and carbons are used for the confirmation of the structure, while the empirical idea about the molecular weight can be obtained by integrating the signals pertaining to different chemical groups present in the copolymer (^{1}H-NMR) [33].

2.2.2 Molecular Weight and Polydispersity Index

The ratio of the weight average molecular weight (M_w) and the number average molecular weight (M_n) of the polymer is known as polydispersity index (PDI), which is used as an indicator of the molecular weight range of the polymer. PDI close to 1 is an indicator of monodispersity in molecular weight. Molecular weight and molecular weight distribution of the synthesized polymers can be determined using gel permeation chromatography (GPC) [12, 35, 59]. For example, Singh et al. [59] have used GPC for determination of the polydispersity index of thermosensitive polymers (i.e., PLGA:PEG:PLGA, PLA:PEG:PLA and PEO:dl-PLA:IPDI:dl-PLA-PEO). It was found to be in the range of 1.09–1.46 with unimodal distribution and a narrow molecular weight distribution. Unimodal GPC trace with low polydispersity values suggests that polymers had sufficient purity for use in drug delivery. Even though GPC is a traditional and most prevalent technique used for the molecular weight determination, it has a limitation that it is calibrated to molecular weights for specific polymers and it has very low mass resolution. For this reason, it is usually coupled with Matrix Assisted Laser Desorption Ionization (MALDI) mass spectroscopy which has high mass range [31].

2.2.3 Micelle Formation, Critical Micelle Concentration and Temperature

Amphiphilic thermosensitive copolymers form a core–shell structure in aqueous environment. The corona is formed by hydrophilic backbone while hydrophobic side chains form a core of the micelle. Micelle formation can be elucidated by a number of analytical techniques such as NMR spectroscopy, DLS, Viscometry, and dye solubilization method [1,6-diphenyl-1,3,5-hexatriene (DPH)] etc. Using deuterated organic/aqueous solvents selective for each block in the copolymer, the micelle formation can be monitored by ^{13}C-NMR spectroscopy. Micelle formed can be visualized using cryo-Transmission Electron Microscopy (cryo-TEM) [60, 61]. Fluorescence spectroscopy using pyrene probe method is the most widely used and successfully employed method for critical micelle concentration (CMC) determination [5]. Dye solubilization is another method where, the hydrophobic dye [e.g. 1,6-diphenyl-1,3,5-hexatriene (DPH)] is dissolved in methanol and injected using a microsyringe into aqueous polymeric solution at various concentrations and allowed to equilibrate at 4°C for a specific time period before measurements. After equilibrium, CMC is determined using UV–visible spectrometry [2, 33]. Equations used for the determination of polymer molecular weight from static light scattering (SLS) can also be employed to micellar systems to obtain the average diameter of a micelle as well as critical micelle temperature (CMT) [60]. DLS is usually employed for determination of hydrodynamic size of the micelle, which is a function of temperature and concentration of the polymeric system [33]. For example, [33], used above mentioned analytical techniques such

as ^{13}C-NMR, dye solubilization, and light scattering to study the micelle formation of PEG–PLGA–PEG block copolymer.

2.2.4 Phase Inversion of Thermosensitive Polymers

Thermosensitive polymers exhibit reverse temperature dependent water solubility, i.e. these polymers are soluble in aqueous solutions at low temperatures and phase separation occurs with increase in temperature [21]. This temperature is known as lower critical solution temperature (LCST). The cloud point which is also known as a measure of thermosensitivity and storage stability of the polymers can be determined using UV spectroscopy and tube inversion method [12, 34, 59]. DSC and strain-controlled rheometers are also useful in determining the sol–gel transition of aqueous polymeric solutions [35, 77].

2.2.5 Rheological Measurements

Type and length of monomers, polymer concentration, pH, and temperature are some important factors which greatly affect the mechanical properties of the thermosensitive hydrogels [68]. Influence of temperature, polymer concentration, and molecular weight on the hydrogel viscosity can be studied using dynamic rheological measurements [68]. Though the rheological characteristics of thermosensitive hydrogels are very important, only few rheological studies using biodegradable thermosensitive polymers have been reported.

2.2.6 Hydrogel Microstructure

Porous morphology of hydrogels and the types of domains that are formed during gel formation can be visualized using SEM, while confocal laser scanning microscopy is also a useful technique for imaging the hydrophobic and hydrophilic regions of hydrogels [69].

2.2.7 In vitro Degradation and Hydrogel Swelling

Hydrolytic degradation of the thermosensitive polymers should be examined in neutral, acidic, and basic conditions by using suitable media. The polymer solutions are incubated at different pH in shaking water bath at 37°C. Time-dependent hydrolytic behavior of the polymer can be determined by monitoring the molecular weight decrease of the polymer using GPC, which gives essential insights into the pH dependency of the degradation pathway [40]. The effect of degradation on the structure of the polymer can be determined using DSC, FT-IR, and by plotting the decrease in number average molecular weight versus time [27].

2.2.8 In vitro Biocompatibility

The ultimate approval of the delivery system by regulatory agencies depends on a number of factors including cytotoxicity, biodegradability and biocompatibility. Though biodegradable polymers degrade into small water soluble molecules which are excreted from the body, good biodegradability does not assure good biocompatibility. Non-biocompatible materials lead to various immune responses, and may cause tissue damage, necrosis and fibrosis at the site of injection. A standard cell viability assay based on mitochondrial succinate dehydrogenase activity measured by 3-(4, 5-dimethylthiazol-2-yl)-2, 5-diphenyltetrazolium bromide (MTT) is the most widely used method for evaluation of in vitro biocompatibility of thermosensitive polymeric delivery systems. In 1996, Ignatius et al. first reported higher sensitivity of polymers cytotoxicity by MTT assay compared to Agar diffusion test [29].

PLGA based polymers have been found to have good biodegradability [58]. Degradation of PLGA polymers mainly relies on non-specific hydrolysis of the polymer backbone by water in surrounding tissue. Lactic acids and glycolic acids produced by polymer degradation are absorbed by surrounding tissue and utilized in the tricarboxylic acid cycle and further metabolized into carbon dioxide and water. Although MTT assay is more sensitive than Agar diffusion test for the intrinsic cytotoxicity of polymer extracts it cannot reveal the effect of decreased pH during polymer degradation on biocompatibility. It is known that degradation of biodegradable polymers results in lowering of pH surrounding the gel depot. The low pH can cause acute inflammation in surrounding tissue. Thus, reports of biocompatibility of biodegradable polymer based in situ gel forming drug delivery systems are controversial. Furthermore, the appearance of bulk gel at injection site may also cause acute inflammation. In order to further address the effect of the two factors on biocompatibility of polymer, in vivo biocompatibility studies are highly suggested.

2.2.9 In vivo Biocompatibility and Biodegradability of the Polymeric Delivery Systems

The in vivo biodegradability and biocompatibility of the delivery systems can be evaluated by observing the extent and duration of tissue inflammatory response after implantation/injection of the delivery system in vivo. Thus, evaluation of in vivo biocompatibility of a biodegradable polymer is based on the timeline of inflammation and results of tissue wound-healing. Polymers with good biocompatibility should only cause a transient inflammation, reversible tissue damage and minimal granulation [65]. Tang and Singh [65] evaluated the in vivo biocompatibility of the thermosensitive polymeric depots of mPEG–PLGA–mPEG in rats. The polymeric hydrogel was injected subcutaneously into the upper portion of neck of rats and the appearance of gel lumps was monitored regularly. Subcutaneous tissue surrounding the injection site was removed at

predetermined time points and examined for the presence of any formulation materials, and any sign of chronic inflammation, granulation tissue, and fibrous capsule formation, and immunological reaction was monitored during the entire period of study [65]. The polymeric delivery systems should comply with the regulations given by the International Organization of Standardization (ISO) [30] for implant materials.

3 In vitro Release of Hormones from the Delivery Systems

A variety of thermosensitive polymers such as Pluronic®, PNIPAAm, have been employed for the controlled delivery of many hormones including insulin, calcitonin, growth hormone etc. [4, 51, 53, 66, 76]. Though Pluronic® gels release drugs slower than solutions, the overall release period rarely exceeds few days, and hence they have been mainly studied for short-term therapies like pain management [49]. One clear advantage of these polymeric delivery systems is their capability to solubilize many peptides/proteins, hormones and to incorporate them uniformly inside the delivery systems. Since copolymer structure, composition and amount are the most important factors which control the release of drugs from thermosensitive polymers, small changes lead to significant effect on sol–gel formation and drug release [79]. Jeong et al. [32], reported a hydrogel consisting of blocks of poly (ethylene oxide) and poly (L-lactic acid) (PEO–PLA–PEO), which can only be loaded with bioactive molecules in an aqueous phase at an elevated temperature ($\sim$45°C), where it forms a sol. This loading procedure limits the nature of the drugs that can be incorporated in the drug delivery system to those that are not prone to degradation at higher temperature. On the other hand, hydrogels made of mPEG–PLGA–mPEG triblocks showed a prolonged release of a peptide hormone, salmon calcitonin when incorporated at room temperature [66].

One of the most encountered challenges during the development of a delivery system for peptide hormones is maintaining their bioactivity throughout the entire release and storage period. In environments other than their physiological ones, peptide hormones may undergo rapid denaturation and lose their conformational stability and biological activity. A Number of analytical techniques such as polyacrylamide gel electrophoresis (PAGE), circular dichroism (CD) spectroscopy, high performance liquid chromatography (HPLC), FT-IR, mass spectroscopy and matrix-assisted laser desorption/ionization (MALDI) can be used to determine the structural integrity and stability of the incorporated hormone. A number of additives are known to increase the protein stability through exclusion of proteins from surrounding harsh environment, limiting proteins spatial movement, and reducing protein–protein interactions [70]. For example Tween 20, and hydroxypropyl-β-cyclodextrin (HP-β-CD), has been shown to prevent the thermal and interfacial denaturation of porcine growth hormone and to stabilize insulin [9, 80].

4 In vivo Absorption and Therapeutic Efficacy of Hormones from Thermosensitive Delivery Systems

This section discusses controlled in vivo delivery of hormones from various thermosensitive polymer based systems.

4.1 PLGA and PEG Based Thermosensitive Systems

An ABA triblock copolymer (PLGA–PEG–PLGA, ReGel®) based thermosensitive drug delivery system was evaluated by Kim et al. [36] for controlled delivery of zinc insulin (0.2 wt% zinc) using Sprague–Dawley (SD) rats. There has been a steady plasma concentration of insulin up to day 15 after a single subcutaneous injection of insulin loaded ReGel® to meet the basal and postprandial insulin requirements.

Choi and Kim [19] designed an insulin (10 wt% zinc carbonate)/ReGel® formulation system for sustained release of basal insulin over a week by a single injection in Zucker Diabetic Fatty rats. In vivo insulin release from the ReGel® depot was almost constant (4–10 μg/L) for a period of 10 days following a single subcutaneous injection. The bioactivity of the released insulin was indicated by the decreased blood glucose level in diabetic animals during insulin release period. These studies indicate the usefulness of ReGel® based insulin delivery systems to maintain basal insulin requirements in diabetic patients for a longer period of time.

A ReGel® (23% w/w) based porcine growth hormone (pGH) formulation was characterized by Zentner et al. [79] in a bio-efficacy study using hypophysectomized rats. A single subcutaneous injection of ReGel®/pGH (70 mg/ml, 1 ml) exhibited similar efficacy (weight gain) equivalent to daily injections of 5 mg of pGH for 14 days (total 70 mg of pGH). The ReGel® polymer based formulation was also evaluated for the controlled release of granulocyte colony-stimulating factor (G-CSF) in rats. Rats administered with a single subcutaneous dose of ReGel®/G-CSF (100 μg/kg of G-CSF) produced similar extent of white cell induction comparable to daily i.v. injection of conventional G-CSF for 10 days (total 100 μg/kg of G-CSF).

Chen and Singh [15] modified the block structure of PLGA–PEG–PLGA (1400–1000–1400) for control delivery of porcine growth hormone (pGH). Formulations containing pGH were prepared by adding the hormone into 30% (w/v) aqueous solution of triblock copolymer. A comparative study was done by different formulations of pGH in New Zealand white rabbits at two different dose levels (4.2 mg/kg and 1.2 mg/kg). Rabbits injected intravenously with 4.2 mg/kg of pGH solution showed very fast clearance of pGH with a maximal serum concentration (C_{max}) of $\sim$1521 ng/mL. The subcutaneous injection of pGH solution resulted in a C_{max} of $\sim$29.3 ng/mL and $\sim$7 ng/mL for high and low dose, respectively. The bioavailability of pGH by subcutaneous injection is only $\sim$8.2%

for high dose and ~6% for low dose. While the subcutaneous injection of thermosensitive triblock polymer based pGH formulation maintain a constant level of exogenous pGH (3–7 ng/mL for high dose and 2–4 ng/mL for low dose) for 4 weeks. The thermosensitive polymer based formulation enhanced 4.5 fold and 14.5 fold bioavailability of pGH from high dose and low dose formulation, respectively compared to pGH solution upon subcutaneous injection.

Chen et al. [11] further extended the application of PLGA–PLE–PLGA (1400–1000–1400) thermosensitive polymer for controlled delivery of levonogestrel (LNG) and testosterone (TSN) in vivo. LNG containing delivery system maintained the constant LNG level in female rabbits for 6 weeks after single subcutaneous injection (Fig. 1). The polymeric delivery system also showed controlled release of TSN in castrated rabbits for more than 2 months (Fig. 2). Significant increase ($p < 0.05$) in relative bioavailability of steroidal hormones was observed in comparison to control solution. These polymeric systems maintained an effective drug concentration in blood for longer duration, which might be useful in reducing the dosage frequency as well as the adverse effects.

The mPEG–PLGA–mPEG copolymer (40% w/v of EG_{12}-$L_{35}G_{12}$-EG_{12}, Mw = 4300 Da) based thermosensitive in situ gel forming drug delivery system was developed for long term controlled release of salmon calcitonin (sCT) after single subcutaneous injection [66]. Polymeric formulation A with higher loading concentration of sCT (0.5% w/v) and formulation B with lower loading concentration (0.25% w/v) were administered to female wistar rats followed by measurement of serum levels of sCT and calcium. Both the polymeric formulations

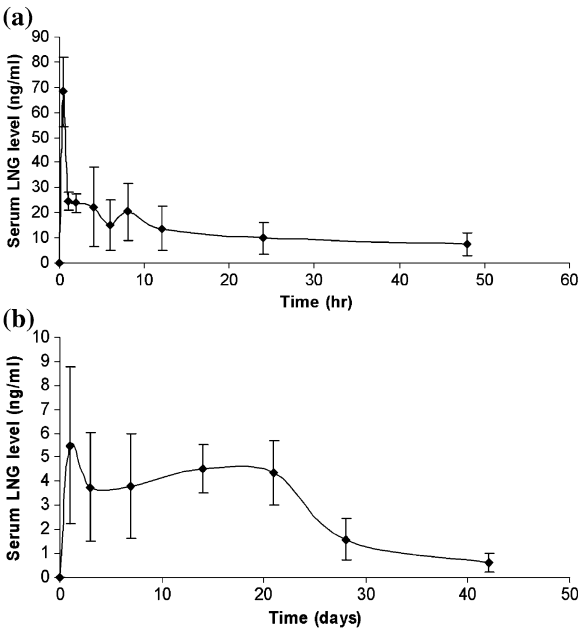

Fig. 1 In vivo absorption of LNG in rabbits after subcutaneous administration of LNG formulations (**a**) control solution (12 mg/ml LNG in DMSO), (**b**) Thermosensitive polymer formulations (12 mg/ml LNG, copolymer PLGA–PEG–PLGA, 30% w/v). All data points are mean ± standard deviation ($n = 4$). [From Chen et al. [11] Reprinted with the permission of Wiley Publishers]

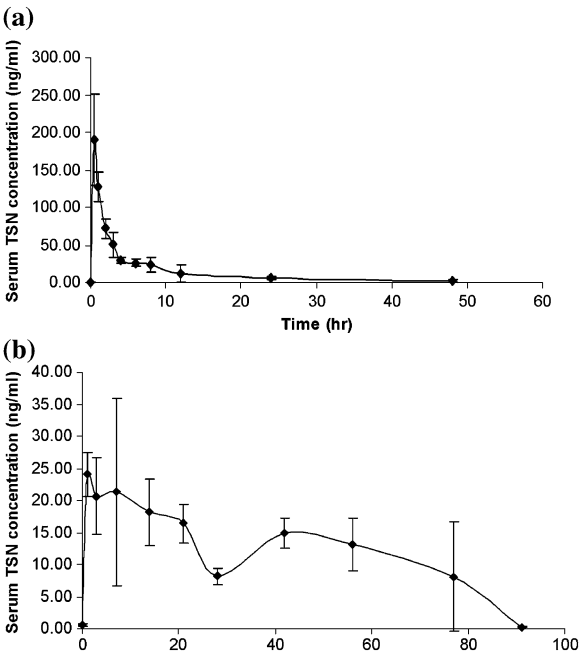

Fig. 2 In vivo absorption of TSN in rabbits after subcutaneous administration of TSN formulations (**a**) Control solution (300 mg/ml TSN in DMSO), (**b**) Thermosensitive polymer formulations (300 mg/ml TSN, copolymer PLGA–PEG–PLGA, 30% w/v). [From Chen et al. [11] Reprinted with the permission of Wiley Publishers]

showed a relatively low initial burst release in comparison to the rats injected with sCT solution in phosphate buffer saline (Fig. 3a, b and c).

Formulation A showed an increased concentration of sCT over a period of $\sim$21 days post subcutaneous administration accompanied with a significant ($p < 0.05$) decline in serum calcium level for $\sim$20 days. At the same time, formulation B showed an increased sCT concentration up to $\sim$40 days and a significantly ($p < 0.05$) lower serum calcium levels for more than a month in comparison to the control group. Formulation A showed a higher initial burst release as compared to formulation B which is attributed to the release of sCT located in the hydrophilic zone of the in situ formed gel and the push-out effect of the system during the gel formation [66]. The therapeutic efficacy of released sCT from polymeric formulations was also evaluated by determining the preventive effect of sCT against methylprednisolone acetate (MPA)-induced osteopenia. Serum level of osteocalcin (a marker for bone formation) and the number of osteoclasts (a marker for bone resorption) were evaluated. It was found that rats administered with a bolus subcutaneous injection of polymeric formulation of sCT in the beginning of the MPA treatment retained their normal serum osteocalcin level for 4 weeks from the administration of formulation A and for 6 weeks from administration of the formulation B. However, there was a significant ($p < 0.05$) decrease in serum osteocalcin level in the MPA treated rats as compared to the blank control. Bone turnover study showed a significant ($p < 0.05$) increase in the number of osteoclasts in MPA treated rats as compared to the blank control group. MPA-induced increase in the number of osteoclasts was prevented, in rat tibia,

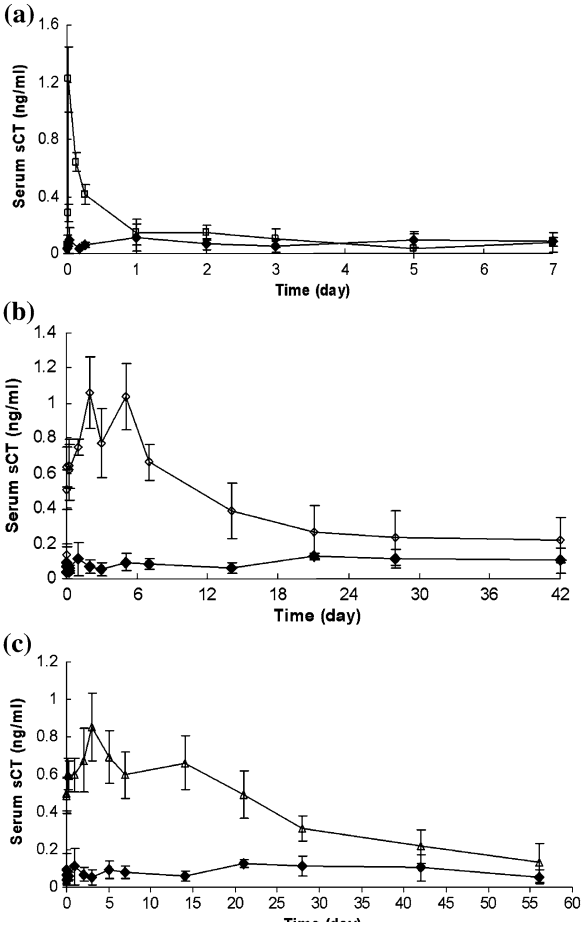

Fig. 3 Serum sCT concentration after administration of **a** sCT solution **b** sCT-loaded polymeric formulation A, and **c** sCT-loaded polymeric formulation B in rats. ($n = 6$) Key: (*filled diamond*) rats administrated with blank polymeric formulation, (*open diamond*) rats administrated with sCT polymeric formulation A, (*open triangle*) rats administrated with sCT polymeric formulation B. [From Tang and Singh, [66] Reprinted with the permission of Springer Publishers]

after administration of formulation A for the first 4 weeks. However, it failed to inhibit the increase in osteoclasts number after 8 weeks of treatment with MPA. In comparison, formulation B significantly ($p < 0.05$) restrained the MPA-induced increase in the number of osteoclasts in rat tibia for 8 weeks.

4.2 Poloxamer Based Thermosensitive Systems (Pluronics)

Pluronic gel (PF127) was administered in vivo and evaluated for delivery of insulin in normal rats [4]. In vivo evaluation of serum insulin and glucose levels was performed after subcutaneous administration of various insulin formulations including insulin solution, PLGA based insulin nanoparticles, insulin-loaded PF127 gels (20 and 30% of PF127) and insulin nanoparticle-loaded PF127 gels (20 and 30% of PF127). PF127 gels showed a prolonged and delayed hypoglycemic effect of insulin which was inversely proportional to the polymer

concentration. The longest hypoglycemic effect was observed using PLGA nanoparticles dispersed in PF127 gel (20 and 30% w/v). This was illustrated by a 3.1 fold increase in the area under curve (AUC) for insulin bioavailability as compared to the simple solution. A reduced absorption rate of insulin was observed at higher concentration of PF127. This could be attributed to the decreased diffusion of insulin as a result of micellar entanglement and increased viscosity of the formulation in body fluids [10, 43]. The formulation with 30% PF127 was evaluated to perform better in controlling the release of insulin among the various formulations studied.

A thermoreversible polymer based suppository system for insulin delivery, which formed bioadhesive gels at body temperature and showed an enhanced bioavailability, was formulated by Yun et al. [78]. Streptozotocin-treated male SD rats were administered with different suppository formulations and subsequently subjected to a comparative pharmacodyanamic study accompanied with a quantitative histological assessment of rectal mucosa. The thermoreversible insulin liquid suppositories [insulin: P407: P188: polycarbophil: sodium salicylate] exhibited the optimal physicochemical properties and showed good safety profile in rats. It also showed significant ($p < 0.05$) reduction in plasma glucose levels than did the solid and liquid suppositories without sodium salicylate in rats, thereby confirming the absorption enhancing effect of sodium salicylate. Thus, thermoreversible insulin liquid suppositories could be potentially developed as a safe, convenient and effective rectal delivery system for insulin.

4.3 Poly(organophosphazenes) Based Thermosensitive Systems

A cationic protamine conjugated poly (organophosphazenes) based thermosensitive drug delivery system was reported for the sustained delivery of human growth hormone (hGH) [52]. To investigate the effect of protamine on hGH release profile, comparative pharmacokinetics studies were performed in male SD rats using various hGH formulations, such as hGH solution, non ionic hydrogel loaded with hGH, and ionic hydrogel loaded with hGH after subcutaneous injection. In non ionic hydrogel, the maximum plasma concentration (C_{max}) was decreased by half and the half-life was increased by more than twice as compared to that of hGH solution alone. However, both the hGH solution and non ionic loaded hGH showed significant ($p < 0.05$) burst release of the hormone. The pharmacokinetics data revealed that with the increasing amount of protamine in the hydrogel, the C_{max} was decreased and the half-life of hGH increased due to the complex formation between the cationic protamine and anionic hGH. In case of ionic hydrogel with higher concentration of protamine, there was 20 fold increase in the half-life as compared to hGH alone and release was sustained for 3 days. The release profile and efficacy of various hGH formulations were also investigated in male cynomolgus monkeys after subcutaneous injection.

Recently, a thermosensitive biodegradable drug delivery system of 2-methoxyestradiol (2-ME) was designed using poly (organophosphazene) polymer [17].

Table 2 Applications of thermosensitive polymers in hormonal delivery

Polymer type	Hormone delivered	Remarks	References
PLGA–PEG–PLGA (Solution: in situ gel)	Porcine growth hormone (pGH)	Controlled release and biocompatible system was formulated	Chen and Singh [15]
Cationic Polyorganophosphazenes (Hydrogel)	Human growth hormone (hGH)	Protamine-hGH complex was conjugated to the polymer. Improved stability, efficacy and sustained release of the hGH were obtained.	Park et al. [52]
N-isopropyl acrylamide (NIPAAm), Butyl methacrylate (BMA) and acrylic acid (Beads)	Insulin	Loaded and released insulin was fully bioactive. Targeting the release of the hormone in colon, small intestine or immediate release in the duodenum may be achieved using different molecular weights of the polymer.	Ramkissoon-Ganorkar et al. [55]
PLA and PLGA–PEG–PLGA (Solution)	Testosterone	Prolonged release injectable implant delivery systems for testosterone were formulated.	Chen and Singh [13]
Ehylene glycol vinyl ether(EGVE):Butyl vinyl ether (BE) (Hydrogel)	Insulin	Bioactive hydrogels were formulated for use in cell culture. Insulin modified gels could support cell growth in the absence of serum.	Gümüsderelioglu et al. [25]
Hexachlorocyclotriphosphazene, methoxy poly(ethylene glycol) (MPEG 350) and oligopeptides (Micelles)	hGH	The trimers self assembled to form stable micelles with a low critical solution temperature of 20–48°C	Toti et al. [67]

(continued)

Table 2 (continued)

Polymer type	Hormone delivered	Remarks	References
Hyaluronic acid/Pluronic [Poly (ethylene glycol)-poly(propylene glycol)-poly(ethylene glycol)] (Hydrogels)	hGH	Pluronic component formed self associating micelles. The hydrogels collapsed with increasing temperature over a range of 5–40°C. Sustained release profile with mass erosion pattern was achieved.	Kim and Park [38]
Chitosan-polyvinyl alcohol (In situ gel)	Insulin	Thermosensitive gel for nasal delivery of insulin could maintain blood glucose for 6 h	Agrawal et al. [1]
PLGA–PEG–PLGA	Levonorgestrel (LNG) and testosterone (TSN)	Controlled release of incorporated hormone and a significantly increased in their bioavailability after single subcutaneous injection in rabbits were achieved.	Chen et al. [11]
Pluronic F127 end capped with D/L lactic acid (Hydrogel)	hGH	Sustained release of the hormone due to erosion of the gel was observed.	Park et al. [51, 53]
Quaternized chitosan, poly(ethylene glycol) and alpha–beta-glycerophosphate (Hydrogel)	Insulin	Thermosensitive hydrogel improved the nasal absorption of macromolecular and hydrophilic drugs.	Wu et al. [75]
Poly(organophosphazenes) (Solution)	hGH	Controlled release of hGH was observed for 3–4 days	Seong et al. [57]
PLGA–PEG–PLGA (Microspheres)	Insulin	Continuous in vitro and in vivo release was observed without any burst or incomplete release.	Kwon and Kim [39]

(continued)

Table 2 (continued)

Polymer type	Hormone delivered	Remarks	References
mPEG-PLGA-mPEG (in situ hydrogel)	Salmon Calcitonin	The polymeric formulation controlled the release of salmon calcitonin for 20–40 days.	Tang and Singh [66]
Poly(organophosphazenes) (Hydrogel)	2-methoxyestradiol	The formulation enhanced the solubility of methoxyestradiol significantly and substantially inhibited tumor growth and angiogenesis.	Cho et al. [17]
PLGA–PEG–PLGA with LA/GA (Hydrogel)	Levonorgestrel (LNG)	Prolonged release of the contraceptive hormone was achieved.	Chen and Singh [14]
ReGel® (Hydrogel)	pGH, Insulin	The gels showed reverse thermal gelation properties and demonstrated a controlled release for 1–6 weeks.	Zentner et al. [79]
ReGel® (Hydrogel)	Glucagon-like peptide 1(GLP-1)	The delivery system provided controlled release for about 2 months and was biocompatible and biodegradable.	Choi et al. [18]
N-isopropylacrylamide (NIPAAM) (Hydrogel)	Insulin like growth factor (IGF 1)	The release IGF 1 from these rapid gelling hydrogel composites remained bioactive during the 2-week release period.	Wang et al. [72]

The efficacy of this delivery system was evaluated in a mouse orthotpic breast tumor (MDA-MB-231) model by monitoring tumor volume and CD31 immunohistochemical staining. The hydrogel containing a relatively low concentration (15 mg/kg) of 2-ME showed the better antitumor and antiangiogenic activity relative to the original formulation.

5 Applications of Thermosensitive Polymeric Delivery Systems

Hormone implants are the most widely administered delivery systems for controlled and long term release of hormones. However, certain issues are associated with implants such as their cost, inconvenience, and discomfort of the minor surgery which is required to insert or remove the device by professionals due to their non-biodegradable nature. Recently, several biodegradable depot formulations have been reported for the controlled delivery of both protein and steroidal hormones. Table 2 depicts the recent applications of temperature sensitive polymeric delivery systems employed for the delivery of hormones.

6 Summary

In conclusion, the primary requirements of a successful controlled release product focuses on increasing patient compliance as well as obtaining a desired release profile of the therapeutic moieties. Various polymeric delivery systems have been approved for bulk production and clinical applications. However, challenges such as bioresponse features, biocompatibility, controlled and optimum release, and stability of the therapeutic moieties in the formulation remain a challenge.

Polymeric in situ gels have a significant advantage over the conventional dosage forms as they provide a sustained and prolonged release of various drugs and have been particularly used for the delivery of protein hormones. In addition, they also possess improved stability and biocompatibility characteristics. Use of biodegradable and water soluble thermosensitive polymers for the in situ gel formulations can make them more acceptable and excellent drug delivery systems.

References

1. Agrawal, A.K., Gupta, P.N., Khanna, A., Sharma, R.K., Chandrawanshi, H.K., Gupta, N., Patil, U.K., Yadav, S.K.: Development and characterization of in situ gel system for nasal insulin delivery. Pharmazie **65**(3), 188–193 (2010)
2. Alexandridis, P., Holzwarth, J.F., Hatton, T.A.: Micellization of Poly(ethylene oxide)-Poly(propylene oxide)-Poly(ethylene oxide) triblock copolymers in aqueous solutions: thermodynamics of copolymer association. Macromolecules **27**(9), 2414–2425 (1994)

3. Al-Tahami, K., Singh, J.: Smart polymer based delivery systems for peptides and proteins. Recent Pat. Drug Deliv. Formul. **1**(1), 65–71 (2007)
4. Barichello, J.M., Morishita, M., Takayama, K., Nagai, T.: Absorption of insulin from pluronic F-127 gels following subcutaneous administration in rats. Int. J. Pharm. **184**(2), 189–198 (1999)
5. Basu Ray, G., Chakraborty, I., Moulik, S.P.: Pyrene absorption can be a convenient method for probing critical micellar concentration (cmc) and indexing micellar polarity. J. Colloid Interface Sci. **294**(1), 248–254 (2006)
6. Behravesh, E., Shung, A.K., Jo, S., Mikos, A.G.: Synthesis and characterization of triblock copolymers of methoxy poly(ethylene glycol) and poly(propylene fumarate). Biomacromolecules **3**(1), 153–158 (2002)
7. Bochot, A., Fattal, E., Gulik, A., Couarraze, G., Couvreur, P.: Liposomes dispersed within a thermosensitive gel: a new dosage form for ocular delivery of oligonucleotides. Pharm. Res. **15**(9), 1364–1369 (1998)
8. Buwalda, S.J., Dijkstra, P.J., Calucci, L., Forte, C., Feijen, J.: Influence of amide versus ester linkages on the properties of eight-armed PEG–PLA star block copolymer hydrogels. Biomacromolecules **11**(1), 224–232 (2010)
9. Charman, S.A., Mason, K.L., Charman, W.N.: Techniques for assessing the effects of pharmaceutical excipients on the aggregation of porcine growth hormone. Pharm. Res. **10**(7), 954–962 (1993)
10. Chen-CHow, P., Frank, S.G.: Comparison of lidocaine release from Pluronic F-127 gels and other formulations. Acta Pharm. Suec **18**(4), 239–244 (1981)
11. Chen, S., Pederson, D., Oak, M., Singh, J.: In vivo absorption of steroidal hormones from smart polymer based delivery systems. J. Pharm. Sci. **99**(8), 3381–3388 (2010)
12. Chen, S., Pieper, R., Webster, D.C., Singh, J.: Triblock copolymers: synthesis, characterization, and delivery of a model protein. Int. J. Pharm. **288**(2), 207–218 (2005)
13. Chen, S., Singh, J.: Controlled delivery of testosterone from smart polymer solution based systems: in vitro evaluation. Int. J. Pharm. **295**(1–2), 183–190 (2005)
14. Chen, S., Singh, J.: In vitro release of levonorgestrel from phase sensitive and thermosensitive smart polymer delivery systems. Pharm. Dev. Technol. **10**(2), 319–325 (2005)
15. Chen, S., Singh, J.: Controlled release of growth hormone from thermosensitive triblock copolymer systems: In vitro and in vivo evaluation. Int. J. Pharm. **352**(1–2), 58–65 (2008)
16. Cho, H., Chung, D., Jeongho, A.: Poly(D, L-lactide-ran-epsilon-caprolactone)-poly(ethylene glycol)-poly(D,L-lactide-ran-epsilon-caprolactone) as parenteral drug-delivery systems. Biomaterials **25**(17), 3733–3742 (2004)
17. Cho, J.-K., Hong, K.-Y., Park, J.W., Yang, H., Song, S.-C.: Injectable delivery system of 2-methoxyestradiol for breast cancer therapy using biodegradable thermosensitive poly(organophosphazene) hydrogel. J. Drug Target (2010) (doi:10.3109/1061186X.2010.499461)
18. Choi, S., Baudys, M., Kim, S.W.: Control of blood glucose by novel GLP-1 delivery using biodegradable triblock copolymer of PLGA–PEG–PLGA in type 2 diabetic rats. Pharm. Res. **21**(5), 827–831 (2004)
19. Choi, S., Kim, S.W.: Controlled release of insulin from injectable biodegradable triblock copolymer depot in ZDF rats. Pharm. Res. **20**(12), 2008–2010 (2003)
20. Cui, Z., Lee, B.H., Vernon, B.L.: New hydrolysis-dependent thermosensitive polymer for an injectable degradable system. Biomacromolecules **8**(4), 1280–1286 (2007)
21. Dimitrov, I., Trzebicka, B., Müller, A.H., Dworak, A., Tsvetanov, C.B.: Thermosensitive water-soluble copolymers with doubly responsive reversibly interacting entities. Prog. Polym. Sci. **32**(11), 1275–1343 (2007)
22. Du, J., Peng, Y., Zhang, T., Ding, X., Zheng, Z.: Study on pH-sensitive and thermosensitive polymer networks containing polyacetal segments. J. Appl. Polym. Sci. Symp. **83**(14), 3002–3006 (2002)

23. Garbern, J.C., Hoffman, A.S., Stayton, P.S.: Injectable pH- and temperature-responsive Poly(N-isopropylacrylamide-co-propylacrylic acid) copolymers for delivery of angiogenic growth factors. Biomacromolecules **11**(7), 1833–1839 (2010)
24. Gong, C., Shi, S., Dong, P., Kan, B., Gou, M., Wang, X., Li, X., Luo, F., Zhao, X., Wei, Y., Qian, Z.: Synthesis and characterization of PEG–PCL–PEG thermosensitive hydrogel. Int. J. Pharm. **365**(1–2), 89–99 (2009)
25. Gümüsderelioglu, M., Müftüoglu, O., Gönen Karakeçili, A.: Biomodification of thermosensitive copolymer of ethylene glycol vinyl ether by RGD and insulin. React. Funct. Polym. **58**(2), 149–156 (2004)
26. Hatefi, A., Amsden, B.: Biodegradable injectable in situ forming drug delivery systems. J. Control Release **80**(1–3), 9–28 (2002)
27. Hu, D.S., Liu, H.: Structural analysis and degradation behavior in polyethylene glycol/poly(L-lactide) copolymers. J. Appl. Polym. Sci. Symp. **51**(3), 473–482 (1994)
28. Hwang, M.J., Suh, J.M., Bae, Y.H., Kim, S.W., Jeong, B.: Caprolactonic poloxamer analog: PEG–PCL–PEG. Biomacromolecules **6**(2), 885–890 (2005)
29. Ignatius, A.A., Claes, L.E.: In vitro biocompatibility of bioresorbable polymers: poly(L, DL-lactide) and poly(L-lactide-co-glycolide). Biomaterials **17**(8), 831–839 (1996)
30. International Organization for Standardization. (2007) Biological evaluation of medical devices. Geneva, Switzerland. Test for local effects after implantation Part 6.
31. Jagtap, R.N., Ambre, A.H.: Overview literature on matrix assisted laser desorption ionization mass spectroscopy (MALDI MS): basics and its applications in characterizing polymeric materials. Bull Mater. Sci. **28**(6), 515–528 (2005)
32. Jeong, B., Bae, Y.H., Lee, D.S., Kim, S.W.: Biodegradable block copolymers as injectable drug-delivery systems. Nature **388**(6645), 860–862 (1997)
33. Jeong, B., Bae, Y.H., Kim, S.W.: Biodegradable thermosensitive micelles of PEG–PLGA–PEG triblock copolymers. Colloids Surf. B Biointerf. **16**(1–4), 185–193 (1999)
34. Jeong, B., Bae, Y.H., Kim, S.W.: Thermoreversible gelation of PEG–PLGA–PEG triblock copolymer aqueous solutions. Macromolecules **32**(21), 7064–7069 (1999)
35. Jeong, B., Kibbey, M.R., Birnbaum, J.C., Won, Y., Gutowska, A.: Thermogelling biodegradable polymers with hydrophilic backbones: PEG-g-PLGA. Macromolecules **33**(22), 8317–8322 (2000)
36. Kim, Y.J., Choi, S., Koh, J.J., Lee, M., Ko, K.S., Kim, S.W.: Controlled release of insulin from injectable biodegradable triblock copolymer. Pharm. Res. **18**(4), 548–550 (2001)
37. Kim, M.S., Hyun, H., Seo, K.S., Cho, Y.H., Won Lee, J., Rae Lee, C., Khang, G., Lee, H.B.: Preparation and characterization of MPEG-PCL diblock copolymers with thermo-responsive sol–gel–sol phase transition. J. Polym. Sci. A. Polym. Chem. **44**, 5413–5423 (2006)
38. Kim, M.R., Park, T.G.: Temperature-responsive and degradable hyaluronic acid/Pluronic composite hydrogels for controlled release of human growth hormone. J. Control Release **80**(1–3), 69–77 (2002)
39. Kwon, Y.M., Kim, S.W.: Biodegradable triblock copolymer microspheres based on thermosensitive sol–gel transition. Pharm. Res. **21**(2), 339–343 (2004)
40. Lee, B.H., Lee, Y.M., Sohn, Y.S., Song, S.: Synthesis and characterization of thermosensitive Poly(organophosphazenes) with methoxy-poly(ethylene glycol) and akylamines as side groups. Bull. Korean Chem. Soc. **23**(4), 549–554 (2002)
41. Lee, S.B., Russell, A.J., Matyjaszewski, K.: ATRP synthesis of amphiphilic random, gradient, and block copolymers of 2-(Dimethylamino)ethyl methacrylate and n-butyl methacrylate in aqueous media. Biomacromolecules **4**(5), 1386–1393 (2003)
42. Loh, X.J., Goh, S.H., Li, J.: New biodegradable thermogelling copolymers having very low gelation concentrations. Biomacromolecules **8**(2), 585–593 (2007)
43. Lu, G., Jun, H.W.: Diffusion studies of methotrexate in Carbopol and Poloxamer gels. Int. J. Pharm. **160**(1), 1–9 (1998)
44. Lutz, J., Akdemir, Ö., Hoth, A.: Point by point comparison of two thermosensitive polymers exhibiting a similar LCST: Is the age of Poly(NIPAM) over? J. Am. Chem. Soc. **128**(40), 13046–13047 (2006)

45. Mahmoud, K.: Recombinant protein production:strategic technology and a vital research tool. Res. J. Cell Mol. Biol. **1**(1), 9–22 (2007)
46. Mori, T., Shiota, Y., Minagawa, K., Tanaka, M.: Alternative approach to the design of thermosensitive polymers: The addition of hydrophobic groups to the ends of hydrophilic polyether. J. Polym. Sci. A Polym. Chem. **43**(5), 1007–1013 (2005)
47. Mortisen, D., Peroglio, M., Alini, M., Eglin, D.: Tailoring thermoreversible hyaluronan hydrogels by "click" chemistry and RAFT polymerization for cell and drug therapy. Biomacromolecules **11**(5), 1261–1272 (2010)
48. Müller, R.H., Rühl, D., Runge, S., Schulze-Forster, K., Mehnert, W.: Cytotoxicity of solid lipid nanoparticles as a function of the lipid matrix and the surfactant. Pharm. Res. **14**(4), 458–462 (1997)
49. Paavola, A., Kilpeläinen, I., Yliruusi, J., Rosenberg, P.: Controlled release injectable liposomal gel of ibuprofen for epidural analgesia. Int. J. Pharm. **199**(1), 85–93 (2000)
50. Packhaeuser, C.B., Schnieders, J., Oster, C.G., Kissel, T.: In situ forming parenteral drug delivery systems: An overview. Eur. J. Pharm. Biopharm. **58**(2), 445–455 (2004)
51. Park, K.M., Bae, J.W., Joung, Y.K., Shin, J.W., Park, K.D.: Nano-aggregate of thermosensitive chitosan-Pluronic for sustained release of hydrophobic drug. Colloids Surf. B Biointerf. **63**(1), 1–6 (2008)
52. Park, M., Chun, C., Ahn, S., Ki, M., Cho, C., Song, S.: Cationic and thermosensitive protamine conjugated gels for enhancing sustained human growth hormone delivery. Biomaterials **31**(6), 1349–1359 (2010)
53. Park, S.Y., Chung, H.J., Lee, Y., Park, T.G.: Injectable and sustained delivery of human growth hormone using chemically modified Pluronic copolymer hydrogels. Biotechnol. J. **3**(5), 669–675 (2008)
54. Park, Y., Yong, C.S., Kim, H., Rhee, J., Oh, Y., Kim, C., Choi, H.: Effect of sodium chloride on the release, absorption and safety of diclofenac sodium delivered by poloxamer gel. Int. J. Pharm. **263**(1–2), 105–111 (2003)
55. Ramkissoon-Ganorkar, C., Liu, F., Baudys, M., Kim, S.W.: Modulating insulin-release profile from pH/thermosensitive polymeric beads through polymer molecular weight. J. Control Release **59**(3), 287–298 (1999)
56. Ruel-Gariépy, E., Leroux, J.: In situ-forming hydrogels-review of temperature-sensitive systems. Eur. J. Pharm. Biopharm. **58**(2), 409–426 (2004)
57. Seong, J., Jun, Y.J., Kim, B.M., Park, Y.M., Sohn, Y.S.: Synthesis and characterization of biocompatible poly(organophosphazenes) aiming for local delivery of protein drugs. Int. J. Pharm. **314**(1), 90–96 (2006)
58. Shive, M.S., Anderson, J.M.: Biodegradation and biocompatibility of PLA and PLGA microspheres. Adv. Drug Deliv. Rev. **28**(1), 5–24 (1997)
59. Singh, S., Webster, D.C., Singh, J.: Thermosensitive polymers: synthesis, characterization, and delivery of proteins. Int. J. Pharm. **341**(1–2), 68–77 (2007)
60. Soga, O., van Nostrum, C.F., Ramzi, A., Visser, T., Soulimani, F., Frederik, P.M., Bomans, P.H., Hennink, W.E.: Physicochemical characterization of degradable thermosensitive polymeric micelles. Langmuir **20**(21), 9388–9395 (2004)
61. Soga, O., van Nostrum, C.F., Fens, M., Rijcken, C.J.F., Schiffelers, R.M., Storm, G., Hennink, W.E.: Thermosensitive and biodegradable polymeric micelles for paclitaxel delivery. J. Control Release **103**(2), 341–353 (2005)
62. Stile, R.A., Burghardt, W.R., Healy, K.E.: Synthesis and characterization of injectable Poly(N-isopropylacrylamide)-based hydrogels that support tissue formation in vitro. Macromolecules **32**(22), 7370–7379 (1999)
63. Tai, H., Howard, D., Takae, S., Wang, W., Vermonden, T., Hennink, W.E., Stayton, P.S., Hoffman, A.S., Endruweit, A., Alexander, C., Howdle, S.M., Shakesheff, K.M.: Photo-cross-linked hydrogels from thermoresponsive PEGMEMA–PPGMA–EGDMA copolymers containing multiple methacrylate groups: mechanical property, swelling, protein release, and cytotoxicity. Biomacromolecules **10**(10), 2895–2903 (2009)

64. Tai, H., Wang, W., Vermonden, T., Heath, F., Hennink, W.E., Alexander, C., Shakesheff, K.M., Howdle, S.M.: Thermoresponsive and photocrosslinkable PEGMEMA–PPGMA–EGDMA copolymers from a one-step ATRP synthesis. Biomacromolecules **10**(4), 822–828 (2009)
65. Tang, Y., Singh, J.: Biodegradable and biocompatible thermosensitive polymer based injectable implant for controlled release of protein. Int. J. Pharm. **365**(1–2), 34–43 (2009)
66. Tang, Y., Singh, J.: Thermosensitive drug delivery system of salmon calcitonin: In vitro release, in vivo absorption, bioactivity and therapeutic efficacies. Pharm. Res. **27**(2), 272–284 (2010)
67. Toti, U.S., Moon, S.H., Kim, H.Y., Jun, Y.J., Kim, B.M., Park, Y.M., Jeong, B., Sohn, Y.S.: Thermosensitive and biocompatible cyclotriphosphazene micelles. J. Control Release **119**(1), 34–40 (2007)
68. Vermonden, T., Besseling, N.A.M., van Steenbergen, M.J., Hennink, W.E.: Rheological studies of thermosensitive triblock copolymer hydrogels. Langmuir **22**(24), 10180–10184 (2006)
69. Vermonden, T., Jena, S.S., Barriet, D., Censi, R., van der Gucht, J., Hennink, W.E., Siegel, R.A.: Macromolecular diffusion in self-assembling biodegradable thermosensitive hydrogels. Macromolecules **43**(2), 782–789 (2010)
70. Wang, W.: Instability, stabilization, and formulation of liquid protein pharmaceuticals. Int. J. Pharm. **185**(2), 129–188 (1999)
71. Wang, F., Li, Z., Khan, M., Tamama, K., Kuppusamy, P., Wagner, W.R., Sen, C.K., Guon, J.: Injectable, rapid gelling and highly flexible hydrogel composites as growth factor and cell carriers. Acta Biomater. **6**(6), 1978–1991 (2010)
72. Wang, Z., Xu, X., Chen, C., Yun, L., Song, J., Zhang, X., Zhuo, R.: In situ formation of thermosensitive PNIPAAm-based hydrogels by Michael-type addition reaction. ACS Appl. Mater. Interf. **2**(4), 1009–1018 (2010)
73. Wasan, K.M., Subramanian, R., Kwong, M., Goldberg, I.J., Wright, T., Johnston, T.P.: Poloxamer 407-mediated alterations in the activities of enzymes regulating lipid metabolism in rats. J. Pharm. Pharm. Sci. **6**(2), 189–197 (2003)
74. Wei, X., Gong, C., Gou, M., Fu, S., Guo, Q., Shi, S., Luo, F., Guo, G., Qiu, L., Qiu, Z.: Biodegradable poly(epsilon-caprolactone)-poly(ethylene glycol) copolymers as drug delivery system. Int. J. Pharm. **381**(1), 1–18 (2009)
75. Wu, J., Wei, W., Wang, L., Su, Z., Ma, G.: A thermosensitive hydrogel based on quaternized chitosan and poly(ethylene glycol) for nasal drug delivery system. Biomaterials **28**(13), 2220–2232 (2007)
76. Xu, X., Wang, B., Wang, Z., Cheng, S., Zhang, X., Zhuo, R.: Fabrication of fast responsive, thermosensitive poly(N-isopropylacrylamide) hydrogels by using diethyl ether as precipitation agent. J. Biomed. Mater. Res. A **86**(4), 1023–1032 (2008)
77. Yu, L., Zhang, Z., Zhang, H., Ding, J.: Biodegradability and biocompatibility of thermoreversible hydrogels formed from mixing a sol and a precipitate of block copolymers in water. Biomacromolecules **11**(8), 2169–2178 (2010)
78. Yun, M., Choi, H., Jung, J., Kim, C.: Development of a thermo-reversible insulin liquid suppository with bioavailability enhancement. Int. J. Pharm. **189**(2), 137–145 (1999)
79. Zentner, G.M., Rathi, R., Shih, C., McRea, J.C., Seo, M.H., Oh, H., Rhee, B.G., Mestecky, J., Moldoveanu, Z., Morgan, M., Weitman, S.: Biodegradable block copolymers for delivery of proteins and water-insoluble drugs. J. Control Release **72**(1–3), 203–215 (2001)
80. Zhang, L., Zhu, W., Song, L., Wang, Y., Jiang, H., Xian, S., Ren, Y.: Effects of hydroxylpropyl-beta-cyclodextrin on in vitro insulin stability. Int. J. Mol. Sci. **10**(5), 2031–2040 (2009)
81. Zhou, G., Harruna, I.I., Ingram, C.W.: Ruthenium-centered thermosensitive polymers. Polymer **46**(24), 10672–10677 (2005)

Intrinsically Conducting Polymer Platforms for Electrochemically Controlled Drug Delivery

Darren Svirskis, Bryon E. Wright, Jadranka Travas-Sejdic and Sanjay Garg

Abstract Intrinsically conducting polymers (ICPs) combine the physical properties of polymers with the electrical properties of metals. This unique group of polymers can be loaded with drugs and then electrochemically stimulated to control the rate at which drug is released. Drug delivery systems based on ICPs have the exciting potential to match treatment requirements with highly controlled drug release using facile electronic control—leading to improved patient outcomes. The application of ICPs to controlled release can be broken into three general types of platform. In ICP matrix systems, drug is directly incorporated into the ICP and release rates are determined by the redox state of the ICP. ICP/hydrogel composite systems are an elaboration in which ICPs are polymerized inside a hydrogel network, actuation of the ICP component drives drug release. In electromechanical systems the ICP can either act as a mechanical actuator or selective membrane to pump or gate the release of drug. This chapter details the basic properties and preparation of ICPs as it relates to controlled drug delivery and considers appropriate drugs for each system. IR and Raman spectroscopy, scanning electron microscopy, and scanning probe microscopy are described as techniques important to the characterization of ICPs. Finally, a discussion of the

D. Svirskis · S. Garg (✉)
School of Pharmacy, Faculty of Medical and Health Sciences and Polymer Electronics Research Centre, Department of Chemistry, Faculty of Science, University of Auckland, Private Bag, Auckland 92019, New Zealand
e-mail: s.garg@auckland.ac.nz

B. E. Wright · J. Travas-Sejdic
Auckland Microfabrication Facility, Department of Chemistry, Faculty of Science, University of Auckland, Private Bag, Auckland 92019, New Zealand

B. E. Wright
Polymer Electronics Research Centre, Department of Chemistry, Faculty of Science, University of Auckland, Private Bag, Auckland 92019, New Zealand

Stud Mechanobiol Tissue Eng Biomater (2011) 8: 481–512
DOI: 10.1007/8415_2010_49

Published Online: 21 January 2011

challenges and prospects faced in the development of ICP systems for controlled release is given.

1 Introduction

Patients with chronic illness or abnormal physiological conditions often have an accompanying high frequency medication regime. Poor compliance with such medication regimes is an obstacle to the successful treatment of chronic health problems including those with an elevated cardio-vascular risk, psychiatric health problems [1, 2], or chronic infectious diseases [3]. Further, frequent dosing with short acting dosage forms can lead to high peak concentrations with toxic drug levels and low trough concentrations where the drug may be ineffective [4]. Controlled release systems providing extended steady levels of drug release help overcome these issues. Whilst many polymeric controlled release formulations have been developed they have predetermined release rates that cannot be easily altered or halted once applied. What is desired is a means to match the dose to the clinical need, even as the need might change; this is the promise of intrinsically conducting polymer (ICP) based drug delivery systems (DDS).

ICPs are a unique class of materials that combine the ease of processing and advantageous physical properties of polymers with the electrical properties of metals. Pioneering work on ICPs by Heeger, MacDiarmid and Shirakawa in the late 1970s led to them being awarded the Nobel Prize in Chemistry in 2000. This exciting group of materials has since been widely researched and applied, e.g., toward light emitting devices, integrated circuits, electromagnetic shielding, corrosion inhibitors, antistatic coatings, field effect transistors and sensing devices [5]. ICPs have also been used in biomedical settings as biosensors, for nerve regeneration, and increasingly as components in DDS [4, 6, 7].

As the name implies, ICPs are intrinsically conductive, without the need for conductive particle or coatings to be added as in earlier conducting polymer formulations. All ICPs share an uninterrupted and ordered π-conjugated polymer backbone that provides the conduction pathway. By analogy with semiconductors, the conductivity of ICPs is dependent on the chemical nature of the material as well as the means by which charge is carried within. This can be tuned by the choice of ionic dopants and by modifying the redox state of the backbone. The alteration in redox state of an ICP results into a movement of ions into and out of the polymer. This can be used to drive ion fluxes and/or to cause mechanical deflections of the polymer, both of which can be exploited to control drug release through the application of an external electronic control signal. The exciting potential of ICP based DDS is this ability to electronically alter the rate of drug delivery in response to patient symptoms, blood results, treatment response or clinician's instruction.

ICPs that have been used for DDS can, in general, be categorized into ICP matrix systems, ICP/hydrogel composite systems and electromechanical systems. The release of drugs from ICP matrix systems can be directly modified by altering the redox state of the ICP, leading to subsequent changes in polymer charge or volume [7] and resulting alterations in drug flux. ICP/hydrogel composite systems are prepared through polymerization of an ICP inside a hydrogel network. This approach has the advantage of increased drug loading and broadening the range of drugs the system can be applied to. Electromechanical systems rely on the use of ICPs as actuators for pumping or gating the release of drug from a reservoir. As actuators for drug release systems, ICPs are highly energy efficient and possess desirable mechanical properties suited to in vivo application [8].

Polypyrrole (PPy) is the ICP most commonly used in drug delivery research; however, other ICPs including PPy derivatives [9], polyanaline (PANI) [10] and PEDOT (poly(3,4-ethylenedioxythiophene)) [11] have also been used. PPy therefore receives the most attention in this chapter and is a suitable model to represent ICPs for DDS. Another reason to highlight PPy is that initial work has shown that PPy is biocompatible [4, 12] while there is limited data available for other ICPs.

This chapter details the general properties and preparation of ICPs as well as specifics relevant to each ICP platform. A discussion is offered concerning the relationship between ICP platform and drug choice. Techniques used for their characterization are described including IR and Raman spectroscopy, scanning electron microscopy and scanning probe microscopy. Finally, a brief discussion of the challenges and prospects faced in the development of ICP systems for the controlled release of bioactive agents is given.

2 Properties of ICPs

2.1 Conductivity

The electrical conductivity of ICPs is attributed to their uninterrupted and ordered π-conjugated backbone. The level of conductivity depends on the density and mobility of electrons to act as charge carriers [13, 5]). In their oxidized state the ICP chains (Fig. 1) contain ‘holes’ following the removal of electrons. Neighboring electrons are free to move into these holes, allowing the progression of charge along the polymer and explaining the resultant conductivity. Charge progression occurs favorably along a polymer chain but can also occur between polymer chains. PPy can be synthesized with conductivities ranging from 10^{-4} to 10^{3} S cm^{-1} [14–19], levels commonly associated with semiconductors. The mobility of charge carriers is affected by conformational and chemical defects within the polymer. The absolute value is often established during synthesis of the

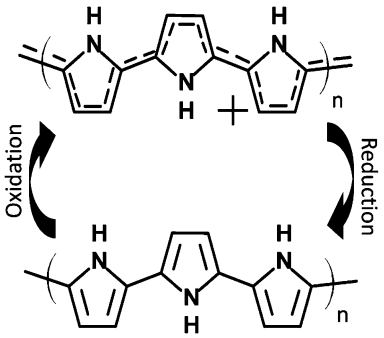

Fig. 1 Reversible redox activity of PPy. Reprinted from [111] with permission from Elsevier

polymer depending on the growth pattern of polymer chains and is influenced by temperature, time, pH, dopant type and concentration [16]. Conductivity has been used as a parameter to assess the quality of the polymer formed and to investigate its stability [14, 19–23].

2.2 Ion Movement in ICP Matrices

When the redox state of an ICP is altered there is a subsequent change in the charge of the polymer backbone (Fig. 1). To balance these charges there will be movement of mobile ions into or out of the polymer bulk. ICPs can be prepared using dopant anions with differing degrees of mobility in the polymer matrix. When smaller, more mobile anions are selected for the preparation of ICPs, these anions are able to leave the polymer on reduction as there is a loss of electrostatic attraction between ion and film [24]. This process is illustrated in Eq. 1.

$$\mathrm{PPy}^{+}/A^{-} \leftrightarrow \mathrm{PPy}^{0} + A^{-} \tag{1}$$

However, if bulkier anions are used as dopants during ICP polymerization, these will be immobilized within the polymer [24]. On redox switching, as the anion is unable to exchange out of the ICP, mobile cations in the surrounding solution will move into the polymer to balance charge according to Eq. 2.

$$\mathrm{PPy}^{+}/A^{-} + B^{+} \leftrightarrow \mathrm{PPy}^{0}/A^{-}/B^{+} \tag{2}$$

2.3 Volume Change

Volume changes in ICPs are due to the movement of solvated ions, into or out of the polymer, in response to a change in net charge when redox state is altered [25]. If highly mobile anions are used in the preparation of ICPs it is

the movement of these anions that drives actuation (Eq. 1); the ICP will be swollen on oxidation due to the increased presence of solvated anions within the polymer matrix and collapsed on reduction. However if immobile anions are use in the preparation of ICPs it is the movement of mobile solvated cations that drives actuation (Eq. 2); with the polymer swollen on reduction and collapsed on oxidation. Frequently actuation can be attributed to neither anion nor cation movement alone, in which case mixed-ion driven actuation is observed [26].

3 Synthesis of ICPs

Conducting polymer synthesis involves the oxidative polymerization of monomer units. Oxidation can be achieved either chemically, using a chemical oxidant, or electrochemically through the application of an oxidizing potential [13]. To create ICP platforms for drug delivery electrochemical oxidation is favorable, as it affords finer control and increased flexibility over the polymerization process. For PPy, polymerization begins when soluble pyrrole monomers are oxidized to radical cations which dimerize with radical–radical coupling at the α-position [27]. Following this coupling, the neutral product can be oxidized to a radical and in turn can react with a monomer, dimer or oligomeric radical to continue polymerization. The electrostatic repulsion of the radicals is balanced in part by the solvent but also requires the presence of anions which are incorporated into the ICP as it forms [28]. When using electrochemical oxidation it is desirable to polymerize the product on the electrode. However, some polymerization will also occur in solution. By controlling the experimental conditions the balance between product forming in solution, or on the electrode, can be influenced. The electropolymerization conditions employed allow the morphological and electromechanical characteristics of the product to be influenced by controlling the amount and rate of polymerization. Figure 2 is a schematic representation of the oxidation of monomer units to PPy. As the oxidation potential of the monomer is greater than the oxidation potential of the polymer, the newly formed polymer will be in the oxidized form [29]. The resulting positive charges on the polymer chain are counterbalanced by incorporation of anionic dopants (A^-). For PPy the ratio of anionic dopant to pyrrole subunits is between 0.25 and 0.33 [29–32].

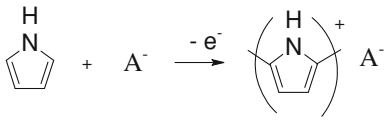

Fig. 2 Polypyrrole synthesis. Reprinted from [111] with permission from Elsevier

3.1 Synthesis Parameters that Influence Polymer Product

Electrochemical oxidation is often favored over chemical oxidation in the preparation of ICP based drug delivery systems as it allows for tighter control over the quantity and properties of polymer produced. Oxidation takes place in a two- or three-electrode cell using a working electrode (WE) and a counter or auxiliary electrode (CE), with or without a reference electrode (RE). Materials used as the WE and CE should be inert, and electrically inactive at the potentials used for polymerization. The material selected to act as the WE will influence the initial polymerization of PPy and will determine the morphology of very thin films [21]. However, as the polymer thickness increases new polymer is formed over an existing polymer layer, decreasing the influence of the WE material. Electrodes should always be carefully cleaned and polished, such as with Al_2O_3 paste, to provide a reliable and repeatable surface. The most common reference electrodes used are either silver/silver chloride (Ag/AgCl) or saturated calomel electrodes (SCE).

Oxidative polymerization can be achieved using different electrochemical methods including constant current density (galvanostatic mode), constant potential (potentiostatic mode) and cyclic voltammetry (CV, or potentiodynamic mode). A benefit of using constant current is to produce homogenous polymers with good mechanical strength and adhesion to the underlying electrode [28, 33]. When a three-electrode synthesis setup is used and constant current applied, the resulting potential can be recorded. It is possible to use constant current to polymerize ICPs with a two-electrode cell, although care must be taken to ensure the potential does not increase to levels where the quality of the polymer produced would be negatively influenced. If the potential is too high overoxidation can occur whereby the conductivity and electroactivity of the polymer are impaired with a loss of mechanical properties and decreased adhesion to the substrate [28, 33]. For a given set of synthesis parameters there will be an anodic activation potential below which polymerization will not occur. This is the minimum potential required to oxidize the monomer units to begin polymer formation. For example, from an aqueous solution containing 0.5 M pyrrole and 0.1 M adenosine triphosphate (ATP), polymerization will not occur at potentials under +0.60 V (vs SCE) [34].

Drug release profiles from a polymer matrix will be affected by polymer morphology. By controlling the parameters of the electrochemical polymerization the morphology of the newly formed polymer can be altered. PPy prepared at lower current densities (<1 mA cm^{-2}), or at lower anodic potentials (<0.8 V), will be dense and compact with smoother surfaces, while PPy films grown at higher charge densities (>5 mA cm^{-2}), or higher anodic potentials (>0.9 V), will form open, porous structures with more irregular surfaces [35–37].

It is often desirable to form polymer as a continuous film on the surface of the working electrode. During initiation of the PPy polymerization process, soluble pyrrole monomers are oxidized to radical cations which dimerize with

radical–radical coupling at the α-position [27]. This neutral dimer can be oxidized to a radical and in turn can react with a monomer, dimer or oligomeric radical to grow the chain. Initially, soluble intermediates form, but as the chains grow in length and exceeds a critical length, the solubility limit is reached and precipitation occurs onto the WE [28]. The electronic efficiency of polymer formation onto the WE is always less than 100%. One reason for this is that some soluble oligomers of PPy will not achieve the critical chain length and so remain soluble in the solvent. In addition, other oligomers will precipitate but in solution rather than onto the WE [27, 29]. Stirring inhibits the electrochemical formation of PPy, likely due to movement of oligomer units away from the WE preventing their precipitation and attachment [38].

While efficiency is below 100%, if synthesis variables are kept constant the amount of charge passed during polymerization can be used to estimate the quantity of polymer produced. Depending on the total thickness of polymer produced and the total polymerization time, estimates of between 240 and 600 mC cm^{-2} charge density have been reported to produce a 1 μm thick film of PPy [33, 37, 39]. While the total amount of charged passed is frequently used to estimate film thickness, it does not account for differences in polymer morphology.

By using different dopant anions in the preparation of ICPs the morphology, properties and function of the final polymers can all be influenced [29, 38]. Fonner et al. compared PPy films prepared with either chloride (Cl), *p*-toluene sulfonate (*p*TS) or poly(styrene sulfonate) (PSS) as the anionic dopant. For the same amount of charge passed during synthesis the Cl doped films were between 2 and 8 times thicker than *p*TS or PSS doped films, profilometry showed PPy-Cl had the roughest surface and PPy-PSS the smoothest surfaces [15].

4 ICP Based Drug Delivery Systems

Various drug delivery systems with an ICP component have been created. This section considers which drugs are appropriate for use in ICP based DDS, then examines different systems. These systems will be discussed in turn and have been categorized into ICP matrix system, ICP/hydrogel composite systems, and electromechanical ICP systems.

4.1 Drug Selection

When considering the suitability of a drug for use in an implantable drug releasing system several factors have to be considered. Drugs with short half lives are desirable as they have a reduced risk of accumulation. An implanted controlled release formulation can improve the efficacy of a drug requiring frequent

administration compared to conventional dosage forms in two ways. Firstly, high rates of non-adherence have been reported in patients requiring chronic therapy and implanted systems are useful to ensure adherence [40]. Secondly, by regulating the rate of drug release, controlled release systems are able to reduce the peak to trough ratio of drug in the body to maintain desirable levels. This reduces the potential for loss of response or toxic effects due to low or high levels of drug, respectively [41]. Parenteral delivery is an attractive option for drugs with poor or variable bioavailability, a lower total quantity of drug can be used to achieve required, predictable blood concentrations. The toxicity of the drug to local tissues must be considered as following implantation of the system drug concentrations can be relatively high in the surrounding area.

In addition to the general considerations when selecting a suitable drug for use in an implantable system, extra factors must be examined if the drug is to find use in an ICP matrix system. To ensure the biological activity of the candidate drug is preserved it should not be electroactive in the window of potentials used during the preparation or operation of the DDS. The drug charge is important during both incorporation and release from the DDS, therefore the pK_a must be taken into account. As high levels of drug loading may not be possible the drug should be relatively potent (require <1 mg release per day) [42]. Drug selection is not so limited for ICP/hydrogel composite systems or for electromechanical systems based on ICPs for two reasons. Firstly, as drug can be loaded into these systems after preparation, the drug avoids the harsh conditions which may be used during manufacture where often an acidic environment and an oxidizing potential predominate. Secondly, theoretically higher levels of drug loading are possible.

4.2 ICP Matrix Systems

4.2.1 Drug Incorporation

Bioactive agents may be incorporated into ICP films either during, or following the polymerization process. For some drugs carrying a negative charge, the drug itself can be used as the dopant molecule allowing polymerization to proceed (Fig. 2). In 1984 Zinger and Miller prepared PPy using ferrocyanide as the anionic dopant [43]. Cationic drugs can also be incorporated into ICPs during synthesis [7]. The mechanism of this incorporation was reported by Thompson et al. to involve a combination of electrostatic and hydrophobic interactions between drug, anionic dopant and polymer, along with physical entrapment [33].

There are limitations to incorporating drug into an ICP during polymerization, such as the bioactive molecule interfering with the polymerization process [43] and difficulty maintaining electrical contact between polymer and the WE [33]. The impact of these limitations can be minimized by using a two-layered

synthesis approach. Here an initial layer of ICP is prepared without the bioactive molecule. Once a complete layer of ICP covers the WE a second layer containing the drug can be polymerized. By using this approach Thomson et al. prepared PPy using *p*TS and a neurotrophin growth factor with the excellent mechanical properties usually expected from PPy and improved adhesion between the polymer and WE [33].

Many researchers choose to incorporate bioactive agents into ICP matrices after the polymer has been prepared. In this way optimal polymerization conditions can be used without having to consider the effect on drug loading or stability. The processes described in Eqs. 1 and 2 help describe the electrostatically controlled incorporation of anionic or cationic drugs. Konturri et al. prepared PPy films using *p*TS as the anionic dopant. In order to incorporate anionic drugs of interest into the ICP, the polymer films were cycled between −0.8 and +0.5 V at 10 mV s^{-1} in a 0.1 M solution of Na^+ and a selected anion. This forced the ICP to repeatedly alternate between reduced and oxidized states and the *p*TS was exchanged for either salicylate, naproxen or nicoside anions [35].

The post-synthesis electrostatic incorporation of several cationic drugs into conducting polymers has been reported [9, 31, 44, 45]. To achieve this PPy films were prepared using large immobilized anions including melanin or poly(styrene sulfonate). Following synthesis cationic drugs were incorporated on reduction of the ICP as described in Eq. 2. When reduced the ICP charges are neutralized, but there will be a net negative charge in the ICP matrix due to the immobilized anions. In this state cationic species will be attracted into the polymer from the surrounding solution. Care must be taken as this is not a selective process and all species present in the environment have the potential to be incorporated into the polymer.

It is also possible to promote the incorporation of neutral drugs into ICP films following synthesis. George et al. used anionic biotin as the primary dopant during PPy synthesis [46]. After preparation, the polymer was incubated with streptavidin which bound to the biotin in the ICP film. This approach greatly increases the range of drugs that can be incorporated into the ICP film as streptavidin has multiple binding sites and the ICP–biotin–streptavidin complex could potentially bind a range of biotin labeled compounds. Biotinylated nerve growth factor (NGF) was used as a model compound and was bound to the PPy film [46]. An alternate approach was reported by Bidan et al. who used anionic *β*-cyclodextrins (CDX) as dopants to prepare PPy [47]. Following polymerization the uncharged antipsychotic drug, *N*-methylphenothiazine (NMP), was loaded into the ICP when the film was submerged in a 0.1 M NMP solution. The mechanism for this loading relied on the hydrophobic tendencies of NMP; the interior of the CDX is hydrophobic relative to the surrounding aqueous solution therefore NMP moved into the CDX interior.

A summary of the polymerization conditions used in published studies to prepare ICP matrix based DDS is given in Table 1.

Table 1 Conditions used for polymer synthesis and drug release from ICP matrices

Reactants/mol L^{-1}	Synthesis conditions	Drug, charge	Release conditions	Reference
Pyrrole/N/A Sodium perchlorate/N/A	N/A	Glutamate, anion	−1.0 V for 2 min	[43]
Pyrrole/0.1 Dexamethasone/0.1	+1.8 V	Dexamethasone, anion	CV −0.8 to +1.4 V (100 mV s^{-1})	[37]
Pyrrole/0.25 ATP/0.02	+0.5 to +1 V, or 0.1–10 mA cm^{-2}	ATP, anion	−0.7 V for 10 min	[36]
Pyrrole/0.25 AQSA/0.025	0.2 mA cm^{-2}	AQSA, anion	−0.8 V	[105]
Pyrrole/0.2 Fluoroscein/0.01	+0.9 V	Model drug fluorescein, anion	−2.0 V	[106, 107]
Pyrrole/0.1 *p*TS/0.1	+1.0 V (observed 2 mA cm^{-2})	Salicylate, naproxen and tosylate, anions	Potential steps between −0.5 and −1.3 V	[35]
Pyrrole/0.1 *p*TS/0.05, 0.1, 0.2	+0.6 V	ATP, anion	−0.6 V	[12]
Pyrrole/0.2 *p*TS/0.05	2 mA cm^{-2}	$NT3^{+}$, cation	CV −0.8 to +1.0 V (50 mV s^{-1}) ±0.6 V (5 Hz) ±0.5 mA (5 Hz) ±20 mA (5 Hz)	[33]
Pyrrole/0.1 ATP/0.02	+0.8 V	ATP, anion	CV 0.0 to −1.1 V (10 mV s^{-1}) Potential steps 0.0 V for 1 min −1.1 V for 1 min	[108]
Pyrrole/0.1 Sodium dodecyl benzene sulfonate/0.02 Biotin/0.0082	2 mA cm^{-2}	Nerve growth factor, neutral	−3 V	[46]

(continued)

Table 1 (continued)

Reactants/mol L^{-1}	Synthesis conditions	Drug, charge	Release conditions	Reference
Pyrrole/0.5 ß-napthalenesulfonic acid/0.4	CV +0.5 to +1.2 V (20 mV s^{-1})	Fluorescein cadaverin, anion	Mechanical pressure	[63]
EDOT/0.02 Phosphate buffered saline	0.9 mA cm^{-2}	Dexamethasone, anion	CV 0.0 to +1.0 V (100 mV s^{-1})	[11]
Pyrrole/0.1 Heptasulfofonated ß-cyclodextrin/0.01	+0.4 V	*N*-methylphenothiazine, neutral/cation	CV −1.2 to +0.4 V (20 mV s^{-1})	[47]
1st layer: Pyrrole/0.1 2-ethylhexylphosphate (EHP)/0.02 2nd layer: *N*-methyl pyrrole/0.1 Poly(styrene sulfonate)/0.1	1st layer: +0.85 V 2nd layer: +0.9 V	EHP, anion	−0.8 V	[109]
N-methyl pyrrole/0.05 Poly(styrene sulfonate)/0.1	4.4 mA cm^{-2}	Dopamine, cation	+0.5 V	[9]
N-methyl pyrrole/0.05 100% sulfonated poly(styrene sulfonate) 0.6% w/w, or 45–55% sulfonated poly(styrene sulfonate) 0.3% w/w	4.4 mA cm^{-2}	Dopamine, cation	Potential step to between +0.4 and +0.6 V	[45]
Pyrrole/0.1 ATP/0.02	+0.8 V	ATP, anion	CV −1.0 to 0.0 V (10 mV s^{-1}) constant −0.5 V	[110]
Pyrrole/0.05 $Fe(CN)_6^{4-}$/0.01 NaCl/0.1	+ 0.7 V	$Fe(CN)_6^{4-}$, anion	Thick films (2 C cm^{-1}) −0.4 V. Thin films (0.22 C cm^{-1}) < −0.6 V.	[38]

(continued)

Table 1 (continued)

Reactants/mol L^{-1}	Synthesis conditions	Drug, charge	Release conditions	Reference
Pyrrole/0.02 Melanin/0.064 g L^{-1} NaCl/0.1	+0.6 V	Chlorpromazine, cation	CV −1.0 to +0.4 V (50 mV s^{-1}) Step change +0.4 to −1.0 V	[31]
Pyrrole/0.2 *p*TS/0.1	2 mA cm^{-2}	Risperidone, cation	+0.6 V −0.6 V ±0.6 V, 0.5 Hz	[7]
Pyrrole/0.2 Sulfosalicylate/0.2 *Or* Pyrrole/0.2 NaCl/0.1	2.5 mA cm^{-2} *Or* 2 mA cm^{-2}	Sulfosalicylate, anion ATP, anion	−0.5, −0.8, −1.0 V *Or* 0, −0.33, −0.5, −0.8 V	[48]

4.2.2 Drug Release

Electrostatic Driven Release

Electrostatic forces can be utilized to control the release of both anionic and cationic bioactive agents according to the processes described in Eqs. 1 and 2. This process was first illustrated by Zinger and Miller in 1984 following incorporation of glutamate anions into PPy films [43]. Release was tested when no electrical stimulation was applied to the PPy films and when a reducing −1.0 V was applied. A 14 times increase was seen in the reduced films compared to the unstimulated films. Similarly Konturri et al. were able to release increased amounts of salicylate, naproxen and *p*TS anions from PPy films on application of a reducing potential [35]. These researchers noted that despite having a smaller molecular weight than naproxen, nicoside anions could not be released from PPy. This suggests that molecular weight is only a partial determinant of whether a species will be mobile in an ICP matrix. An alternative approach to using electrical stimulation to alter the redox state of ICP films is to use a chemical approach [36]. Pernaut and Reynolds used a chemical reducing agent to promote the release of ATP anions, however lower levels were released compared to electrochemical reduction of the ICP. This may have been due in part to the impermeable nature of the chemical reductant into the ICP, allowing for only surface reduction of the PPy film, but not of the bulk material. Moreover, with a chemical reductant fine control of the redox state of an ICP is lost, as is the ability to cycle between redox states. The applicability of such an approach must also be questioned when designing a system for in vivo use as a sufficiently powerful reducing environment may not be present.

Ge et al. investigated drug release from gold microelectrode arrays consisting of 36 microelectrodes [48]. Each of the microelectrodes was covered in either PPy-ATP or PPy-sulfosalicylate. The electrical stimulus to each microelectrode could be individually controlled. In this way the release of 1 or 2 drugs could be achieved in a pulsatile fashion from a single silicon chip. One issue with using an ICP matrix to achieve controlled drug delivery is the inability to completely shut off release. Often in the absence of electrical stimulation ICP matrices still release drug due to diffusion processes. Ge et al. were able to reduce the open circuit release of sulfosalicylate from PPy-sulfosalicylate films by polymerizing a layer of PPy-Cl on top of the drug containing layer [48]. This greatly reduced the spontaneous release of sulfosalicylate whilst the electrically stimulated release could still be achieved.

Release of cationic drugs can be driven by the electrostatic oxidation of ICP matrices. When oxidized, electrons are removed from the ICP backbone creating a positive charge; the resulting electrostatic repulsion will encourage the cationic drug to leave the polymer. This was initially demonstrated by Miller et al. who prepared PPy and PPy derivatives with immobilized anions [9, 44, 45]. Following synthesis cationic dopamine was incorporated into the ICP on reduction according to Eq. 2. Subsequently, when the polymer was oxidized dopamine was released from the film. Interestingly the polymer film could then be reloaded with dopamine on reduction and released on oxidation. Similarly, Hepel and Mahdavi prepared

PPy-melanin films and were able to incorporate the cationic drug chlorpromazine on reduction, and release the drug when the ICP was oxidized [31].

Novel approaches have allowed even neutral drugs to be released under electrostatic control. Following preparation of PPy with biotin as the primary dopant streptavidin was introduced followed by the biotinylated drug [46]. On subsequent electrochemically driven reduction, release of the biotin–streptavidin–biotinylated drug complex was observed. A nerve growth factor was used as the model drug and the biological activity of this entity was retained following biotinylation. An alternative approach was taken by Bidan et al. where uncharged NMP drug was incorporated into a PPy film doped with CDX [47]. The bioactive agent was seen to release on oxidation of the ICP. When the oxidizing stimulus was applied NMP was oxidized to NMP^+. Two possible release mechanisms were proposed; firstly, release was due to electrostatic repulsion between PPy^+ and NMP^+, and secondly, NMP^+ is more polar than NMP promoting drug to leave the hydrophobic CDX core and enter the surrounding aqueous media. It is likely that both proposed mechanisms play a role in drug release.

Actuation Driven Release

ICPs can undergo volume changes following electrochemically driven alterations in redox state [26]. The actuating properties of ICPs have been utilized in various ways to control drug release. Bidan et al. prepared dexamethasone containing poly(lactic-*co*-glycolic acid) fibers and coated these with the ICP PEDOT [11]. The PEDOT coating was partially permeable to the bioactive agent; under 25% of total dexamethasone was released after 54 days. However, following electrical stimulation which cycled PEDOT between redox states, up to 75% of incorporated dexamethasone could be released in a controllable fashion. The observed increase in drug release may have been due to cracks opening in the PEDOT coating on actuation increasing the permeability of drug through the ICP coating.

Actuation has been identified as a driving mechanism for drug release from ICP matrices [7]. Release of cationic risperidone from PPy films doped with *p*TS did not follow the expected release pattern attributable to electrostatic forces following electrochemically driven redox stimulation. Instead, an increase in release of cationic drug was seen on reduction with a decrease in release on oxidation. AFM characterization allowed a correlation to be made between increased drug release and expansion of the polymer film. It was concluded the faster rates of drug release observed may have been due to the expanded film being more permeable to risperidone.

4.3 ICP/Hydrogel Composite Systems

Hydrogels are a cross-linked networks of hydrophilic polymers [49]. These polymeric materials are able to absorb a great deal of water (>20% with some

capable of 99% + (w/w)) whilst maintaining their 3D structure. Hydrogels, like ICPs, are capable of responding to environmental changes—physical properties can be altered in response to temperature, pH, electrical signal, light and mechanical pressure [50]. However, the speed of response is often slower than ICPs. By creating composite ICP/hydrogel materials researchers have attempted to overcome some of the limitations usually noted with straight ICP systems, namely; large drug molecules may be unable to be released, only low levels of drug loading can be achieved, drug charge may be incompatible with system design.

The first ICP/hydrogel composite was created when PPy was electropolymerized inside a polyacrylamide hydrogel by Gilmore et al. Table 2 [51]. This technique allowed an ICP to be grown with a total volume of *ca.* 36 cm^3, far greater than could be produced from a straight ICP due to mechanical constraints. To form these composite materials contact is required between a working electrode and the hydrogel (Fig. 3). If the hydrogel contains ICP monomer, on commencement of electropolymerization the ICP will be polymerised first on the WE then start to grow through the hydrogel using the gel fibres as a template. Kim et al. formed PPy inside a polyacrylamide hydrogel when a constant 0.5 mA cm^{-2} was applied to a three electrode setup with the WE immersed in the hydrogel [52]. PPy was seen to grow out from the electrode through the hydrogel (Fig. 4). After 2 h the hydrogel was completely permeated, however even after 24 h the total PPy content was reported as <5% (w/w). At these relatively high levels of PPy the structure of the hydrogel was compromised due to excessive water ingress in response to the increase in osmotic pressure caused by PPy and counterions. By controlling the extent of ICP polymerization within the hydrogel supporting network the water content of the gel could be maintained, while the composite material was conductive and redox active. It should be noted that the speed of response to redox activation was slower compared to an intact ICP which may be due to reduced ion mobility or reduced conductivity in the composite materials.

Small et al. prepared composite ICP/polyacrylamide materials by growing PPy or PANI with various counterions [53]. Following polymerization of the ICP inside the gel a high proportion of water (80–95% (w/w)) was maintained. A model drug calcon was released from the composite materials following application of −0.75 V, demonstrating the open pore structure of the hydrogel was maintained after ICP polymerization. The pore size of the hydrogel can be influenced by controlling the gelation process which has implications for drug mobility inside the composite matrix [10].

Lira and de Torressi prepared a PANI-polyacrylamide composite to test the release of safranin dye as a model drug [10]. To incorporate safranin the composite material was placed in 5 mM safranin solution for 24 h. Release was tested at open circuit, and when either −0.2 V or +0.6 V was applied. An increase in safranin was noted when an oxidizing +0.6 V was applied to the composite system. This was accompanied by expansion of PANI within the hydrogel pores and a corresponding increase in the efflux of water and safranin [10]. The same researchers have also examined PPy grown inside a polyacrylamide hydrogel [54]. Raman spectroscopy proved a useful tool to examine the distribution of PPy inside the gel.

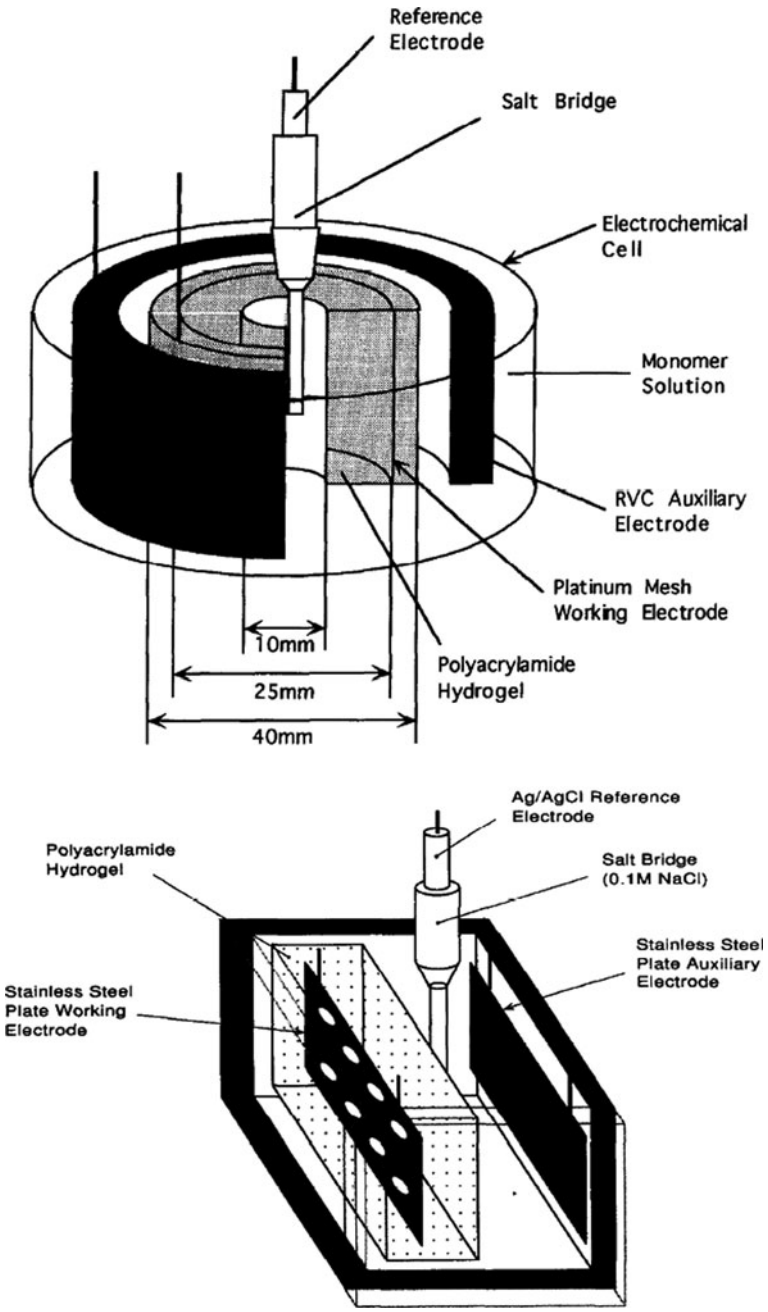

Fig. 3 Three electrode cells allowing for the polymerisation of ICP/hydrogel composite material with flexible geometries. Reprinted from [53] with permission from Elsevier

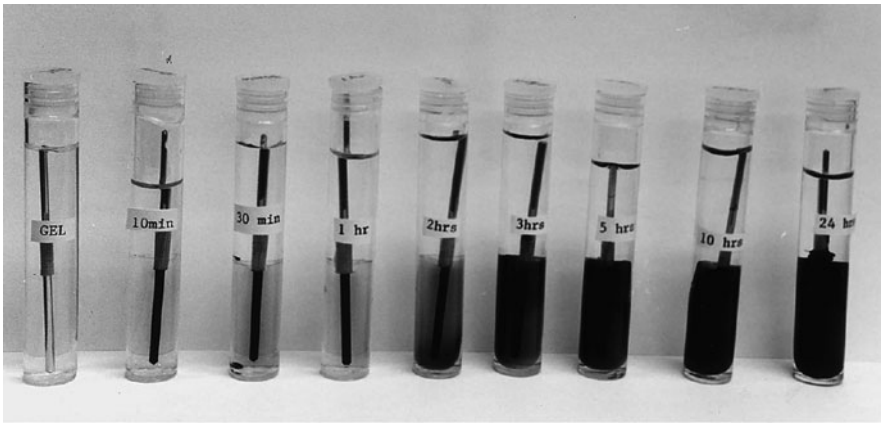

Fig. 4 ICP polymerisation inside a hydrogel. Reprinted from [52] with permission from Elsevier

Polyacrylamide gels were prepared with larger or smaller pore sizes. PPy distribution was far more uniform in the larger pore sizes (2.0 nm) compared to irregular distribution observed in hydrogels with smaller pore sizes (0.5 nm).

In other work, a poly(vinyl alcohol)-heparin hydrogel was covalently bound to a PPy film [55]. Although the ICP and hydrogel were not intimately interwoven, heparin release was found to be twofold greater when the system was stimulated with electrical current compared to when it was not. The increase in drug release was not fully elucidated but was attributed to actuation effects of the ICP swelling and contracting altering the water content of the hydrogel and affecting the release of heparin from the hydrogel. These results are somewhat surprising as PPy was reported to have been polymerised by applying a constant +8 V. This high voltage would have been expected to severely overoxidize the polymer and would have reduced its actuating properties [28].

Recently, neural electrodes were coated with ICP/hydrogel composites to provide materials for implantation which were soft, with low impedance and high charge density, which could provide for the controlled release of the anti-inflammatory drug dexamethasone [56]. When drug release from an ICP coating was tested without the hydrogel component a burst release pattern was seen, with 95% of the dexamethasone releasing within the first 5 weeks. However when the composite ICP/hydrogel system was used this burst release was decreased with only 60% releasing within 5 weeks, allowing for more prolonged sustained release.

Compared to using straight ICP matrices for the controlled release of drugs, ICP/hydrogel composite systems offer the possibility of higher drug loading and the ability to apply the system to a wide range of bioactive agents with differing physicochemical parameters. ICP actuation appears to be the main mechanism of controlling drug release from ICP/hydrogel composite systems [10]. However there are possible drawbacks including slower response to redox stimulation, alterations in mechanical properties, and issues with electrode to ICP contact.

Table 2 Polymerisation conditions for ICP/hydrogel composites

Hydrogel	ICP reactants/mol L^{-1}	Synthesis conditions	Drug	Release conditions	Reference
Polyacrylamide	Pyrrole/0.2 $NaNO_3$/0.5	Constant current	N/A	N/A	[51]
Poly(vinyl alcohol)	Pyrrole/0.1 *p*TS/0.1	+8 V	Heparin	1 mA	[55]
Polyacrylamide	Anline/0.5 HCl/1	+0.75 V	Safranin (model drug)	−0.2 V +0.6 V	[10]
Polyacrylamide	PPy composites from: Pyrrole/0.2 Nitrate or dextran sulfate or chondroitin sulfate or tiron or polyvinylsulfonate or dodecylsulfate or chloride or pTS/0.05 PANI composites from: Aniline/0.2 Chloride or nitrate or pTS/1.0		Calcon (model drug)	−0.75 V	[53]
Polyacrylamide	Pyrrole/N/A pTS/0.1 or $NaNO_3$/1	0.5 mA cm^{-2}	N/A	N/A	[52]
Alginate	EDOT/0.01 $LiClO_4$/0.1	0.5 mA cm^{-2}	Dexamethasone	Open circuit	[56]
Polyacrylamide	Pyrrole/0.4 or 0.5 Sodium nitrate/1.0 or 1.2	0.6 or 0.7 V	Safranin	−0.5 V +0.5 V	[54]

4.4 Electromechanical ICP Systems

The controlled release of drugs from electromechanical systems have several potential advantages over other ICP platforms including better reproducibility, increased applicability of the system to a wide range of drugs, increased reliability and the ability to completely shut off release. ICPs actuators have found biomedical application and have been researched extensively as artificial muscles [57]. These same actuating properties can be utilized to control the release of drugs from electromechanical systems by operating values or in a pump arrangement. ICPs are promising materials to use as actuating components in biomechanical systems as they perform reliably in body fluids, are highly energy efficient with low power requirements, are inexpensive and are biocompatible [4, 8].

Low et al. investigated the ICP PANI for use as a microactuator, both as a single material and in combination with the hydrogel poly(2-hydroxyethylmethacrylate) [58]. Different combinations of these microactuators and electrodes could be used to

control the movement of drug containing fluid from a reservoir (Fig. 5). Electrochemically controlled volume changes were observed in both materials but the combinational material occupied a larger volume and had a smoother morphology, both desirable properties for sealing valves.

An electromechanical system was assembled by Tsai and Madou consisting of a drug reservoir, circuitry and microbatteries [59]. Release of drug from the reservoir was controlled by a PPy/gold bilayer valve. On application of +1.2 V, the valve opened an aperture and allowed drug to escape from the reservoir. There is the possibility of constructing a device containing multiple drug reservoirs, each containing the same drug, or different drugs. Xu et al. demonstrated that the controlled release of dye from an array of reservoirs could be achieved by

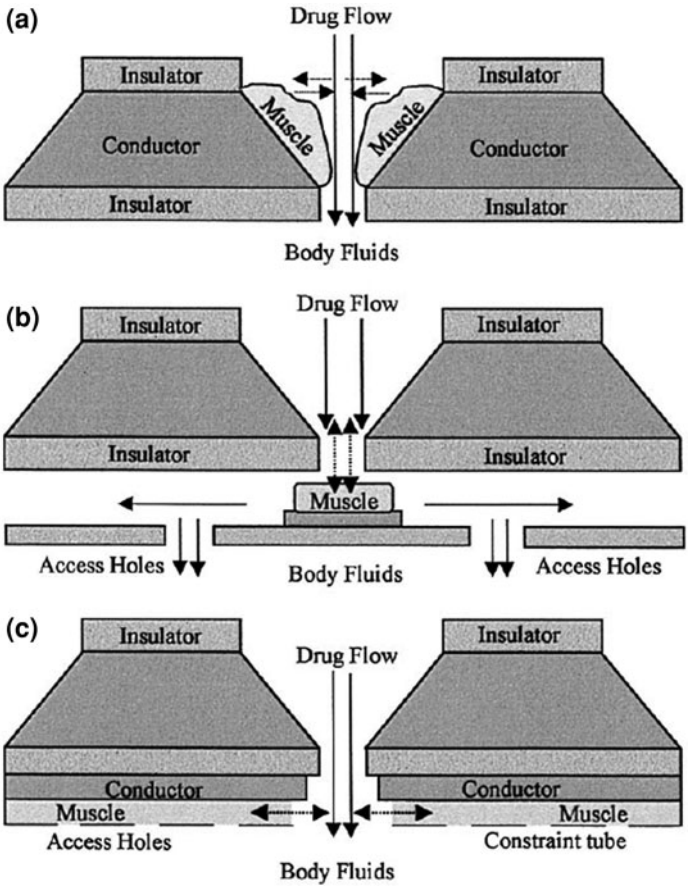

Fig. 5 Alternate arrangements of ICP actuators to control the flow of fluid though an opening; (**a**) sphincter configuration, (**b**) plunger configuration, (**c**) tube configuration. Reprinted from [58] with permission from Elsevier

actuating individual valves consisting of PPy/gold bilayers [8]. By using multiple drug reservoirs complex release patterns could be achieved.

A different approach was taken by Stassen et al. who used the ICP poly (3-hexylthiophene) to control the movement of dopamine through a membrane [60]. A membrane containing pores of a determined size was coated with a thin layer of ICP, sufficient to cover the membrane whilst maintaining the open pores. On oxidation of the ICP the polymer coating expanded reducing the permeability of the membrane to the bioactive agent. On reduction the ICP contracted rendering the membrane more permeable to dopamine, 40% more drug was able to pass through the membrane with the ICP in the reduced state.

5 Characterization

5.1 Infrared and Raman Spectroscopy

Infrared (IR) and Raman spectroscopy are complementary techniques useful to examine the various stretching and bending modes indicative of certain intramolecular bonds and are used to identify functional groups. These techniques can be used in isolation or together to identify and characterize ICPs. Raman spectroscopy was used by Kilmartin et al. to provide information on the oxidation state of PPy films [61] and by Chiu et al. to study dopants' effect on PEDOT oxidation. Typical absorption peaks of PPy seen with Raman spectroscopy are displayed in Table 3. A strong band at 1,580 cm^{-1} is attributed to C=C backbone stretching, a shift in this band to higher wave numbers can be used to indicate lower doping levels of PPy, or shorter polymer chain lengths [17, 62]. IR spectroscopy bands typical of PPy are often observed between 1,400 and 1,650 cm^{-1} and are attributed to C=C and C–N bonds [37, 63–65]. Both IR and Raman spectroscopy can be used to detect overoxidation of PPy, due to the formation of carbonyl groups, seen around 1,700 cm^{-1} on IR spectra [63, 66], or around 1,620 cm^{-1} on Raman spectra [28]. In addition, both techniques can be used to identify species present in the ICP matrix [12, 37, 63, 65]. An alternate application of Raman spectroscopy has involved the examination of PPy penetration as it is grown inside a

Table 3 Raman absorption bands observed in PPy [17, 28]

Bonding	Absorption peak (cm^{-1})
C–H out of plane bending (oxidized PPy)	927
C–H in-plane deformation	Doublet at 1,050 and 1,080
C–H or N–H in plane bending	1,240
PPy ring stretching	Doublet at 1,320 and 1,380
C=C backbone stretching	1,580
C=O	1,620

polyacrylamide hydrogel network [54]. By looking at the spectra at different locations of the polymer, Raman data suggested PPy was able to distribute more homogeneously inside the hydrogel with pore diameters of *ca.* 2.0 nm compared to those gels with pore diameters *ca.* 0.5 nm.

5.2 Scanning Electron Microscopy

Scanning Electron Microscopy (SEM) can be used to examine the surface morphology of a polymer. The surface morphology displayed has been used to explain different cell interactions with ICP and can have a bearing on cell adhesion and compatibility [67]. Figure 6 displays a typical image of PPy, the surface of which is often described as 'cauliflower like' with multiple small projections coming off larger projections [7, 33]. The surface morphology of polymer films often changes during the polymerization process. Thin PPy films containing different dopants may appear similar, but differences are noticeable as the films grow to greater thicknesses [67]. Indeed great variation in polymer surfaces can be produced by adjusting the polymerization parameters [17], or when different dopant anions are used during polymerization [68]. Unfortunately SEM is only able to image dry samples. This is may provide false representations of a surface that will find in vivo use in an aqueous environment.

5.3 Atomic Force Microscopy

Atomic Force Microscopy (AFM) is a high resolution technique for studying ICP surfaces in situ and to provide information on morphological changes during oxidation and reduction events. AFM involves measuring the surface forces

Fig. 6 SEM image of PPy-*p*TS [7]

between a sharp stylus probe and a surface [69]. In the fundamental mode of AFM a cantilevered probe is raster-scanned over the sample while maintaining constant force between the probe and sample. The basic information gained is a map of the surface topography. The standard spatial resolution for AFM scans is in the nanometer range in plane and Ångstroms in height and a single scan can cover hundreds of micrometers on a side. As in other scanning probe microscopies an AFM can be modified to gain additional information about the sample composition, mechanical, electrical, magnetic and other properties [70]. An important advantage of using AFM to study ICPs over other high resolution techniques such as SEM is the ability to scan in situ and within electrochemical liquid cells (Fig. 7). The ability to scan a film under liquid allows for greater correlation with in vivo performance as a drug delivery system.

AFM has been widely applied to the study of ICPs starting from about 1994. Early studies concentrated on general morphology and roughness measurements resulting from changes in polymerisation or oxidation conditions [71–77]. In 1999 several groups introduced AFM as a means to study the out-of-plane actuation of thin film ICPs [25, 78, 79]. This was a substantial breakthrough as the volume changes that ICPs undergo upon oxidation and reduction cycling could be directly measured with high spatial and temporal resolution. This complemented measurements from quart crystal microbalance (QCM) and ellipsometry studies and led to a more general understanding of ICP chemomechanical actuation [80, 81]. Other studies have used AFM for the study of ICP nucleation and mechanical properties, for nanoscale characterization and patterned deposition [82–87].

Different ions used in the preparation of PPy have resulted in films with vastly differing % strain [25, 88]. AFM measurement of volume changes during ICP actuation have been directly linked to drug release rates from an ICP matrix formulation [7]. By modelling the system as linear and time-invariant (LTI), a simple model describing actuation was proposed [89] as per Eq. 3

$$Z(t) = Z_{\infty}\left(1 - e^{-t/\tau}\right) \tag{3}$$

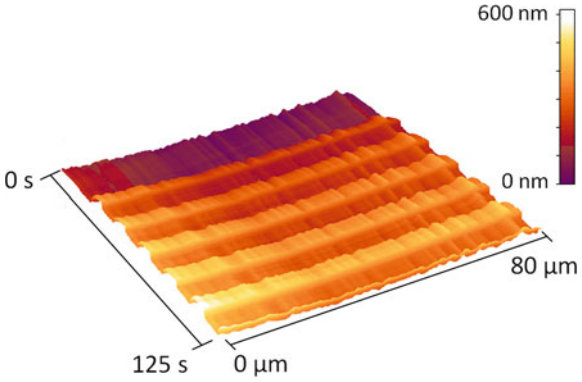

Fig. 7 AFM image of an 80 µm line of PPy-dodecylbenzene sulfonate film immersed in phosphate buffered saline (PBS). Height changes *vs* time are shown when ±0.6 V is applied at 0.05 Hz

Where $Z(t)$ is the function describing the height of the film over time. The characteristic time constant, τ, is the time it takes the system height to reach $\sim 67\%$ of its final actuation magnitude.

This equation has been used to describe both oxidation and reduction forced actuation and improves upon the standard description using constant strain rates which only take into account a linear actuation pattern. This description will allow the use of control theory for both open loop quantification of drug release and closed-loop feedback control of drug dosing for implantable systems.

5.4 Scanning Ion Conductance Microscopy

Scanning ion conductance microscopy (SICM) [90–92] is another scanning probe technique that is being applied to the characterization of conducting polymers in our laboratory. Instead of a sharp stylus, SICM probes the local ionic conductance near the pore opening of a drawn capillary, which can be very small—from micrometers to nanometers. Like AFM, SICMs can be operated in situ and to measure topography; however, the real advantage of SICM is the ability to read out and/or change the ionic composition near a conducting polymer. The possibilities are therefore twofold. Firstly, SICM produces spatially and temporally resolved information about the localized ionic conductance which gives a measure of the movement of dopants including ionic drugs, allowing a map of the polymers ability to release drugs to be produced. Secondly, by driving a current through the SICM probe ICPs can be deposited or modified with high spatial resolution (Fig. 8).

6 Stability

There is limited data available on the stability of ICPs. To be clinically useful an ICP based DDS must be able to be prepared in advance and stored until administration to the patient. Conductivity measurements have been used as an indicating parameter

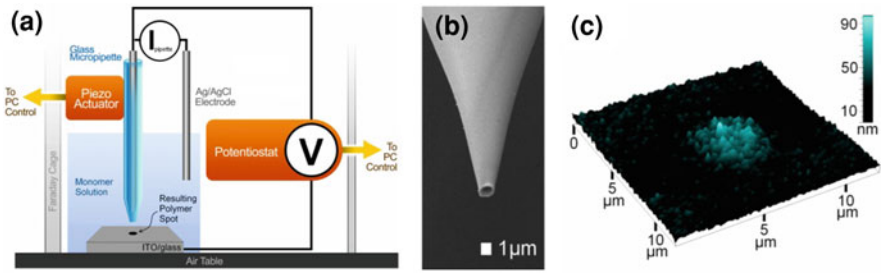

Fig. 8 Representative scanning ion conductance microscopy (SICM) setup (**a**), SEM image of the capillary pore (**b**) and AFM image of an electrodeposited ICP spot using this setup (**c**) (unpublished, courtesy of C. Laslau)

to assess stability [14, 19–23]. This is an easily measured parameter that gives an indication of alterations in polymer structure that may occur over time. The dopant anion used, and its concentration during synthesis, have been shown to influence the stability of the final product. PPy films prepared with *p*TS appear more stable than PPy prepared with either ClO_4^-, BF_4^-, NO_3^- [14] or dodecyl sulfate [18]. PPy-*p*TS prepared from solutions containing *p*TS at concentrations of 0.05 M or higher have shown enhanced stability compared to polymers prepared from lower *p*TS concentrations [19]. Not surprisingly, temperature during storage affects stability. Brie et al. reported PPy-*p*TS films stored at ambient temperatures showed an increase in conductivity for *ca.* 2 weeks followed by a slow loss of conductivity [14]. At temperatures between 80 and 120°C a similar pattern was reported by separate investigators but the decline in conductivity began after a shorter time [20]. PPy-*p*TS films containing risperidone stored at 40°C also showed an increase in conductivity after 6 days, followed by a subsequent decline [23]. The conductivity observed in ICPs is known to be reliant on the presence of conjugated polymer chains [93]. In addition to the propagation of charge along polymer chains, 'charge-hopping' between polymer chains also occurs [94]. The initial increase in conductivity reported may be due to a realignment of polymer chains promoting the 'charge-hopping' between chains. Over time a decline in conductivity is reported in the literature. This appears to be due to the irreversible loss of conjugation of the ICP backbone when PPy reacts with oxygen producing carbonyl defects [14, 95]. Supporting data for this hypothesis can be found in FTIR investigations which have noted the appearance of a band at 1,690 cm^{-1} characteristic of α, β-unsaturated ketones due to the oxidation of PPy [16]. To add to this body of evidence Truong et al. reported an experiment where PPy-*p*TS films were stored at 150°C either in air or an oxygen free environment [18]. The conductivity of the films stored in air began to fall immediately, however the films stored in an oxygen free environment showed no decrease in conductivity after 3 days. If oxygen was subsequently introduced to the system conductivity started to fall immediately.

Recently the actuation parameters of PPy-*p*TS films containing risperidone were used to assess the stability of the DDS. ICP films were stored at 40°C and the amplitude of actuation of these films was seen to decline over a 6 day period [23]. As actuation was attributed as a driving force behind drug release this helped explain the observed decline in drug releasing rates with time. If ICP based DDS are to find use in the clinical setting the stability of these devices needs to be fully investigated and the stability profile improved, to ensure the DDS remains functional on storage.

7 Considerations for the Design of ICP Based Drug Delivery Systems

There is a great opportunity for using drug-eluting ICPs in controlled release formulations, especially in standalone applications, but their success will ultimately rely on the means used to control release. Therefore consideration must

be given to the design of the DDS. The basic release process relies on the controlled oxidation and reduction of the ICP, leading to the redox-coupled release or retention of the drug. The redox state of the polymer can be controlled chemically or electrically—leading to two different potential means to control release.

It would be difficult to transfer techniques used in vitro to chemically oxidize or reduce ICPs for in vivo use. However, there is the possibility that redox control of the drug eluting ICP could be coupled to changes to the in vivo redox potential, e.g. in response to increases in H_2O_2 during dermal wound inflammation [96]. However, the magnitude of chemical redox potential required to actuate drug release in ICPs is of a scale larger than that normally utilized by biological systems and so it is unlikely that redox changes in vivo could be used to control release directly. Instead, amplification of biological signals to produce substantial redox activity in the ICP would be required—for example consider wound inflammation. Reactive oxygen species such as hydrogen peroxide are a component of the local inflammation response at micromolar concentrations [97]. This spike in the hydrogen peroxide concentration during wound inflammation occurs at levels insufficient to oxidize ICP for drug release, nor would one want to disrupt the normal paracrine signaling function. However, by analogy with redox-amplified biosensors, small amounts of the oxidant could be coupled to a redox species in an ICP-based drug delivery formulation applied to the wound, leading to amplification of the oxidizing signal [98, 99]. Hence, the drug would be released during the inflammation event and turned off as it subsides. A related strategy would be to use the response of a stimulus-sensitive hydrogel in an ICP/hydrogel composite to biological signals lacking electrochemical activity to trigger actuation of the ICP and release of a drug [100].

On the other hand, facile electrical stimulation of drug-eluting ICPs has been demonstrated but applications will require a device to protect the drug releasing ICP from uncontrolled release and provide controlled electrical stimulation. A listing of the desired characteristics for an implantable device can be substantial and would include: small size, localized delivery, appropriate lifetime and stability, limitation of the secondary effects on surrounding tissue, inherent safety from overdosing, and convenient loading, powering and programming.

Implantable electronic devices with some or all of the above characteristics have been developed for clinical use; examples include pacemakers, drug pumps, and biosensors. One exciting possibility would be to use telemetry to communicate with and power an implanted device [41, 101, 102]. The basic setup involves a small transmitter that is implanted into the animal and a receiver that is, in this case, kept underneath the animal's cage. The transmitter can be made very small, with volumes close to 1 mL, and with batteries and electronics sufficient to send signals back to the receiver via telemetry for months on end.

It should be noted that a strong correlation between electrical stimulation and drug release needs to be established in vitro in order to implement an electrically controlled dose. As an example, the link between actuation and dosing established

using AFM and in vitro release was described using simple control theory that can be directly used for dosing control [89]. An alternative for controlling dose would be to create a large array of small, 'all-or-nothing' doses using ICP microfabrication and then using electrical stimulation to selectively trigger release of individual or sets of doses [103]. Finally, a dose regime requiring large volumes of drugs would make an ICP matrix formulation less attractive, however alternatives to direct loading of the ICP with drug are possible. For instance, the ICP could be used as an electromechanical valve or as a switchable selective membrane as a gate on a drug-containing reservoir, allowing the reservoir could be reloaded externally via syringe injection [104].

8 Conclusion

ICPs are an expanding class of materials and one of the more exciting applications is for ICP based DDS. The driving motivation is to realize exact control of drug release by the application of an external electronic control signal. Three general platforms of application are being currently pursued: ICP matrix systems, ICP/hydrogel systems, and electromechanical systems. Whether based on direct control of the ion flux or by indirect control of release from hydrogels or reservoirs, the basic principle is the same: alterations in the redox state of the ICP provide the crucial link between the facile control afforded by electronics and tunable drug release. There are, however, significant hurdles to overcome before ICP-based DDS could be fully realized. Future research should aim to increase the quantities of drug that can be released as current levels of release may be sufficient for localized effects but are generally insufficient if systemic delivery of drug is required. Devices with ICPs as drug-releasing components need to be designed. While these could simply receive external control signals an exciting prospect is to use inherent or external feedback signals to create a closed loop, self regulating system. And for long term application, more research needs to address the in vivo stability and biocompatibility of ICPs developed for DDS. Certainly, the advancement of these exciting materials within DDS is expanding and will continue to do so because the final outcome is a compelling one: exact matching of drug release to treatment requirements, thereby fully optimizing patient treatment outcomes.

Acknowledgements Thanks to Cosmin Laslau for providing the SICM figure.

References

1. Irani, F., Dankert, M., Brensinger, C., Bilker, W.B., Nair, S.R., Kohler, C.G., Kanes, S.J., Turetsky, B.I., Moberg, P.J., Ragland, J.D., Gur, R.C., Gur, R.E., Siegel, S.J.: Patient attitudes towards surgically implantable, long-term delivery of psychiatric medicine. Neuropsychopharmacology **29**(5), 960–968 (2004)

2. Marder, S.R.: Overview of partial compliance. J. Clin. Psychiatry **64**(Suppl 16), 3–9 (2003)
3. Pandey, R., Khuller, G.K.: Polymer based drug delivery systems for mycobacterial infections. Curr. Drug. Deliv. **1**(3), 195–201 (2004)
4. Geetha, S., Rao, C.R., Vijayan, M., Trivedi, D.: Biosensing and drug delivery by polypyrrole. Anal. Chim. Acta **568**, 119–125 (2006)
5. Norden, B., Krutmeijer, E.: The nobel prize in chemistry, 2000: conductive polymers. Kungl. Vetenskapsakademien. http://nobelprize.org/nobel_prizes/chemistry/laureates/2000/chemadv.pdf (2000). Accessed 25 Mar 2009
6. Richardson, R., Thompson, B., Moulton, S., Newbold, C., Lum, M.G., Cameron, A., Wallace, G., Kapsa, R., Clark, G., O'Leary, S.: The effect of polypyrrole with incorporated neurotrophin-3 on the promotion of neurite outgrowth from auditory neurons. Biomaterials **28**, 513–523 (2007)
7. Svirskis, D., Wright, B.E., Travas-Sejdic, J., Rodgers, A., Garg, S.: Development of a controlled release system for risperidone using polypyrrole: mechanistic studies. Electroanalysis **22**(4), 439–444 (2010)
8. Xu, H., Wang, C., Wang, C., Zoval, J., Madou, M.: Polymer actuator valves toward controlled drug delivery application. Biosens. Bioelectron. **21**, 2094–2099 (2006)
9. Miller, L.L., Zhou, Q.X.: Poly(*N*-methylpyrrolylium) poly(styrenesulfonate). A conductive, electrically switchable cation exchanger that cathodically binds and anodically releases dopamine. Macromolecules **20**, 1594–1597 (1987)
10. Lira, L.M., Cordoba de Torresi, S.I.: Conducting polymer-hydrogel composites for electrochemical release devices: synthesis and characterization of semi-interpenetrating polyaniline-polyacrylamide networks. Electrochem. Commun. **7**, 717–723 (2005)
11. Abidian, M.R., Kim, D.-H., Martin, D.C.: Conducting-polymer nanotubes for controlled drug release. Adv. Mater. **18**, 405–409 (2006)
12. Xiao, Y., Che, J., Li, C.M., Sun, C.Q., Chua, Y.T., Lee, V.S., Luong, J.H.: Preparation of nano-tentacle polypyrrole with pseudo-molecular template for ATP incorporation. J. Biomed. Mater. Res. A **80A**(4), 925–931 (2007)
13. Conjugated Polymers: Theory, Synthesis, Properties and Characterization: Handbook of Conducting Polymers, vol. 1, 3rd edn. Taylor & Francis Group, Boca Raton (2007)
14. Brie, M., Turcu, R., Mihut, A.: Stability study of conducting polypyrrole films and polyvinylchloride-polypyrrole composites doped with different counterions. Mater. Chem. Phys. **49**, 174–178 (1997)
15. Fonner, J.M., Forciniti, L., Nguyen, H., Byrne, J.D., Kou, Y.-F., Syeda-Nawaz, J., Schmidt, C.E.: Biocompatibility implications of polypyrrole synthesis techniques. Biomed. Mater. **3**, 034124 (2008)
16. Kaynak, A., Rintoul, L., George, G.A.: Change of mechanical and electrical properties of polypyrrole films with dopant concentration and oxidative aging. Mater. Res. Bull. **35**, 813–824 (2000)
17. Sui, J., Travas-Sejdic, J., Chu, S.Y., Li, K.C., Kilmartin, P.A.: The actuation behaviour and stability of *p*-toluene sulfonate doped polypyrrole films formed at different deposition current densities. J. Appl. Polym. Sci. **111**, 876–882 (2009)
18. Truong, V.-T., Ennis, B.C., Turner, T.G., Jenden, C.M.: Thermal stability of polypyrroles. Polym. Int. **27**, 187–195 (1992)
19. Waynne, K.J., Street, G.B.: Poly(pyrrol-2-ylium tosylate): electrochemical synthesis and physical and mechanical properties. Macromolecules **18**, 2361–2368 (1985)
20. Kaynak, A.: Decay of electrical conductivity in *p*-toluene sulfonate doped polypyrrole films. Fibers Polym. **10**(5), 590–593 (2009)
21. Li, J., Wang, E.: Scanning tunnelling microscopy (STM) and lateral force microscopy (LFM) investigation of the structure and character of conductive polypyrrole film. Synth. Metals **66**, 67–74 (1994)
22. Suarez, M.F., Compton, R.G.: In situ atomic force microscopy study of polypyrrole synthesis and the volume changes induced by oxidation and reduction of the polymer. J. Electroanal. Chem. **462**, 211–221 (1999)

23. Svirskis, D., Wright, B.E., Travas-Sejdic, J., Rodgers, A., Garg, S.: Evaluation of physical properties and performance over time of an actuating polypyrrole based drug delivery system. Sens. Actuators B **151**, 97–102 (2010)
24. Gade, V., Shirale, D., Gaikwad, P., Kakde, K., Savale, P., Kharat, H., Shirsat, M.: Synthesis and characterization of Ppy-PVS, Ppy-pTS, and Ppy-DBS composite films. Int. J. Polym. Mater. **56**, 107–114 (2007)
25. Smela, E., Gadegaard, N.: Surprising volume change in PPy(DBS): an atomic force microscopy study. Adv. Mater. **11**(11), 953–957 (1999). doi:10.1002/(sici)1521-4095(199908)11:11<953:aid-adma953>3.0.co;2-h
26. Kiefer, R., Chu, S.Y., Kilmartin, P.A., Bowmaker, G.A., Cooney, R.P., Travas-Sejdic, J.: Mixed-ion linear actuation behaviour of polypyrrole. Electrochim. Acta **52**, 2386–2391 (2007)
27. John, R., Wallace, G.: The use of microelectrodes to probe the electropolymerisation mechanism of heterocyclic conducting polymers. J. Electroanal. Chem. **306**, 157–167 (1991)
28. Wallace, G.G., Spinks, G.M., Kane-Maguire, L.A., Teasdale, P.R.: Conductive electroactive polymers: intelligent polymer systems, 3rd edn. Taylor & Francis Group, Boca Raton (2009)
29. Vernitskaya, T., Efimov, O.: Polypyrrole: a conducting polymer; its synthesis, properties and applications. Russ. Chem. Rev. **66**(5), 443–457 (1997)
30. Genies, E., Pernaut, J.: Spectroelectrochemical studies of the redox and kinetic behaviour of polypyrrole film. Synth. Metals **10**, 117–129 (1984/1985)
31. Hepel, M., Mahdavi, F.: Application of the electrochemical quartz crystal microbalance for electrochemically controlled binding and release of chlorpromazine from conductive polymer matrix. Microchem. J. **56**, 54–64 (1997)
32. Kanazawa, K., Diaz, A., Geiss, R., Gill, W., Kwak, J., Logan, J., Rabolt, J., Street, G.: 'Organic metals': polypyrrole, a stable synthetic 'metallic' polymer. J. Chem. Soc. Chem. Commun. **19**, 854–855 (1979)
33. Thompson, B.C., Moulton, S.E., Ding, J., Richardson, R., Cameron, A., O'Leary, S., Wallace, G.G., Clark, G.M.: Optimising the incorporation and release of a neurotrophic factor using conducting polypyrrole. J. Control. Release **116**(3), 285–294 (2006)
34. Boyle, A., Genies, E., Fouletier, M.: Electrochemical behaviour of polypyrrole films doped with ATP anions. J. Electroanal. Chem. **279**, 179–186 (1990)
35. Kontturi, K., Pentti, P., Sundholm, G.: Polypyrrole as a model membrane for drug delivery. J. Electroanal. Chem. **453**, 231–238 (1998)
36. Pernaut, J.-M., Reynolds, J.R.: Use of conducting electroactive polymers for drug delivery and sensing of bioactive molecules. A redox chemistry approach. J. Phys. Chem. B **104**, 4080–4090 (2000)
37. Wadhwa, R., Lagenaur, C.F., Cui, X.T.: Electrochemically controlled release of dexamethasone from conducting polymer polypyrrole coated electrode. J. Control. Release **110**, 531–541 (2006)
38. Miller, L.L., Zinger, B., Zhou, Q.-X.: Electrically controlled release of $Fe(CN)_6^{4-}$ from polypyrrole. J. Am. Chem. Soc. **109**, 2267–2272 (1987)
39. Diaz, A.F., Castillo, J.I.: A polymer electrode with variable conductivity: polypyrrole. J. Chem. Soc. Chem. Commun. **9**, 397–398 (1980)
40. Turner, M.S., Stewart, D.W.: Review of evidence for the long-term efficacy of atypical antipsychotic agents in the treatment of patients with schizophrenia and related psychoses. J. Psychopharmacol. **20**(6), 20–37 (2006)
41. Langer, R.: New methods of drug delivery. Science **249**(4976), 1527–1533 (1990)
42. Staples, M., Daniel, K., Cima, M.J., Langer, R.: Application of micro- and nano-electromechanical devices to drug delivery. Pharm. Res. **23**(5), 847–863 (2006)
43. Zinger, B., Miller, L.L.: Timed release of chemicals from polypyrrole films. J. Am. Chem. Soc. **106**, 6861–6863 (1984)
44. Miller, L.L., Smith, G.A., Chang, A.-C., Zhou, Q.-X.: Electrochemically controlled release. J. Control. Release **6**, 293–296 (1987)

45. Zhou, Q.-X., Miller, L.L., Valentine, J.R.: Electrochemically controlled binding and release of protonated dimethyldopamine and other cations from poly(*N*-methyl-pyrrole)/polyanion composite redox polymers. J. Electroanal. Chem. **261**, 147–164 (1989)
46. George, P.M., LaVan, D.A., Burdick, J.A., Chen, C.-Y., Liang, E., Langer, R.: Electrically controlled drug delivery from biotin-doped conductive polypyrrole. Adv. Mater. **18**, 577–581 (2006)
47. Bidan, G., Lopez, C., Mendes-Viegas, F., Vieil, E.: Incorporation of sulphonated cyclodextrins into polypyrrole: an approach for the electro-controlled delivering of neutral drugs. Biosens. Bioelectron. **9**, 219–229 (1994)
48. Ge, D., Tian, X., Qi, R., Huang, S., Mu, J., Hong, S., Ye, S., Zhang, X., Li, D., Shi, W.: A polypyrrole-based microchip for controlled drug release. Electrochim. Acta **55**, 271–275 (2009)
49. Gupta, P., Vermani, K., Garg, S.: Hydrogels: from controlled release to pH-responsive drug delivery. Drug Discov. Today **7**(10), 569–579 (2002)
50. Qiu, Y., Park, K.: Environmental-sensitive hydrogels for drug delivery. Adv. Drug Deliv. Rev. **53**, 321–339 (2001)
51. Gilmore, K., Hodgson, A., Luan, B., Small, C., Wallace, G.: Preparation of hydrogel/conducting polymer composites. Polym. Gels Netw. **2**, 135–143 (1994)
52. Kim, B., Spinks, G., Wallace, G., John, R.: Electroformation of conducting polymers in a hydrogel support matrix. Polymer **41**, 1783–1790 (2000)
53. Small, C., Too, C., Wallace, G.: Responsive conducting polymer-hydrogel composites. Polym. Gels Netw. **5**, 251–265 (1997)
54. Barthus, R.C., Lira, L.M., Cordoba de Torresi, S.I.: Conducting polymer-hydrogel blends for electrochemically controlled drug release devices. J. Brazil. Chem. Soc. **19**(4), 630–636 (2008)
55. Li, Y., Neoh, K., Kang, E.: Controlled release of heparin from polypyrrole-poly(vinylalcohol) assembly by electrical stimulation. J. Biomed. Mater. Res. **73A**, 171–181 (2005)
56. Abidian, M.R., Martin, D.C.: Multifunctional nanobiomaterials for neural interfaces. Adv. Funct. Mater. **19**, 573–585 (2009)
57. Smela, E.: Conjugated polymer actuators for biomedical applications. Adv. Mater. **15**, 481–494 (2003)
58. Low, L.-M., Seetharaman, S., He, K.-Q., Madou, M.J.: Microactuators toward microvalves for responsive controlled drug delivery. Sens. Actuators B **67**, 149–160 (2000)
59. Tsai, H.-K.A., Madou, M.: Microfabrication of bilayer polymer actuator valves for controlled drug delivery. JALA J. Assoc. Lab. Auto. **12**(5), 291–295 (2007)
60. Stassen, I., Sloboda, G., Hambitzer, G.: Membrane with controllable permeability for drugs. Synth. Metals **71**, 2243–2244 (1995)
61. Kilmartin, P.A., Li, K.C., Bowmaker, G.A., Vigar, N.A., Cooney, R.P., Travas-Sejdic, J.: Spectroscopic studies of doping reactions in polypyrrole actuators. Curr. Appl. Phys. **6**, 567–570 (2006)
62. Liu, Y.-C.: Evaluation of the conductivity of the polypyrrole film via its CC bonds stretching on surface-enhanced Raman spectrum. Electroanalysis **15**, 1134–1138 (2003)
63. Bajpai, V., He, P., Dai, L.: Conducting-polymer microcontainers: controlled synthesis and potential applications. Adv. Funct. Mater. **14**(2), 145–151 (2004)
64. Lamprakopoulos, S., Yfantis, D., Yfantis, A., Schmeisser, D., Anastassopoulou, J., Theophanides, T.: An FTIR study of the role of H_2O and D_2O in the aging mechanism of conducting polypyrroles. Synth. Metals **144**, 229–234 (2004)
65. Merz, A., Haimerl, A.: Free-standing, conducting films of polypyrrole/*N*-(4-ferrocenylbutyl-) pyrrole benzenesulphonate copolymers. Synth. Metals **25**, 89–102 (1988)
66. Qu, L., Shi, G., Chen, Fe., Zhang, J.: Electrochemical growth of polypyrrole microcontainers. Macromolecules **36**, 1063–1067 (2003)
67. Ateh, D.D., Navsaria, H.A., Vadgama, P.: Polypyrrole-based conducting polymers and interactions with biological tissues. J. R. Soc. Interface **3**, 741–752 (2006)

68. Ateh, D.D., Vadgama, P., Navsaria, H.A.: Culture of human keratinocytes on polypyrrole-based conducting polymers. Tissue Eng. **12**(4), 645–655 (2006)
69. Binnig, G., Quate, C.F., Gerber, C.: Atomic force microscope. Phys. Rev. Lett. **56**(9), 930 (1986)
70. Eaton, P., West, P.: Atomic Force Microscopy. Oxford University Press, Oxford (2010)
71. Avlyanov, J.K., Josefowicz, J.Y., MacDiarmid, A.G.: Atomic force microscopy surface morphology studies of 'in situ' deposited polyaniline thin films. Synth. Metals **73**(3), 205–208 (1995)
72. Froeck, C., Bartl, A., Dunsch, L.: STM- and AFM-investigations of one- and two-dimensional polypyrrole structures on electrodes. Electrochim. Acta **40**(10), 1421–1425 (1995)
73. Kaynak, A.: Effect of synthesis parameters on the surface morphology of conducting polypyrrole films. Mater. Res. Bull. **32**(3), 271–285 (1997)
74. Li, J., Wang, E., Green, M., West, P.E.: In situ AFM study of the surface morphology of polypyrrole film. Synth. Metals **74**(2), 127–131 (1995)
75. Silk, T., Hong, Q., Tamm, J., Compton, R.G.: AFM studies of polypyrrole film surface morphology I. The influence of film thickness and dopant nature. Synth. Metals **93**(1), 59–64 (1998)
76. Silk, T., Hong, Q., Tamm, J., Compton, R.G.: AFM studies of polypyrrole film surface morphology II. Roughness characterization by the fractal dimension analysis. Synth. Metals **93**(1), 65–71 (1998)
77. Xie, L., Buckley, L.J., Josefowicz, J.Y.: Observations of polyaniline surface morphology modification during doping and de-doping using atomic force microscopy. J. Mater. Sci. **29**(16), 4200–4204 (1994)
78. Smela, E.: Microfabrication of PPy microactuators and other conjugated polymer devices. J. Micromech. Microeng. **9**(1), 1 (1999)
79. Suárez, M.F., Compton, R.G.: In situ atomic force microscopy study of polypyrrole synthesis and the volume changes induced by oxidation and reduction of the polymer. J. Electroanal. Chem. **462**(2), 211–221 (1999)
80. Bay, L., Jacobsen, T., Skaarup, S., West, K.: Mechanism of actuation in conducting polymers: osmotic expansion. J. Phys. Chem. B **105**(36), 8492–8497 (2001). doi: 10.1021/jp003872w
81. Smela, E., Gadegaard, N.: Volume change in polypyrrole studied by atomic force microscopy. J. Phys. Chem. B **105**(39), 9395–9405 (2001). doi:10.1021/jp004126u
82. Charrier, D.S.H., Janssen, R.A.J., Kemerink, M.: Large electrically induced height and volume changes in poly(3,4-ethylenedioxythiophene)/poly(styrenesulfonate) thin films. Chem. Mater. **22**(12), 3670–3677 (2010). doi:10.1021/cm100452a
83. Higgins, M.J., McGovern, S.T., Wallace, G.G.: Visualizing dynamic actuation of ultrathin polypyrrole films. Langmuir **25**(6), 3627–3633 (2009). doi:10.1021/La803874r
84. Kemp, N.T., Cochrane, J.W., Newbury, R.: Patterning of conducting polymer nanowires on gold/platinum electrodes. Nanotechnology **18**(14), 145610 (2007)
85. Kim, J., Sohn, D., Sung, Y., Kim, E.-R.: Fabrication and characterization of conductive polypyrrole thin film prepared by in situ vapor-phase polymerization. Synth. Metals **132**(3), 309–313 (2003)
86. Shimomura, T., Akai, T., Abe, T., Ito, K.: Atomic force microscopy observation of insulated molecular wire formed by conducting polymer and molecular nanotube. J Chem. Phys. **116**(5), 1753–1756 (2002)
87. Venancio, E.C., Costa, C.A.R., Machado, S.A.S., Motheo, A.J.: AFM study of the initial stages of polyaniline growth on ITO electrode. Electrochem. Commun. **3**(5), 229–233 (2001)
88. Gelmi, A., Higgins, M.J., Wallace, G.G.: Physical surface and electromechanical properties of doped polypyrrole biomaterials. Biomaterials **31**, 1974–1983 (2010)

89. Svirskis, D., Wright, B.E., Travas-Sejdic, J., Rodgers, A., Garg, S.: Evaluation of physical properties and performance over time of an actuating polypyrrole based drug delivery system. Sens. Actuators B: Chem. **151**, 97–102 (2010)
90. Hansma, P., Drake, B., Marti, O., Gould, S., Prater, C.: The scanning ion-conductance microscope. Science **243**(4891), 641–643 (1989). doi:10.1126/science.2464851
91. Korchev, Y.E., Bashford, C.L., Milovanovic, M., Vodyanoy, I., Lab, M.J.: Scanning ion conductance microscopy of living cells. Biophys. J. **73**(2), 653–658 (1997)
92. Schäffer, T.E., Anczykowski, B., Fuchs, H.: Scanning ion conductance microscopy. In: Bhushan, B., Fuchs, H. (eds.) Applied Scanning Probe Methods II. NanoScience and Technology, pp. 91–119. Springer, Berlin (2006). doi:10.1007/3-540-27453-7_3
93. MacDiarmid, A.G.: "Synthetic metals": a novel role for organic polymers (Nobel lecture). Angew. Chem. Int. Ed. **40**, 2581–2590 (2001)
94. Kaynak, A.: Electrical conductivity of polypyrrole films at a temperature range of 70 K to 350 K. Mater. Res. Bull. **33**(1), 81–88 (1998)
95. Uyar, T., Toppare, L., Hacaloglu, J.: Spectroscopic investigation of oxidation of *p*-toluene sulfonic acid doped polypyrrole. Synth. Metals **123**, 335–342 (2001)
96. Roy, S., Khanna, S., Nallu, K., Hunt, T.K., Sen, C.K.: Dermal wound healing is subject to redox control. Mol. Ther. **13**(1), 211–220 (2006)
97. Niethammer, P., Grabher, C., Look, A.T., Mitchison, T.J.: A tissue-scale gradient of hydrogen peroxide mediates rapid wound detection in zebrafish. Nature **459**(7249):996–999. http://www.nature.com/nature/journal/v459/n7249/suppinfo/nature08119_S1.html (2009)
98. Fare, T.L., Cabelli, M.D., Dallas, S.M., Herzog, D.P.: Functional characterization of a conducting polymer-based immunoassay system. Biosens. Bioelectron. **13**(3–4), 459–470 (1998). doi:10.1016/s0956-5663(97)00091-2
99. Schuhmann, W.: Electron-transfer pathways in amperometric biosensors. Ferrocene-modified enzymes entrapped in conducting-polymer layers. Biosens. Bioelectron. **10**(1–2):181–193 (1995). doi:10.1016/0956-5663(95)96805-9
100. Qiu, Y., Park, K.: Environment-sensitive hydrogels for drug delivery. Adv. Drug Deliv. Rev. **53**(3), 321–339 (2001)
101. Budgett, D.M., Hu, A.P., Si, P., Pallas, W.T., Donnelly, M.G., Broad, J.W.T., Barrett, C.J., Guild, S.-J., Malpas, S.C.: Novel technology for the provision of power to implantable physiological devices. J. Appl. Physiol. **102**(4), 1658–1663 (2007). doi:10.1152/japplphysiol.00105.2006
102. Cools, A., Lambrechts, P., van Bommel, J.: Wireless power-supplying system for implanted electronic circuits in freely moving animals. Med. Biol. Eng. Comput. **16**(5), 559–563 (1978). doi:10.1007/bf02457809
103. LaVan, D.A., McGuire, T., Langer, R.: Small-scale systems for in vivo drug delivery. Nat. Biotech. **21**(10), 1184–1191 (2003)
104. Kontturi, K., Pentti, P., Sundholm, G.: Polypyrrole as a model membrane for drug delivery. J. Electroanal. Chem. **453**(1–2), 231–238 (1998)
105. Lin, Y., Wallace, G.G.: Factors influencing electrochemical release of 2,6-anthraquinone disulphonic acid from polypyrrole. J. Control. Release **30**, 137–142 (1994)
106. Luo, X., Cui, X.T.: Electrochemically controlled release based on nanoporous conducting polymers. Electrochem. Commun. **11**, 402–404 (2009)
107. Luo, X., Cui, X.T.: Sponge-like nanostructured conducting polymers for electrically controlled drug release. Electrochem. Commun. **11**, 1956–1959 (2009)
108. Li, L., Huang, C.: Electrochemical/electrospray mass spectrometric studies of electrochemically stimulated ATP release from PP/ATP films. J. Am. Soc. Mass Spectrom. **18**(5), 919–926 (2007)
109. Massoumi, B., Entezami, A.A.: Electrochemically stimulated 2-ethylhexylphosphate (EHP) release through redox switching of conducting polypyrrole film and polypyrrole/poly (*N*-methylpyrrole) or self-doped polyaniline bilayers. Polym. Int. **51**, 555–560 (2002)

110. Pyo, M., Maeder, G., Kennedy, R.T., Reynolds, J.R.: Controlled release of biological molecules from conducting polymer modified electrodes. The potential dependent release of adenosine 5′-triphosphate from poly(pyrrole adenosine 5′-triphosphate) films. J. Electroanal. Chem. **368**, 329–332 (1994)
111. Svirskis, D., Travas-Sejdic, J., Rodgers, A., Garg, S.: Electrochemically controlled drug delivery based on intrinsically conducting polymers. J. Control. Release **146**, 6–15 (2010)

Author Index